frontiers | Research Topics

Chilling tolerance and regulation of horticultural crops: physiological, molecular, and genetic perspectives

Edited by
Shifeng Cao, Diane Maria Beckles, Maria F. Drincovich, Isabel Lara, Julian C. Verdonk, Qiong Lin, Chongde Sun and Reinaldo Campos-Vargas

Published in
Frontiers in Plant Science

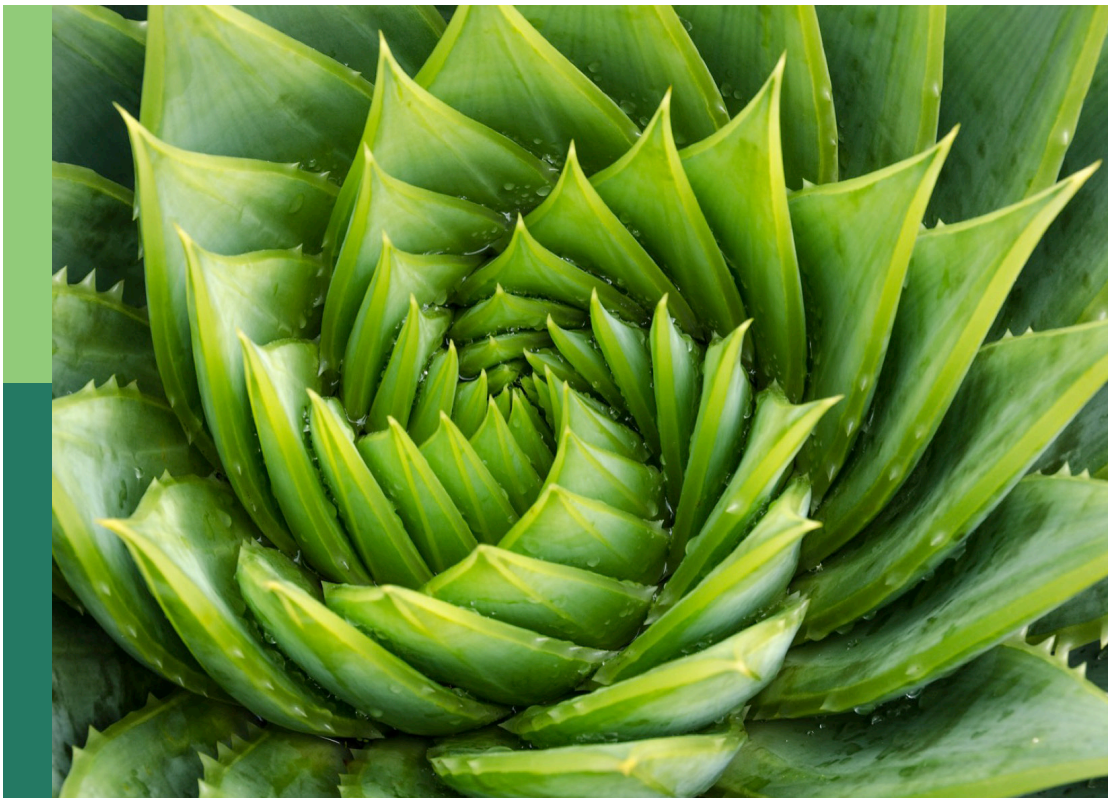

ISSN 1664-8714
ISBN 978-2-8325-5939-0
DOI 10.3389/978-2-8325-5939-0

About Frontiers

Frontiers is more than just an open access publisher of scholarly articles: it is a pioneering approach to the world of academia, radically improving the way scholarly research is managed. The grand vision of Frontiers is a world where all people have an equal opportunity to seek, share and generate knowledge. Frontiers provides immediate and permanent online open access to all its publications, but this alone is not enough to realize our grand goals.

Frontiers journal series

The Frontiers journal series is a multi-tier and interdisciplinary set of open-access, online journals, promising a paradigm shift from the current review, selection and dissemination processes in academic publishing. All Frontiers journals are driven by researchers for researchers; therefore, they constitute a service to the scholarly community. At the same time, the *Frontiers journal series* operates on a revolutionary invention, the tiered publishing system, initially addressing specific communities of scholars, and gradually climbing up to broader public understanding, thus serving the interests of the lay society, too.

Dedication to quality

Each Frontiers article is a landmark of the highest quality, thanks to genuinely collaborative interactions between authors and review editors, who include some of the world's best academicians. Research must be certified by peers before entering a stream of knowledge that may eventually reach the public - and shape society; therefore, Frontiers only applies the most rigorous and unbiased reviews. Frontiers revolutionizes research publishing by freely delivering the most outstanding research, evaluated with no bias from both the academic and social point of view. By applying the most advanced information technologies, Frontiers is catapulting scholarly publishing into a new generation.

What are Frontiers Research Topics?

Frontiers Research Topics are very popular trademarks of the *Frontiers journals series*: they are collections of at least ten articles, all centered on a particular subject. With their unique mix of varied contributions from Original Research to Review Articles, Frontiers Research Topics unify the most influential researchers, the latest key findings and historical advances in a hot research area.

Find out more on how to host your own Frontiers Research Topic or contribute to one as an author by contacting the Frontiers editorial office: frontiersin.org/about/contact

Chilling tolerance and regulation of horticultural crops: physiological, molecular, and genetic perspectives

Topic editors

Shifeng Cao — Zhejiang Wanli University, China
Diane Maria Beckles — University of California, Davis, United States
Maria F. Drincovich — Centro de Estudios Fotosintéticos y Bioquímicos (CEFOBI), Argentina
Isabel Lara — Universitat de Lleida, Spain
Julian C. Verdonk — Wageningen University and Research, Netherlands
Qiong Lin — Chinese Academy of Agricultural Sciences (CAAS), China
Chongde Sun — Zhejiang University, China
Reinaldo Campos-Vargas — Andres Bello University, Chile

Citation

Cao, S., Beckles, D. M., Drincovich, M. F., Lara, I., Verdonk, J. C., Lin, Q., Sun, C., Campos-Vargas, R., eds. (2025). *Chilling tolerance and regulation of horticultural crops: physiological, molecular, and genetic perspectives*.
Lausanne: Frontiers Media SA. doi: 10.3389/978-2-8325-5939-0

Table of contents

frontiers | Frontiers in Plant Science

TYPE Editorial
PUBLISHED 14 January 2025
DOI 10.3389/fpls.2024.1549259

OPEN ACCESS

EDITED AND REVIEWED BY
Luisa M. Sandalio,
Spanish National Research Council (CSIC), Spain

*CORRESPONDENCE
Isabel Lara
isabel.lara@udl.cat

RECEIVED 20 December 2024
ACCEPTED 30 December 2024
PUBLISHED 14 January 2025

CITATION
Lara I, Beckles DM, Drincovich MF, Cao S, Verdonk JC and Campos-Vargas R (2025) Editorial: Chilling tolerance and regulation of horticultural crops: physiological, molecular, and genetic perspectives. *Front. Plant Sci.* 15:1549259. doi: 10.3389/fpls.2024.1549259

Editorial: Chilling tolerance and regulation of horticultural crops: physiological, molecular, and genetic perspectives

Isabel Lara[1]*, Diane M. Beckles[2], Maria F. Drincovich[3], Shifeng Cao[4], Julian C. Verdonk[5] and Reinaldo Campos-Vargas[6]

[1]Departament de Química, Física i Ciències Ambientals i del Sòl, Universitat de Lleida, Lleida, Spain, [2]Department of Plant Sciences, University of California, Davis, Davis, CA, United States, [3]Centro de Estudios Fotosintéticos y Bioquímicos (CEFOBI), CONICET, Universidad Nacional de Rosario, Rosario, Argentina, [4]Zhejiang Wanli University, Ningbo, China, [5]Horticulture and Product Physiology, Plant Science Group, Wageningen University and Research, Wageningen, Netherlands, [6]Departamento de Producción Agrícola, Universidad de Chile, Santiago, Chile

KEYWORDS

chilling response, chilling stress, chilling tolerance, horticultural crop, metabolomics, transcriptomics

Editorial on the Research Topic
Chilling tolerance and regulation of horticultural crops: physiological, molecular, and genetic perspectives

Introduction

Crops of tropical and subtropical origin are cold-sensitive at every stage of the lifecycle, including postharvest cold storage. Chilling-induced damage leads to diverse symptoms which manifest as external alterations (surface pitting, discolouration), internal disorders (browning, water soaking) and/or impaired physiological processes (ripening and growth inhibition, wilting, altered flavour, decay).

Plants have developed complex tolerance mechanisms to counteract or to minimize chilling injury (CI), including stress perception, signal transduction, transcriptional activation of stress-responsive target genes, and the synthesis of stress-related proteins and other molecules. The integration of molecular and *omics*-based approaches has provided new *loci* for marker-assisted breeding toward chilling tolerance. Thus, understanding the physiological, biochemical and molecular responses underlying these tolerance mechanisms, and the causal genes, is paramount to engineering strategies for enhanced tolerance to chilling stress.

This Research Topic was launched to gather recent investigations in this field. Fourteen papers were finally compiled, which examined a wide range of edible and non-edible plant species, including climacteric and non-climacteric fruit species, herbs, and edible corms or seedlings belonging to different botanical families. They explored general mechanisms involved in plant cold tolerance and the suitability of exogenous treatments for alleviating CI-related disorders.

Mechanisms involved in tolerance to cold stress

Plants employ sophisticated molecular mechanisms to perceive and respond to cold stress through cold tolerance and/or cold avoidance. However, the specific physiological and molecular mechanisms driving these protective effects remain poorly understood. Jahed et al. surveyed recent literature on these mechanisms and their potential impact on crop productivity and sustainability. One key adaptive strategy identified was the production of cryoprotectant molecules, which have antioxidant and reactive oxygen species (ROS) activity. These processes prevent protein denaturation, mitigate cell damage and minimize cell dehydration, which preserves cellular function under low temperatures.

Sun et al. explored the biological mechanisms underlying the response to cold in the seedling roots of 'Jinyou 35', a cold-tolerant cucumber (*Cucumis sativus* L.) cultivar. Hormonal analysis revealed high auxin accumulation and roles for jasmonic acid and strigolactone in the cold-tolerant response. Metabolite profiling identified phenolic acids as the most abundant metabolites under chilling conditions, with potential roles for triterpenes. Seedling transcript analysis pointed to *AP2/ERF* transcription factor gene induction under both suboptimal and low-temperature stress. Interestingly, the benzoxazinoid biosynthesis pathways were upregulated at the transcript and metabolite level.

In a large-scale study, Zhang et al. investigated the metabolic mechanisms underlying the cold-induced flavour loss in melon (*Cucumis melo* L.). The key finding was the reduced emission of acetate esters due to transcriptional regulation. Several transcription factors, such as *NOR*, *MYB*, and *AP2/ERF*, were also suppressed. These results might provide insights into the regulation of flavour-associated pathways and the physiological chilling response in melon fruit. In addition, Lv et al. investigated the role of actin depolymerizing factors (ADFs) in different melon tissues in a low temperature-tolerant cultivar ('LT-6'). Depolymerization of actin filaments in the cytoskeleton can improve plant tolerance to cold. Nine *ADF* genes (*CmADF*s) were identified, all responsive to temperature stress. The most responsive of them, *CmADF1*, was functionally characterized using transgenic approaches – virus-induced gene silencing of *CmADF1* increased sensitivity to low temperatures in melon. Accordingly, ectopic *CmADF1* expression in *Arabidopsis* improved cold tolerance, likely through actin filament depolymerization. The expression of *CmADF*s in abscisic acid (ABA)- and salicylic acid (SA)-treated melon leaves supports a role for *CmADF*s genes in stress responses mediated by these hormones.

Lignification may occur during postharvest storage, which in loquat (*Eriobotrya japonica* (Thunb.) Lindl.), a non-climacteric fruit, results in significant quality and economic losses. Ge et al. used transcriptomic analyses and identified the senescence-specific MADS-box gene (*EjAGL15*) as a positive regulator of postharvest flesh lignification in loquats. This study thus provided new information that may help improving loquat fruit management after harvest.

Low-temperature stress in tea (*Camellia sinensis* L.) shrubs causes growth inhibition and leaf senescence. Expression analysis by Wu et al. implicated cell wall-associated receptor-like kinase CsWAK12 in the cold response pathway. Ectopic expression of *CsWAK12* in Arabidopsis was associated with better growth but greater sensitivity to cold, and this response was linked to decreased expression of key cold-stress response genes, such as *C-repeat binding factors* (CBF) genes. CsWAK12 negatively modulates plant cold tolerance by interfering with CBF transcription while simultaneously promoting growth. Hence it may be a key sensor that redirects plant resources for growth under normal conditions, or to adaptive/tolerance responses under cold stress.

Potential strategies for the alleviation of cold stress

There is great interest in exploring postharvest treatments that may allow the extension of storage and shelf life of commodities for higher consumption and reduced loss. Khaliq et al. applied γ-aminobutyric acid (GABA) to papaya (*Carica papaya* L.) fruit and showed enhanced oxidative stress tolerance and antioxidant defence systems in treated fruit stored under cold temperatures. GABA treatment effectively improved the chilling tolerance of papaya fruit, likely by reducing oxidative damage, which strengthened defence systems. Treated fruit were lower in lipid peroxidation, ion leakage, H_2O_2 content, and antioxidant enzyme activities, and had higher contents of proline, endogenous GABA, and total phenolics, which may have helped to maintain plasma membrane fluidity and integrity. Melatonin applications have shown beneficial effects against cold stress across plant species. Wang et al. applied exogenous melatonin to papaya fruit prior to cold storage and showed reduced decay compared with the untreated controls. Most ripening- and quality-related features were enhanced in the treated samples, correlating with ROS levels and enhanced activity of antioxidant enzymes. Considering increasing consumers' concerns about the use of synthetic agrochemicals, exogenous GABA and melatonin treatments emerge as promising non-toxic alternatives to preserve papaya fruit quality during cold storage.

Dai et al. examined the potential of exogenous glycine betaine (GB) to improve tomato (*Solanum lycopersicon* L.) seedling chilling-tolerance. GB treatment activated genes related to the antioxidant system, photosynthesis, calcium signalling, energy metabolism, and cold-responsive pathways, thereby enhancing cold tolerance. GB treatment triggered higher proline content and increased activity of antioxidant enzymes while lowering the levels of malondialdehyde, an indicator of oxidative stress. Exogenous GB can act as a cryoprotectant to favour tomato seedling growth under cold stress.

Chilling injury of zucchini (*Cucurbita pepo* L.), a non-climacteric fruit species, manifests as pits, damaged areas, and fungal growth on the exocarp. Strigolactones (SL) are plant hormones that modulate plant responses to stresses, among other roles. Wang et al. showed that postharvest SL treatments improved zucchini fruit quality by maintaining membrane and oxidative status under cold treatment compared to the untreated controls. Reduced CI was associated with increased proline, arginine, ascorbic acid and ABA contents.

Paprika (*Capsicum annuum* L.), also a non-climacteric fruit species, shows CI primarily as surface pitting. Park et al. applied 20% and 30% CO_2 shocks to mature 'Sirocco' paprika fruit to assess their impact on fruit quality after cold storage. Treatments preserved fruit quality during and after cold storage, with a lower incidence of surface pitting. Transcriptomic and metabolomic analyses of the fruit suggest that activation of sucrose metabolism and phosphatidic acid biosynthesis were key. These metabolites in turn induced stress signalling pathways, lipid processes and antioxidant defence mechanisms, favouring membrane stability and reducing pitting.

Basil (*Ocimum* spp.) is a high-value aromatic culinary herb with a short shelf-life, but the chilling temperatures used for postharvest preservation alter the key volatile compounds critical for desirable aroma and flavour. Rodeo et al. investigated the response of two chilling-sensitive basil genotypes (*O. basilicum* L., cv. 'Genovese' and *O. citriodorum* Vis., cv. 'Lemon') to low temperatures and atmosphere modification. Basil leaves suffered severe CI and greater loss of aroma volatiles at 5°C compared to 10°C and 15°C, which was attenuated in 'Genovese' but not in 'Lemon' samples stored under 5% CO_2. The differentially expressed volatiles might be potential biochemical markers of chilling stress in these genotypes.

Two of the studies compiled in this Research Topic explored possible strategies to maintain the postharvest quality of Chinese water chestnuts (*Eleocharis dulcis* (Burm.f.) Trin.). Peeling the corm is necessary for consumption but leads to discoloration and quality loss. Chen et al. applied eugenol to fresh-peeled Chinese water chestnut corms, which delayed surface discolouration during storage. Eugenol enhanced antioxidant and ROS-scavenging capacity by inhibiting phenolic metabolism. In turn, Lu et al. investigated the effects of methyl jasmonate (MeJa) dips on the quality of fresh-cut Chinese water chestnuts. MeJa delayed yellowing and quality loss. Similarly to applied eugenol, MeJA treatment enhanced antioxidant capacity, inhibited ROS generation and reduced the accumulation of flavonoids, thus delaying surface discoloration.

Conclusions

This Research Topic highlighted the conserved pathways underlying CI responses across diverse species and tissues, and illustrated the suitability of some hormonal and physical treatments to mitigate CI damage; these lines of research are necessary to support robust breeding programs and to improve postharvest management to reduce commercial losses due to CI.

Author contributions

IL: Conceptualization, Visualization, Writing – original draft, Writing – review & editing. DB: Writing – original draft, Writing – review & editing. MD: Writing – original draft, Writing – review & editing. SC: Writing – original draft, Writing – review & editing. JV: Writing – original draft, Writing – review & editing. RC-V: Writing – original draft, Writing – review & editing.

Acknowledgments

The Guest Editors would like to express their gratitude to all the authors who considered this Research Topic for the submission of their work.

Conflict of interest

The authors declare that the research was conducted in the absence of any commercial or financial relationships that could be construed as a potential conflict of interest.

The author(s) declared that they were an editorial board member of Frontiers, at the time of submission. This had no impact on the peer review process and the final decision.

Publisher's note

frontiers | Frontiers in Plant Science

TYPE Original Research
PUBLISHED 28 September 2022
DOI 10.3389/fpls.2022.965723

OPEN ACCESS

EDITED BY
Reinaldo Campos-Vargas,
University of Chile, Chile

REVIEWED BY
Murat Dikilitas,
Harran University, Turkey
Poonam Mishra,
Tezpur University, India

*CORRESPONDENCE
Ting Min
email@uni.edu
minting1323@163.com

SPECIALTY SECTION
This article was submitted to Crop and Product Physiology, a section of the journal Frontiers in Plant Science

RECEIVED 10 June 2022
ACCEPTED 13 September 2022
PUBLISHED 28 September 2022

CITATION
Chen Z, Xu Y, Lu Y, Miao Z, Yi Y, Wang L, Hou W, Ai Y, Wang H and Min T (2022) Effect and mechanism of eugenol on storage quality of fresh-peeled Chinese water chestnuts. *Front. Plant Sci.* 13:965723. doi: 10.3389/fpls.2022.965723

Effect and mechanism of eugenol on storage quality of fresh-peeled Chinese water chestnuts

Zhe Chen[1], Yuhan Xu[1], Yang Lu[1], Zeyu Miao[1], Yang Yi[1], Limei Wang[2], Wenfu Hou[1], Youwei Ai[1], Hongxun Wang[2] and Ting Min[1]*

[1]College of Food Science and Engineering, Wuhan Polytechnic University, Wuhan, China, [2]College of Biology and Pharmaceutical Engineering, Wuhan Polytechnic University, Wuhan, China

The study aimed to investigate the effect and mechanism of eugenol treatment on fresh-peeled Chinese water chestnuts (CWCs). The results found that eugenol treatment maintained the appearance of fresh-peeled CWCs, accompanied by higher L* value, total solids and O_2 contents, as well as lower browning degree, weight loss rate, CO_2 content, a* and b* values. In addition, eugenol treatment significantly reduced the activities of peroxidase, phenylalanine ammonia-lyase, and polyphenol oxidase, as well as the total content of soluble quinone in fresh-peeled CWCs. Meanwhile, fresh-peeled CWCs treated with eugenol showed markedly lower content of total flavonoids, which may be related to yellowing. Furthermore, eugenol treatment suppressed the rates of $O_2^{\cdot -}$ and $OH^{\cdot -}$ production as well as the contents of H_2O_2 and malondialdehyde in fresh-peeled CWCs. During the storage, eugenol treatment not only increased the activities of catalase, superoxide dismutase, ascorbate peroxidase and glutathione reductase as well as the DPPH free radical scavenging rate, but also increased the total phenolics, ascorbic acid and glutathione contents. In summary, eugenol treatment delayed the surface discoloration of fresh-peeled CWCs by improving the antioxidant capacity, inhibiting the phenolic compound metabolism and scavenging ROS, thus effectively maintaining the quality of fresh-peeled CWCs while extending their shelf life.

KEYWORDS

eugenol, reactive oxygen metabolism, phenolic metabolism, storage quality, fresh-peeled Chinese water chestnut

Introduction

Chinese water chestnuts (CWCs) grow mainly in the south area of the Yangtze River in China (Nie et al., 2021), and are rich in starch, vitamins, minerals, and proteins (Jiang et al., 2004). CWCs are usually peeled before being eaten, due to a certain quantity of pathogenic microorganisms are attached to their peels (Jiang et al., 2004). As a result, fresh-peeled CWCs are increasingly welcomed among consumers for deliciousness and convenience. However, CWCs are often vulnerable to mechanical damage in the fresh cutting process, resulting in the decline of quality and reduction of the shelf life. Surface discoloration is an important phenomenon indicating a quality decrease in fresh-peeled CWCs (Song et al., 2019).

There are hypotheses on the discoloration of fresh-peeled CWCs. One hypothesis is that the surface discoloration is yellowing. Flavonoids, especially naringin and eriodictyol, are the main yellowing substances in fresh-peeled CWCs (Pan et al., 2015). The other hypothesis is that enzymatic browning contributes to surface discoloration, and phenylalanine ammonia-lyase (PAL), peroxidase (POD), and polyphenol oxidase (PPO) are key enzymes (Li et al., 2020). The senescence of fresh-cut vegetables and fruits has been reported to be closely related to ROS, like H_2O_2, $O_2\cdot^-$ and $OH\cdot^-$. Excessive accumulation of ROS disrupts the balance of the scavenging system, which gives rise to malondialdehyde (MDA) accumulation and membrane lipid peroxidation, further exacerbating the senescence process (Dou et al., 2021). Moreover, ROS metabolism is also closely related to the activities of antioxidant enzymes (Li et al., 2021). The antioxidant system is mainly composed of ascorbic acid (AsA), glutathione (GSH), catalase (CAT), superoxide dismutase (SOD), ascorbate peroxidase (APX) and glutathione reductase (GR) and other enzymes. The main function of CAT is to generate H_2O and O_2 by specifically catalyzing the decomposition of H_2O_2. The catalytic effect of SOD is to inhibit the damage of $O_2\cdot^-$ to the plant, establishing the first defensive line of the antioxidant system. The important antioxidant enzymes in the ascorbic acid-glutathione cycle are APX and GR, which work together with antioxidants to remove ROS and protect the integrity of cell membranes. And it is reported that lower accumulation of ROS and higher antioxidative enzyme activity play a role in alleviating the discoloration of fresh-peeled CWCs treated with hydrogen sulfide (Dou et al., 2021).

Therefore, it is a matter of great concern to seek effective methods to delay the discoloration and quality deterioration of fresh-peeled CWCs. Various methods have been currently adopted to maintain the appearance of fresh-peeled CWCs and to prolong the shelf life. Anoxic treatment contributes to alleviating lipid peroxidation and maintaining storage quality in fresh-peeled CWCs by reducing the activity of malondialdehyde, H_2O_2 and lipoxygenase and increasing the activity of ascorbate peroxidase and superoxide dismutase (You et al., 2012). Pen and colleagues used chitosan coating treatment to delay discoloration of fresh-peeled CWCs, reducing the activity of PAL, PPO, and POD as well as the content of total phenolics (Jiang et al., 2004). Hydrogen-rich water treatment delayed the yellowing of fresh-peeled CWCs, alleviated oxidative damage, and decreased the PAL activity and accumulation of flavonoids (Li et al., 2022). Moreover, ferulic acid is effective in inhibiting yellowing and eriodictyol and naringenin levels in fresh-peeled CWCs (Song et al., 2019). Salicylic acid also inhibits the browning of fresh-peeled CWCs and reduces the activity of PPO, POD, and PAL (Peng and Jiang, 2006). At present, the main treatment method is concentrated on chemical preservatives. Today, with the increasing requirements for food safety, the development of pure natural plant extracts from plants to extract antibacterial and bactericidal active substances has been put on the agenda (Fernández-Pan et al., 2012; Alshaikh and Perveen, 2017).

As a natural plant extract, eugenol is the main component of clove oil and has strong insecticidal, antibacterial, and antiseptic effects (Devi et al., 2013; Ma et al., 2016). EUG is a food additive approved by the U.S. FDA (Food and Drug Administration), with the LD_{50} value being 3000 mg kg^{-1} oral mice (Gong et al., 2016). Eugenol is superior to hydrogen sulfide in safety and antimicrobial activity. And the production cost of eugenol is lower than those of ferulic acid and hydrogen-rich water. In the food industry, eugenol is mainly used for retaining the texture, sensory properties, and moisture of shrimp (Sharifimehr et al., 2019) and pork (Wan et al., 2018). However, there is little research on the storage and preservation of fresh-cut vegetables and fruits treated with eugenol. Fresh-cut lettuce treated with eugenol at the concentration of 0.5 g/L inhibited the browning of fresh-cut lettuce and the activity of PAL, PPO, and POD enzymes (Chen et al., 2017). Edible coatings with 1 g/L eugenol and 1.5 g/L citral on raspberries (Guerreiro et al., 2016) and fresh-cut apples (Guerreiro et al., 2016) have high Trolox equivalent antioxidant activity. Moreover, 15 g/L eugenol emulsion treatment delayed the browning of fresh-cut CWCs, enhanced the activities of ROS scavenging enzymes, and increased the contents of phenolic substances, thereby reducing the damage to the cell membrane (Teng et al., 2020; Zhu et al., 2022). Previous studies have shown that antioxidant and ROS metabolism are involved in the browning and senescence of fresh-cut CWCs (Dou et al., 2021). In addition to the direct antioxidant system, the ascorbic acid-glutathione (AsA-GSH) cycle plays an important role in maintaining the quality of fresh-cut fruits and vegetables. Therefore, the mechanism of eugenol on inhibiting discoloration and quality deterioration of fresh-peeled CWCs needs to be further investigated, especially the combined study of direct and indirect antioxidant processes.

This study investigated the effect of 1 g/L eugenol treatment on the quality of fresh-peeled CWCs during storage, and its underlying mechanism on phenolics and ROS metabolism. The quality change (color difference, browning degree, total soluble solids, weight loss rate, and headspace gas composition) of packaged fresh-peeled CWCs were evaluated first. To further understand the possible mechanism for discoloration of fresh-peeled CWCs, the phenolic metabolism (total flavonoid, total phenolic and total quinone contents, and activities of POD, PPO, and PAL), ROS metabolism ($O_2^{\cdot-}$ and $OH^{\cdot}$ production rates, H_2O_2 and MDA contents), and antioxidant substances (activities of CAT, SOD APX, GR and DPPH free radical scavenging rate) were studied. This study aims to provide a theoretical basis for storing and preserving fresh-peeled CWCs with eugenol.

Materials and methods

Materials and reagents

CWCs were bought from the Southeast Fruit Wholesale Market in Wuhan, Hubei. Severely damaged CWCs were removed and fruits with uniform size and appearance were selected as experimental materials. After pre-cooling at 4°C for 24 h, the CWCs were manually washed and peeled. Later, fresh-peeled CWCs were soaked in 0.1 g/L sodium hypochlorite for 5 min. The four eugenol concentrations were selected to be 0.75, 1, 2, and 4 g/L, and the five eugenol treatment times were 1, 3, 5, 7, and 10 min, respectively. It can be seen from Figure 1A and B that the optimal concentration of eugenol treatment is 1 g/L and the optimal time was 5 min. Therefore, one group was soaked in 1 g/L eugenol solution (Yuanye, Wuhan Feiyang Biological Technology Co., Ltd.) for 5 min, one group as the control was soaked in distilled water for 5 min, and the other group as the ethanol control was soaked in 5% ethanol for 5 min. Eugenol solution (1 g/L) was dissolved in a small amount of ethanol (5%) and diluted with distilled water. After draining the water, three groups of fresh-peeled CWCs were sealed in polyethylene bags (200 × 280 mm) after being placed in food-grade polyethylene trays (180 × 120 × 25 mm). At last, samples were stored at 10°C with a relative humidity of 85-90% (Fan et al., 2018) for 5 d and used for analysis at 1 d interval.

Color difference, browning degree, total soluble solid content, weight loss rate, and headspace gas composition

An EOS550D camera was used to record the appearance of fresh-peeled CWCs. According to Du et al. (2009), a JZ-300 colorimeter was used to measure color differences (L*, a*, and b* values) of fresh-peeled CWCs.

The degree of browning fresh-peeled CWCs was measured using the method of Min et al. (2017). Three grams of fresh-peeled CWCs pulp was homogenized in 30 mL of distilled water, followed by centrifugation of the mixture at 10,000 ×g for 10 min. Later, the supernatant (3.5 mL) was incubated at 25°C for 5 min and the absorbance was determined at 410 nm by an A360 UV-Vis spectrophotometer (Aoyi Instrument Shanghai Co., Ltd).

The total soluble solid content of fresh-peeled CWCs pulp was determined using the method of Liu et al. (2018), followed by grinding and pestling 10 g of fresh-peeled CWCs pulp. An

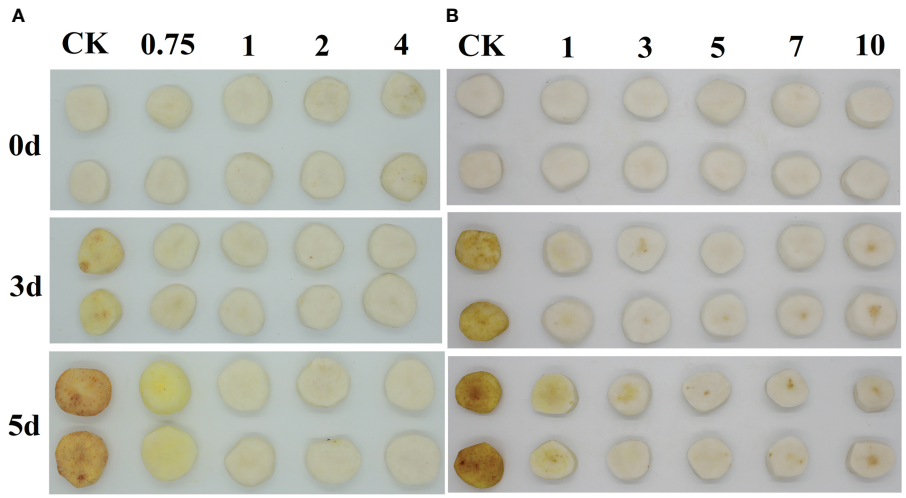

FIGURE 1
Images of 0, 0.75, 1, 2, and 4 g/L EUG treatment on fresh-peeled CWC **(A)**, and 0, 1, 3, 5, 7 and 10 min EUG treatment on fresh-peeled CWC **(B)**.

LQ80T portable refractometer was used to measure the total soluble solid content.

The weight loss rate was measured using the method of Chen et al. (2022). The mass weighed on the 0th day was M_0, and the weight weighed on the n day was M_n. The weight loss rate of CWCs was calculated by $\frac{M_0-M_n}{M_0} \times 100\,\%$.

Headspace gas composition in CWCs packages was measured using the method of Chen et al. (2022). Checkpoint 3 Portable Headspace Analyzer was used to measure O_2 and CO_2 contents.

Total flavonoid, total phenolic, and soluble quinone content

The total flavonoid content was measured by referring to a modified method by Liu et al. (2018). Fresh-peeled CWCs pulp (5 g) was homogenized in 50 mL of 0.6 mL/mL ethanol, followed by centrifugation at 4°C for 10 min (10,000 ×g). Later, the supernatant (4 mL) was incubated with 0.3 mL of 50 g/L $NaNO_2$ for 6 min and then 0.3 mL of 100 g/L Al $(NO_3)_3$ was added. After 6 min, 4 mL of 1 mol/L NaOH was added to the mixture with 0.8 mL/mL ethanol and incubated for 15 min. The absorbance was measured at 510 nm. The content of total flavonoids was indicated as mg kg^{-1}.

The total phenolic content was quantified by using the method of Min et al. (2017). Fresh-peeled CWCs pulp (3 g) was mixed with 30 mL of 0.6 mL/mL ethanol, followed by homogenization for 6 min and centrifugation at 4 °C for 5 min (10,000 ×g). Then 0.125 mL of Folin-Ciocalteau and 1.25 mL of 7% Na_2CO_3 and 1 mL of distilled water were added, till the temperature reached 25°C for 90 min in the dark. The standard curve was determined with gallic acid solution. The absorbance was measured at 760 nm and the content of total phenolics was indicated as mg kg^{-1}.

The soluble quinone content was determined by referring to the method of Homaida et al. (2017). Fresh-peeled CWCs pulp (3 g) was mixed with 20 mL of methanol, followed by homogenization for 1 min and centrifugation at 4°C for 10 min. The soluble quinone content was measured at 437 nm and indicated as A_{437nm} g^{-1}.

Enzyme activity assay (PAL, PPO, and POD)

The extraction and assay of PAL, PPO, and POD activity were conducted based on our previous paper (Min et al., 2019).

The PAL activity was measured using the Phenylalanine Ammonia Lyase Kit. Fresh-peeled CWCs pulp (0.3 g) was mixed with precooled reagent 1 (2.7 mL), followed by centrifugation at 4°C for 10 min (10,000 ×g). The subsequent procedures were conducted according to the manufacturer's instructions. A unit of PAL activity was defined as a change in absorbance of 0.1 at 290 nm per fresh weight per min.

To determine the PPO activity, three grams of fresh-peeled CWCs pulp was mixed in 50 mL of phosphate buffer. Then they were centrifuged at 4 °C for 15 min (6,000 ×g). A unit of PPO activity was defined as a change in absorbance of 0.001 at 420 nm per min per fresh weight.

To determine the POD activity, five grams of fresh-peeled CWCs pulp was mixed with 5 mL of extraction buffer (1 mmol/L MPEG, 40 g/L PVPP, and 10 g/L Tritonx-100). Then they were ground and homogenized, followed by centrifugation at 4°C for 30 min (12,000 ×g). A unit of POD activity was defined as a change in absorbance of 0.01 at 470 nm per min per fresh weight.

H_2O_2 content, $O_2\cdot^-$ generation rate, $OH\cdot^-$ production rate, and MDA content

The hydrogen peroxide test kit was used to determine the H_2O_2 content. Two grams of fresh-peeled CWCs pulp and 18 mL of 8.5 g/L NaCl were diluted 10 times in an ice bath. Then they were centrifuged for 10 min at 4°C (10,000 ×g) and the supernatant was taken as the reaction solution. Finally, the absorbance value was measured at 405 nm and expressed as mmol g^{-1}. $O_2\cdot^-$ generation rate was measured by referring to the method (Zou et al., 2019). Two grams of fresh-peeled CWCs pulp was mixed with 5 mL of 50 mmol/L phosphate buffer and were ground in an ice bath. After that, they were centrifuged for 10 min at 4°C (12,000 ×g). Later, the supernatant was centrifuged at 12,000 ×g for 20 min. 1 mL of the supernatant was incubated with 10 mmol/L hydroxylamine hydrochloride and 5 mL of 50 mmol/L of phosphate buffer at 25°C for 20 min. They were then incubated at 25°C with 1 mL of 7 mmol/L α-naphthylamine and 1 mL of 17 mmol/L p-aminobenzene sulfonic acids. Finally, the absorbance value was measured at a wavelength of 530 nm and expressed as μmol g^{-1} min^{-1}.

$OH\cdot^-$ production rate was measured using the hydroxyl radical kit (Nanjing Jiancheng Biological Engineering Co., Ltd., Nanjing, China). Five grams of fresh-peeled CWCs pulp was ground and homogenized with 20 mL of absolute ethanol, and they were centrifuged at for 10 min at 4°C (10,000 ×g). Then the supernatant was taken for experiments according to the kit instructions. Finally, the absorbance value was measured at a wavelength of 550 nm and expressed in nmol g^{-1} min^{-1}.

The MDA content was determined by referring to the method of Kong et al. (2020). Three grams of fresh-peeled CWCs pulp was mixed with 15 mL of 100 g/L trichloroacetic acids, followed by centrifugation at 4°C for 20 min at 10,000 ×g. After that, 2 mL of the supernatant (corresponding to the blank control tube, added with 2 mL of 100 g/L trichloroacetic acid solution and 2 mL of 6.7 g/L thiobarbituric acids were mixed and placed in a water bath at 100 °C for 20 min. After cooling, the above centrifugation step was repeated. The absorbance was

determined at 450, 532, and 600 nm, respectively. The MDA content was indicated as nmol g^{-1}.

CAT, SOD activity and DPPH free radical scavenging rate

The CAT activity was measured using a catalase test box kit (Nanjing Jiancheng Biological Engineering Co., Ltd., Nanjing, China). Two grams of fresh-peeled CWCs pulp and 18 mL of 8.5 g/L NaCl were diluted 10 times in an ice bath. They were then centrifuged for 10 min at 4°C (10,000 ×g) and the supernatant was taken as the reaction solution. Finally, the absorbance value was measured at 405 nm and indicated as U g^{-1}.

The total superoxide dismutase test kit was used to measure the SOD activity. Five grams of fresh-peeled CWCs pulp was mixed with 20 mL of 0.15 mol/L phosphate buffer in the mortar. Next, they were ground under the condition of the ice bath and centrifuged at 10,000 ×g for 10 min. Then the supernatant was taken and diluted 7 times. The subsequent procedures were conducted according to the manufacturer's instructions. Finally, the absorbance value was measured at a wavelength of 550 nm and indicated as U g^{-1}.

The DPPH radical scavenging rate was measured using the method of Chen et al. (2022).Two grams of fresh-peeled CWCs pulp was homogenized in 25 mL of absolute ethanol in an ice bath, sonicated at 50°C for 30 min. After being centrifuged at 10,000 × g for 10 min at 4°C, and the supernatant were collected. The supernatant, DPPH alcohol solution and absolute ethanol solution were mixed in pairs. Then the reaction was performed at room temperature for 30 min in the dark, and the absorbance was measured at 517 nm.

AsA, GSH content and APX, GR activity

The AsA content was measured using an ascorbate test kit (Nanjing Jiancheng Biological Engineering Co., Ltd., Nanjing, China). Five grams of fresh-peeled CWCs pulp and 20 mL of phosphate buffer, followed by homogenization for 3 min and centrifugation at 4 °C for 15 min (4,000 ×g). The supernatant was collected for testing. The subsequent procedures were conducted according to the manufacturer's instructions. Finally, the absorbance value was measured at the wavelength of 536 nm and the results were indicated as μg g^{-1}.

The GSH content was performed using a reduced glutathione test kit (Beijing Solarbio Science and Technology Co., Ltd., Beijing, China). The pulp of fresh-peeled CWCs were first washed twice with phosphate buffer, then 2 g of fresh-peeled CWCs pulp were homogenized in 5 mL of reagent 1 in an ice bath. They were then centrifuged for 10 min at 4°C (8,000 ×g). Then the supernatant was taken for experiments according to the kit instructions. Finally, the absorbance value was measured at 412 nm and the results were expressed as μg g^{-1}.

The APX activity was measured using an ascorbate peroxidase test kit (Beijing Solarbio Science and Technology Co., Ltd., Beijing, China). Fresh-peeled CWCs pulp (1 g) was homogenized in 5 mL of reagent 1 in an ice bath and centrifuged at 13,000 ×g for 20 min at 4°C. Then the supernatant was taken for experiments according to the kit instructions. Finally, the absorbance value was measured at 290 nm and the results were indicated as U g^{-1}.

The GR activity was measured using a glutathione reductase test kit (Beijing Solarbio Science and Technology Co., Ltd., Beijing, China). Fresh-peeled CWCs pulp (0.5 g) was homogenized in 5 mL of reagent 1 in an ice bath and centrifuged at 10,000 ×g for 10 min at 4°C. Then the supernatant was taken for experiments according to the kit instructions. Finally, the absorbance value was measured at 340 nm and the results were expressed as U g^{-1}.

Statistical analysis

The experiment was conducted three times and the findings were indicated as mean ± standard error. Before Duncan's multiple range test, variance analysis (ANOVA) was used to compare means among groups. Analyses were performed by using the SPSS 19.0 software. Significance was expressed at $p<0.05$.

Results

The effect of EUG on quality indicators of fresh-peeled CWCs

Color difference is a key indicator for measuring the degree of the surface color change of fresh-cut vegetables and fruits (Valverde et al., 2005). Fresh-peeled CWCs treated with eugenol at a concentration of 0.75 g/L showed a slight discoloration (Figure 1A), while fresh-peeled CWCs treated with 1, 2 and 4 g/L eugenol had no obvious color change. Therefore, considering the effect and actual cost, 1 g/L eugenol was chosen for follow-up experiments. As shown in Figure 1B, eugenol treatment at a concentration of 1 g/L for 5 min delayed the discoloration of fresh-peeled CWCs in an effective manner.

The photos of the fresh-peeled CWCs soaked in distilled water, ethanol (5%) and eugenol solution (1 g/L) for 0-5 d (Figure 2A). L* values of all the eugenol, ethanol treatments and control groups showed a downward trend during storage (Figure 2B). The L* value of the control group (86.3-76.3) and the ethanol treatment group (86.3-78.4) were much lower than that of the eugenol treatment group (86.3-83.1) on 0-5 d, and

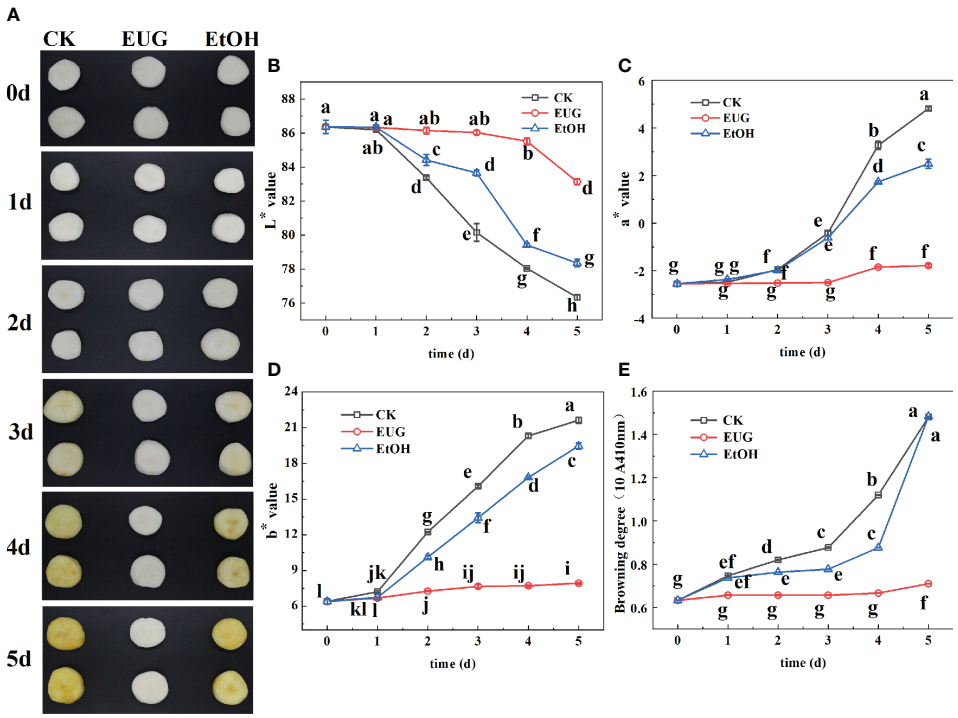

FIGURE 2
Effects of eugenol treatment on the visual quality **(A)**, color difference **(B–D)**, browning degree **(E)** of fresh-peeled CWC. Fresh-peeled CWCs were treated with tap water (CK), ethanol (EtOH) or eugenol (EUG). Error bars denote a standard error of the mean of triplicate assays. Different lowercase letters have shown significant differences (P<0.05).

there were significant differences from the second day. Throughout the storage, a* and b* values of fresh-peeled CWCs tended to increase, while a* and b* values of the eugenol treatment group were markedly lower than that of the control and ethanol treatment groups on 2-5 d (Figure 2C, D). After 5 d of storage, a* value in the control, ethanol treatment and eugenol treatment groups increased by 73.6%, 50.5% and 7.7%, respectively. And the b* value of the control and the ethanol treatment groups was 2.7 and 2.5-fold higher than that of the eugenol treatment group on 5 d.

The browning degree is one of the most important indicators to evaluate the quality of fruits and vegetables (Yang et al., 2021). The browning degree of fresh-peeled CWCs continued rising (Figure 2E), the control and ethanol-treated groups were significantly higher than those of the eugenol-treated group throughout the storage. The browning degree of the control and ethanol treatment group was 2.08-fold as high as that of the eugenol treatment on 5 d.

Total soluble solids reflect the content of soluble sugar and other nutrients in fresh-peeled CWCs (Guerreiro et al., 2015). As shown in Figure 3A, the content of soluble solids in all groups increased rapidly on the 1st day and then decreased gradually on 2-5 d. The content of soluble solids in the eugenol treatment group was significantly higher than that of the control and ethanol treatment groups during the whole storage. By the end of storage, the total soluble solid content of fresh-peeled CWCs in the control and ethanol-treated groups decreased to 18.5 and 21.6%, while that of eugenol-treated fresh-peeled CWCs was 26%.

Fresh-peeled CWCs are mechanically damaged, resulting in the outflow of intracellular juices, and the weight continues to decrease during storage (Chen et al., 2017). As shown in Figure 3B, the weight loss rate of fresh-peeled CWCs in the three groups showed an upward trend during the whole storage period, the control and the ethanol treatment groups were significantly higher than the eugenol treatment group at the later storage period. The weight loss rates of the control and ethanol-treated groups on 5 d were 1.27% and 1.25% compared to 1.02% in the eugenol-treated group.

The partial pressures of O_2 and CO_2 reflect the respiration intensity of fresh-peeled CWCs (Chen et al., 2022). During the whole storage, the O_2 content first decreased and then increased slowly (Figure 3C). From the first day, the eugenol-treated group was significantly higher than the control and ethanol-treated groups. The CO_2 content showed a trend of first increase and then a slight decrease, and the eugenol treatment group was significantly lower than the control and ethanol treatment groups in the late storage period (Figure 3D).

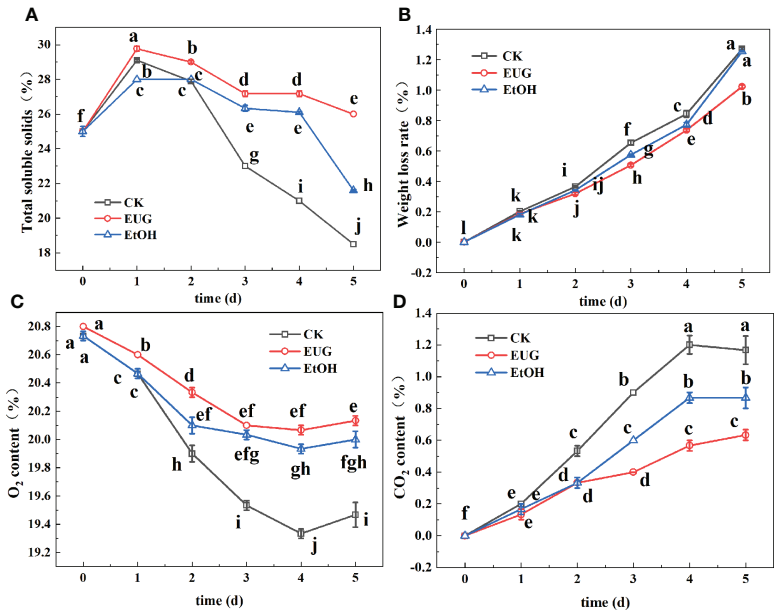

FIGURE 3
Effects of eugenol treatment on the total soluble solids **(A)**, weight loss rate **(B)**, O_2 content **(C)** and CO_2 content **(D)** of fresh-peeled CWC. Fresh-peeled CWCs were treated with tap water (CK), ethanol (EtOH) or eugenol (EUG). Error bars denote a standard error of the mean of triplicate assays. Different lowercase letters have shown significant differences (P<0.05).

The effect of EUG on total flavonoids, total phenolics, and soluble quinones of fresh-peeled CWCs

The yellowing of fresh-peeled CWCs may be due to the presence of total flavonoids (Pan et al., 2015). It can be seen from Figure 4A that the total flavonoid content of the control and ethanol-treated groups was significantly higher than that of the eugenol-treated group during the whole storage. Compared with eugenol-treated fresh-peeled CWCs, the total flavonoid content of the control and ethanol-treated groups increased rapidly during the later storage period. On the last day of storage, the total flavonoid content of the control and ethanol-treated groups rose to 63.7 and 55.3 mg kg^{-1}, while that of the eugenol treatment group was 37.7 mg kg^{-1}.

Phenolics are not key substrates of enzymatic browning in vegetables and fruits, but also have antioxidant effects (Teng et al., 2020). The total phenolic content of fresh-peeled CWCs showed an increasing trend (Figure 4B). The control and ethanol-treated groups were significantly lower than those of the eugenol-treated group in the early storage period. However, in the later storage period, the control group was lower than the eugenol-treated group but higher than the ethanol-treated group.

Quinones are the oxidation products of phenols during the enzymatic browning reaction (Saltveit, 2000). As shown in Figure 4C, the content of soluble quinone in the three groups showed a trend of first decreasing and then increasing, and the control and ethanol treatment group were significantly higher than eugenol treatment during the whole storage. For example, the content of soluble quinones in the control and ethanol-treated groups was 3.5-fold higher than that in the eugenol-treated group on 5 d.

The effect of EUG on the enzymatic activity of fresh-peeled CWCs

PAL is an important enzyme in the phenylpropane pathway for producing secondary metabolites such as flavonoids (Chen et al., 2017). It can be found from Figure 5A that the PAL activity of fresh-peeled CWCs showed an upward trend during the entire storage, and the PAL activity of the control and ethanol-treated groups was markedly higher than that of the eugenol-treated group. On the last day of storage, the PAL activity of the control and ethanol-treated groups rose to 5.4 and 4.7 U g^{-1}, while the eugenol-treated group was only 2.75 U g^{-1}.

PPO is one of the main causes of the enzymatic browning of vegetables and fruits (Teng et al., 2020). During the whole storage, the PPO activity of fresh-peeled CWCs in both the control and ethanol-treated groups was higher than that in the eugenol-treated group. Moreover, the control group was significantly higher than the eugenol-treated group (Figure 5B). The PPO activity in the control and ethanol

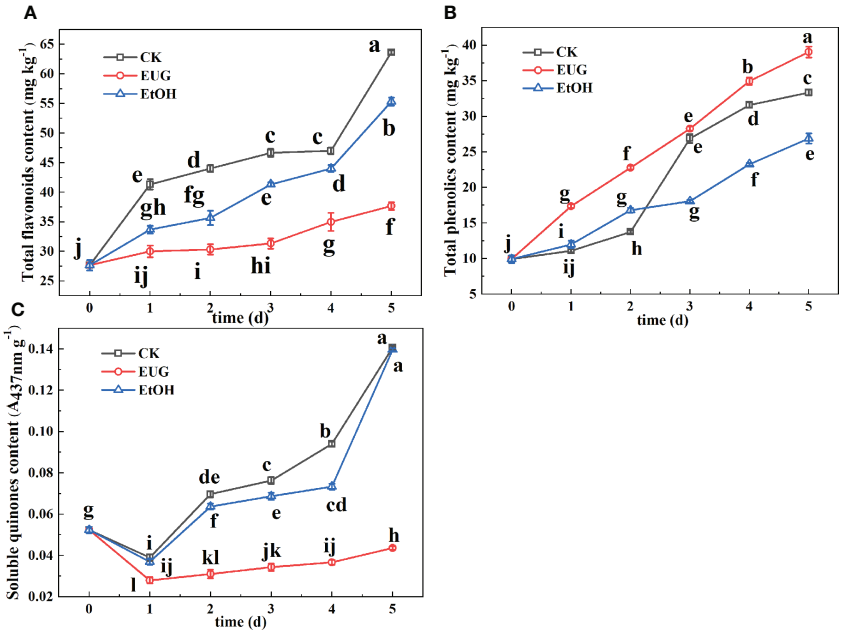

FIGURE 4
Effects of eugenol treatment on the total flavonoids **(A)**, total phenolics **(B)**, and soluble quinones **(C)** of fresh-peeled CWC. Fresh-peeled CWCs were treated with tap water (CK), ethanol (EtOH) or eugenol (EUG). Error bars denote a standard error of the mean of triplicate assays. Different lowercase letters have shown significant differences ($P<0.05$).

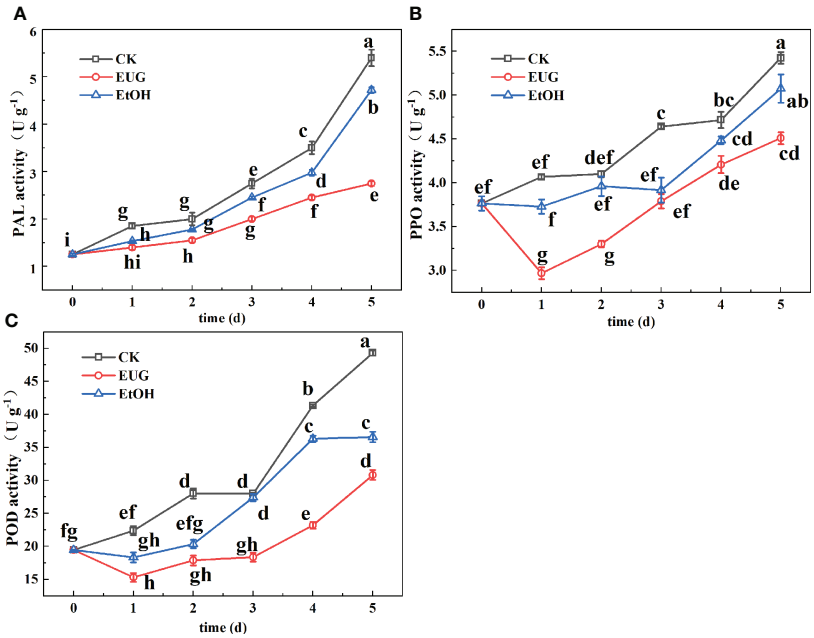

FIGURE 5
Effects of eugenol treatment on the activities of PAL **(A)**, PPO **(B)**, and POD **(C)** of fresh-peeled CWC. Fresh-peeled CWCs were treated with tap water (CK), ethanol (EtOH) or eugenol (EUG). Error bars denote a standard error of the mean of triplicate assays. Different lowercase letters have shown significant differences ($P<0.05$).

treatment groups reached 5.4 and 5.1 U g^{-1} on 5 d, while that of the eugenol treatment group was 4.5 U g^{-1}.

POD is an important enzyme in the process of enzymatic browning and melanin synthesis (Toivonen and Brummell, 2008). As shown in Figure 5C, the POD activity of the control and ethanol-treated groups was higher than that of the eugenol-treated group throughout the storage. There were significant differences between the eugenol-treated group and the control and ethanol-treated groups in the late storage. By the end of storage, the POD activity of the control and ethanol-treated groups increased by 60.6 and 46.9%, while the eugenol-treated group increased by 36.9%.

The effect of EUG on H_2O_2 content, $O_2\cdot^-$ generation rate, $OH\cdot^-$ production rate, and MDA content of fresh-peeled CWCs

H_2O_2 can directly or indirectly oxidize biological macromolecules in the cell and destroy the cell membrane, accelerating cell senescence and disintegration (Asaeda et al., 2018). It can be seen from Figure 6A that throughout the whole storage, the H_2O_2 content of the control and ethanol treatment groups was markedly higher than that of the eugenol treatment group. And the H_2O_2 content of the control and the ethanol-treated group was 3.7 and 1.9-fold as high as that of the eugenol-treated group on 5 d, respectively. $O_2\cdot^-$ is one of the most important reactive oxygen species (Kong et al., 2020). During the whole storage period, the $O_2\cdot^-$ production rate of fresh-peeled CWCs showed a downward trend (Figure 6B). The $O_2\cdot^-$ generation rate of the control and ethanol treatment groups was markedly higher than that of the eugenol treatment group on 2-5 d. During the whole storage, the $O_2\cdot^-$ production rate in the control and ethanol-treated groups decreased from 1.15 to 0.29 and 0.30 μmol g^{-1} min^{-1}, while that of the eugenol-treated group decreased from 1.15 to 0.05 μmol g^{-1} min^{-1}.

$OH\cdot^-$ is one of the most oxidative free radicals in ROS, which can react with almost all cellular components and cause great damage to plants (Dou et al., 2021). It can be seen from Figure 6C that the $OH\cdot^-$ generation rate showed a trend of increasing first and then decreasing. And the eugenol-treated group was significantly lower than that of the control and ethanol-treated groups. In the last two days of storage, the $OH\cdot^-$ generation rate of the control and ethanol treatment groups was about 1.4-fold that of the eugenol treatment group.

MDA is one of the membrane lipid peroxidation products of the cell membrane (Kong et al., 2020). The MDA content of the control and ethanol-treated groups steadily rose during the storage (Figure 6D), but that of the eugenol-treated group first decreased and then increased. The control and ethanol-treated groups were significantly higher than the eugenol-treated groups

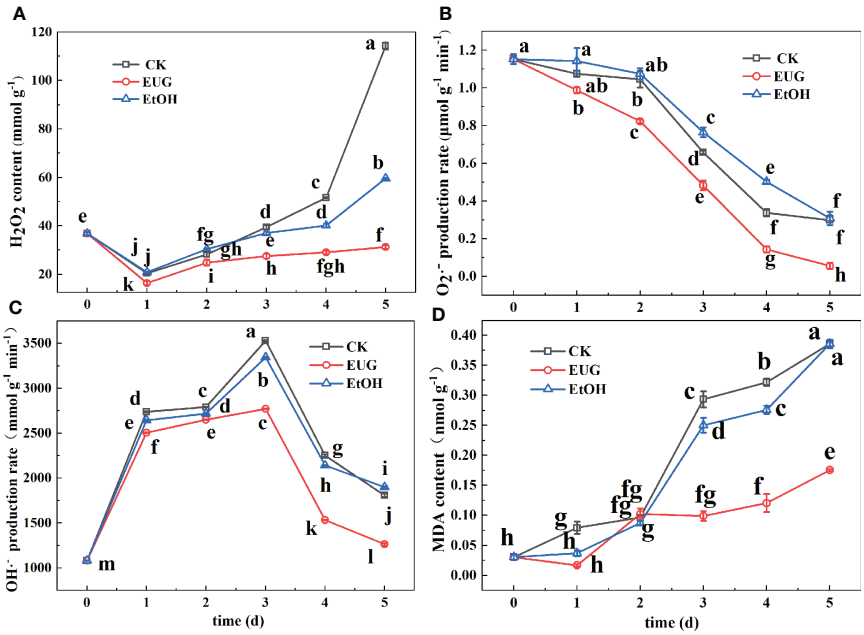

FIGURE 6
Effects of eugenol treatment on the H_2O_2 content **(A)**, $O_2\cdot^-$ production rate **(B)**, $OH\cdot^-$ production rate **(C)** and MDA content **(D)** of fresh-peeled CWC. Fresh-peeled CWCs were treated with tap water (CK), ethanol (EtOH) or eugenol (EUG). Error bars denote a standard error of the mean of triplicate assays. Different lowercase letters have shown significant differences (P<0.05).

on 3-5 d. On 5 d, the MDA content of the control and ethanol-treated groups was 2.17-fold that of the eugenol-treated group.

The effect of EUG on CAT, SOD activity and DPPH free radical scavenging rate of fresh-peeled CWCs

CAT is present in peroxides, and its main function is to specifically catalyze the decomposition of H_2O_2 to generate H_2O and O_2 (Li et al., 2021). The CAT activity of fresh-peeled CWCs witnessed a fluctuation during the storage (Figure 7A). However, the CAT activity of the eugenol treatment group was significantly higher than that of the control and ethanol treatment groups throughout the storage. On 5 d, the eugenol-treated group was 1.9 and 1.8-fold more than the control and ethanol-treated groups.

The catalytic effect of SOD is to inhibit the damage of $O_2^{\cdot-}$ to the plant body and establish the first line of defense to the antioxidant system (Peskin and Winterbourn, 2000). The SOD activity of the control and ethanol-treated fresh-peeled CWCs decreased first and then increased during the storage (Figure 7B), while the eugenol-treated group showed significantly higher SOD activity compared with that of the control and ethanol-treated groups. By the end of storage, the SOD activity in the eugenol treatment group reached 55.28 U g^{-1}, while the control and ethanol-treated groups were 51.87 and 49.99 U g^{-1}. Eugenol treatment increased SOD activity, inhibited the production of harmful substances and enhanced antioxidant capacity in fresh-peeled CWCs.

DPPH free radical scavenging rate is one of the indicators to evaluate the antioxidant capacity of plants (Chen et al., 2022). The DPPH free radical scavenging rate of fresh-peeled CWCs showed a fluctuating upward trend (Figure 7C). During the whole storage, the eugenol treatment group was consistently higher than the control and ethanol treatment groups, and there was a significant difference between the eugenol-treated group and the control group. On 5 d, the DPPH free radical scavenging rate in the eugenol-treated group was 51.5%, compared with 33.73% in the control group.

The effect of EUG on AsA, GSH content and APX, GR activity of resh-peeled CWCs

The AsA-GSH cycle is mainly composed of the interaction of AsA, GSH, APX and GR, and plays an important role in scavenging ROS. AsA is a vitamin substance widely distributed in plant tissues. It participates in the redox effect in the electron transport system in plants and is an important reducing agent in non-enzymatic antioxidant system of plants (Xu et al., 2022).

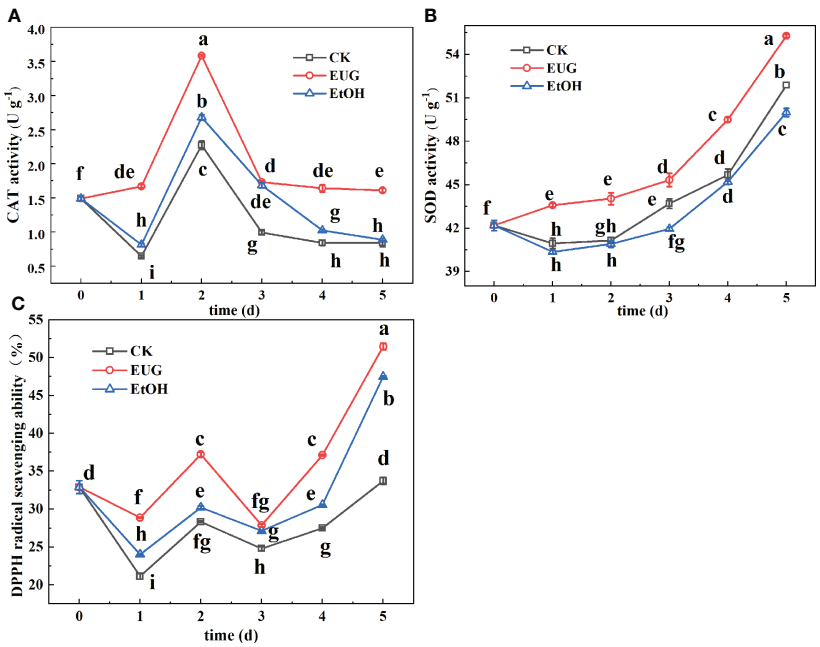

FIGURE 7
Effects of eugenol treatment on the activities of CAT **(A)**, SOD **(B)** and DPPH radical scavenging ability **(C)** of fresh-peeled CWC. Fresh-peeled CWCs were treated with tap water (CK), ethanol (EtOH) or eugenol (EUG). Error bars denote a standard error of the mean of triplicate assays. Different lowercase letters have shown significant differences (P<0.05).

The AsA content in fresh-peeled CWCs generally showed a downward trend (Figure 8A). The eugenol-treated group was higher than the control and ethanol-treated groups, and there was a significant difference between the eugenol-treated group and the control group from the third day to the end of storage. On the last day, the AsA content decreased by 39.3% and 40.2% in the control and ethanol-treated groups, respectively, while the eugenol-treated group decreased by 32.5%.

As a common non-enzymatic antioxidant, GSH not only directly scavenges a range of ROS, but also participates in many other functions that keep cells in a favorable state (Wang et al., 2021). It can be seen from Figure 8B that the GSH content in fresh-peeled CWCs first increased and then decreased. During the entire storage period, the GSH content of the eugenol-treated group was higher than that of the other two groups, and there were significant differences between the control and eugenol-treated groups. On 5 d, the eugenol treatment group was 1.5 and 1.3-fold as high as the control and ethanol treatment groups.

APX and GR are antioxidant enzymes that work together with antioxidant substances to remove ROS to protect the integrity of the cell membrane (Xu et al., 2022). The APX activity of eugenol treatment group was higher than the other two groups. During the whole storage, and there was a significant difference in the later storage (Figure 8C). On 5 d, the eugenol-treated groups were 1.3 and 1.4-fold as high as the control and ethanol-treated groups, respectively.

The GR activity in the three groups showed an upward trend, and the eugenol-treated group was significantly higher than the control and ethanol-treated groups during the entire storage (Figure 8D). On the last day of storage, the eugenol-treated group rose to 1.55 U g^{-1}, while the control and ethanol-treated groups were 0.68 and 0.73 U g^{-1}.

Correlation analysis

The color change of fresh-peeled CWCs could directly reflect its storage quality (Valverde et al., 2005). As can be seen from Figure 9, the color difference L* value of fresh-peeled CWCs treated with eugenol was significantly positively correlated with O_2 content, $O_2\cdot^-$ generation rate and AsA content. This suggests that eugenol treatment may delay the quality deterioration of fresh-peeled CWCs by inhibiting the rate of $O_2\cdot^-$ generation, reducing respiration intensity and loss of ascorbic acid. The color difference L* value was significantly negatively correlated with a*, b* value, browning degree, weight loss rate, the contents of CO_2, total flavonoids, total phenolics, and MDA, antioxidant enzyme activities (PAL, PPO, SOD, and GR). This indicated that the eugenol treatment may reduce the degree of browning and weight loss rate, and improving the antioxidant capacity, thereby inhibiting the discoloration of fresh-peeled CWCs and prolonging its shelf life.

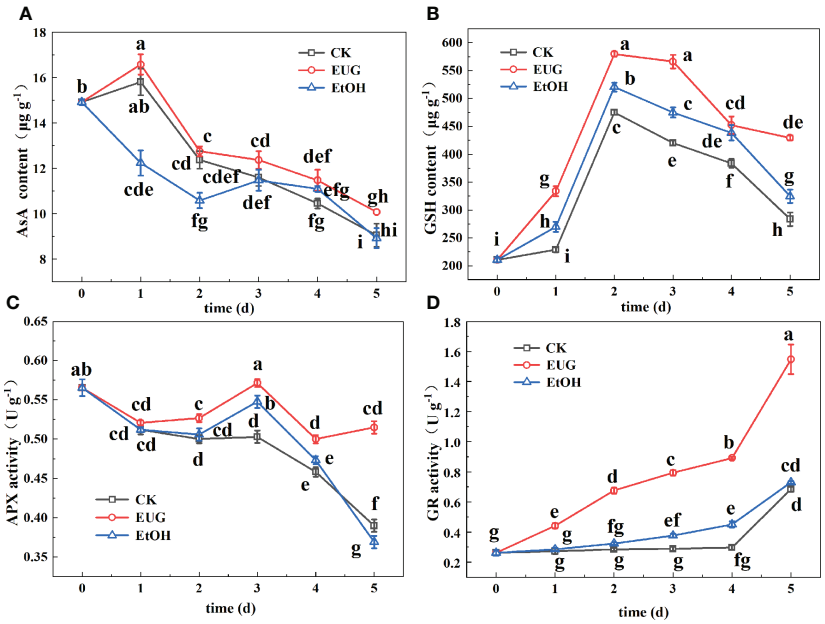

FIGURE 8
Effects of eugenol treatment on the AsA content **(A)**, GSH content **(B)**, APX activity **(C)** and GR activity **(D)** of fresh-peeled CWC. Fresh-peeled CWCs were treated with tap water (CK), ethanol (EtOH) or eugenol (EUG). Error bars denote a standard error of the mean of triplicate assays. Different lowercase letters have shown significant differences (P<0.05).

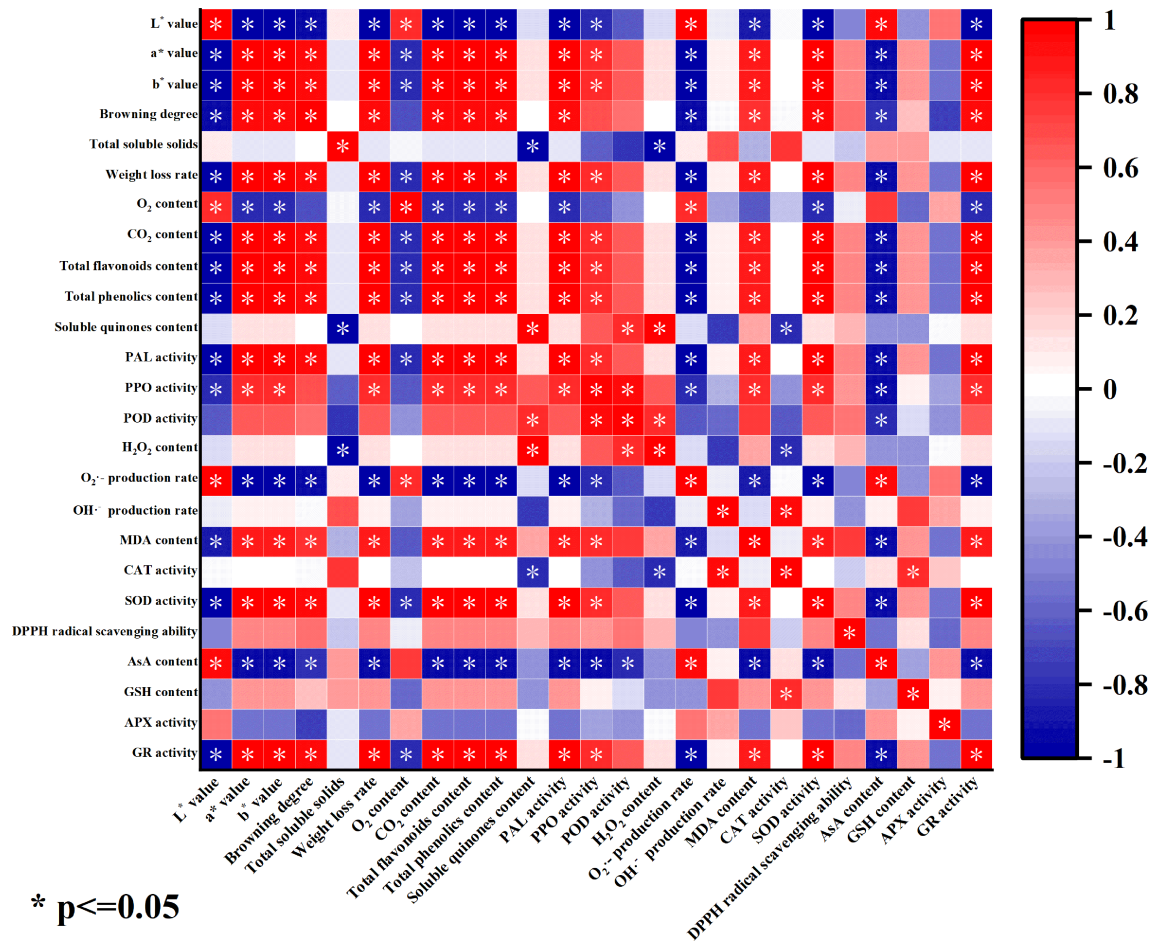

FIGURE 9
Correlation heat map of each index of fresh-peeled CWCs treated with eugenol. (The color depth indicates the strength of the correlation, the redder the color, the stronger the positive correlation, and the bluer the color, the stronger the negative correlation).

Discussion

Due to the mechanical damage during the fresh-cut processing, fresh-peeled CWCs suffer quality deterioration, such as discoloration and nutrient loss (Song et al., 2019). The appearance of fresh-peeled CWCs gradually deteriorated during storage, which is consistent with the increase in a* and b* values and the decrease in the L* value. These results accorded with the changes in browning degree in fresh-peeled CWCs. Thus, eugenol treatment delayed the discoloration of fresh-peeled CWCs, which is similar to the results of eugenol treatment in eggplant fruit (Huang et al., 2019), fresh-cut lettuce (Chen et al., 2017), citrus fruit (Yang et al., 2021) and cucumber (Li et al., 2021). Meanwhile, the total soluble solids reflect the content of soluble sugar and other nutrients in fresh-peeled CWCs (Song et al., 2019). It is found that eugenol treatment effectively maintained the total soluble solids level of fresh-peeled CWCs, which is consistent with the results of eugenol treatment in eggplant fruit (Huang et al., 2019) and citrus fruit (Yang et al., 2021). It may be due to that eugenol treatment accelerates the converting of organic acids and starches to soluble sugars (Yang et al., 2021). However, fresh-peeled CWCs are susceptible to mechanical damage, and the respiration and transpiration are enhanced, so the water loss will increase and the weight loss rate will increase. Eugenol treatment not only delayed the loss of the total soluble solids content in fresh-peeled CWCs, but also reduced the loss of juice of its fruit, which reduced the weight loss rate of fresh-peeled CWCs treated with eugenol. Eugenol treatment reduced the weight loss rate of fresh-peeled CWCs, which was similar to the findings of eugenol-treated fresh-cut lettuce (Chen et al., 2017) and cucumber fruit (Li et al., 2021). The headspace gas composition could reflect the respiration intensity of fresh-peeled CWCs. The O_2 content was higher and the CO_2 content was lower after eugenol treatment. Therefore, eugenol treatment inhibited the respiration intensity of fresh-peeled CWCs and delayed the quality deterioration. And this is

consistent with the results of eugenol-treated grape fruit (Valverde et al., 2005). In addition, many researchers have found that eugenol treatment can inhibit the growth of microorganisms, indicating that eugenol treatment has antiseptic and antibacterial effects (Zheng et al., 2013). Therefore, eugenol treatment could inhibit the respiration intensity of fresh-cut fruits and vegetables to maintain the quality of fresh-cut fruits and vegetables.

Phenolic metabolism is another important cause of discoloration (Pen and Jiang, 2003). After mechanical damage, the phenolic metabolism of fresh-cut fruits and vegetables will be activated (Pen and Jiang, 2003). PAL is an important enzyme in the metabolic pathway of phenylpropane for connecting phenylpropane metabolism with primary metabolism and catalyzing phenylalanine to generate cinnamic acids, followed by the production of flavonoids and other secondary metabolites (Min et al., 2017). Likewise, according to the study treating fresh-cut water chestnuts with exogenous ascorbic acid and ferulic acid, PAL is the key enzyme to promoting discoloration (Song et al., 2019). Throughout the storage, the PAL activity of fresh-peeled CWCs treated with eugenol was markedly lower than that of the control group (P<0.05). The total phenolics are key substrates that cause discoloration of fresh-cut vegetables and fruits, and also play antioxidant effects (Dou et al., 2021). In our study, eugenol treatment increased the total phenolic content of fresh-peeled CWCs, which is consistent with the results of eugenol treatment in eggplants (Huang et al., 2019) and tomatoes (Mirdehghan and Valero, 2017), and the active package containing eugenol for organic ready-to-eat iceberg lettuce (Wieczyńska and Cavoski, 2018). Moreover, in the study of fresh-peeled CWCs treated with 15 g/L eugenol emulsion, the eugenol emulsion treatment group exhibited higher content of p-hydroxybenzoic acid and chlorogenic acid (Teng et al., 2020). It may be that the increase in the content of these monophenols such as p-hydroxybenzoic acid and chlorogenic acid led to the increase in the total phenolic content of fresh-peeled CWCs. Under normal circumstances, the browning of vegetables and fruits is caused by the oxidation of phenolic substances into quinones, catalyzed by POD and PPO in the presence of oxygen (Huang et al., 2019). Quinones polymerize spontaneously and react with the side-chain groups of protein amino acid residues to produce black or brown substances (Toivonen and Brummell, 2008). The POD and PPO activity of fresh-peeled CWCs treated with eugenol were markedly lower than those of the control group during the whole storage (P<0.05), which is consistent with the results of fresh-cut lettuce treated with eugenol (Chen et al., 2017). Similar to the suppressed PPO and POD activity, fresh-peeled CWCs treated with eugenol showed lower total content of soluble quinones. However, some researchers believe that the cause of fresh-peeled CWCs discoloration is yellowing instead of enzymatic browning and that flavonoids such as naringenin and eriodictyol are the major substances of yellowing (Pan et al., 2015; Song et al., 2019). Throughout the storage, the total flavonoid content of fresh-peeled CWCs treated with eugenol was markedly lower than that of the control group (P<0.05). This suggests that eugenol treatment may delay the discoloration of fresh-peeled CWCs by inhibiting the production of total flavonoids. Therefore, eugenol treatment not only inhibited the production of flavonoids and quinones to a certain extent, but also reduced the production of PAL, PPO, POD. Moreover, eugenol treatment promoted the production of some phenolic substances, improved the antioxidant capacity of fresh-cut fruits and vegetables, and inhibited their discoloration.

The imbalance of ROS metabolism is an important reason for causing discoloration of vegetables and fruits during fresh-cutting (Tripathy and Oelmüller, 2012; Li et al., 2022). ROS mainly consists of H_2O_2, superoxide radicals ($O_2\cdot^-$), hydroxyl radicals ($OH\cdot^-$) and lipid peroxides (MDA). H_2O_2 can directly or indirectly oxidize biological macromolecules in cells, such as nucleic acids and proteins, thereby accelerating cell senescence and disintegration (Asaeda et al., 2018). The increase in $O_2\cdot^-$ generation will cause membrane lipid peroxidation, thereby accelerating the senescence of plant tissues (Kong et al., 2020). $OH\cdot^-$ is one of the most oxidative free radicals that can react with all cells and cause damage to the plant body (Dou et al., 2021). As one of the membrane lipid peroxidation products of cell membranes, MDA can damage the cell membrane of plant tissues and accelerate discoloration (Kong et al., 2020). During the whole storage process, the contents of H_2O_2 and MDA and the production rate of $O_2\cdot^-$ and $OH\cdot^-$ in fresh-peeled CWCs treated with eugenol were markedly lower than those in the control group (P<0.05). This finding is consistent with research results of eugenol treated eggplant fruit (Huang et al., 2019) and cucumbers treated by double layer membrane loading eugenol (Li et al., 2021). So, the eugenol treatment inhibited the accumulation of these harmful substances. There is a complete ROS scavenging system in vegetables and fruits. It mainly including antioxidant enzymes and antioxidants (Li et al., 2021), which can not only exert their own antioxidant effects, but also coordinate with each other to scavenge ROS. A main function of CAT is to catalyze the decomposition of H_2O_2 to generate H_2O and O_2 (Li et al., 2021). SOD is the first line of defense to inhibit the damage of $O_2\cdot^-$ on plant bodies and establish an antioxidant system (Yang et al., 2021). During the whole storage process, the fresh-peeled CWCs treated with eugenol showed higher CAT and SOD activities than the control group (P<0.05). Similarly, SOD and CAT activity were markedly enhanced in citrus fruits treated by eugenol nano-emulsion (Yang et al., 2021) and eugenol emulsion-treated fresh-cut water chestnuts (Zhu et al., 2022). DPPH free radical scavenging rate is closely related to plant antioxidant capacity (Chen et al., 2022). It can be seen from the experimental results that the DPPH free radical scavenging rate in the eugenol treatment group was significantly higher than that in the control group (P<0.05). This result was similar to that of

strawberry treated with eugenol (Wang et al., 2007), which also enhanced the DPPH free radical scavenging rate. Therefore, eugenol treatment improved the antioxidant capacity of fresh-peeled CWCs. The AsA-GSH cycle is mainly composed of the interaction of AsA, APX, GSH and GR, and plays an important role in scavenging ROS. During the whole storage process, the AsA and GSH contents and APX and GR activities of fresh-peeled CWCs treated with eugenol were higher than those of the control and ethanol-treated groups. This is similar to the results of treating fresh-cut CWCs with hydrogen sulfide (Dou et al., 2021), fresh-cut pears treated with high carbon dioxide (Wang et al., 2021), and fresh-cut pitaya fruit pretreated with hot air (Li et al., 2022). Therefore, eugenol treatment results in an increase the contents of these antioxidants and the activities of antioxidant enzymes in fresh-peeled CWCs. Moreover, eugenol treatment could inhibit the production of ROS metabolism, thereby inhibiting the spoilage and aging of fresh-cut fruits and vegetables, and reducing the accumulation of harmful substances. Meanwhile, eugenol treatment could promote the generation of antioxidant enzymes and antioxidants in the ROS scavenging system to maintain the quality of fresh-cut fruits and vegetables, and play a very important role in extending their shelf life.

Conclusions

This study indicated that eugenol treatment could effectively delay the surface discoloration, reduce the degree of browning, weight loss rate and the loss of soluble solids and increase the O_2 content, reduce the CO_2 content in fresh-peeled CWCs. Moreover, eugenol treatment markedly decreased the content of total flavonoids and soluble quinones and inhibited the activity of POD, PPO, and PAL of fresh-peeled CWCs. In addition, eugenol treatment increased the total phenolic content and DPPH radical scavenging rate, and improved the antioxidant ability of fresh-peeled CWCs. In particular, the ROS production (H_2O_2, $O_2\cdot^-$ and $OH\cdot^-$) and MDA level were suppressed by eugenol treatment, while promoting the production of antioxidants (AsA and GSH), and enhanced the activities of antioxidant enzymes (CAT, SOD, APX and GR). In summary, the fresh-peeled CWCs after eugenol treatment can effectively maintain the storage quality by inhibiting the phenolic metabolism, improving the antioxidant capacity and scavenging the ROS. Thus, eugenol treatment has broad potential for the preservation of fresh-cut vegetables and fruits in future.

Data availability statement

The original contributions presented in the study are included in the article/Supplementary Material. Further inquiries can be directed to the corresponding author.

Author contributions

ZC and TM designed the study; ZC, YL and ZM carried out the experiments; ZC, TM, YX and YY made the data analysis; TM, ZC and WH drafted the manuscript; LW, TM, YA and HW reviewed the final manuscript. All authors contributed to the article and approved the submitted version.

Funding

Supported by National Natural Science Foundation of China (no. 32001764).

Conflict of interest

The authors declare that the research was conducted in the absence of any commercial or financial relationships that could be construed as a potential conflict of interest.

Publisher's note

All claims expressed in this article are solely those of the authors and do not necessarily represent those of their affiliated organizations, or those of the publisher, the editors and the reviewers. Any product that may be evaluated in this article, or claim that may be made by its manufacturer, is not guaranteed or endorsed by the publisher.

References

Alshaikh, N., and Perveen, K. (2017). Anti-candidal activity and chemical composition of essential oil of clove (Syzygium aromaticum). *J. Essential Oil Bearing Plants* 20 (4), 951–958. doi: 10.1080/0972060X.2017.1375867

Asaeda, T., Jayasanka, S. M. D. H., Xia, L. P., and Barnuevo, A. (2018). Application of hydrogen peroxide as an environmental stress indicator for vegetation management. *Engineering* 4 (5), 610–616. doi: 10.1016/j.eng.2018.09.001

Chen, X., Ren, L., Li, M., Qian, J., Fan, J., and Du, B. (2017). Effects of clove essential oil and eugenol on quality and browning control of fresh-cut lettuce. *Food Chem.* 214, 432–439. doi: 10.1016/j.foodchem.2016.07.101

Chen, J., Xu, Y., Yi, Y., Hou, W., Wang, L., Ai, Y., et al. (2022). Regulations and mechanisms of 1-methylcyclopropene treatment on browning and quality of fresh-cut lotus (Nelumbo nucifera gaertn.) root slices. *Postharvest Biol. Technol.* 185, 111782. doi: 10.1016/j.postharvbio.2021.111782

Devi, K. P., Sakthivel, R., Nisha, S. A., Suganthy, N., and Pandian, S. K. (2013). Eugenol alters the integrity of cell membrane and acts against the nosocomial pathogen Proteus mirabilis. *Arch. Pharmacal Res.* 36 (3), 282–292. doi: 10.1007/s12272-013-0028-3

Dou, Y., Chang, C., Wang, J., Cai, Z., Zhang, W., Du, H., et al. (2021). Hydrogen sulfide inhibits enzymatic browning of fresh-cut Chinese water chestnuts. *Front. Nutr.* 8, 652984. doi: 10.3389/fnut.2021.652984

Du, J., Fu, Y., and Wang, N. (2009). Effects of aqueous chlorine dioxide treatment on browning of fresh-cut lotus root. *LWT-Food Sci. Technol.* 42 (2), 654–659. doi: 10.1016/j.lwt.2008.08.007

Fan, P., Huber, D. J., Su, Z., Hu, M., Gao, Z., Li, M., et al. (2018). Effect of postharvest spray of apple polyphenols on the quality of fresh-cut red pitaya fruit during shelf life. *Food Chem.* 243, 19–25. doi: 10.1016/j.foodchem.2017.09.103

Fernández-Pan, I., Royo, M., and Ignacio Mate, J. (2012). Antimicrobial activity of whey protein isolate edible films with essential oils against food spoilers and foodborne pathogens. *J. Food Sci.* 77 (7), M383–M390. doi: 10.1111/j.1750-3841.2012.02752.x

Gong, L., Li, T., Chen, F., Duan, X., Yuan, Y., Zhang, D., et al. (2016). An inclusion complex of eugenol into β-cyclodextrin: Preparation, and physicochemical and antifungal characterization. *Food Chem.* 196, 324–330. doi: 10.1016/j.foodchem.2015.09.052

Guerreiro, A. C., Gago, C. M., Faleiro, M. L., Miguel, M. G., and Antunes, M. D. (2015). The use of polysaccharide-based edible coatings enriched with essential oils to improve shelf-life of strawberries. *Postharvest Biol. Technol.* 110, 51–60. doi: 10.1016/j.postharvbio.2015.06.019

Guerreiro, A. C., Gago, C. M., Faleiro, M. L., Miguel, M. G., and Antunes, M. D. (2016). Edible coatings enriched with essential oils for extending the shelf-life of 'Bravo de esmolfe' fresh-cut apples. *Int. J. Food Sci. Technol.* 51 (1), 87–95. doi: 10.1111/ijfs.12949

Guerreiro, A. C., Gago, C. M., Miguel, M. G., Faleiro, M. L., and Antunes, M. D. (2016). The influence of edible coatings enriched with citral and eugenol on the raspberry storage ability, nutritional and sensory quality. *Food Packaging Shelf Life* 9, 20–28. doi: 10.1016/j.fpsl.2016.05.004

Homaida, M. A., Yan, S., and Yang, H. (2017). Effects of ethanol treatment on inhibiting fresh-cut sugarcane enzymatic browning and microbial growth. *LWT* 77, 8–14. doi: 10.1016/j.lwt.2016.10.063

Huang, Q., Qian, X., Jiang, T., and Zheng, X. (2019). Effect of eugenol fumigation treatment on chilling injury and CBF gene expression in eggplant fruit during cold storage. *Food Chem.* 292, 143–150. doi: 10.1016/j.foodchem.2019.04.048

Jiang, Y., Pen, L., and Li, J. (2004). Use of citric acid for shelf life and quality maintenance of fresh-cut Chinese water chestnut. *Journal of food engineering. 63(3)*, 325–328. doi: 10.1016/j.jfoodeng.2003.08.004

Kong, X. M., Ge, W. Y., Wei, B. D., Zhou, Q., Zhou, X., Zhao, Y. B., et al. (2020). Melatonin ameliorates chilling injury in green bell peppers during storage by regulating membrane lipid metabolism and antioxidant capacity. *Postharvest Biol. Technol.* 170, 111315. doi: 10.1016/j.postharvbio.2020.111315

Li, F., Hu, Y., Shan, Y., Liu, J., Ding, X., Duan, X., et al. (2022). Hydrogen-rich water maintains the color quality of fresh-cut Chinese water chestnut. *Postharvest Biol. Technol.* 183, 111743. doi: 10.1016/j.postharvbio.2021.111743

Li, Z., Li, B., Li, M., Fu, X., Zhao, X., Min, D., et al. (2022). Hot air pretreatment alleviates browning of fresh-cut pitaya fruit by regulating phenylpropanoid pathway and ascorbate-glutathione cycle. *Postharvest Biol. Technol.* 190, 111954. doi: 10.1016/j.postharvbio.2022.111954

Li, H., Shui, Y., Li, S., Xing, Y., Xu, Q., Li, X., et al. (2020). Quality of fresh cut lemon during different temperature as affected by chitosan coating with clove oil. *Int. J. Food Properties* 23 (1), 1214–1230. doi: 10.1080/10942912.2020.1792924

Liu, C., Zheng, H., Sheng, K., Liu, W., and Zheng, L. (2018). Effects of melatonin treatment on the postharvest quality of strawberry fruit. *Postharvest Biol. Technol.* 139, 47–55. doi: 10.1016/j.postharvbio.2018.01.016

Li, M., Yu, H., Xie, Y., Guo, Y., Cheng, Y., Qian, H., et al. (2021). Effects of double layer membrane loading eugenol on postharvest quality of cucumber. *LWT* 145, 111310. doi: 10.1016/j.lwt.2021.111310

Ma, Q., Davidson, P. M., and Zhong, Q. (2016). Nanoemulsions of thymol and eugenol co-emulsified by lauric arginate and lecithin. *Food Chem.* 206, 167–173. doi: 10.1016/j.foodchem.2016.03.065

Min, T., Liu, E. C., Xie, J., Yi, Y., Wang, L. M., Ai, Y. W., et al. (2019). Effects of vacuum packaging on enzymatic browning and ethylene response factor (ERF) gene expression of fresh-cut lotus root. *HortScience* 54 (2), 331–336. doi: 10.21273/HORTSCI13735-18

Min, T., Xie, J., Zheng, M., Yi, Y., Hou, W., Wang, L., et al. (2017). The effect of different temperatures on browning incidence and phenol compound metabolism in fresh-cut lotus (Nelumbo nucifera g.) root. *Postharvest Biol. Technol.* 123, 69–76. doi: 10.1016/j.postharvbio.2016.08.011

Mirdehghan, S. H., and Valero, D. (2017). Bioactive compounds in tomato fruit and its antioxidant activity as affected by incorporation of aloe, eugenol, and thymol in fruit package during storage. *Int. J. Food Properties* 20 (sup2), 1798–1806. doi: 10.1080/10942912.2016.1223128

Nie, H., Chen, H., Li, G., Su, K., Song, M., Duan, Z., et al. (2021). Comparison of flavonoids and phenylpropanoids compounds in Chinese water chestnut processed with different methods. *Food Chem.* 335, 127662. doi: 10.1016/j.foodchem.2020.127662

Pan, Y. G., Li, Y. X., and Yuan, M. Q. (2015). Isolation, purification and identification of etiolation substrate from fresh-cut Chinese water-chestnut (Eleocharis tuberosa). *Food Chem.* 186, 119–122. doi: 10.1016/j.foodchem.2015.03.070

Peng, L., and Jiang, Y. (2006). Exogenous salicylic acid inhibits browning of fresh-cut Chinese water chestnut. *Food Chem.* 94 (4), 535–540. doi: 10.1016/j.foodchem.2004.11.047

Pen, L. T., and Jiang, Y. M. (2003). Effects of chitosan coating on shelf life and quality of fresh-cut Chinese water chestnut. *LWT-Food Sci. Technol.* 36 (3), 359–364. doi: 10.1016/S0023-6438(03)00024-0

Peskin, A. V., and Winterbourn, C. C. (2000). A microtiter plate assay for superoxide dismutase using a water-soluble tetrazolium salt (WST-1). *Clinica Chimica Acta* 293 (1-2), 157–166. doi: 10.1016/S0009-8981(99)00246-6

Saltveit, M. E. (2000). Wound induced changes in phenolic metabolism and tissue browning are altered by heat shock. *Postharvest Biol. Technol.* 21 (1), 61–69. doi: 10.1016/S0925-5214(00)00165-4

Sharifimehr, S., Soltanizadeh, N., and Hossein Goli, S. A. (2019). Effects of edible coating containing nano-emulsion of aloe vera and eugenol on the physicochemical properties of shrimp during cold storage. *J. Sci. Food Agric.* 99 (7), 3604–3615. doi: 10.1002/jsfa.9581

Song, M., Wu, S., Shuai, L., Duan, Z., Chen, Z., Shang, F., et al. (2019). Effects of exogenous ascorbic acid and ferulic acid on the yellowing of fresh-cut Chinese water chestnut. *Postharvest Biol. Technol.* 148, 15–21. doi: 10.1016/j.postharvbio.2018.10.005

Teng, Y., Murtaza, A., Iqbal, A., Fu, J., Ali, S. W., Iqbal, M. A., et al. (2020). Eugenol emulsions affect the browning processes, and microbial and chemical qualities of fresh-cut Chinese water chestnut. *Food Bioscience* 38, 100716. doi: 10.1016/j.fbio.2020.100716

Toivonen, P. M., and Brummell, D. A. (2008). Biochemical bases of appearance and texture changes in fresh-cut fruit and vegetables. *Postharvest Biol. Technol.* 48 (1), 1–14. doi: 10.1016/j.postharvbio.2007.09.004

Tripathy, B. C., and Oelmüller, R. (2012). Reactive oxygen species generation and signaling in plants. *Plant Signaling Behav.* 7 (12), 1621–1633. doi: 10.4161/psb.22455

Valverde, J. M., Guillén, F., Martínez-Romero, D., Castillo, S., Serrano, M., and Valero, D. (2005). Improvement of table grapes quality and safety by the combination of modified atmosphere packaging (MAP) and eugenol, menthol, or thymol. *J. Agric. Food Chem.* 53 (19), 7458–7464. doi: 10.1021/jf050913i

Wang, D., Li, W., Li, D., Li, L., and Luo, Z. (2021). Effect of high carbon dioxide treatment on reactive oxygen species accumulation and antioxidant capacity in fresh-cut pear fruit during storage. *Scientia Hortic.* 281, 109925. doi: 10.1016/j.scienta.2021.109925

Wang, C. Y., Wang, S. Y., Yin, J. J., Parry, J., and Yu, L. L. (2007). Enhancing antioxidant, antiproliferation, and free radical scavenging activities in strawberries with essential oils. *J. Agric. Food Chem.* 55 (16), 6527–6532. doi: 10.1021/jf070429a

Wan, J., Hu, Y., Ai, T., Ye, S., Huang, Q., Yang, Q., et al. (2018). Preparation of thermo-reversible eugenol-loaded emulgel for refrigerated meat preservation. *Food Hydrocolloids* 79, 235–242. doi: 10.1016/j.foodhyd.2018.01.002

Wieczyńska, J., and Cavoski, I. (2018). Antimicrobial, antioxidant and sensory features of eugenol, carvacrol and trans-anethole in active packaging for organic ready-to-eat iceberg lettuce. *Food Chem.* 259, 251–260. doi: 10.1016/j.foodchem.2018.03.137

Xu, Y., Yu, J., Chen, J., Gong, J., Peng, L., Yi, Y., et al. (2022). Melatonin maintains the storage quality of fresh-cut Chinese water chestnuts by regulating phenolic and reactive oxygen species metabolism. *Food Qual. Saf.* 6, 1–9. doi: 10.1093/fqsafe/fyac002

Yang, R., Miao, J., Shen, Y., Cai, N., Wan, C., Zou, L., et al. (2021). Antifungal effect of cinnamaldehyde, eugenol and carvacrol nanoemulsion against penicillium digitatum and application in postharvest preservation of citrus fruit. *LWT* 141, 110924. doi: 10.1016/j.lwt.2021.110924

You, Y., Jiang, Y., Sun, J., Liu, H., Song, L., and Duan, X. (2012). Effects of short-term anoxia treatment on browning of fresh-cut Chinese water chestnut in relation to antioxidant activity. *Food Chem.* 132 (3), 1191–1196. doi: 10.1016/j.foodchem.2011.11.073

Zheng, L., Bae, Y. M., Jung, K. S., Heu, S., and Lee, S. Y. (2013). Antimicrobial activity of natural antimicrobial substances against spoilage bacteria isolated from fresh produce. *Food Control* 32 (2), 665–672. doi: 10.1016/j.foodcont.2013.01.009

Zhu, L., Hu, W., Murtaza, A., Iqbal, A., Li, J., Zhang, J., et al. (2022). Eugenol treatment delays the flesh browning of fresh-cut water chestnut (Eleocharis tuberosa) through regulating the metabolisms of phenolics and reactive oxygen species. *Food Chemistry: X* 14, 100307. doi: 10.1016/j.fochx.2022.100307

Zou, J. N., Jin, X. J., Zhang, Y. X., Ren, C. Y., Zhang, M. C., and Wang, M. X. (2019). Effects of melatonin on photosynthesis and soybean seed growth during grain filling under drought stress. *Photosynthetica* 57 (2), 512–520. doi: 10.32615/ps.2019.066

frontiers | Frontiers in Plant Science

TYPE Original Research
PUBLISHED 06 December 2022
DOI 10.3389/fpls.2022.1039373

OPEN ACCESS

EDITED BY
Qiong Lin,
Chinese Academy of Agricultural Sciences (CAAS), China

REVIEWED BY
Walid Badawy Abdelaal,
Agricultural Research Center, Egypt
Muhammad Azher Nawaz,
University of Sargodha, Pakistan
Asgar Ali,
University of Nottingham Malaysia Campus, Malaysia

*CORRESPONDENCE
Muhammad Azam
muhammad.azam@uaf.edu.pk
Hongru Liu
hear2008dream@163.com

†These authors have contributed equally to this work

SPECIALTY SECTION
This article was submitted to Crop and Product Physiology, a section of the journal Frontiers in Plant Science

RECEIVED 08 September 2022
ACCEPTED 16 November 2022
PUBLISHED 06 December 2022

CITATION
Wang D, Randhawa MS, Azam M, Liu H, Ejaz S, Ilahy R, Qadri R, Khan MI, Umer MA, Khan MA and Wang K (2022) Exogenous melatonin treatment reduces postharvest senescence and maintains the quality of papaya fruit during cold storage. *Front. Plant Sci.* 13:1039373. doi: 10.3389/fpls.2022.1039373

Exogenous melatonin treatment reduces postharvest senescence and maintains the quality of papaya fruit during cold storage

Dengliang Wang[1†], Mazhar Saeed Randhawa[2†], Muhammad Azam[2*], Hongru Liu[3*], Shaghef Ejaz[4], Riadh Ilahy[5], Rashad Qadri[2], Muhammad Imran Khan[6], Muhammad Ali Umer[2], Muhammad Arslan Khan[2] and Ke Wang[7]

[1]1Institute of Fruit Tree Research, Quzhou Academy of Agriculture and Forestry Science, Quzhou, China, [2]Pomology Laboratory, Institute of Horticultural Sciences, University of Agriculture, Faisalabad, Pakistan, [3]Institute of Crop Breeding & Cultivation Research, Shanghai Academy of Agricultural Sciences, Shanghai, China, [4]Department of Horticulture, Bahauddin Zakariya University, Multan, Pakistan, [5]Laboratory of Horticulture, National Agricultural Research Institute of Tunisia (INRAT), University of Carthage, Ariana, Tunisia, [6]Institute of Soil and Environmental Sciences, University of Agriculture, Faisalabad, Pakistan, [7]Key Laboratory of Jianghuai Agricultural Product Fine Processing and Resource Utilization, Ministry of Agriculture and Rural Affairs/Anhui Engineering Laboratory for Agro-products Processing, Anhui Agricultural University, Hefei, China

Introduction: Exogenous melatonin (EMT) application has been used to reduce postharvest senescence and improve the quality and antioxidant enzyme activities of papaya fruits during cold storage.

Methods: The effects of exogenous melatonin application (1. 5 mM) were investigated on papaya fruits during cold storage (10°C ± 2°C) for 28 days in the present study.

Results and discussion: The EMT treatment delayed postharvest senescence significantly with lower maturing status compared with untreated papaya fruits (control). In addition, EMT treatment maintained substantially higher titratable acidity values and ascorbic acid content but significantly lower soluble solids content and lower weight loss compared with the untreated fruits. Concerning the antioxidant capacity, the EMT-treated papaya fruit exhibited markedly higher total phenolic content and, consequently, higher DPPH-radical scavenging activity than the control group. The EMT treatment not only kept a higher enzyme activity of superoxide dismutase, peroxidase, and catalase but also significantly inhibited the accumulation of hydrogen peroxide and malondialdehyde, along with satisfying sensory attributes.

Conclusion: The findings of this study indicated that EMT application could be commercially used as an eco-friendly strategy to reduce postharvest senescence and maintain the fresh-like quality traits of papaya fruit during cold storage.

KEYWORDS

Papaya, biochemical assays, antioxidant capacity, ROS, sensory attributes, postharvest storage, melatonin

Introduction

Papaya (*Carica papaya* L.) is an economically important fruit that is mostly grown in tropical and subtropical zones of many countries (Wu et al., 2019). It is considered a rich source of bioactive compounds, phytochemicals, and minerals (Oloyede, 2005). Papaya is a climacteric fruit and ripens rapidly after postharvest. Several physical and biochemical changes cause pulp softening, skin discoloration, and fungal infection, significantly limiting papaya's postharvest life (Escamilla-García et al., 2018; de Vasconcellos Santos Batista et al., 2020). Additionally, papaya fruits are prone to chilling injury during cold storage and fast quality deterioration during transportation due to the higher vulnerability of their delicate skin to mechanical damage (Nunes et al., 2006; Zerpa-Catanho et al., 2017). Papaya incurs up to 25% postharvest losses from the field to the retail level, where fungal diseases cause the majority (93%) of these losses. Similarly, 5% to 40% losses may occur during air and sea transit, depending on papaya handling and packaging methods (Nunes et al., 2006; Gajanana et al., 2010). Generally, ripe papaya fruits maintain fresh-like quality for 1 week at 25°C and for 14 days at 12°C (Wu et al., 2019). Most of the approaches adapted to control the postharvest deterioration of papayas either have high economic costs or require a high input of synthetic chemicals which posed a high risk to the environment and human health. Therefore, there is a need for an efficient and eco-friendly strategy to prolong the shelf life of papaya.

Recently, several methods, such as the application of putrescine (Hanif et al., 2020b), ozone (Ong et al., 2013a), bioactive extracts (Albertini et al., 2016) alone or combined with hot water treatment (Vilaplana et al., 2020), gamma and UV-C irradiation (Zhao et al., 1996; Cia et al., 2007), and edible coatings (Maqbool et al., 2011; Hamzah et al., 2013; Dotto et al., 2015; Dos Passos et al., 2020), have been extensively employed to enhance the postharvest storage quality of papaya fruits. Ong et al. (2013b) reported variations in physicochemical traits and antioxidant concentration during the postharvest ripening of papaya cv. Frangi. Moreover, the quality of fresh-cut products was kept by using postharvest green and innovative chemical treatments, which substantially inhibited microbial infestation (Ali et al., 2018). An increasing trend has recently been noticed which is using melatonin treatment to delay ripening and postharvest decay and to increase resistance against oxidative stress in stored fruits (Huang and Vanyo, 2020; Li et al., 2017). Fan et al. (2022) reported that melatonin application has safe commercial use in addition to enhancing storage potential and maintaining postharvest quality traits of various fruits.

Melatonin (N-acetyl-5-methoxytryptamine) has been implicated in abiotic and biotic stress tolerance in plants. Melatonin is an important pleiotropic molecule with multiple physiological and cellular actions in plants and is considered an efficient antioxidant and nutritional supplement for humans (Galano et al., 2011; Reiter et al., 2015; Sun et al., 2015; Liu et al., 2018; Yan et al., 2020). Wang et al. (2020) reported that melatonin is a ubiquitous signaling molecule involved in different plant growth and development processes, leading to improved crop yield and fruit storage life. Recently, the impact of exogenous melatonin (EMT) application to delay postharvest senescence and its effect on the biochemical and antioxidative defense system of fruits have gained extensive consideration. EMT application has been used to delay ripening and senescence, maintain quality, and increase postharvest life during storage in various fresh products such as tomato, peach, and strawberry fruits (Gao et al., 2016; Ma et al., 2016; Aghdam and Fard, 2017). EMT treatment also increased the endogenous melatonin level and improved the nutraceutical properties of various fruits including sweet cherries, bananas, and litchis (Hu et al., 2017; Wang et al., 2019; Wu et al., 2021). Melatonin treatments decreased fruit senescence by trapping reactive oxygen species (ROS) and malondialdehyde (MDA) content while improving the antioxidant activities and phenolic concentration (Li et al., 2017; Wang et al., 2019). EMT application significantly decreased the content of MDA and hydrogen peroxide (H_2O_2) and maintained higher superoxide dismutase (SOD), peroxidase (POD), catalase (CAT), and glutathione reductase (GR) enzyme activities than control and retained the integrity of the membrane wall in sweet cherry fruits (Sharafi et al., 2021). Wang et al. (2021) found that EMT application also delayed low-temperature injury, lowered peel browning, and increased the antioxidant defense system which contributed to lower H_2O_2 and O_2^- production rates in banana fruit. Based on the abovementioned advantages, EMT treatment might be safe and eco-friendly and a better alternative to various chemical treatments in maintaining fresh-like fruit quality during storage. However, such studies on papaya fruit during cold storage are very limited and not complete.

Therefore, the aim of this research was to investigate the effect of EMT treatment in reducing postharvest senescence and maintaining the fresh-like quality of papaya fruit during cold storage (10°C for 28 days).

Materials and methods

Fruit materials and treatment

Papaya (*C. papaya* L. Cv. Red Lady) fruits were harvested at two physiological stages of maturation (with green and a trace of yellow) from a local orchard located at Faisalabad, Punjab, Pakistan, and kept under shade. Healthy and uniformly sized (450– 550 g) papaya fruits were selected and immediately delivered to the laboratory. The papaya fruits were washed with water to remove dirt before soaking in a disinfectant [sodium hypochlorite (0.1%, v/v)] solution for 2 min. Then, the fruits were rinsed and air-dried. For melatonin treatment, the fruits were divided into two groups. The first group of papaya

fruits (control) was dipped only in distilled water, whereas the second group was treated with 1. 5 mM of melatonin for 10 min. A preliminary experiment on papaya fruits was conducted with four melatonin concentrations of 0.5, 1, 1.5, and 2 mM. Finally, 1. 5 mM of melatonin concentration was screened out for further experiments. The fruits were air-dried for 30 min and then stored at 10° C ± 2°C and 90%–95% relative humidity (RH) for 28 days after the treatments. Papaya fruits were sampled at 7-day intervals. Each treatment was comprised of three biological replications, each consisting of 20 fruits. The samples were frozen with liquid nitrogen and kept at −40°C for further analysis. The data were recorded at each sampling point through the storage period.

Determination of decay incidence and weight loss

Papaya fruits with visible symptoms of rot and fungal or bacterial infections were considered as decay. In each treatment, the decay rate was measured by dividing the number of decaying fruits in relation to the total quantity of fruits. The results were expressed in percentage of decayed fruit. Regarding weight loss, three papaya fruits were marked and weighed at each interval using a digital electronic balance (EK-600H, Japan). The outcomes were presented as a percentage of weight reduction with respect to the initial weight.

Determination of soluble solids content, titratable acidity, ripening index, and ascorbic acid content

The juice of the papaya fruits was prepared using a juicer machine (DN-DOB, DEURON, Japan) for chemical analysis. To determine the soluble solids content (SSC), a drop of juice was placed on the cleaned prism plate of a digital refractometer (RX 5000, Atago, Japan). Prior to taking reading, distilled water was used to calibrate the refractometer at room temperature (27°C). After measurements, distilled water was used to clean up the prism of the refractometer for further analysis and SSC was expressed as °Brix.

The measurement of titratable acidity (TA) was obtained according to the procedure of Hortwitz (1960). For TA measurement, 10 ml of fresh juice and 50 ml of distilled water were added to a 100-ml conical flask. TA was measured by the titration method using 0. 1 N of NaOH in the presence of phenolphthalein (one to two drops) as a pH indicator. Titration was continued until the achievement of the endpoint of pink color and the data were expressed as percent TA. The ripening index was determined by taking the ratio between SSC and TA (SSC: TA ratio).

The content of ascorbic acid (AsA) in papaya fruits was measured according to the method of Ruck (1961) by using 2, 6-dichlorophenolindophenol as a dye. For this, the samples were prepared by taking 5 ml of papaya juice extracted from three fruits per replication. Furthermore, 90 ml of 0.4% oxalic acid solution was added to the juice in a volumetric flask (100 ml). After filtration, an aliquot of 5 ml was titrated against the dye until a pink color appeared and remained at least for a period of 15 s. The results were expressed as mg of ascorbic acid per 100 ml of fruit juice.

Determination of total sugar, reducing sugar, and non-reducing sugar (%)

Total, reducing, and non-reducing sugars of papaya fruits were evaluated using the standard method of Hortwitz (1960) by using a specified titration procedure.

Measurement of total phenolic content and DPPH-radical scavenging activity

The total phenolic content in papaya fruit was estimated using the Folin–Ciocalteu reagent as suggested by Razzaq et al. (2013) with slight modification. The supernatant was extracted, vortexed, incubated, and then centrifuged at 13,000 × *g*. Finally, the absorbance was measured by using a spectrophotometer at 765 and 517 nm. The results were reported as mg of gallic acid equivalent (GAE)/100 g FW.

DPPH-radical scavenging activity (DPPH-RSA) was determined using the free radical 2,2-diphenyl-1-picrylhydrazyl as reported by Brand-Williams et al. (1995), and the results were expressed in percentage.

Measurement of malondialdehyde and hydrogen peroxide contents

The determination of MDA content was conducted by using the thiobarbituric acid (TBA) assay (Hodges et al., 1999) with slight changes. Two grams of papaya pulp was mixed with 5 ml of 30 mM trichloroacetic acid and centrifuged (10,000 × *g* for 10 min at 4°C). The supernatant (1 ml) was mixed with 3 ml of 0.67% TBA and heated for 20 min. After cooling at room temperature, the absorbance was recorded at 450, 532, and 600 nm. MDA values were expressed as nmol g^{-1} FW. The measurement of H_2O_2 content was performed using the method of Ferguson et al. (1983) with minor modifications. Shortly, papaya pulp (1 g) was weighed, and 5 ml of precooled acetone was added to the sample, followed by homogenizing the sample and centrifuging (10,000 × *g*) for 10 min at 4°C. Afterward, 0.5 ml of the supernatant was mixed with

precooled acetone (0. 5 ml), $TiCl_4$–HCl (0. 1 ml, 10%), and concentrated ammonia (0. 2 ml). Then, the mixture was centrifuged (10,000 × *g* at 4°C for 15 min), the precipitate was then mixed with H_2SO_4 (3 ml, 2 mol L^{-1}), and the absorbance of the solution was measured at 412 nm. H_2O_2 production rate was expressed as mmol kg^{-1}.

Determination of antioxidant enzyme activities

For the determination of antioxidant enzyme activities, the papaya pulp sample (1 g) was homogenized with phosphate buffer (pH 7.2), and then the homogenate was centrifuged at 10,000 × *g* for 10 min at 4°C. The supernatant was collected for further assessment of enzymatic activities.

The SOD activity of papaya was determined according to the method of Stajner and Popovic (2009) with slight modifications. Shortly, the reaction mixture consisted of 500 µl of phosphate buffer (50 mM, pH 5), 200 µl of methionine (22 µM), 100 µl of NBT (20 µM), 200 µl of Triton X (0. 1 µM), and 100 µl of riboflavin (0. 6 µM), along with 800 µl of distilled water and 100 µl of enzyme extract. Then, the mixture was incubated in a box under luminous lamps for 15 min. The changes in absorbance were monitored and recorded at 560 nm, and SOD activity was calculated as U mg^{-1} protein. The POD activity of papaya fruit extract was determined according to Liu et al. (2014) with minor changes. Briefly, the reaction mixture, containing 0. 5 ml of crude extract and 2 ml of guaiacol substrate, was incubated at 30°C for 5 min, and 1 ml of H_2O_2 (24 mM) was added to it. The change in absorbance at 460 nm was monitored, and POD activity was expressed as U mg^{-1} protein. Catalase activity was measured as outlined by Lafuente et al. (2004). The reaction mixture, comprised of enzyme extract (100 µl), 50 mM of sodium phosphate buffer (pH 7.0), and 130 mM of H_2O_2, was incubated at 37°C for 1 min. Furthermore, ammonium molybdate (32. 4 mM) was added to the mixture and shaken for 1 min. The absorbance fluctuation of 0. 01 units per minute was considered as one catalase activity unit (U mg^{-1} protein).

Sensory evaluation

The changes in the appearance, staste, aroma, and sweetness of papaya fruits during the storage period were evaluated by using a 9-point hedonic scoring scale (Lawless and Heymann, 2010). Papaya fruits were peeled off, sliced, and presented to the trained panel on randomly arranged white plates for the scoring. The hedonic score points varied from 1 = dislike extremely and 5 = neither like/nor dislike to 9 = like extremely. However, to indicate the acceptability of the fruit, a score of ≥ 6 "I like it slightly" was considered.

Statistics

The experiment was conducted according to a completely randomized block design with the factorial arrangement. The data were subjected to the analysis of variance (ANOVA) procedure by using Statistix 8.1 (USA) statistical software, and significant differences among treatment means were calculated using the least significance difference test ($P \leq 0.05$).

Results

Effect of EMT treatment on decay incidence and weight loss rate

In the present study, the decay incidence gradually increased across the two treatments in papaya fruits during storage. However, a higher decay incidence was recorded in the control than in EMT-treated papaya fruits ($P < 0.05$). Moreover, EMT treatment substantially reduced fruit decay, and the incidence was 66% lower than that of untreated fruits on 28 days of cold storage (Figure 1A). Irrespective of the treatments, there was an increased weight loss in papaya fruits during postharvest storage (Figure 1B). However, the EMT-treated fruits exhibited significantly reduced weight loss (49% less) compared with the control on 28 days of storage.

Effect of EMT treatment on soluble solids content, titratable acidity, ripening index, and ascorbic acid content

The SSC content increased regardless of treatments throughout the storage duration (Figure 2A). However, the EMT-treated papaya fruits showed a substantially ($P < 0.05$) limited increase with respect to the control fruits throughout the storage. The EMT-treated fruits had 20% lower SSC content than the control group on 28 days of storage. Overall, melatonin treatment inhibited SSC accumulation in papaya fruits (Figure 2A). Moreover, EMT treatment significantly decelerated the decrease in TA during the whole storage period ($P < 0.05$). The EMT-treated papaya fruits exhibited significantly higher (96% higher) TA values than the control group on 28 days of storage (Figure 2B).

Following EMT application, the ripening index was significantly ($P < 0.05$) reduced in treated papaya fruits during the storage duration (Figure 2C). The EMT-treated fruits showed a lower (14% to 48%) ripening index from 7 to 28 days of storage as compared with the untreated fruits, respectively. AsA content exhibited a decreasing trend regardless of the applied treatments (Figure 2D). However, EMT treatment maintained a considerably ($P < 0.05$) higher

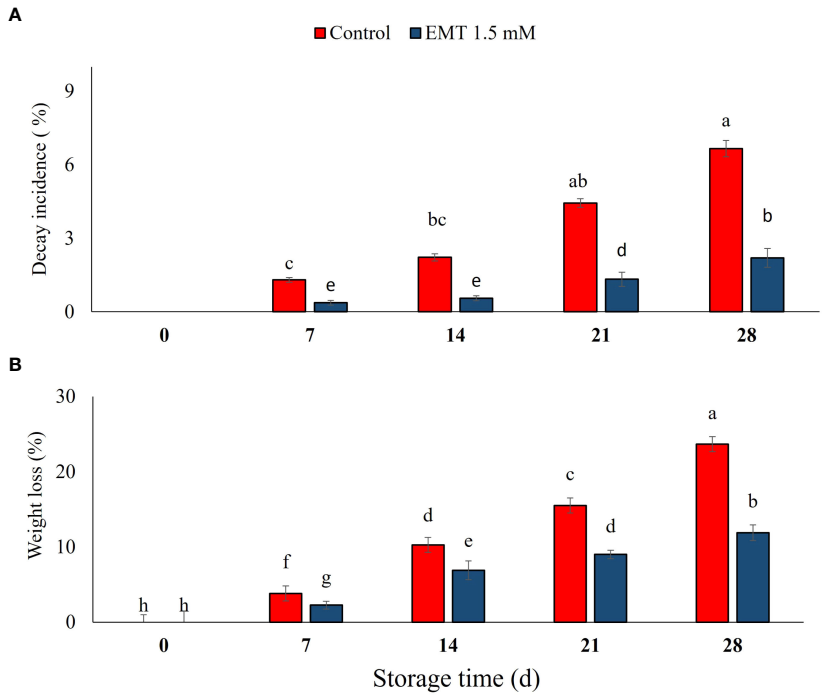

FIGURE 1
Effect of exogenous melatonin (EMT) treatment on fruit decay **(A)** and weight loss **(B)** of papaya fruits during cold storage. Data collected from the mean of three replicates, and vertical bars indicate the standard error of the means. Mean values with different letters show significant differences, and those with similar letters show no statistical difference according to the least significant difference test ($P < 0.05$).

(14% to 43%) concentration of ascorbic acid than the control group between 7 and 28 days of storage.

Effect of EMT treatment on total sugar, reducing sugar, and non-reducing sugar

Total sugar, reducing sugar, and non-reducing sugar contents changed gradually in papaya fruits throughout the storage period ($P < 0.05$; Figures 3A–C). All the three kinds of sugar content were increased in the control during the storage, while the EMT-treated fruits were not changed so obviously except for 7 and 28 days as compared with the 0 days. The EMT-treated fruits had considerably less total sugar (38%), reducing sugar (19%), and non-reducing sugar (59%) as compared with the control fruits on 28 days of storage (Figures 3A–C).

Effect of EMT treatment on malondialdehyde and hydrogen peroxide content

In this study, MDA content increased significantly during the storage, while the EMT treatment significantly inhibited the accumulation of MDA compared with the control from 14 to 28 days ($P < 0.05$; Figure 4A). In addition, the EMT-treated papaya fruits showed 18% lower MDA content with respect to the untreated fruits on 28 days of cold storage. As shown in Figure 4B, the H_2O_2 contents were increased in both EMT-treated papaya and control fruits throughout the cold storage period. However, the EMT-treated papaya fruits delayed the increase of H_2O_2 contents and exhibited 30% lower H_2O_2 contents than the control group on 28 days of storage ($P < 0.05$; Figure 4B).

Effect of EMT application on total phenolic content and DPPH-RSA

Total phenolic contents (TPCs) were moderately enhanced from 7 to 28 days in both EMT-treated and untreated fruits ($P < 0.05$). However, the EMT-treated papaya fruits displayed 15% higher TPC than the untreated fruits on 28 days of storage (Figure 5A). DPPH-RSA activity in the stored papaya fruits was significantly ($P < 0.05$) increased up to 21 days and then decreased up to 28 days of storage. However, DPPH-RSA activity was significantly higher in the EMT-treated fruits and peaked on 21 days of storage (33% higher) as compared with that

10.3389/fpls.2022.1039373

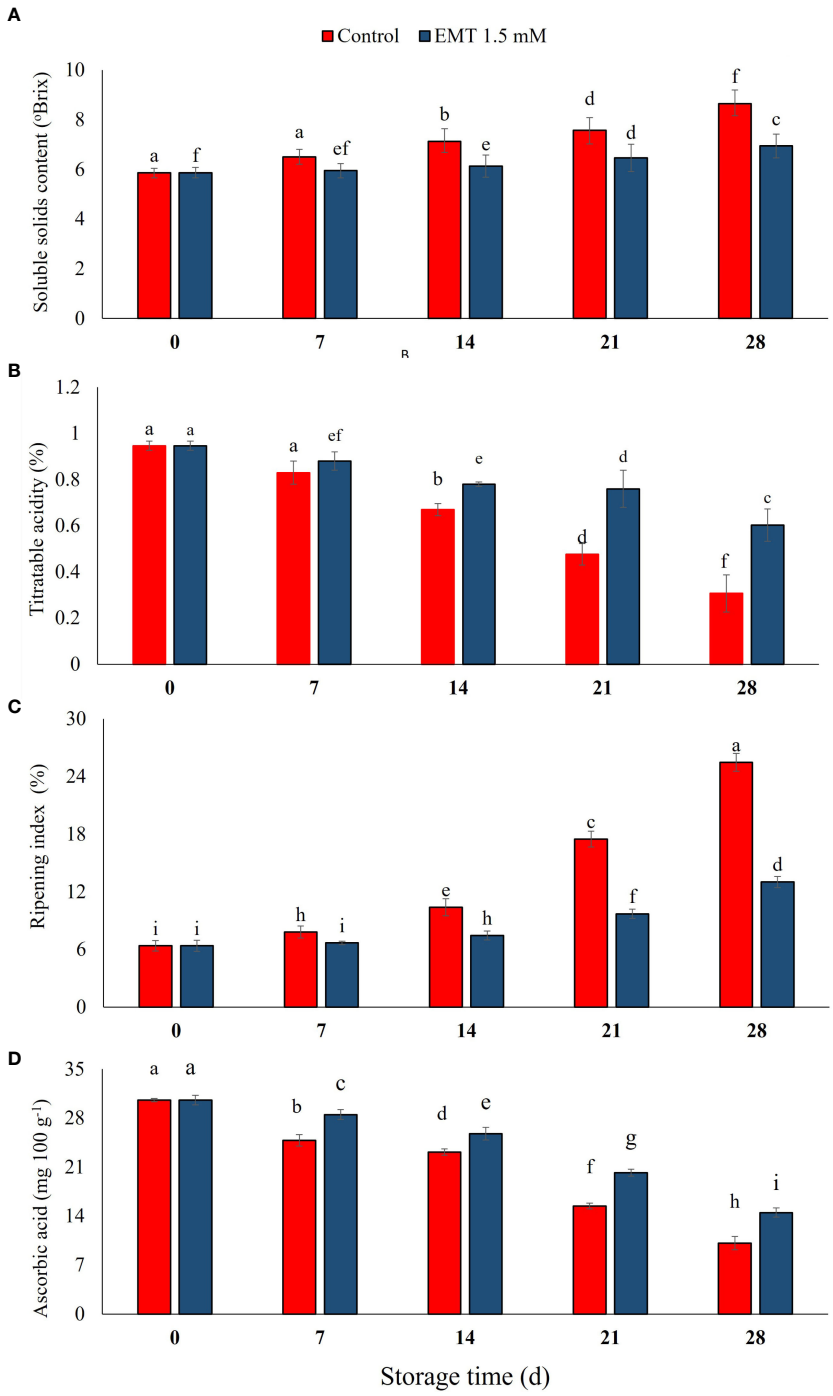

FIGURE 2
Effect of EMT treatment on soluble solids content **(A)**, titratable acidity **(B)**, ripening index **(C)**, and ascorbic acid **(D)** of papaya fruits during cold storage. Data collected from the mean of three replicates, and vertical bars indicate the standard error of the means. Mean values with different letters show significant differences, and those with the same letters show no statistical difference according to the least significant difference test ($P < 0.05$).

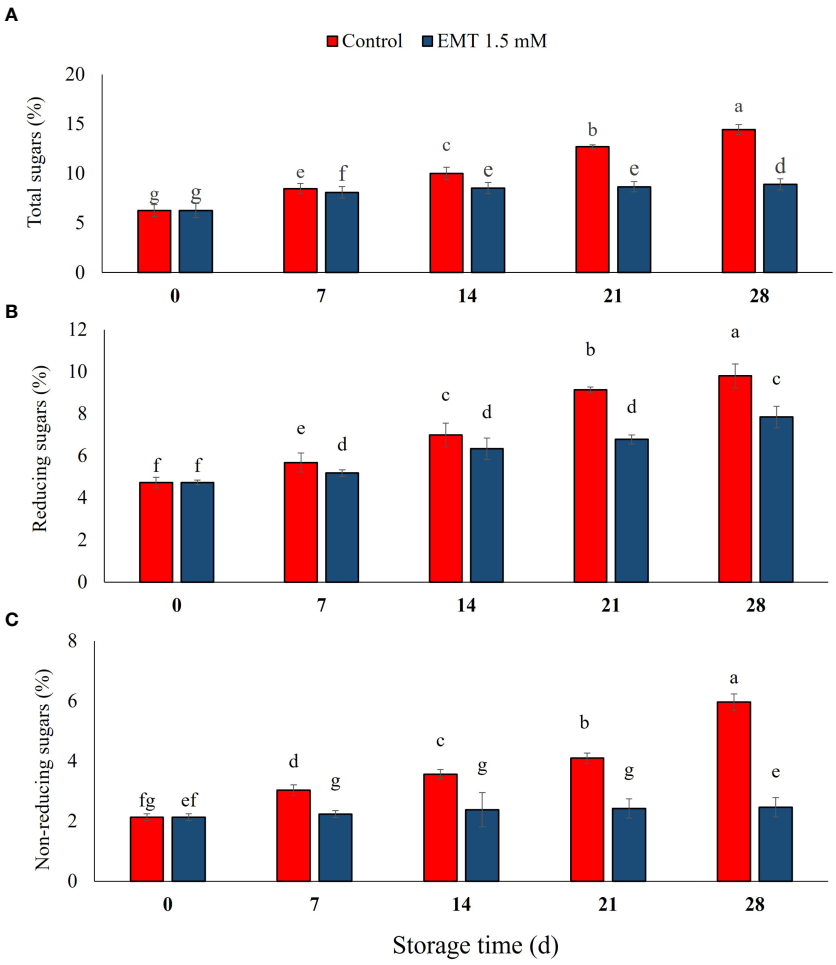

FIGURE 3
Effect of EMT treatment on total sugar **(A)**, reducing sugar **(B)**, and non-reducing sugar **(C)** of papaya fruits during cold storage. Data collected from the mean of three replicates, and vertical bars indicate the standard error of the means. Mean values with different letters show significant differences, and those with the same letters show no statistical difference according to the least significant difference test ($P < 0.05$).

of the untreated fruits (Figure 5B). DPPH-RSA in the EMT-treated papaya fruits remained 27% higher than in the untreated fruits on 28 days of storage.

Effect of EMT treatment on antioxidant enzymes

The activity of SOD substantially ($P < 0.05$) increased in the EMT-treated papaya fruits compared with the control group during the storage period (Figure 6A). EMT treatment enhanced SOD activity by almost 14% compared with the control papaya fruits on 28 days of storage. Peroxidase activity gradually increased in both EMT-treated and control fruits during the entire storage duration (Figure 6B). However, the EMT-treated fruits showed significantly higher (25%) levels of POD activity than the untreated fruits on 28 days of storage ($P < 0.05$). CAT activity significantly increased during the storage except for the interval between 7 and 14 days in the EMT-treated fruits, while the activity only increased slightly from 0 to 14 days in the control (Figure 6C). The EMT treatment significantly induced CAT activity from 14 to 28 days of storage and promoted CAT activity by 12% as compared with the control on 28 days of storage ($P < 0.05$; Figure 6C).

Effect of EMT treatment on sensory attributes

The EMT-treated fruits had significantly improved sensory attributes such as taste, sweetness, aroma, and overall acceptability as compared with the untreated papaya fruits on

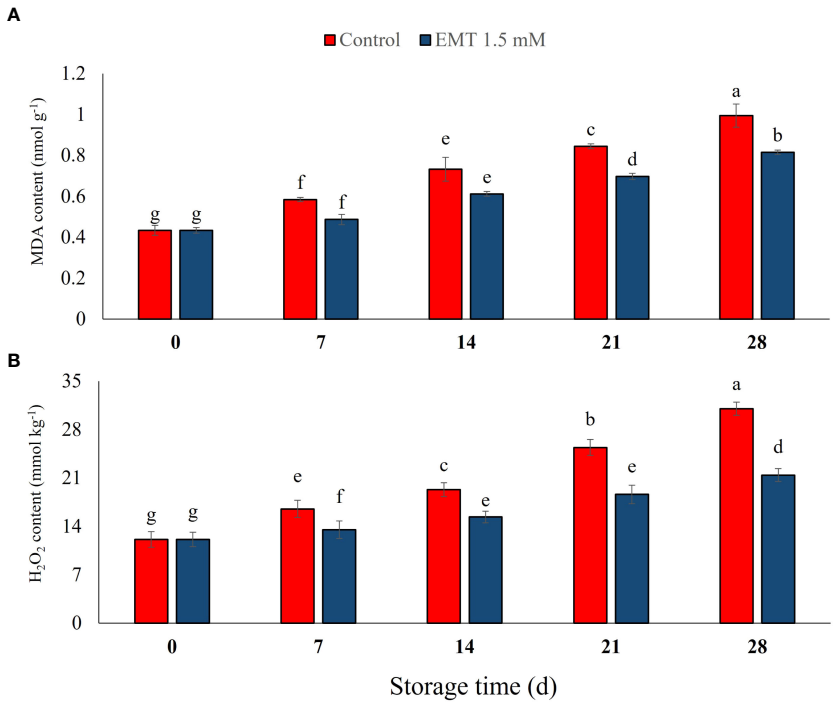

FIGURE 4
Effect of EMT treatment on MDA **(A)** and H_2O_2 content **(B)** of papaya fruits during cold storage. Data collected from the mean of three replicates, and vertical bars indicate the standard error of the means. Mean values with different letters show significant differences, and those with the same letters show no statistical difference according to the least significant difference test ($P < 0.05$).

28 days of storage (Figures 7A–F). While most of the sensory attributes gradually decreased in both EMT-treated and control papaya fruits, the EMT-treated papaya fruits maintained higher taste (38%), sweetness (28%), aroma (49%), and overall acceptability (36%) than the untreated fruits at the end of the storage period ($P < 0.05$; Figures 7C–F).

Correlation analysis

The correlation analysis of different parameters showed that decay incidence was positively correlated with weight loss, soluble solids contents, ripening index, total sugar, reducing sugar, non-reducing sugar, MDA, H_2O_2, SOD, POD, and CAT ($P < 0.05$; Figure 8). Moreover, decay incidence was significantly negatively correlated with titratable acidity, ascorbic acid, taste, sweetness, aroma, and overall acceptability ($P < 0.05$; Figure 8). Our results suggest that EMT treatment substantially reduced decay incidence and weight loss rate and maintained the higher antioxidant enzyme activities (SOD, POD, CAT) by inhibiting the rate of MDA and H_2O_2 contents. This indicated that EMT treatment maintained the sensory quality and prolonged the shelf life of papaya during cold storage.

Discussion

Mostly, postharvest decay incidence and weight loss occur because of increased respiration rate and fungal pathogen infection in papaya fruits. Different fungicides have been used to manage and control fruit decay; however, consumers are increasingly concerned about the use of synthetic chemicals because of their negative effects (Hanif et al., 2020a). Consequently, melatonin, a ubiquitous molecule, has shown great potential for extending the postharvest life of fresh produces (Nawaz et al., 2016; Aghdam et al., 2019; Tiwari et al., 2020; Bose and Howlader, 2020). Fruit decay during storage is one of the major problems for the fresh food industry, which results in high losses and inferior fruit quality, hampering the fruits' marketability. Higher respiration and ethylene production rapidly increase weight loss in fruits and vegetables during storage. Likewise, Ong et al. (2013b) reported a significant increase in weight loss during the postharvest ripening of papaya. In the present study, EMT treatment significantly decreased the senescence and weight loss rate in comparison to the control during the whole storage period. Similar findings have been reported, where EMT-treated strawberry fruits exhibited substantially lower senescence and

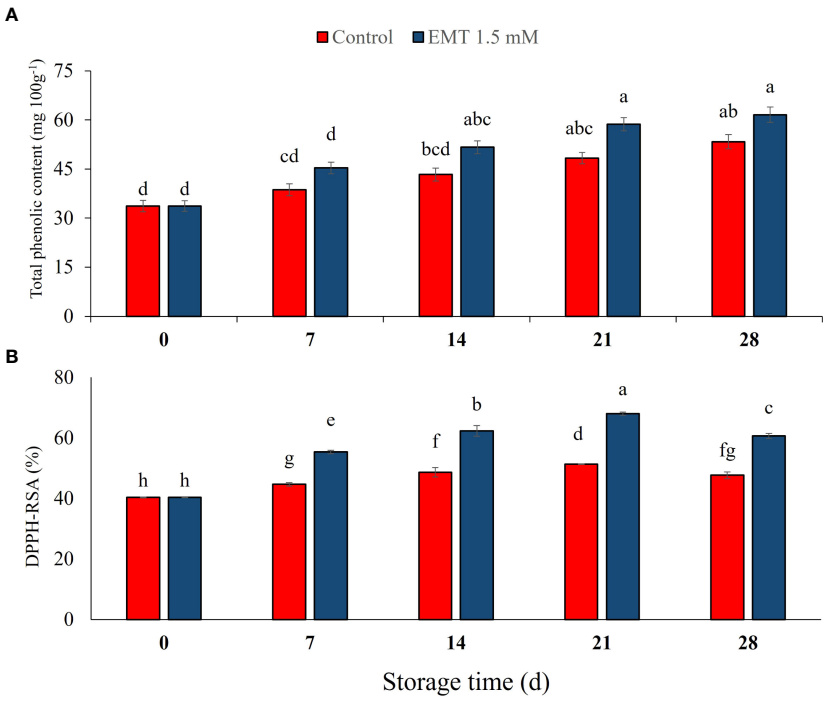

FIGURE 5
Effect of EMT treatment on total phenolic content **(A)** and DPPH-RSA activity **(B)** of papaya fruits during cold storage. Data collected from the mean of three replicates, and vertical bars indicate the standard error of the means. Mean values with different letters show significant differences, and those with the same letters show no statistical difference according to the least significant difference test ($P < 0.05$).

weight loss rates during cold storage (Liu et al., 2018). In papaya fruits (Hanif et al., 2020b) and cherries (Correia et al., 2017), weight loss increases during storage due to higher respiration and evaporation rate and fast utilization of stored metabolites for cellular metabolic activities. Likewise, Gao et al. (2016) reported that exogenous EMT treatment markedly reduced peach quality deterioration and weight loss during storage. Recently, studies have demonstrated that EMT treatment significantly reduced weight loss, delayed senescence, and improved the resistance against abiotic stress in sweet cherry fruits (Wang et al., 2019).

In this study, melatonin treatment effectively maintained higher titratable acidity and ascorbic acid content during storage, whereas it significantly reduced the change in SSC, ripening index, and sugar contents in stored papaya fruits. Our results agreed with the earlier studies of Liu et al. (2018) who noticed that EMT treatment at 0. 1 mM substantially reduced SSC and higher acidity which contributed to the delay in the senescence of strawberry fruits under cold storage conditions. Similarly, Gao et al. (2016) determined that EMT treatment significantly maintained the levels of ascorbic acid content in peach fruits as compared with the control. Likewise, ozone treatments effectively reduce the microbial population and maintained the quality traits of papaya fruit during storage (Kying and Ali, 2016). Bal (2019) reported that exogenous EMT (1 mM) treatment on plum fruits caused lower SSC and higher titratable acidity values which contributed to the slowing down of senescence in the treated fruits. The sugar–acid ratio is considered an important indicator of fruit flavor and consumer acceptance and appreciation (Gao et al., 2016). Meanwhile, a low ripening index indicated the suitability of treated fruits for a prolonged storage period. In our study, the EMT-treated fruits led to reduced ripening index values and a slow ripening process which resulted in an extended storage life of the papaya fruit. This is in agreement with previous studies on papaya and plum fruits (Bal, 2019; Hanif et al., 2020b).

Starch breakdown increases the accumulation of simple sugars during the ripening of fruits (Hanif et al., 2020b). In this study, total, reducing, and non-reducing sugars exhibited a higher accumulation trend in the control than in the EMT-treated fruits. A lower accumulation of sugars is an important indicator of delayed postharvest ripening and senescence due to the inhibition of amylase and phosphorylase enzyme activity (Hanif et al., 2020a). In addition, sugars influenced fruit flavor and consumers' acceptability for sweetness, and organic acids contributed to the increase of sugar levels as respiratory substrates (Hu et al., 2017).

Total antioxidants and TPC are important nutritional quality traits for stored fruits and vegetables. Our results showed that following EMT treatment, TPC content and DPPH scavenging

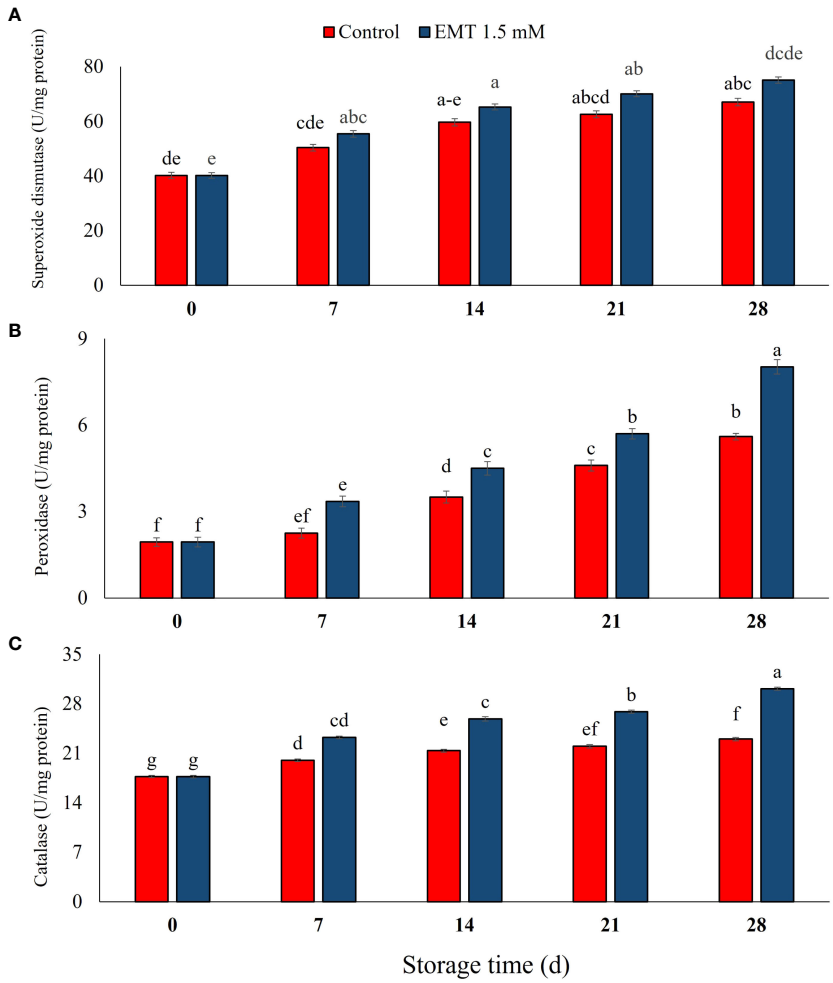

FIGURE 6
Effect of EMT treatment on superoxide dismutase (U mg^{-1} protein) **(A)**, peroxidase (U mg^{-1} protein) **(B)**, and catalase (U mg^{-1} protein) **(C)** of papaya fruits during cold storage. Data collected from the mean of three replicates, and vertical bars indicate the standard error of the means. Mean values with different letters show significant differences, and those with the same letters show no statistical difference according to the least significant difference test ($P < 0.05$).

activity gradually increased and remained high during the entire storage. Ghasemnezhad et al. (2010) reported that chitosan-coated peach fruits with higher TPC and DPPH scavenging activity showed higher anti-senescence properties than the control group during cold storage. The salicylic acid treatment increased the levels of TPC and DPPH scavenging activity in papaya fruits stored at 12°C for 28 days (Hanif et al., 2020b). The EMT treatment increased DPPH scavenging potential that ultimately stimulated non-enzymatic antioxidative defense levels. EMT application delayed senescence and led to a higher accumulation of TPC and flavonoid compounds that induced a higher antioxidant potential and inhibited the synthesis of H_2O_2 in stored strawberry (Liu et al., 2018), sweet cherry (Sharafi et al., 2021), and tomato fruits (Sharafi et al., 2019) under cold storage. Recently, various researchers have suggested that higher activities of phenylpropanoid pathway enzymes along with lower activities of polyphenoloxidase enzymes improve phytochemical accumulation and DPPH scavenging capacity in fresh produce (Gao et al., 2016; Aghdam et al., 2019).

Exogenous melatonin application plays an important role in enhancing the activity of ROS scavenging enzymes that combat various ROS, thereby maintaining the membrane's integrity within fruit tissues (Zhao et al., 2013; Zhang et al., 2018). Antioxidant enzymes (SOD, POD, CAT, APX) regulate lipid peroxidation and accumulation of ROS (Xu et al., 2019). Enhanced antioxidant enzyme activities may reduce the peroxidation of lipids which consequently delays senescence in peach fruits (Flores et al., 2008). In the present study, EMT application promoted the activity of antioxidant enzymes in stored papaya fruits. Similar results have been observed by Gao et al. (2016), who reported that

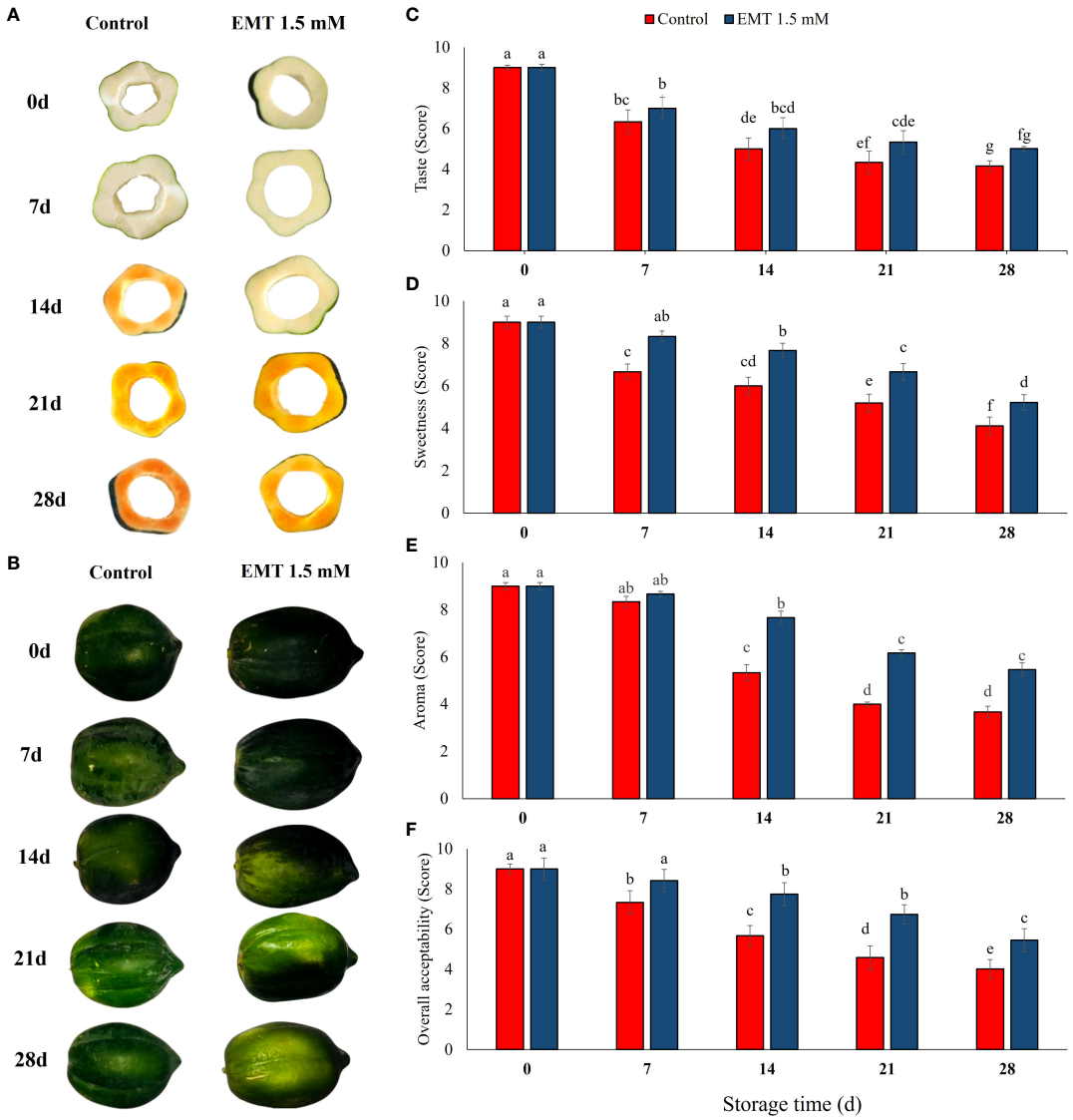

FIGURE 7
Effect of EMT treatment on visual quality **(A, B)**, taste **(C)**, sweetness **(D)**, aroma **(E)**, and overall acceptability **(F)** of papaya fruits during cold storage. Data collected from the mean of three replicates, and vertical bars indicate the standard error of the means. Mean values with different letters show significant differences, and those with the same letters show no statistical difference according to the least significant difference test ($P < 0.05$).

delayed fruit decay and higher antioxidant enzyme activities were related to the increased cell wall integrity and lower cell wall-degrading enzyme activities in EMT-treated peach fruits. Likewise, our findings are in line with previous studies whereby SOD, POD, and CAT activities increased in sweet cherries following EMT treatment (Wang et al., 2019). A similar result was also obtained by Arnao and Hernandez-Ruiz (2018), who reported that EMT treatment increased antioxidant enzyme activities and reduced the biosynthesis of ROS which inhibited ethylene biosynthesis and, consequently, halted the fruit ripening process. A similar observation has been reported in blueberry and pear (Zhai et al., 2018; Shang et al., 2021) and banana (Hu et al., 2017) fruits during storage. So, EMT treatment reduced oxidative stress which contributed to slowing down senescence and maintaining the fresh-like quality of papaya fruit for an extended storage duration.

The disintegration of cellular membranes is highly related to elevated electrolyte leakage and, consequently, rapid fruit senescence (Duan et al., 2011). Excessive accumulation of MDA levels is often related to the loss of cellular membrane integrity during fruit storage (Duan et al., 2011; Yang et al., 2014). The activities of antioxidant enzymes in plants are important in reducing the level of MDA, delaying senescence, and maintaining

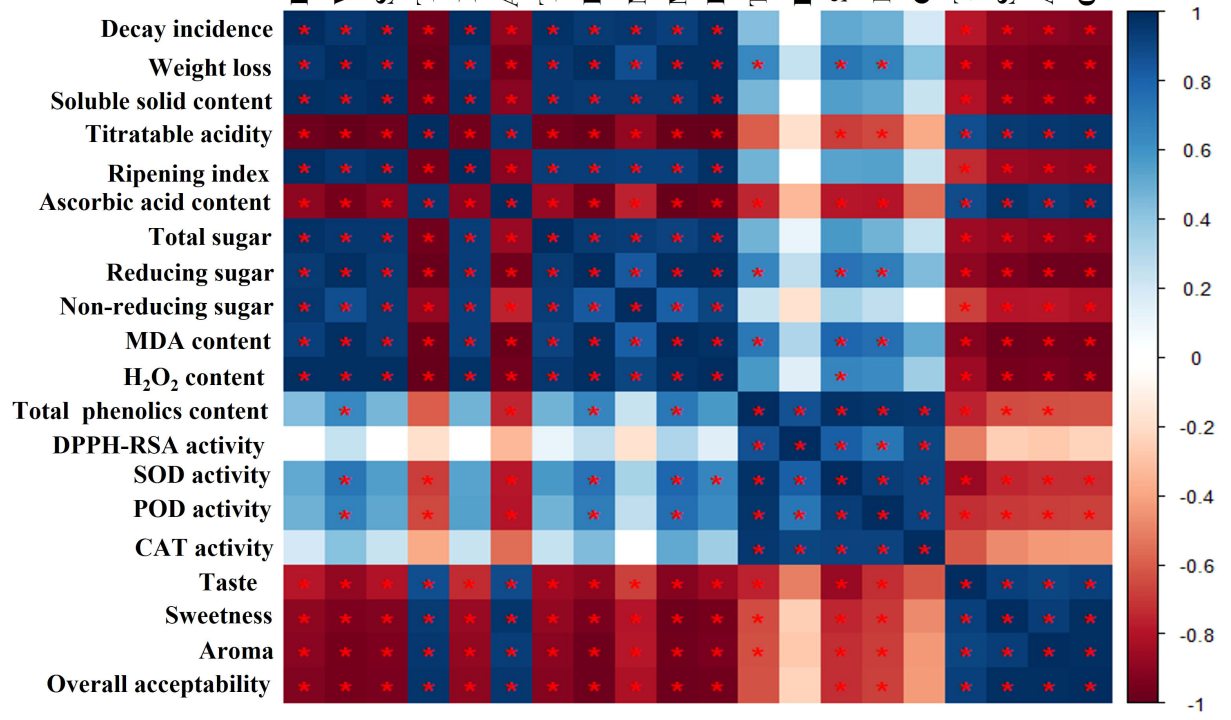

FIGURE 8
Correlation heat map analysis of each variable of EMT-treated papaya fruits during cold storage. The intensity of color represents the strength of the correlation: the blue color indicates a positive correlation, and the red color displays a negative correlation. The symbol * expresses significant correlations

cellular redox status (Jimenez et al., 2002). In the present study, EMT treatment reduced H_2O_2 and MDA levels as compared with the untreated papaya fruits. Melatonin was considered an antioxidant compound which improved the storage quality and life of cherry fruits by limiting oxidative stress (Yu et al., 2013). In the same context, Shang et al. (2021) reported that EMT treatment significantly decreased H_2O_2 and MDA biosynthesis, the main oxidative stress markers, which delayed senescence in blueberry fruits during storage. Recently, Xu et al. (2019) reported multifaceted mechanisms, following the EMT treatment of fruits and vegetables, such as ROS neutralization, an increase in antioxidant enzyme activities and non-enzymatic antioxidant levels, and protein repairs. It has been reported that the loss of subcellular compartmentalization following cellular breakdown resulted in higher utilization of phenolics as substrates and led to the reduction of postharvest storage quality of various horticultural produces (Yang et al., 2014; Wang et al., 2019). Similarly, Fu et al. (2017) reported that EMT treatment of *Elymus nutans* improved the antioxidant enzyme activities, suppressed the MDA content, and exhibited higher tolerance to cold stress.

Sensory attributes are important quality parameters for consumers' acceptance of fruits and vegetables (Radi et al., 2017). In our study, EMT application maintained higher sensory quality traits compared with the untreated papaya fruits. Generally, there is a loss of consumer acceptance for fresh produce following unsatisfactory sensory quality or a decline in phytochemical and nutritional quality, especially after storage. Liu et al. (2018) noticed lower SSC and higher titratable acidity which significantly delayed the postharvest senescence process and preserved the sensory attributes of EMT-treated strawberry fruits stored at 4°C. Similarly, Onik et al. (2021) noticed a better skin appearance of stored apples following EMT treatment. Our results are in

agreement with the studies on peaches (Cao et al., 2018), pears (Zhai et al., 2018), and banana fruits (Hu et al., 2017), which noticed that EMT treatments significantly delayed decay incidence and senescence, improved nutritional profiles, and conserved the sensory attributes. Recently, Wang et al. (2019) reported that EMT treatment may lead to a higher accumulation of endogenous melatonin and phenolic compounds, an improvement in overall nutritional quality, and a decline in H_2O_2 and MDA concentrations in sweet cherry fruits. The application of EMT enhanced the shelf life of fresh produces and was generally recognized as safe for human health (Zhai et al., 2018; Ze et al., 2021). Therefore, EMT treatment might be an efficient tool for boosting ROS scavenging abilities and improving the quality attributes of papaya fruits during cold storage.

Conclusion

In this study, the comprehensive beneficial effects of EMT treatment on papaya fruit quality were evaluated, including the assessment of the main physicochemical traits, bioactive compound content, antioxidant activity, and ROS scavenging enzyme activities during cold storage. EMT application effectively delayed postharvest senescence, reduced weight loss, and maintained higher TA, lower SSC, and ripening index compared with the control. Furthermore, EMT application stimulated the accumulation of phenolic content and higher DPPH-scavenging abilities in papaya fruits. In addition, EMT treatment markedly suppressed the levels of ROS and MDA by enhancing the antioxidant enzyme activities in papaya fruits during cold storage. Therefore, EMT application is a promising method for delaying senescence, maintaining quality attributes, and extending the postharvest life of papaya during cold storage.

Data availability statement

The original contributions presented in the study are included in the article/supplementary material. Further inquiries can be directed to the corresponding authors.

Author contributions

DW, MSR, MA, KW: Data curation, Formal analysis, Investigation, Methodology, Writing–original draft. MA, SE, HL: Conceptualization, Funding acquisition, Methodology, Supervision, Writing – review and editing. RI, SE, RQ, MAU: Formal analysis, Investigation, Methodology, Writing – original draft. MIK, RQ, MAK: Methodology, Writing – review and editing. All authors contributed to the article and approved the submitted version.

Funding

This study was partially funded from the project number TT-119/17 by Endowment Fund Secretariat, University Agriculture, Faisalabad, Pakistan, and partially funded by Shanghai Agricultural Products Preservation and Processing Engineering Technology Research Center (19DZ2251600), and Shanghai Professional Service Platform for Agriculture Products Preservation and Processing (21 DZ2292200).

Conflict of interest

The authors declare that the research was conducted in the absence of any commercial or financial relationships that could be construed as a potential conflict of interest.

Publisher's note

All claims expressed in this article are solely those of the authors and do not necessarily represent those of their affiliated organizations, or those of the publisher, the editors and the reviewers. Any product that may be evaluated in this article, or claim that may be made by its manufacturer, is not guaranteed or endorsed by the publisher.

References

Aghdam, M. S., and Fard, J. R. (2017). Melatonin treatment attenuates postharvest decay and maintains nutritional quality of strawberry fruits (Fragaria× anannasa cv. selva) by enhancing GABA shunt activity. *Food Chem.* 221, 1650–1657. doi: 10.1016/j.foodchem.2016.10.123

Aghdam, M. S., Luo, Z., Jannatizadeh, A., Sheikh-Assadi, M., Sharafi, Y., Farmani, B., et al. (2019). Employing exogenous melatonin applying confers chilling tolerance in tomato fruits by upregulating giving rise to promoting endogenous polyamines, proline, and nitric oxide accumulation by triggering arginine pathway activity. *Food Chem.* 275, 549–556. doi: 10.1016/j.foodchem.2018.09.157

Albertini, S., Reyes, A. E. L., Trigo, J. M., Sarriés, G. A., and Spoto, M. H. F. (2016). Effects of chemical treatments on fresh-cut papaya. *Food Chem.* 190, 1182–1189. doi: 10.1016/j.foodchem.2015.06.038

Ali, A., Yeoh, W. K., Forney, C., and Siddiqui, M. W. (2018). Advances in postharvest technologies to extend the storage life of minimally processed fruits and vegetables. *Crit. Rev. Food Sci. Nutr.* 58 (15), 2632–2649. doi: 10.1007/s11694-019-00088-6

Arnao, M. B., and Hernandez-Ruiz, J. (2018). Melatonin and its relationship to plant hormones. *Ann. Bot.* 121 (2), 195–207. doi: 10.1093/aob/mcx114

Bal, E. (2019). Physicochemical changes in 'Santa rosa'plum fruit treated with melatonin during cold storage. *J. Food Meas. Charact* 13 (3), 1713–1720.

Bose, S. K., and Howlader, P. (2020). Melatonin plays multifunctional role in horticultural crops against environmental stresses: A review. *Environ. Exp. Bot.* 176, 104063. doi: 10.1016/j.envexpbot.2020.104063

Brand-Williams, W., Cuvelier, M. E., and Berset, C. (1995). Use of a free radical method to evaluate antioxidant activity. *LWT - Food Sci. Technol.* 28, 25–30. doi: 10.1016/S0023-6438(95)80008-5

Cao, S., Shao, J., Shi, L., Xu, L., Shen, Z., Chen, W., et al. (2018). Melatonin increases chilling tolerance in postharvest peach fruit by alleviating oxidative damage. *Sci. Rep.* 8 (1), 1–11. doi: 10.1038/s41598-018-19363-5

Cia, P., Pascholati, S. F., Benato, E. A., Camili, E. C., and Santos, C. A. (2007). Effects of gamma and UV-c irradiation on the postharvest control of papaya anthracnose. *Postharvest Biol. Technol.* 43 (3), 366–373. doi: 10.1016/j.postharvbio.2006.10.004

Correia, S., Schouten, R., Silva, A. P., and Gonçalves, B. (2017). Factors affecting quality and health promoting compounds during growth and postharvest life of sweet cherry (*Prunus avium* l.). *Front. Plant Sci.* 8. doi: 10.3389/fpls.2017.02166

de Vasconcellos Santos Batista, D., Reis, R. C., Almeida, J. M., Rezende, B., Bragança, C. A. D., and da Silva, F. (2020). Edible coatings in post-harvest papaya: impact on physical–chemical and sensory characteristics. *Food Sci. Technol.* 57 (1), pp.274–pp.281. doi: 10.1007/s13197-019-04057-1

Dos Passos, B. S., Magnani, M., Madruga, M. S., de Souza Galvão, M., de Medeiros, L. L., Batista, A. U. D., et al. (2020). Characterization of edible coatings formulated with chitosan and mentha essential oils and their use to preserve papaya (*Carica papaya* l.). *Innov. Food Sci. Emerg. Technol.* 65, 102472. doi: 10.1016/j.ifset.2020.102472

Dotto, G. L., Vieira, M. L., and Pinto, L. A. (2015). Use of chitosan solutions for the microbiological shelf-life extension of papaya fruits during storage at room temperature. *Food Sci. Technol.* 64 (1), 126–130. doi: 10.1016/j.lwt.2015.05.042

Duan, X., Liu, T., Zhang, D., Su, X., Lin, H., and Jiang, Y. (2011). Effect of pure oxygen atmosphere on antioxidant enzyme and antioxidant activity of harvested litchi fruit during storage. *Int. Food Res. J.* 44, 1905–1911. doi: 10.1016/j.foodres.2010.10.027

Escamilla-García, M., Rodríguez-Hernández, M. J., Hernández-Hernández, H. M., Delgado-Sánchez, L. F., García-Almendárez, B. E., Amaro-Reyes, A., et al. (2018). Effect of an edible coating based on chitosan and oxidized starch on shelf life of *Carica papaya* l., and its physicochemical and antimicrobial properties. *Coatings* 8 (9), 318. doi: 10.3390/coatings8090318

Fan, Y., Li, C., Li, Y., Huang, R., Guo, M., Liu, J., et al. (2022). Postharvest melatonin dipping maintains quality of apples by mediating sucrose metabolism. *Plant Physiol. Biochem.* 174, 43–50. doi: 10.1016/j.plaphy.2022.01.034

Ferguson, I. B., Watkins, C. B., and Harman, J. E. (1983). Inhibition by calcium of senescence of detached cucumber cotyledons: effect on ethylene and hydroperoxide production. *Plant Physiol.* 71 (1), 182–186. doi: 10.1104/pp.71.1.182

Flores, F. B., Sánchez-Bel, P., Valdenegro, M., Romojaro, F., Martínez-Madrid, M. C., and Egea, M. I. (2008). Effects of a pretreatment with nitric oxide on peach (*Prunus persica* l.) storage at room temperature. *Eur. Food Res. Technol.* 227 (6), 1599–1611. doi: 10.1007/s00217-008-0884-0

Fu, J., Wu, Y., Miao, Y., Xu, Y., Zhao, E., Wang, J., et al. (2017). Improved cold tolerance in elymus nutans by exogenous application of melatonin may involve ABA-dependent and ABA-independent pathways. *Sci. Rep.* 7 (1), 1–11. doi: 10.1038/srep39865

Gajanana, T. M., Sudha, M., Saxena, A. K., and Dakshinamoorthy, V. (2010). Post-harvest handling, marketing and assessment of losses in papaya. *In II Int. Symposium Papaya* 851, 519–526. doi: 10.17660/ActaHortic.2010.851.79

Galano, A., Tan, D. X., and Reiter, R. J. (2011). Melatonin as a natural ally against oxidative stress: a physicochemical examination. *J. Pineal Res.* 51 (1), 1–16. doi: 10.1111/j.1600-079X.2011.00916.x

Gao, H., Zhang, Z. K., Chai, H. K., Cheng, N., Yang, Y., Wang, D. N., et al. (2016). Melatonin treatment delays postharvest senescence and regulates reactive oxygen species metabolism in peach fruit. *Postharvest Bio. Technol.* 118, 103–110. doi: 10.1016/j.postharvbio.2016.03.006

Ghasemnezhad, M., Shiri, M. A., and Sanavi, M. (2010). Effect of chitosan coatings on some quality indices of apricot (*Prunus armeniaca* l.) during cold storage. *J. Environ. Sci.* 8 (1), 25–33.

Hamzah, H. M., Osman, A., Tan, C. P., and Ghazali, F. M. (2013). Carrageenan as an alternative coating for papaya (*Carica papaya* l. cv. eksotika). *Postharvest Biol. Technol.* 75, 142–146. doi: 10.1016/j.postharvbio.2012.08.012

Hanif, A., Ahmad, S., Jaskani, M. J., and Ahmad, R. (2020a). Papaya treatment with putrescine maintained the overall quality and promoted the antioxidative enzyme activities of the stored fruit. *Sci. Hortic.* 268, 109367. doi: 10.1016/j.scienta.2020.109367

Hanif, A., Ahmad, S., Shahzad, S., Liaquat, M., and Anwar, R. (2020b). Postharvest application of salicylic acid reduced decay and enhanced storage life of papaya fruit during cold storage. *J. Food Meas. Charact.* 14 (6), 3078–3088. doi: 10.1007/s11694-020-00555-5

Hodges, D. M., DeLong, J. M., Forney, C. F., and Prange, R. K. (1999). Improving the thiobarbituric acid-reactive-substances assay for estimating lipid peroxidation in plant tissues containing anthocyanin and other interfering compounds. *Planta* 207 (4), 604–611 doi: 10.1007/s00425-017-2699-3.

Hortwitz, W. (1960). *Official and tentative methods of analysis* (Washington, DC: Association of Official Agricultural Chemists), 314–320.

Huang, T. Y., and Vanyo, M. (2020). Trends in the airglow temperatures in the MLT region part 1: Model simulations. *Atmosphere* 11 (5), 468. doi: 10.3390/atmos11050468

Hu, W., Yang, H., Tie, W., Yan, Y., Ding, Z., Liu, Y., et al. (2017). Natural variation in banana varieties highlights the role of melatonin in postharvest ripening and quality. *J. Agric. Food Chem.* 65 (46), 9987–9994. doi: 10.1021/acs.jafc.7b03354

Jimenez, A., Creissen, G., Kular, B., Firmin, J., Robinson, S., Verhoeyen, M., et al. (2002). Changes in oxidative processes and components of the antioxidant system during tomato fruit ripening. *Planta* 214 (5), 751–758. doi: 10.1007/s004250100667

Kying, O. M., and Ali, A. (2016). Effect of ozone exposure on microbial flora and quality attributes of papaya (*Carica papaya* l) fruit. *J. Agr. Agric. Aspec.* 104, 1–7 ISSN: 2574-2914.

Lafuente, M. T., Sala, J. M., and Zacarias, L. (2004). Active oxygen detoxifying enzymes and phenylalanine ammonia-lyase in the ethylene-induced chilling tolerance in citrus fruit. *J. Agric. Food Chem.* 52 (11), 3606–3611. doi: 10.1021/jf035185i

Lawless, H. T., and Heymann, H. (2010). *Sensory evaluation of food: principles and practices* Vol. Vol. 2 (New York: Springer), ISBN: .

Li, R. Q., Mao, Z. Q., Rong, L., Wu, N., Lei, Q., Zhu, J. Y., et al. (2017). A two-photon fluorescent probe for exogenous and endogenous superoxide anion imaging *in vitro* and *in vivo*. *Biosens. Bioelectron* 87, 73–80. doi: 10.1016/j.bios.2016.08.008

Liu, K., Yuan, C., Chen, Y., Li, H., and Liu, J. (2014). Combined effects of ascorbic acid and chitosan on the quality maintenance and shelf life of plums. *Sci. Hortic.* 176, 45–53. doi: 10.1016/j.scienta.2014.06.027

Liu, C., Zheng, H., Sheng, K., Liu, W., and Zheng, L. (2018). Effects of melatonin treatment on the postharvest quality of strawberry fruit. *Postharvest Biol. Technol.* 139, 47–55. doi: 10.1016/j.postharvbio.2018.01.016

Maqbool, M., Ali, A., Alderson, P. G., and Zahid, N. (2011). "Exploring the new applications of gum arabic obtained from acacia species to preserve fresh fruits and vegetables," in *II international symposium on underutilized plant species: Crops for the future-beyond food security*, ISHS vol. 979, 127–130. doi: 10.17660/ActaHortic.2013.979.10

Ma, Q., Zhang, T., Zhang, P., and Wang, Z. Y. (2016). Melatonin attenuates postharvest physiological deterioration of cassava storage roots. *J. Pineal Res.* 60, 424–434. doi: 10.1111/jpi.12325

Nawaz, M. A., Huang, Y., Bie, Z., Ahmed, W., Reiter, R. J., Niu, M., et al. (2016). Melatonin: current status and future perspectives in plant science. *Front. Plant Sci.* 6. doi: 10.3389/fpls.2015.01230

Nunes, M. C. N., Emond, J. P., and Brecht, J. K. (2006). Brief deviations from set point temperatures during normal airport handling operations negatively affect the quality of papaya (*Carica papaya*) fruit. *Postharvest Biol. Technol.* 41 (3), 328–340. doi: 10.1016/j.postharvbio.2006.04.013

Oloyede, O. I. (2005). Chemical profile of unripe pulp of *Carica papaya*. pak. J. *Nutr.* 4 (6), 379–381. doi: 10.3923/pjn.2005.379.381

Ong, M. K., Forney, C. F., Alderson, P. G., and Ali, A. (2013b). Postharvest profile of a solo variety 'Frangi'during ripening at ambient temperature. *Sci. Hortic.* 160, 12–19. doi: 10.1016/j.scienta.2013.05.026

Ong, M. K., Kazi, F. K., Forney, C. F., and Ali, A. (2013a). Effect of gaseous ozone on papaya anthracnose. *Food Bioproc. Tech.* 6 (11), 2996–3005. doi: 10.1007/s11947-012-1013-4

Onik, J. C., Wai, S. C., Li, A., Lin, Q., Sun, Q., Wang, Z., et al. (2021). Melatonin treatment reduces ethylene production and maintains fruit quality in apple during postharvest storage. *Food Chem.* 337, 127753. doi: 10.1016/j.foodchem.2020.127753

Radi, M., Firouzi, E., Akhavan, H., and Amiri, S. (2017). Effect of gelatin-based edible coatings incorporated with aloe vera and black and green tea extracts on the shelf life of fresh-cut oranges. *J. Food Qual.* 2017. doi: 10.1155/2017/9764650

Razzaq, K., Khan, A. S., Malik, A. U., and Shahid, M. (2013). Ripening period influences fruit softening and antioxidative system of 'Samar bahisht chaunsa'mango. *Sci. Hortic.* 160, 108–114. doi: 10.1016/j.scienta.2013.05.018

Reiter, R. J., Tan, D. X., Zhou, Z., Cruz, M. H. C., Fuentes-Broto, L., and Galano, A. (2015). Phytomelatonin: assisting plants to survive and thrive. *Molecules* 20 (4), 7396–7437. doi: 10.3390/molecules20047396

Ruck, J. A. (1961). *Chemical methods for analysis of fruits and vegetables no. 1154* (Research Station Summerland, Research Branch Canada, Department of Agriculture, Canada).

Shang, F., Liu, R., Wu, W., Han, Y., Fang, X., Chen, H., et al. (2021). Effects of melatonin on the components, quality and antioxidant activities of blueberry fruits. *LWT-Food Sci. Technol.* 147, 111582. doi: 10.1016/j.lwt.2021.111582

Sharafi, Y., Aghdam, M. S., Luo, Z., Jannatizadeh, A., Razavi, F., Fard, J. R., et al. (2019). Melatonin treatment promotes endogenous melatonin accumulation and triggers GABA shunt pathway activity in tomato fruits during cold storage. *Sci. Hortic.* 254, 222–227. doi: 10.1016/j.scienta.2019.04.056

Sharafi, Y., Jannatizadeh, A., Fard, J. R., and Aghdam, M. S. (2021). Melatonin treatment delays senescence and improves antioxidant potential of sweet cherry fruits during cold storage. *Sci. Hortic.* 288, 110304. doi: 10.1016/j.scienta.2021.110304

Stajner, D., and Popovic, B. (2009). Comparative study of antioxidant capacity in organs of different allium species. *Cent. Eur. J. Biol.* 4 (2), 224–228. doi: 10.2478/s11535-009-0010-8

Sun, Q., Zhang, N., Wang, J., Zhang, H., Li, D., Shi, J., et al. (2015). Melatonin promotes ripening and improves quality of tomato fruit during postharvest life. *J. Exp. Bot.* 66 (3), 657–668. doi: 10.1093/jxb/eru332

Tiwari, R. K., Lal, M. K., Naga, K. C., Kumar, R., Chourasia, K. N., Subhash, S., et al. (2020). Emerging roles of melatonin in mitigating abiotic and biotic stresses of horticultural crops. *Sci. Hortic.* 272, 109592. doi: 10.1016/j.scienta.2020.109592

Vilaplana, R., Chicaiza, G., Vaca, C., and Valencia-Chamorro, S. (2020). Combination of hot water treatment and chitosan coating to control anthracnose in papaya (*Carica papaya* l.) during the postharvest period. *J. Crop Prod.* 128, 105007. doi: 10.1016/j.cropro.2019.105007

Wang, X., Liu, S., Liu, C., Liu, Y., Lu, X., Du, G., et al. (2020). Biochemical characterization and expression analysis of lignification in two pear (*Pyrus ussuriensis* maxim.) varieties with contrasting stone cell content. *Protoplast* 257 (1), 261–274. doi: 10.1007/s00709-019-01434-7

Wang, Z., Pu, H., Shan, S., Zhang, P., Li, J., Song, H., et al. (2021). Melatonin enhanced chilling tolerance and alleviated peel browning of banana fruit under low temperature storage. *Postharvest Biol. Technol.* 179, 111571. doi: 10.1016/j.postharvbio.2021.111571

Wang, F., Zhang, X., Yang, Q., and Zhao, Q. (2019). Exogenous melatonin delays postharvest fruit senescence and maintains the quality of sweet cherries. *Food Chem.* 301, 125311. doi: 10.1016/j.foodchem.2019.125311

Wu, C., Cao, S., Xie, K., Chi, Z., Wang, J., Wang, H., et al. (2021). Melatonin delays yellowing of broccoli during storage by regulating chlorophyll catabolism and maintaining chloroplast ultrastructure. *Postharvest Biol. Technol.* 172, 111378. doi: 10.1016/j.postharvbio.2020.111378

Wu, Q., Li, Z., Chen, X., Yun, Z., Li, T., and Jiang, Y. (2019). Comparative metabolites profiling of harvested papaya (*Carica papaya* l.) peel in response to chilling stress. *J. Sci. Food Agric.* 99 (15), 6868–6881. doi: 10.1002/jsfa.9972

Xu, T., Chen, Y., and Kang, H. (2019). Melatonin is a potential target for improving post-harvest preservation of fruits and vegetables. *Front. Plant Sci.* 10. doi: 10.3389/fpls.2019.01388

Yang, X., Sun, G. Y., Eckert, G. P., and Lee, J. C. (2014). Cellular membrane fluidity in amyloid precursor protein processing. *Mol. Neurobiol.* 50 (1), 119–129. doi: 10.1007/s12035-014-8652-6

Yan, Y., Shi, Q., and Gong, B. (2020). Review of melatonin in horticultural crops: In melatonin-the hormone of darkness and its therapeutic potential and perspectives. Marilena Vlachou, ed. London: IntechOpen. 2020, 1–23 doi: 10.5772/intechopen.90935

Yu, H., Nie, E., Xu, J., Yan, S., Cooper, W. J., and Song, W. (2013). Degradation of diclofenac by advanced oxidation and reduction processes: kinetic studies, degradation pathways and toxicity assessments. *Water Res.* 47 (5), 1909–1918. doi: 10.1016/j.watres.2013.01.016

Ze, Y., Gao, H., Li, T., Yang, B., and Jiang, Y. (2021). Insights into the roles of melatonin in maintaining quality and extending shelf life of postharvest fruits. *Trends Food Sci. Technol.* 109, 569–578. doi: 10.1016/j.tifs.2021.01.051

Zerpa-Catanho, D., Esquivel, P., Mora-Newcomer, E., Sáenz, M. V., Herrera, R., and Jiménez, V. M. (2017). Transcription analysis of softening-related genes during postharvest of papaya fruit (*Carica papaya* L.'Pococí'hybrid). *Postharvest Biol. Technol.* 125, 42–51. doi: 10.1016/j.postharvbio.2016.11.002

Zhai, R., Liu, J., Liu, F., Zhao, Y., Liu, L., Fang, C., et al. (2018). Melatonin limited ethylene production, softening and reduced physiology disorder in pear (*Pyrus communis* l.) fruit during senescence. *Postharvest Biol. Technol.* 139, 38–46. doi: 10.1016/j.postharvbio.2018.01.017

Zhang, Y., Huber, D. J., Hu, M., Jiang, G., Gao, Z., Xu, X., et al. (2018). Delay of postharvest browning in litchi fruit by melatonin *via* the enhancing of antioxidative processes and oxidation repair. *J. Agric. Food Chem.* 66 (28), 7475–7484. doi: 10.1021/acs.jafc.8b01922

Zhao, M., Moy, J., and Paull, R. E. (1996). Effect of gamma-irradiation on ripening papaya pectin. *Postharvest Biol. Technol.* 8 (3), 209–222. doi: 10.1016/0925-5214(96)00004-X

Zhao, Y., Tan, D. X., Lei, Q., Chen, H., Wang, L., Li, Q. T., et al. (2013). Melatonin and its potential biological functions in the fruits of sweet cherry. *J. Pineal Res.* 55 (1), 79–88. doi: 10.1111/jpi.12044

frontiers | Frontiers in Plant Science

TYPE Original Research
PUBLISHED 06 January 2023
DOI 10.3389/fpls.2022.1067680

OPEN ACCESS

EDITED BY
Qiong Lin,
Chinese Academy of Agricultural Sciences (CAAS), China

REVIEWED BY
Ke Wang,
Anhui Agricultural University, China
Natasha Damiana Spadafora,
University of Calabria, Italy

*CORRESPONDENCE
Xiang Li
xiangli1@ufl.edu

SPECIALTY SECTION
This article was submitted to Crop and Product Physiology, a section of the journal Frontiers in Plant Science

RECEIVED 12 October 2022
ACCEPTED 01 December 2022
PUBLISHED 06 January 2023

CITATION
Zhang H, Zhu X, Xu R, Yuan Y, Abugu MN, Yan C, Tieman D and Li X (2023) Postharvest chilling diminishes melon flavor *via* effects on volatile acetate ester biosynthesis. *Front. Plant Sci.* 13:1067680. doi: 10.3389/fpls.2022.1067680

Postharvest chilling diminishes melon flavor *via* effects on volatile acetate ester biosynthesis

Huijun Zhang[1], Xiuxiu Zhu[1], Runzhe Xu[1], Yushu Yuan[1], Modesta N. Abugu[2], Congsheng Yan[3], Denise Tieman[4] and Xiang Li[4]*

[1]School of Life Science, Huaibei Normal University, Huaibei, Anhui, China, [2]Horticultural Sciences, North Carolina State University, Raleigh, NC, United States, [3]Horticultural Institute, Anhui Academy of Agricultural Sciences, Hefei, China, [4]Horticultural Sciences, Genetics Institute, University of Florida, Gainesville, FL, United States

In postharvest handling systems, refrigeration can extend fruit shelf life and delay decay *via* slowing ripening progress; however, it selectively alters the biosynthesis of flavor-associated volatile organic compounds (VOCs), which results in reduced flavor quality. Volatile esters are major contributors to melon fruit flavor. The more esters, the more consumers enjoy the melon fruit. However, the effects of chilling on melon flavor and volatiles associated with consumer liking are yet to be fully understood. In the present study, consumer sensory evaluation showed that chilling changed the perception of melon fruit. Total ester content was lower after chilling, particularly volatile acetate esters (VAEs). Transcriptomic analysis revealed that transcript abundance of multiple flavor-associated genes in fatty acid and amino acid pathways was reduced after chilling. Additionally, expression levels of the transcription factors (TFs), such as *NOR*, *MYB*, and *AP2*/*ERF*, also were substantially downregulated, which likely altered the transcript levels of ester-associated pathway genes during cold storage. VAE content and expression of some key genes recover after transfer to room temperature. Therefore, chilling-induced changes of VAE profiles were consistent with expression patterns of some pathway genes that encode specific fatty acid- and amino acid-mobilizing enzymes as well as TFs involved in fruit ripening, metabolic regulation, and hormone signaling.

KEYWORDS

melon, chilling, fruit flavor, volatile acetate esters, transcriptome, alcohol acyltransferase

Introduction

Melon is one of the most important and popular horticultural crops worldwide because of its excellent flavor and rich nutrition (Pereira et al., 2018; Yano et al., 2020; Zhang et al., 2021). The unique flavor of melon fruit (*Cucumis melo* L.) is a sum of interactions among soluble sugars, acids, and various volatile organic compounds (VOCs). VOCs are critical contributors to fruit quality and consumer preference (Schwab et al., 2008). In climacteric melon, approximately 240 VOCs have been identified, including aldehydes, alcohols, terpenes, esters, and sulfur-containing aroma compounds (Beaulieu and Grimm, 2001; Fallik et al., 2001; El-Sharkawy et al., 2005; Kourkoutas et al., 2006; Obando-Ulloa et al., 2008; Gonda et al., 2016; Esteras et al., 2018). High levels of sulfur-containing compounds may cause undesirable aromas in melon fruit (Gonda et al., 2013). Volatile esters, generally described as fruity or floral-like, are the most abundant VOCs and make a positive contribution to melon flavor and consumer liking (Gonda et al., 2016; Esteras et al., 2018). In contrast, non-climacteric melons show a lack of esters (Aubert and Pitrat, 2006; Sangster et al., 2006; Obando–Ulloa et al., 2008).

The flavor-related VOCs are mostly derived from amino acid, fatty acid, and carotenoid precursors (Schwab et al., 2008; Klee and Tieman, 2018). Most of the VOCs in climacteric melon are esters derived from fatty acids and amino acids (Gonda et al., 2016). Multiple flavor-impacting genes have been identified in melon. In the fatty acid pathway, lipoxygenases (LOXs) are classified into two groups, including 9-LOX and 13-LOX, generating 9(*S*)- and 13(*S*)-hydroperoxides of linoleic and linolenic acid. Hydroperoxide lyases (HPLs) can catalyze 13 (*S*)-hydroperoxides to generate corresponding C6 aldehydes (2017; Chen et al., 2004; Shen et al., 2014; Zhang et al., 2015; Zhang et al., 2017). Additionally, pyruvate decarboxylases (PDCs) are prominent enzymes and associate with the decarboxylation of keto-acids generating acetaldehyde, propanal, pentanal from their corresponding carboxylic acids (Wang et al., 2019). In the amino acid pathway, branched-chain amino transferases (BCATs) and aromatic amino transferases (ArATs) are involved in the initial step in the formation of amino acid-derived aldehydes (Gonda et al., 2010). Alcohol dehydrogenases (ADHs) can catalyze the reduction of aldehydes to generate alcohols (Speirs et al., 1998; Chen et al., 2016). Esters are the most important VOCs that contribute to melon flavor, and they are mainly derived from fatty acids and amino acids (Gonda et al., 2016). The most abundant esters include acetate, butyrate, hexanoate and benzoate esters of fatty acids and amino acids, with acyl-coenzyme A (2 carbons), butyryl-CoA (4 carbons), hexanoyl-CoA (6 carbons) and benzoyl-CoA (7 carbons) as the co-substrate, respectively. In the final step, alcohol acyltransferases (AATs) can catalyze the esterification of an acyl moiety from an acyl-CoA donor onto alcohol, to form the corresponding esters (Goulet et al., 2015; Peng et al., 2020). In addition to formation of esters, degradation is also an important step to balance ester levels in fruit. In tomato, carboxylesterases (CXEs) catalyze the removal of the ester group to release the corresponding alcohol (Goulet et al., 2012; Cao et al., 2019).

In addition to the biosynthetic enzymes directly involved in production of volatile esters, transcription factors (TFs) also play key roles in the biosynthesis of flavor-associated VOCs in fruit crops. *Colorless nonripening* (*CNR*) and *nonripening* (*NOR*) genes are important fruit development and ripening regulators in plants. In tomato, levels of the fatty acid-derived VOCs in the ripening *cnr* and *nor* mutants are substantially lower than those in the wild-type (Zhang et al., 2016; Gao et al., 2022). Hormones also play important roles in fruit VOC biosynthesis *via* impacting the expressions of VOC-associated genes (Jin et al., 2016). An ethylene-responsive AP2/ERF family member, CitERF71 was associated with volatile terpene synthesis by activating transcription of a terpene synthase gene (*CitTPS16*) in sweet orange (Li et al., 2017). An ERF#9-MYB98 complex is involved in furaneol production *via* transactivation of quinone oxidoreductase *FaQR* (Zhang et al., 2018). For flavor-associated esters, MYB and bZIP have been shown to interact with the promoters of ester-related AATs in apple and banana, respectively (Li et al., 2014; Guo et al., 2018). Additionally, recent research revealed a peach NAC transcription factor homologous to tomato NOR (*PpNAC1*), positively regulates ester biosynthesis *via* activation of *PpAAT1* (Cao et al., 2019). In melon, a ripening regulator, CmNOR involved in ethylene production also activates the production of esters (Santo Domingo et al., 2022).

Deterioration in fruit flavor quality has become a major cause of consumer dissatisfaction (Whiteside. 1977; Bruhn et al., 1991; Fernqvist and Hunter., 2012; Klee and Tieman, 2018; Colantonio et al., 2022). For example, modern commercial tomato varieties are generally substantially less flavorful than heirloom varieties. Human selection plays an important role in fruit flavor quality (Tieman et al., 2017; Klee and Tieman, 2018; Li et al., 2020). Fruit of wild melons have very thin light green flesh, are not sweet, are sometimes bitter and without aroma. In contrast, domesticated melon cultivars have larger fruit, non-bitter and thicker flesh, with considerably improved flavor (Pitrat, 2013). In terms of cultivated melons, postharvest handling and the retail system seem to be major contributors to poor fruit flavor. For example, heat treatment changes the aroma profiles of melons, causing a reduced “fresh” aroma as well as increased unpleasant “sulfurous” and “fermented” aroma (Yu et al., 2021). Additionally, total volatiles in melon juice are reduced significantly after 10°C storage for 20 d (Sun et al., 2022). In tomato, chilling results in loss of fruit flavor through impacting various flavor-associated VOCs (Zhang et al., 2016). Different fruit have different suites of VOCs, which contribute to their unique flavor. Thus, understanding how postharvest

handling affects the flavor of different fruits is an important step to restore and maintain superior fruit flavor.

The aim of the present work is to study the effect of cold storage on melon fruit flavor quality and VOCs associated with human preference and to understand molecular mechanisms responsible for flavor loss in the chilled climacteric background of melon. Here, comprehensive metabolomic and transcriptomic analyses were performed in melon fruit. Altered flavor-associated VAEs in response to chilling and following a recovery period were associated with expression changes of some key pathway genes and multiple TFs, particularly ripening-related TFs.

Materials and methods

Melon materials

Melon 'HT' (Huai Tian No. 1, a climacteric cultivar of oriental melon, *Cucumis melon* var. *Makuwa* Makino) fruit were grown in a greenhouse on the Huaibei Normal University campus in Huaibei, China. Fruits were harvested at the ripe stage (30 days after pollination). Fruits of uniform size and without mechanical damage were selected, washed and dried at room temperature.

Fruit treatment

Fruit treatment was performed as described by Zhang et al. (2016). Briefly, melon fruits were divided into three groups: (A) stored at 4°C for 7 d (without chilling injury), and then transferred to room temperature (~22°C) for 1 d; (B) held at 4°C for 8 d until use (without chilling injury); (C) harvested on day 8 (8 d after the fruits of first two groups). Three replicates of each group were performed, and each replicate has three fruits.

Consumer preference test and analysis

A triangle test was performed according to the method described previously (Radovich et al., 2004). The test consisted of 58 untrained panelists, including twenty-eight males and thirty females, aged 20-45 years. Panelists were not trained but received instructions regarding the evaluation procedure. Panelists were presented with three samples of chilled (Group B) or unchilled (Group C) fruit, two were identical, and one was different. The samples were assigned blinding codes and randomized before testing. Panelists were instructed to identify the odd sample among the three by tasting all in the order presented. Panelists were provided with bottled water and sugar-free biscuits for palate cleansing, which they used between samples. Finally, they were asked to comment on the flavor and taste variation observed. The critical number of correct and incorrect responses for significance analysis was determined as described by Civille and Carr (2015). A binomial test was used to test for significance based on the correct number of accessors (Lawless and Heymann, 2010). The number of correct responses greater or equal to 27 of 60 panelists was considered a significant difference. Ambiguous responses were removed from the data. A plot of the frequency of the flavor descriptors for the chilled and unchilled fruit were obtained using the ggplot2 package in R (Wickham, 2016).

Volatile analysis by gas chromatograpghy-ion mobility spectrometry

GC-IMS is a powerful technique for the separation and sensitive detection of VOCs and is widely used to analyze VOC changes during food storage (Wang et al., 2020). To investigate the volatile changes of HT1 melon cultivar during cold storage, the analysis of volatile fingerprints was performed on an HS-GC-IMS system (FlavourSpec® Gesellschaft für Analytische Sensorsysteme mbH, Dortmund, Germany) as described by Yu et al. (2021). Three pooled fruit (three replicates for each group) were homogenized in a blender. For each replicate of melon sample, 10 g of melon juice was combined with 3 ml 200 mM ethylenediaminetetraacetic acid (EDTA) and 3 ml 20% $CaCl_2$ (m/v) in a 20 ml headspace vial, the samples were stored at -80°C and mixed well before use. The GC system is equipped with an automatic headspace sampler unit (CTC Analytics AG, Switzerland), which can collect samples from the headspace vials with a heated air-tight syringe (1 ml). Next, the prepared 'HT1' samples in a 20 ml headspace vial were incubated at 40°C for 20 min with an agitation speed of 450 rpm, and 500 µl of headspace was injected into the GC injector at 80°C using a heated gas-tight syringe (45°C) with an injection speed of 30 ml min^{-1} and the GC program was as follow: 2 ml min^{-1} for 2 min, ramped up to 100 ml min^{-1} over 18 min, and held for 10 min. The separation was carried out on both a nonpolar FS-SE-54-CB capillary column (15 m × 0.53 mm × 0.25 µm, CS-Chromatographie Service GmbH, Durem, Germany) and a polar DB-Wax column (15 m × 0.53 mm × 0.25 µm, Agilent, Santa Clara, CA, USA) at isothermal condition of 60°C. Nitrogen was the gas at a flow rate of 150 ml min^{-1}. The drift tube is 5 cm in length, and it was operated at a constant voltage of 400 V cm^{-1} at 45°C with a 150 ml min^{-1} N_2 flow. Each IMS spectrum is an average of 12 scans. Each GC-IMS analysis was run in triplicate. To eliminate cross-contamination, the syringe was purged by an N_2 flow for 30 s before every analysis and another 5 min after every analysis. n-ketones C_3-C_9 (Sinopharm Chemical Reagent Beijing Co., Ltd., China) were employed as external references to calculate the retention index (RI) of each compound. All volatile compounds were identified by comparing RI and normalized

drift time (RIP relative) with the authentic reference compounds in the GC-IMS library. Analysis was performed on three replicates of each group.

cDNA preparation, quantitative PCR, and sequencing

Total RNA from different treatments was extracted using TRIzol reagent (Life Technologies) and first-strand cDNAs were synthesized using the ReverTra Ace quantitative real-time PCR (qRT-PCR) Kit (Toyobo, Osaka, Japan) according to the manufacturer's instructions. qRT-PCR was performed using the SuperReal PreMix Plus Kit (Tiangen, Beijing, China) in CFX Connect real-time PCR detection system (Bio-Rad, Hercules, CA, USA) according to the manufacturers' instructions. Actin was used as the internal control (Primers used are listed in Supplementary Table S13). Total RNA samples were submitted for Next-Generation Sequencing (NGS) using Illumina NovaSeq (Shanghai Personal Biotechnology Co., Ltd, China). Briefly, the paired-end (PE) method was applied for RNA sequencing and the read length was 150 base pairs. The mapped reads for each sample ranged from 37,300,202 to 46,422,461 and the transcriptome coverage varied from 94.72% to 95.15%.

RNA-Seq data analysis

The procedure of analysis was performed as described by (Guo et al., 2021). Briefly, the adapter sequence and low-quality value (QV < 20) from the raw reads in FastQ format were removed using Cutadapt (Version 1.1) software (Kim et al., 2015). The pruned clean reads were aligned to the melon reference genomic sequence Melon (DHL92) v3.5.1 Genome database (http://cucurbitgenomics.org/organism/18) using HISAT2 software (v. 2.1.0). HTSeq (v. 0.1.1) was used to calculate the read count as the original gene expression. The transcript abundance was indicated by normalized Fragments Per Kilo bases per Million fragments (FPKM), and genes with an average value higher than 1 were considered as expressed genes, while the genes expressed at very low levels were removed. Pearson correlation coefficient was estimated to examine the correlation of gene expression levels among samples. Based on principal component analysis (PCA) in "DESeq" package in R software, samples in each treatment group were clustered according to relative expression. Absolute log2 fold change (FC) > 1 and adjusted p-value < 0.05 were differentially expressed genes (DEGs) in each treatment. Expression levels of DEGs in each group were visualized as a heat map using "Pheatmap" package. The DEGs in each treatment group were further submitted for functional enrichment analysis of gene ontology (GO) and transcription factor (TF). For GO enrichment analyses performed in "TopGO" package, DEGs were divided into GO molecular function (MF), biological process (BP), and cellular component (CC). The TF information and relative family classification were predicted according to Plant Transcription Factor Database (PlantTFDB).

Metabolite extraction and analysis

Metabolite profiling was performed using a non-targeted metabolome method by Personal Biotechnology Co. Ltd. (Shanghai, China). The materials used for the transcriptomic analysis were the same as those in metabolite profiling. Extraction and analysis of metabolites were performed as previously described (Sangster et al., 2006; De Vos et al., 2007). 200 mg (± 1%) of melon fruit was accurately weighed in an EP tube, and then 0.6 ml 2-chlorophenylalanine (4 ppm) methanol (-20°C) was added, followed by vortexing, grinding, and centrifugation. Finally, 20 µl from each sample was taken to the quality control (QC) samples (These QC samples were used to monitor deviations of the analytical results from these pool mixtures and compare them to the errors caused by the analytical instrument itself), and the samples were used for LC-MS detection.

Chromatographic separation was accomplished in a Vanquish system (Thermo, USA) equipped with an ACQUITY UPLC® HSS T3 (150 mm x 2.1 mm, Waters, USA) column maintained at 40°C. The temperature of the autosampler was 8°C. Gradient elution of analytes was carried out with 0.1% formic acid in water (A2) and 0.1% formic acid in acetonitrile (B2) or 5 mM ammonium formate in water (A3) and acetonitrile (B3) at a flow rate of 0.25 ml min^{-1}. Injection of 2 µl of each sample was done after equilibration. An increasing linear gradient of solvent B2/B3 (v/v) was used as follows: 0-1 min, 2% B2/B3; 1-9 min, 2%-50% B2/B3; 9-12 min, 50%-98% B2/B3; 12-13.5 min, 98% B2/B3; 13.5-14 min, 98%-2% B2/B3; 14-20 min, 2% B2-positive model (14-17 min, 2% B3-negative model). The ESI-MSn experiments were executed on the Thermo Q Exactive HF-X mass spectrometer with the spray voltage of 3.5 kV and -2.5 kV in positive and negative modes, respectively. Sheath gas and auxiliary gas were set at 30 and 10 arbitrary units, respectively. The capillary temperature was 325° C. The analyzer scanned over a mass range of m/z 81-1,000 for a full scan at a mass resolution of 60,000. Data dependent acquisition (DDA) MS/MS experiments were performed with HCD scan. The normalized collision energy was 30 eV. Dynamic exclusion was implemented to remove some unnecessary

information in MS/MS spectra.

Weighted gene co-expression network analysis

Co-expression networks were created using WGCNA (v1.29) package in R as described by (Langfelder and Horvath, 2008). The data used for WGCNA were performed on aroma components (alcohols, aldehydes, ketones, and esters) produced during storage. All genes and TFs were used as input to the signed WGCNA network construction. Modules were identified using "one-step network construction and module detection function" method with a soft thresholding power of 6 and a relatively large minimum module size of 30, and the threshold for merging modules was 0.25.

Promoter analysis

Promoter sequences (base pairs -1,500 to -1) were obtained from Melon (DHL92) v3.5.1 Genome (http://cucurbitgenomics.org/organism/3). Transcription binding motifs were analyzed with plantCARE (http://bioinformatics.psb.ugent.be/webtools/plantcare/html/) and PlantPAN 3.0 (http://plantpan.itps.ncku.edu.tw/promoter.php) (Lescot et al., 2002; Li et al., 2020).

Statistical analysis

Student *t*-test analysis was applied to compare the variation of volatile content and gene expression between Group A & B, B & C and A & C (Graphpad Prism 9). Letters and asterisks indicate significant differences (p-value < 0.05) for treatments at each measure time. PCA, DEGs, and GO enrich were described in each method section.

Accession numbers

All accession numbers were obtained from the Melon (DHL92) v3.5.1 Genome database. *CmLOX18* (MELO3C024348.2), *CmADH1/2* (MELO3C023685.2/MELO3C014897.2), *CmHPL1/2* (MELO3C010910.2/MELO3C018413.2), *CmAAT1/3* (MELO3C024771.2/MELO3C024762.2), *CmMGL* (MELO3C013774.2), *CmPDC1/2* (MELO3C009145.2/MELO3C007227.2), *CmCXE1/2* (MELO3C010887.2/MELO3C014690.2), *CmBCAT1* (MELO3C010776.2), *CmArAT1* (MELO3C025613.2), *CmAADC1* (MELO3C008357.2), *CmACO1* (MELO3C014437.2), *CmACS1* (MELO3C021182.2), *CmNOR* (MELO3C016540.2), *CmMYB44* (MELO3C007586.2), *CmbZIP1* (MELO3C013408.2), *CmCBF1* (MELO3C006869.2).

Results

Chilling resulted in changes of melon VOC profiles and consumer liking

To gain insight into how chilling affects flavor of melon fruit and consumer liking, we performed a triangle test to evaluate the flavor differences between chilled and unchilled fruit. Twenty-seven of fifty-eight panelists were able to identify significant differences in the flavor of the chilled compared to the unchilled (n > 26, p = 0.02 < 0.05) (Figure 1A). In addition, they described the unchilled melon as sweeter, juicier, and more aromatic than the chilled fruit, indicating that chilling had an adverse effect on flavor (Figure 1B).

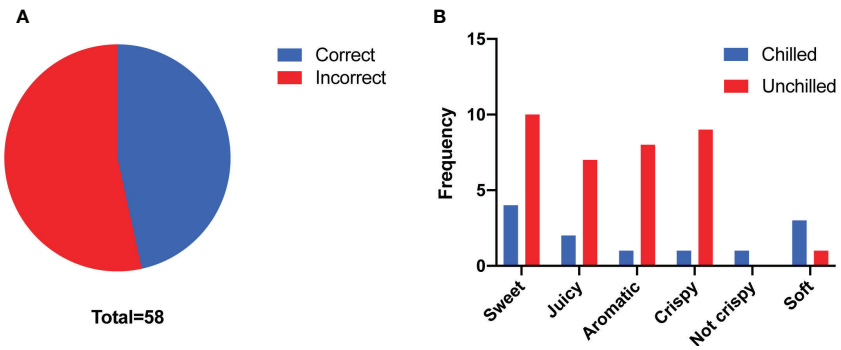

FIGURE 1
Consumer panel analyses. **(A)** Number of correct answers (n = 27) and incorrect answers (n = 31) from triangle test. **(B)** Taste descriptors for the chilled and unchilled melon fruit according to their frequency of use. Fewer panelists rated the chilled melon fruit as sweet, juicy and aromatic compared to the unchilled melon fruit.

Subsequently, VOCs extracted from melon fruit after 7 d chilling followed by 1-d recovery at room temperature (Group A), after 8 d chilling only (Group B), and harvested on day 8 (Group C) were quantified. Sixty known and nine unknown VOCs were detected in fruit from all three groups and used for further analysis (Supplementary Table S1). These VOCs consist of nine alcohols, twelve aldehydes, six ketones, twenty-four esters, and eighteen others (Figure 2A). Among the VOCs, esters are the most abundant (> 70% of total VOC content) in all groups, and ~70% of the esters are VAEs. Based on the VOC content, melon fruit from the three different groups were separated by PCA, and biological replicates clustered together (Supplementary Figure S1). 2D ion mobility spectrums of volatiles in fruit from these three groups were shown (Supplementary Figure S2). In general, the concentration of volatiles in 8-d chilled fruit (Group B) was lower in comparison with unchilled fruit (Group C). Total amount of volatiles in 8-d chilled fruit decreased by ~73% relative to the unchilled. After 1-d recovery at room temperature (Group A), total VOC content increased, but was still lower compared to the unchilled (Figure 2B). In particular, content of VAEs was lower after chilling and recovery at room temperature for 1 d. However, total content of volatile alcohols or aldehydes was not substantially affected after cold storage compared to the unchilled (Figures 2B, C). Additionally, no significant differences were observed in fructose, glucose and citrate between the chilled and the unchilled fruit (Supplementary Figure S3).

A gallery plot was performed to better visualize major chilling-induced changes to VOC profiles. A total of eighty-two detected signal peaks were characterized (Figure 2D). Although total content of alcohols or aldehydes was not altered after cold storage compared to the unchilled fruit, content of several alcohols and aldehydes was lower, including 3-methylpentanol, nonanal and (*E*, *E*)-2,4-nonadienal. In addition, total ketone content was also reduced in 8-d chilled fruit. Among the ketones, content of 3-hepten-2-one and 2-propanone was lower. Total content of VAEs in the chilled fruit was ~30% lower compared to that in unchilled fruit and those recovered after transfer to the room temperature. Content of multiple VAEs was reduced after cold storage, including propyl acetate, isobutyl acetate, pentyl acetate, hexyl acetate, and benzyl acetate. Chilling-induced decreases were also observed for other esters, including isopentyl isopentanoate, butyl butanoate, isobutyl butanoate, and isopentyl hexanoate. Content of the aforementioned VAEs increased after 1-d recovery. However, some VOCs were found to increase after cold storage compared to the unchilled. Interestingly, these VOCs mainly included methyl esters, such as methyl butanoate, methyl hexanoate, methyl 3-methylbutanoate, and methyl 2-methylpropanoate (Supplementary Table S1). In addition, content of these

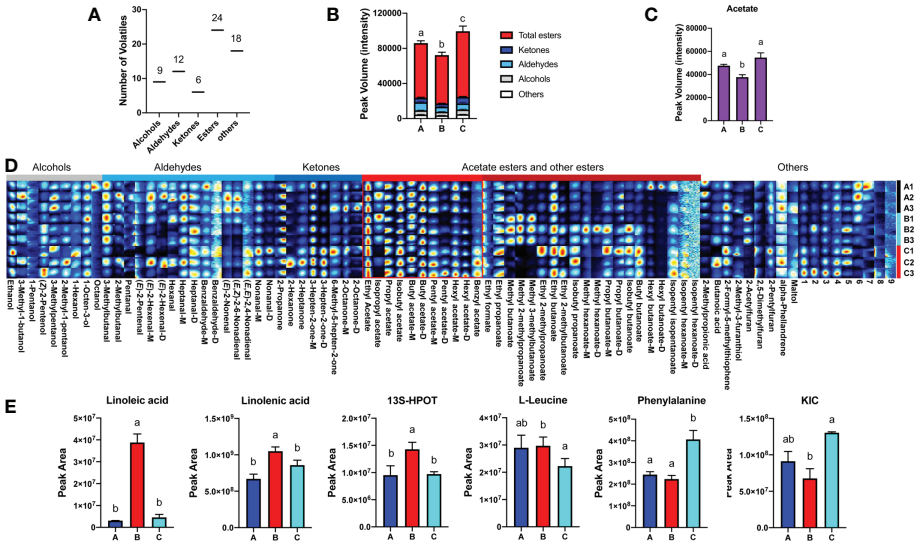

FIGURE 2
Changes of melon volatile content and metabolites in response to chilling. **(A)** Classification and numbers of all volatiles detected. **(B)** Statistical analysis of changes in VOC content after chilling (± SE, n = 3). **(C)** Chilling-induced changes in total VAE content (± SE, n = 3). **(D)** Fingerprint of all volatiles detected in three groups. Each row represents all signal peaks in each sample, and each column represents the signal peak of the same VOC in different samples. The intensity of the ion signal is described by different colors, red indicates high intensity. VOC names are listed below each column, and some volatiles are followed by M and D, which are the monomer and dimer of the same volatile. The numbers indicate unidentified VOC peaks. Information of all volatiles is listed in Supplementary Table S1. **(E)** Statistical analysis of metabolites in fatty acid and amino acid pathways after chilling (± SE, n = 6). Significant differences in volatiles and metabolites are denoted by different letters (p-value < 0.05). HPOT, Hydroperoxy octadecatrienoic acid; KIC, Ketoisocaprorate. Group A, stored at 4°C for 7 d, and then transferred to room temperature (~22°C) for 1 d; Group B, held at 4°C for 8 d; Group C, melon fruit were harvested 8 d after the fruit of first two groups.

methyl esters was reduced after return to room temperature. These results indicate that chilling affects the flavor of melon fruit, and chilling-induced changes to melon VOC profiles are mainly involved in flavor-associated esters, particularly VAEs.

Metabolomic analysis on the VAE-related pathways in response to chilling

The aforementioned VAEs are derived from fatty acid and amino acid pathways. In response to chilling, metabolic flux throughout these two pathways is critical for downstream VAE biosynthesis. Therefore, multiple intermediate metabolites were investigated, including linoleic acid, linolenic acid, 9(*S*)-hydroperoxy-10(*E*),12(*Z*),15(*Z*)-octadecatrienoic acid (9(*S*)-HPOT), and 13(*S*)-hydroperoxy-9(*Z*),11(*E*),15(*Z*)-octadecatrienoic acid (13(*S*)-HPOT) from the fatty acid pathway, in addition to isoleucine, L-leucine, valine, phenylalanine, 3-Methyl-2-oxovaleric acid and Ketoisocaprorate (KIC) from the amino acid pathway. According to the analysis of differentially accumulated metabolites, we found that content of linoleic acid, linolenic acid, and 13*S*-HPOT increased after chilling and was reduced after 1-d recovery at room temperature (Figure 2E; Supplementary Table S2). However, content of metabolites from the amino acid pathway showed inconsistent patterns in response to chilling. Content of L-leucine was higher in the chilled fruit than the unchilled and remained high after cold storage followed by 1-d recovery. Content of KIC, a ketoacid generated from L-leucine, was reduced after chilling and slightly increased after recovery. Phenylalanine content was lower after cold storage and remained at a low level after 1 d returning to room temperature (Figure 2E; Supplementary Table S2). These results suggested that chilling affects VAE biosynthesis *via* regulation of metabolic flux.

Transcriptomic response to cold storage

RNA-Seq data was generated for transcriptomic analysis. After discarding adaptor and low-quality reads, ~6.2 Gb clean reads (>90% of total reads) on average were produced (Supplementary Table S3). Principle components analysis (PCA) of RNA-Seq data revealed the relationship between experimental samples, which exhibited clear separation for the samples of the aforementioned three groups (Figure 3A). Pearson correlation coefficient analysis indicated that, in general, replicates after chilling followed by 1-d recovery at room temperature (Group A) and harvested on day 8 (Group C) were less correlated with the replicates after chilling (Group B) (Figure 3B).

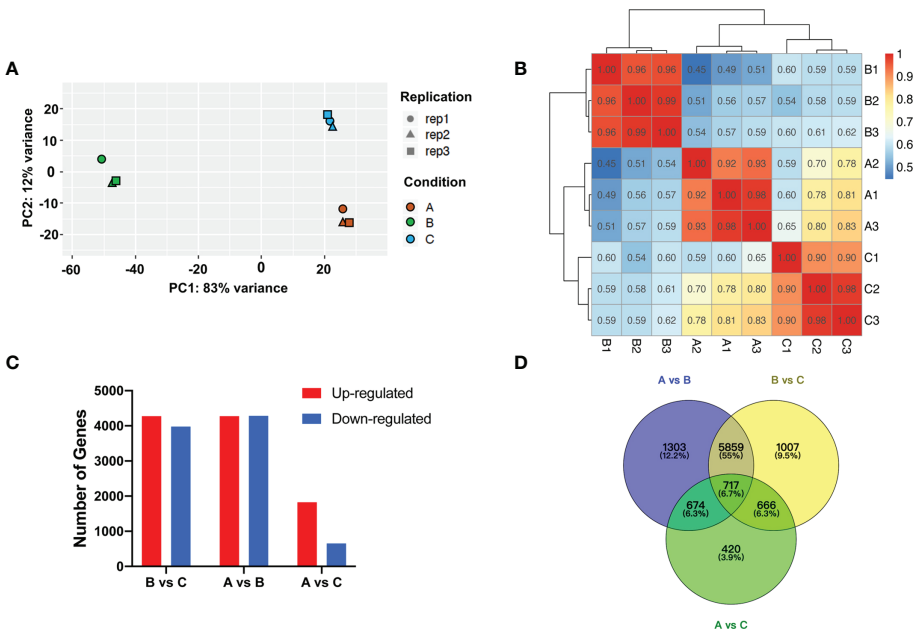

FIGURE 3
Transcriptomic analysis after cold storage. **(A)** Principal component analysis of differential expressed genes. Different symbols and colors represent different replicates and treatment conditions, respectively. **(B)** Correlation analysis of patterns of RNA-Seq in each group. **(C)** Number of up- and downregulated genes among groups. **(D)** Venn diagram of number of DEGs among groups.

Analysis of Group A & B, and Group B & C identified 8553 (4272 upregulated and 4281 downregulated) and 8249 (4272 upregulated and 3977 downregulated) DEGs, respectively. However, only 1824 upregulated and 653 downregulated DEGs were identified *via* analysis of Group A and C (Figures 3C, D). Based on the expression levels of genes from each group, correlation among the samples was calculated and hierarchical clustering was visualized in a heatmap. Consistent with PCA analysis, gene expression clusters in Group B were distinguishable from that in Group A and Group C (Supplementary Figure S4). These results indicate that expression levels of many genes are sensitive to temperature shift. The C-repeat binding factor (CBF)/dehydration responsive-element binding (DREB) TFs are known to be sensitive to low temperature (Thomashow, 2010; Zhang et al., 2016). In the present study, we found that transcript levels of multiple melon CBFs/DREBs were higher in the chilled melon and returned to unchilled levels after transfer to room temperature (Supplementary Figure S5).

Responses of VAE biosynthetic genes to chilling

To understand the molecular basis of the reduction of melon flavor-associated VAEs during cold storage, we investigated the relevant biosynthetic pathways and genes involved in the biosynthesis of VAEs. As observed in the aromatic melon fruit that we used, content of volatile esters was much higher than other characterized VOCs, such as alcohols and aldehydes (Figure 2B; Supplementary Table S1). Alcohol dehydrogenase (ADH) and alcohol acyltransferase (AAT) are able to convert volatile aldehydes to their corresponding alcohols and esters (Figure 4A). The expression levels of two ADH family members (*CmADH1* and *CmADH2*) were downregulated after 8-d cold storage and upregulated to higher levels after 1-d recovery at room temperature, and the transcript levels after recovery were higher than day 8. Similarly, the transcript abundance of two members of AAT family (*CmAAT1* and *CmAAT3*) was lower in the chilled melon and recovered after 1 d at room temperature (Figure 4B; Supplementary Tables S4, S5).

In the fatty acid pathway, biosynthesis of C5 and C6 green leafy volatiles depends upon LOX and HPL activities (Figure 4A). Here, we observed *CmLOX18* expression level was lower after chilling and recovered after 1 d at room temperature. In addition, expression levels of *CmLOX8* and a 9-lipoxygenase (*CmLOX9*) were also altered after chilling. Transcript levels of two CmHPLs were lower in the chilled melon. *CmHPL2* expression was recovered after return to the room temperature, while *CmHPL1* remained at low level. CmPDC1 involved in aldehyde biosynthesis through catalyzing straight-chain ketoacids was reduced after chilling and recovered to higher level after 1 d at room temperature (Figure 4B; Supplementary Tables S4, S5). In the amino acid pathway,

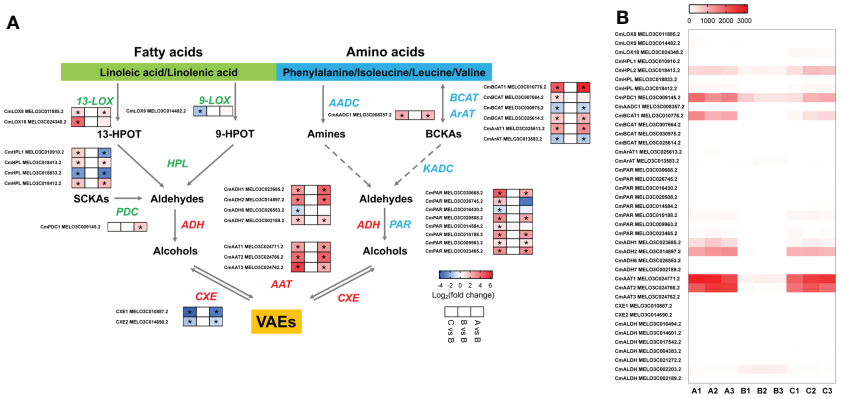

FIGURE 4
The analysis of differentially expressed genes in VAE biosynthesis pathway. **(A)** VAE biosynthesis in fatty acid and amino acid pathways. **(B)** A heatmap of DEGs involved in these pathways. Values of log2(foldchange) and FPKM are used in the heatmap of A and B, respectively. 13-HPOT, 13(*S*)-hydroperoxy-9(*Z*),11(*E*),15(*Z*)-octadecatrienoic acid; 9-HPOT, 9(*S*)-hydroperoxy-10(*E*),12(*Z*),15(*Z*)-octadecatrienoic acid; SCKAs, straight-chain ketoacids; BCKAs, branched-chain ketoacids; LOX, lipoxygenase; HPL, hydroperoxide lyase; PDC, pyruvate decarboxylase; BCAT, branched chain amino transferase; ArAT, aromatic amino transferase; AADC, amino acid decarboxylase; ADH, alcohol dehydrogenase; PAR, phenylacetaldehyde reductase; AAT, alcohol acyltransferase; CXE, carboxylesterase; ALDH, aldehyde dehydrogenase; KADC, ketoacid decarboxylase; VAEs, volatile acetate esters. Asterisks indicate significant differences (p-value < 0.05).

CmBCAT1 and *CmArAT1* expression levels were reduced in the chilled melon fruit and upregulated after 1 d of recovery. Moreover, multiple aldehyde dehydrogenases (ALDHs) were also sensitive to low temperatures (Figure 4B; Supplementary Tables S4, S5). Therefore, reduced production of VAEs after chilling cannot be directly explained by a single enzyme activity alone.

Chilling-induced expression variations in transcription factors and hormone regulators

According to the expression patterns of DEGs among the three groups, clustering analysis was carried out, and DEGs were divided into nine clusters (Supplementary Figure S6). Based on the Plant/Animal Transcription Factor Database (Plant/AnimalTFDB), thirty TF families were identified (Supplementary Figure S7; Supplementary Table S6). To narrow the scope of differentially expressed TFs, we removed the genes without significance (p-value > 0.01), and 375 TFs were selected. 246 TFs belong to Cluster 1 and 5, indicating that their expression levels were higher after chilling and recovered after 1 d at room temperature. On the contrary, 129 TFs were clustered in Cluster 6 and 8, indicating that their expression levels were lower after chilling and increased after 1-d recovery (Supplementary Table S7).

Clusters 6 and 8 identified melon *NONRIPENING* (*CmNOR*) which is a key ripening regulator, and its expression was reduced (~30-fold reduction) after chilling and upregulated (~40-fold increase) after 1-d recovery at room temperature, which is consistent with the pattern of ester levels and flavor intensity (Supplementary Tables S4, S5). In the same cluster with *CmNOR*, *CmMYB44*, an ester-associated apple MdMYB6 homolog, had lower expression during cold storage and increased transcript after 1-d recovery (Supplementary Tables S4, S5). In addition, Cluster 1 and 5 identified a bZIP family gene (named *CmbZIP1*, ester-associated MabZIP4 homolog in banana) with the highest expression during chilling and reduced transcript levels after recovery (Supplementary Tables S4, S5).

Ethylene also regulates various aspects of ripening, including VOC biosynthesis in fruit. Ethylene biosynthesis genes, including aminocyclopropane carboxylate synthase (ACS) and oxidase (ACO), were investigated. The transcript levels of *CmACS1* and *CmACO1* were the highest among the family members, respectively. The expression of *CmACO1* was lower in the chilled melon and increased after 1 d at room temperature. Conversely, much higher transcript levels of *CmACS1* was observed after cold storage and declined after returning to room temperature (Supplementary Figure S8; Supplementary Tables S4, S5).

WGCNA identified the aforementioned ester-associated genes in response to temperature changes

To gain further insight into the regulation of ester biosynthesis after temperature shift, WGCNA was performed to investigate the co-expression networks of key DEGs. According to the similarity of expression patterns, genes were grouped into a total of eighteen co-expression modules (Figure 5A). Based on the top three coefficient values shown in the heatmap of module-trait correlations, content of esters was positively correlated with gene expressions in the blue, turquoise and green-yellow modules (Figure 5B; Supplementary Table S8). Subsequently, GO annotation analysis was performed to summarize functions of the DEGs identified in the modules, and DEGs in response to chilling were investigated. The functional categories of the DEGs included biological process, molecular function and cellular component. Top twenty GO terms indicated that cellular process in the biological process ranked the highest, and 753 DEGs were divided into the group of cellular aromatic compound metabolic process (Figure 6; Supplementary Table S9).

Based on the analyses of transcriptome and metabolome, multiple genes involved in ester biosynthesis were preliminarily identified. Notably, WGCNA further narrowed the scope of DEGs correlated with ester biosynthesis. Two lipoxygenases (*CmLOX8* and *CmLOX18*), one hydroperoxide lyase (*CmHPL2*), one alcohol acyltransferase (*CmAAT1*), one carboxylesterase (*CmCXE1*), and one amino acid decarboxylase (*CmAADC1*) were identified. These DEGs were confirmed by qRT-PCR using RNA from fruit after chilling followed by 1-d recovery at room temperature (Group A), chilled (Group B) and unchilled fruit (Group C) (Figure 7). Additionally, WGCNA was also performed to investigate the correlation between differentially expressed TFs and ester content during chilling and 1-d recovery after chilling. Seventeen key TFs (GS > 0.85, GS < -0.85) were identified, including twelve positive regulators (one C3H, one CPP, one ERF, two GATAs, one GeBP, one LBD, one MYB, one STAT and three WRKYs) and five negative regulators (one ARR-B, two bHLHs, one DBB and one MYB-related) (Table 1). These positive regulators exhibited lower expression levels in the chilled fruit and were upregulated after 1-d recovery at room temperature, which was consistent with the pattern of altered ester content. However, the negative regulators exhibited higher levels after chilling and were downregulated after 1-d recovery. Although the aforementioned three TFs, *CmNOR*, *CmMYB44*, and *CmbZIP1* were not included in the list of top TFs, WGCNA revealed that the relative GS values were higher than 0.7 or lower than -0.7, indicating significant correlations between expression and ester content (Supplementary Table S10).

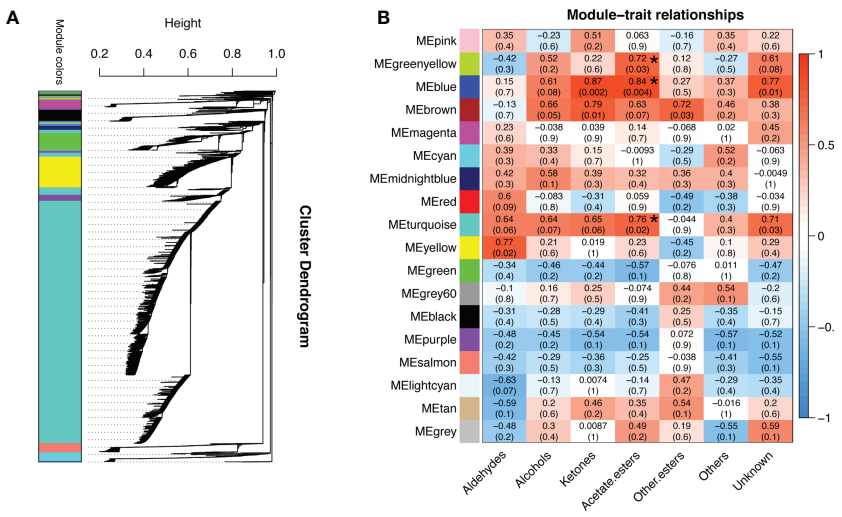

FIGURE 5
Analysis of gene co-expression and the relationships between genes and volatile content in response to cold storage. **(A)** Hierarchical cluster tree exhibits 18 modules of co-expressed genes. Each branch represents one gene in the tree. **(B)** Module-trait correlations and gene co-expression network analysis performed by weighted gene co-expression network analysis during cold storage. The green-yellow, blue and turquoise modules with asterisks significantly related to the content of volatile acetate esters. The corresponding *p*-values are shown in parentheses. The left to right panel represents the module-trait correlations from -1 to 1.

Analysis of potential transcriptional binding motifs in *CmAAT1* and *CmAAT3* promoter sequence

Under chilling conditions, volatile aldehydes and alcohols were not substantially affected, and the last step of ester biosynthesis catalyzed by AAT seems to be an important control point. *cis*-regulatory elements in promoter regions containing TF binding sites play a critical role in regulation of gene expressions. Thus, 1.5-kb putative promoter sequences of *CmAAT1* and *CmAAT3* were investigated.

The analysis of *CmAAT1* and *CmAAT3* promoter regions identified motifs mainly involved in response to stress and hormone levels. For *CmAAT1*, stress responses included anaerobic induction (ARE), stress (STRE), wounding (WUN-motif), and hormone response consists of ethylene (ERE), MeJA

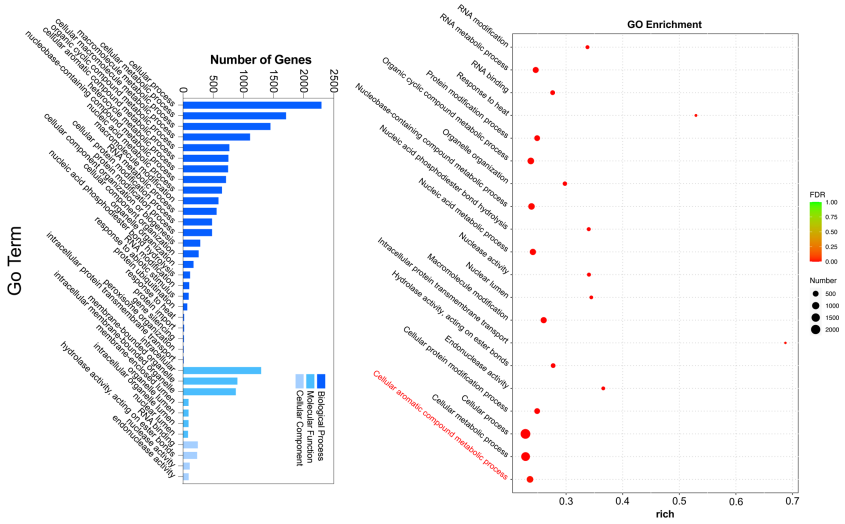

FIGURE 6
GO functional enrichment analysis of DEGs in chilled and unchilled melon fruit.

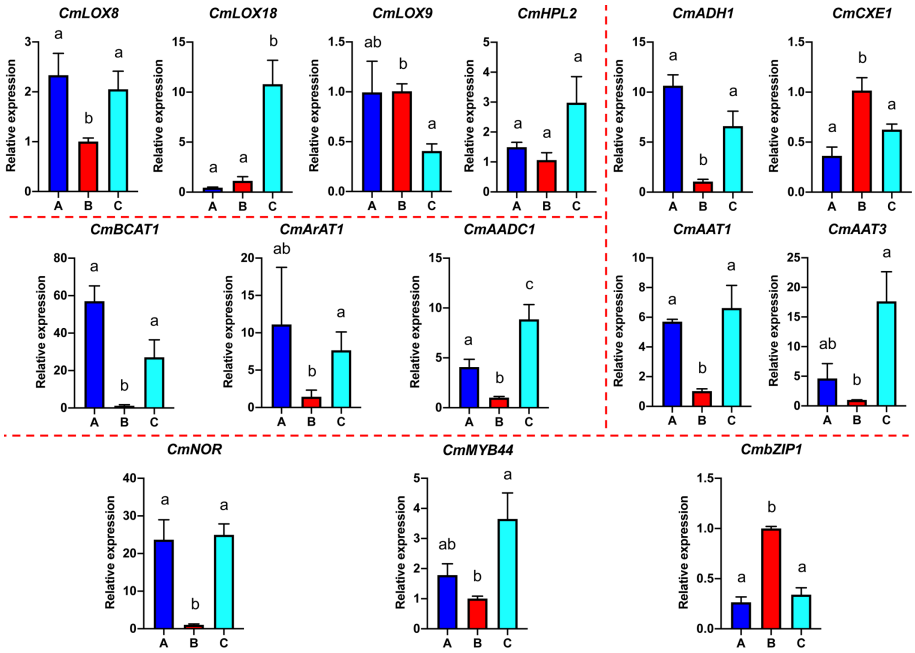

FIGURE 7
Quantitative real-time PCR analysis of select VAE-related DEGs. Significant differences in gene expression are denoted by different letters (± SE, n = 3, *p*-value < 0.05).

(MYC and TGACG-motif) and salicylic acid (TCA-element). For *CmAAT3*, anaerobic induction (ARE), light (AE-box), wounding (WRE3) and ethylene (ERE), gibberellin (TATC-box), MeJA (MYC), salicylic acid (TCA-element) were found to be involved in stress and hormone responsiveness, respectively. In addition, various conserved motifs were found in the promoter region of *CmAAT1*, including G-box (bZIP binding site), MYB and 'ACCGAC' (DREB/CBF) and 'TTA/GCGT' (NAC). MBSI (MYB) and 'TTA/GCGT' (NAC) were found in the *CmAAT3* promoter region.

After temperature shift, we found that expression levels of many TFs exhibited the same pattern with the *CmAAT1* and *CmAAT3*. These TFs included Dof, ERF, WRKY and TCP, in addition to the aforementioned bZIP, MYB, MYC and NAC (Table 1; Supplementary Tables S4, S5). The putative binding sites of some selected TFs were also found in the 1.5-kb promoter sequence of *CmAAT1* and *CmAAT3* (Figure 8), and all putative motifs were shown in Supplementary Table S11 and S12. These observations indicated potential roles of the aforementioned TFs in regulation of VAE-related *AAT* expression during cold storage.

Discussion

For decades, consumers have complained about the flavor of commercial fruit. In addition to breeding of modern cultivars with poor flavor, postharvest chilling treatment is known to result in fruit flavor loss (Zhang et al., 2016; Tieman et al., 2017; Klee and Tieman, 2018). VOCs are critical contributors to fruit flavor quality. Although different fruit often share many aroma characteristics, each fruit has a distinctive aroma determined by the proportions of key volatiles as well as the presence or absence of unique components (Gonda et al., 2010). Therefore, chilling-induced changes to flavor-associated VOCs can be various among fruit species. In our present study, we found that chilling resulted in reduction of flavor-associated esters, particularly VAEs in melon fruit, while other VOCs were only slightly altered. Finally, comparative metabolomic and transcriptomic analyses during temperature shift from 4°C to room temperature were performed to uncover the causes of melon flavor deterioration after chilling.

In climacteric melon, fatty acid- and amino acid-derived esters are the most abundant as well as the most important contributors to fruit flavor (Gonda et al., 2016). Approximately 50% of VOCs are VAEs at a ripe stage in the climacteric melon fruit used in this study. A previous study revealed that content of VAEs was reduced at the later maturity of the oriental melon (Guo et al., 2017). As known, low temperature can slow ripening progress (Zhang et al., 2021). Here, we found that total content of VAEs was remarkably lower in the chilled ripe melon than the unchilled fruit. Thus, chilling-induced reduction of VAE content is more likely caused by transcriptional regulation of the metabolic pathways.

TABLE 1 The candidate transcription factors potentially involved in VAE biosynthesis.

TF family	Gene ID	Description	Correlation with VAEs	*p*-value
ARR-B	MELO3C016975.2	two-component response regulator ARR12-like	-0.9043733	0.00080999
bHLH	MELO3C023532.2	transcription factor bHLH130-like isoform X2	-0.8627904	0.00274777
	MELO3C020781.2	transcription factor bHLH121 isoform X1	-0.8782129	0.00183893
C3H	MELO3C015665.2	zinc finger CCCH domain-containing protein 14-like	0.86642181	0.00251085
CPP	MELO3C006510.2	Protein tesmin/TSO1-like CXC 2	0.86381782	0.00267924
DBB	MELO3C016115.2	B-box zinc finger protein 22	-0.8500681	0.00369915
ERF	MELO3C014181.2	ethylene-responsive transcription factor 3	0.85900818	0.00301046
GATA	MELO3C011079.2	GATA transcription factor 25	0.87782345	0.00185886
	MELO3C007882.2	GATA transcription factor	0.87543688	0.00198426
GeBP	MELO3C022945.2	mediator-associated protein 1-like	0.86541279	0.0025752
LBD	MELO3C005013.2	Lob domain-containing protein 1	0.87612233	0.00194767
MYB	MELO3C012077.2	Myb family transcription factor family protein	0.93648017	0.0001998
MYB-Related	MELO3C020620.2	telomere repeat-binding protein 5-like	-0.9271353	0.00032002
STAT	MELO3C016678.2	SH2 domain protein B	0.85480225	0.00332233
WRKY	MELO3C016966.2	WRKY transcription factor	0.90052453	0.00092635
	MELO3C018717.2	WRKY protein	0.86917051	0.00234117
	MELO3C014066.2	WRKY transcription factor	0.85615109	0.00322

Multiple flavor-associated pathway genes have been identified, and each of them plays an important role in regulating flux of metabolites throughout respective pathways (2012; Speirs et al., 1998; Chen et al., 2004; Gonda et al., 2010; Goulet et al., 2012; Goulet et al., 2015; Wang et al., 2019). However, flavor-associated VOCs and molecular regulation in response to chilling are still not fully understood in many fruit crops such as melon. In addition to the well-known pathway genes, we found that additional genes involved in flavor-associated VOC synthesis were also sensitive to chilling. An aromatic amino acid decarboxylase gene (named *CmAADC1*) was expressed in a lower level during chilling and partially recovered after 1 d at room temperature. Its homolog, tomato LeAADC2 plays a critical role in the initial step of biosynthesis of 2-phenylethanol and 2-phenylacetaldehyde (Tieman et al., 2006). Additionally, a methionine-gamma-lyase gene (*CmMGL*) associated with the presence of sulfur volatiles in melon was upregulated during cold storage and returned to a considerably lower level after transfer to room temperature (Supplementary Tables S4, S5). GC-IMS analysis identified only sixty known VOCs and nine unknown VOCs (Supplementary Table S1). However, multiple VOCs that contribute to the fruit flavor were not measured in the used melon fruit, including 2-phenylethanol and sulfur volatiles. Sulfur volatiles are important contributors to melon aroma and can be detected in many melon varieties, but high levels may cause undesirable aroma (Gonda et al., 2013). Thus, it will be interesting to determine whether these flavor-associated VOCs are altered during temperature shift in melon fruit, other than VAEs.

In addition, expression levels of multiple TFs were altered in response to low temperature. In particular, some associated with fruit development were downregulated, including ripening-associated NOR and ethylene-responsive ERF (Supplementary Tables S4, S5). Altered expression of these TFs during temperature shift would be expected to change numerous ripening processes, permitting the organ to redirect metabolic resources into more suitable stress responses (Zhang et al., 2016). Additionally, ripening has been a major focus of plant breeding in fleshy fruits, with special effort on the improvement of organoleptic quality and post-harvest durability (Ríos et al., 2017). Ripening-associated ETHQV6.3 encoded by a NAC domain TF (CmNOR) advances the ethylene production and activates the production of esters, changing the aroma profile of melon fruit (Santo Domingo et al., 2022). Thus, the altered expression levels of ripening-associated TFs cannot be ignored when examining melon flavor loss after cold storage. Besides, TFs are able to regulate expression of downstream genes *via* binding to elements in the promoter region (Schwechheimer et al., 1998). Notably, NAC and ERF binding motifs were observed in the promoter sequences of ester-associated *CmAAT1* and *CmAAT3* (Figure 8). Motifs involved in stress and hormone responsiveness were also found in the aforementioned promoter regions.

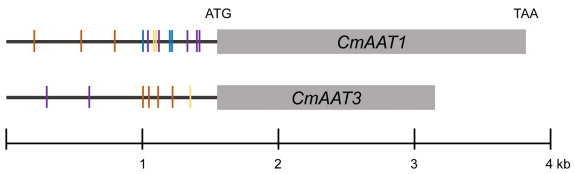

FIGURE 8
Analysis of *CmAAT1* and *CmAAT3* promoter sequences. TF binding motifs were shown in the 1.5-kb promoter regions. Purple, NAC (TTA/GCGT, (Lindemose et al., 2014); Blue, AP2/ERF (ACCGAC, Suzuki et al., 2005); Yellow, MYB (AACTG, Prouse and Campbell, 2012); Orange, AP2/RAV (CAACA, Zhang et al., 2020).

Climacteric ripening is characterized by the autocatalytic biosynthesis of plant hormone ethylene (Ríos et al., 2017). Ethylene synthesis was reduced after chilling with partial recovery after transfer to room temperature in tomato (Zhang et al., 2016). In melon, low temperature treatments inhibited ethylene production during storage (Zhang et al., 2015). Ethylene biosynthesis genes included aminocyclopropane carboxylate synthase (ACS) and oxidase (ACO). Conversion of S-adenosylmethionine to 1-aminocyclopropane-1-carboxylic acid by ACS is the first and committal step in the ethylene biosynthesis pathway, and ACO is involved in the final step of ethylene production in plant tissues (Pech et al., 2008). Of the multiple ACS and ACO enzymes reported in the melon genome, *CmACS1* and *CmACO1* are specific to fruit ripening as their expression increases in climacteric fruit after the burst of ethylene (Miki et al., 1995; Saladié et al., 2015). Initially, it was postulated that not ACO, but ACS is the rate-limiting enzyme in ethylene biosynthesis pathway (Adams and Yang, 1979; Houben and Van de Poel, 2019). However, an increasing amount of evidence has been gathered over the years, which demonstrates the importance of ACO, and not ACS, in controlling ethylene production in plants (English et al., 1995; Vriezen et al., 1999; Shi et al., 2006; Love et al., 2009; Van de Poel et al., 2012; Chen et al., 2016). In our study, *CmACO1* expression was downregulated after chilling. However, *CmACS1* displayed an opposite expression pattern in response to low temperature. The last step of ethylene biosynthesis is likely to be controlled by rate-limiting enzyme CmACO1, rather than CmACS1 involved in the initial step.

Sugar and organic acid accumulation were ethylene-independent (Pech et al., 2008; Ríos et al., 2017). Accordingly, fructose, glucose and citrate were not substantially affected after chilling (Figure S3). Conversely, the production of aroma volatiles was strictly ethylene-dependent. Ethylene has an important role in ester biosynthesis in climacteric fruit including peach and apple (Wang et al., 2018; Cao et al., 2021; Santo Domingo et al., 2022). A previous study revealed that ethylene levels were lower in chilled oriental melon (Zhang et al., 2015), showing the same pattern as we observed for VAEs. Climacteric melon has a peak of ripening, controlled by increased ethylene (Pech et al., 2008; Santo Domingo et al., 2022). Multiple genes involved in ester biosynthesis were regulated by ethylene production in melon. The expression of *CmAAT1* was severely reduced in ethylene-suppressed antisense 1-aminocyclopropane-1-carboxylic acid oxidase fruit and in wild-type fruit treated with the ethylene antagonist 1-methylcyclopropene (1-MCP) (Yahyaoui et al., 2002). In addition, both 1-MCP and low temperature downregulated *CmLOX18* expression (Zhang et al., 2015). As observed in our work, a key ethylene regulator, *CmACO1* was downregulated after cold storage, which likely resulted in reduced ethylene production. Consistently, expression of *CmLOX18*, *CmAAT1* and *CmAAT3* were found to be decreased after chilling and recovered after a return to room temperature.

VAEs were remarkably altered in response to chilling. However, total volatile aldehydes and alcohols derived from fatty acids and amino acids were only slightly affected by chilling. During cold storage, the reduced *CmAAT1* and *CmAAT3* expression can be responsible for the lower VAE content, in turn resulting in higher volatile alcohols. Similarly, reduced transcript of *CmADH1* and *CmADH2* resulted in less conversion of volatile aldehydes. GC-IMS analysis showed that content of some aldehydes even increased after chilling. In addition, CXEs are responsible for conversion of VAEs to alcohols (Goulet et al., 2015). Interestingly, the transcripts of two tomato homologs in melon, *CmCXE1* and *CmCXE2*, were higher in chilled melon fruit and downregulated after 1-d recovery at room temperature (Supplementary Tables S4, S5), which indicated that CXE-catalyzed biosynthesis of volatile alcohols might increase during cold storage. Additionally, content of some upstream metabolites in the fatty acid pathway increased after cold storage. Thus, a metabolic balance of intermediate products occurred during cold storage, and it seems that chilling reduced VAE content was a result of transcriptional regulation.

Conclusion

We combined sensory evaluation, transcriptomic and metabolomic analyses to determine the impact of postharvest chilling on the flavor of melon fruit. In summary, consumer panel tests indicated a negative change in the flavor of the chilled melon fruit in comparison with the unchilled. Melon flavor-associated VAEs derived from fatty acids and amino acids represents the dominant esters, showing considerably lower content after cold storage. Additionally, metabolomic analysis suggested that the corresponding upstream metabolites including linoleic acid, linolenic acid, phenylalanine and KIC were also altered in the chilled fruit. Transcripts for various key VAE synthesis genes, such as *CmLOX18*, *CmADH1*, *CmAAT1*,

CmCXE1, *CmArAT1* and *CmBCAT1*, ripening-related TF, such as *CmNOR* and hormone regulators, such as *CmACO1* were significantly changed during cold storage. Most of the chilling-induced changes recovered after transfer to the room temperature. In general, chilling resulted in flavor loss of melon fruit, in large part due to the reduced VAE content. Our study provided a molecular basis for the understanding of melon fruit flavor loss during cold storage.

Data availability statement

The RNASeq data presented in the study are deposited in the NCBI-GEO (Gene Expression Omnibus) repository, accession number GSE220934.

Author contributions

HZ and XL designed and performed the experiments, also analyzed data and contributed to the writing of the manuscript. XZ, RX and YY contributed to part of data analysis. MA contributed to the consumer preference analysis and revised the manuscript. CY supervised part of the research and reviewed the manuscript. DT reviewed and revised the manuscript. XL supervised the research. All authors contributed to the article and approved the submitted version.

Funding

This work was supported by the National Natural Science Foundation of China (31640069), Huaibei major science and technology projects (Z2020011), Anhui Key Research and Development Project (202104a06020024), Anhui Provincial University Super Talents Funding Programme (gxyqZD2021141) and Major Science and Technology Project of Anhui Province (202203a06020018). Science Fund for Distinguished Young Scholars Higher Education of Anhui (2022AH020037).

Acknowledgments

We thank Fu Beiling for the WGCNA analysis.

Conflict of interest

The authors declare that the research was conducted in the absence of any commercial or financial relationships that could be construed as a potential conflict of interest.

Publisher's note

Supplementary material

The Supplementary Material for this article can be found online at: https://www.frontiersin.org/articles/10.3389/fpls.2022.1067680/full#supplementary-material

References

Adams, D. O., and Yang, S. F. (1979). Ethylene biosynthesis: Identification of 1-aminocyclopropane-1-carboxylic acid as an intermediate in the conversion of methionine to ethylene. *Proc. Natl. Acad. Sci. U.S.A.* 76, 170–174. doi: 10.1073/pnas.76.1.170

Aubert, C., and Pitrat, M. (2006). Volatile compounds in the skin and pulp of queen anne's pocket melon. *J. Agric. Food Chem.* 54, 8177–8182. doi: 10.1021/jf061415s

Beaulieu, J. C., and Grimm, C. C. (2001). Identification of volatile compounds in cantaloupe at various developmental stages using solid phase microextraction. *J. Agric. Food Chem.* 49, 1345–1352. doi: 10.1021/jf0005768

Bruhn, C. M., Feldman, N., Garlitz, C., Harwood, J., Ivans, E., Marshall, M., et al. (1991). Consumer perceptions of quality: apricots, cantaloupes, peaches, pears, strawberries and tomatoes. *J. Food. Qual.* 14, 187–195. doi: 10.1111/j.1745-4557.1991.tb00060.x

Cao, X., Wei, C., Duan, W., Gao, Y., Kuang, J., Liu, M., et al. (2021). Transcriptional and epigenetic analysis reveals that NAC transcription factors regulate fruit flavor ester biosynthesis. *Plant J.* 106, 785–800. doi: 10.1111/tpj.15200

Cao, X., Xie, K., Duan, W., Zhu, Y., Liu, M., Chen, K., et al. (2019). Peach carboxylesterase PpCXE1 is associated with catabolism of volatile esters. *J. Agric. Food Chem.* 67, 5189–5196. doi: 10.1021/acs.jafc.9b01166

Chen, H., Cao, S., Jin, Y., Tang, Y., and Qi, H. (2016). The relationship between CmADHs and the diversity of volatile organic compounds of three aroma types of melon (Cucumis melo). *Front. Physiol.* 7. doi: 10.3389/fphys.2016.00254

Chen, G., Hackett, R., Walker, D., Taylor, A., Lin, Z., and Grierson, D. (2004). Identification of a specific isoform of tomato lipoxygenase (TomloxC) involved in the generation of fatty acid-derived flavor compounds. *Plant Physiol.* 136, 2641–2651. doi: 10.1104/pp.104.041608

Chen, H., Sun, J., Li, S., Cui, Q., Zhang, H., Xin, F., et al. (2016). An ACC oxidase gene essential for cucumber carpel development. *Mol. Plant* 9, 1315–1327. doi: 10.1016/j.molp.2016.06.018

Civille, G. V., and Carr, B. T. (2015). *Sensory evaluation techniques. 5th ed* (CRC press). Available at: https://www.routledge.com/Sensory-Evaluation-Techniques/Civille-Carr/p/book/9781482216905.

Colantonio, V., Ferrão, L. F. V., Tieman, D. M., Bliznyuk, N., Sims, C., Klee, H. J., et al. (2022). Metabolomic selection for enhanced fruit flavor. *Proc. Natl. Acad. Sci. U.S.A.* 119. doi: 10.1073/pnas.2115865119

De Vos, R. C. H., Moco, S., Lommen, A., Keurentjes, J. J. B., Bino, R. J., and Hall, R. D. (2007). Untargeted large-scale plant metabolomics using liquid chromatography coupled to mass spectrometry. *Nat. Protoc.* 2, 778–791. doi: 10.1038/nprot.2007.95

El-Sharkawy, I., Manriquez, D., Flores, F. B., Regad, F., Bouzayen, M., Latché, A., et al. (2005). Functional characterization of a melon alcohol acyl-transferase gene family involved in the biosynthesis of ester volatiles. identification of the crucial role of a threonine residue for enzyme activity*. *Plant Mol. Biol.* 59, 345–362. doi: 10.1007/s11103-005-8884-y

English, P. J., Lycett, G. W., Roberts, J. A., and Jackson, M. B. (1995). Increased 1-aminocyclopropane-1-carboxylic acid oxidase activity in shoots of flooded tomato plants raises ethylene production to physiologically active levels. *Plant Physiol.* 109, 1435–1440. doi: 10.1104/pp.109.4.1435

Esteras, C., Rambla, J. L., Sánchez, G., López-Gresa, M. P., González-Mas, M. C., Fernández-Trujillo, J. P., et al. (2018). Fruit flesh volatile and carotenoid profile analysis within the cucumis melo l. species reveals unexploited variability for future genetic breeding. *J. Sci. Food Agric.* 98, 3915–3925. doi: 10.1002/jsfa.8909

Fallik, E., Alkali-Tuvia, S., Horev, B., Copel, A., Rodov, V., Aharoni, Y., et al. (2001). Characterisation of 'Galia' melon aroma by GC and mass spectrometric sensor measurements after prolonged storage. *Postharvest Biol. Technol.* 22, 85–91. doi: 10.1016/S0925-5214(00)00185-X

Fernqvist, F., and Hunter, E. (2012). Who's to blame for tasteless tomatoes? the effect of tomato chilling on consumers' taste perceptions. *Eur. J. Hortic. Sci.* 77, 193–198.

Gao, Y., Lin, Y., Xu, M., Bian, H., Zhang, C., Wang, J., et al. (2022). The role and interaction between transcription factor NAC-NOR and DNA demethylase SlDML2 in the biosynthesis of tomato fruit flavor volatiles. *New Phytol.* 235, 1913–1926. doi: 10.1111/nph.18301

Gonda, I., Bar, E., Portnoy, V., Lev, S., Burger, J., Schaffer, A. A., et al. (2010). Branched-chain and aromatic amino acid catabolism into aroma volatiles in cucumis melo l. fruit. *J. Exp. Bot.* 61, 1111–1123. doi: 10.1093/jxb/erp390

Gonda, I., Burger, Y., Schaffer, A. A., Ibdah, M., Tadmor, Y., Katzir, N., et al. (2016). "Biosynthesis and perception of melon aroma," in *Biotechnology in flavor production*. Eds. D. Havkin-Frenkel and N. Dudai (Chichester, UK: John Wiley & Sons, Ltd), 281–305. doi: 10.1002/9781118354056.ch11

Gonda, I., Lev, S., Bar, E., Sikron, N., Portnoy, V., Davidovich-Rikanati, R., et al. (2013). Catabolism of l-methionine in the formation of sulfur and other volatiles in melon (Cucumis melo l.) fruit. *Plant J.* 74, 458–472. doi: 10.1111/tpj.12149

Goulet, C., Kamiyoshihara, Y., Lam, N. B., Richard, T., Taylor, M. G., Tieman, D. M., et al. (2015). Divergence in the enzymatic activities of a tomato and solanum pennellii alcohol acyltransferase impacts fruit volatile ester composition. *Mol. Plant* 8, 153–162. doi: 10.1016/j.molp.2014.11.007

Goulet, C., Mageroy, M. H., Lam, N. B., Floystad, A., Tieman, D. M., and Klee, H. J. (2012). Role of an esterase in flavor volatile variation within the tomato clade. *Proc. Natl. Acad. Sci. U.S.A.* 109, 19009–19014. doi: 10.1073/pnas.1216515109

Guo, J., Ma, Z., Peng, J., Mo, J., Li, Q., Guo, J., et al. (2021). Transcriptomic analysis of raphidocelis subcapitata exposed to erythromycin: The role of DNA replication in hormesis and growth inhibition. *J. Hazard. Mater.* 402, 123512. doi: 10.1016/j.jhazmat.2020.123512

Guo, X., Xu, J., Cui, X., Chen, H., and Qi, H. (2017). iTRAQ-based protein profiling and fruit quality changes at different development stages of oriental melon. *BMC Plant Biol.* 17, 28. doi: 10.1186/s12870-017-0977-7

Guo, Y. F., Zhang, Y. L., Shan, W., Cai, Y. J., Liang, S. M., Chen, J. Y., et al. (2018). Identification of two transcriptional activators MabZIP4/5 in controlling aroma biosynthetic genes during banana ripening. *J. Agric. Food Chem.* 66, 6142–6150. doi: 10.1021/acs.jafc.8b01435

Houben, M., and Van de Poel, B. (2019). 1-Aminocyclopropane-1-Carboxylic acid oxidase (ACO): The enzyme that makes the plant hormone ethylene. *Front. Plant Sci.* 10. doi: 10.3389/fpls.2019.00695

Jin, Y., Zhang, C., Liu, W., Tang, Y., Qi, H., Chen, H., et al. (2016). The alcohol dehydrogenase gene family in melon (Cucumis melo l.): Bioinformatic analysis and expression patterns. *Front. Plant Sci.* 7. doi: 10.3389/fpls.2016.00670

Kim, D., Langmead, B., and Salzberg, S. L. (2015). HISAT: a fast spliced aligner with low memory requirements. *Nat. Methods* 12, 357–360. doi: 10.1038/nmeth.3317

Klee, H. J., and Tieman, D. M. (2018). The genetics of fruit flavour preferences. *Nat. Rev. Genet.* 19, 347–356. doi: 10.1038/s41576-018-0002-5

Kourkoutas, D., Elmore, J. S., and Mottram, D. S. (2006). Comparison of the volatile compositions and flavour properties of cantaloupe, galia and honeydew muskmelons. *Food Chem.* 97, 95–102. doi: 10.1016/j.foodchem.2005.03.026

Langfelder, P., and Horvath, S. (2008). WGCNA: an r package for weighted correlation network analysis. *BMC Bioinf.* 9, 559. doi: 10.1186/1471-2105-9-559

Lawless, H. T., and Heymann, H. (2010). *Sensory evaluation of food: Principles and practices* Vol. 2 (New York: Springer). doi: 10.1007/978-1-4419-6488-5

Lescot, M., Déhais, P., Thijs, G., Marchal, K., Moreau, Y., Van de Peer, Y., et al. (2002). PlantCARE, a database of plant cis-acting regulatory elements and a portal to tools for *in silico* analysis of promoter sequences. *Nucleic Acids Res.* 30, 325–327. doi: 10.1093/nar/30.1.325

Lindemose, S., Jensen, M. K., Van de Velde, J., O'Shea, C., Heyndrickx, K. S., Workman, C. T., et al. (2014). A DNA-binding-site landscape and regulatory network analysis for NAC transcription factors in arabidopsis thaliana. *Nucleic Acids Res.* 42, 7681–7693. doi: 10.1093/nar/gku502

Li, X., Tieman, D., Liu, Z., Chen, K., and Klee, H. J. (2020). Identification of a lipase gene with a role in tomato fruit short-chain fatty acid-derived flavor volatiles by genome-wide association. *Plant J.* 104, 631–644. doi: 10.1111/tpj.14951

Li, X., Xu, Y., Shen, S., Yin, X., Klee, H., Zhang, B., et al. (2017). Transcription factor CitERF71 activates the terpene synthase gene CitTPS16 involved in the synthesis of e-geraniol in sweet orange fruit. *J. Exp. Bot.* 68, 4929–4938. doi: 10.1093/jxb/erx316

Li, P. C., Yu, S. W., Shen, J., Li, Q. Q., Li, D. P., Li, D. Q., et al. (2014). The transcriptional response of apple alcohol acyltransferase (MdAAT2) to salicylic acid and ethylene is mediated through two apple MYB TFs in transgenic tobacco. *Plant Mol. Biol.* 85, 627–638. doi: 10.1007/s11103-014-0207-8

Love, J., Björklund, S., Vahala, J., Hertzberg, M., Kangasjärvi, J., and Sundberg, B. (2009). Ethylene is an endogenous stimulator of cell division in the cambial meristem of populus. *Proc. Natl. Acad. Sci. U.S.A.* 106, 5984–5989. doi: 10.1073/pnas.0811660106

Miki, T., Yamamoto, M., Nakagawa, H., Ogura, N., Mori, H., Imaseki, H., et al. (1995). Nucleotide sequence of a cDNA for 1-aminocyclopropane-1-carboxylate synthase from melon fruits. *Plant Physiol.* 107, 297–298. doi: 10.1104/pp.107.1.297

Obando-Ulloa, J. M., Moreno, E., García-Mas, J., Nicolai, B., Lammertyn, J., Monforte, A. J., et al. (2008). Climacteric or non-climacteric behavior in melon fruit. *Postharvest Biol. Technol.* 49, 27–37. doi: 10.1016/j.postharvbio.2007.11.004

Pech, J. C., Bouzayen, M., and Latché, A. (2008). Climacteric fruit ripening: Ethylene-dependent and independent regulation of ripening pathways in melon fruit. *Plant Sci.* 175, 114–120. doi: 10.1016/j.plantsci.2008.01.003

Peng, B., Yu, M., Zhang, B., Xu, J., and Ma, R. (2020). Differences in PpAAT1 activity in high- and low-aroma peach varieties affect γ-decalactone production. *Plant Physiol.* 182, 2065–2080. doi: 10.1104/pp.19.00964

Pereira, L., Ruggieri, V., Pérez, S., Alexiou, K. G., Fernández, M., Jahrmann, T., et al. (2018). QTL mapping of melon fruit quality traits using a high-density GBS-based genetic map. *BMC Plant Biol.* 18, 324. doi: 10.1186/s12870-018-1537-5

Pitrat, M. (2013). Phenotypic diversity in wild and cultivated melons (Cucumis melo). *Plant Biotechnol.* 30, 273–278. doi: 10.5511/plantbiotechnology.13.0813a

Prouse, M. B., and Campbell, M. M. (2012). The interaction between MYB proteins and their target DNA binding sites. *Biochim. Biophys. Acta* 1819, 67–77. doi: 10.1016/j.bbagrm.2011.10.010

Radovich, T. J. K., Kleinhenz, M. D., Delwiche, J. F., and Liggett, R. E. (2004). Triangle tests indicate that irrigation timing affects fresh cabbage sensory quality. *Food Qual. Prefer.* 15, 471–476. doi: 10.1016/j.foodqual.2003.08.003

Ríos, P., Argyris, J., Vegas, J., Leida, C., Kenigswald, M., Tzuri, G., et al. (2017). ETHQV6.3 is involved in melon climacteric fruit ripening and is encoded by a NAC domain transcription factor. *Plant J.* 91, 671–683. doi: 10.1111/tpj.13596

Saladié, M., Cañizares, J., Phillips, M. A., Rodriguez-Concepcion, M., Larrigaudière, C., Gibon, Y., et al. (2015). Comparative transcriptional profiling analysis of developing melon (Cucumis melo l.) fruit from climacteric and non-climacteric varieties. *BMC Genomics* 16, 440. doi: 10.1186/s12864-015-1649-3

Sangster, T., Major, H., Plumb, R., Wilson, A. J., and Wilson, I. D. (2006). A pragmatic and readily implemented quality control strategy for HPLC-MS and GC-MS-based metabonomic analysis. *Analyst* 131, 1075–1078. doi: 10.1039/b604498k

Santo Domingo, M., Areco, L., Mayobre, C., Valverde, L., Martín-Hernández, A. M., Pujol, M., et al. (2022). Modulating climacteric intensity in melon through QTL stacking. *Hortic. Res.* 9, uhac131. doi: 10.1093/hr/uhac131

Schwab, W., Davidovich-Rikanati, R., and Lewinsohn, E. (2008). Biosynthesis of plant-derived flavor compounds. *Plant J.* 54, 712–732. doi: 10.1111/j.1365-313X.2008.03446.x

Schwechheimer, C., Zourelidou, M., and Bevan, M. W. (1998). Plant transcription factor studies. *Annu. Rev. Plant Physiol. Plant Mol. Biol.* 49, 127–150. doi: 10.1146/annurev.arplant.49.1.127

Shen, J., Tieman, D., Jones, J. B., Taylor, M. G., Schmelz, E., Huffaker, A., et al. (2014). A 13-lipoxygenase, TomloxC, is essential for synthesis of C5 flavour volatiles in tomato. *J. Exp. Bot.* 65, 419–428. doi: 10.1093/jxb/ert382

Shi, Y.-H., Zhu, S.-W., Mao, X.-Z., Feng, J.-X., Qin, Y.-M., Zhang, L., et al. (2006). Transcriptome profiling, molecular biological and physiological studies reveal a major role for ethylene in cotton fiber cell elongation. *Plant Cell* 18, 651–664. doi: 10.1105/tpc.105.040303

Speirs, J., Lee, E., Holt, K., Yong-Duk, K., Steele Scott, N., Loveys, B., et al. (1998). Genetic manipulation of alcohol dehydrogenase levels in ripening tomato fruit affects the balance of some flavor aldehydes and alcohols1. *Plant Physiol.* 117, 1047–1058. doi: 10.1104/pp.117.3.1047

Sun, X., Baldwin, E. A., Manthey, J., Dorado, C., Rivera, T., and Bai, J. (2022). Effect of preprocessing storage temperature and time on the physicochemical properties of winter melon juice. *J. Food Qual.* 2022, 1–6. doi: 10.1155/2022/3237639

Suzuki, M., Ketterling, M. G., and McCarty, D. R. (2005). Quantitative statistical analysis of cis-regulatory sequences in ABA/VP1- and CBF/DREB1-regulated genes of arabidopsis. *Plant Physiol.* 139, 437–447. doi: 10.1104/pp.104.058412

Thomashow, M. F. (2010). Molecular basis of plant cold acclimation: insights gained from studying the CBF cold response pathway. *Plant Physiol.* 154, 571–577. doi: 10.1104/pp.110.161794

Tieman, D., Taylor, M., Schauer, N., Fernie, A. R., Hanson, A. D., and Klee, H. J. (2006). Tomato aromatic amino acid decarboxylases participate in synthesis of the flavor volatiles 2-phenylethanol and 2-phenylacetaldehyde. *Proc. Natl. Acad. Sci. U.S.A.* 103, 8287–8292. doi: 10.1073/pnas.0602469103

Tieman, D., Zhu, G., Resende, M. F. R., Lin, T., Nguyen, C., Bies, D., et al. (2017). A chemical genetic roadmap to improved tomato flavor. *Science* 355, 391–394. doi: 10.1126/science.aal1556

Van de Poel, B., Bulens, I., Markoula, A., Hertog, M. L. A. T. M., Dreesen, R., Wirtz, M., et al. (2012). Targeted systems biology profiling of tomato fruit reveals coordination of the yang cycle and a distinct regulation of ethylene biosynthesis during postclimacteric ripening. *Plant Physiol.* 160, 1498–1514. doi: 10.1104/pp.112.206086

Vriezen, W. H., Hulzink, R., Mariani, C., and Voesenek, L. A. (1999). 1-aminocyclopropane-1-carboxylate oxidase activity limits ethylene biosynthesis in rumex palustris during submergence. *Plant Physiol.* 121, 189–196. doi: 10.1104/pp.121.1.189

Wang, S., Chen, H., and Sun, B. (2020). Recent progress in food flavor analysis using gas chromatography-ion mobility spectrometry (GC-IMS). *Food Chem.* 315, 126158. doi: 10.1016/j.foodchem.2019.126158

Wang, S., Saito, T., Ohkawa, K., Ohara, H., Suktawee, S., Ikeura, H., et al. (2018). Abscisic acid is involved in aromatic ester biosynthesis related with ethylene in green apples. *J. Plant Physiol.* 221, 85–93. doi: 10.1016/j.jplph.2017.12.007

Wang, M., Zhang, L., Boo, K. H., Park, E., Drakakaki, G., and Zakharov, F. (2019). PDC1, a pyruvate/α-ketoacid decarboxylase, is involved in acetaldehyde, propanal and pentanal biosynthesis in melon (Cucumis melo l.) fruit. *Plant J.* 98, 112–125. doi: 10.1111/tpj.14204

Whiteside, T. (1977). *Tomatoes* (The New Yorker), 36–61. Available at: https://www.newyorker.com/magazine/1977/01/24/tomatoes.

Wickham, H. (2016). Data Transformation. In: *ggplot2: Elegant graphics for data analysis* (Springer). doi: 10.1007/978-3-319-24277-4_10

Yahyaoui, F. E. L., Wongs-Aree, C., Latché, A., Hackett, R., Grierson, D., and Pech, J. C. (2002). Molecular and biochemical characteristics of a gene encoding an alcohol acyl-transferase involved in the generation of aroma volatile esters during melon ripening. *Eur. J. Biochem.* 269, 2359–2366. doi: 10.1046/j.1432-1033.2002.02892.x

Yano, R., Ariizumi, T., Nonaka, S., Kawazu, Y., Zhong, S., Mueller, L., et al. (2020). Comparative genomics of muskmelon reveals a potential role for retrotransposons in the modification of gene expression. *Commun. Biol.* 3, 432. doi: 10.1038/s42003-020-01172-0

Yu, W., Zhang, Y., Lin, Y., Pang, X., Zhao, L., and Wu, J. (2021). Differential sensitivity to thermal processing of two muskmelon cultivars with contrasting differences in aroma profile. *LWT* 138, 110769. doi: 10.1016/j.lwt.2020.110769

Zhang, C., Cao, S., Jin, Y., Ju, L., Chen, Q., Xing, Q., et al. (2017). Melon13-lipoxygenase CmLOX18 may be involved in C6 volatiles biosynthesis in fruit. *Sci. Rep.* 7, 2816. doi: 10.1038/s41598-017-02559-6

Zhang, C., Shao, Q., Cao, S. X., Tang, Y. F., Liu, J. Y., Jin, Y. Z., et al. (2015). Effects of postharvest treatments on expression of three lipoxygenase genes in oriental melon (Cucumis melo var. makuwa makino). *Postharvest Biol. Technol.* 110, 229–238. doi: 10.1016/j.postharvbio.2015.08.024

Zhang, Z., Shi, Y., Ma, Y., Yang, X., Yin, X., Zhang, Y., et al. (2020). The strawberry transcription factor FaRAV1 positively regulates anthocyanin accumulation by activation of FaMYB10 and anthocyanin pathway genes. *Plant Biotechnol. J.* 18, 2267–2279. doi: 10.1111/pbi.13382

Zhang, X., Tang, N., Zhang, H., Chen, C., Li, L., Dong, C., et al. (2021). Comparative transcriptomic analysis of cantaloupe melon under cold storage with ozone treatment. *Food Res. Int.* 140, 109993. doi: 10.1016/j.foodres.2020.109993

Zhang, B., Tieman, D. M., Jiao, C., Xu, Y., Chen, K., Fei, Z., et al. (2016). Chilling-induced tomato flavor loss is associated with altered volatile synthesis and transient changes in DNA methylation. *Proc. Natl. Acad. Sci. U.S.A.* 113, 12580–12585. doi: 10.1073/pnas.1613910113

Zhang, Y., Yin, X., Xiao, Y., Zhang, Z., Li, S., Liu, X., et al. (2018). An ETHYLENE RESPONSE FACTOR-MYB transcription complex regulates furaneol biosynthesis by activating QUINONE OXIDOREDUCTASE expression in strawberry. *Plant Physiol.* 178, 189–201. doi: 10.1104/pp.18.00598

frontiers | Frontiers in Plant Science

TYPE Original Research
PUBLISHED 10 May 2023
DOI 10.3389/fpls.2023.1166262

OPEN ACCESS

EDITED BY
Reinaldo Campos-Vargas,
University of Chile, Chile

REVIEWED BY
Hong Ru Liu,
Shanghai Academy of Agricultural Sciences, China
Muhammad Azam,
University of Agriculture, Faisalabad, Pakistan

*CORRESPONDENCE
Junwei Chen
chenjunwei@zaas.ac.cn

RECEIVED 15 February 2023
ACCEPTED 21 April 2023
PUBLISHED 10 May 2023

CITATION
Ge H, Xu H, Li X and Chen J (2023) The MADS-box gene *EjAGL15* positively regulates lignin deposition in the flesh of loquat fruit during its storage.
Front. Plant Sci. 14:1166262.
doi: 10.3389/fpls.2023.1166262

The MADS-box gene *EjAGL15* positively regulates lignin deposition in the flesh of loquat fruit during its storage

Hang Ge, Hongxia Xu, Xiaoying Li and Junwei Chen*

Institute of Horticulture, Zhejiang Academy of Agricultural Sciences, Hangzhou, Zhejiang, China

Introduction: Lignification of fruit flesh is a common physiological disorder that occurs during post-harvest storage, resulting in the deterioration of fruit quality. Lignin deposition in loquat fruit flesh occurs due to chilling injury or senescence, at temperatures around 0°C or 20°C, respectively. Despite extensive research on the molecular mechanisms underlying chilling-induced lignification, the key genes responsible for the lignification process during senescence in loquat fruit remain unknown. MADS-box genes, an evolutionarily conserved transcription factor family, have been suggested to play a role in regulating senescence. However, it is still unclear whether MADS-box genes can regulate the lignin deposition that arises from fruit senescence.

Methods: Both senescence- and chilling-induced flesh lignification were simulated by applying temperature treatments on loquat fruits. The flesh lignin content during the storage was measured. Transcriptomic, quantitative reverse transcription PCR and correlation analysis were employed to identify key MADS-box genes that may be involved in flesh lignification. The Dual-luciferase assay was utilized to identify the potential interactions between MADS-box members and genes in phenylpropanoid pathway.

Results and Discussion: The lignin content of the flesh samples treated at 20°C or 0°C increased during storage, but at different rates. Results from transcriptome analysis, quantitative reverse transcription PCR, and correlation analysis led us to identify a senescence-specific MADS-box gene, EjAGL15, which correlated positively with the variation in lignin content of loquat fruit. Luciferase assay results confirmed that EjAGL15 activated multiple lignin biosynthesis-related genes. Our findings suggest that EjAGL15 functions as a positive regulator of senescence-induced flesh lignification in loquat fruit.

KEYWORDS

loquat, lignin, MADS-box, postharvest storage, senescence

1 Introduction

Loquat fruit (*Eriobotrya japonica* Lindl.) has a delicious taste and is rich in carotenoids, two features which make it popular among consumers in Asia and Europe. However, the taste of loquat fruit rapidly deteriorates once harvested if it is stored at room temperature, which reduces the feasibility of both its long-term storage and long-distance transportation. The flesh of loquat fruit becomes less juicy and harder to chew when such postharvest deterioration takes place (Cai et al., 2006a). Recent research has clarified that the deposition of lignin in loquat flesh is the leading cause for its diminished taste (Huang et al., 2019). Accordingly, developing effective and inexpensive methods to alleviate the fruity flesh lignification is imperative for securing and promoting the loquat industry.

In the last decade, cold chain has been gradually applied to the transportation and storage of fruits and vegetables, significantly delaying their postharvest spoilage via the precise management of air temperature and suppression of senescence (Mercier et al., 2017; Yang et al., 2020). Yet fruits can also often exhibit physiological disorders, such as internal browning and loss of aromatic flavors, when they undergo inappropriate cold storage (Ding et al., 2002; Zheng et al., 2022). Unfortunately, loquat fruit not only exhibits all the above symptoms but also incurs lignin deposition in its flesh when the temperature drops below its threshold for chilling injury (Cai et al., 2006c), which greatly limits the application of cold chain technology. Hence, suitable conditions that would not cause chilling injury are needed to maintain the commodity properties (and thus market value) of loquat fruits. Nevertheless, the lignification of loquat flesh could also be advanced by senescence under room temperature conditions (Yang et al., 2010), which complicates the optimization of a suitable storage temperature range. Consequently, both chilling and senescence effects should be taking into consideration when trying to balance the benefits versus losses of using cold chain storage.

To precisely define the temperature that best minimizes or stalls the lignification of loquat's flesh during its storage, the molecular mechanism by which flesh is lignified should be first elucidated. Key genes that regulate the deposition of lignin require robust identification for guiding the invention of convenient and inexpensive storage methods. Current studies on loquat lignification have revealed that several genes account for chilling-induced lignin deposition, together with the conditions that initial their transcription, which provides a promising basis to estimate the optimal temperature interval. For example, *EjMYB1*, *EjNAC3*, and *EjHAT1* participate in lignin biosynthesis by interacting with genes in the phenylpropanoid pathway, and their transcripts at 0°C are more abundant than that at 5°C, consistent with a chilling-induced expression pattern (Xu et al., 2014; Ge et al., 2017; Xu et al., 2019). Nonetheless, comparatively little attention has been paid to senescence- induced lignification. Although the abnormal deposition of lignin during fruit senescence has been attributed to the activation of enzymes in phenylpropanoid pathway like Phenylalanine ammonia-lyase (PAL) and Cinnamyl alcohol dehydrogenase (CAD) which is identical to that during chilling injury (Cai et al., 2006b; Chong et al., 2006; Li et al., 2017), the mechanism underlying the temperature-dependent regulation of that pathway remains poorly clarified with an insufficient characterization of the key regulators involved. It was recently shown that multiple regulators are recruited when chilling-induced lignification occurs (Shi et al., 2022), but none of them have been proven to play roles in the lignification process at room temperature. In fact, the transcripts of *EjERF39* and *EjMYB8*, two vital regulators of chilling-induced lignification, remain at low abundance during loquat fruit's storage at room temperature (Zhang et al., 2020). These findings imply the existence of a unique regulation pathway underpinning senescence-induced lignification that differs from chilling-induced lignification.

Lignin deposition is a process during plant development that is mainly controlled by NAC and MYB transcription factors, known as master switches of the secondary cell wall (Wang et al., 2011; Zhong and Ye, 2012; Nakano et al., 2015). However, regulation of stress-induced lignification in different plant tissues is believed to entail novel players other than NAC and MYB (Cesarino, 2019). MADS-box is a conserved gene family found in plants as well as animals. Many studies have presented evidence for linkages between MADS-box members and senescence in different plant species; for example, *Arabidopsis thaliana* (Fang and Fernandez, 2002), *Solanum lycopersicum* (Xie et al., 2014), *Medicago truncatula* (De Michele et al., 2009), and *Brassica rapa* (Yi et al., 2021). The overexpression of MADS-box genes usually results in a delayed senescence process in different organs, which demonstrates the role of negative regulators of senescence. During senescence, lignin deposition is activated in certain kinds of fruit and vegetables besides loquat, such as in wax apple (Hao et al., 2016) and bamboo (Li et al., 2019). But it is unclear whether tissue lignification process during senescence is controlled by MADS-box genes. Interestingly, recent studies found that MADS-box genes are capable of controlling lignin deposition in specific plant tissues such as the stem (Cosio et al., 2017) and fruit flesh (Ge et al., 2021), which expands the scope of MADS-box genes' molecular functioning. By synthesizing the available information, a hypothesis may be deduced: that MADS-box genes are somehow involved in senescence-triggered lignification in loquat flesh.

In this study, both senescence- and chilling-induced lignification of flesh during the storage of loquat fruits were simulated by temperature treatments. The lignin content of flesh samples under two treatments, 20°C and 0°C, was measured. Transcriptome and correlation analysis were carried out to distinguish the MADS-box genes associated with senescence-induced lignification; a MADS-box gene, named *EjAGL15*, was found to be positively related to the variation in lignin content of loquat flesh. Meanwhile, the biological function of the identified MADS-box gene for regulating lignin deposition was investigated via the dual luciferase assay.

2 Materials and methods

2.1 Plant materials and treatment

Loquat fruits (*E. japonica* cultivar 'Luoyangqing') were harvested in Luqiao, Zhejiang Province, China, then packaged in plastic foam boxes, and taken to the laboratory by vehicle. Upon

arrival the fruits were immediately sorted and selected according to the color of their pericarp, ensuring uniformity of maturity, and transferred to atmosphere chambers. Two chambers were set respectively to 20°C and 0°C, as two treatment groups, thus emulating shelf storage and cold storage conditions, respectively. Fruits were sampled at the beginning of storage, and then again after 2, 6, and 10 days. Each time-point had three biological replicates, with each replicate consisting of four fruits. These fruit flesh samples without the pericarp were immediately frozen in liquid nitrogen for status fixation, then stored at –80°C.

2.2 Lignin content analysis

Total lignin content was measured based on the methodology described by Lowry et al. (1994) with minor modifications applied. The 1-g lyophilized sample was ground into powder and mixed with 100 mL of acidic wash buffer (0.5 mol/L sulfuric acid, 0.05 mol/L hexadecyl trimethyl ammonium Bromide), 2 mL of decahydronaphthalene, and 0.5 g of sodium sulfite in a beaker, then boiled for 60 min. After discarding the acidic wash buffer, the residual material was washed with distilled water until the flow-through became neutral; this was followed by another washing step using about 20 mL of acetone. The washed residual material was transferred into an oven and dried at 105°C for 2 h. This dried residue, which mainly consisted of acid detergent fiber (ADF), was put in a desiccator for 30 min, and cooled to room temperature. The ADF was hydrolyzed in 10 mL of 72% H_2SO_4 for 3 h then incubated overnight after adding 45 mL of distilled water. The hydrolyzed ADF was weighed (W_1) following filtration and a washing step. The residual material was transferred to a muffle furnace and burned for 2.5 h at 550°C, and then weighed (W_2). The lignin content was equal to the weight loss (W_1–W_2) of the residual material.

2.3 Detection of guaiacyl and syringyl lignin units

The 20-mg well-ground sample was mixed with 1 mL of a freshly prepared dioxane solution containing 2.5% boron trifluoride and 10% ethyl mercaptan. The mixture was then incubated at 100°C for 4 h, and the reaction ended by rapid cooling at –20°C for 5 min. Tetracosane was added, as an internal standard, to yield final concentration of 0.1 mg/mL. Meanwhile, each sample was thoroughly mixed with dichloromethane (1 mL) and water (2 mL) for separation. The organic phase was carefully transferred to a new tube into which sodium sulfate was added to remove the water. After complete volatilization, the solute was redissolved in 0.4 mL of dichloromethane. Before its gas chromatography analysis, pyrimidine (50 µL) and bovine serum albumin (100 µL) were added to the sample solution, and it incubated at 25°C for 4 h.

The degraded lignin units were determined by GC/MS (Trace1310 ISQ, Thermo) with a TG-5MS column (Thermo, 30 m × 0.25 mm × 0.25 µm). The GC conditions were set as follows: initial column temperature of 60°C; ramped at 35°C/min, 0.5°C/min, and 50°C/min to 220°C, 230°C, and 280°C respectively, then held for 7 min; injection temperature of 250°C; flow rate of carrier gas: 1.2 mL/min; sample loading volume of 2 µL; injection model: split, using a split ratio of 20:1. The MS conditions were as follows: an EI voltage of 70 eV; ion source temperature of 200°C; interface temperature of 250°C; solvent delay, 5 min; and, monitoring range: 40–650 amu.

2.4 Total RNA extraction and quantitative reverse transcription PCR

Total RNA in the flesh of each replicate sample was extracted using CTAB methods (Shan et al., 2008). Genomic DNA was removed by implementing the TURBO DNA-free kit (Ambion). The quality of extracted RNA was determined by gel electrophoresis and spectrophotometry (Implen), after which the corresponding first-strand cDNA was synthesized using the PrimeScript™ RT reagent kit (Takara). The gene transcripts were quantified on a CFX384 Real-Time System (Biorad), with SsoFast EvaGreen Supermix (Biorad). The primers for quantitative reverse transcription PCR were designed based on the 3' region of coding sequence, using Primer3 software (v4.0.0; http://bioinfo.ut.ee/primer3/), and are listed in Supplementary Table S1. The PCR program was set to 30 s at 95°C, followed by 45 cycles at 95°C for 5 s and 60°C for 5 s, and completed with a melting curve analysis program. The *EjACT* (Fu et al., 2012) gene served as an internal control and relative gene expression levels were calculated using the $2^{-\Delta CT}$ method.

2.5 Phylogenetic analysis

The amino acid sequences of Arabidopsis and loquat MADS-box genes were respectively downloaded from TAIR (www.arabidopsis.org) and NCBI (www.ncbi.nlm.nih.gov). The phylogenetic tree was constructed using MEGA 11 (Tamura et al., 2021), by applying the Neighbor-Join and BioNJ algorithms to a matrix of pairwise distances estimated using the JTT (Jones-Taylor-Thornton) model, and then selecting the topology having the superior log-likelihood value. A discrete Gamma distribution was used to model the differences in evolutionary rate among sites. The branches and gene names were then labeled with different colors, using the 'ggtree' (Yu et al., 2017) and 'treeio' (Wang et al., 2020) R packages.

2.6 Dual luciferase assay

The dual luciferase assay was performed as previously described (Xu et al., 2014). The coding sequence of *EjAGL15* was amplified using the primer listed in Supplementary Table S2 and inserted into the pGreen II 0029 62-SK vector (SK). The promoters of lignin

deposition-related genes from both loquat and Arabidopsis were delivered to the pGreen II 0800-LUC vector (LUC). All the recombinant SK and LUC vectors were individually transfected into *Agrobacterium tumefaciens* GV3101. The glycerol stocks with transfected *Agrobacterium* were grown in a lysogeny broth (LB) plates with kanamycin (50 μg/mL) and gentamycin (25 μg/mL) for 2 days, and then restreaked onto new LB plates for 1 day. *Agrobacterium* cells were suspended in an infiltration buffer (10 mM MES, 10 mM $MgCl_2$, 150 mM acetosyringone, pH 5.6) to an optimal density (OD_{600} = 0.75), then 1 mL of *Agrobacterium* cultures containing *EjAGL15* were mixed with 100 μL of *Agrobacterium* containing the promoters. The mixtures were then injected into tobacco (*Nicotiana tabacum*) leaves, via needleless syringes; 3 days after that infiltration, both LUC and REN fluorescence intensities were measured using the dual luciferase assay reagents (Promega). Five replicates were conducted for *EjAGL15* and each promoter combination.

2.7 Statistical analyses

Pearson's correlation coefficient and *p*-values between the transcript abundance of MADS-box genes and lignin content flesh were first calculated and then arranged in the form of a matrix, using R software (v4.2.2). This matrix was then visualized using the R package 'corrplot'. Statistical differences were tested by two-tailed, unpaired Student's *t*-test and ANOVA followed by Fisher's LSD test using Origin 2023. For all these analyses, a significance level $p < 0.05$ was used.

3 Results

3.1 Distinct pattern of lignin accumulation under contrasting temperatures

The amounts of total lignin and the three units consisting of differing monolignols in the flesh of loquat fruits were monitored during their storage under the 20°C and 0°C treatments. The fruits stored at 20°C continuously accumulated lignin in flesh during the whole storage period, increasing their content from 10.15 to 40.6 mg/g, a phenomenon typical of postharvest flesh lignification. On the contrary, lignin accumulation was effectively alleviated by storage at 0°C, though the lignin content did slowly increase from 10.15 to 16.18 mg/g due to chilling injury (Figure 1A). As a kind of dicot plant, loquat's fruit flesh contains the guaiacyl (G) and syringyl (S) lignin units, but the *p*-hydroxyphenyl (H) lignin unit was beyond the detection limit (Figures 1B, C). The content of both G and S units changed in a temperature-dependent manner, which again confirmed the stalled lignification by cold storage. The greatest difference in lignin units arose on day 6 of storage, when the G and S units were 52.9% and 66.7% higher than at the onset of storage, respectively, indicating the continuous activation of the lignin biosynthesis pathway.

3.2 Quantified transcripts of MADS-box family genes

Because the lignin content of flesh differed significantly between the 20°C and 0°C conditions at 6 days of storage, samples from two time-points (the 1st and 6th day under storage) of each condition were collected for their transcriptome analysis. Although about 89 MADS-box members were annotated in the loquat genome database (Liu et al., 2022), we found only 28 MADS-box genes active above the detection limit of high-throughput sequencing. Next, we tried to trace the transcripts of those MADS-box genes detected in the transcriptome data at all time-points during the storage experiment, as this could provide more information. Due to the low abundance of transcripts, 10 pairs of primers met the requirements for successful measurements. The changed transcript levels of loquat's MADS-box genes during the storage period are shown in Figure 2. Despite all these genes being expressed differently between the two time-points under the same storage condition, or between the two storage temperatures within the same time-point based on transcriptome data, some of them were statistically insignificant. Actually, the transcript abundances of *EVM0016672*, *EVM0029116*, *EVM0043458*, and *EVM0020139* were not significantly different at any time-points within or between storage conditions, whereas *EVM003568*, *EVM0040152*, and *EVM0068673* were expressed differently only at time-points of a certain storage condition. Additionally, the transcripts of *EVM0041929* and *EVM0010237* were induced in loquat fruits during their storage under 0°C but maintained at a stable level under 20°C. Meanwhile, their difference in transcripts between temperatures was significant when fruits were stored for 6 days or longer. In contrast to *EVM0041929* and *EVM0010237*, the transcript abundance of *EVM0033729* continually increased at 20°C, significantly exceeding that at 0°C after 6 days of storage (Figure 2). The differential responses to temperature of loquat MADS-box genes may point to their distinctive functions in the lignification process under different storage conditions. However, further analysis of differentially expressed MADS-box genes (DEGs) using transcriptome data revealed four genes which exceeded the threshold of both the fold change and *p*-value between the comparison groups (Supplementary Figures 1A–C), of which *EVM0033729* was the only gene differentially expressed in all comparison groups (Supplementary Figure 1D). Thus, *EVM0033729* exhibited a unique temperature-dependent expression pattern in loquat flesh during fruit storage, which suggested it was highly involved in the lignification process.

3.3 Phylogenetic analysis of MADS-box genes

The sequences of the 10 quantified MADS-box genes were analyzed according to the Conserved Domain Database (https://www.ncbi.nlm.nih.gov/Structure/cdd/cdd.shtml), and all of them scored hits with specific motifs. All sequences harbored the

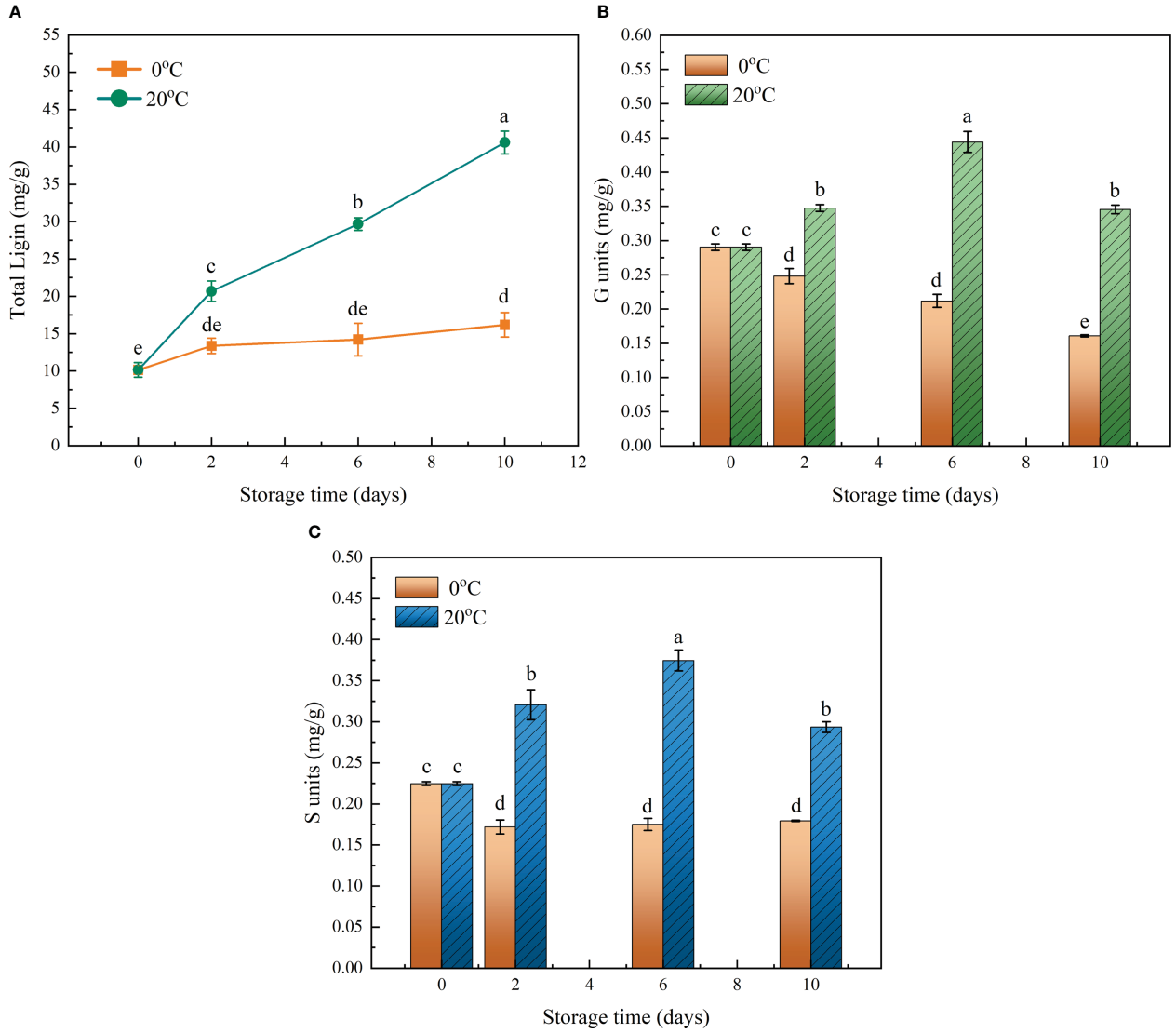

FIGURE 1
Effects of two contrasting storage temperatures on the lignin content of flesh in loquat fruit during its storage. **(A)** Change of total lignin content during the storage period. **(B)** Content of the guaiacyl (G) lignin unit. **(C)** Content of the syringyl (S) lignin unit. Error bars are the SE of the mean, based on n = 3 biological replicates. Different letters indicate significantly different means of groups in the comparison ($p < 0.05$).

conserved MADS-box domain at their N terminal (Supplementary Figure 2), which is a homolog to the SRF domain in mammals. But three of the sequences lacked the K domain, as symbolized in the MIKC subgroup of the MADS-box family. The gene structure of each of these MADS-box genes was visualized next, according to the genome data. Genes with or without the K domain differ in the number and length of introns (Supplementary Figure 3). Generally, genes without the K domain have fewer or shorter introns than genes with the K domain. Even *EVM0008673* had no introns, implying the conservation of its gene functions during the evolution of loquat plants.

To better predict their biological function, we built a phylogenetic tree using the sequences of the 10 MADS-box genes, together with four previously reported loquat MADS-box genes and Arabidopsis MADS-box analogs, whose functions are well elucidated. Multiple models for describing the substitution pattern were first evaluated and the JTT with a discrete Gamma distribution (JTT+G+F) mixed model yielded the lowest Bayesian Information Criterion (BIC) score (Supplementary Table S3). As Figure 3 shows, the Arabidopsis MADS-box genes were divided into five clades (Mα, Mβ, Mγ, Mδ, MIKC), which is consistent with the findings of an earlier report (Parenicova et al., 2003). Different colors were used to distinguish species and subgroups to enhance their visualization. Evidently, the loquat MADS-box genes are dispersed in a different subgroup of the tree, but the number of loquat genes in each clade varies considerably. Most loquat MADS-box genes are localized at the MIKC group, while the Mα, Mβ, Mγ, and Mδ group included 0,

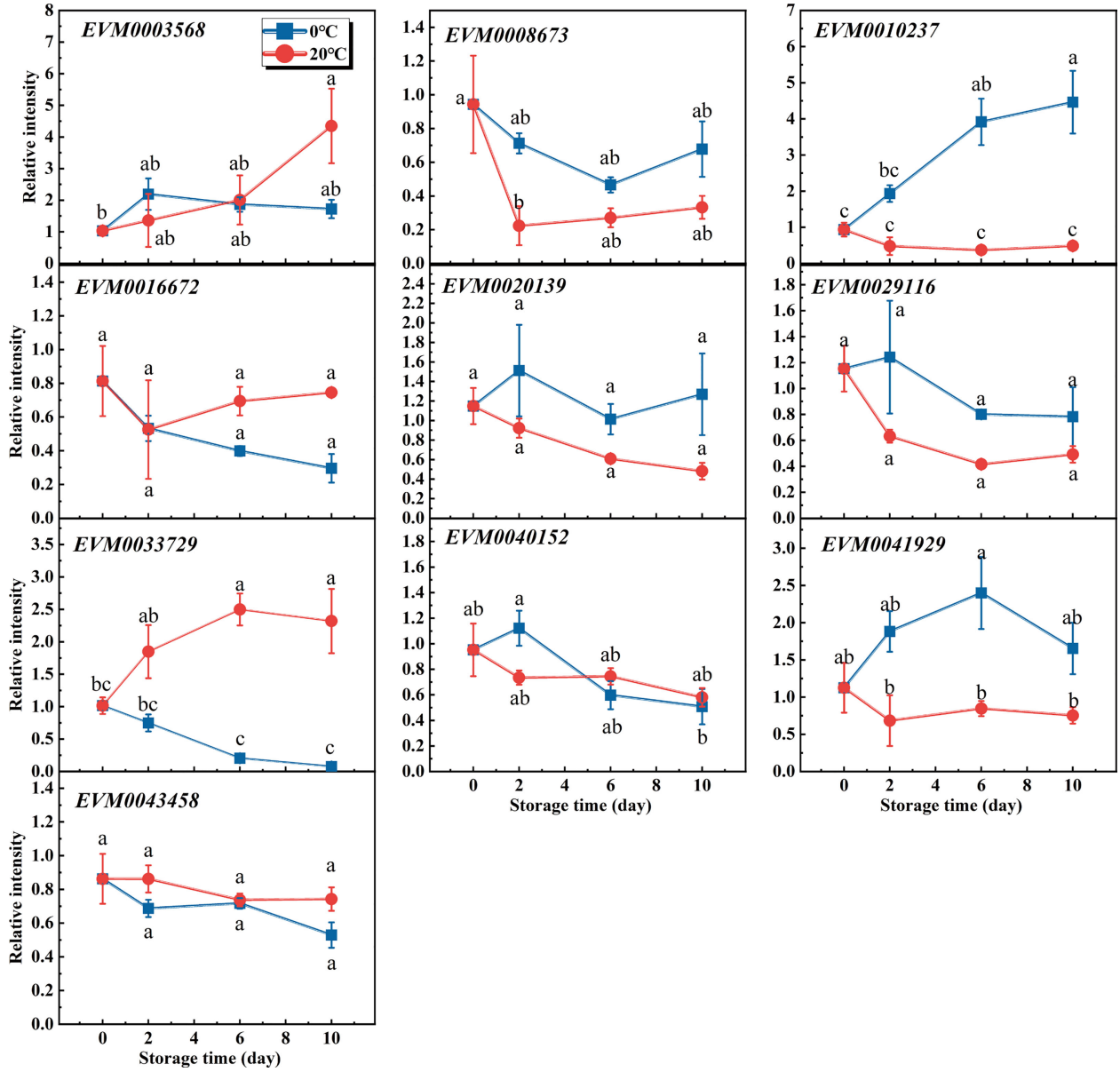

FIGURE 2
Characterization of the differentially expressed MADS-box genes by quantitative reverse transcription PCR and the transcriptome analysis. Transcripts of 10 MADS-box genes were monitored during the storage of loquat fruit under 20°C versus 0°C. Error bars are the SE of the mean, based on n = 3 biological replicates. Different letters indicate significantly different means of groups in the comparison ($p < 0.05$).

0, 1, and 2 genes, respectively. This constructed tree provided general structural and evolutionary information about loquat's MADS-box genes extracted from its genome, but clues concerning lignin-related MADS-box gene were limited. The MADS-box members are mainly considered as key regulators of flowering; hence, the relation between MADS-box genes and lignin content remains poorly elucidated. In fact, Arabidopsis AGL15 is the only member confirmed as involved in lignin deposition (Cosio et al., 2017). Thus, EVM0033729 may have a similar function to AGL15 due to their short evolutionary distance and was renamed *EjAGL15* for the follow-up investigation.

3.4 Relationship between *EjAGL15* transcripts and lignin content during storage

Correlations were tested given that the transcript levels of MADS-box genes and the lignin content of flesh both varied in a temperature-dependent pattern. Genes except *EVM0043458* and *EVM0040152* had a positive or negative correlation with either the content of monolignols or total lignin (Figure 4 all p-values < 0.05). To obtain more convincing results, the correlations were re-evaluated using a lower threshold p-value. Correspondingly, we

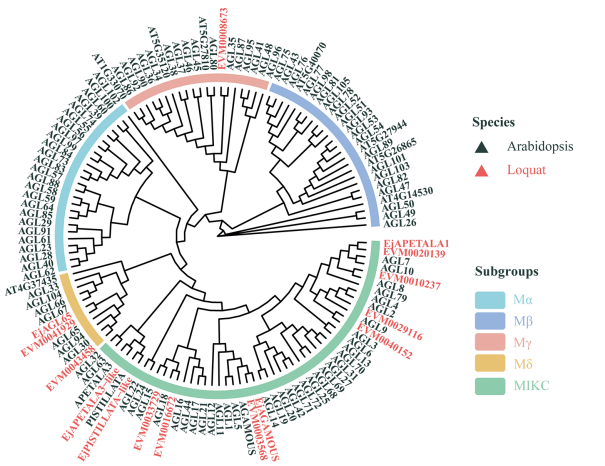

FIGURE 3
Phylogenetic analysis of loquat and Arabidopsis MADS-box genes. The tree was constructed using the Jones-Taylor-Thornton model. Genes belonging to loquat and Arabidopsis are in red and black, respectively. Arcs with different colors represent the five subgroups of Arabidopsis MADS-box genes.

uncovered five highly significant correlations (all p-values < 0.01). Specifically, *EVM0010237* and *EVM0020139* were negatively correlated with the G unit and total lignin content, respectively, while *EVM0033729* and *EVM0003568* had positive correlations with the either G unit, S unit, or total lignin content. Moreover, when applying a stricter threshold of $p < 0.001$, the correlation between *EVM0033729* and the G or S unit were still significant. Besides, among these MADS-box genes, the coefficient values for the correlations of *EVM0033729* were the highest ($r = 0.81$ and $r = 0.79$ with the G and S unit, respectively). These empirical clues strongly implied that a close relationship between *EjAGL15* and lignin deposition exists in the flesh of loquat fruit.

3.5 Interactions between EjAGL15 and lignin biosynthesis-related genes

Altogether, the above results pinpointed a MADS-box gene, *EjAGL15*, as being likely involved in regulating the lignification process in fleshy tissues of loquat. Next, the dual luciferase assay was performed to reveal the potential protein-DNA interactions *in vivo*. As Figure 5A shows, EjAGL15 had a strong activation effect on the promoters of four genes: *EjPAL1*, *Ej4CL1*, *EjCAD3*, and *EjCAD4*. In addition to the induction of genes participating in the lignin biosynthesis pathway, *EjAGL15* also significantly activated certain transcriptional regulators, like *EjMYB8*, which is a key activator of flesh lignin deposition, suggesting its role as a positive regulator. However, another activator, *EjMYB1*, was inhibited by transient overexpression of *EjAGL15*; this runs counter to an increased lignin content of flesh. Meanwhile, activation of the *EjMYB2*'s promoter could have a negative influence on the rate of lignin deposition as well. Further, the expression of *EjPRX12*, which is known to be involved in the polymerization of monolignols (Zhang et al., 2022), is inhibited by EjAGL15. This inconsistent influence on positive or negative regulators of the flesh lignification process means that *EjAGL15* probably fulfills complex roles in the manipulation of lignin deposition in loquat fruit during the senescence process.

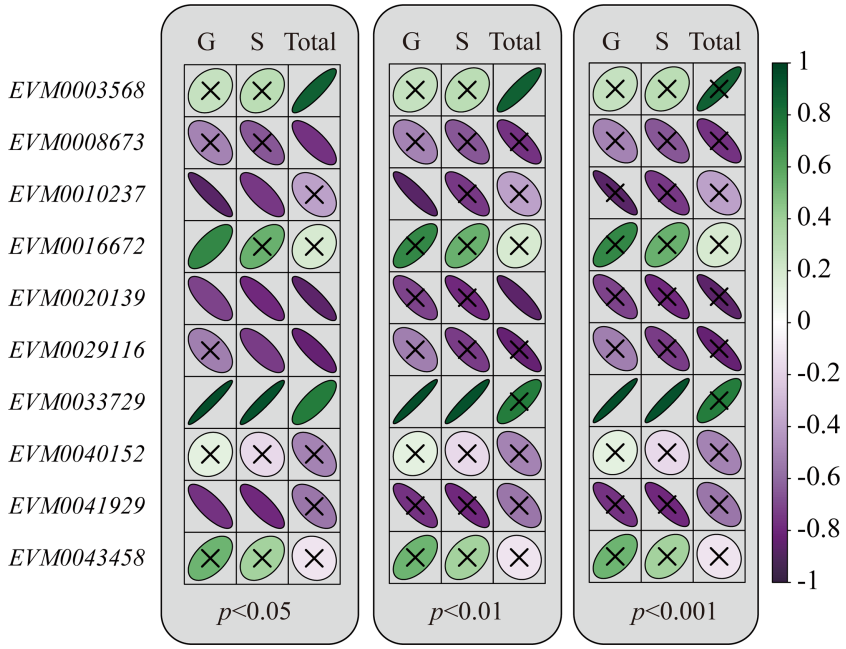

FIGURE 4
Relationship between the change in transcripts abundance and lignin content during the storage of loquat fruit. The Pearson correlation coefficients are visualized by the color gradient (far right). Green color indicates a positive value while purple refers to a negative value for Pearson's *r*. The significance of each correlation was visualized by the focal distance of ellipse. A flatter ellipse represents a lower p-value for the correlation. Insignificant correlations under a certain significant level are labeled with the cross symbol.

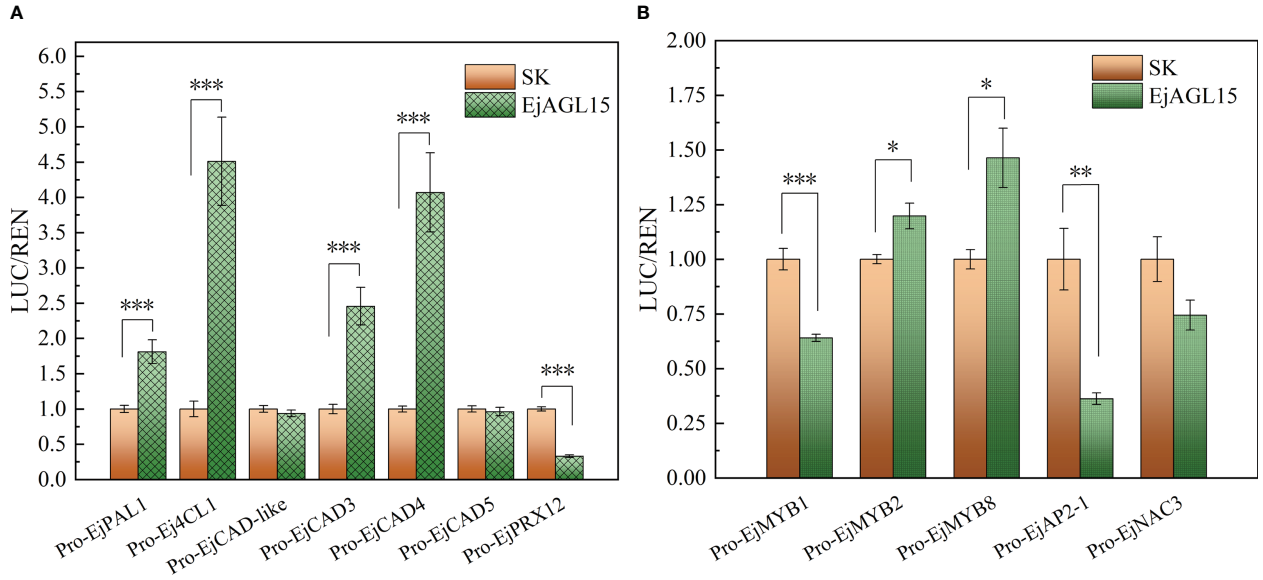

FIGURE 5
Biological effect of EjAGL15 on the promoter region of genes in the phenylpropanoid pathway **(A)** and lignification-related transcription factors **(B)**. Error bars are the SE of means based on five biological replicates. The number of asterisks corresponds to a more stringent significant level (Student's *t*-test; "*", "**" and "***" mean p<0.05, 0.01 and 0.001 respectively).

4 Discussion

4.1 *EjAGL15* positively modulates lignin deposition in loquat flesh

Fruits generally contain less lignin when compared to other parts of plants. However, the fruit of loquat (*E. japonica*) accumulates lignin in its flesh during postharvest storage, being a typical example of fruit lignification. Extensive studies have focused on revealing the molecular mechanism behind flesh lignification. A series of transcription factors have been characterized as regulators of flesh lignification in loquat, notably the MYB (Xu et al., 2014; Zhang et al., 2020) and NAC (Ge et al., 2017) family members. Recently, novel regulators other than NAC and MYB have been uncovered, providing new perspectives and insight for understanding the complicated regulatory mechanism of fruity flesh lignification (Xu et al., 2019; Ge et al., 2021; Zhang et al., 2022). Here, we found that the MADS-box family gene *EjAGL15* is involved in lignin deposition in fruit flesh. Unlike other regulators of flesh lignification, *EjAGL15* is an activator of multiple genes in the phenylpropanoid pathway, including *EjPAL1*, *Ej4CL1*, *EjCAD3*, and *EjCAD4*. Both *EjPAL1* and *Ej4CL1* are located upstream of the phenylpropanoid pathway and are responsible for the removal of an amino group of phenylalanine and the addition of coenzyme A, respectively (Boerjan et al., 2003; Vanholme et al., 2019). The *EjCAD3* gene encodes an enzyme that catalyzes the conversion of coniferyl aldehyde to coniferyl alcohol (Xu et al., 2019). Accordingly, the strong activation of these genes by *EjAGL15* would facilitate the flux of metabolites directed toward monolignol synthesis, which accords with the augmented G and S lignin units observed during loquat fruits' postharvest storage. Despite its role in lignin biosynthesis, *EjAGL15* also regulates lignin monomer polymerization to some extent. Interestingly, *EjAGL15* impairs the promoter activity of *EjPRX12*, which is inconsistent with other monolignol biosynthesis-related genes. Given the molecular functions of enzyme-encoding genes that *EjAGL15* activates, the expression of *EjAGL15* should lead to the accumulation of coniferyl alcohol and sinapyl alcohol, both being substrates for lignin polymerization. Nevertheless, the repression of *EjPRX12*'s promoter indicates a negative effect on the polymerization of monolignols, which seems contrary to the lignin content increasing during the postharvest storage period. This contradiction may be explained by the redundancy of genes that encode peroxidase. It has been confirmed that multiple PRXs are associated with lignin content in the stem tissue of Arabidopsis, such as *AtPRX52* (Fernandez-Perez et al., 2015b), *AtPRX71* (Shigeto and Tsutsumi, 2016), and *AtPRX72* (Herrero et al., 2013; Fernandez-Perez et al., 2015a). In loquat, EjPRX12 is able to specifically catalyze sinapyl alcohol (Zhang et al., 2022), and other lignin-related PRX genes have yet to be reported. Considering our findings that the G lignin content continually increases during loquat storage, but EjPRX12 does not use coniferyl alcohol as a substrate, we may infer that other genes encoding peroxidase are required for biosynthesis of the G unit. This circumstantial evidence proves that *EjPRX12* alone is insufficient for complete polymerization of all lignin units present in loquat flesh. Meanwhile, those genes responsible for lignin biosynthesis are strongly activated by *EjAGL15* and this leads to the accumulation of monolignols. Hence, the sole inhibition of *EjPRX12* may not slow the rate of monolignol polymerization enough to significantly reduce the flesh lignin content.

Apart from genes in the phenylpropanoid pathway, *EjAGL15* also affects multiple regulators of loquat flesh lignification (Figure 5B). According to the luciferase assay, the EjAGL15 had an activation or repression effect on the promoters of MYB, AP2, and NAC family members. Both *EjMYB2* and *EjMYB8* are

significantly up-regulated by EjAGL15 whereas *EjMYB1* and *EjAP2*-1 are repressed. Interestingly, the regulatory effects of EjAGL15 on different lignification regulators does not lead to a consistent influence upon *Ej4CL1*, which is the direct target of *EjMYB1*, *EjMYB2*, and *EjMYB8*. For instance, *EjMYB2* and *EjMYB8* are a repressor and activator of *Ej4CL1*, respectively, and yet both are activated by *EjAGL15*. In general, *EjAGL15* functions more like a positive regulator of flesh lignification due to its strong activation of genes encoding lignin biosynthesis-related enzymes and its significant positive correlation with lignin content.

Although *EjAGL15* has biological functions vis-à-vis multiple lignin-related genes, the direct linkage between *EjAGL15* and them or regulators of lignification have not been established. Intriguingly, the abundance of *EjMYB8* and *EjERF39* transcripts remained at a markedly low level at 20°C versus 0°C (Zhang et al., 2020), which presumably limits their activation effect on *Ej4CL1*'s promoter. Hence, we suspect the strong activation on *Ej4CL1* by *EjAGL15* should be mediated by genes other than *EjMYB8* and *EjERF39*, this corresponding to the existence of a senescence-specific signal transduction routine in which *EjAGL15* acts as one of the key nodes.

4.2 *EjAGL15* is involved in senescence-induced flesh lignification

In loquat fruits, lignin gets deposited in their flesh during postharvest storage at either 20°C or 0°C and the responsible mechanisms are thought differ (Yang et al., 2010). Generally, senescence and chilling injury are considered crucial factors that account for the postharvest lignification of loquat at 20°C and 0°C, respectively, in that both processes entail genes being activated in the phenylpropanoid pathway, such as *Ej4CL1* and *EjCAD5* (Li et al., 2017; Xu et al., 2019). According to previous reports, the lignin deposition in loquat flesh in response to chilling injury is mainly regulated by various transcription factors, such as those in the MYB family (Xu et al., 2014; Zhang et al., 2020); however, it remains unclear whether senescence-induced lignin deposition is likewise under control of that same set of genes. Actually, transcript profiles during loquat fruit's storage at 20°C have not been characterized for most of its transcription factors active in the regulation of chilling-induced flesh lignification, with the exception of *EjMYB8* and *EjERF39*. However, the abundance of *EjERF39* and *EjMYB8* transcripts is low during storage at 20°C (Zhang et al., 2020), indicating their absence in modulating lignin deposition during senescence. The limited results discovered previously left it difficult to reliably identify key regulators of senescence-induced lignin deposition in loquat flesh. In this study, we discovered a MADS-box gene, *EjAGL15*, whose transcription was induced during storage at 20°C but at 0°C it declined continually. The expression pattern of *EjAGL15* indicates this gene has a close relationship with senescence, as confirmed by the Pearson correlations with the flesh lignin data. Further, *EjAGL15* probably fulfills its function only at 20°C given the low abundance of its gene transcripts at 0°C. Collectively, these clues indicate that *EjAGL15* drives a rapid augmentation of lignin content under loquat fruit's storage at 20°C, but not so at 0°C. Thus, *EjAGL15* tends to activate lignin biosynthesis via senescence-induced lignification rather than a reliance on chilling.

The senescence-related expression pattern of *EjAGL15* is consistent with its homologs in Arabidopsis. The Arabidopsis *AGL15* is a repressor of senescence and overexpressing this gene leads to the increase of perianth longevity (Fang and Fernandez, 2002). The delay in perianth abscission originates from the repression of abscission-related genes, like the receptor-like protein kinases *HAESA*, by AGL15 in Arabidopsis (Patharkar and Walker, 2015). On the other hand, *AGL15* has been suggested to function as a regulator in lignified tissue formation (Cosio et al., 2017). Although it could be hypothesized that *AGL15* postpones the senescence-induced abscission of perianth by regulating lignin deposition in the abscission zone, the detailed mechanism by which *AGL15* manipulates lignin deposition has not been fully revealed. Thus, it is hard to predict the exact targets of *EjAGL15* based on its Arabidopsis homologs. Here, we identified several potential targets of the *EjAGL15*, including *Ej4CL1*, *EjCAD3*, *EjCAD4* and *EjPRX12*, which explains how senescence can trigger flesh lignification in loquat. *EjPRX12* most resembles the homolog of Arabidopsis *PRX17*, which is reportedly under regulation by *AGL15*. Similarly, in this study, we find that *EjAGL15* significantly inhibits the promoter of *EjPRX12*. However, the activation effect of *EjAGL15* upon lignin biosynthesis-related genes such as *Ej4CL1*, *EjCAD3*, and *EjCAD4* has not been found in Arabidopsis. Our data indicate *EjAGL15* may regulate not only polymerization but also the biosynthesis of monolignol. The discovery of *EjAGL15* provides a node that had been missing in the complex network used to regulate senescence-induced lignification, making it now possible to screen other genes that work synergistically or antagonistically with *EjAGL15*.

4.3 The discovery of *EjAGL15* extends our understandings of the regulatory mechanism of lignin-related MADS-box gene in loquat

Generally, MADS-box genes are considered to operate as regulators of flower morphogenesis or pollen maturation (Michaels and Amasino, 1999; Yu et al., 2014). For example, the loquat MADS-box genes *EjCAL* can promote the flower bud differentiation process (Xu et al., 2022). The connection between MADS-box genes and fruit lignification could not be established until the loquat *EjAGL65* was first identified (Ge et al., 2021). The *EjAGL65* gene is responsive to chilling injury but not senescence, and it negatively regulates lignin biosynthesis. As the second lignin-related MADS-box gene found in loquat, *EjAGL15* differs from *EjAGL65* in many aspects. Firstly, *EjAGL15* is not a member of the Mδ subgroup to which EjAGL65 belongs. Through phylogenetic analysis we find that *EjAGL15* is assigned to the MIKC subgroup of Arabidopsis, as per the classification by Parenicova et al. (2003). Members of that MIKC subgroup have been proven to play pivotal roles in plant development (Gramzow and Theissen, 2010; Schilling et al., 2020) and plant responses to stress (Arora et al., 2007; Jia et al., 2018). Interestingly, *EjAGL15* is a close homolog of

Arabidopsis *AGL15*, which participates in age-dependent lignified tissue formation (Cosio et al., 2017). Overexpressing *AGL15* leads to the deposition of lignin in the dehiscent zone of petal and sepal parts in Arabidopsis, thus delaying the senescence of perianth (Fang and Fernandez, 2002). The results of the present study imply a similar role for *EjAGL15* as a positive regulator of lignin deposition. But the increased abundance of *EjAGL15* transcripts in flesh tissue results in the deposition of lignin in the same area, which unexpectedly changed the function of *EjAGL15*: from delaying senescence to deteriorating fruit quality. Secondly, *EjAGL15* was able to activate lignin biosynthesis-related genes and its transcript abundance is positively correlated with lignin content, which suggests an effect opposite that exerted from *EjAGL65* on regulating flesh lignification. In addition, *EjAGL15* exacts a biological effect on multiple targets in the phenylpropanoid pathway, but the target of *EjAGL65* is limited to *Ej4CL1*. Furthermore, *EjAGL15* and *EjAGL65* are induced by different storage temperatures and regulate lignin deposition under differing physiological disorders. All the above lines of evidence point to *EjAGL15* and *EjAGL65* respectively having a positive and negative influence upon flesh lignin deposition, for which the genes recruited by them for transducing the signal from senescence and chilling injury also differ. Considering the fact that the lignin content of loquat fruit flesh increased so rapidly under the 20°C treatment condition, in tandem with key regulators of chilling-induced lignification like *EjMYB8* and *EjERF39* not being highly transcribed, *EjAGL15* probably activates lignin biosynthesis via a pathway that is independent of the currently discovered transcription factors. Altogether then, the MADS-box family genes *EjAGL15* and *EjAGL65* are deeply involved in manipulating senescence- and chilling-induced lignin deposition, respectively.

5 Conclusion

This study identified a MADS-box gene, *EjAGL15*, induced by senescence. *EjAGL15* belongs to the MIKC subgroup of the MADS-box family and shows a positive correlation with the lignin content of loquat fruit flesh. The dual-luciferase assay revealed *EjPAL1*, *Ej4CL1*, *EjCAD3*, *EjCAD4*, and *EjPRX12* as potential targets of *EjAGL15*. Similar to its Arabidopsis homolog *AGL15*, *EjAGL15* functions in facilitating lignin deposition. However, in contrast to *AGL15* which delays the abscission of perianth by depositing lignin in the dehiscent zone, *EjAGL15* expression is induced in the flesh of loquat fruit, contributing to the deterioration of its fruit quality during storage.

Data availability statement

The datasets presented in this study can be found in online repositories. The names of the repository/repositories and accession number(s) can be found below: https://www.ncbi.nlm.nih.gov/genbank/, OQ435240.

Author contributions

JC and HG conceived the study and supervised the experiments. HG and XL performed the experiments and analysis. HG wrote the article. HX and JC was involved in the discussion of the manuscript organization and revised the manuscript. All authors contributed to the article and approved the submitted version.

Funding

This work is supported by the National Natural Science Foundation of China (grant no. 31901740) and the Key Scientific and Technological Grant of Zhejiang for Breeding New Agricultural Varieties (2021C02066-3).

Conflict of interest

The authors declare that the research was conducted in the absence of any commercial or financial relationships that could be construed as a potential conflict of interest.

Publisher's note

Supplementary material

The Supplementary Material for this article can be found online at: https://www.frontiersin.org/articles/10.3389/fpls.2023.1166262/full#supplementary-material

References

Arora, R., Agarwal, P., Ray, S., Singh, A. K., Singh, V. P., Tyagi, A. K., et al. (2007). MADS-box gene family in rice: genome-wide identification, organization and expression profiling during reproductive development and stress. *BMC Genomics* 8, 21. doi: 10.1186/1471-2164-8-242

Boerjan, W., Ralph, J., and Baucher, M. (2003). Lignin biosynthesis. *Annu. Rev. Plant Biol.* 54, 519–546.

Cai, C., Chen, K., Lu, J., Li, X., and Gong, M. (2006a). Texture changes and regulation of postharvest loquat fruit. *Acta Hortic. Sin.* 33 (4), 731–736.

Cai, C., Xu, C., Li, X., Ferguson, I., and Chen, K. (2006b). Accumulation of lignin in relation to change in activities of lignification enzymes in loquat fruit flesh after harvest. *Postharvest Biol. Technol.* 40 (2), 163–169. doi: 10.1016/j.postharvbio.2005.12.009

Cai, C., Xu, C., Shan, L., Li, X., Zhou, C., Zhang, W., et al. (2006c). Low temperature conditioning reduces postharvest chilling injury in loquat fruit. *Postharvest Biol. Technol.* 41 (3), 252–259. doi: 10.1016/j.postharvbio.2006.04.015

Cesarino, I. (2019). Structural features and regulation of lignin deposited upon biotic and abiotic stresses. *Curr. Opin. Biotechnol.* 56, 209–214. doi: 10.1016/j.copbio.2018.12.012

Chong, C., Xian, L., and KunSong, C. (2006). Acetylsalicylic acid alleviates chilling injury of postharvest loquat (Eriobotrya japonica lindl.) fruit. *Eur. Food Res. Technol.* 223 (4), 533–539. doi: 10.1007/s00217-005-0233-5

Cosio, C., Ranocha, P., Francoz, E., Burlat, V., Zheng, Y., Perry, S. E., et al. (2017). The class III peroxidase PRX17 is a direct target of the MADS-box transcription factor AGAMOUS-LIKE15 (AGL15) and participates in lignified tissue formation. *New Phytol.* 213 (1), 250–263. doi: 10.1111/nph.14127

De Michele, R., Formentin, E., Todesco, M., Toppo, S., Carimi, F., Zottini, M., et al. (2009). Transcriptome analysis of medicago truncatula leaf senescence: similarities and differences in metabolic and transcriptional regulations as compared with arabidopsis, nodule senescence and nitric oxide signalling. *New Phytol.* 181 (3), 563–575. doi: 10.1111/j.1469-8137.2008.02684.x

Ding, C. K., Wang, C. Y., Gross, K. C., and Smith, D. L. (2002). Jasmonate and salicylate induce the expression of pathogenesis-related-protein genes and increase resistance to chilling injury in tomato fruit. *Planta* 214 (6), 895–901. doi: 10.1007/s00425-001-0698-9

Fang, S. C., and Fernandez, D. E. (2002). Effect of regulated overexpression of the MADS domain factor AGL15 on flower senescence and fruit maturation. *Plant Physiol.* 130 (1), 78–89. doi: 10.1104/pp.004721

Fernandez-Perez, F., Pomar, F., Pedreno, M. A., and Novo-Uzal, E. (2015a). Suppression of arabidopsis peroxidase 72 alters cell wall and phenylpropanoid metabolism. *Plant Sci.* 239, 192–199. doi: 10.1016/j.plantsci.2015.08.001

Fernandez-Perez, F., Pomar, F., Pedreno, M. A., and Novo-Uzal, E. (2015b). The suppression of AtPrx52 affects fibers but not xylem lignification in arabidopsis by altering the proportion of syringyl units. *Physiologia Plantarum* 154 (3), 395–406. doi: 10.1111/ppl.12310

Fu, X., Kong, W., Peng, G., Zhou, J., Azam, M., Xu, C., et al. (2012). Plastid structure and carotenogenic gene expression in red- and white-fleshed loquat (Eriobotrya japonica) fruits. *J. Exp. Bot.* 63 (1), 341–354.

Ge, H., Shi, Y. N., Zhang, M. X., Li, X., Yin, X. R., and Chen, K. S. (2021). The MADS-box transcription factor EjAGL65 controls loquat flesh lignification via direct transcriptional inhibition of EjMYB8. *Front. Plant Sci.* 12, 652959. doi: 10.3389/fpls.2021.652959

Ge, H., Zhang, J., Zhang, Y. J., Li, X., Yin, X. R., Grierson, D., et al. (2017). EjNAC3 transcriptionally regulates chilling-induced lignification of loquat fruit via physical interaction with an atypical CAD-like gene. *J. Exp. Bot.* 68 (18), 5129–5136. doi: 10.1093/jxb/erx330

Gramzow, L., and Theissen, G. (2010). A hitchhiker's guide to the MADS world of plants. *Genome Biol.* 11 (6), 11. doi: 10.1186/gb-2010-11-6-214

Hao, Y., Chen, F., Wu, G., and Gao, W. (2016). Impact of postharvest nitric oxide treatment on lignin biosynthesis-related genes in wax apple (Syzygium samarangense) fruit. *J. Agric. Food Chem.* 64 (45), 8483–8490. doi: 10.1021/acs.jafc.6b03281

Herrero, J., Fernandez-Perez, F., Yebra, T., Novo-Uzal, E., Pomar, F., Pedreno, M. A., et al. (2013). Bioinformatic and functional characterization of the basic peroxidase 72 from arabidopsis thaliana involved in lignin biosynthesis. *Planta* 237 (6), 1599–1612. doi: 10.1007/s00425-013-1865-5

Huang, W., Zhu, N., Zhu, C., Wu, D., and Chen, K. (2019). Morphology and cell wall composition changes in lignified cells from loquat fruit during postharvest storage. *Postharvest Biol. Technol.* 157, 110975. doi: 10.1016/j.postharvbio.2019.110975

Jia, J. T., Zhao, P. C., Cheng, L. Q., Yuan, G. X., Yang, W. G., Liu, S., et al. (2018). MADS-box family genes in sheepgrass and their involvement in abiotic stress responses. *BMC Plant Biol.* 18, 11. doi: 10.1186/s12870-018-1259-8

Li, D., Limwachiranon, J., Li, L., Zhang, L., Xu, Y., Fu, M., et al. (2019). Hydrogen peroxide accelerated the lignification process of bamboo shoots by activating the phenylpropanoid pathway and programmed cell death in postharvest storage. *Postharvest Biol. Technol.* 153, 79–86. doi: 10.1016/j.postharvbio.2019.03.012

Li, X., Zang, C., Ge, H., Zhang, J., Grierson, D., Yin, X. R., et al. (2017). Involvement of PAL, C4H, and 4CL in chilling injury-induced flesh lignification of loquat fruit. *Hortscience* 52 (1), 127–131. doi: 10.21273/HORTSCI11304-16

Liu, N., Kou, Y., Li, X., Chen, X., Gao, H., Zhang, J., et al. (2022). Genome-wide identification and analysis of MADS-box gene family in loquat and its potential role in fruit ripening. *J. Fujian Agric. Forestry Univ.* 51 (3), 351–360.

Lowry, J. B., Conlan, L. L., Schlink, A. C., and McSweeney, C. S. (1994). Acid detergent dispersible lignin in tropical grasses. *J. Sci. Food Agric.* 65 (1), 41–49.

Mercier, S., Villeneuve, S., Mondor, M., and Uysal, I. (2017). Time-temperature management along the food cold chain: a review of recent developments. *Compr. Rev. Food Sci. Food Saf.* 16 (4), 647–667. doi: 10.1111/1541-4337.12269

Michaels, S. D., and Amasino, R. M. (1999). FLOWERING LOCUS c encodes a novel MADS domain protein that acts as a repressor of flowering. *Plant Cell* 11 (5), 949–956. doi: 10.1105/tpc.11.5.949

Nakano, Y., Yamaguchiz, M., Endo, H., Rejab, N. A., and Ohtani, M. (2015). NAC-MYB-based transcriptional regulation of secondary cell wall biosynthesis in land plants. *Front. Plant Sci.* 6. doi: 10.3389/fpls.2015.00288

Parenicova, L., de Folter, S., Kieffer, M., Horner, D. S., Favalli, C., Busscher, J., et al. (2003). Molecular and phylogenetic analyses of the complete MADS-box transcription factor family in arabidopsis: new openings to the MADS world. *Plant Cell* 15 (7), 1538–1551. doi: 10.1105/tpc.011544

Patharkar, O. R., and Walker, J. C. (2015). Floral organ abscission is regulated by a positive feedback loop. *Proc. Natl. Acad. Sci. U. S. A.* 112 (9), 2906–2911. doi: 10.1073/pnas.1423595112

Schilling, S., Kennedy, A., Pan, S., Jermiin, L. S., and Melzer, R. (2020). Genome-wide analysis of MIKC-type MADS-box genes in wheat: pervasive duplications, functional conservation and putative neofunctionalization. *New Phytol.* 225 (1), 511–529. doi: 10.1111/nph.16122

Shan, L. L., Li, X., Wang, P., Cai, C., Zhang, B., De Sun, C., et al. (2008). Characterization of cDNAs associated with lignification and their expression profiles in loquat fruit with different lignin accumulation. *Planta* 227 (6), 1243–1254.

Shi, Y., Li, B. J., Su, G., Zhang, M., Grierson, D., and Chen, K. S. (2022). Transcriptional regulation of fleshy fruit texture. *J. Integr. Plant Biol.* 64 (9), 1649–1672. doi: 10.1111/jipb.13316

Shigeto, J., and Tsutsumi, Y. (2016). Diverse functions and reactions of class III peroxidases. *New Phytol.* 209 (4), 1395–1402. doi: 10.1111/nph.13738

Tamura, K., Stecher, G., and Kumar, S. (2021). MEGA11: Molecular evolutionary genetics analysis version 11. *Mol. Biol. Evol.* 38, 3022–3027.

Vanholme, R., De Meester, B., Ralph, J., and Boerjan, W. (2019). Lignin biosynthesis and its integration into metabolism. *Curr. Opin. Biotechnol.* 56, 230–239.

Wang, L. G., Lam, T. T. Y., Xu, S. B., Dai, Z. H., Zhou, L., Feng, T. Z., et al. (2020). Treeio: an r package for phylogenetic tree input and output with richly annotated and associated data. *Mol. Biol. Evol.* 37 (2), 599–603. doi: 10.1093/molbev/msz240

Wang, H., Zhao, Q., Chen, F., Wang, M., and Dixon, R. A. (2011). NAC domain function and transcriptional control of a secondary cell wall master switch. *Plant J.* 68 (6), 1104–1114. doi: 10.1111/j.1365-313X.2011.04764.x

Xie, Q., Hu, Z., Zhu, Z., Dong, T., Zhao, Z., Cui, B., et al. (2014). Overexpression of a novel MADS-box gene SlFYFL delays senescence, fruit ripening and abscission in tomato. *Sci. Rep.* 4, 4367. doi: 10.1038/srep04367

Xu, H.-X., Meng, D., Yang, Q., Chen, T., Qi, M., Li, X.-Y., et al. (2022). Sorbitol induces flower bud formation via the MADS-box transcription factor EjCAL in loquat. *J. Integr. Plant Biol*, 1–21. doi: 10.1111/jipb.13439

Xu, Q., Yin, X. R., Zeng, J. K., Ge, H., Song, M., Xu, C. J., et al. (2014). Activator- and repressor-type MYB transcription factors are involved in chilling injury induced flesh lignification in loquat via their interactions with the phenylpropanoid pathway. *J. Exp. Bot.* 65 (15), 4349–4359. doi: 10.1093/jxb/eru208

Xu, M., Zhang, M. X., Shi, Y. N., Liu, X. F., Li, X., Grierson, D., et al. (2019). EjHAT1 participates in heat alleviation of loquat fruit lignification by suppressing the promoter activity of key lignin monomer synthesis gene EjCAD5. *J. Agric. Food Chem.* 67 (18), 5204–5211. doi: 10.1021/acs.jafc.9b00641

Yang, C., Duan, W., Xie, K., Ren, C., Zhu, C., Chen, K., et al. (2020). Effect of salicylic acid treatment on sensory quality, flavor-related chemicals and gene expression in peach fruit after cold storage. *Postharvest Biol. Technol.* 161, 111089. doi: 10.1016/j.postharvbio.2019.111089

Yang, Z., Wang, Z., and Jin, X. (2010). Effect of storage temperature on quality of loquat fruits from different cultivars. *Food Sci.* 31 (20), 481–484.

Yi, S. Y., Rameneni, J. J., Lee, M., Song, S. G., Choi, Y., Lu, L., et al. (2021). Comparative transcriptome-based mining of senescence-related MADS, NAC, and WRKY transcription factors in the rapid-senescence line DLS-91 of brassica rapa. *Int. J. Mol. Sci.* 22 (11), 6017. doi: 10.3390/ijms22116017

Yu, L. H., Miao, Z. Q., Qi, G. F., Wu, J., Cai, X. T., Mao, J. L., et al. (2014). MADS-box transcription factor AGL21 regulates lateral root development and responds to multiple external and physiological signals. *Mol. Plant* 7 (11), 1653–1669. doi: 10.1093/mp/ssu088

Yu, G. C., Smith, D. K., Zhu, H. C., Guan, Y., and Lam, T. T. Y. (2017). GGTREE: an r package for visualization and annotation of phylogenetic trees with their covariates and other associated data. *Methods Ecol. Evol.* 8 (1), 28–36. doi: 10.1111/2041-210X.12628

Zhang, M., Shi, Y., Liu, Z., Zhang, Y., Yin, X., Liang, Z., et al. (2022). An EjbHLH14-EjHB1-EjPRX12 module is involved in methyl jasmonate alleviation of chilling-induced lignin deposition in loquat fruit. *J. Exp. Bot.* 73 (5), 1668–1682. doi: 10.1093/jxb/erab511

Zhang, J., Yin, X. R., Li, H., Xu, M., Zhang, M. X., Li, S. J., et al. (2020). ETHYLENE RESPONSE FACTOR39-MYB8 complex regulates low-temperature-induced lignification of loquat fruit. *J. Exp. Bot.* 71 (10), 3172–3184. doi: 10.1093/jxb/eraa085

Zheng, Y., Liu, Z., Wang, H., Zhang, W., Li, S., and Xu, M. (2022). Transcriptome and genome analysis to identify C2H2 genes participating in low-temperature conditioning-alleviated postharvest chilling injury of peach fruit. *Food Qual. Saf.* 6, 1–10. doi: 10.1093/fqsafe/fyac059

Zhong, R., and Ye, Z.-H. (2012). MYB46 and MYB83 bind to the SMRE sites and directly activate a suite of transcription factors and secondary wall biosynthetic genes. *Plant Cell Physiol.* 53 (2), 368–380. doi: 10.1093/pcp/pcr185

frontiers | Frontiers in Plant Science

TYPE Original Research
PUBLISHED 03 July 2023
DOI 10.3389/fpls.2023.1218734

OPEN ACCESS

EDITED BY
Isabel Lara,
Universitat de Lleida, Spain

REVIEWED BY
Brian Farneti,
Fondazione Edmund Mach, Italy
Anne Plotto,
Agricultural Research Service (USDA),
United States

*CORRESPONDENCE
Elizabeth J. Mitcham
ejmitcham@ucdavis.edu
Arlan James D. Rodeo
adrodeo@up.edu.ph

RECEIVED 08 May 2023
ACCEPTED 15 June 2023
PUBLISHED 03 July 2023

CITATION
Rodeo AJD and Mitcham EJ (2023) Chilling temperatures and controlled atmospheres alter key volatile compounds implicated in basil aroma and flavor.
Front. Plant Sci. 14:1218734.
doi: 10.3389/fpls.2023.1218734

Chilling temperatures and controlled atmospheres alter key volatile compounds implicated in basil aroma and flavor

Arlan James D. Rodeo[1,2*] and Elizabeth J. Mitcham[1*]

[1]Department of Plant Sciences, University of California, Davis, Davis, CA, United States, [2]Institute of Crop Science, College of Agriculture and Food Science, University of the Philippines Los Baños, College, Laguna, Philippines

Use of basil in its fresh form is increasingly popular due to its unique aromatic and sensory properties. However, fresh basil has a short shelf life and high chilling sensitivity resulting in leaf browning and loss of characteristic aroma. Moderate CO_2 atmospheres have shown potential in alleviating symptoms of chilling injury in basil during short-term storage but its effect on the flavor volatiles is unclear. Moreover, studies on basil volatile profile as impacted by chilling temperatures are limited. We investigated the response of two basil genotypes to low temperatures and atmosphere modification, with emphasis on the volatile organic compounds responsible for basil aroma and flavor. Leaves were stored for 6 days at 5, 10, or 15°C combined with three different CO_2 atmospheres (0.04%, 5% or 10%). Basil volatile profile was assessed using headspace solid phase microextraction (HS-SPME) coupled with gas chromatography-mass spectrometry (GC-MS). Leaves suffered severe chilling injury and greater loss of aroma volatiles at 5°C compared to 10°C and 15°C. More than 70 volatiles were identified for each genotype, while supervised multivariate analysis revealed 26 and 10 differentially-accumulated volatiles for 'Genovese' and 'Lemon' basil, respectively, stored at different temperatures. Storage in 5% CO_2 ameliorated the symptoms of chilling injury for up to 3 days in 'Genovese', but not in 'Lemon' basil. Both chilling temperatures and controlled atmospheres altered key volatile compounds implicated in basil aroma and flavor, but temperature had a bigger influence on the observed changes in volatile profile.

KEYWORDS

basil, chilling injury, volatile profile, controlled atmosphere, low temperature storage, aroma, flavor

1 Introduction

Basil (*Ocimum* spp.) is one of the most popular aromatic herbs grown in several regions of the world. It is considered an ultra-niche crop, one of exceptionally high-value that can provide a significant source of income to growers while using minimal land area (Matthews et al., 2018). As a culinary herb, basil leaves provide a crisp and aromatic element to a

variety of food and beverage preparations. It is also a source of essential oils, aroma compounds, and valuable phytonutrients known for their antioxidant properties (Simon et al., 1999; Filip, 2017). With the expanding market for fresh aromatic herbs, basil leaves have emerged as a significant segment in the global food ingredients market. The demand for fresh basil has increased immensely through the years due to the shift to healthier and better-tasting food preparations (Curutchet et al., 2014). However, fresh basil has a relatively short shelf life and is very sensitive to chilling temperatures (Cantwell and Reid, 1993; Lange and Cameron, 1997). Storage of basil at temperatures below 12°C during postharvest handling and transport results in chilling injury, characterized by brown discoloration of the interveinal areas of the leaf, stem browning and collapse, loss of glossy appearance, wilting of the leaves and loss of characteristic aroma (Lange and Cameron, 1994; Aharoni et al., 2010).

In basil, a range of management approaches at the farm level have been shown to lessen the severity of chilling injury, such as harvesting in the afternoon (Lange and Cameron, 1994; Aharoni et al., 2010), acclimating plants with less severe low temperatures before and after harvest (Lange and Cameron, 1994; Lange and Cameron, 1997), applying plant hormone treatments (Satpute et al., 2019) or applying artificial lighting during production (Dudai et al., 2017; Jensen et al., 2018). These methods can be supplemented by postharvest strategies to maximize the effect. Controlled atmospheres (CA) and modified atmosphere packaging (MAP) are some techniques used to alleviate chilling injury during transit and storage (Kader et al., 1989). Lowered O_2 and increased CO_2 concentrations achieved by atmosphere modification retard deterioration of harvested produce due to effects on physiological processes, including respiration, ethylene production, cellular composition, pathological breakdown, and other metabolic changes (Cantwell and Reid, 1993). Most atmosphere modification studies on basil have centered on extending the shelf life and delaying senescence at or above optimum temperatures for storage, i.e. 12°C (Lange and Cameron, 1998; Amodio et al., 2005; Kenigsbuch et al., 2009; Jirapong et al., 2010; Patiño et al., 2018). However, there is a need to explore the potential of CA storage at chilling temperatures, especially since basil is a chilling-sensitive crop and is being transported commercially in refrigerated vans with other chilling-tolerant commodities. Storage at moderate CO_2 atmospheres showed promise in alleviating chilling injury in 'Genovese' and 'Thai' basil (Rodeo and Mitcham, 2022). Whether this alleviation impacts basil aroma and flavor remains unknown.

Volatile organic compounds (VOCs) are responsible for the characteristic aroma and flavor of basil (Chang et al., 2007). Basil volatile profile consists mostly of monoterpenes, sesquiterpenes, and phenylpropenes, and a large number of these secondary metabolites are produced and stored in the glandular trichomes on the surface of the leaves (Gang et al., 2001; Iijima et al., 2004a). Different *Ocimum* species and cultivars vary in their essential oil components, which confer distinct taste and aroma. The sweet basil cultivars have a rich spicy pungent aroma due to the presence of compounds such as linalool, estragole (methylchavicol), 1,8-cineole and eugenol (Simon, 1995; Simon et al., 1999). The aroma of estragole can be compared to that of anise. Linalool and 1,8-cineole respectively give the floral and camphoraceous notes while eugenol is reminiscent of cloves (Burdock and Fenaroli, 2010). Lesser known types and some cultivars of commercial importance can contain a wide range of aromas and unique flavors, including lemon, licorice, or cinnamon (Simon, 1995; Simon et al., 1999).

Since basil is most commonly used as a culinary herb, it is vital that sensory attributes, particularly its aroma and flavor, are preserved because these contribute to the overall eating quality and consumer satisfaction. It is, therefore, important to find the best storage conditions that will limit significant alterations in volatile constituents and hence, flavor. Loss of these volatile organic compounds is among the consequences of chilling injury in fresh herbs (Xiao et al., 2015). Aroma and flavor loss could precede visible chilling symptoms manifestation, and assessment of volatile changes can be utilized as a diagnostic marker for imminent stress which can affect the condition of fresh produce (Cozzolino et al., 2016). Yet, information on the changes in volatile compounds of fresh basil subjected to chilling temperatures is limited. Moreover, the ability of controlled atmospheres to modulate the impacts of low temperature storage on basil volatile compounds has not been documented.

In the present work, we analyzed changes in the volatile compounds of two chilling-sensitive basil genotypes, 'Genovese' (*Ocimum basilicum*) and 'Lemon' (*Ocimum* × *citriodorum*), stored at different temperatures in an attempt to identify volatile markers implicated in the chilling response of the said basil types. We also explored the potential of moderate CO_2 atmospheres to alleviate chilling injury in both 'Genovese' and 'Lemon' and the impact of controlled atmospheres and low temperatures on the concentration of key basil flavor volatiles.

2 Materials and methods

2.1 Plant material

'Genovese' and 'Lemon' basil seeds were obtained from Botanical Interests® (Broomfield, CO, USA) and sown in a mixture of peat and sand (1:1 ratio by volume). Approximately 2 weeks after germination, seedlings were transplanted into 3-L pots with the same media and grown inside a climate chamber (BioChambers, Winnipeg, MB, Canada) set at 27 ± 0.2°C and 86 ± 5.6% RH with a 16-h photoperiod and canopy irradiance of 200 μmol m^{-2} s^{-1} provided by cool-white fluorescent lamps (Philips, Cambridge, MA, USA). Sixty days after sowing, leaves from the first four nodes starting from the apex were harvested and randomly packed inside a vented plastic clamshell (18.7 × 12.1 × 8.3 cm). Three clamshells per treatment, each containing approximately 15-30 leaves, depending on leaf size, were used for storage experiments.

2.2 Storage conditions

Clamshells containing basil leaves were stored at 5, 10 or 15°C. For each temperature, the leaves were exposed to three atmospheres: 10% CO_2 + 11% O_2; 5% CO_2 + 16% O_2; and 0.04% CO_2 + 21% O_2. Gas mixtures were passed through a gas flow board

at a continuous flow rate of 100 mL min^{-1}, bubbled through water for humidification, then supplied to plastic bags containing three clamshells each. One flow board delivered gas mixtures to three bags, each serving as a replicate. Gas concentration inside each bag was measured periodically using a CO_2/O_2 gas analyzer (Bridge Analyzers, Bedford Heights, OH, USA). Three clamshells (one from each bag) were withdrawn from storage for assessment of chilling injury and analysis of volatile changes after 3 and 6 days, and after an additional 2 days of storage at 20°C in air following 6 days of controlled atmosphere exposure.

2.3 Assessment of chilling injury

Visual damage due to chilling injury (i.e. browning of leaves) was assessed using the following scale (Wongsheree et al., 2009): (1) no damage, (2) several dark spots, (3) less than 30% of total leaf area brown, (4) 30–50% of leaf area brown, and (5) more than 50% of leaf area brown. Electrolyte leakage was determined according to the method described by Cozzolino et al. (2016) with slight modification. In brief, approximately 0.5 g of square leaf segments (0.5 cm^2), collected from three random leaf samples in clamshells previously stored at 5, 10, or 15°C, were washed with ultrapure water and placed in 10 mL of an isotonic solution of 0.1 M mannitol. Sample electrical conductivity was measured using a dual channel benchtop meter (Mettler Toledo, Columbus, OH, USA), after incubation for 30 min on a rotary shaker (Hoefer Scientific Instruments, San Francisco, CA, USA). Total conductivity was recorded following a 48-hour freeze/thaw cycle. Electrolyte leakage was recorded as the percentage ratio of initial over total conductivity.

2.4 Volatile analysis by gas chromatography-mass spectrometry

Headspace volatile compound analysis was performed using solid phase microextraction (SPME). Approximately 0.75 g of square leaf segments (0.5 cm^2) from three random basil leaf samples in a clamshell were immediately placed in a 20-mL headspace vial with a magnetic screw cap lined with a PTFE/silicon septum (Agilent Technologies, Santa Clara, CA, USA). SPME was performed using a divinylbenzene/carboxen on a polydimethylsiloxane (DVB/CAR/PDMS) 50/30 µm fiber (Supelco, Bellefonte, PA, USA) for 30 min at 40°C. The SPME fiber was injected into a gas chromatograph (Agilent Technologies 6890N Network GC System) paired with a 5975B inert XL EI/CI mass selective detector (Agilent Technologies, Santa Clara, CA, USA). The injection port was maintained at 250°C and the volatile compounds were separated in an Agilent DB-WAX Ultra Inert (30 m × 0.25 mm × 0.5 µm) capillary column using helium as the carrier gas at 1.2 mL min^{-1} flow rate. The initial oven temperature was set at 40°C and held for 5 min, then increased to 80°C at a rate of 5°C min^{-1} followed by a 200°C-ramp up at a rate of 10°C min^{-1}, and finally up to 250°C at 20°C min^{-1}, where it was held for 10 min. Total GC run time was 37.5 min with 1 min post-run time at 260°C. The mass selective detector was operated in electron ionization mode (70 eV) with a full scan mass range of 30–300 m/z (threshold: 150). The transfer line, ion source, and quadrupole temperatures were set at 280, 230, and 150°C, respectively.

Data collection and processing were done with Agilent MSD ChemStation. Volatile compounds were identified by matching their mass spectra to the NIST05 mass spectral database and comparison of their retention times with authentic standards, when available. Further identification was done by comparing their linear retention indices (RI) with those found in the literature, determined relative to the retention time of a C_8-C_{20} n-alkane series run under the same GC conditions. Relative quantification of volatiles was carried out by comparison of their peak areas to that of stable isotope external standards. Hexanol-d_{13} (alcohols), octanal-d_{16} (aldehydes, ketones, and esters), and α-methylstyrene-d_{10} (terpenoids and phenylpropanoids) (C/D/N Isotopes, Pointe-Claire, QC, Canada) were used to represent the range of compounds found in basil. Standards were run externally to avoid potential competition for SPME adsorption sites between internal standards and native headspace compounds, and to limit any interference with the natural equilibrium that might happen during extraction (Franklin et al., 2017).

2.5 Statistical analysis

Volatile concentration data was log-transformed and auto-scaled prior to comprehensive downstream analysis using the web-based software MetaboAnalyst 5.0 (Xia et al., 2009). Univariate analysis was performed to determine the statistical significance and fold change of volatile compounds between chilling and non-chilling temperatures. Multivariate analyses such as Principal Component Analysis (PCA) and Orthogonal Projections to Latent Structures-Discriminant Analysis (OPLS-DA) were also employed to visualize patterns and maximize separation of differential metabolites. Leave-one-out cross-validation (LOOCV) and permutation tests (1000 permutations) were performed to assess the quality of the model and the tendency for data overfitting. The Variable Importance in Projection (VIP) was used to determine the relative importance of each volatile in the OPLS-DA model. Differential volatiles were screened based on the combination of three parameters: VIP ≥ 1, fold change ≥ 2 or ≤ 0.5, and p-value (≤ 0.05) adjusted for false discovery rate (FDR).

A three-way ANOVA was performed to determine the effect of storage temperature, atmosphere treatments, and storage duration on the volatile compounds. *Post hoc* analysis was carried out by Tukey's Honest Significant Difference. PCA, hierarchical cluster analysis, and heat maps were performed and built using R 4.2.0 in RStudio (Posit, PBC).

3 Results

3.1 Chilling injury parameters as affected by temperature

Chilling injury (CI) development in basil leaves was affected by temperature and the duration of storage, in 'Genovese', and by the

interaction of both factors in 'Lemon' basil. To highlight the sole effect of temperature without atmosphere modification, a separate plot was presented considering only air storage (Figure 1). Browning and blackening as a symptom of chilling injury was higher in leaves stored at 5°C compared to the ones held at 10 or 15°C for both basil genotypes throughout storage (Figures 1A, B). Electrolyte leakage followed the same trend as CI index, except that after 2 days at 20°C following 6 days storage at chilling temperatures, no difference was found between leaves stored at 5 and 10°C.

3.2 Temperature and atmosphere treatment effects on chilling injury parameters

The development of browning symptoms in 'Genovese' basil was affected by the atmosphere and the interaction between temperature and duration of storage. Browning symptoms, as a manifestation of CI, were greater at 5°C compared to 10 or 15°C, regardless of atmosphere and duration of storage. There was no significant difference in CI index between basil leaves held at 10 and 15°C, except during post-storage at 20°C for leaves stored under 0.04% CO_2. Storage in 5% CO_2 alleviated chilling injury for up to 3 days at 5°C, as shown by lower CI index and electrolyte leakage (Figure 2A).

In 'Lemon' basil, browning symptom development was affected by the interaction of temperature, atmosphere, and duration of storage. On the other hand, electrolyte leakage was influenced by the duration of storage and the interaction of atmosphere treatment and temperature. Neither 5% nor 10% CO_2 alleviated chilling injury in leaves stored at 5°C since no differences were observed in browning symptoms or electrolyte leakage among the atmosphere treatments (Figure 2B). Storage at 10% CO_2 even resulted in higher browning development and electrolyte leakage after 6 days of storage at 10°C and after 2 days post-storage at 20°C following storage at 15°C. Unlike 'Genovese', leaf browning was observed in 'Lemon' basil even at 15°C.

3.3 Effect of chilling temperatures on volatile profile

More than 70 volatile compounds were identified for each of the basil genotypes under study (Supplementary Tables 1, 2). Unsupervised multivariate analysis was done to determine the internal structures of several variables and how these relate based on the principal components. PCA scores plots showed the effect of temperature on the biological replicates (Figures 3A, B). For both 'Genovese' and 'Lemon', there was considerable overlap between samples stored at temperatures of 10 and 15°C, as exemplified by the clustering together of the different replicates. On the other hand, these two groups were held distinct to that of samples stored at 5°C, which tended to move away from the clustering. To further maximize the separation and determine what caused this distinction, orthogonal projections to latent structures-discriminant analysis (OPLS-DA) was done. For both genotypes, a distinct separation in volatile constituents was observed between

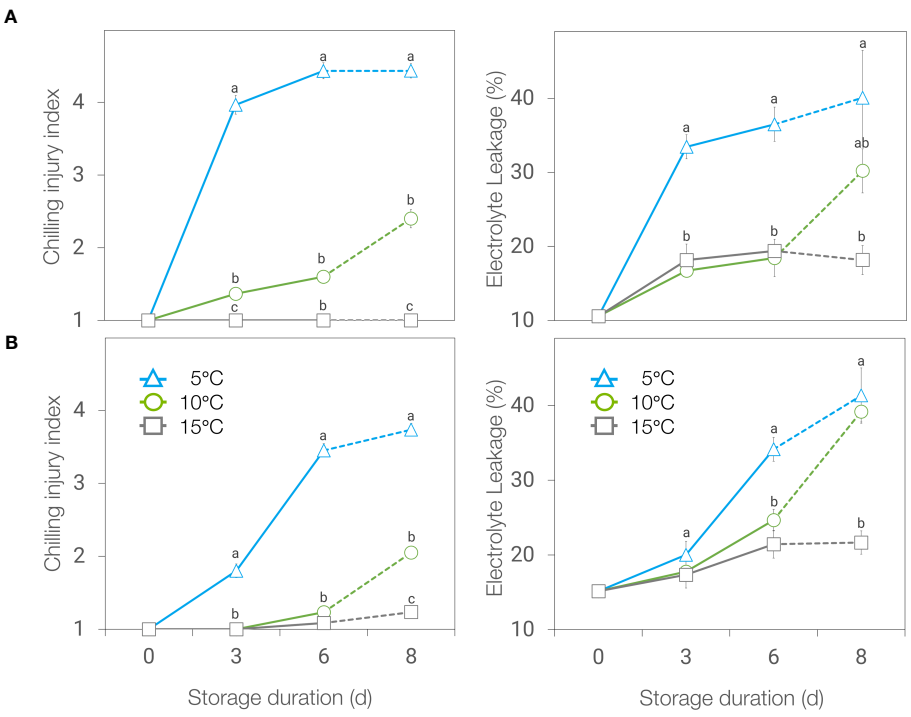

FIGURE 1
Chilling injury (CI) index (left) and electrolyte leakage (right) of 'Genovese' **(A)** and 'Lemon' **(B)** basil stored at 5, 10 and 15°C for 6 days + additional 2 days at 20°C (broken lines). Means with the same letter within a storage period are not significantly different ($p < 0.05$).

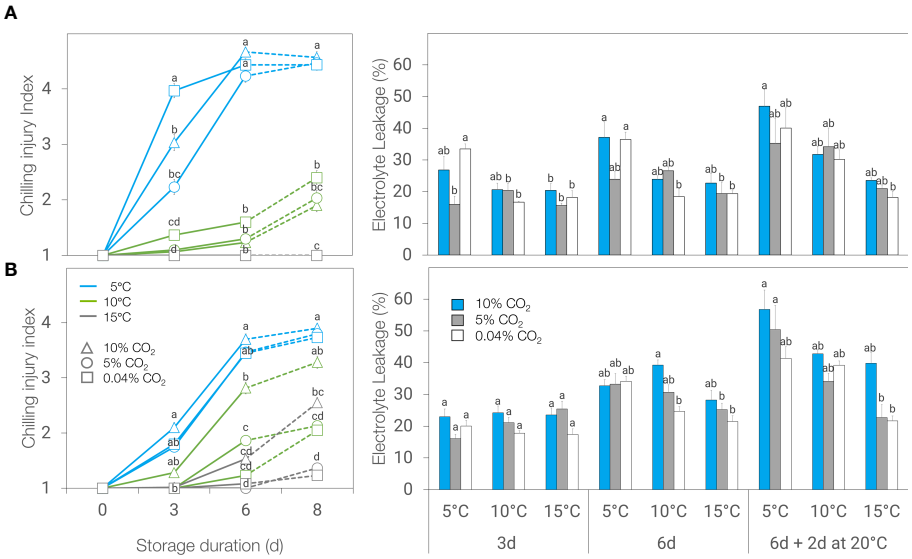

FIGURE 2
Chilling injury (CI) index (left) and electrolyte leakage (right) of 'Genovese' **(A)** and 'Lemon' **(B)** basil stored under various CO_2 atmospheres (0.04, 5 or 10% CO_2) and temperatures (5, 10, or 15°C) for 3 days, 6 days, and 6 days + additional 2 days at 20°C (broken lines). Means with the same letter within a storage period are not significantly different ($p < 0.05$).

10 and 5°C, and between 15 and 5°C, but not between 10 and 15°C (Figures 3A, B). Q^2 values greater than 0.5 in cross-validation and permutation tests suggested an adequately reliable model for both 'Genovese' and 'Lemon' (data not shown). To screen for differentially accumulated volatiles (DAVs) at different temperatures, the VIP parameter (≥ 1) from the OPLS-DA model was used together with fold change (≥ 2 or ≤ 0.5) and FDR-adjusted *p*-value (≤ 0.05). Based on the thresholds set, there were 28 DAVs

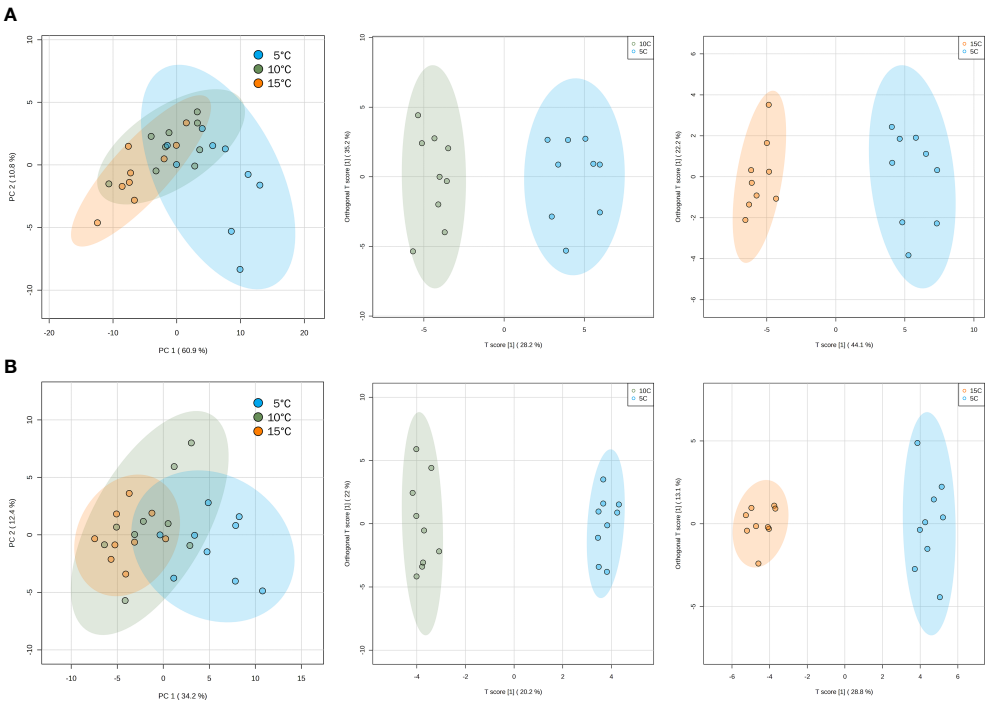

FIGURE 3
Principal component analysis (PCA) scores plots (left) and orthogonal projections to latent structures discriminant analysis (OPLS-DA) scores plots (middle and right) for 'Genovese' **(A)** and 'Lemon' **(B)** basil, separated according to the accumulation of volatile compounds at different temperatures. OPLS-DA scores plots are showing 10°C vs 5°C (middle) and 15°C vs 5°C (right) comparison groups, respectively. Confidence regions (95%) are shown in colored ellipses.

between 10 and 5°C and 42 DAVs between 15 and 5°C in the 'Genovese' variety, all of which were downregulated when stored at 5°C (Supplementary Tables 3A, B). In 'Lemon' basil, there were 12 DAVs between 10 and 5°C (9 downregulated and 3 upregulated at 5°C) and 23 DAVs between 15 and 5°C (18 downregulated and 5 upregulated at 5°C) (Supplementary Tables 4A, B). There were 26 DAVs found common in both comparison groups for 'Genovese', while 10 DAVs were common in both comparison groups for 'Lemon'. These volatile compounds could play potential roles in the chilling injury response at 5°C and can be starting points for volatile markers to indicate chilling injury in the said genotypes.

3.4 VOCs response to combined temperature and controlled atmosphere treatments

The loss of volatile compounds in both genotypes was greater at lower temperatures. A sudden decline in volatile constituents was observed after 3 days at 5°C and continued until day 8 (i.e. withdrawal after 6 days at chilling temperatures and then holding for 2 days at 20°C) (Supplementary Figure 1). No significant differences were observed in total combined volatiles among the three CO_2 atmosphere treatments in 'Genovese' (p = 0.955) and 'Lemon' (p = 0.795). More than half of the reduction in volatile compounds was due to decreases in the monoterpenes and sesquiterpenes.

Three-way ANOVA revealed that some VOCs were affected by the interactions between temperature, atmosphere treatment, and duration of storage. However, a lot of variations can be explained by a stronger effect of temperature and duration of storage compared to the controlled atmosphere treatment (Supplementary Tables 1, 2). PCA scores plots also supported this observation, separating atmosphere treatments into clusters depending on the accompanying temperature (Figure 4). In 'Genovese' basil, the first principal component (PC1) explained 77.3% of the variation in the data, clearly separating the 10°C and 15°C temperature groups from the 5°C group. The second principal component (PC2) explained 11.7% of the variation and separated the 10°C group from the 15°C group, as well as the CO_2 treatment groups at 5°C and 10°C. In 'Lemon' basil, PC1 and PC2 explained 56.9% and 13.5% of the variation in the data, respectively, with PC1 separating the 10°C and 15°C temperature groups from the 5°C group, and PC2 separating the atmosphere groups at 5°C. Temperature and CO_2 treatment groups at 10°C and 15°C tended to cluster together in 'Lemon' compared to in 'Genovese'.

Cluster dendogram and heat maps provided insights on the changes in VOC profile expression in the different temperature and atmosphere treatment combinations. Based on the similarities in volatile compound expression in 'Genovese' basil, temperature groups were clustered together, as exemplified by the greater loss of terpenoid compounds at 5°C than at 10°C, and higher expression of these volatiles at 15°C (Figure 5A). Differences among CO_2 atmosphere treatments within a temperature group can best be seen at 10°C, with 5% CO_2 treatment showing higher production of terpenoid compounds and 10% CO_2 showing high expression of aliphatic alcohols and aldehydes. In 'Lemon' basil, cluster separation was observed between the 5°C temperature group and the 10 and 15°C temperature groups, the latter being clustered together, as we observed in the PCA scores plot. Similar to 'Genovese', cluster separation was underscored by the largest reductions in most terpenoid compounds and the largest increases of aliphatic and terpene alcohols at 5°C (Figure 5B).

3.5 Impact of temperature and CO_2 atmospheres on key flavor volatiles

Out of more than 70 volatile compounds detected and identified for each genotype under study, our analysis was focused mostly on

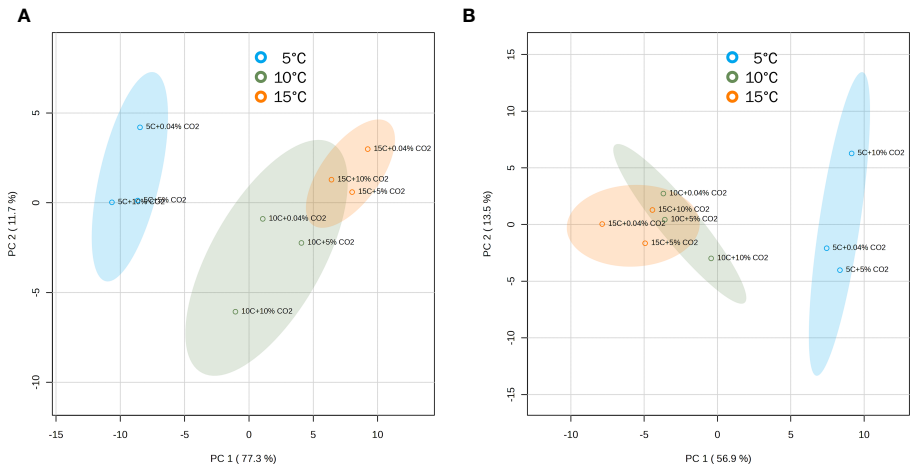

FIGURE 4
Principal component analysis (PCA) scores plots for 'Genovese' **(A)** and 'Lemon' **(B)** basil separated according to the accumulation of volatile compounds at different temperature and CO_2 atmosphere combinations. Leaves are stored under various CO_2 atmospheres (0.04, 5 or 10% CO_2) and temperatures (5, 10, or 15°C) for 6 days + additional 2 days at 20°C. Confidence regions (95%) are shown in colored ellipses.

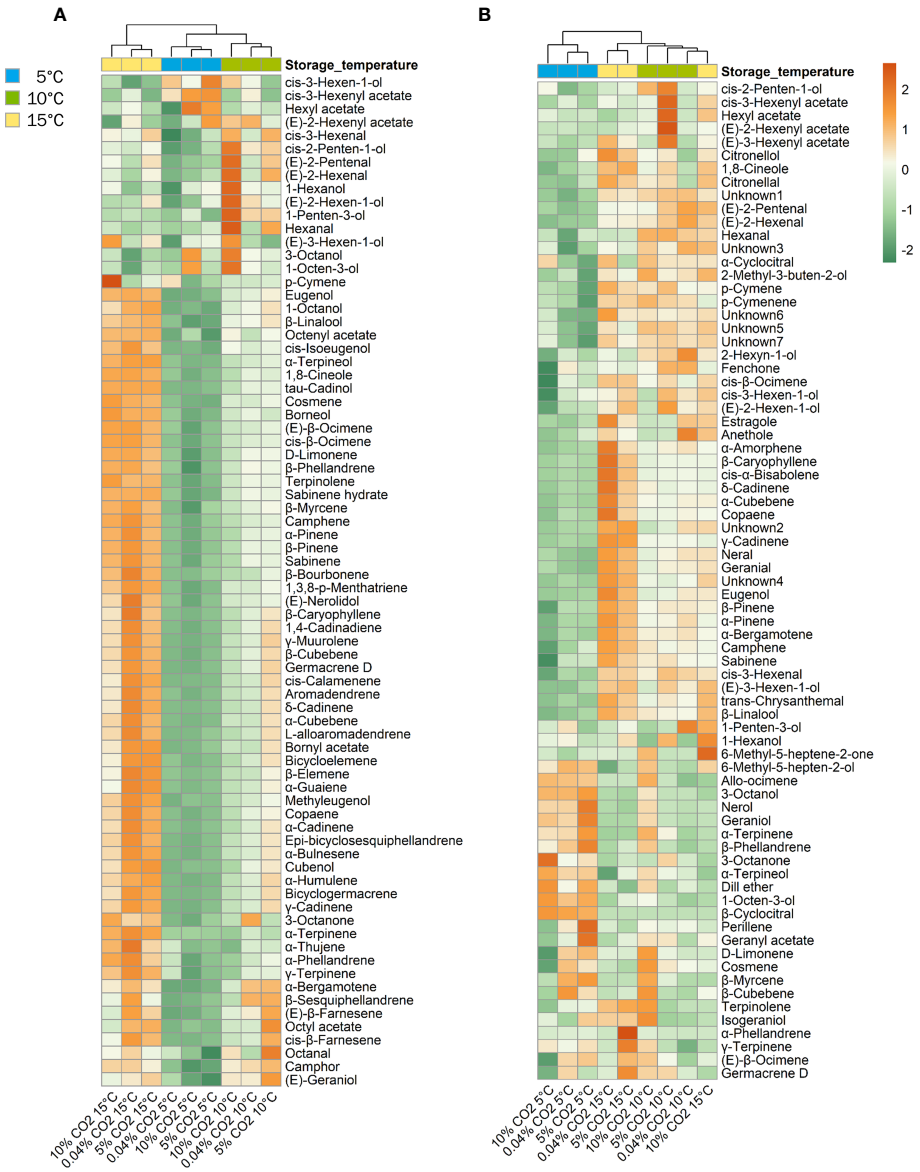

FIGURE 5
Heatmap of volatile expression for 'Genovese' **(A)** and 'Lemon' **(B)** basil stored under various CO_2 atmospheres (0.04, 5 or 10% CO_2) and temperatures (5, 10, or 15°C) for 6 days + additional 2 days at 20°C. Orange and green colors correspond to upregulation and downregulation, respectively.

key compounds responsible for basil's characteristic aroma and flavor. These compounds confer green, woody, fresh, floral and clove aroma and flavor to 'Genovese' and a citrusy with a hint of woody, green, spicy, anethole, fresh, floral, and sweet rose aroma to 'Lemon' basil (Simon et al., 1999; Al-Kateb and Mottram, 2014; Hammock et al., 2021; Patel et al., 2021).

3.5.1 'Genovese' basil

The concentration of key flavor volatile compounds α-pinene, β-pinene, β-myrcene, 1,8-cineole, *cis*-β-ocimene, linalool, and eugenol decreased with storage duration and were mostly affected by storage temperature (Figure 6; Supplementary Table 1). When stored in 0.04% CO_2, levels of these volatiles were generally lower at 5°C compared to 15°C, although the trend was only statistically significant in α-pinene and β-pinene after 6 days, in *cis*-β-ocimene for all storage periods, and in eugenol after 3 and 8 days (6 days + additional 2 days at 20°C) (Figures 6A–G). When stored in 10% CO_2, the concentrations of α-pinene, β-pinene, β-myrcene, 1,8-cineole, *cis*-β-ocimene, linalool, and eugenol were significantly lower at 5°C compared to 15°C after 6 days (Figures 6A–G), while only *cis*-β-ocimene was significantly lower after 3 days (Figure 6E). In 5% CO_2, *cis*-β-ocimene concentration showed a significant decrease when stored at 5°C compared to 15°C after 6 days. Following 2 days of post-storage at 20°C, the levels of *cis*-β-ocimene, linalool, and eugenol were significantly lower at 5°C compared to 15°C whether leaves were held in 5% or 10% CO_2 (Figures 6E–G).

The concentration of *cis*-3-hexenal was affected by the atmosphere, temperature, and the duration of storage. An increase in concentration was observed after 3 days of storage regardless of temperature (Supplementary Table 1). Although *cis*-3-

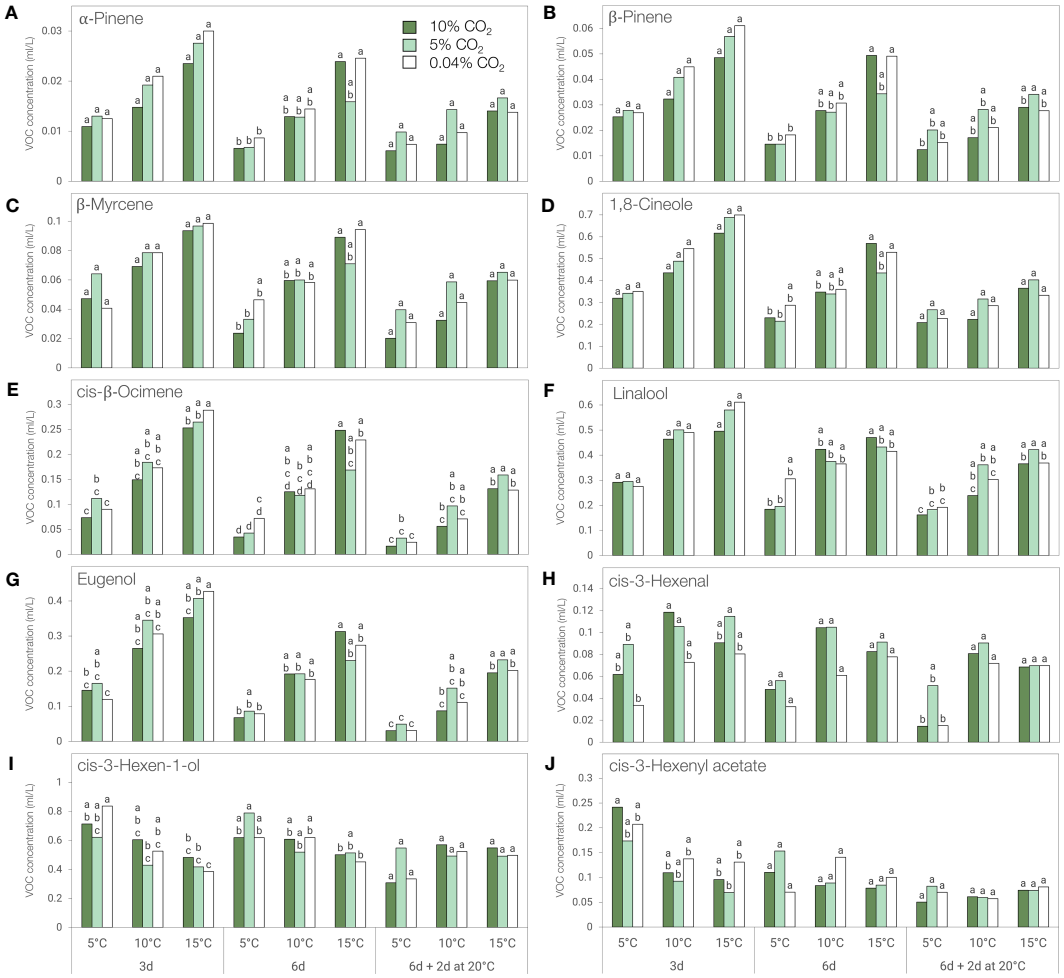

FIGURE 6
Concentration of key flavor volatiles of 'Genovese' basil stored at different temperatures (5, 10, or 15°C) and CO_2 atmospheres (0.04, 5 or 10% CO2) for 3 days, 6 days, or 6 days + additional 2 days at 20°C. **(A)** α-Pinene, **(B)** β-Pinene, **(C)** β-Myrcene, **(D)** 1,8-Cineole, **(E)** *cis*-β-Ocimene, **(F)** Linalool, **(G)** Eugenol, **(H)** *cis*-3-Hexenal, **(I)** *cis*-3-Hexen-1-ol, **(J)** *cis*-3-Hexenyl acetate. Means with the same letter within a storage period are not significantly different ($p < 0.05$).

hexenal levels were generally higher in 5% and 10% CO_2, no significant differences were observed between atmospheres for a specific temperature. However, leaves stored at 5°C had significantly lower *cis*-3-hexenal content compared to 15°C in 0.04% CO_2 and 10% CO_2 during post-storage at 20°C (Figure 6H).

The concentrations of *cis*-3-hexen-1-ol and *cis*-3-hexenyl acetate were affected by the interaction between temperature and duration of storage. A sudden increase was also observed after 3 days but unlike other key volatiles mentioned above, the concentration of these two compounds were generally higher at lower temperatures during the first 6 days of storage (Figures 6I, J). Nonetheless, only the levels of *cis*-3-hexen-1-ol in 0.04% CO_2 showed a statistically significant result after 3 days of storage (Figure 6I).

3.5.2 'Lemon' basil

Neral (*cis*-citral) and geranial (*trans*-citral) were the two most abundant volatile compounds in 'Lemon' basil, with 10-fold higher concentrations than other volatile compounds. The concentrations of these citral geometric isomers and green leaf volatile *cis*-3-hexen-1-ol were affected by the interaction between the atmosphere, temperature, and duration of storage (Supplementary Table 2). Linalool and estragole concentration were affected by temperature and duration of storage, that of β-caryophyllene by the two-way interactions between atmosphere and temperature, and temperature and duration of storage, while *cis*-3-hexenal, and (*E*)-2-hexenal content were influenced by the respective interaction of atmosphere and temperature with duration of storage. Nerol and geraniol concentrations were influenced by the two-way interactions between atmosphere, temperature, and duration of storage.

The concentration of these key volatile compounds decreased during storage and was generally lower at 5°C compared to 15°C, except for nerol and geraniol which showed a reverse trend following post-storage at 20°C (Figure 7; Supplementary Table 2). β-caryophyllene concentration was significantly lower at 5°C compared to 15°C following 3 and 6 days of storage in 0.04% CO_2 (Figure 7E) while a similar trend was observed for neral, geranial, estragole and *cis*-3-hexenal, but only after 6 days of storage in in 0.04% CO_2 (Figures 7A, B, D, G). The concentration of (*E*)-2-

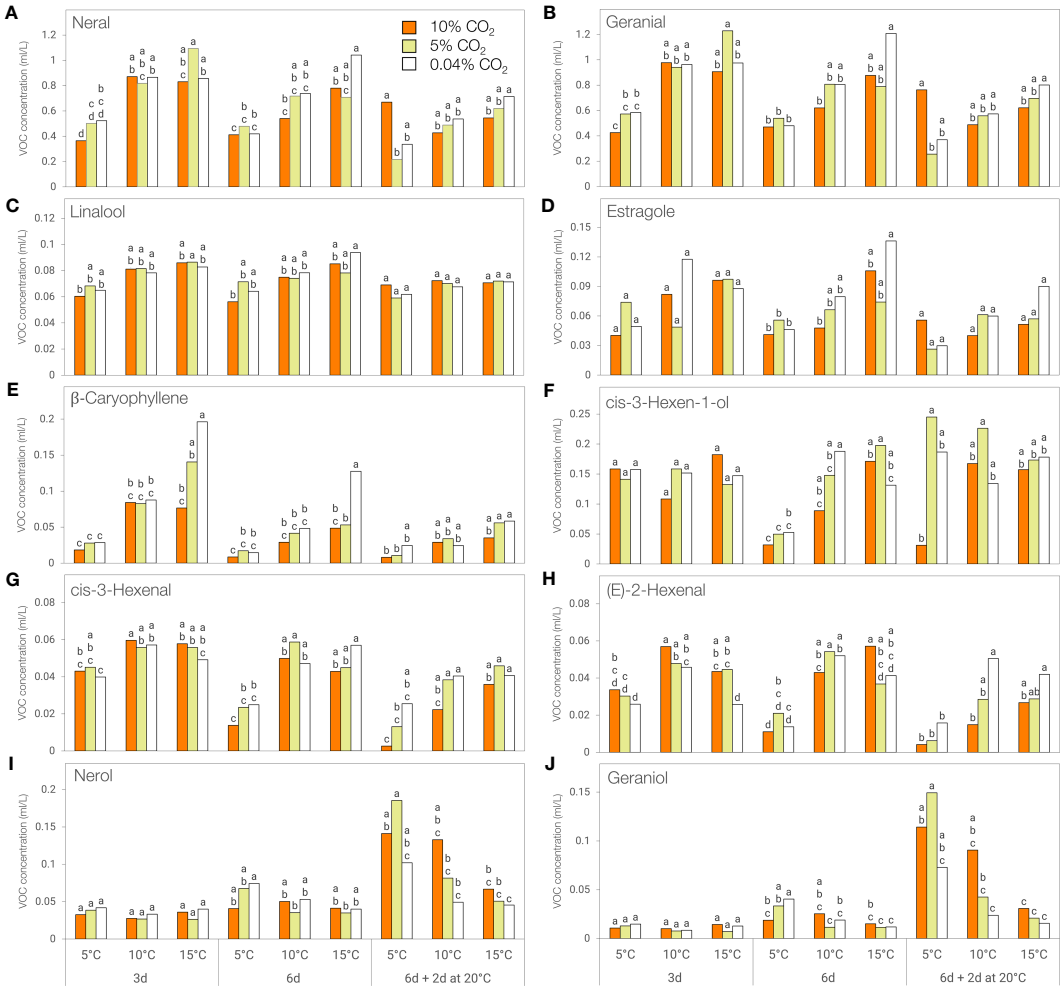

FIGURE 7
Concentration of key flavor volatiles of 'Lemon' basil stored at different temperatures (5, 10, or 15°C) and CO_2 atmospheres (0.04, 5 or 10% CO_2) for 3 days, 6 days, or 6 days + additional 2 days at 20°C. **(A)** Neral, **(B)** Geranial, **(C)** Linalool, **(D)** Estragole, **(E)** β-Caryophyllene, **(F)** *cis*-3-Hexen-1-ol, **(G)** *cis*-3-Hexenal, **(H)** **(E)**-2-Hexenal, **(I)** Nerol, **(J)** Geraniol. Means with the same letter within a storage period are not significantly different ($p < 0.05$).

hexenal was higher at 10°C compared to 5°C in 0.04% CO_2 for all storage periods while the same trend was observed in *cis*-3-hexen-1-ol levels but only after 6 days of storage (Figures 7F, H).

When stored in 10% CO_2, significantly lower volatile concentrations were observed at 5°C compared to 15°C in neral and geranial after 3 days, in neral, *cis*-3-hexen-1-ol, and (*E*)-2-hexenal after 6 days, and in *cis*-3-hexenal after 6 and 8 days (6 days + additional 2 days at 20°C) (Figures 7A, B, F, G, H). In addition, *cis*-3-hexenal and (*E*)-2-hexenal concentrations were significantly lower at 5°C compared to 10°C after 3 days of storage (Figures 7G, H).

When stored in 5% CO_2, significantly lower volatile concentrations were observed at 5°C compared to 15°C in neral, geranial, and β-caryophyllene after 3 days, in *cis*-3-hexen-1-ol after 6 days, and in *cis*-3-hexenal after 6 and 8 days (6 days + additional 2 days at 20°C) (Figures 7A, B, E, F, G). The concentration of (*E*)-2-hexenal was significantly lower at 5°C compared to 10°C after 3 and 6 days of storage (Figure 7H). In contrast, nerol and geraniol concentrations were significantly higher at 5°C compared to 10 and 15°C following 2 days post-storage at 20°C (Figures 7I, J).

4 Discussion

Basil is one of a few chilling-sensitive culinary herbs (Cantwell and Reid, 1993). Chilling injury in basil is characterized by brown discoloration of the interveinal areas of the leaf, stem browning and collapse, loss of glossy appearance, wilting of the leaves and loss of characteristic aroma (Lange and Cameron, 1994; Aharoni et al., 2010). In this study, 'Genovese' and 'Lemon' basil leaves incurred chilling injury when stored at temperatures below 15°C, with browning symptoms increasing according to the duration of storage. Severe chilling damage, manifested by leaf darkening, was observed at 5°C and this is accompanied by an increase in electrolyte leakage. Progressive loss of membrane integrity and eventual leakage of ions and solutes are among the many physiological disruptions following chilling stress, the manifestations in leaves of which include browning and discoloration. Chilling damage in basil has previously been shown to correlate well with electrolyte leakage (Wongsheree et al., 2009; Cozzolino et al., 2016) and our results also support this finding.

The relative susceptibility of basil to chilling temperatures limits safe transport and storage with other culinary herbs. Since basil is usually transported in packages, atmosphere modification can be easily applied to potentially combat chilling effects. Controlled and modified atmospheres have been found to alleviate chilling injury in a variety of fruits and vegetables (Wang, 1989; Thompson, 2018). In basil, a controlled atmosphere of 1.5% O_2 + 5% CO_2 did not prevent the occurrence of chilling injury (Lange and Cameron, 1998). Our previous experiment on 'Genovese' and 'Thai' basil using 5% and 10% CO_2 mixed with 16% and 11% O_2, respectively, showed promise in chilling injury alleviation (Rodeo and Mitcham, 2022). In the current study, 5% and 10% CO_2 atmospheres alleviated browning symptoms in 'Genovese' basil for up to 3 days at 5°C compared to air (0.04% CO_2) storage. Other than inhibiting ethylene action by acting as a competitive inhibitor (Kader et al., 1989), elevated CO_2 levels were also found to inhibit the accumulation of reactive oxygen species (ROS), enhance the activities and expression of genes of antioxidant enzymes, and increased accumulation of known antioxidants such as ascorbic acid and glutathione (Liang et al., 2021; Wang et al., 2021). Generation of ROS is one of the key events in chilling injury and its overproduction can lead to progressive loss of membrane integrity due to lipid peroxidation (Sevillano et al., 2009; Heyes, 2018). The aforementioned effects of CO_2 could have resulted in chilling injury amelioration until such time as the production of ROS exceeded the capacity of the scavenging process, at which time chilling injury symptoms developed.

However, elevated CO_2 atmospheres were not effective in ameliorating chilling symptoms in 'Lemon' basil. Instead, 10% CO_2 aggravated browning symptoms at 10°C after 6 days and at 15°C following 2 days of post-storage at 20°C. Wongsheree et al. (2009) found that 'Lemon' basil was more prone to leaf blackening than holy and sweet basil types. This was also confirmed in our previous experiments comparing five different commercial basil varieties and species, including 'Lemon' and 'Genovese', that indicated there is a differential chilling sensitivity among basil types (unpublished data). The current study revealed that 'Lemon' basil is also more sensitive to high CO_2 atmospheres. The browning symptoms observed cannot be solely ascribed to the effect of chilling, but also to CO_2 injury. The combination of the two stresses could be too much for a sensitive genotype such as 'Lemon', resulting in intensified symptoms. In 'Napoletano' basil, 10% CO_2 likewise caused serious leaf browning even when stored at an otherwise safe temperature of 12°C (Amodio et al., 2005). Sweet basil stored at 20°C under atmospheres containing more than 10% CO_2 was found to have a reduced shelf life due to brown spotting and CO_2 injury (Lange and Cameron, 1998). The relative susceptibility of different basil types to elevated levels of CO_2 that resulted in injury underscored the need for dynamic CA or MAP systems that will not only cater to changing environmental conditions and a commodity's metabolic state, but also to species and cultivar differences (Saltveit, 2003).

Aside from leaf browning and discoloration, chilling injury is also accompanied by the loss of volatile organic compounds (Farneti et al., 2015; Wang et al., 2015). Major alterations in the contents of these compounds can result in a significant reduction in flavor quality, a characteristic that is most valued in culinary herbs such as basil (Zhang et al., 2016). Our present work revealed significant changes in the volatile profile of two chilling-sensitive basil genotypes, 'Genovese' and 'Lemon'. Compared to 10 and 15°C, storage at 5°C resulted in lower concentration of a number of volatile compounds deemed important for basil flavor. Differentially expressed volatiles between 5°C and relatively higher chilling temperatures (10°C and 15°C) suggested that fold decreases in storage temperature can lead to greater reductions in volatile constituents. Cozzolino et al. (2016) identified 10 volatile compounds considered to be potential markers of chilling injury in three sweet basil cultivars ('Italico a foglia larga', 'Cammeo' and 'Italiano classico'). Our results indicated 26 and 10 differentially accumulated volatiles (DAVs) in 'Genovese' and 'Lemon', respectively. These compounds were found to be downregulated in 'Genovese' and 'Lemon' stored at 5°C, with the exception of 6-methyl-5-hepten-2-ol, which was upregulated in 'Lemon' basil at 5°C. Since these volatiles were found to be greatly affected by chilling based on the variable importance in projection (VIP) and fold-changes, we can therefore consider them as potential volatile markers for chilling stress in 'Genovese' and 'Lemon' basil. It is interesting to note that 80% of DAVs in 'Genovese' and 50% of DAVs in 'Lemon' were sesquiterpenes which could suggest that the synthesis of this group of volatile compounds can be greatly affected by chilling. Sesquiterpenes (C_{15}) are derived from isopentenyl diphosphate (IPP) and its isomer dimethylallyl diphosphate (DMAPP), produced by the cytosolic mevalonate (MVA) pathway. On the other hand, monoterpenes (C_{10}) are derived from IPP and DMAPP, produced by the parallel methylerythritol (MEP) pathway situated in the plastids (Dudareva et al., 2004; Iijima et al., 2004a). Compartmentalization and synthesis location might have played a role in the relative differences between the response of these two groups of terpenoid compounds.

Studies on the ability of controlled atmospheres to modulate the impacts of chilling temperatures on volatile and flavor compounds of fresh basil are very limited, if not non-existent. Several factors can influence the fate of volatile compounds in the harvested plant; among these are storage methods and postharvest techniques employed (Figueiredo et al., 2008). In basil, controlled atmospheres (3% CO_2 + 2% O_2) did not alter volatile composition, but concentrations decreased with duration of storage at 12°C (Amodio et al., 2005). Storage at 4°C compared to 12°C resulted in lower concentrations of volatile compounds in three basil cultivars (Cozzolino et al., 2016). Our results agree with the above studies where volatile abundance generally decreased with time and lower storage temperatures. Storage at 5% CO_2 was able to mitigate some volatile losses resulting from chilling, especially during the first 3 days of storage, which coincided with visible chilling symptom alleviation in 'Genovese' (Figures 2, 6). This was also evident in 10°C storage as shown by the upregulation of volatile abundance with 5% CO_2 compared to air or 10% CO_2 (Figure 5A).

While volatile changes in fruits post-harvest depend on maturity and ripening processes, this does not apply to basil and other herbs. Instead, storage conditions and leaf morphology could play critical roles in volatile compound dynamics. Most volatile compounds in basil are synthesized and stored in the glandular

trichomes and released following environmental cues and mechanical damage (Holopainen and Gershenzon, 2010). Having these external secretory structures makes basil more vulnerable to evaporative volatile losses and transformations, especially during handling and storage (Combrinck et al., 2007; Figueiredo et al., 2008). In this study, multivariate analyses also revealed that temperature was the major driving force for basil volatile changes rather than atmosphere. Storage at 15°C in air resulted in a gradual loss of volatile compounds with time, capped with a further decline following transfer to 20°C. On the other hand, storage at lower temperatures led to a sudden reduction in volatile compounds. This pattern was generally true even for higher CO_2 atmosphere storage. PCA and cluster analysis showed groupings mostly according to storage temperature. There was a very distinct separation between basil stored at 5°C and those that were held at relatively higher temperatures of 10 and 15°C in the 3 atmospheres (Figures 4, 5). This suggests that for a chilling-sensitive commodity such as basil, most of the volatile losses can be attributed to storage at temperatures significantly below the chilling threshold. Most studies on basil chilling injury denote the critical temperature as 12°C, below which chilling damage will be expressed (Lange and Cameron, 1994; Meir et al., 1997; Wongsheree et al., 2009; Aharoni et al., 2010; Cozzolino et al., 2016), be it visible (browning and wilting) or invisible (loss of volatiles and characteristic aroma). Holding basil closer to this threshold temperature is important for volatile compound preservation. Interestingly, controlled atmosphere storage at 10°C led to an increase in volatile aldehydes and their alcohol derivatives which are mostly products of the oxylipin pathway. In mango peel, chilling stress also increased the production of these volatiles and was suggested to be implicated in abiotic stress signaling (Sivankalyani et al., 2017). This might also be the case in basil. The elevated production of these volatiles at median temperatures could signal impending stress to enable activation of defense responses.

The characteristic aroma and flavor of 'Genovese' basil leaves can be attributed to the presence of key volatile compounds. Consistent with the findings of Chang et al. (2007), the major volatile compounds observed in 'Genovese' basil consisted of a 3:3:2 ratio of 1,8-cineole, linalool, and eugenol. A pure standard mixture of these volatiles that we made in a similar ratio recreated the major aroma notes of 'Genovese' basil, as perceived by a trained panel (unpublished data). Cineole (eucalyptol) has a camphoraceous aroma and a fresh, cooling taste, suggestive of mint. Linalool is responsible for the sweet floral aroma in basil, while eugenol has a strong clove-like odor and a spicy, pungent taste (Burdock and Fenaroli, 2010). Other compounds that have a significant impact on the aroma and flavor of 'Genovese' basil are α-pinene and β-pinene (earthy/pine/woody), β-myrcene (spicy/balsamic), and *cis*-β-ocimene (floral/woodsy). Green leaf volatiles such as *cis*-3-hexenal, *cis*-3-hexen-1-ol, and *cis*-3-hexenyl acetate provide basil with green, grassy, and fruity aroma, respectively. Since culinary herbs such as basil do not have a substantial amount of sugars and acids, loss of these volatile compounds leads to a significant amount of flavor loss (Zhang et al., 2016).

Storage at low temperature, especially at 5°C, accelerated the decrease in the levels of 1,8-cineole, linalool, eugenol, β-myrcene, *cis*-β-ocimene, α-pinene and β-pinene in 'Genovese'. With the exception of eugenol, all the other volatile compounds mentioned are monoterpenes and therefore share the same biosynthetic pathway. Monoterpenes are derived from geranyl diphosphate (GDP), and produced from the condensation of IPP and DMAPP that are mainly formed in the plastid through the MEP pathway. GDP then undergoes several transformations by a large family of enzymes known as terpene synthases giving rise to different monoterpenes (Bohlmann et al., 1998; Dudareva et al., 2004). Eugenol, on the other hand, is derived from the amino acid, phenylalanine, through the phenylpropanoid pathway, and its biosynthesis proceeds *via* the reduction of a coniferyl alcohol ester by the eugenol synthase enzyme (Gang et al., 2001; Koeduka et al., 2006). The loss of these volatile compounds during subsequent low temperature storage is related to reduced expression levels of genes coding for important enzymes in the metabolic pathway. For instance, the expression of a linalool synthase gene coding for the enzyme responsible for the formation of linalool in a single-stage reaction from GDP was downregulated by chilling temperature in papaya fruit, resulting in impaired linalool production (Gomes et al., 2016). In tomato, significant reduction in volatile concentrations at 5°C was correlated with lower transcript abundance of genes coding for enzymes and products essential for volatile biosynthesis, leading to reduced flavor quality (Zhang et al., 2016).

In contrast, the concentrations of *cis*-3-hexen-1-ol and *cis*-3-hexenyl acetate were generally higher after 3 days at 5°C than at 15°C, while storage in 5% CO_2 generally maintained the levels of *cis*-3-hexenal regardless of temperature. These green leaf volatiles are derived from the oxygenation of C_{18} unsaturated fatty acids through the action of lipoxygenase (LOX), hydroperoxide lyase (HPL), and alcohol dehydrogenase (ADH) enzymes *via* the oxylipin pathway (Schwab et al., 2008; Bai et al., 2011). The increase in these volatiles at low temperatures might be due to an increase in substrate concentration during chilling since C_6 volatile aldehydes production is likely determined by substrate availability rather than HPL activity abundance (Vancanneyt et al., 2001). Moreover, the levels of C_{18} unsaturated fatty acids increased in basil leaves after 2 days of storage at 4°C (Wongsheree et al., 2009). Eventual conversion of *cis*-3-hexenal to *cis*-3-hexen-1-ol by ADH activity, and a decrease in ester levels could also explain the high levels of volatile alcohol particularly in leaves stored at 0.04% CO_2 (Schwab et al., 2008; Farcuh and Hopfer, 2023).

Unlike in 'Genovese' basil, green leaf volatiles in 'Lemon' basil were affected by controlled atmosphere storage, aside from temperature and duration of storage. Higher CO_2 atmospheres of 10% resulted in increased leaf browning in 'Lemon' basil, even at 10°C, and this highly impacted the levels of *cis*-3-hexenal, (*E*)-2-hexenal, and *cis*-3-hexen-1-ol which impart fresh green and grassy aromas to basil leaves. Lower concentrations of C_6 volatile aldehydes and alcohol after 6 days of storage at 5°C might be due to downregulation of LOX and HPL gene expression, as has been previously observed in other fresh commodities (Bai et al., 2011; Zhang et al., 2011). Moreover, the increase in *cis*-3-hexen-1-ol after 2 days at 20°C following 6 days of chilling exposure was accompanied by a decrease in the concentration of *cis*-3-hexenal,

which hinted to a possible recovery of function of ADH, enabling the conversion of said C_6 aldehyde to its corresponding alcohol.

Linalool concentration in 'Lemon' basil was also reduced by lower temperature, and storage in 10% CO_2, which enhanced leaf browning, also led to a significant loss in linalool content. Similarly, estragole, a volatile with anise-like flavor, was also significantly reduced in basil leaves after 6 days of storage at 5°C. Just like eugenol, estragole is derived from phenylalanine through the phenylpropanoid pathway and is synthesized by an additional transfer of a methyl group to chavicol by a specific *o*-methyltransferase (Lewinsohn et al., 2000; Gang et al., 2002). Aside from activity suppression of enzymes in the phenylpropanoid pathway, it is highly possible that *o*-methyltransferase activity was also downregulated resulting in a decrease in estragole levels since some methyltransferases have been found to be repressed by chilling in other crops, such as wheat (Onyemaobi et al., 2022).

β-Caryophyllene, one of the volatile compounds associated with the flavor of black pepper, gives 'Lemon' basil a spicy and woody note (Burdock and Fenaroli, 2010). The concentration of this volatile declined significantly following chilling exposure early in storage, when visible chilling symptoms were still limited. Thus, β-caryophyllene can be considered as an early diagnostic marker of chilling injury in 'Lemon' basil. As a sesquiterpene, this volatile is derived from farnesyl diphosphate (FDP), another condensation product of IPP and DMAPP, which are mainly produced in the cytosol *via* the mevalonate pathway. A caryophyllene synthase from the large terpene synthases family then generates caryophyllene from FDP, and is likely downregulated during chilling exposure (Bohlmann et al., 1998; Dudareva et al., 2004).

Chilling temperatures also led to a significant reduction in citral concentration in 'Lemon' basil. Citral, which exists in two geometric isomers, neral and geranial, is the most abundant volatile compound and is mainly responsible for the lemon-like aroma and flavor of 'Lemon' basil. In 'Sweet Dani', another basil cultivar known for its lemony flavor, more than 99% of the monoterpenes found are comprised of neral and geranial, along with the monoterpene alcohols nerol and geraniol (Iijima et al., 2004b). Nerol and geraniol have a characteristic sweet, rose-like odor and bitter flavor (Burdock and Fenaroli, 2010). Geranial is produced from the oxidation of geraniol by alcohol dehydrogenases, which then undergo non-enzymatic conversion *via* keto-enol tautomerization to neral. The reduction of neral by dehydrogenase enzymes will in turn produce nerol (Iijima et al., 2004b; Iijima et al., 2006). Storage of 'Lemon' basil leaves at 5°C could have resulted in reduced activity of geraniol synthase and alcohol dehydrogenases, resulting in lower concentrations of citral. It is noteworthy that the concentrations of nerol and geraniol increased after 2 days post-storage at 20°C following 6 days at 5°C, especially after storage in elevated CO_2 atmospheres. Chilling injury may have triggered accumulation of said monoterpene alcohols through increased concentrations of reduced cofactors, such as NADPH, facilitating the reduction of neral and geranial to their corresponding alcohols (Iijima et al., 2006).

5 Conclusion

Chilling injury in basil can be manifested both by visible (browning and leaf discoloration) and invisible (loss of volatile compounds responsible for aroma and flavor) damage. Chilling damage is more severe when leaves are stored at temperatures far lower than the threshold temperature. Storage at 5°C resulted in more chilling injury than at 10°C or 15°C, but injury occurred in all three temperatures. Storage at 5°C also resulted in differential accumulation of 26 and 10 volatiles in 'Genovese' and 'Lemon' basil leaves, respectively. Out of these differentially expressed volatiles, *cis*-3-hexenal, eugenol, and germacrene D have significant potential as diagnostic markers for chilling stress in 'Genovese' based on their VIP values and relative importance to flavor perception. For 'Lemon' basil, *cis*-α-bisabolene, β-caryophyllene, and estragole have similar marker potential. Controlled atmosphere storage with 5% CO_2 alleviated chilling injury by reducing visible symptoms and maintaining volatile concentrations in 'Genovese' basil for up to 3 days, but did not have a similar effect in 'Lemon' basil. Volatile changes were more influenced by storage temperature than the accompanying atmosphere. Our study demonstrated that the impact of low temperatures on volatile abundance can be modulated by moderate CO_2 atmospheres (i.e., 5%), albeit for a short period. This modulation was also found to be cultivar- and species-dependent, as susceptibility to CO_2 injury limits its potential application. Sensory evaluation based on descriptive analysis can be done to further evaluate this effect on basil flavor quality in relation to actual human perception.

Data availability statement

The original contributions presented in the study are included in the article/Supplementary Material. Further inquiries can be directed to the corresponding author.

Author contributions

AR and EM conceptualized the research and designed the experiments. AR carried out the experiments, analyzed the data, and wrote the original draft. EM reviewed and revised the manuscript. Both authors contributed to manuscript revision and approved the submitted version.

Funding

AR was supported by the Department of Science and Technology-Science Education Institute (DOST-SEI), Philippines for his PhD. Additional support was provided by the Henry A. Jastro Research Award.

Conflict of interest

The authors declare that the research was conducted in the absence of any commercial or financial relationships that could be construed as a potential conflict of interest.

Publisher's note

All claims expressed in this article are solely those of the authors and do not necessarily represent those of their affiliated organizations, or those of the publisher, the editors and the reviewers. Any product that may be evaluated in this article, or claim that may be made by its manufacturer, is not guaranteed or endorsed by the publisher.

Supplementary material

The Supplementary Material for this article can be found online at: https://www.frontiersin.org/articles/10.3389/fpls.2023.1218734/full#supplementary-material

References

Aharoni, N., Kenigsbuch, D., Chalupowicz, D., Faura-Mlinski, M., Aharon, Z., Maurer, D., et al. (2010). Reducing chilling injury and decay in stored sweet basil. *Isr. J. Plant Sci.* 58, 167–181. doi: 10.1560/IJPS.58.3-4.167

Al-Kateb, H., and Mottram, D. S. (2014). The relationship between growth stages and aroma composition of lemon basil ocimum citriodorum vis. *Food Chem.* 152, 440–446. doi: 10.1016/j.foodchem.2013.12.001

Amodio, M. L., Peri, G., Colelli, G., Centonze, D., and Quinto, M. (2005). Effects of atmosphere composition on postharvest quality of fresh basil leaves (Ocimum basilicum l.). *Acta Hortic.* 682, 731–736. doi: 10.17660/ActaHortic.2005.682.95

Bai, J., Baldwin, E. A., Imahori, Y., Kostenyuk, I., Burns, J., and Brecht, J. K. (2011). Chilling and heating may regulate C6 volatile aroma production by different mechanisms in tomato (Solanum lycopersicum) fruit. *Postharvest Biol. Technol.* 60, 111–120. doi: 10.1016/j.postharvbio.2010.12.002

Bohlmann, J., Meyer-Gauen, G., and Croteau, R. (1998). Plant terpenoid synthases: molecular biology and phylogenetic analysis. *Proc. Natl. Acad. Sci.* 95, 4126–4133. doi: 10.1073/pnas.95.8.4126

Burdock, G. A., and Fenaroli, G. (2010). *Fenaroli's handbook of flavor ingredients. 6th ed* (Boca Raton: CRC Press/Taylor & Francis Group).

Cantwell, M. I., and Reid, M. S. (1993). Postharvest physiology and handling of fresh culinary herbs. *J. Herbs Spices Med. Plants* 1, 93–127. doi: 10.1300/J044v01n03_09

Chang, X., Alderson, P. G., Hollowood, T. A., Hewson, L., and Wright, C. J. (2007). Flavour and aroma of fresh basil are affected by temperature. *J. Sci. Food Agric.* 87, 1381–1385. doi: 10.1002/jsfa.2869

Combrinck, S., Du Plooy, G. W., McCrindle, R. I., and Botha, B. M. (2007). Morphology and histochemistry of the glandular trichomes of lippia scaberrima (Verbenaceae). *Ann. Bot.* 99, 1111–1119. doi: 10.1093/aob/mcm064

Cozzolino, R., Pace, B., Cefola, M., Martignetti, A., Stocchero, M., Fratianni, F., et al. (2016). Assessment of volatile profile as potential marker of chilling injury of basil leaves during postharvest storage. *Food Chem.* 213, 361–368. doi: 10.1016/j.foodchem.2016.06.109

Curutchet, A., Dellacassa, E., Ringuelet, J. A., Chaves, A. R., and Viña, S. Z. (2014). Nutritional and sensory quality during refrigerated storage of fresh-cut mints (Mentha×piperita and m. spicata). *Food Chem.* 143, 231–238. doi: 10.1016/j.foodchem.2013.07.117

Dudai, N., Naharan, O., Bernstein, N., Shachter, A., Rud, R., and Chaimovitsh, D. (2017). Reduction of visible chilling injury in sweet basil (Ocimum basilicum l.) using artificial illumination. *J. Appl. Res. Med. Aromat. Plants* 6, 15–21. doi: 10.1016/j.jarmap.2016.12.002

Dudareva, N., Pichersky, E., and Gershenzon, J. (2004). Biochemistry of plant volatiles. *Plant Physiol.* 135, 1893–1902. doi: 10.1104/pp.104.049981

Farcuh, M., and Hopfer, H. (2023). Aroma volatiles as predictors of chilling injury development during peach (Prunus persica (L) batsch) cold storage and subsequent shelf-life. *Postharvest Biol. Technol.* 195, 112137. doi: 10.1016/j.postharvbio.2022.112137

Farneti, B., Alarcón, A. A., Papasotiriou, F. G., Samudrala, D., Cristescu, S. M., Costa, G., et al. (2015). Chilling-induced changes in aroma volatile profiles in tomato. *Food Bioprocess Technol.* 8, 1442–1454. doi: 10.1007/s11947-015-1504-1

Figueiredo, A. C., Barroso, J. G., Pedro, L. G., and Scheffer, J. J. C. (2008). Factors affecting secondary metabolite production in plants: volatile components and essential oils. *Flavour Fragr. J.* 23, 213–226. doi: 10.1002/ffj.1875

Filip, S. (2017). Basil (Ocimum basilicum l.) a source of valuable phytonutrients. *Int. J. Clin. Nutr. Diet* 3. doi: 10.15344/2456-8171/2017/118

Franklin, L. M., Chapman, D. M., King, E. S., Mau, M., Huang, G., and Mitchell, A. E. (2017). Chemical and sensory characterization of oxidative changes in roasted almonds undergoing accelerated shelf life. *J. Agric. Food Chem.* 65, 2549–2563. doi: 10.1021/acs.jafc.6b05357

Gang, D. R., Lavid, N., Zubieta, C., Chen, F., Beuerle, T., Lewinsohn, E., et al. (2002). Characterization of phenylpropene o-methyltransferases from sweet basil. *Plant Cell* 14, 505–519. doi: 10.1105/tpc.010327

Gang, D. R., Wang, J., Dudareva, N., Nam, K. H., Simon, J. E., Lewinsohn, E., et al. (2001). An investigation of the storage and biosynthesis of phenylpropenes in sweet basil. *Plant Physiol.* 125, 539–555. doi: 10.1104/pp.125.2.539

Gomes, B. L., Fabi, J. P., and Purgatto, E. (2016). Cold storage affects the volatile profile and expression of a putative linalool synthase of papaya fruit. *Food Res. Int.* 89, 654–660. doi: 10.1016/j.foodres.2016.09.025

Hammock, H. A., Kopsell, D. A., and Sams, C. E. (2021). Narrowband blue and red led supplements impact key flavor volatiles in hydroponically grown basil across growing seasons. *Front. Plant Sci.* 12. doi: 10.3389/fpls.2021.623314

Heyes, J. A. (2018). Chilling injury in tropical crops after harvest. *Annual Plant Reviews online* 1, 149–180. doi: 10.1002/9781119312994.apr0605

Holopainen, J. K., and Gershenzon, J. (2010). Multiple stress factors and the emission of plant VOCs. *Trends Plant Sci.* 15, 176–184. doi: 10.1016/j.tplants.2010.01.006

Iijima, Y., Davidovich-Rikanati, R., Fridman, E., Gang, D. R., Bar, E., Lewinsohn, E., et al. (2004a). The biochemical and molecular basis for the divergent patterns in the biosynthesis of terpenes and phenylpropenes in the peltate glands of three cultivars of basil. *Plant Physiol.* 136, 3724–3736. doi: 10.1104/pp.104.051318

Iijima, Y., Gang, D. R., Fridman, E., Lewinsohn, E., and Pichersky, E. (2004b). Characterization of geraniol synthase from the peltate glands of sweet basil. *Plant Physiol.* 134, 370–379. doi: 10.1104/pp.103.032946

Iijima, Y., Wang, G., Fridman, E., and Pichersky, E. (2006). Analysis of the enzymatic formation of citral in the glands of sweet basil. *Arch. Biochem. Biophys.* 448, 141–149. doi: 10.1016/j.abb.2005.07.026

Jensen, N. B., Clausen, M. R., and Kjaer, K. H. (2018). Spectral quality of supplemental LED grow light permanently alters stomatal functioning and chilling tolerance in basil (Ocimum basilicum l.). *Sci. Hortic.* 227, 38–47. doi: 10.1016/j.scienta.2017.09.011

Jirapong, C., Sriraveeroj, N., and Wongs-Aree, C. (2010). Abscission of sweet basil leaves induced by ethylene under modified atmosphere packaging. *Acta Hortic.* 875, 431–434. doi: 10.17660/ActaHortic.2010.875.56

Kader, A. A., Zagory, D., Kerbel, E. L., and Wang, C. Y. (1989). Modified atmosphere packaging of fruits and vegetables. *Crit. Rev. Food Sci. Nutr.* 28, 1–30. doi: 10.1080/10408398909527490

Kenigsbuch, D., Ovadia, A., Chalupowicz, D., Maurer, D., Aharon, Z., and Aharoni, N. (2009). Post-harvest leaf abscission in summer-grown basil (Ocimum basilicum l.) may be controlled by combining a pre-treatment with 1-MCP and moderately raised CO2. *J. Hortic. Sci. Biotechnol.* 84, 291–294. doi: 10.1080/14620316.2009.11512519

Koeduka, T., Fridman, E., Gang, D. R., Vassão, D. G., Jackson, B. L., Kish, C. M., et al. (2006). Eugenol and isoeugenol, characteristic aromatic constituents of spices, are biosynthesized *via* reduction of a coniferyl alcohol ester. *Proc. Natl. Acad. Sci.* 103, 10128–10133. doi: 10.1073/pnas.0603732103

Lange, D. D., and Cameron, A. C. (1994). Postharvest shelf life of sweet basil (Ocimum basilicum). *HortScience* 29, 102–103. doi: 10.21273/HORTSCI.29.2.102

Lange, D. L., and Cameron, A. C. (1997). Pre- and postharvest temperature conditioning of greenhouse-grown sweet basil. *HortScience* 32, 114–116. doi: 10.21273/HORTSCI.32.1.114

Lange, D. L., and Cameron, A. C. (1998). Controlled-atmosphere storage of sweet basil. *HortScience* 33, 741–743. doi: 10.21273/HORTSCI.33.4.741

Lewinsohn, E., Ziv-Raz, I., Dudai, N., Tadmor, Y., Lastochkin, E., Larkov, O., et al. (2000). Biosynthesis of estragole and methyl-eugenol in sweet basil (Ocimum basilicum l). developmental and chemotypic association of allylphenol o-methyltransferase activities. *Plant Sci.* 160, 27–35. doi: 10.1016/S0168-9452(00)00357-5

Liang, Z., Luo, Z., Li, W., Yang, M., Wang, L., Lin, X., et al. (2021). Elevated CO2 enhanced the antioxidant activity and downregulated cell wall metabolism of wolfberry (Lycium barbarum l.). *Antioxidants* 11, 16. doi: 10.3390/antiox11010016

Matthews, J., Melendez, M., Simon, J., and Wyenandt, A. (2018) *Ultra-niche crops series: fresh-market basil* (Rutgers Coop. Ext). Available at: https://njaes.rutgers.edu/fs1279/ (Accessed 9.9.22).

Meir, S., Ronen, R., Lurie, S., and Philosoph-Hadas, S. (1997). Assessment of chilling injury during storage: chlorophyll fluorescence characteristics of chilling-susceptible and triazole-induced chilling tolerant basil leaves. *Postharvest Biol. Technol.* 10, 213–220. doi: 10.1016/S0925-5214(97)01410-5

Onyemaobi, O., Sangma, H., Garg, G., Wallace, X., Kleven, S., and Dolferus, R. (2022). Transcriptome profiling of the chilling response in wheat spikes: II, response to short-term cold exposure. *Curr. Plant Biol.* 32, 100264. doi: 10.1016/j.cpb.2022.100264

Patel, M., Lee, R., Merchant, E. V., Juliani, H. R., Simon, J. E., and Tepper, B. J. (2021). Descriptive aroma profiles of fresh sweet basil cultivars (Ocimum spp.): relationship to volatile chemical composition. *J. Food Sci.* 86, 3228–3239. doi: 10.1111/1750-3841.15797

Patiño, L. S., Castellanos, D. A., and Herrera, A. O. (2018). Influence of 1-MCP and modified atmosphere packaging in the quality and preservation of fresh basil. *Postharvest Biol. Technol.* 136, 57–65. doi: 10.1016/j.postharvbio.2017.10.010

Rodeo, A. J. D., and Mitcham, E. J. (2022). Alleviating postharvest chilling injury in fresh basil by storage temperature and atmosphere manipulation (abstr). *HortScience* 57, S150.

Saltveit, M. E. (2003). Is it possible to find an optimal controlled atmosphere? *Postharvest Biol. Technol.* 27, 3–13. doi: 10.1016/S0925-5214(02)00184-9

Satpute, A., Meyering, B., and Albrecht, U. (2019). Preharvest abscisic acid application to alleviate chilling injury of sweet basil (Ocimum basilicum l.) during cold storage. *HortScience* 54, 155–161. doi: 10.21273/HORTSCI13556-18

Schwab, W., Davidovich-Rikanati, R., and Lewinsohn, E. (2008). Biosynthesis of plant-derived flavor compounds. *Plant J.* 54, 712–732. doi: 10.1111/j.1365-313X.2008.03446.x

Sevillano, L., Sanchez-Ballesta, M. T., Romojaro, F., and Flores, F. B. (2009). Physiological, hormonal and molecular mechanisms regulating chilling injury in horticultural species. postharvest technologies applied to reduce its impact. *J. Sci. Food Agric.* 89, 555–573. doi: 10.1002/jsfa.3468

Simon, J. E. (1995). *Basil (fact sheet), new crop* (West Lafayette, IN: Purdue University, Center for New Crops & Plant Products).

Simon, J. E., Morales, M. R., Phippen, W. B., Vieira, R. F., and Hao, Z. (1999). "Basil: a source of aroma compounds and a popular culinary and ornamental her," in *Perspectives on new crops and new uses*. Ed. J. Janick (Alexandria, Virginia: ASHS Press), 499–505.

Sivankalyani, V., Maoz, I., Feygenberg, O., Maurer, D., and Alkan, N. (2017). Chilling stress upregulates α-linolenic acid-oxidation pathway and induces volatiles of C6 and C9 aldehydes in mango fruit. J. *Agric. Food Chem.* 65, 632–638. doi: 10.1021/acs.jafc.6b04355

Thompson, A. K. (2018). *Controlled atmosphere storage of fruit and vegetables. 3rd ed.* (Boston, MA: CABI).

Vancanneyt, G., Sanz, C., Farmaki, T., Paneque, M., Ortego, F., Castañera, P., et al. (2001). Hydroperoxide lyase depletion in transgenic potato plants leads to an increase in aphid performance. *Proc. Natl. Acad. Sci.* 98, 8139–8144. doi: 10.1073/pnas.141079498

Wang, C. Y. (1989). Chilling injury of fruits and vegetables. *Food Rev. Int.* 5, 209–236. doi: 10.1080/87559128909540850

Wang, L., Baldwin, E. A., Zhao, W., Plotto, A., Sun, X., Wang, Z., et al. (2015). Suppression of volatile production in tomato fruit exposed to chilling temperature and alleviation of chilling injury by a pre-chilling heat treatment. *LWT - Food Sci. Technol.* 62, 115–121. doi: 10.1016/j.lwt.2014.12.062

Wang, D., Li, W., Li, D., Li, L., and Luo, Z. (2021). Effect of high carbon dioxide treatment on reactive oxygen species accumulation and antioxidant capacity in fresh-cut pear fruit during storage. *Sci. Hortic.* 281, 109925. doi: 10.1016/j.scienta.2021.109925

Wongsheree, T., Ketsa, S., and van Doorn, W. G. (2009). The relationship between chilling injury and membrane damage in lemon basil (Ocimum×citriodourum) leaves. *Postharvest Biol. Technol.* 51, 91–96. doi: 10.1016/j.postharvbio.2008.05.015

Xia, J., Psychogios, N., Young, N., and Wishart, D. S. (2009). MetaboAnalyst: a web server for metabolomic data analysis and interpretation. *Nucleic Acids Res.* 37, W652–W660. doi: 10.1093/nar/gkp356

Xiao, Z., Lester, G. E., Park, E., Saftner, R. A., Luo, Y., and Wang, Q. (2015). Evaluation and correlation of sensory attributes and chemical compositions of emerging fresh produce: microgreens. *Postharvest Biol. Technol.* 110, 140–148. doi: 10.1016/j.postharvbio.2015.07.021

Zhang, B., Tieman, D. M., Jiao, C., Xu, Y., Chen, K., Fei, Z., et al. (2016). Chilling-induced tomato flavor loss is associated with altered volatile synthesis and transient changes in DNA methylation. *Proc. Natl. Acad. Sci.* 113, 12580–12585. doi: 10.1073/pnas.1613910113

Zhang, B., Xi, W., Wei, W., Shen, J., Ferguson, I., and Chen, K. (2011). Changes in aroma-related volatiles and gene expression during low temperature storage and subsequent shelf-life of peach fruit. postharvest biol. *Technol.* 60, 7–16. doi: 10.1016/j.postharvbio.2010.09.012

frontiers | Frontiers in Plant Science

TYPE Review
PUBLISHED 15 August 2023
DOI 10.3389/fpls.2023.1246093

OPEN ACCESS

EDITED BY
Shifeng Cao,
Zhejiang Wanli University, China

REVIEWED BY
Klára Kosová,
Crop Research Institute (CRI), Czechia
Jiban Shrestha,
Nepal Agricultural Research Council, Nepal

*CORRESPONDENCE
Sherif M. Sherif
ssherif@vt.edu

RECEIVED 24 June 2023
ACCEPTED 31 July 2023
PUBLISHED 15 August 2023

CITATION
Jahed KR, Saini AK and Sherif SM (2023) Coping with the cold: unveiling cryoprotectants, molecular signaling pathways, and strategies for cold stress resilience. *Front. Plant Sci.* 14:1246093. doi: 10.3389/fpls.2023.1246093

Coping with the cold: unveiling cryoprotectants, molecular signaling pathways, and strategies for cold stress resilience

Khalil R. Jahed, Amolpreet Kaur Saini and Sherif M. Sherif*

Alson H. Smith Jr. Agricultural Research and Extension Center, School of Plant and Environmental Sciences, Virginia Tech, Winchester, VA, United States

Low temperature stress significantly threatens crop productivity and economic sustainability. Plants counter this by deploying advanced molecular mechanisms to perceive and respond to cold stress. Transmembrane proteins initiate these responses, triggering a series of events involving secondary messengers such as calcium ions (Ca^{2+}), reactive oxygen species (ROS), and inositol phosphates. Of these, calcium signaling is paramount, activating downstream phosphorylation cascades and the transcription of cold-responsive genes, including cold-regulated (COR) genes. This review focuses on how plants manage freeze-induced damage through dual strategies: cold tolerance and cold avoidance. Tolerance mechanisms involve acclimatization to decreasing temperatures, fostering gradual accumulation of cold resistance. In contrast, avoidance mechanisms rely on cryoprotectant molecules like potassium ions (K^+), proline, glycerol, and antifreeze proteins (AFPs). Cryoprotectants modulate intracellular solute concentration, lower the freezing point, inhibit ice formation, and preserve plasma membrane fluidity. Additionally, these molecules demonstrate antioxidant activity, scavenging ROS, preventing protein denaturation, and subsequently mitigating cellular damage. By forming extensive hydrogen bonds with water molecules, cryoprotectants also limit intercellular water movement, minimizing extracellular ice crystal formation, and cell dehydration. The deployment of cryoprotectants is a key adaptive strategy that bolsters plant resilience to cold stress and promotes survival in freezing environments. However, the specific physiological and molecular mechanisms underlying these protective effects remain insufficiently understood. Therefore, this review underscores the need for further research to elucidate these mechanisms and assess their potential impact on crop productivity and sustainability, contributing to the progressive discourse in plant biology and environmental science.

KEYWORDS

cryoprotectants, low temperature stress, ROS, AFPs, transmembrane proteins, antioxidants, ice crystals, cell dehydration

1 Introduction

Spring frost is a major environmental stress caused by low temperature combined with dewpoints below freezing points (≤ 0°C), posing substantial economic threat on plants. While the terms "frost damage" and "freeze damage" are commonly used interchangeably, there are slight distinctions between them. Freeze damage is attributed to temperature below freezing points, whereas frost damage is caused by dewpoints below freezing points irrespective of temperature being at or below freezing points (Perry, 1998). However, the damage mechanisms at organ level are comparable in both cases. Consequently, for the purpose of this review, the term "freeze damage" will be employed. At the organ level, the damage occurs when water within plant tissues freezes, forming extracellular ice crystals that result in cell dehydration. Freezing-induced cellular dehydration is the predominant cause of damage in which the cell membranes are disrupted when the dehydration exceeds cell dehydration-tolerance (Pearce, 2001). The severity of damage is determined by multiple factors including plants species, their genetic makeup, dewpoint, surface moisture, probability of an extracellular ice nucleation event, pre-frost environmental conditions, and developmental stage – with flowering being the most susceptible developmental stage (Centinari et al., 2016). Crops can be exposed to two types of frost: radiation and advective – with the former being more common (Liu and Sherif, 2019). Radiation frost is a meteorological phenomenon resulting from the release of thermal energy stored in the soil. This thermal energy is radiated back into the atmosphere during the nocturnal period, characterized by a stable atmosphere and a low wind regime, allowing the formation of a temperature inversion. This atmospheric condition, in conjunction with a reduced dewpoint temperature, leads to a sharp reduction in the air temperature, which falls below the freezing point of water. Advective frost, on the other hand, occurs when a massive system of cold air moves into an area from polar and arctic regions, typically accompanied by wind ≥ 8 km/h. The resultant wind-driven turbulent mixing and cold advection lead to a significant reduction in the air temperature, resulting in the formation of frost.

Crop losses resulting from frost damage represent a significant economic threat to the crop production industry, with frost-related yield reduction being ranked highest among all weather-related disasters in the United States (Centinari et al., 2016; Snyder and de Melo-Abreu, 2005). For example, the one-week Easter freeze in 2007 led to over 2 billion dollars in economic losses due to reduced production of wheat (*Triticum aestivum*) by 19%, peach (*Prunus persica*) by 75%, apple (*Malus domestica*) by 67%, and pecan (*Carya illinoinensis*) by 66% (Liu et al., 2018). Additionally, based on our observations, even a brief frost event persisting only for a few hours can cause substantial damage to various crops. A recent hard freeze event in 2022, lasting 2.5 hours in Virginia, U.S., resulted in an 80% rate of damage to the sweet cherry crop, 15 – 35% damage to apple floral buds, and 15% damage to peach crops (Sherif, 2023). Climate change, leading to increasing global temperatures, exacerbates this threat (Liu et al., 2018), causing alterations in plant phenology such as shortened dormancy and early budburst and flowering (Augspurger, 2013; Ma et al., 2019). Economic losses vary in severity, ranging from partial to complete loss of valuable crops, and can have detrimental impacts on crop quality. Frost-related losses are not limited to specific regions or species; rather, they are a global phenomenon. Notable incidents such as the Easter freeze of 2007 (Liu et al., 2018), the Mother's Day Freeze (2010), the Killer Frost (2012), and the Polar Vortex (2014) have inflicted billions of dollars in damages on the agricultural industry across North America.

The critical temperature at which crop damage occurs depends on multiple factors, including species specificity, duration of the frost event, and developmental stage (Centinari et al., 2016). For instance, the lower temperature limit at which 90% of floral buds are damaged ranges from -17.6°C to -3.0°C for tree fruits like apples, -19.4°C to -2.8°C for grapes, -6.1°C to -0.6°C for small fruits like strawberries, and -2.8°C to -0.8°C for citrus (Snyder and de Melo-Abreu, 2005). Plants at the dormant stage are less susceptible to low temperatures compared to advanced developmental stages. For example, apple floral buds at the silver-tip stage, characterized by slight separation and a shimmery gray color, can tolerate temperatures as low as -17.6°C. However, at the post-bloom stage, 90% flower mortality can occur at -3°C. Furthermore, the duration and severity of a frost event have a significant impact on the extent of damage – the more severe and longer it persists, the more damage occurs. Our research, involving a series of experiments investigating frost mitigation strategies, showed that a deleterious frost event in 2023, persisting for 1.5 hours, resulted in approximately 87% damage to apple floral buds, while a 2-hour long frost event in 2021 caused around 65% bud mortality. However, a relatively longer frost event in 2022, lasting around 2.5 hours, resulted in approximately 15 – 35% damage to floral buds. Interestingly, although the duration of frost in 2022 was relatively longer, it coincided with the early developmental stage of the crops, resulting in comparatively lower damage to the crops (Sherif, 2023). These observations suggest that crops at an early developmental stage exhibit increased resilience to extended frost exposure.

Frost protection methods for plants can be categorized into passive and active methods. Passive methods are considered preventive measures applied before the occurrence of frost events (Liu and Sherif, 2019). These methods are more economically efficient compared to active ones and are intended to provide protection over an extended period. Examples of passive methods include site selection, enhancing plant tolerance to frost through the application of cryoprotectant compounds and growth regulators, and the selection of frost-tolerant varieties (cold-hardy and/or late-blooming varieties). On the other hand, active frost protection methods are those applied during or immediately before a frost event with the aim of preventing the temperature from dropping below the freezing point. These methods involve various techniques including heaters (i.e., solid fuel, propane), wind machines, helicopters, surface irrigation, and sprinklers (i.e., over- and under-tree sprinklers). These approaches are designed to actively counteract the effects of frost in real-time.

Specific weather conditions, including wind speed, humidity, and the severity and duration of a frost event, significantly influence the efficacy of both active and passive methods of frost mitigation (Unterberger et al., 2018). For example, wind machines are beneficial for countering radiation frost, but they fail to provide

protection against advective frost. Moreover, active methods frequently carry considerable costs, such as those involved in the acquisition and upkeep of necessary equipment. Implementing heaters is one such method, which, while effective, necessitates energy consumption and regular maintenance expenses. Another example is the use of helicopters, the operation and fueling of which can be significantly costly. Certain practical constraints may also emerge, causing some methods to be unsuitable in particular agricultural contexts. An example is the implementation of surface irrigation or sprinkler systems, which might not be feasible in regions with scarce water resources. In addition to these considerations, the environmental impact of these methods, particularly in terms of their energy and water usage, should be evaluated to determine their sustainability. A comprehensive understanding of these limitations is indispensable for making informed decisions about frost protection strategies, as this allows for the consideration of the specific needs and restrictions unique to each agricultural system.

A relatively recent strategy to mitigate frost damage in plants involves the application of chemical compounds, specifically plant growth regulators (PGRs). Over the past half-century, researchers have extensively probed PGRs for their potential in bolstering plant frost tolerance and delaying blooming periods, thereby averting late-spring freezes. Ethephon (2-chloroethylphosphonic acid), for example, is an ethylene-based PGR compound that has shown promising results in delaying bloom and increasing cold hardiness in various fruit and nut trees (Liu and Sherif, 2019; Liu et al., 2021a). Our research involved conducting a set of experiments to investigate the impact of ethephon applications on bloom delay. Our findings revealed that applying ethephon in the fall resulted in a bloom delay of 5-6 days in peaches, varying based on application timing and concentration (Liu et al., 2021a). Such a delay could notably lower the risk of frost damage. Furthermore, our results indicated that ethephon could enhance the cold hardiness of dormant buds, thereby promoting their survival through winter. However, ethephon application does have its drawbacks. For instance, it has been associated with adverse effects like gummosis, terminal dieback, and yield reduction (Liu et al., 2021a). Another frost damage mitigation approach involves applying exogenous cryoprotectant compounds. Yet, the specific physiological and molecular mechanisms that enable these compounds to offer frost protection remain relatively unclear. In this article, we present an in-depth overview of the physiological and molecular mechanisms associated with cryoprotectant compounds. However, gaining a robust understanding of these mechanisms requires a comprehensive grasp of plant cold-sensing mechanisms, natural plant defenses against freezing, and the damaging effects of freezing on plant tissues. Therefore, we also provide a detailed examination of these defense mechanisms and the impact of freezing on plants.

2 Cold sensing mechanisms

Plants have evolved intricate mechanisms to identify and respond to abiotic stresses such as cold stress. They perceive shifts in their physical and chemical surroundings like water availability, ion concentration, and temperature, and translate these changes into a biological signal via primary sensory mechanisms (Lamers et al., 2020). Each sensor is typically designed to detect a specific feature of the stress, potentially playing a role in a unique branch of the stress signaling pathway. In this context, the cold-signaling pathway is our focal point for this article. Plants deploy sophisticated multilevel processes in response to a decrease in temperature (Örvar et al., 2000). At the cellular level, cold stress signals are perceived via a variety of receptors that include plasma membrane (PM) rigidification, PM-bound G-protein-associated receptors, and other cold sensors such as Ca^{2+} influx channels, two-component histidine kinases, and changes in protein and nucleic acid conformations or metabolite concentrations (Figure 1) (Kazemi-Shahandashti and Maali-Amiri, 2018). These signals give rise to secondary messengers like Ca^{2+}, ROS, and inositol phosphates. These messengers subsequently adjust the intracellular Ca^{2+} level. Changes in the cytosolic Ca^{2+} level are detected by calcium-binding proteins, also known as Ca^{2+} sensors. These sensors engage with their target proteins to relay the calcium signal within the cell. These proteins coordinate the transfer of the cold stress signal, trigger protein phosphorylation cascades, and manage the expression of transcription factors and cold-regulated (COR) genes in plants (Figure 1, Table 1) (Drerup et al., 2013; Zhang et al., 2014; Ma et al., 2015; Zhu, 2016; Guo et al., 2018).

Plant cold signaling perception and transduction have been extensively studied in recent years, leading to significant advances in our understanding of this complex process (Zhang et al., 2017; Zhao et al., 2017; Ding et al., 2018; Guo et al., 2018). Plants perceive the environmental stimuli and transduce the signal into downstream biological responses by decreasing membrane fluidity, which in turn affects membrane-associated cellular functions (Hou et al., 2014). Different microdomains with specific lipid compositions, including sphingolipids in the plasma membrane, have been identified for their crucial roles in sensing particular temperature ranges (Fabri et al., 2020). Additionally, multiple cold sensors associated with sending temperature changes and cold signaling, such as putative calcium channels, PM-bound G-protein-associated receptors, and plasma membrane-localized receptor-like kinases (RLKs), have been identified in plants (Figure 1). Calcium ions enter the cell primarily through transmembrane proteins complex, known as calcium channels, which are crucial sensors for abiotic stress (Görlach et al., 2015). The rigidification of the membrane due to cold stress activates mechanosensitive or ligand-activated calcium channels, leading to a transient Ca^{2+} influx into the cytosol (Wei et al., 2021).

After perceiving cold stress, plants initiate a series of intricate signal transduction events within the cytosol and nucleus. These events rely on secondary messengers like Ca^{2+}, ROS, and nitric oxide (NO) to facilitate intracellular signaling and cell-to-cell communication (Marcec et al., 2019). Cold stress-induced Ca^{2+} signatures are deciphered through various pathways involving specific groups of Ca^{2+} sensors such as CaM (calmodulin) and CMLs (CaM-like), CDPKs (Ca^{2+}-dependent protein kinases), CCaMK (Ca^{2+}-and Ca^{2+}/CaM-dependent protein kinase),

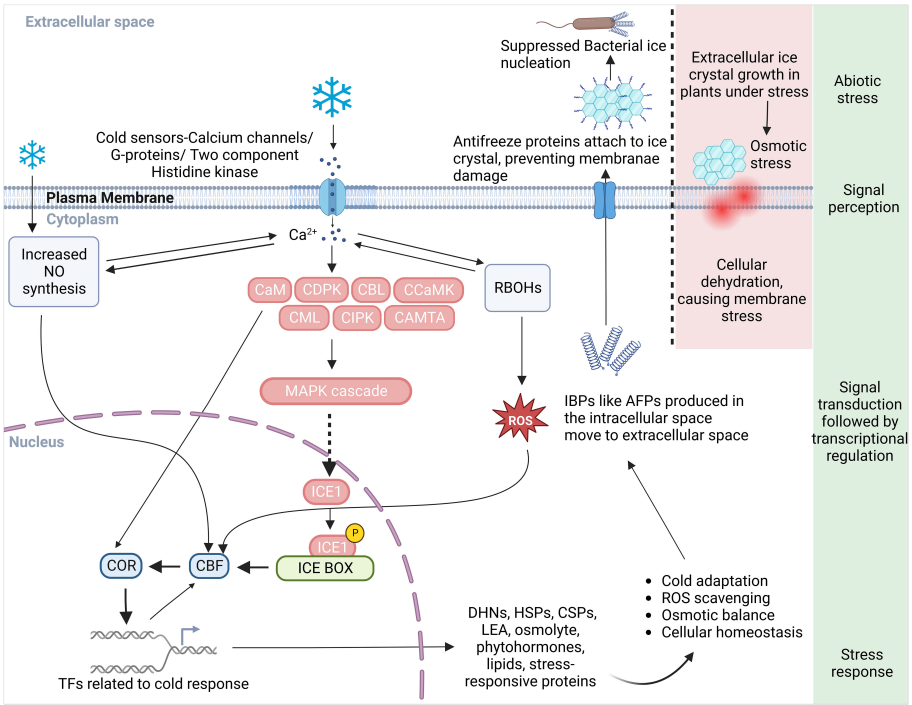

FIGURE 1
A schematic diagram illustrating an overview of the cold perception and the Ca^{2+} mediated cold responsive signal transduction and response pathways in plant. Plasma membrane receptors and membrane rigidification sense the cold stress and initiate a series of downstream reactions. This cascade activates calcium channels/G-proteins, a two-component histidine kinase, and increases Ca^{2+} influx in the cytoplasm, subsequently stimulating Ca^{2+}-related proteins such as CaM, CDPK, CBL, CCaMK, CML, CIPK, CAMTA, and the MAPK signaling pathway. ICE1 interaction with the signaling cascade instigates the ICE-CBF-COR transcriptome machinery's response. Proteins responsible for the synthesis of cryoprotectants, PKs, phytohormones, and protective proteins like DHNs, AFPs, HSPs, and CSPs, all crucial in cold adaptation, are encoded by the COR genes. For freeze protection in cold-acclimated plants, the process involves IBP induction, secretion of AFPs into the extracellular space, and attachment to ice crystals to inhibit their growth and to prevent freezing linked with bacterial ice nucleation. In non-acclimated plants lacking IBP, large damaging ice crystals form that can rupture the plasma membrane due to cellular dehydration caused by an osmotic gradient that sequesters intracellular water. An increase in Ca^{2+} level due to cold stress also activates RBOHs to produce more ROS and prompts NO synthesis necessary for cold adaptation response. The crosstalk between ROS and Ca^{2+} controls the expression of defense related genes in nucleus. ROS, reactive oxygen species; NO, nitric oxide; RBOH, respiratory burst oxidase homologues; CaM, calmodulin; CDPKs, Ca^{2+} dependent protein kinases; CBLs, calcineurin B-like proteins; CCaMK, Ca^{2+}/calmodulin-dependent protein kinase; CML, CaM like; CIPK, CBL-interacting protein kinases; CaMTA, CaM-binding transcription activator; MAPK, mitogen-activated protein kinase; CBFs, C-repeat binding factors; ICE, inducer of CBF expression; COR, cold-responsive; AFP, anti-freeze proteins; IBP, ice-binding proteins; DHN, dehydrin, HSP, heat shock proteins; CSP, cold shock protein; LEA, late embryogenesis abundant protein; TFs, transcription factors.

CAMTA (CaM-binding transcription activator), CBLs (calcineurin B-like proteins) and CIPKs (CBL-interacting protein kinases) (Kudla et al., 2018). The Calcium/CaM-Regulated Receptor-Like Kinase 1, CRLK1, actively modulates MAPK kinase activity and exerts regulatory control over C-repeat Binding Factors (CBFs) regulons, as well as freezing tolerance (Yang et al., 2010). Subsequent downstream reactions in plants are triggered by cold stress encompass the ICE-CBF/DREB1 pathway, the intricate regulation of cold-responsive genes (Miura and Furumoto, 2013), and post-transcriptional and post-translational modifications (Vyse et al., 2020).

In addition to the plasma membrane, chloroplasts may also serve as important sensors for ambient temperature. When temperatures drop, the equilibrium between the ability to capture light energy and the ability to disperse this energy through metabolic processes is disturbed. This disruption results in enhanced excitation pressure on photosystem II (PSII) and subsequently hinders the photosynthetic capacity by inhibiting it (Ivanov et al., 2012). This phenomenon, known as photoinhibition, results in redox imbalances in photosynthetic electron transport and photosynthetic carbon reduction cycles. Eventually, the photosynthetic apparatus is destroyed, and ROS are generated, serving as a secondary messenger (Bhattacharjee, 2019). Disruption of the photosynthesis process under cold-stress conditions significantly reduces crop yield through various mechanisms. The maximum attainable yield, which represents the optimal conversion of captured light energy into biomass, known as photosynthetic efficiency, is compromised under cold stress (Simkin et al., 2019). This reduction in photosynthetic efficiency is primarily attributed to the impairment of key enzymes involved in the carbon fixation cycle, namely fructose-1,6-bisphosphatase (FBPase) and sedoheptulose-1,7-bisphosphatase (SBPase) (Sassenrath et al.,1990; Kingston-Smith et al., 1997; Hutchison et al., 2000). The decreased activity of ribulose-1,5-bisphosphate carboxylase/oxygenase (Rubisco), the primary enzyme involved in carbon fixation, and the reduction in bisphosphate (RuBP) levels are processes observed at low temperatures. Multiple causes contribute to the diminished RuBP regeneration, such as limitations in linear electron transport,

TABLE 1 A comprehensive list of cold acclimatization genes, transcription factors, and proteins, along with the species of identification, their mode of action, and references, is provided.

Gene/Transcription Factor/Protein	Species	Mode of Action	References
Fruit Trees and Shrubs			
MdCPK1a	*Malus domestica* (apple)	Overexpression in tobacco increased freezing, salt, and cold tolerance, root length, and antioxidants, while reducing membrane damage and lipid peroxidation	(Dong et al., 2020)
PpCBF6	*Prunus persica* (peach)	Transient overexpression prevented sucrose degradation and increased chilling tolerance in peach fruit.	(Cao et al., 2021)
PpCBF1		Overexpression in apple increased freezing tolerance in both non-acclimated and acclimated conditions	(Wisniewski et al., 2011)
PpyCBF1-3	*Pyrus pyrifolia* (Asian pear)	Overexpression in Arabidopsis enhanced tolerance to low temperature, salt, and drought stresses while reducing ROS production	(Ahmad et al., 2019)
BB-*CBF*	*Vaccinium corymbosum* (Highbush blueberry)	Overexpression in Arabidopsis enhanced freezing tolerance and induced certain COR genes	(Polashock et al., 2010)
VvCBF2	*Vitis vinifera* (grape)	Overexpression in Arabidopsis enhanced cold tolerance	(Takuhara et al 2011)
VvCBF4			
VvCBFL			
VvCZFPL			
PgCBF3	*Punica granatum* (pomegranate)	Overexpression in Arabidopsis increased cold resilience by raising proline, total soluble sugar levels, and enzymatic activity (CAT, SOD, and peroxidase), while reducing electrolyte leakage, MDA content, and ROS production	(Wang et al., 2022)
PgCBF7			
PtCBF	*Poncirus trifoliata* (trifoliate orange)	Exhibited increased accumulation in response to low temperature	(He et al., 2012)
MaPIP2-7	*Musa acuminata* L. (banana)	Overexpression enhanced tolerance to multiple abiotic stresses (low temperature, drought, salt) by maintaining osmotic balance, reducing membrane injury, and increasing chlorophyll, proline, soluble sugar, and ABA	(Xu et al., 2020)
MusaPIP1;2		Overexpression improved cold resilience by reducing MDA levels, increasing proline and relative water content, and enhancing photosynthetic efficiency	(Sreedharan et al., 2013)
DlCBF1-3	*Dimocarpus longan* (longan)	Overexpression in Arabidopsis improved cold tolerance by increasing proline accumulation, reducing ROS content, and upregulating cold-responsive genes in the CBF pathway	(Yang et al., 2020)
Solanum			
LeCOR413PM2	*Lycopersicon esculentum* (tomato)	Overexpression prevented membrane damage by increasing antioxidant enzymes, ROS scavenging, reducing PSII photoinhibition, and improving osmotic regulation, while suppressing by RNAi resulted in increased sensitivity of plans to cold	(Zhang et al., 2021)
LeGPA1		Overexpression increased cold tolerance by inducing ICE-CBF pathway genes and enhancing SOD, peroxidase, CAT, proline, and total soluble sugar levels, while reducing ROS production and lipid peroxidation	(Guo et al., 2020)
AtCBF1		Heterology expression of the Arabidopsis *AtCBF1* in tomato improved plant resilience to low temperature by inducing CAT1 gene expression and reducing H_2O_2 levels. It also enhanced tolerance to oxidative damage from methyl viologen	(Hsieh et al., 2002)
AtCBF1-3	*Solanum tuberosum* (potato)	Overexpression of Arabidopsis *AtCBF* genes resulted in improved freezing tolerance in potato	(Pino et al., 2007)
Field Crops			
ZmDREB1A	*Zea mays* (maize)	Overexpression in Arabidopsis induced COR genes and conferred plant's tolerance to cold, drought and high salinity stresses	(Qin et al., 2004)
OsDREB1A	*Oryza sativa* (rice)	Overexpression in Arabidopsis conferred plant's tolerance to cold, drought and high salinity stresses	(Dubouzet et al., 2003)
OsDREB1A/B		Overexpression in Arabidopsis improved tolerance to drought, high-salt and low-temperature. Also, it increased the contents of osmoprotectants such as free proline and various soluble sugars	(Ito et al., 2006)

(Continued)

TABLE 1 Continued

Gene/Transcription Factor/Protein	Species	Mode of Action	References
GmDREB1B	*Glycine max* (soybean)	Overexpression in Arabidopsis resulted in elevated tolerance to abiotic and environmental stresses such as cold, drought, salinity, and heat	(Kidokoro et al., 2015)
BaAFP-1	*Hordeum vulgare* (malting barley)	Increased accumulation observed after cold acclimatization	(Ding et al., 2015)
IbCBF3	*Ipomoea batatas* (sweet potato)	Overexpression led to enhanced tolerance to cold, drought and oxidative stress, and showed improved photosynthesis efficiency and reduced hydrogen peroxide levels	(Jin et al., 2017)
BnCBF5, BnCBF 17	*Brassica napus* (rapeseed)	Overexpression improved freezing tolerance, COR genes mRNA accumulation, photosynthesis-related gene transcript levels accumulation, and chloroplast development resulting in increased photosynthetic efficiency and capacity	(Savitch et al., 2005)
MfLEA3	*Medicago falcata* (yellow alfalfa)	*MfLEA3* was induced by cold, dehydration, and ABA. Its constitutive expression enhanced tolerance to cold, drought, and high-light stress in transgenic tobacco plants, along with higher CAT activity.	(Shi et al., 2020)
Ornamental Plants			
SikCOR413PM1	*Saussurea involucrata* (snow lotus)	Overexpression in tobacco enhanced cold tolerance through Ca^{2+} signaling and membrane stabilization	(Guo, et al., 2019a)
SiDHN		Overexpression in tomato enhanced cold tolerance by preserving cell membrane integrity, increasing chlorophyll a and b contents, carotenoid, reducing chlorophyll photo-oxidation and ROS accumulation, and improving antioxidant enzyme activity and photochemical electron transfer efficiency	(Guo, et al., 2019b)
Herbaceous Plants			
AtCBF2	*Arabidopsis thaliana*	Loss-of-function mutants resulted sensitivity to freezing after cold acclimatization and high salinity	(Zhao et al., 2016)
OST1		Overexpression enhanced freezing tolerance, while *ost1* mutants showed freezing hypersensitivity. Cold-activated OST1 phosphorylates ICE1 and boosts its stability and transcriptional activity in the CBF pathway.	(Ding et al., 2018)
Phospholipase Dδ (PLDδ)		Overexpression increased freezing tolerance, while knockout increased sensitivity. PLDδ gene is involved in membrane lipid hydrolysis, contributing ~20% to phosphatidic acid production; its overexpression enhanced phosphatidic acid production	(Li et al., 2004)
AtDREB1A	*Nicotiana tabacum* (tobacco)	Overexpression of Arabidopsis *AtDREB1A* gene enhanced drought and cold stress tolerance in tobacco by inducing abiotic stress-related genes and interacting with the dehydration responsive element	(Kasuga et al., 2004)
PpCBF3	*Poa pratensis* (kentucky bluegrass)	Transient overexpression in Arabidopsis increased freezing tolerance by reducing electrolyte leakage, H_2O_2 and O_2•− contents, increasing chlorophyll content and photochemical efficacy, and upregulating cold tolerance genes	(Zhuang et al., 2015)
BdIRI-7	*Brachypodium distachyon* (Purple false brome)	Knockdown mutants exhibited reduced freezing survival and impaired ice-crystal growth restriction in plants, while showing increased membrane damage and electrolyte leakage.	(Bredow et al., 2016)
PsCOR413PM2	*Phlox subulate* (creeping phlox)	Overexpression in Arabidopsis improved low-temperature tolerance by modulating Ca^{2+} flux and influencing the expression of stress-related COR and CBF genes	(Zhou et al., 2018)
Others			
PttLHY1, PttLHY2	*Populus tremula* × *Populus tremuloides* (poplar)	RNAi knockdown compromised freezing tolerance during winter dormancy	(IbÁñez et al., 2010)
EgCBF3	*Elaeis guineensis* var. Dura × Pisisfera (oil palm)	Overexpression in tomato improved abiotic stress tolerance under *in vitro* conditions	(Ebrahimi et al., 2016)

chronic photoinactivation, deactivation of stromal bisphosphatases, and end-product limitation. In the case of end-product limitation, the limited synthesis of sucrose, starch, and amino acids leads to the accumulation of phosphorylated intermediates, depletion of the inorganic phosphate pool, and inhibition of ATP synthesis (Leegood and Furbank, 1986; Sharkey et al., 1986; Lemoine et al., 2013). Furthermore, imbalances in the source-sink relationship, where the plant's source activity surpasses the sink demand, result in decreased mRNA levels, degradation of photosynthetic proteins, and ultimately reduced productivity (Adams et al., 2013; Kurepin et al., 2015). These combined effects contribute to lower crop yields under cold stress conditions.

3 Freeze-induced damage in plants: mechanisms and consequences

At freezing temperatures, the aggregation of water molecules within plant cells leads to the formation of stable ice nuclei, which is a critical step in initiating the freezing process. Ice nucleation occurs when these small ice nuclei form a group of membrane proteins known as ice-nucleating proteins (INPs), which act as nucleation sites. These sites promote the formation of extracellular ice crystals by facilitating the proper arrangement of water molecules. In the absence of ice-binding proteins (IBPs), large ice crystals form in the apoplast, which can physically damage plasma membranes. The formation of ice crystals and the subsequent sequestration of intracellular water create an osmotic gradient, leading to cellular dehydration. This loss of cell volume can result in cell collapse or rupture (Pearce, 2001; Larcher, 2003; Snyder and de Melo-Abreu 2005; Zhang et al., 2019). Freeze damage also occurs due to alterations in membrane fluidity caused by the transition of lipid components from liquid into a gel state. This transition reduces membrane selectivity, increases permeability, destabilizes metabolic activities, and inhibits photosynthesis (Larcher, 2003; Zhang et al., 2019).

The magnitude of damage depends on the intensity and duration of freezing conditions and the developmental stage of the plant (Larcher, 2003; Centinari et al., 2016). In some cases, plants can delay the formation of extracellular ice crystals through a process called supercooling, where water in plant tissues remain in a liquid state below the freezing point of water. Supercooling in plants is a sophisticated process, involving various mechanisms working synergistically. It prevents the transition of intercellular water from a liquid to a solid state, effectively suppressing water nucleation and thereby avoiding ice crystallization (Wisniewski et al., 2004; Londo and Kovaleski, 2019). Supercooling is a common phenomenon in woody plants, manifesting in both leaves and the living cells of the xylem, including the xylem ray parenchyma cells. This phenomenon readily takes place in small volumes of water, where the free energy of water is influenced by surface properties, especially in the absence of nucleation particles or agents responsible for initiating ice-crystal formation. This process allows cells to maintain their function, albeit at a relatively reduced rate, and become more tolerant to freeze damage (Cavender-Bares, 2005). However, even in supercooled parts of the plant, progressive dehydration can still occur, indicating that the avoidance of freezing-induced dehydration through deep supercooling is only partial (Pearce, 2001; Larcher, 2003).

Another equally important factor that influences the extent of damage caused by dehydration is the ratio of bound water to free water within plant cells. As freezing-induced dehydration progresses, it can disrupt cell structures associated with the bound water compartment, which is involved in the structural organization of membranes, organelles, and proteins. This disruption can result in irreversible injury to the cells (Elliott et al., 2017). Negative osmotic pressure induces a net movement of water towards the extracellular space, reducing cell volume. In non-acclimated cells, this reduction in cell volume leads to invagination of the plasma membrane and formation of endocytic vesicles, resulting in loss of surface area of the plasma membrane. Upon rewarming, melted water from the extracellular space re-enters the cell, causing the cell to burst before it can regain its original volume (Ambroise et al., 2020).

The antioxidant system in plants also scavenges the excessive amount of ROS, including superoxide ($O_2^{\bullet-}$), hydroxyl radicals ($OH^{\bullet}$), hydrogen peroxide (H_2O_2) and singlet oxygen ($^1O_2$) in response to cold stress. The antioxidant compounds play a critical role in maintaining redox homeostasis during cold stress, as optimal levels of ROS are necessary for normal progression of fundamental biological processes including cellular proliferation and differentiation (Tsukagoshi et al., 2010; Mittler, 2017). Under normal conditions, excessive ROS is neutralized through various enzymatic and non-enzymatic antioxidative defense mechanisms. However, when plants are exposed to cold stress, the equilibrium between ROS production and scavenging is disrupted, leading to mitochondrial membrane rigidification (Saha et al., 2015), loss of complex IV (Prasad et al., 1994), DNA damage, and impaired regulation of physiological cell death (Xie et al., 2014; Berni et al., 2019). These disruptive events can cause severe damage to plant cells and their functions, which may affect their survival and reproduction.

4 Plant defense mechanisms against freezing: insights and perspectives

Plants possess avoidance and tolerance strategies to mitigate the detrimental effects of freezing temperatures and prevent damage to their cellular structures (Larcher, 2003; Hoermiller et al., 2018). Avoidance mechanisms rely on a variety of cryoprotectant molecules to reduce the intracellular freezing temperature through a plant-specific process called supercooling (Francko et al., 2011). These molecules help maintain the intracellular liquids at sub-zero temperatures supercooled and delay or inhibit the formation of extracellular ice crystals (Larcher, 2003; Wisniewski et al., 2018). Certain plant species have developed sophisticated mechanisms to mitigate freezing damage by utilizing IBPs as a part of their survival strategy. IBPs, also known as antifreeze proteins (AFPs) or ice recrystallization inhibition (IRI) proteins, are a group of low temperature-associated proteins found in various cold-adapted organisms, including plants such as *Lolium perenne, Loliurn perenne and Ammopiptanthus nanus* (Yu et al., 2021), animals, and microorganisms. Plant IBPs possess unique structural features and functional properties that enable them to interact with ice crystals, thereby impeding their growth and inhibiting the movement of water molecules from the intracellular to extracellular space. This binding ability helps prevent cell dehydration and maintains cellular integrity during freezing conditions. Additionally, IBPs exhibit the ability to suppress ice recrystallization, a process that can lead to tissue damage and disrupt plasma membranes. By effectively limiting ice crystal growth and inhibiting ice recrystallization, IBPs play a crucial role in safeguarding plant tissues against freezing

temperatures (Bredow and Walker, 2017; Wisniewski et al., 2020). Numerous AFPs have been identified in various plant species, highlighting the diversity of these ice-binding proteins. For example, fpAFP has been discovered in *Festuca pratensis* (Muthukumaran et al., 2011), LpAFP and LpIRI2/3 in *Lolium perenne* (Bredow et al., 2017), BdIRI1-7 in *Brachypodium distachyon* (Bredow et al., 2016), daAFP in *Daucus carota* (Cid et al., 2018) and rsAFP in *Raphanus sativus* (Wisniewski et al., 2020). These specific IBPs exemplify the adaptations of plants to withstand freezing stress and highlight the intricate molecular strategies employed by these organisms to protect themselves from the detrimental effects of low temperatures.

Cold tolerance mechanisms involve acquiring tolerance to low, non-freezing temperatures through a process known as cold acclimation. It is a complex physiological process where plants gradually adapt to decreasing temperatures, resulting in enhanced hardiness and adaptive responses that enable them to withstand freezing conditions. Cold acclimation encompasses coordinated molecular, physiological, and biochemical changes that enhance plant tolerance to cold stress, crucial for survival under low temperature conditions. These adaptations include diverse morphological modifications such as reduced plant height, decreased leaf number, and increased epidermal thickness. Biochemical alterations involve the accumulation of sugars, amino acids, and secondary metabolites. Physiological adjustments encompass decreased photosynthesis, reduced water use efficiency, and altered pigment synthesis. Collectively, these mechanisms enhance a plant's ability to thrive in cold environments (Fürtauer et al., 2019; Wang et al., 2020; Fang et al., 2021; Guo et al., 2021; Liu et al., 2021b; Satyakam et al., 2022). The regulation of gene expression during cold stress response is a complex network triggered by multiple factors including Ca^{2+} and plant hormones, particularly brassinosteroids (BRs), gibberellins, abscisic acid, jasmonic acid, and ethylene (Arias et al., 2015; Eremina et al., 2016; Hu et al., 2017; Li et al., 2017:1; Juurakko et al., 2021; Mishra et al., 2022; Sarkar and Sadhukhan, 2022). Additionally, plants synthesize secondary metabolites in response to cold stress, such as proline, betaine, and putrescine. These osmolytes act as protective compounds, helping to mitigate the effects of cold stress on plant cells (Lee et al., 2019). Plants also accumulate low-molecular-weight compatible solutes or osmolyte cryoprotectants, such as sucrose, glucose, raffinose, fructose and trehalose. These molecules assist in maintaining cellular osmotic balance and protect cellular structures from cold-induced damage (Karabudak et al., 2014; Lunn et al., 2014; Judy and Kishore, 2016; Roychoudhury and Banerjee, 2016; Suo et al., 2017; Siddique et al., 2018; Liu et al., 2019; Chen et al., 2022). In addition, plants respond to cold stress by increasing the accumulation of suberin and lignin, which contribute to the reinforcement of cell walls and the protection of plant tissues against freezing injury. These modifications are essential for reducing the adverse effects of cold stress on plant growth and development (Trache et al., 2017; Jian et al., 2020; Sun et al., 2021).

The process of cold acclimation in plants also involves plasma membrane rigidification and rearrangement of the cytoskeleton (Knight and Knight, 2012; Ambroise et al., 2020; Satyakam et al., 2022). These alterations trigger increased metabolic activities, initiating signaling pathways that regulate the expression of COR genes (Iqbal et al., 2022; Satyakam et al., 2022). The induction of COR genes is mediated by transcriptional activators known as C-repeat Binding Factors (CBFs), which are controlled by the regulatory module involving the Inducer of CBF Expression (ICE). This regulatory module, referred to as ICE-CBF-COR, represents a central pathway responsible for initiating the cold response in plants (Chinnusamy et al., 2003; Jin et al., 2018). Upon activation, COR genes regulate the synthesis of various protective molecules, including compatible solutes such as soluble sugars and proline, pigments like xanthophylls and carotenoids, amino acids, and cold-responsive proteins such as AFPs, late embryogenesis abundant (LEA) proteins, heat shock proteins (HSPs), cold shock proteins (CSPs), as well as antioxidants and stabilizing proteins like chaperones and dehydrins (DHNs) (Rinehart et al., 2007; Latowski et al., 2011; Yu et al., 2017; Meena et al., 2019; Ambroise et al., 2020). The synthesis and accumulation of these molecules collectively contribute to the development of cold tolerance in plants.

5 Cryoprotectants: mechanisms of action and insights in frost mitigation

Over the past two decades, agrochemical companies have developed multiple cryoprotectants (such as KDL, Glacier, diKap, Anti-Stress 550, ThermoMax, FrostGard, etc.) for frost protection – a comprehensive list of the artificial cryoprotectants has recently been summarized in a review by (Román-Figueroa et al., 2021). These compounds, when externally applied to plants, enhance plant's freezing avoidance ability through various methods. They create a physical barrier around plant tissues, increase the concentration of endogenous cryoprotectants like metabolites and proteins, and boost the intercellular solute concentration. This elevated solute concentration leads to a depression in freezing point, preventing the formation of extracellular ice crystals and reducing cell dehydration-induced damage caused by apoplastic freezing. It has also been suggested that solute accumulation stabilizes cell membranes and macromolecules, either through direct interaction with the membrane surface or through strong interplay with the surrounding water. The precise mechanism by which these molecules prevent ice crystal formation and cell dehydration is intricate and varies depending on the specific type of cryoprotectant. In this summary, we outline some general mechanisms through which cryoprotectants alleviate freezing damage to plant tissues.

5.1 Physical barrier: plant tissue protection using cellulose nanocrystals

Cellulose nanocrystals (CNCs) are nanoscale biomaterials with unique structural characteristics and impressive physicochemical properties. These properties include biocompatibility, biodegradability, renewability, low density, versatile surface

chemistry, optical transparency, and enhanced mechanical properties (Trache et al., 2017). CNCs serve as the foundational polymeric motifs of macroscopic cellulosic fibers produced through the acid hydrolysis of cellulose materials. CNCs exhibit a needle-like or rod-like shape and have dimensions on the nanometer scale, typically ranging from a few to several hundred nanometers in length and a few nanometers in width. These materials can be obtained from various sources such as higher plants, marine animals (such as tunicates), and, to a lesser extent, algae, fungi, bacteria, invertebrates, and even amoeba like *Dictyostelium discoideum* (Habibi et a., 2010; Grishkewich et al., 2017). Due to their exceptional attributes, CNCs find applications in diverse fields, including automotive, medicine, construction, marine, aerospace, barrier materials, flexible displays, antimicrobial coatings, biomedical implants, transparent films, pharmaceuticals, drug delivery, electronic component templates, fibers and textiles, separation membranes, supercapacitors, batteries, and electroactive polymers (Trache et al., 2017).

Recently, researchers have explored the use of CNCs as a cryoprotectant for grape and sweet cherry reproductive buds (Alhamid et al., 2018). The application of sprayable CNCs forms a thermal insulation coating around the buds and flowers, resulting in enhanced cold hardness and effective mitigation of frost damage. The protective properties of CNCs can be attributed to their low thermal conductivity (0.061 W m^{-1} K^{-1}), which surpasses that of other commonly used frost protection materials. In this study, CNC treatment significantly reduced the damage temperature of grape and sweet cherry buds and improved their resistance to frost damage by 2 – 4°C. Moreover, the application of CNCs delayed the formation of ice nucleation in the buds when exposed to freezing temperatures. The freezing temperature at which ice nucleation occurred was lowered by approximately 3°C in CNC-treated buds compared to untreated buds (Alhamid and Mo 2021). These findings highlight the extensive potential of CNCs as cryoprotectants in enhancing plants' protective mechanisms and their capacity for freeze protection.

5.2 Reducing freezing point

Certain cryoprotectants exhibit cryohydricity, which refers to their ability to depress the freezing point of water. This phenomenon enables plants to endure lower temperatures by modifying the colligative properties of water, including osmotic potential and increased intracellular solute concentration. Solute compounds, such as sugars, salts, and other dissolved substances, disrupt ice crystal formation and impede the progress of freezing. As a result, the freezing temperature of water within plant tissues is reduced below the standard freezing point of pure water (0°C), known as freezing point depression (Ginot et al., 2020) (Figure 2). The extent of this depression depends on the concentration and nature of the solutes involved, with higher solute concentrations yielding greater reductions in freezing point. This reduced freezing point enables plant cells to remain in a liquid state even at sub-zero temperatures, thus preventing or delaying ice crystal formation. At the cellular level, cryoprotectants modify water properties through hydrogen bonding interactions between water and cryoprotectant molecules. This hydrogen bonding plays a crucial role in hindering the movement of intracellular water into the extracellular space, effectively reducing ice crystal formation and minimizing cellular damage (Weng et al., 2011; Elliott et al., 2017) (Figure 2).

An example of an exogenous cryoprotectant capable of lowering the freezing point of plant tissues is FreezePruf, a commercially available product. FreezePruf is formulated using polyethylene glycol, potassium silicate, glycerol, silicone polyether surfactant, and a bicyclic oxazolidine anti-desiccant. These constituent molecules act as solutes or osmolytes, and their application increases solute concentration in the intracellular cytoplasmic compartments, leading to a reduction in the freezing point of these cellular regions. Francko et al. (2011) conducted a study to evaluate the effectiveness of FreezePruf on various monocot herbaceous and dicot fruit crops. Their experimental results demonstrated that the treatment with FreezePruf significantly decreased freezing-induced injury and lowered the mortality temperature by approximately 7 degrees when applied to foliage and about 1 degree when applied to open flowers. This reduction in freezing temperature is primarily attributed to the active ingredients present in FreezePruf, which act colligatively via freezing point depression as solutes. Moreover, these ingredients exert non-colligative effects by stabilizing cell membranes, thereby providing protection against freeze damage caused by ice crystal formation (Francko et al., 2011).

5.3 Stabilizing cellular structures

Plasma membranes are highly vulnerable to damage caused by freezing. This damage arises from several factors, including increased levels of ROS, the transition of the lipid bilayer from a fluid state to a solid-gel state, cell dehydration, and the formation of extracellular ice crystals. Collectively, these factors compromise the integrity, fluidity, and functionality of the membrane, leading to cellular damage and impaired plant survival under freeze stress. The temperature-dependent phase transition of the lipid bilayer plays a critical role in freeze-induced membrane damage. This transition reduces water diffusion across the membrane (Eze, 1991) and disrupts lipid-protein interactions, impacting membrane integrity and function (Iivonen et al., 2004). The composition of lipids, specifically the number of carbon atoms and double bonds in the lipid tail, influences the phase transition temperature. Lipids with higher unsaturation, characterized by an increased number of double bonds, exhibit a lower phase transition temperature, thereby reducing the occurrence of phase transition, leading to reduced freeze-induced membrane damage (Ambroise et al., 2020).

Cryoprotectants have been demonstrated to stabilize cellular structures and plasma membranes through various mechanisms. These mechanisms include modulating the membrane lipid phase transition, preventing protein denaturation, interacting with membrane proteins to stabilize their conformation and function, inducing membrane repair mechanisms, enhancing membrane flexibility, reducing mechanical stress, and acting as osmoregulators (Fürtauer et al., 2019). Furthermore, the osmoregulatory properties of

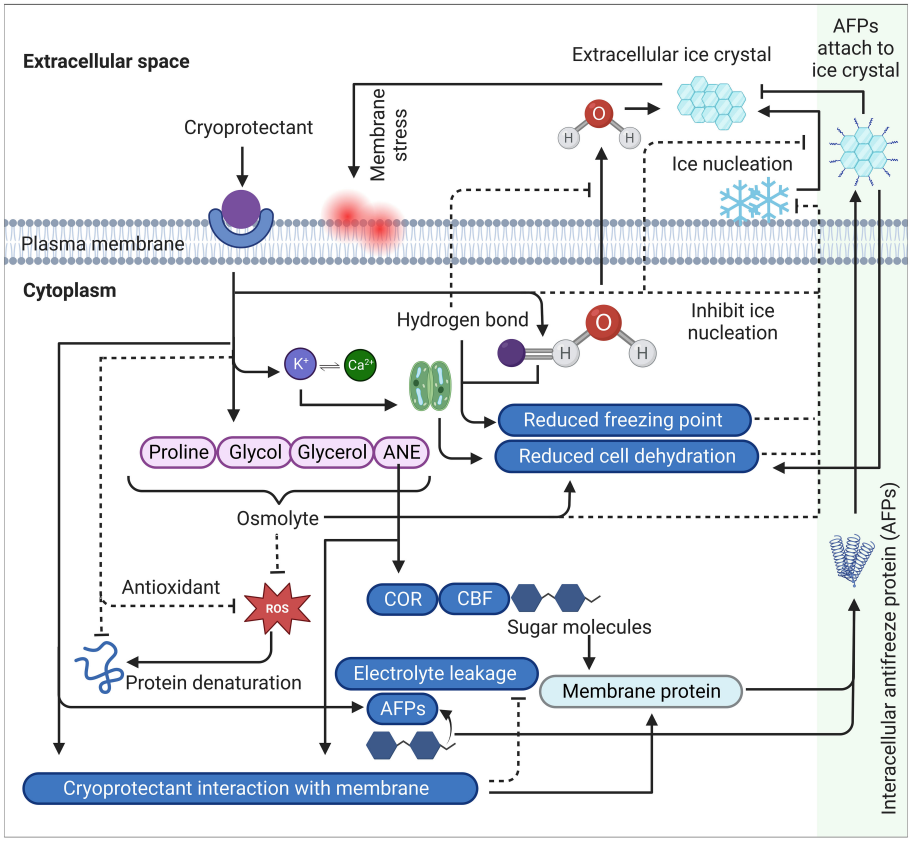

FIGURE 2
A comprehensive schematic summary of cryoprotectants mechanism of action and cold stress modulation in plants. Cryoprotectants regulate osmolytes such as proline, glycol, glycerol and ANE. The increased accumulation of these osmolytes triggers the induction of cold regulating (COR) genes through the activation of transcriptional activators called C-repeat Binding Factors (CBFs), which are involved in reducing cell dehydration, regulating membrane proteins and synthesizing antifreeze proteins (AFPs). Sugar molecules also participate in this regulation by reducing cell dehydration and modulating membrane proteins, including antifreeze proteins (AFPs). AFPs are secreted into extracellular spaces, attaching to ice crystals to prevent ice aggregation, resulting in suppressing recrystallization and reducing cell dehydration. Additionally, cryoprotectants trigger K^+ interacting with Ca^{2+} that plays an important role in the hydrodynamic stomatal closure mechanism, leading to reduced cell dehydration. Furthermore, cryoprotectants establish hydrogen bonds with intracellular water molecules, restricting their movement into extracellular spaces and inhibiting its conversion into ice crystals. This hydrogen bonding lowers the freezing point of water. In addition, certain cryoprotectants scavenge ROS either through their antioxidant properties or through its osmoregulatory properties that contributes to maintaining cellular osmotic balance and integrity by regulating water movement across the membrane, resulting in enhanced plasma membrane stability. Collectively, these mechanisms prevent the formation of ice-nucleation sites on the membrane surface, which is a critical step in the initiation of extracellular ice crystal formation and subsequent freezing stress. Arrows indicate positive regulation while dashed line with a perpendicular line at the end indicates negative regulation. ROS, reactive oxygen species; CBF, C-repeat Binding Factors, COR, cold-responsive, AFP, antifreeze proteins, ANE, *Ascophyllum nodosum* (Seaweed) extract.

these compounds contribute to maintaining cellular osmotic balance and integrity by regulating water movement across the membrane, resulting in enhanced plasma membrane stability (Sami et al., 2016; Arakawa et al., 2018; Fürtauer et al., 2019).

Certain commercially available cryoprotectants, such as KDL, FrostGard, and Superkelp/Vitazyme, utilize *Ascophyllum nodosum* (Seaweed) extract (ANE) as an active ingredient. ANE has been reported to alleviate low-temperature stress in plants by mitigating freezing-induced electrolyte leakage through the preservation of membrane integrity (Figure 2). Notably, ANE application on winter barley has been found to enhance winter hardiness and augment cold resistance (Shukla et al., 2019). Additionally, treatment with the lipophilic fraction (LPC) of ANE in Arabidopsis plants improved cold tolerance, as evidenced by the suppression of chlorosis and recovery from freezing-induced tissue damage (Rayirath et al., 2009).

Furthermore, a comprehensive analysis of the transcriptome and metabolome of LPC-treated Arabidopsis plants revealed that ANE treatment induces the expression of cold-responsive genes, including *COR15A*, *RD29A*, and *CBF* (Rayirath et al., 2009), as well as genes associated with sugar accumulation and lipid metabolism (Nair et al., 2012). Metabolite profiling of LPC-treated plants showed that the observed protection against freezing stress is mediated by the regulation of soluble sugars, sugar alcohols, organic acids, and lipophilic components such as fatty acids (Nair et al., 2012). The accumulation of sugars plays a crucial role in mitigating freezing stress by stabilizing various biological components, such as cellular membranes and membrane-bound organelles (Tarkowski and Van den Ende 2015). Interestingly, ANE treatment did not improve freezing tolerance in the *sfr4* (sensitive to freezing) mutant of Arabidopsis, which is defective in the

accumulation of free sugars, suggesting that ANE-induced accumulation of soluble sugars prior to freezing stress exposure is critical for its protective effects (Nair et al., 2012).

At the molecular level, ANE-mediated cold tolerance in plants is attributed to the regulation of key transcription factors and genes encoding cryoprotective proteins. For instance, ANE-treated Arabidopsis plants showed increased cold tolerance due to the downregulation of chlorophyll degradation genes, including *AtCLH1* and *AtCLH2*, resulting in an increased chlorophyll content. ANE-mediated cryoprotectants also upregulated genes responsible for proline biosynthesis, such as *5CS1* and *P5CS2*, while downregulating *ProDH*, a gene involved in proline degradation. Moreover, ANE treatment upregulated genes responsible for polysaccharide degradation (*9SEX1* and *SEX4*) and carbohydrate biosynthesis (*GOLS2* and *GOLS3*), while downregulating genes involved in sucrose degradation. ANE treatment also induced key genes involved in freezing tolerance, including galactinol synthase 2, pyrroline 5-carboxylate synthase, and acetyl-CoA carboxylase (Zamani-Babgohari et al., 2019; Ali et al., 2021). These findings provide compelling evidence supporting the role of ANE-based cryoprotectants in enhancing cellular stabilization in plants through molecular, biochemical, and physiological mechanisms.

Another class of cryoprotectants, such as Superkelp/Vitazyme, confer cold protection in plants by increasing the levels of endogenous proline. Proline is naturally accumulated compound in plants in response to cold stress as it is water-soluble and electrically neutral at neutral pH, which helps maintaining cell osmotic potential and protecting against cold damage (Verbruggen and Hermans, 2008). The application of exogenous cryoprotectants containing proline significantly elevates the endogenous proline levels and enhances cold tolerance. Studies have shown that proline-mediated cryoprotectant treatments in rapeseed shoots increase cold tolerance and reduce electrolyte leakage, which is an indicator of membrane injury (Jonytiene et al., 2012). Additionally, proline-treated *Brassica juncea* has been shown to protect isolated thylakoid membranes from photoinhibition (Bhandari and Nayyar, 2014) and improve the maintenance of chloroplast ultrastructure and membrane integrity in tobacco plants (Van Rensburg et al., 1993). Moreover, proline-stimulating cryoprotectants exert their protective effects by interacting with plasma membrane-bound proteins and enzymes. These compounds act as hydrotropes to stabilize enzymes and biomembranes, owing to the ability of proline to form hydrophilic colloids with water and a hydrophobic backbone for protein interactions. This helps maintain the structure and conformation of proteins necessary for their functional integrity. Additionally, proline functions as a chaperone to prevent membrane proteins from denaturation (Rajendrakumar et al., 1994; Zhang et al., 2011).

5.4 Cryoprotectant interactions with ice crystals: inhibiting nucleation and their growth

Certain cryoprotectants possess the ability to inhibit the formation of ice nuclei, which serve as the initial points for ice crystal growth. These cryoprotectants also prevent the fusion of smaller ice crystals into larger ones, which could otherwise lead to cellular damage. For example, cryoprotectants containing antifreeze proteins (AFPs) have been shown to bind to the surface of ice crystals and inhibit their growth, thus preventing the formation of large ice crystals in the extracellular space (Figure 2). These molecules can also inhibit ice recrystallization, a phenomenon that can occur during repeated freeze-thaw cycles or prolonged exposure to low temperatures (Meyer et al., 1999; Wisniewski and Fuller, 1999; Griffith and Yaish, 2004). The effect of three synthetic analogues based on naturally occurring antifreeze peptides, AFPW, DCR26, DCR39, was investigated on carrot and cherry fruits (Kong et al., 2016; Kong et al., 2017). The *in vitro* experimental results showed that these compounds modified ice crystal morphology, resulting in reduced cell damage by ice crystals (Kong et al., 2017). Interestingly, certain plant AFPs share sequence homology with plant pathogenesis-related (PR) proteins including endochitinases (PR3), endo-β-1,3-glucanases (PR2), and thaumatines (PR5) (Antikainen et al., 1996; Pearce, 2001). This suggests that AFPs may serve a dual role in cold survival by mitigating freeze-related damage and providing defense against psychrophilic pathogens (e.g., ice-nucleating bacteria) (Griffith and Yaish, 2004).

The precise molecular mechanism underlying the interaction between cryoprotectants, particularly those containing AFPs, and ice crystals is not yet fully understood. Several factors that facilitate the binding of AFPs to ice nuclei have been identified. These include the amino acid composition of AFPs, with specific residues playing a role in the binding process (Davies and Sykes, 1997). Additionally, the secondary structure of these compounds, such as beta-strand-rich proteins, has been implicated in their ice-binding ability (Lu et al., 2002). Motifs such as the presence of N-acetyl groups at C-2 peptide chains with O-glycosidic linkages and gamma-methyl groups at threonine have also been identified as potential contributors to the ice-binding mechanism (Urbańczyk et al., 2017; Chakraborty and Jana, 2018). These ice-binding sites are primarily hydrophobic, although recent molecular studies have shown that both hydrophobic and hydrophilic properties contribute to the ice-binding mechanism (Hudait et al., 2018). Furthermore, AFPs and AFP-mediated cryoprotectants are known to form cages around the methyl groups on the ice-binding surface, organizing surrounding water molecules into an ice-like lattice and creating a quasi-liquid-like layer between water and the already formed ice crystals (Satyakam et al., 2022). However, despite these insights, the precise molecular mechanism by which certain cryoprotectants interact with ice crystals remains to be fully elucidated, and further research is needed to better understand this intriguing phenomenon.

In some cases, exogenously applied cryoprotectants can inhibit ice-nucleating bacteria by using inorganic salts or organic polymers to create a vapor barrier on the leaf surface, offering modest frost and freeze protection (Francko et al., 2011). An example of such cryoprotectants is a successful patent by Glenn et al. (2001), which describes a slurry comprising particulate materials that prevent ice crystal formation on the leaf surface at freezing temperatures. Ice-nucleating active (INA) bacteria, such as *Pseudomonas syringae* van Hall and *Erwinia herbicola* (Lihnis) Dye, possess a unique capability

to catalyze ice formation at temperatures slightly below the freezing point (approximately -2°C) (Lindow et al., 1982). The ice-nucleation capability of INA bacteria is attributed to their specialized hydrophilic-hydrophobic ice-active sites (Pandey et al., 2016). In natural conditions, frost damage to plants typically occurs between -2°C and -5°C. Within this temperature range, ice crystals form from supercooled water within the plants, propagating throughout the intercellular and intracellular spaces and causing damage. In the absence of ice nucleation sites, water in plant tissues can remain in a supercooled state without freezing until the temperature becomes low enough for the most active ice nucleation site associated with the plant to catalyze the crystallization of supercooled water (Lindow et al., 1982). INA bacteria, found ubiquitously on plant surfaces, prevent supercooling by initiating the ice nucleation process using specialized ice-nucleating proteins (INPs) attached to their outer cellular membrane (Pandey et al., 2016), ultimately leading to freeze injury alleviation (Roeters et al., 2021; Lukas et al., 2022).

5.5 Reducing cell dehydration

At sub-zero temperatures, freeze-induced dehydration stress triggers changes in the lipid bilayer configuration of cell membranes, leading to a transition from a lamellar phase to a hexagonal II phase. The formation of hexagonal II phase membranes is facilitated by decreased water content, an increased number of intracellular membranes, and the presence of specific lipids such as phosphatidylethanolamine and sterols in the bilipid membrane (Uemura et al., 1995). Lipid unsaturation in plant cells plays a pivotal role in mitigating freeze damage and enhancing cold resistance. This is largely due to the properties of unsaturated fatty acids within the phospholipids of the cell membrane. These fatty acids have double bonds that introduce kinks in the fatty acid chains, preventing them from packing tightly and solidifying at low temperatures. Consequently, a higher degree of lipid unsaturation typically decreases freeze damage in plants. This is an adaptive strategy that many cold-tolerant plant species employ, synthesizing and accumulating unsaturated fatty acids under low-temperature exposure.

Alongside the structural changes in the lipid bilayer, dehydration stress can also induce expansion-induced lysis, where negative osmotic pressure drives water movement from the cell interior towards the extracellular space, resulting in a reduction in cell volume. This phenomenon causes the plasma membrane to invaginate and form endocytic vesicles, leading to a loss of plasma membrane surface area. Upon rewarming, the melted extracellular water reenters the cell, causing the cell to burst before regaining its original volume. In contrast, in cold-acclimated cell protoplasts, the volume reduction triggers the formation of exocytotic extrusions that do not decrease the membrane surface area and do not cause cell bursting upon rewarming (Uemura et al., 1995; Ambroise et al., 2020).

The application of specific exogenous cryoprotectants, such as Anti-Stress 2000 (Terra Tech, Eugene, OR) and Wilt-Pruf (Wilt-Pruf Products, Essex, CT), has been demonstrated to mitigate dehydration risk in plants during freezing and thawing cycles. This protective effect is attributed to the anti-desiccant properties of these compounds, which reduce water loss from plant tissues resulting from osmotic stress induced by ice crystal formation (Figure 2). By preserving cellular integrity and preventing dehydration-induced damage, these cryoprotectants play a vital role in plant protection. As discussed earlier, certain cryoprotectants contain molecules capable of lowering the freezing points of plant tissues. Additionally, these compounds contribute significantly to the prevention of cellular dehydration. For instance, potassium, a key component of several cryoprotectants, plays a crucial role in the hydrodynamic stomatal closure mechanism and helps maintain cellular osmotic balance (Figure 2). This regulatory mechanism of potassium is essential for preserving cellular integrity during freezing and thawing cycles (Cakmak, 2005; Wang et al., 2013).

5.6 Scavenging reactive oxygen species

Reactive Oxygen Species (ROS) are partially reduced or excited derivatives of molecular oxygen (O_2), which naturally arise as a normal byproduct of aerobic life (Mittler, 2017; Sies and Jones, 2020). In contrast to O_2, ROS are highly reactive and autonomously produced in various cellular compartments, leading to the oxidation of lipids, proteins, DNA, RNA, and many small cellular molecules. The high reactivity of ROS is attributed to their altered chemical composition, enabling them to engage in electron donation or transfer an excited energy states to accepter molecules (Mittler et al., 2022). The major forms of ROS in cells include free radicals like superoxide anion radical (O_2•−) and hydroxyl radical (OH•), and non-radicals like hydrogen peroxide (H_2O_2) and singlet oxygen ($^1O_2$), and various forms of organic and inorganic peroxides (Mittler, 2017; Sies and Jones, 2020). ROS are primarily formed in chloroplast, mitochondria and peroxisomes. There are secondary sites including endoplasmic reticulum, cell membrane, cell wall and the apoplast, typically equipped with molecules having a high redox potential to reduced or excite molecular oxygen (Das and Roychoudhury, 2014; Mittler, 2017). ROS can be produced both passively by housekeeping enzyme or as by-products of metabolic pathways such as photosynthesis and respiration, and actively by specialized oxidase enzymes such as the respiratory burst oxidase homologues (RBOHs) proteins, which are the functional equivalent of mammalian NADPH oxidase (NOX proteins) (Mittler et al., 2022). Superoxide radical is the first by-product produced at the apoplast through the function of RBOHs proteins, which is subsequently dismutated by the action of superoxide dismutase (SOD) to H_2O_2. The membrane permeable H_2O_2 is the premier signaling molecule, playing an important role in regulating various cellular metabolic activities associated with growth, development, cell expansion and response to environmental stimuli (Baxter et al., 2014; Smirnoff and Arnaud, 2019). Hydrogen peroxide interacts with ferrous ions (Fe^{2+}), forming OH•, the highly reactive form of ROS, through Fenton reaction (Mittler, 2017).

ROS display a dual role in plant cells, depending on their accumulation levels. A moderate, “steady-state” level of ROS is

required for the progression of various fundamental biological processes, including cellular proliferation, differentiation and important signaling reactions in cells, but are also the unavoidable toxic byproducts of aerobic metabolism. As signaling molecules, ROS enables cells to rapidly respond to environmental stimuli and triggers plant's cellular defense signaling cascade (Chi et al., 2013). Under optimal growth conditions, plants maintain a basal level of ROS serving as signaling molecules to sense elevated atmospheric oxygen levels and to monitor different metabolic reactions. However, different biotic and abiotic stress (i.e., freezing stress) disrupt the cellular homeostasis, uncouple metabolic pathways and leads to an increased production of ROS (Suzuki and Mittler, 2006; Miller et al., 2010). The elevated accumulation of ROS in cells leads to toxic oxidative stress, which adversely damages cellular components including protein denaturation, membrane lipids degradation through peroxidation (Heidarvand and Maali-Amiri, 2013) and oxidation and damaging of DNA, RNA, protein and membrane (Mittler, 2002; Mittler, 2017; Sharma et al., 2021), leading to cell death. The ROS-induced cell death is mediated through a programmed physiological and genetic pathway such as ferroptosis or regulated necrosis (Mittler, 2017). Plants pose ROS-scavenging mechanisms to detoxify the excessive ROS and maintain the balance between scavenging and production. This include the various antioxidative enzymes such as superoxide dismutase (SOD), ascorbate peroxidase (APX), catalase (CAT), glutathione peroxidase (GPX), peroxiredoxin (PRX), monodehydroascorbate reductase (MDHAR), and dehydroascorbate reductase (DHAR), and non-enzymatic antioxidants including ascorbic acid (AsA), reduced glutathione (GSH), α-tocopherol, carotenoids, flavonoids, and the osmolyte proline. The presence of these antioxidative systems in plants helps maintain a basal non-toxic level of ROS in cells, which serve as signaling molecules and promotes normal cellular processes (Miller et al., 2010; Das and Roychoudhury, 2014).

The application of certain cryoprotectants, such as Basfoliar® Frost Protect or COMPO® Frost Protect, has been shown to effectively mitigate ROS toxicity in plant cells. These cryoprotectants contain α-tocopherol, a lipophilic antioxidant that exhibit ROS and lipid radicals scavenging properties (Gill and Tuteja, 2010; Das and Roychoudhury, 2014) (Figure 2). Among the four isoforms of tocopherol (α-, β-, γ-, δ-), α-tocopherol has the highest antioxidant capability (Das and Roychoudhury, 2014). The antioxidant activity of tocopherol is primarily attributed to its ability of donating phenolic hydrogens to lipid free-radicals (Kamal-Eldin and Appelqvist, 1996). These compounds are known for their ability to inhibit lipid peroxidation, preserve the integrity and fluidity of photosynthesizing membranes and prevent membrane damage by interacting with O_2 molecule and quenching reactive oxidative anions in which the reactivity of the highly reactive ROS, such as $^1O_2$, is substantially reduced. It has been estimated that a single molecule of α-tocopherol can neutralize up to 120 molecules of $^1O_2$ through resonance energy transfer (Gill and Tuteja, 2010; Das and Roychoudhury, 2014; Sadiq et al., 2019). Multiple studies demonstrated that increased accumulation of α-tocopherol in winter wheat leaves was associated with enhanced frost tolerance (Janeczko et al., 2018). Additionally, the application of exogenous α-tocopherol cryoprotectants has been found to enhance abiotic stress tolerance in onions by reducing the level of endogenous H_2O_2 and lipid peroxidation, and increasing the activity of antioxidative enzymes (i.e., SAD, CAT, APX, and GPX) and non-enzymatic antioxidants (i.e., AsA and GSH) (Semida et al., 2016).

Additionally, cryoprotectants, such as Frost Shield® (Maz-Zee S.A. International) and *CROPAID® NPA®* (Natural Plant Antifreeze, Bimas, Turkey), can enhance plant tolerance to excessive ROS levels through sequestering or replacing cellular free iron with other minerals. These cryoprotectants contain minerals and amino acids in their composition. Minerals, such as Mn^{2+} that is found in complex with amino acid, peptides, nucleotides and carbohydrates, can replace iron to prevent its toxicity during oxidative stress (Mittler, 2017). The presence of free iron in the form of Fe^{2+} is considered crucial for ROS toxicity due to its role in the Fenton reaction, where it catalyzes the generation of highly reactive hydroxyl radicals. By sequestering or substituting free iron with alternative minerals (i.e., Mn^{2+}), cryoprotectants can disrupt the Fenton reaction and attenuate the production of damaging hydroxyl radicals. In addition, these manganese complexes are shown to effectively scavenge $O_2^{\bullet-}$, H_2O_2 and $OH^{\bullet}$ (Slade and Radman, 2011; Mittler, 2017). Overall, cryoprotectants modulate the equilibrium between ROS production through NADPH and ROS scavenging through various enzymatic and non-enzymatic antioxidants. However, it should be acknowledged that the specific molecular mechanisms can vary based on the type of cryoprotectant, plant species, and cellular conditions. Further research is required to gain a comprehensive understanding of these mechanisms.

6 Conclusion

Plants utilize advanced molecular mechanisms to perceive and respond to cold stress. Transmembrane proteins function as initial sensors for cold stress signals, triggering a cascade of molecular events that involve the generation of secondary messengers such as calcium ions (Ca^{2+}), reactive oxygen species (ROS), and inositol phosphates. Among these, calcium signaling plays a critical role, activating downstream phosphorylation cascades and inducing the transcription of cold-responsive genes, including the cold-regulated (COR) genes. Cold stress imposes significant challenges on plant tissues, leading to membrane rigidification and dehydration caused by freeze-induced damage. In an effort to mitigate these adverse effects, plants have evolved strategies encompassing both avoidance and tolerance mechanisms. Tolerance mechanisms involve the gradual acclimatization of plants to decreasing temperatures, allowing them to incrementally accumulate cold tolerance. In contrast, avoidance mechanisms are predicted on the presence of cryoprotectant molecules such as potassium ions (K^+), proline, glycerol, and antifreeze proteins (AFPs).

Cryoprotectants operate by increasing intracellular solute concentration, thereby lowering the freezing point and obstructing ice formation. These molecules also exhibit potent antioxidant properties, efficiently scavenging ROS and preventing protein denaturation. By forming extensive hydrogen bonds with water molecules, cryoprotectants can also alter water properties,

limiting intercellular water movement, and minimizing extracellular ice crystal formation (Figure 2). This action consequently reduces cell dehydration and mitigates freeze-induced cellular damage. In addition, cryoprotectants aid in the preservation of plasma membrane fluidity and the reduction of electrolyte leakage, effectively shielding plant cells against freeze-induced injury. The intricate relationship between these cryoprotectant molecules and cellular processes enhances the plant's resilience to cold stress and bolsters survival in freezing environments. Taken together, the deployment of cryoprotectants represents a sophisticated adaptive strategy utilized by plants to counter the damaging effects of cold stress, thereby facilitating their acclimation and survival in freezing conditions. Nevertheless, a comprehensive understanding of these mechanisms warrants further research. It is essential to elucidate the physiological and molecular mechanisms of these compounds and evaluate their potential impact on crop productivity and sustainability. Such efforts will undoubtedly contribute to the ongoing advancement of plant biology and the broader field of environmental science.

Author contributions

KJ conducted literature searches, prepared schematic diagrams, and wrote the first draft. AS contributed to figure preparation and literature review. SS oversaw the study, provided edits to improve clarity and readability, and ensured the overall quality of the manuscript. All authors contributed to the article and approved the submitted version.

Funding

This research was supported partially by funding to SMS from VA-Specialty Crop Block Grant Program (SCBGP) (Grant # 419842) and NIFA-AFRI (Grant# 13367799).

Conflict of interest

The authors declare that the research was conducted in the absence of any commercial or financial relationships that could be construed as a potential conflict of interest.

Publisher's note

References

Adams, W. W., Muller, O., Cohu, C. M., and Demmig-Adams, B. (2013). May photoinhibition be a consequence, rather than a cause, of limited plant productivity? *Photosynthesis Res.* 117 (1), 31–44. doi: 10.1007/s11120-013-9849-7

Ahmad, M., Li, J., Yang, Q., Jamil, W., Teng, Y., and Bai, S. (2019). Phylogenetic, molecular, and functional characterization of ppyCBF proteins in asian pears (Pyrus pyrifolia). *Int. J. Mol. Sci.* 20 (9), 2074. doi: 10.3390/ijms20092074

Alhamid, J. O., and Mo, C. (2021). Numerical analysis of cellulose nanocrystals CNC for reducing cold damage to reproductive buds in fruit crops." *Thermal Sci. Eng. Prog.* 26, 101123. doi: 10.1016/j.tsep.2021.101123

Alhamid, J. O., Mo, C., Zhang, X., Wang, P., Whiting, M. D., and Zhang, Q. (2018). Cellulose nanocrystals reduce cold damage to reproductive buds in fruit crops." *Biosyst. Eng.* 172, 124–133 doi: 10.1016/j.biosystemseng.2018.06.006

Ali, O., Ramsubhag, A., and ayaraman, J. J. (2021). Biostimulant properties of seaweed extracts in plants: implications towards sustainable crop production. *Plants* 10 (3), 531. doi: 10.3390/plants10030531

Ambroise, V., Legay, S., Guerriero, G., Hausman, J.-F., Cuypers, A., and Sergeant, K. (2020). The roots of plant frost hardiness and tolerance. *Plant Cell Physiol.* 61 (1), 3–20. doi: 10.1093/pcp/pcz196

Antikainen, M., Griffith, M., Zhang, J., Hon, W.-C., Yang, D. S. C., and Pihakaski-Maunsbach, K. (1996). Immunolocalization of antifreeze proteins in winter rye leaves, crowns, and roots by tissue printing. *Plant Physiol.* 110 (3), 845–857. doi: 10.1104/pp.110.3.845

Arakawa, K., Kasuga, J., and Takata, N. (2018). "Mechanism of overwintering in trees," in *Survival strategies in extreme cold and desiccation: adaptation mechanisms and their applications, advances in experimental medicine and biology*. Eds. M. Iwaya-Inoue, M. Sakurai and M. Uemura (Singapore: Springer), 129–147.

Arias, N. S., Bucci, S. J., Scholz, F. G., and Goldstein, G. (2015). Freezing avoidance by supercooling in olea europaea cultivars: the role of apoplastic water, solute content and cell wall rigidity. *Plant Cell Environ.* 38 (10), 2061–2070. doi: 10.1111/pce.12529

Augspurger, C. K. (2013). Reconstructing patterns of temperature, phenology, and frost damage over 124 years: spring damage risk is increasing. *Ecology* 94 (1), 41–50. doi: 10.1890/12-0200.1

Baxter, A., Mittler, R., and Suzuki, N. (2014). ROS as key players in plant stress signalling. *J. Exp. Bot.* 65 (5), 1229–1240. doi: 10.1093/jxb/ert375

Berni, R., Luyckx, M., Xu, X., Legay, S., Sergeant, K., Hausman, J.-F., et al. (2019). Reactive oxygen species and heavy metal stress in plants: impact on the cell wall and secondary metabolism." *Environ. Exp. Bot.* 161, 98–106. doi: 10.1016/j.envexpbot.2018.10.017

Bhandari, K., and Nayyar, H. (2014). "Low temperature stress in plants: an overview of roles of cryoprotectants in defense," in *Physiological mechanisms and adaptation strategies in plants under changing environment*, vol. 1 . Eds. P. Ahmad and M. R. Wani (New York, NY: Springer), 193–265.

Bhattacharjee, S. (2019). "ROS and regulation of photosynthesis," in *Reactive oxygen species in plant biology*, (New Delhi: Springer India) 107–125.

Bredow, M., Vanderbeld, B., and Walker, V. K. (2016). Knockdown of ice-binding proteins in brachypodium distachyon demonstrates their role in freeze protection. *PloS One* 11 (12), e0167941. doi: 10.1371/journal.pone.0167941

Bredow, M., Vanderbeld, B., and Walker, V. K. (2017). Ice-binding proteins confer freezing tolerance in transgenic arabidopsis thaliana. *Plant Biotechnol. J.* 15 (1), 68–81. doi: 10.1111/pbi.12592

Bredow, M., and Walker, V. K. (2017). Ice-binding proteins in plants. *Front. Plant Sci.* 8. doi: 10.3389/fpls.2017.02153

Cakmak, I. (2005). The role of potassium in alleviating detrimental effects of abiotic stresses in plants. *J. Plant Nutr. Soil Sci.* 168 (4), 521–530. doi: 10.1002/jpln.200420485

Cao, K., Wei, Y., Chen, Yi, Jiang, S., Chen, X., Wang, X., et al. (2021). PpCBF6 is a low-temperature-sensitive transcription factor that binds the ppVIN2 promoter in peach fruit and regulates sucrose metabolism and chilling injury. *Postharvest Biol. Technol.* 181, 111681. doi: 10.1016/j.postharvbio.2021.111681

Cavender-Bares, J. (2005). Impacts of freezing on longdistance transport in woody plants. In: Holbrook NM, Zwieniecki M, eds. *Vascular transport in plants*. (Oxford, UK: Elsevier) 401–424. doi: 10.1016/B978-012088457-5/50021-6

Centinari, M., Smith, M. S., and Jason P., L. (2016). Assessment of freeze injury of grapevine green tissues in response to cultivars and a cryoprotectant product. *HortScience* 51 (7), 856–860. doi: 10.21273/HORTSCI.51.7.856

Chakraborty, S., and Jana, B. (2018). Antifreeze proteins: an unusual tale of structural evolution, hydration and function. *Proc. Indian Natl. Sci. Acad.* 100, 169–187. doi: 10.16943/ptinsa/2018/49553

Chen, D., Mubeen, B., Hasnain, A., Rizwan, M., Adrees, M., Naqvi, S. A. H., et al. (2022). Role of promising secondary metabolites to confer resistance against environmental stresses in crop plants: current scenario and future perspectives. *Front. Plant Sci.* 13. doi: 10.3389/fpls.2022.881032

Chi, Y. H., Paeng, S. Ki, Kim, M. Ji, Hwang, G. Y., Melencion, S. M., Oh, H. T., et al. (2013). Redox-dependent functional switching of plant proteins accompanying with their structural changes. *Front. Plant Sci.* 4. doi: 10.3389/fpls.2013.00277

Chinnusamy, V., Ohta, M., Kanrar, S., Lee, B.-h., Hong, X., Agarwal, M., et al. (2003). ICE1: A regulator of cold-induced transcriptome and freezing tolerance in arabidopsis. *Genes Dev.* 17 (8), 1043–1054. doi: 10.1101/gad.1077503

Cid, F. P., Maruyama, F., Murase, K., Graether, S. P., Larama, G., Bravo, L. A., et al. (2018). Draft genome sequences of bacteria isolated from the deschampsia Antarctica phyllosphere. *Extremophiles* 22 (3), 537–552. doi: 10.1007/s00792-018-1015-x

Das, K., and Roychoudhury, A. (2014). Reactive oxygen species (ROS) and response of antioxidants as ROS-scavengers during environmental stress in plants." *Front. Environ. Sci.* 2. doi: 10.3389/fenvs.2014.00053

Davies, P. L., and Sykes, B. D. (1997). Antifreeze proteins. *Curr. Opin. Struct. Biol.* 7 (6), 828–834. doi: 10.1016/S0959-440X(97)80154-6

Ding, Y., Jia, Y., Shi, Y., Zhang, X., Song, C., Gong, Z., et al. (2018). OST1-mediated BTF3L phosphorylation positively regulates CBFs during plant cold responses. *EMBO J.* 37 (8), e98228. doi: 10.15252/embj.201798228

Ding, X., Zhang, H., Chen, H., Wang, Li, Qian, H., and Qi, X. (2015). Extraction, purification and identification of antifreeze proteins from cold acclimated malting barley (Hordeum vulgare L.)." *Food Chem.* 175, 74–81. doi: 10.1016/j.foodchem.2014.11.027

Dong, H., Wu, C., Luo, C., Wei, M., Qu, S., and Wang, S. (2020). Overexpression of mdCPK1a gene, a calcium dependent protein kinase in apple, increase tobacco cold tolerance via scavenging ROS accumulation. *PloS One* 15 (11), e0242139. doi: 10.1371/journal.pone.0242139

Drerup, M. M., Schlücking, K., Hashimoto, K., Manishankar, P., Steinhorst, L., Kuchitsu, K., et al. (2013). The calcineurin B-like calcium sensors CBL1 and CBL9 together with their interacting protein kinase CIPK26 regulate the arabidopsis NADPH oxidase RBOHF. *Mol. Plant* 6 (2), 559–569. doi: 10.1093/mp/sst009

Dubouzet, J. G., Sakuma, Y., Ito, Y., Kasuga, M., Dubouzet, E. G., Miura, S., et al. (2003). OsDREB genes in rice, oryza sativa L., encode transcription activators that function in drought-, high-salt- and cold-responsive gene expression. *Plant J.* 33 (4), 751–763. doi: 10.1046/j.1365-313X.2003.01661.x

Ebrahimi, M., Abdullah, S. N. A., Aziz, M. A., and Namasivayam, P. (2016). Oil palm egCBF3 conferred stress tolerance in transgenic tomato plants through modulation of the ethylene signaling pathway. *J. Plant Physiol.* 202, 107–120. doi: 10.1016/j.jplph.2016.07.001

Elliott, G. D., Wang, S., and Fuller, B. J. (2017). Cryoprotectants: A review of the actions and applications of cryoprotective solutes that modulate cell recovery from ultra-low temperatures. *Cryobiology* 76, 74–91. doi: 10.1016/j.cryobiol.2017.04.004

Eremina, M., Unterholzner, S. J., Rathnayake, A. I., Castellanos, M., Khan, M., Kugler, K. G., et al. (2016). Brassinosteroids participate in the control of basal and acquired freezing tolerance of plants. *Proc. Natl. Acad. Sci.* 113 (40), E5982–E5991. doi: 10.1073/pnas.1611477113

Eze, M. O. (1991). Phase transitions in phospholipid bilayers: lateral phase separations play vital roles in biomembranes. *Biochem. Educ.* 19 (4), 204–208. doi: 10.1016/0307-4412(91)90103-F

Fabri, JoãoH. T. M., de Sá, N. P., Malavazi, I., and Poeta, M. D. (2020). The dynamics and role of sphingolipids in eukaryotic organisms upon thermal adaptation. *Prog. Lipid Res.* 80, 101063. doi: 10.1016/j.plipres.2020.101063

Fang, J.-C., Tsai, Y.-C., Chou, W.-L., Liu, H.-Y., Chang, C.-C., Wu, S.-J., et al. (2021). A CCR4-associated factor 1, osCAF1B, confers tolerance of low-temperature stress to rice seedlings. *Plant Mol. Biol.* 105 (1), 177–192. doi: 10.1007/s11103-020-01079-8

Francko, D. A., Wilson, K. G., Li, Q. Q., and Equiza, M. A. (2011). A topical spray to enhance plant resistance to cold injury and mortality. *HortTechnology* 21 (1), 109–118. doi: 10.21273/HORTTECH.21.1.109

Fürtauer, L., Weiszmann, J., Weckwerth, W., and Nägele, T. (2019). Dynamics of plant metabolism during cold acclimation. *Int. J. Mol. Sci.* 20 (21), 5411. doi: 10.3390/ijms20215411

Gill, S. S., and Tuteja, N. (2010). Reactive oxygen species and antioxidant machinery in abiotic stress tolerance in crop plants. *Plant Physiol. Biochem.* 48 (12), 909–930. doi: 10.1016/j.plaphy.2010.08.016

Ginot, Félix, Lenavetier, Théo, Dedovets, D., and Deville, S. (2020). Solute strongly impacts freezing under confinement. *Appl. Phys. Lett.* 116 (25), 253701. doi: 10.1063/5.0008925

Glenn, D. M., Wisniewski, M., Puterka, G. J., and Sekutowski, D. G. (2001). *Method for enhanced supercooling of plants to provide frost protection*.

Görlach, A., Bertram, K., Hudecova, S., and Krizanova, O. (2015). Calcium and ROS: A mutual interplay. *Redox Biol.* 6, 260–271. doi: 10.1016/j.redox.2015.08.010

Griffith, M., and Yaish, M. W.F. (2004). Antifreeze proteins in overwintering plants: A tale of two activities. *Trends Plant Sci.* 9 (8), 399–405. doi: 10.1016/j.tplants.2004.06.007

Grishkewich, N., Mohammed, N., Tang, J., and Tam, K. C. (2017). Recent advances in the application of cellulose nanocrystals. *Curr. Opin. Colloid Interface Sci.* 29, 32–45. doi: 10.1016/j.cocis.2017.01.005

Guo, Q., Li, X., Niu, Li, Jameson, P. E., and Zhou, W. (2021). Transcription-associated metabolomic adjustments in maize occur during combined drought and cold stress. *Plant Physiol.* 186 (1), 677–695. doi: 10.1093/plphys/kiab050

Guo, X., Li, J., Zhang, Li, Zhang, Z., He, P., Wang, W., et al. (2020). Heterotrimeric G-protein α Subunit (LeGPA1) confers cold stress tolerance to processing tomato plants (Lycopersicon esculentum mill). *BMC Plant Biol.* 20 (1), 394. doi: 10.1186/s12870-020-02615-w

Guo, X., Liu, D., and Chong, K. (2018). Cold signaling in plants: insights into mechanisms and regulation. *J. Integr. Plant Biol.* 60 (9), 745–756. doi: 10.1111/jipb.12706

Guo, X., Zhang, Li, Dong, G., Xu, Z., Li, G., Liu, N., et al. (2019a). A novel cold-regulated protein isolated from saussurea involucrata confers cold and drought tolerance in transgenic tobacco (Nicotiana tabacum). *Plant Sci.* 289, 110246. doi: 10.1016/j.plantsci.2019.110246

Guo, X., Zhang, Li, Wang, X., Zhang, M., Xi, Y., Wang, A., et al. (2019b). Overexpression of saussurea involucrata dehydrin gene siDHN promotes cold and drought tolerance in transgenic tomato plants. *PloS One* 14 (11), e0225090. doi: 10.1371/journal.pone.0225090

Habibi, Y., Lucia, L. A., and Rojas, O. J. (2010). Cellulose nanocrystals: chemistry, self-assembly, and applications. *Chem. Rev.* 110 (6), 3479–3500. doi: 10.1021/cr900339w

He, L. G., Wang, H. L., Liu, D. C., Zhao, Y. J., Xu, M., Zhu, M., et al. (2012). Isolation and expression of a cold-responsive gene ptCBF in poncirus trifoliata and isolation of citrus CBF promoters. *Biol. Plantarum* 56 (3), 484–492. doi: 10.1007/s10535-012-0059-5

Heidarvand, L., and Maali-Amiri, R. (2013). Physio-biochemical and proteome analysis of chickpea in early phases of cold stress. *J. Plant Physiol.* 170 (5), 459–469. doi: 10.1016/j.jplph.2012.11.021

Hoermiller, I. I., Ruschhaupt, M., and Heyer, A. G. (2018). Mechanisms of frost resistance in arabidopsis thaliana. *Planta* 248 (4), 827–835. doi: 10.1007/s00425-018-2939-1

Hou, C., Tian, W., Kleist, T., He, K., Garcia, V., Bai, F., et al. (2014). DUF221 proteins are a family of osmosensitive calcium-permeable cation channels conserved across eukaryotes. *Cell Res.* 24 (5), 632–635. doi: 10.1038/cr.2014.14

Hsieh, T.-H., Lee, J.-T., Yang, P.-T., Chiu, L.-H., Charng, Y.-y., Wang, Y.-C., et al. (2002). Heterology expression of the arabidopsis C-repeat/dehydration response element binding factor 1 gene confers elevated tolerance to chilling and oxidative stresses in transgenic tomato. *Plant Physiol.* 129 (3), 1086–1094. doi: 10.1104/pp.003442

Hu, Y., Jiang, Y., Han, X., Wang, H., Pan, J., and Yu, D. (2017). Jasmonate regulates leaf senescence and tolerance to cold stress: crosstalk with other phytohormones. *J. Exp. Bot.* 68 (6), 1361–1369. doi: 10.1093/jxb/erx004

Hudait, A., Odendahl, N., Qiu, Y., Paesani, F., and Molinero, V. (2018). Ice-nucleating and antifreeze proteins recognize ice through a diversity of anchored clathrate and ice-like motifs. *J. Am. Chem. Soc.* 140 (14), 4905–4912. doi: 10.1021/jacs.8b01246

Hutchison, R. S., Groom, Q., and Ort, D. R. (2000). Differential effects of chilling-induced photooxidation on the redox regulation of photosynthetic enzymes. *Biochemistry* 39 (22), 6679–6688. doi: 10.1021/bi0001978

IbÁñez, C., Kozarewa, I., Johansson, M., Ögren, E., Rohde, A., and Eriksson, M. E. (2010). Circadian clock components regulate entry and affect exit of seasonal dormancy as well as winter hardiness in populus trees. *Plant Physiol.* 153 (4), 1823–1833. doi: 10.1104/pp.110.158220

Iivonen, S., Saranpää, P., Sutinen, M.-L., and Vapaavuori, E. (2004). Effects of temperature and nutrient availability on plasma membrane lipid composition in scots pine roots during growth initiation. *Tree Physiol.* 24 (4), 437–446. doi: 10.1093/treephys/24.4.437

Iqbal, Z., Memon, A. G., Ahmad, A., and Iqbal, M. S. (2022). Calcium mediated cold acclimation in plants: underlying signaling and molecular mechanisms. *Front. Plant Sci.* 13. doi: 10.3389/fpls.2022.855559

Ito, Y., Katsura, K., Maruyama, K., Taji, T., Kobayashi, M., Seki, M., et al. (2006). Functional analysis of rice DREB1/CBF-type transcription factors involved in cold-responsive gene expression in transgenic rice. *Plant Cell Physiol.* 47 (1), 141–153. doi: 10.1093/pcp/pci230

Ivanov, A. G., Allakhverdiev, S. I., Huner, N. P. A., and Murata, N. (2012). Genetic decrease in fatty acid unsaturation of phosphatidylglycerol increased photoinhibition of photosystem I at low temperature in tobacco leaves. *Biochim. Biophys. Acta (BBA) - Bioenergetics* 1817 (8), 1374–1379. doi: 10.1016/j.bbabio.2012.03.010

Janeczko, A., Dziurka, Michał, and Pociecha, E. (2018). Increased leaf tocopherol and β-carotene content is associated with the tolerance of winter wheat cultivars to frost. *J. Agron. Crop Sci.* 204 (6), 594–602. doi: 10.1111/jac.12287

Jian, H., Xie, L., Wang, Y., Cao, Y., Wan, M., Lv, D., et al. (2020). Characterization of cold stress responses in different rapeseed ecotypes based on metabolomics and transcriptomics analyses. *PeerJ* 8, e8704. doi: 10.7717/peerj.8704

Jin, R., Kim, B. H., Ji, C. Y., Kim, Ho S., Li, H. M., Ma, D. Fu, et al. (2017). Overexpressing ibCBF3 increases low temperature and drought stress tolerance in transgenic sweetpotato. *Plant Physiol. Biochem.* 118, 45–54. doi: 10.1016/j.plaphy.2017.06.002

Jin, Ya'nan, Zhai, S., Wang, W., Ding, X., Guo, Z., Bai, L., et al. (2018). Identification of genes from the ICE–CBF–COR pathway under cold stress in aegilops–triticum composite group and the evolution analysis with those from triticeae. *Physiol. Mol. Biol. Plants* 24 (2), 211–229. doi: 10.1007/s12298-017-0495-y

Jonytiene, V., Burbulis, N., Kuprienė, Ramunė, and Blinstrubienė, Aušra (2012). Effect of exogenous proline and de-acclimation treatment on cold tolerance in brassica napus shoots cultured in vitro. *J. Food Agric. Environ.* 1010, 327–330.

Judy, E., and Kishore, N. (2016). Biological wonders of osmolytes: the need to know more. *Biochem. Anal. Biochem.* 5 (4), 1–5. doi: 10.4172/2161-1009.1000304

Juurakko, C. L., diCenzo, G. C., and Walker, V. K. (2021). Cold acclimation and prospects for cold-resilient crops. *Plant Stress* 2, 100028. doi: 10.1016/j.stress.2021.100028

Kamal-Eldin, A., and Appelqvist, Lars-Åke (1996). The chemistry and antioxidant properties of tocopherols and tocotrienols. *Lipids* 31 (7), 671–701. doi: 10.1007/BF02522884

Karabudak, T., Bor, M., Özdemir, F., and Türkan, İ. (2014). Glycine betaine protects tomato (Solanum lycopersicum) plants at low temperature by inducing fatty acid desaturase7 and lipoxygenase gene expression. *Mol. Biol. Rep.* 41 (3), 1401–1410. doi: 10.1007/s11033-013-2984-6

Kasuga, M., Miura, S., Shinozaki, K., and Yamaguchi-Shinozaki, K. (2004). A combination of the arabidopsis DREB1A gene and stress-inducible rd29A promoter improved drought- and low-temperature stress tolerance in tobacco by gene transfer. *Plant Cell Physiol.* 45 (3), 346–350. doi: 10.1093/pcp/pch037

Kazemi-Shahandashti, S.-S., and Maali-Amiri, R. (2018). Global insights of protein responses to cold stress in plants: signaling, defence, and degradation. *J. Plant Physiol.* 226, 123–135. doi: 10.1016/j.jplph.2018.03.022

Kidokoro, S., Watanabe, K., Ohori, T., Moriwaki, T., Maruyama, K., Mizoi, J., et al. (2015). Soybean DREB1/CBF-type transcription factors function in heat and drought as well as cold stress-responsive gene expression. *Plant J.* 81 (3), 505–518. doi: 10.1111/tpj.12746

Kingston-Smith, A. H., Harbinson, J., Williams, J., and Foyer, C. H. (1997). Effect of chilling on carbon assimilation, enzyme activation, and photosynthetic electron transport in the absence of photoinhibition in maize leaves. *Plant Physiol.* 114 (3), 1039–1046. doi: 10.1104/pp.114.3.1039

Knight, M. R., and Knight, H. (2012). Low-temperature perception leading to gene expression and cold tolerance in higher plants. *New Phytol.* 195 (4), 737–751. doi: 10.1111/j.1469-8137.2012.04239.x

Kong, C. H. Z., Hamid, N., Liu, T., and Sarojini, V. (2016). Effect of antifreeze peptide pretreatment on ice crystal size, drip loss, texture, and volatile compounds of frozen carrots. *J. Agric. Food Chem.* 64 (21), 4327–4335. doi: 10.1021/acs.jafc.6b00046

Kong, C. H.Z., Hamid, N., Ma, Q., Lu, J., Wang, B.-G., and Sarojini, V. (2017). Antifreeze peptide pretreatment minimizes freeze-thaw damage to cherries: an in-depth investigation. *LWT* 84, 441–448. doi: 10.1016/j.lwt.2017.06.002

Kudla, Jörg, Becker, D., Grill, E., Hedrich, R., Hippler, M., Kummer, U., et al. (2018). Advances and current challenges in calcium signaling. *New Phytol.* 218 (2), 414–431. doi: 10.1111/nph.14966

Kurepin, L. V., Ivanov, A. G., Zaman, M., Pharis, R. P., Allakhverdiev, S. I., Hurry, V., et al. (2015). Stress-related hormones and glycinebetaine interplay in protection of photosynthesis under abiotic stress conditions. *Photosynthesis Res.* 126 (2), 221–235. doi: 10.1007/s11120-015-0125-x

Lamers, J., Meer, T. v. d., and Testerink, C. (2020). How plants sense and respond to stressful environments1. *Plant Physiol.* 182 (4), 1624–1635. doi: 10.1104/pp.19.01464

Larcher, W. (2003). *Physiological plant ecology: ecophysiology and stress physiology of functional groups* (Berlin, Germany: Springer Science & Business Media).

Latowski, D., Kuczyńska, P., and Strzałka, K. (2011). Xanthophyll cycle – a mechanism protecting plants against oxidative stress. *Redox Rep.* 16 (2), 78–90. doi: 10.1179/174329211X13020951739938

Lee, J.-H., Kwon, M. C., Jung, E. S., Lee, C. H., and Oh, M.-M. (2019). Physiological and metabolomic responses of kale to combined chilling and UV-A treatment. *Int. J. Mol. Sci.* 20 (19), 4950. doi: 10.3390/ijms20194950

Leegood, R. C., and Furbank, R. T. (1986). Stimulation of photosynthesis by 2% Oxygen at low temperatures is restored by phosphate. *Planta* 168 (1), 84–93. doi: 10.1007/BF00407013

Lemoine, R., Camera, S. La, Atanassova, R., Dédaldéchamp, F., Allario, T., Pourtau, N., et al. (2013). Source-to-sink transport of sugar and regulation by environmental factors. *Front. Plant Sci.* 4. doi: 10.3389/fpls.2013.00272

Li, W., Li, M., Zhang, W., Welti, R., and Wang, X. (2004). The plasma membrane–bound phospholipase Dδ Enhances freezing tolerance in arabidopsis thaliana. *Nat. Biotechnol.* 22 (4), 427–433. doi: 10.1038/nbt949

Li, H., Ye, K., Shi, Y., Cheng, J., Zhang, X., and Yang, S. (2017). BZR1 positively regulates freezing tolerance via CBF-dependent and CBF-independent pathways in arabidopsis. *Mol. Plant* 10 (4), 545–559. doi: 10.1016/j.molp.2017.01.004

Lindow, S. E., Arny, D. C., and Upper, C. D. (1982). Bacterial ice nucleation: A factor in frost injury to plants. *Plant Physiol.* 70 (4), 1084–1089. doi: 10.1104/pp.70.4.1084

Liu, X., Fu, L., Qin, P., Sun, Y., Liu, J., and Wang, X. (2019). Overexpression of the wheat trehalose 6-phosphate synthase 11 gene enhances cold tolerance in arabidopsis thaliana. *Gene* 710, 210–217. doi: 10.1016/j.gene.2019.06.006

Liu, J., Islam, Md T., Sapkota, S., Ravindran, P., Kumar, P. P., Artlip, T. S., et al. (2021a). Ethylene-mediated modulation of bud phenology, cold hardiness, and hormone biosynthesis in peach (Prunus persica). *Plants* 10 (7), 1266. doi: 10.3390/plants10071266

Liu, J., Islam, Md T., Sapkota, S., Ravindran, P., Kumar, P. P., Artlip, T. S., et al. (2021b). Ethylene-mediated modulation of bud phenology, cold hardiness, and hormone biosynthesis in peach (Prunus persica). *Plants* 10 (7), 1266. doi: 10.3390/plants10071266

Liu, Q., Piao, S., Janssens, I. A., Fu, Y., Peng, S., Lian, Xu, et al. (2018). Extension of the growing season increases vegetation exposure to frost. *Nat. Commun.* 9 (1), 426. doi: 10.1038/s41467-017-02690-y

Liu, J., and Sherif, S. M. (2019). Combating spring frost with ethylene. *Front. Plant Sci.* 10. doi: 10.3389/fpls.2019.01408

Londo, J. P., and Kovaleski, A. P. (2019). Deconstructing cold hardiness: variation in supercooling ability and chilling requirements in the wild grapevine vitis riparia. *Aust. J. Grape Wine Res.* 25 (3), 276–285. doi: 10.1111/ajgw.12389

Lu, M., Wang, B., Li, Zh., Fei, Y., Wei, L., and Gao, Sh. (2002). Differential scanning calorimetric and circular dichroistic studies on plant antifreeze proteins. *J. Thermal Anal. Calorimetry* 67 (3), 689–698. doi: 10.1023/A:1014369208229

Lukas, M., Schwidetzky, R., Eufemio, R. J., Bonn, M., and Meister, K. (2022). Toward understanding bacterial ice nucleation. *J. Phys. Chem. B* 126 (9), 1861–1867. doi: 10.1021/acs.jpcb.1c09342

Lunn, J. E., Delorge, I., Figueroa, C. María, Dijck, P. V., and Stitt, M. (2014). Trehalose metabolism in plants. *Plant J.* 79 (4), 544–567. doi: 10.1111/tpj.12509

Ma, Y., Dai, X., Xu, Y., Luo, W., Zheng, X., Zeng, D., et al. (2015). COLD1 confers chilling tolerance in rice. *Cell* 160 (6), 1209–1221. doi: 10.1016/j.cell.2015.01.046

Ma, Q., Huang, J.-G., Hänninen, H., and Berninger, F. (2019). Divergent trends in the risk of spring frost damage to trees in europe with recent warming. *Global Change Biol.* 25 (1), 351–360. doi: 10.1111/gcb.14479

Marcec, M. J., Gilroy, S., Poovaiah, B. W., and Tanaka, K. (2019). Mutual interplay of ca2+ and ROS signaling in plant immune response. *Plant Sci.* 283, 343–354. doi: 10.1016/j.plantsci.2019.03.004

Meena, M., Divyanshu, K., Kumar, S., Swapnil, P., Zehra, A., Shukla, V., et al. (2019). Regulation of L-proline biosynthesis, signal transduction, transport, accumulation and its vital role in plants during variable environmental conditions. *Heliyon* 5 (12), e02952. doi: 10.1016/j.heliyon.2019.e02952

Meyer, K., Keil, M., and Naldrett, M. J. (1999). A leucine-rich repeat protein of carrot that exhibits antifreeze activity. *FEBS Lett.* 447 (2), 171–178. doi: 10.1016/S0014-5793(99)00280-X

Miller, G., Suzuki, N., Ciftci-Yilmaz, S., and Mittler, R. (2010). Reactive oxygen species homeostasis and signalling during drought and salinity stresses. *Plant Cell Environ.* 33 (4), 453–467. doi: 10.1111/j.1365-3040.2009.02041.x

Mishra, B. S., Sharma, M., and Laxmi, A. (2022). Role of sugar and auxin crosstalk in plant growth and development. *Physiologia Plantarum* 174 (1), e13546. doi: 10.1111/ppl.13546

Mittler, R. (2002). Oxidative stress, antioxidants and stress tolerance. *Trends Plant Sci.* 7 (9), 405–410. doi: 10.1016/S1360-1385(02)02312-9

Mittler, R. (2017). ROS are good. *Trends Plant Sci.* 22 (1), 11–19. doi: 10.1016/j.tplants.2016.08.002

Mittler, R., Zandalinas, S. I., Fichman, Y., and Breusegem, F. V. (2022). Reactive oxygen species signalling in plant stress responses. *Nat. Rev. Mol. Cell Biol.* 23 (10), 663–679. doi: 10.1038/s41580-022-00499-2

Miura, K., and Furumoto, T. (2013). Cold signaling and cold response in plants. *Int. J. Mol. Sci.* 14 (3), 5312–5337. doi: 10.3390/ijms14035312

Muthukumaran, J., Manivel, P., Kannan, M., Jeyakanthan, J., and Krishna, R. (2011). A framework for classification of antifreeze proteins in over wintering plants based on their sequence and structural features. *J. Bioinform. Seq. Anal.* 3, 70–88. doi: 10.5897/JBSA11.003

Nair, P., Kandasamy, S., Zhang, J., Ji, X., Kirby, C., Benkel, B., et al. (2012). Transcriptional and metabolomic analysis of ascophyllum nodosum mediated freezing tolerance in arabidopsis thaliana. *BMC Genomics* 13 (1), 643. doi: 10.1186/1471-2164-13-643

Örvar, BjörnLárus, Sangwan, V., Omann, F., and Dhindsa, R. S. (2000). Early steps in cold sensing by plant cells: the role of actin cytoskeleton and membrane fluidity. *Plant J.* 23 (6), 785–794. doi: 10.1046/j.1365-313x.2000.00845.x

Pandey, R., Usui, K., Livingstone, R. A., Fischer, S. A., Pfaendtner, J., Backus, E. H.G., et al. (2016). Ice-nucleating bacteria control the order and dynamics of interfacial water. *Sci. Adv.* 2 (4), e1501630. doi: 10.1126/sciadv.1501630

Pearce, R. (2001). Plant freezing and damage. *Ann. Bot.* 87 (4), 417–424. doi: 10.1006/anbo.2000.1352

Perry, K. B. (1998). Basics of frost and freeze protection for horticultural crops. *HortTechnology* 8 (1), 10–15. doi: 10.21273/HORTTECH.8.1.10

Pino, María-Teresa, Skinner, J. S., Park, E.-J., Jeknić, Z., Hayes, P. M., Thomashow, M. F., et al. (2007). Use of a stress inducible promoter to drive ectopic atCBF expression improves potato freezing tolerance while minimizing negative effects on tuber yield. *Plant Biotechnol. J.* 5 (5), 591–604. doi: 10.1111/j.1467-7652.2007.00269.x

Polashock, J. J., Arora, R., Peng, Y., Naik, D., and Rowland, L. J. (2010). Functional identification of a C-repeat binding factor transcriptional activator from blueberry associated with cold acclimation and freezing tolerance. *J. Am. Soc. Hortic. Sci.* 135 (1), 40–48. doi: 10.21273/JASHS.135.1.40

Prasad, T. K., Anderson, M. D., and Stewart, C. R. (1994). Acclimation, hydrogen peroxide, and abscisic acid protect mitochondria against irreversible chilling injury in maize seedlings. *Plant Physiol.* 105 (2), 619–627. doi: 10.1104/pp.105.2.619

Qin, F., Sakuma, Y., Li, J., Liu, Q., Li, Y.-Q., Shinozaki, K., et al. (2004). Cloning and functional analysis of a novel DREB1/CBF transcription factor involved in cold-responsive gene expression in zea mays L. *Plant Cell Physiol.* 45 (8), 1042–1052. doi: 10.1093/pcp/pch118

Rajendrakumar, C. S. V., Reddy, B. V. B., and Reddy, A. R. (1994). Proline-protein interactions: protection of structural and functional integrity of M4 lactate dehydrogenase. *Biochem. Biophys. Res. Commun.* 201 (2), 957–963. doi: 10.1006/bbrc.1994.1795

Rayirath, P., Benkel, B., Hodges, D.M., Allan-Wojtas, P., MacKinnon, S., Critchley, A. T., et al. (2009). Lipophilic components of the brown seaweed, ascophyllum nodosum, enhance freezing tolerance in arabidopsis thaliana. *Planta* 230 (1), 135–147. doi: 10.1007/s00425-009-0920-8

Rinehart, J. P., Li, A., Yocum, G. D., Robich, R. M., Hayward, S. A.L., and Denlinger, D. L. (2007). Up-regulation of heat shock proteins is essential for cold survival during insect diapause. *Proc. Natl. Acad. Sci.* 104 (27), 11130–11137. doi: 10.1073/pnas.0703538104

Roeters, S. J., Golbek, T. W., Bregnhøj, M., Drace, T., Alamdari, S., Roseboom, W., et al. (2021). Ice-nucleating proteins are activated by low temperatures to control the structure of interfacial water. *Nat. Commun.* 12 (1), 1183. doi: 10.1038/s41467-021-21349-3

Román-Figueroa, Celián, Bravo, León, Paneque, M., Navia, R., and Cea, M. (2021). Chemical products for crop protection against freezing stress: A review. *J. Agron. Crop Sci.* 207 (3), 391–403. doi: 10.1111/jac.12489

Roychoudhury, A., and Banerjee, A. (2016). Endogenous glycine betaine accumulation mediates abiotic stress tolerance in plants. *Trop. Plant Res.* 3 (1), 105–111.

Sadiq, M., Akram, N. A., Ashraf, M., Al-Qurainy, F., and Ahmad, P. (2019). Alpha-tocopherol-induced regulation of growth and metabolism in plants under non-stress and stress conditions. *J. Plant Growth Regul.* 38 (4), 1325–1340. doi: 10.1007/s00344-019-09936-7

Saha, J., Brauer, E. K., Sengupta, A., Popescu, S. C., Gupta, K., and Gupta, B. (2015). Polyamines as redox homeostasis regulators during salt stress in plants. *Front. Environ. Sci.* 3. doi: 10.3389/fenvs.2015.00021

Sami, F., Yusuf, M., Faizan, M., Faraz, A., and Hayat, S. (2016). Role of sugars under abiotic stress. *Plant Physiol. Biochem.* 109, 54–61. doi: 10.1016/j.plaphy.2016.09.005

Sarkar, A. K., and Sadhukhan, S. (2022). Imperative role of trehalose metabolism and trehalose-6-phosphate signaling on salt stress responses in plants. *Physiologia Plantarum* 174 (1), e13647. doi: 10.1111/ppl.13647

Sassenrath, G. F., Ort, D. R., and Portis, A. R. (1990). Impaired reductive activation of stromal bisphosphatases in tomato leaves following low-temperature exposure at high light. *Arch. Biochem. Biophysics* 282 (2), 302–308. doi: 10.1016/0003-9861(90)90121-e

Satyakam, G. Z., Singh, R. K., and Kumar, R. (2022). Cold adaptation strategies in plants—An emerging role of epigenetics and antifreeze proteins to engineer cold resilient plants. *Front. Genet.* 13. doi: 10.3389/fgene.2022.909007

Savitch, L. V., Allard, G., Seki, M., Robert, L. S., Tinker, N. A., Huner, N. P.A., et al. (2005). The effect of overexpression of two brassica CBF/DREB1-like transcription factors on photosynthetic capacity and freezing tolerance in brassica napus. *Plant Cell Physiol.* 46 (9), 1525–1539. doi: 10.1093/pcp/pci165

Semida, W. M., Abd, E.-M. T. A., Howladar, S. M., and Rady, M. M. (2016). Foliar-applied alpha-tocopherol enhances salt-tolerance in onion plants by improving antioxidant defence system. *Aust. J. Crop Sci.* 10 (7), 1030–1039. doi: 10.3316/informit.327621977858527

Sharkey, T. D., Stitt, M., Heineke, D., Gerhardt, R., Raschke, K., and Heldt, H. W. (1986). Limitation of photosynthesis by carbon metabolism 1: II. O2-insensitive CO2 uptake results from limitation of triose phosphate utilization. *Plant Physiol.* 81 (4), 1123–1129. doi: 10.1104/pp.81.4.1123

Sharma, P., Jha, A. B., Dubey, R. S., and Pessarakli, M. (2021). "Reactive oxygen species generation, hazards, and defense mechanisms in plants under environmental (Abiotic and biotic) stress conditions," in *Handbook of plant and crop physiology* (Boca Raton, FL, USA: CRC Press) (2021). pp. 509–548.

Sherif, S. M. (2023) *Tree fruit horticulture updates*. Available at: https://blogs.ext.vt.edu/tree-fruit-horticulture/.

Shi, H., He, X., Zhao, Y., Lu, S., and Guo, Z. (2020). Constitutive expression of a group 3 LEA protein from medicago falcata (MfLEA3) increases cold and drought tolerance in transgenic tobacco. *Plant Cell Rep.* 39 (7), 851–860. doi: 10.1007/s00299-020-02534-y

Shukla, P. S., Mantin, E. G., Adil, M., Bajpai, S., Critchley, A. T., and Prithiviraj, B. (2019). Ascophyllum nodosum-based biostimulants: sustainable applications in agriculture for the stimulation of plant growth, stress tolerance, and disease management. *Front. Plant Sci.* 10. doi: 10.3389/fpls.2019.00655

Siddique, A., Kandpal, G., and Kumar, P. (2018). Proline accumulation and its defensive role under diverse stress condition in plants: an overview. *J. Pure Appl. Microbiol.* 12 (3), 1655–1659. doi: 10.22207/JPAM.12.3.73

Sies, H., and Jones, D. P. (2020). Reactive oxygen species (ROS) as pleiotropic physiological signalling agents. *Nat. Rev. Mol. Cell Biol.* 21 (7), 363–383. doi: 10.1038/s41580-020-0230-3

Simkin, A. J., López-Calcagno, P. E., and Raines, C. A. (2019). Feeding the world: improving photosynthetic efficiency for sustainable crop production. *J. Exp. Bot.* 70 (4), 1119–1140. doi: 10.1093/jxb/ery445

Slade, D., and Radman, M. (2011). Oxidative stress resistance in deinococcus radiodurans. *Microbiol. Mol. Biol. Reviews: MMBR* 75 (1), 133–191. doi: 10.1128/MMBR.00015-10

Smirnoff, N., and Arnaud, D. (2019). Hydrogen peroxide metabolism and functions in plants. *New Phytol.* 221 (3), 1197–1214. doi: 10.1111/nph.15488

Snyder, R. L., and de Melo-Abreu, J.P. (2005). Frost protection: fundamentals, practice and economics. *Food Agric. Organ. United Nations* 1, 1–240.

Sreedharan, S., Shekhawat, U. K.S., and Ganapathi, T. R. (2013). Transgenic banana plants overexpressing a native plasma membrane aquaporin musaPIP1;2 display high tolerance levels to different abiotic stresses. *Plant Biotechnol. J.* 11 (8), 942–952. doi: 10.1111/pbi.12086

Sun, S., Fang, J., Lin, M., Hu, C., Qi, X., Chen, J., et al. (2021). Comparative metabolomic and transcriptomic studies reveal key metabolism pathways contributing to freezing tolerance under cold stress in kiwifruit. *Front. Plant Sci.* 12. doi: 10.3389/fpls.2021.628969

Suo, J., Zhao, Qi, David, L., Chen, S., and Dai, S. (2017). Salinity response in chloroplasts: insights from gene characterization. *Int. J. Mol. Sci.* 18 (5), 1011. doi: 10.3390/ijms18051011

Suzuki, N., and Mittler, R. (2006). Reactive oxygen species and temperature stresses: A delicate balance between signaling and destruction. *Physiologia Plantarum* 126 (1), 45–51. doi: 10.1111/j.0031-9317.2005.00582.x

Takuhara, Y., Kobayashi, M., and Suzuki, S. (2011). Low-temperature-induced transcription factors in grapevine enhance cold tolerance in transgenic arabidopsis plants. *J. Plant Physiol.* 168 (9), 967–975. doi: 10.1016/j.jplph.2010.11.008

Tarkowski, ŁukaszP., and Van den Ende, W. (2015). Cold tolerance triggered by soluble sugars: A multifaceted countermeasure. *Front. Plant Sci.* 6. doi: 10.3389/fpls.2015.00203

Trache, D., Hussin, M.H., Mohamad Haafiz, M. K., and Thakur, V. K. (2017). Recent progress in cellulose nanocrystals: sources and production. *Nanoscale* 9 (5), 1763–1786. doi: 10.1039/C6NR09494E

Tsukagoshi, H., Busch, W., and Benfey, P. N. (2010). Transcriptional regulation of ROS controls transition from proliferation to differentiation in the root. *Cell* 143 (4), 606–616. doi: 10.1016/j.cell.2010.10.020

Uemura, M., Joseph, R. A., and Steponkus, P. L. (1995). Cold acclimation of arabidopsis thaliana (Effect on plasma membrane lipid composition and freeze-induced lesions). *Plant Physiol.* 109 (1), 15–30. doi: 10.1104/pp.109.1.15

Unterberger, C., Brunner, L., Nabernegg, S., Steininger, K. W., Steiner, A. K., Stabentheiner, E., et al. (2018). Spring frost risk for regional apple production under a warmer climate. *PloS One* 13 (7), e0200201. doi: 10.1371/journal.pone.0200201

Urbańczyk, Małgorzata, Góra, J., Latajka, Rafał, and Sewald, N. (2017). Antifreeze glycopeptides: from structure and activity studies to current approaches in chemical synthesis. *Amino Acids* 49 (2), 209–222. doi: 10.1007/s00726-016-2368-z

Van Rensburg, L., Krüger, G. H. J., and Krüger, H. (1993). Proline accumulation as drought-tolerance selection criterion: its relationship to membrane integrity and chloroplast ultrastructure in nicotiana tabacum L. *J. Plant Physiol.* 141 (2), 188–194. doi: 10.1016/S0176-1617(11)80758-3

Verbruggen, N., and Hermans, C. (2008). Proline accumulation in plants: A review. *Amino Acids* 35 (4), 753–759. doi: 10.1007/s00726-008-0061-6

Vyse, K., Faivre, Léa, Romich, M., Pagter, M., Schubert, D., Hincha, D. K., et al. (2020). Transcriptional and post-transcriptional regulation and transcriptional memory of chromatin regulators in response to low temperature. *Front. Plant Sci.* 11. doi: 10.3389/fpls.2020.00039

Wang, B., Chai, H., Zhong, Y., Shen, Y., Yang, W., Chen, J., et al. (2020). The DEAD-box RNA helicase SHI2 functions in repression of salt-inducible genes and regulation of cold-inducible gene splicing. *J. Exp. Bot.* 71 (4), 1598–1613. doi: 10.1093/jxb/erz523

Wang, L., Wang, Sa, Tong, R., Wang, S., Yao, J., Jiao, J., et al. (2022). Overexpression of pgCBF3 and pgCBF7 transcription factors from pomegranate enhances freezing tolerance in arabidopsis under the promoter activity positively regulated by pgICE1. *Int. J. Mol. Sci.* 23 (16), 9439. doi: 10.3390/ijms23169439

Wang, M., Zheng, Q., Shen, Q., and Guo, S. (2013). The critical role of potassium in plant stress response. *Int. J. Mol. Sci.* 14 (4), 7370–7390. doi: 10.3390/ijms14047370

Wei, X., Liu, S., Sun, C., Xie, G., and Wang, L. (2021). Convergence and divergence: signal perception and transduction mechanisms of cold stress in arabidopsis and rice. *Plants* 10 (9), 1864. doi: 10.3390/plants10091864

Weng, L., Chen, C., Zuo, J., and Li, W. (2011). Molecular dynamics study of effects of temperature and concentration on hydrogen-bond abilities of ethylene glycol and glycerol: implications for cryopreservation. *J. Phys. Chem. A* 115 (18), 4729–4737. doi: 10.1021/jp111162w

Wisniewski, M., and Fuller, M. (1999). "Ice nucleation and deep supercooling in plants: new insights using infrared thermography," in *Cold-Adapted Organisms: Ecology, Physiology, Enzymology and Molecular biology*. Ed. R. Margesin and F. Schinner. Berlin (Heidelberg: Springer), 105–118.

Wisniewski, M., Fuller, M. I. C. K., Palta, J., Carter, J., and Arora, R. (2004). Ice nucleation, propagation, and deep supercooling in woody plants. *J. Crop Improvement* 10 (1–2), 5–16. doi: 10.1300/J411v10n01_02

Wisniewski, M., Nassuth, A., and Arora, R. (2018). Cold hardiness in trees: A mini-review. *Front. Plant Sci.* 9. doi: 10.3389/fpls.2018.01394

Wisniewski, M., Norelli, J., Bassett, C., Artlip, T., and Macarisin, D. (2011). Ectopic expression of a novel peach (Prunus persica) CBF transcription factor in apple (Malus × Domestica) results in short-day induced dormancy and increased cold hardiness. *Planta* 233 (5), 971–983. doi: 10.1007/s00425-011-1358-3

Wisniewski, M., Willick, I. R., Duman, J. G., Livingston, D., and Newton, S. S. (2020). "Plant Antifreeze Proteins," in *Antifreeze Proteins Volume 1: Environment, Systematics and Evolution*. Eds. H. Ramløv and D. S. Friis (Cham: Springer International Publishing), 189–226.

Xie, H.-T., Wan, Z.-Y., Li, S., and Zhang, Y. (2014). Spatiotemporal production of reactive oxygen species by NADPH oxidase is critical for tapetal programmed cell death and pollen development in arabidopsis. *Plant Cell* 26 (5), 2007–2023. doi: 10.1105/tpc.114.125427

Xu, Yi, Hu, W., Liu, J., Song, S., Hou, X., Jia, C., et al. (2020). An aquaporin gene maPIP2-7 is involved in tolerance to drought, cold and salt stresses in transgenic banana (Musa acuminata L.). *Plant Physiol. Biochem.* 147, 66–76. doi: 10.1016/j.plaphy.2019.12.011

Yang, T., Ali, G. S., Yang, L., Du, L., Reddy, A. S. N., and Poovaiah, B. W. (2010). Calcium/calmodulin-regulated receptor-like kinase CRLK1 interacts with MEKK1 in plants. *Plant Signaling Behav.* 5 (8), 991–994. doi: 10.4161/psb.5.8.12225

Yang, X., Wang, R., Jing, H., Chen, Q., Bao, X., Zhao, J., et al. (2020). Three novel C-repeat binding factor genes of dimocarpus longan regulate cold stress response in arabidopsis. *Front. Plant Sci.* 11. doi: 10.3389/fpls.2020.01026

Yu, T.-F., Xu, Z.-S., Guo, J.-K., Wang, Y.-X., Abernathy, B., Fu, J.-D., et al. (2017). Improved drought tolerance in wheat plants overexpressing a synthetic bacterial cold shock protein gene seCspA. *Sci. Rep.* 7 (1), 44050. doi: 10.1038/srep44050

Yu, H., Zheng, H., Liu, Y., Yang, Q., Li, W., Zhang, Y., et al. (2021). Antifreeze protein from ammopiptanthus nanus functions in temperature-stress through domain A. *Sci. Rep.* 11 (1), 8458. doi: 10.1038/s41598-021-88021-0

Zamani-Babgohari, M., Critchley, A. T., Norrie, J., and Prithiviraj, B. (2019). Increased freezing stress tolerance of nicotiana tabacum L. Cv. Bright yellow-2 cell cultures with the medium addition of ascophyllum nodosum (L.) le jolis extract. *In Vitro Cell. Dev. Biol. - Plant* 55 (3), 321–333. doi: 10.1007/s11627-019-09972-8

Zhang, Qi, Chen, Q., Wang, S., Hong, Y., and Wang, Z. (2014). Rice and cold stress: methods for its evaluation and summary of cold tolerance-related quantitative trait loci. *Rice* 7 (1), 24. doi: 10.1186/s12284-014-0024-3

Zhang, S., Gottschalk, C., and Nocker, S. v. (2019). Genetic mechanisms in the repression of flowering by gibberellins in apple (Malus x domestica borkh.). *BMC Genomics* 20 (1), 747. doi: 10.1186/s12864-019-6090-6

Zhang, Li, Guo, X., Zhang, Z., Wang, A., and Zhu, J. (2021). Cold-regulated gene leCOR413PM2 confers cold stress tolerance in tomato plants." *Gene* 764, 145097. doi: 10.1016/j.gene.2020.145097

Zhang, Z., Li, J., Li, F., Liu, H., Yang, W., Chong, K., et al. (2017). OsMAPK3 phosphorylates osbHLH002/osICE1 and inhibits its ubiquitination to activate osTPP1 and enhances rice chilling tolerance. *Dev. Cell* 43 (6), 731–743.e5. doi: 10.1016/j.devcel.2017.11.016

Zhang, L.-L., Zhao, M.-G., Tian, Q.-Y., and Zhang, W.-H. (2011). Comparative studies on tolerance of medicago truncatula and medicago falcata to freezing. *Planta* 234 (3), 445–457. doi: 10.1007/s00425-011-1416-x

Zhao, C., Wang, P., Si, T., Hsu, C.-C., Wang, Lu, Zayed, O., et al. (2017). MAP kinase cascades regulate the cold response by modulating ICE1 protein stability. *Dev. Cell* 43 (5), 18–629.e5. doi: 10.1016/j.devcel.2017.09.024

Zhao, C., Zhang, Z., Xie, S., Si, T., Li, Y., and Zhu, J.-K. (2016). Mutational evidence for the critical role of CBF transcription factors in cold acclimation in arabidopsis. *Plant Physiol.* 171 (4), 2744–2759. doi: 10.1104/pp.16.00533

Zhou, A., Liu, E., Li, He, Li, Y., Feng, S., Gong, S., et al. (2018). PsCor413pm2, a plasma membrane-localized, cold-regulated protein from phlox subulata, confers low temperature tolerance in arabidopsis. *Int. J. Mol. Sci.* 19 (9), 2579. doi: 10.3390/ijms19092579

Zhu, J.-K. (2016). Abiotic stress signaling and responses in plants. *Cell* 167 (2), 313–324. doi: 10.1016/j.cell.2016.08.029

Zhuang, L., Yuan, X., Chen, Yu, Xu, B., Yang, Z., and Huang, B. (2015). PpCBF3 from cold-tolerant kentucky bluegrass involved in freezing tolerance associated with up-regulation of cold-related genes in transgenic arabidopsis thaliana. *PloS One* 10 (7), e0132928. doi: 10.1371/journal.pone.0132928

frontiers | Frontiers in Plant Science

TYPE Original Research
PUBLISHED 16 November 2023
DOI 10.3389/fpls.2023.1287997

OPEN ACCESS

EDITED BY
Isabel Lara,
Universitat de Lleida, Spain

REVIEWED BY
George Manganaris,
Cyprus University of Technology, Cyprus
Natasha Damiana Spadafora,
University of Calabria, Italy

*CORRESPONDENCE
Siva Kumar Malka
malka@korea.kr

RECEIVED 03 September 2023
ACCEPTED 30 October 2023
PUBLISHED 16 November 2023

CITATION
Park M-H, Ku K-M, Do K-R, Eum HL, Cho JH, Park PH and Malka SK (2023) Carbon dioxide treatment modulates phosphatidic acid signaling and stress response to improve chilling tolerance and postharvest quality in paprika. *Front. Plant Sci.* 14:1287997. doi: 10.3389/fpls.2023.1287997

Carbon dioxide treatment modulates phosphatidic acid signaling and stress response to improve chilling tolerance and postharvest quality in paprika

Me-Hea Park[1], Kang-Mo Ku[2], Kyung-Ran Do[3], Hyang Lan Eum[1], Jae Han Cho[1], Pue Hee Park[1] and Siva Kumar Malka[1]*

[1]Postharvest Research Division, National Institute of Horticultural and Herbal Science, Wanju, Republic of Korea, [2]Department of Plant Biotechnology, College of Life Sciences and Biotechnology, Korea University, Seoul, Republic of Korea, [3]Planning and Coordination Division, National Institute of Horticultural & Herbal Science, Wanju, Republic of Korea

Introduction: Paprika (*Capsicum annuum* L.) is prone to chilling injury (CI) during low-temperature storage. Although recent findings suggest that CO_2 treatment may protect against CI, the effects of short-term CO_2 treatment on CI and the underlying molecular mechanisms in paprika remain unknown. Therefore, this study aimed to examine the effect of short-term CO_2 treatment on CI and postharvest quality in paprika during storage at cold storage and retail condition at physio-biochemical-molecular level.

Methods: Paprika was treated with 20 and 30% CO_2 for 3 h and stored at 4°C for 14 days, followed by additional storage for 2 days at 20°C (retail condition). Fruit quality parameters, including weight loss, firmness, color, and pitting were assessed, and the molecular mechanism of the treatment was elucidated using transcriptomic and metabolomic analyses.

Results: Short-term treatment with 20 and 30% CO_2 effectively maintained paprika quality during cold storage and retailer conditions, with reduced surface pitting, a common symptom of CI. Additionally, transcriptomic and metabolomic analyses revealed that 20% CO_2 treatment induced genes associated with biosynthesis of phosphatidic acid (PA), diacylglycerol, triacylglycerol, and stress response, metabolites associated with phasphatidyl inositol signaling, inositol phosphate metabolism, and starch and sucrose metabolism.

Conclusion: CO_2 treatment activates PA biosynthesis through PLD and PLC-DGK pathways, and induces inositol phosphate, starch, and sucrose metabolism, thereby regulating chilling stress response via the ICE-CBF pathway. These

findings suggest that short-term CO_2 treatment enhances resistance to cold-induced injury and preserves postharvest quality in non-climacteric fruits, such as paprika, through activation of PA signaling, which improves membrane stability during cold storage and distribution.

KEYWORDS

Capsicum annum L., chilling injury, membrane integrity, postharvest quality, lipid metabolism, phosphatidic acid, stress response, DREB

1 Introduction

Postharvest storage and transportation of fresh produce are crucial stages in the supply chain that substantially affect product quality and shelf life. Among the various factors affecting the postharvest quality of fruits and vegetables, chilling injury (CI) remains a persistent challenge, particularly for chilling-sensitive crops, such as paprika (*Capsicum annuum* L.). CI is a physiological disorder characterized by the development of various symptoms, including tissue softening, water soaking, discoloration, and increased susceptibility to decay, leading to considerable economic losses for producers and retailers (Biswas et al., 2016; Park et al., 2021; Rai et al., 2022). Conventional approaches to mitigate CI often involve controlling storage temperatures above the chilling threshold, which is typically around 10°C for paprika (Lim et al., 2007). However, maintaining high temperatures during storage can result in accelerated deterioration and reduced shelf life (Rao et al., 2011). Therefore, it is critical to explore alternative strategies that can effectively alleviate CI, while preserving the quality attributes and extending the postharvest life of paprika.

Recently, carbon dioxide (CO_2) treatment has emerged as a promising strategy for preserving the post-harvest quality of various horticultural products. For instance, continuous exposure to CO_2 (5%) effectively maintained the postharvest quality of tomatoes during storage at 10°C (Taye et al., 2017). Similarly, strawberries exposed to 18% CO_2 for 48 h prior to storage at 1°C exhibited enhanced resistance to softening and oxidative stress (del Olmo et al., 2022). Additionally, treatment with 95% CO_2 for 36 h prior to storage at 1°C reduced the susceptibility of persimmons to CI (Besada et al., 2015). Moreover, treatment with 10% CO_2 for 24 h in combination with modified atmosphere packaging effectively maintained the quality of sweet peppers stored at 10°C (Afolabi et al., 2023). Furthermore, treatment with 30% CO_2 for 6 h prior to storage at 0°C reduced CI, extended storability, and preserved the sensory quality and antioxidant capacity of Madoka peach fruit (Tilahun et al., 2022). However, it is imperative to minimize the treatment duration to enhance the feasibility and cost-effectiveness of postharvest treatments for producers and distributors. Notably, studies have shown that exposing strawberries and tomatoes to 30% CO_2 for only 3 h can effectively maintain quality and mitigate CI (Eum et al., 2021; Park et al., 2021).

The mechanism underlying CO_2-induced postharvest quality preservation is attributed to its ability to reduce respiration rate and ethylene production. For instance, apples, melons, tomatoes, and bananas showed respiratory reduction following high CO_2 treatment (Kubo et al., 1989; Park et al., 2021). CO_2 pretreatment coupled with cold storage synergistically reduced ethylene production, leading to delayed ripening in tomatoes (Park et al., 2021). At the molecular level, ethylene biosynthesis and signaling genes are suppressed by CO_2 pretreatment in tomatoes (Rothan et al., 1997; Park et al., 2021), and CO_2 treatment can modulate genes encoding cell wall-degrading enzymes in strawberries (Eum et al., 2021). Additionally, CO_2 pretreatment triggers the expression of genes involved in stress and the activity of antioxidant enzymes in several fruits and vegetables, including tomatoes, grapes, peaches, and strawberries (Rothan et al., 1997; Romero et al., 2016; Park et al., 2021; del Olmo et al., 2022; Tilahun et al., 2022). CI often disrupts membrane integrity due to altered fluidity and rigidity caused by temperature fluctuations during storage, resulting in cellular leakage, compromised physiological functions, and decrease in overall quality (Biswas et al., 2016; Valenzuela et al., 2017). Moreover, chilling stress can induce oxidative stress by triggering the production of reactive oxygen species (ROS) owing to disrupted electron transport chains and impaired antioxidant systems (Biswas et al., 2016; Valenzuela et al., 2017). Therefore, developing postharvest technologies that target membrane lipid metabolism and stress responses would be highly beneficial for inhibiting CI and maintaining the postharvest quality of fresh produce.

Despite the positive effects of short-term CO_2 treatment in tomato and strawberry, its impact on the quality of stored paprika remains unexplored. Moreover, the molecular mechanisms of CO_2-induced quality preservation and CI resistance remains unclear, particularly in non-climacteric fruits, such as paprika. Therefore, this study aimed to comprehensively evaluate the effect and molecular mechanism of short-term CO_2 pretreatment on postharvest quality in paprika under cold storage and retail conditions, using transcriptomic and metabolomic analyses.

2 Materials and methods

2.1 Plant materials and treatments

Paprika fruits (cv. Sirocco, red color) were harvested at approximately 80–85% maturity stage. After arrival to the laboratory, the fruits were immediately treated with 20 and 30% CO_2 (mixed with ambient air) or left untreated in a commercial

cardboard box for 3 h in a closed chamber at room temperature (~20°C). After the treatment period, the chamber was flushed with air to remove CO_2. In total, 30 boxes per treatment were used for the study, with each box containing 30 fruits. The CO_2 concentration in the closed chamber was measured using a portable headspace analyzer (Dansensor, Ringsted, Denmark). Samples in the control group were flushed with ambient air, and the damaged fruits were discarded. The fruits were stored in a covered cardboard box at 4°C (cold storage) for 14 d or at 4°C for 14 d, followed by additional 2 d at 20°C (14 + 2 d; retail condition). Relative humidity was maintained at 90 ± 5% during the storage period.

2.2 Fruit quality evaluation

Briefly, 20 fruits were sampled per treatment for fruit quality assessment. The fruits were weighed to determine weight loss using an electronic weighing balance. Skin color was monitored using a color meter (Minolta CR-400; Konica Minolta, Osaka, Japan), and values were reported based on Hunter's redness scale (a*). Firmness was analyzed using a texture analyzer (TA Plus Lloyd Instruments Ltd., Fareham, Hamshire, UK) equipped with a 5-mm plunger head (diameter) at a speed of 2 mm/s. Total soluble solid content (SSC) was analyzed using a digital refractometer (PAL-1, Atago Co. Ltd., Tokyo, Japan). Fruit pitting was expressed as the percentage of fruits that exhibited pitting. The final reported quality attributes were obtained from three independent replicates per treatment per day.

2.3 Light microscopy for tissue structure analysis

Tissue analysis was performed as previously described (Clément et al., 1996), with some modifications. Briefly, paprika tissues were fixed in 2.5% glutaraldehyde (v/v in a 0.1 M phosphate buffer) at pH of 7.2 with 4% sucrose (w/v) for 24 h. After three rinses with the above fixing buffer (30 min each), the samples were post-fixed with 1% OsO4 w/v in the same buffer with 4% sucrose (w/v) for 4 h. After rinsing three times (30 min each), the tissues were dehydrated in alcohol gradient series, transferred to propylene oxide, and embedded in Epon epoxy resin. Semi-thin sections (2.5 µm) were prepared using an ultra-microtome and placed on glass slides. The polysaccharide-specific reaction was performed using periodic acid-Schiff (PAS) and the tissue structures are shown in red. Sections for staining were first immersed in 1% periodic acid (w/v) for 30 min, followed by immersion in Schiff's reagent for 40 min and in 5% sodium bisulfite (w/v) for 35 min. Thereafter, the sections were rinsed with distilled water, dried on a warm plate, and mounted on Histomount. The negative control was prepared by omitting the oxidation step using periodic acid. The samples were observed under a light microscope (Axioscop 2; Carl Zeiss, Germany).

2.4 Transcriptome analysis

Paprika fruits were sampled at days 0, 7, and 14 + 2 from the untreated control and 20% CO_2-treated groups. Thereafter, five fruits were pooled from each sample, and the peel tissue was used for RNA isolation using the Qiagen RNA mini prep (Qiagen, USA). RNA purity and integrity were verified using an Agilent 2100 Bioanalyzer (Agilent Technologies, Santa Clara, CA, USA USA), and only RNA with an RNA integrity value (RIN) > 8 were used for library preparation. Library preparation and RNA sequencing (RNA-seq) were performed at C&K Genomics in Seoul, South Korea. The processed reads were aligned to the sequence of *Capsicum annuum* (AVRZ02) using HISAT v2.1.0 (Kim et al., 2015). Aligned reads were counted using featureCounts in the Subread package version 1.6.0100 (Liao et al., 2014). Count data were analyzed for differential gene expression using the EdgeR package (Robinson et al., 2010). The expression level of each transcript was normalized to the TMM (trimmed mean) using the M-value normalization method (Robinson and Oshlack, 2010). The filtered data were log2-transformed and subjected to quantile normalization. Differentially expressed genes (DEGs) were selected using $p \leq 0.05$ and log2-fold change (FC) ≥ 1 as thresholds. Gene ontology (GO) enrichment sets of the DEGs were obtained using the DAVID (Databank for Annotation, Visualization, and Integrated Discovery) database (Dennis et al., 2003).

2.5 Quantitative real-time PCR

Quantitative real-time PCR (qRT-PCR) was performed as described by Park et al. (2021). Target genes were amplified on a CFX96 TouchTM Real-Time PCR Detection System (Bio-Rad, USA) using the iQTM SYBR Green Supermix (Bio-Rad) with specific primers (Supplementary Table S1). The qRT-PCR conditions were as follows: 95°C for 30 s, followed by 40 cycles of 95°C for 10 s and 55°C or 58°C for 40 s. The relative gene expression was calculated using the ΔΔCt method and normalized to that of the housekeeping genes *actin* and *elongation factor 1*. The qRT-PCR was performed using at least three biological replicates and two technical replicates.

2.6 Metabolome analysis using gas chromatography–mass spectrometry

Samples were prepared for primary metabolites profiling following previously described methods (Lisec et al., 2015; Song and Ku, 2021), with some modifications. Briefly, freeze-dried paprika powder was extracted in methanol. Ribitol and tetracosane were used as internal standards for water- and lipid-soluble compounds, respectively. Water- and lipid-soluble compounds were separated into two phases via liquid-to-liquid extraction using deionized water and chloroform, respectively. Each organic phase was fully dried using a SpeedVac. Thereafter, methoxyamide (in anhydrous pyridine) was added to a tube containing dried water-soluble phase and incubated at 37°C for 90 min under constant shaking at 800 rpm. For derivatization of the water-soluble metabolites, N-methyl-N-(trimethylsilyl)trifluoroacetamide and 1% trimethylchlorosilane (TMCS) were added, and the sample was incubated at 50°C for 20 min under constant shaking at 800 rpm.

10.3389/fpls.2023.1287997

For derivatization of the lipid-soluble metabolites, N, O-bis (trimethylsilyl)trifluoroacetamide + TMCS was added to the sample. The mixture was incubated at 60°C for 60 min under constant shaking at 800 rpm. The sample was transferred to vials with an insert and 1 µL was injected into a gas chromatograph (Nexis GC-2030, Shimadzu, Kyoto, Japan) coupled to a gas chromatograph–mass spectrometer (GC/MS-QP 2020 NX, Shimadzu) and an autosampler with injector (AOC-20i PLUS, Shimadzu). Chromatographic separation was performed in a capillary column (DB-5MS, Agilent, CA, USA; 30 m × 0.25 mm coated with 0.25 µm film). The flow rate of the carrier gas (helium) was set to 1.2 mL·min^{-1}. The mass spectrophotometry parameters were as follows: ion source temperature, interface temperature, and mass scan range were set to 300°C, 250°C, and 40-600 m/z, respectively. For analysis of water-soluble metabolites, the initial oven temperature was set at 80°C for 2 min, then increased to 330°C at a rate of 12°C·min^{-1}, and maintained at 330°C for 5 min. For analysis of lipid-soluble metabolites, the initial oven temperature was set at 150°C for 1 min, then increased to 320°C at a rate of 12°C·min^{-1}, and maintained at 320°C for 7 min. Metabolites were identified based on the library from National Institute of Standards and Technology (NIST) or standard compounds (Supplementary Table S4).

2.7 Statistical analyses

Data are presented as the mean ± standard error. Significant differences were determined using analysis of variance (ANOVA), followed by *t*-test for comparisons between groups. Partial least squares discriminant analysis (PLS–DA) and pathway analysis were performed using MetaboAnalyst (https://www.metaboanalyst.ca/). All analyses were performed using SAS v.9.2 (SAS Institute, Cary, NC, USA).

3 Results

3.1 CO_2 treatment reduces chilling injury and maintains quality in paprika

Compared with that in the control group, treatment with 20 and 30% CO_2 increased the respiration rate at day 0, indicating the successful absorption of CO_2 in treated paprika (Supplementary Figure S1). However, there was a decrease in respiration rate during cold storage (4°C) for 14 days with respiration rate peaking at day 5 of storage at 20°C (Supplementary Figure S1). Notably, there was no significant difference in respiration rate between the treatment and control groups during storage at 4 and 20°C regardless of the CO_2 treatment concentration. Additionally, treatment with 20% CO_2 caused a decrease in hue value and fresh weight during cold storage (Supplementary Table S2). Figure 1A represents the images of CO_2 -treated and untreated fruits stored at 14 days of cold storage at 4°C and additional 2 days of storage under retails condition at 20°C. Moreover, 20% CO_2 - and 30% CO_2 -treated paprika were significantly firmer than untreated fruits at 14 days cold storage at 4°C and 5 days at 20°C (Figure 1B; Supplementary Table S2). Specifically, fruits treated with 20% CO_2 were 18.2% firmer than

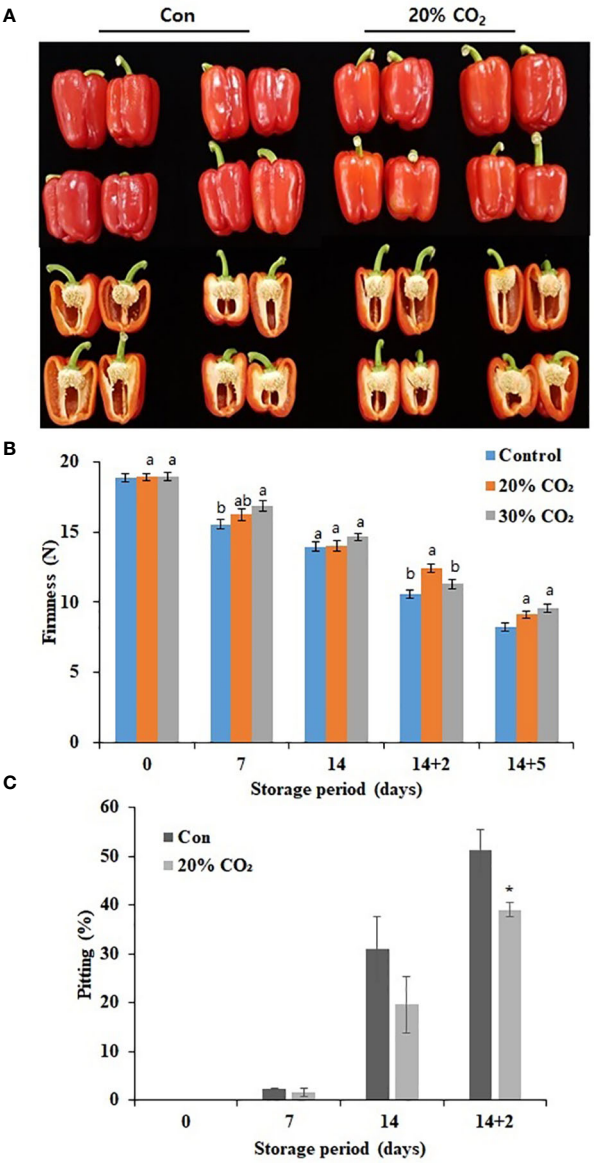

FIGURE 1
Effect of short-term CO_2 treatment on postharvest quality and chilling injury in paprika. Representative images of CO_2-treated and untreated fruits at 4°C for 14 days, followed by storage for 2 days at 20°C **(A)**, firmness **(B)**, and pitting **(C)** in paprika treated with CO_2 and stored at 4°C for 14 days, and retail condition. Data represents the mean ± standard error of three replicates. At **(B)**, different letters on the graphs represent significant differences between the control and CO_2 treatments (DMRT, $P < 0.05$). and at **(C)**, * represent t-test for comparisons between groups($p<0.1$,**$p < 0.05$ and ***$p < 0.0005$).

those in the control group after 14 days of cold storage and additional 2 days of storage under retails condition (14 + 2 days) (Figure 1B). There was no significant difference in SSC between CO_2-treated and untreated fruits (Supplementary Table S2). The Pitting rate is a primary symptom of CI in paprika, fruits treated with 20 and 30% CO_2 (Supplementary Figure S3) showed significantly lower surface pitting after transfer from cold storage to retail conditions. Specifically, only 39% of fruits treated with 20% CO_2 showed surface pitting at day 2 after transfer from cold storage (14 days) to

retail conditions compared with a rate of 51% in the control group (Figure 1C). CO_2 treatment reduced the loss rate by about 12% during distribution, which is an economic benefit depending on the market price (Supplementary Table S3) Overall, these results suggest that CO_2 treatment effectively delayed ripening and senescence and maintained fruit firmness during storage, which improved quality and reduced CI in paprika. As there were no notable differences between 20 and 30% CO_2 treatments, 20% CO_2 treatment was selected for further experiments.

3.2 CO_2 treatment affects the transcriptome profile of paprika

RNA sequencing was performed at days 0, 14, and 14 + 2 after CO_2 treatment using pericarp tissues. Heatmap revealed remarkable changes in the transcriptome of the fruits following 20% CO_2 treatment (Figure 2A). Differential expression analysis identified 3,511 DEGs in the treated vs. untreated groups, among which 2,996 DEGs were expressed at day 0, 56 DEGs at day 14, and 459 DEGs at

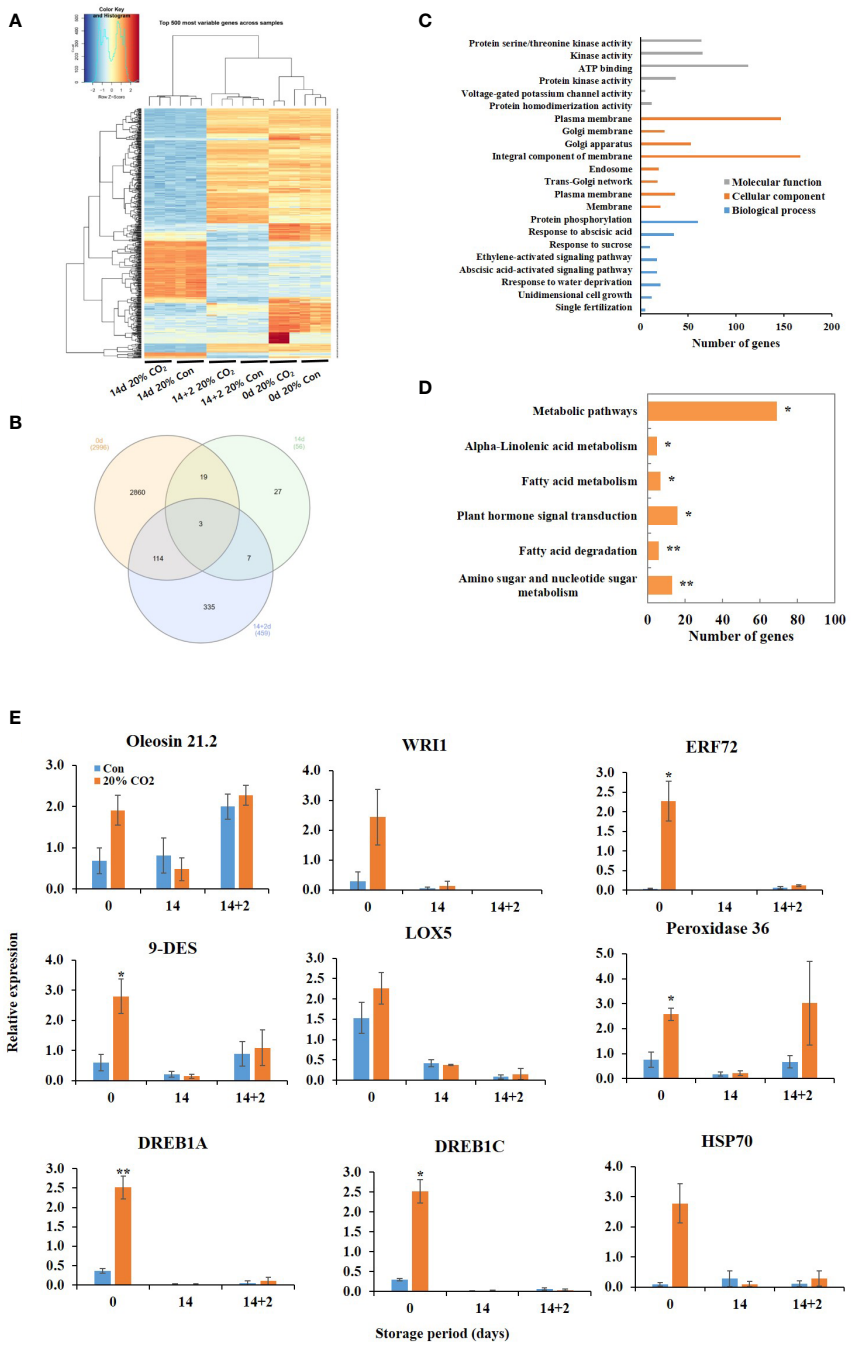

FIGURE 2
Transcriptome analysis of CO_2-treated tomatoes. Heatmap **(A)** and Venn diagram **(B)** of differentially expressed genes (DEGs); Gene ontology functional categorization of DEGs **(C)**; KEGG pathway enrichment analysis of DEGs **(D)**; quantitative real-time PCR validation of lipid metabolism- and stress-related genes **(E)** in paprika treated with CO_2 and stored at 4°C for 14 days, followed by storage for 2 days at 20°C (14 + 2). *p < 0.1, and **p < 0.01.

10.3389/fpls.2023.1287997

day 14 + 2 after CO_2 treatment (Figure 2B). GO functional annotation showed that the DEGs were enriched in different functional terms in the cellular components, biological processes, and molecular functions categories (Figure 2C). Kyoto Encyclopedia of Genes and Genomes (KEGG) enrichment analysis showed that the DEGs were enriched in amino sugar and nucleotide sugar metabolism, fatty acid degradation, fatty acid metabolism, alpha-linoleic acid metabolism, plant hormone signal transduction, and metabolic pathways (Figure 2D). All upregulated and downregulated genes in response to CO_2 treatment are shown in Tables S5, S6, S7.

Membrane lipid metabolism plays an important role in the cold stress response. DEGs involved in lipid processes, such as phospholipases (*phospholipase D delta* and *phospholipase A1-II 1*), *diacylglycerol kinase 5* (*DGK5*), *diacylglycerol O-acyltransferase 1* (*DGAT1), omega-6 fatty acid desaturase* (*FAD*), *GDSL esterase/lipases* (*GDSL esterase/lipase At5g18430*, *GDSL esterase/lipase At1g71250*), *non-specific lipid-transfer proteins*, *oleosins (oleosin 21.2 kDa*, *oleosin 18 kDa*, *oleosin 18.5 kDa*), and *WRI1* were upregulated at day 0 (Table 1). Additionally, DEGs encoding the lipid-body membrane proteins, including *oleosins* (*oleosin 21.2 kDa*, *oleosin 18 kDa*, *oleosin 18.5 kDa*), were strongly induced at day 0. Moreover, DEGs encoding *glycerol-3-phosphate acyltransferase 3*, *FAD*, *enoyl-CoA delta isomerase 1*, and *lipid phosphate phosphatase 3* (*LPP3*) were upregulated in the CO_2-treated fruits at day 14 + 2 (Table 1). At day 14, only 18 DEGs showed expression of more than 1.5 fold, and where mainly involved in encoding unknown proteins, except for cardiolipin synthase, which was downregulated. Additionally, DEG related to lipid-derived molecules, including oxylipins and jasmonates (*alpha-dioxygenase 1, 9-divinyl ether synthase*, *linolenate hydroperoxide lyase*, and *linoleate 9S-lipoxygenase*), were induced by CO_2 treatment at days 0 and 14 + 2 after treatment (Table 1).

Furthermore, CO_2 treatment modulated the expression of various stress-related genes, including dehydration-responsive element-binding proteins (*DREB1A* and *DREB1C*), *MYBs*, *heat shock 70 kDa protein*, *peroxidase 36*, *proline-rich protein 4*, *desiccation-related protein*, and *pathogenesis-related proteins*, at days 0 and 14 + 2 (Table 2). However, one DEG encoding *NAC domain-containing protein 7* was suppressed at day 14 after CO_2 treatment (Table 2). qRT-PCR was performed to confirm the effects of CO_2 treatment on *oleosin*, *9-DES*, *LOX5*, *ERF72*, *WRI1*, *peroxidase 36*, *HSP70*, *DREB1A*, and *DREB1C*. There were no significant differences in the expression levels of *lipoxygenase*, *oleosin*, *WRI*, and *HSP70* between CO_2-treated and untreated fruits (Figure 2E). Notably, these genes, except for *oleosin* and *peroxidase36*, were specifically induced in CO_2-treated fruits at day 0 (Figure 2E).

TABLE 1 Differentially expressed genes (DEGs) involved in lipid processes in paprika treated with CO_2.

Gene ID	Annotation	Fold change (log 2 ratio)
0 d		
CA.PGAv.1.6.scaffold1148.6	Oleosin 21.2 kDa	13.43
CA.PGAv.1.6.scaffold206.50	Alpha-dioxygenase 1	10.77
CA.PGAv.1.6.scaffold1716.8	9-divinyl ether synthase	9.74
CA.PGAv.1.6.scaffold338.13	Oleosin 18 kDa	8.69
CA.PGAv.1.6.scaffold1856.8	Oleosin 18.5 kDa	8.42
CA.PGAv.1.6.scaffold1361.7	Short-chain dehydrogenase reductase 4	7.81
CA.PGAv.1.6.scaffold174.20	Oleosin 1	7.71
CA.PGAv.1.6.scaffold338.15	Oleosin 5	7.68
CA.PGAv.1.6.scaffold1344.22	AP2-like ethylene-responsive transcription factor AIL6	7.43
CA.PGAv.1.6.scaffold386.6	Poly [ADP-ribose] polymerase 3	7.37
CA.PGAv.1.6.scaffold134.49	Ethylene-responsive transcription factor WRI1	6.73
CA.PGAv.1.6.scaffold732.20	11-beta-hydroxysteroid dehydrogenase 1A	6.43
CA.PGAv.1.6.scaffold4.13	GDSL esterase/lipase At5g18430	6.01
CA.PGAv.1.6.scaffold781.9	GDSL esterase/lipase At1g71250	5.74
CA.PGAv.1.6.scaffold712.2	AP2-like ethylene-responsive transcription factor AIL6	5.58
CA.PGAv.1.6.scaffold508.5	Diacylglycerol kinase 5-like isoform X1	5.14
CA.PGAv.1.6.scaffold644.44	Putative phospholipid: diacylglycerol acyltransferase 2	5.00
CA.PGAv.1.6.scaffold1529.2	Peroxisomal fatty acid beta-oxidation multifunctional protein AIM1-like	4.72
CA.PGAv.1.6.scaffold508.7	Diacylglycerol kinase 5-like isoform X1	4.53
CA.PGAv.1.6.scaffold345.6	Non-specific lipid-transfer protein 2	4.34
CA.PGAv.1.6.scaffold508.6	Diacylglycerol kinase 5-like isoform X1	4.23
CA.PGAv.1.6.scaffold798.35	Phospholipase D delta-like	2.33
CA.PGAv.1.6.scaffold290.8	Linolenate hydroperoxide lyase, chloroplastic	1.77
CA.PGAv.1.6.scaffold1583.4	Diacylglycerol O-acyltransferase 1-like	1.58
CA.PGAv.1.6.scaffold702.15	Phospholipase A1-II 1-like	1.58

(Continued)

3.3 CO_2 treatment affects the metabolome of paprika

The metabolite profiles of CO_2-treated and untreated fruits were analyzed at days 0, 14, and 14 + 2 after CO_2 treatment. In total,

10.3389/fpls.2023.1287997

TABLE 1 Continued

Gene ID	Annotation	Fold change (log 2 ratio)
CA.PGAv.1.6.scaffold62.12	Phospholipase A1-Ibeta2, chloroplastic	1.02
14 d		
CA.PGAv.1.6.scaffold3104.1	Cardiolipin synthase (CMP-forming), mitochondrial	-2.22
14 + 2		
CA.PGAv.1.6.scaffold1152.14	Probable linoleate 9S-lipoxygenase 5	5.46
CA.PGAv.1.6.scaffold338.55	Glycerol-3-phosphate acyltransferase 3-like isoform X1	5.36
CA.PGAv.1.6.scaffold869.25	Enoyl-CoA delta isomerase 1, peroxisomal	5.21
CA.PGAv.1.6.scaffold575.39	Omega-6 fatty acid desaturase, endoplasmic reticulum	4.94
CA.PGAv.1.6.scaffold575.39	Omega-6 fatty acid desaturase, endoplasmic reticulum	4.94
CA.PGAv.1.6.scaffold1235.27	Lysine histidine transporter-like 8	4.00
CA.PGAv.1.6.scaffold575.29	Omega-6 fatty acid desaturase, endoplasmic reticulum	2.44
CA.PGAv.1.6.scaffold610.20	Lipid phosphate phosphatase 3, chloroplastic-like	2.09
CA.PGAv.1.6.scaffold103.21	Omega-6 fatty acid desaturase, endoplasmic reticulum	1.58

Bold value means paprika treated with CO2 and stored at 4°C for 14 days (14d), followed by storage for 2 days at 20°C (14 + 2). Od means before storage after treatment.

36 metabolites, including 28 water-soluble and 8 lipid-soluble metabolites including 2 internal standards, were identified (Supplementary Table S4). PLS-DA was conducted to explore the effect of CO_2 and the relationship between the metabolites. The two PLS-DA components collectively accounted for 85.4 and 86.4% of the total variance in the dataset at days 14 and 14 + 2, respectively (Figures 3A, B). Additionally, there was a clear separation of the two clusters, indicating the significant impact of CO_2 on metabolites in paprika during storage (Figures 3A, B).

Further analysis indicated changes in pathways analysis at days 14 and 14 + 2 after CO_2 treatment (Figures 3C, D). At day 14, the most significantly affected pathway was starch and sucrose metabolism' pathway. At day 14 + 2, the most significantly affected pathway was the phosphatidylinositol signaling system and inositol phosphate metabolism. Furthermore, CO_2 treatment significantly reduced the levels of the metabolites valine, asparagine, citric acid, sucrose, myoinositol, and oxyproline at days 14 and 14 + 2 after CO_2 treatment (Figure 3E), indicating potential

TABLE 2 Differentially expressed genes (DEGs) involved in stress response in paprika treated with CO_2.

Gene ID	Annotation	Fold change (log 2 ratio)
0 d		
CA.PGAv.1.6.scaffold1129.55	Pathogenesis-related protein 5	8.37
CA.PGAv.1.6.scaffold104.8	Proline-rich protein 4	8.12
CA.PGAv.1.6.scaffold793.22	1-aminocyclopropane-1-carboxylate oxidase homolog 2	8.07
CA.PGAv.1.6.scaffold305.57	Desiccation-related protein PCC13-62	7.57
CA.PGAv.1.6.scaffold165.2	Cytochrome P450 81E8	7.41
CA.PGAv.1.6.scaffold160.28	Heat shock 70 kDa protein	7.11
CA.PGAv.1.6.scaffold851.27	Dehydration-responsive element-binding protein 2C	6.94
CA.PGAv.1.6.scaffold1129.23	Transcription factor MYB3-like	6.94
CA.PGAv.1.6.scaffold1239.15	Growth-regulating factor 8	6.11
CA.PGAv.1.6.scaffold927.3	Peroxidase 36	5.86
CA.PGAv.1.6.scaffold48.44	Leucine-rich repeat receptor-like protein kinase TDR	5.74
CA.PGAv.1.6.scaffold610.67	Transcription factor MYB48-like	5.50
CA.PGAv.1.6.scaffold862.63	Ethylene-responsive transcription factor RAP2-3	5.48
CA.PGAv.1.6.scaffold1297.5	Laccase-16	5.17
CA.PGAv.1.6.scaffold352.24	Cytochrome P450 94B3	4.21
CA.PGAv.1.6.scaffold138.3	Transcription factor MYB82-like	3.92
CA.PGAv.1.6.scaffold26.31	Dehydration-responsive element-binding protein 1C	2.47
CA.PGAv.1.6.scaffold1711.13	Probable WRKY transcription factor 72-like	2.45
CA.PGAv.1.6.scaffold809.26	Transcription factor MYB86-like	2.30
CA.PGAv.1.6.scaffold548.14	Dehydration-responsive element-binding protein 1A	2.15
CA.PGAv.1.6.scaffold907.9	MYB family transcription factor family protein	-1.14
CA.PGAv.1.6.scaffold362.14	Transcription repressor MYB4-like	-1.18
CA.PGAv.1.6.scaffold492.68	NAC domain-containing protein 21/22-like	-1.32

(Continued)

10.3389/fpls.2023.1287997

TABLE 2 Continued

Gene ID	Annotation	Fold change (log 2 ratio)
14 d		
CA.PGAv.1.6.scaffold330.12	NAC domain-containing protein 7	-2.69
14 + 2		
CA.PGAv.1.6.scaffold981.3	Thaumatin-like protein-like	5.49
CA.PGAv.1.6.scaffold2357.1	5-epiaristolochene synthase	3.67
CA.PGAv.1.6.scaffold566.15	Pathogenesis-related protein STH-21	3.60
CA.PGAv.1.6.scaffold1495.1	4-coumarate–CoA ligase 1	3.11
CA.PGAv.1.6.scaffold134.86	Pathogenesis-related protein PR-4B	3.02

Bold value means paprika treated with CO2 and stored at 4°C for 14 days (14d), followed by storage for 2 days at 20°C (14 + 2). Od means before storage after treatment.

alteration of the TCA cycle, electron transport chain, and stress tolerance mechanisms in CO_2-treated fruits. Decreased citric acid and sucrose levels in CO_2-treated fruits (Figure 3E) suggest their channelizing into GABA shunt pathway.

3.4 Anatomical analysis of pericarp of paprika treated with CO_2

In this study, surface pitting was observed on the fruits at day 14 + 2 of storage (Figure 1C). Microscopic examination of cross-sections of pericarp tissues of the fruits at days 0 and 14 + 2 showed that the epidermis and hypodermis of the pericarp tissues appeared to have a compact cell size and shrinking cell morphology, suggesting severe water loss in the hypodermal layer (Figure 4). Notably, hypodermal cells were substantially shirked and appeared to collapse compared with epidermal cells (Figure 4), suggesting cell membrane impairment in hypodermal cells during long-term low-temperature storage.

4 Discussion

4.1 Short-term CO_2 treatment enhances postharvest quality and reduces CI in paprika

The primary CI symptoms in paprika such as surface pitting, calyx discoloration remains a major concern, leading to substantial economic losses. CI is initiated in fruits exposed to cold temperatures; however, the symptoms are more evident when the fruits are shifted from cold storage temperatures to non-chilling temperatures (Biswas et al., 2016). In the present study, short-term treatment with 20 and 30% CO_2 for 3 h prior to cold storage delayed ripening progression, enhanced firmness, reduced weight loss, and minimized surface pitting (Figure 1), which was consistent with previous findings in CO_2-treated crops, including tomatoes, strawberries, persimmons, peaches, and sweet peppers (Besada et al., 2015; Eum et al., 2021; Park et al., 2021; Tilahun et al., 2022; Afolabi et al., 2023). Notably, our study differs from previous approaches that utilized longer treatment durations, ranging from 6 to 48 h or continuous. Although the effect of CO_2 treatment for 3 h on tomato and strawberries has been previously examined, this is the first study to best of our knowledge to examine the effects of short-term CO_2 treatment on postharvest quality and CI in paprika. The results of the present study are attributed to the ability of CO_2 to modulate respiration rates and ethylene production, as observed in studies on tomatoes and other fruits (Kubo et al., 1989; Taye et al., 2017; Park et al., 2021; Tilahun et al., 2022).

4.2 Short-term CO_2 treatment activates genes associated with phosphatidic acid biosynthesis and stress response

Transcriptomic and metabolomic analyses revealed the intricate molecular responses triggered by CO_2 treatment in paprika. Specifically, CO_2 treatment activated specific DEGs and metabolites associated with lipid processes and stress responses, shedding light on the underlying mechanisms. Particularly, CO_2 treatment activated genes involved in phosphatidic acid (PA) biosynthesis, a central precursor for glycerophospholipids, galactolipids, and triacylglycerol (TAG) biosynthesis; moreover, PA plays a pivotal role in cellular responses to stress conditions (Hong et al., 2016; Perlikowski et al., 2016; Yu et al., 2019; Wu et al., 2022). PA is produced through the acylation of lysophosphatidic acid (LPA), which is derived from glycerol 3-phosphate by the enzyme glycerol 3-phosphate acyltransferase (GPAT) (Nakamura, 2017). PA biosynthesis via acylation steps is the start of the glycerolipid *de novo* biosynthesis. In this study, CO_2 treatment induced the expression of *GPAT* (Table 1), indicating the induction of PA production in these fruits. Alternatively, PA levels are controlled by phospholipase (PL) D and PLC-DGK (diacylglycerol kinase) pathways, involving PLs, phosphates, and lipid kinases (Wu et al., 2022). In the PLD pathway, the structural phospholipids are hydrolyzed by PLD to produce PA and soluble head groups (Wu et al., 2022). In the PLC-DGK pathway, PLC acts on phosphatidylinositol 4,5-bisphosphate (PtdInsP2) to produce DAG and inositol phosphate (IP) 3. Notably, DAG can be phosphorylated by DGK to form PA (Wu et al., 2022). Additionally, PA can be dephosphorylated back into DAG by lipid phosphate phosphatases (LPP) (Craddock et al., 2017; Su et al., 2021). In this study, CO_2 treatment enhanced the expression of *PLDδ*, *DGK5s*, and *LPP3*, indicating the activation of PLD and PLC-DGK pathways. These pathways are the two principal routes that produce signaling PA and have been extensively studied for their early response to cold stress (Vergnolle et al., 2005; Wu et al., 2022). For instance, *PLDs* and *DGKs* were responsive to low temperature in peppers (Kong et al., 2019). Deactivating *PLDδ* makes Arabidopsis plants more sensitive to freezing, while its

10.3389/fpls.2023.1287997

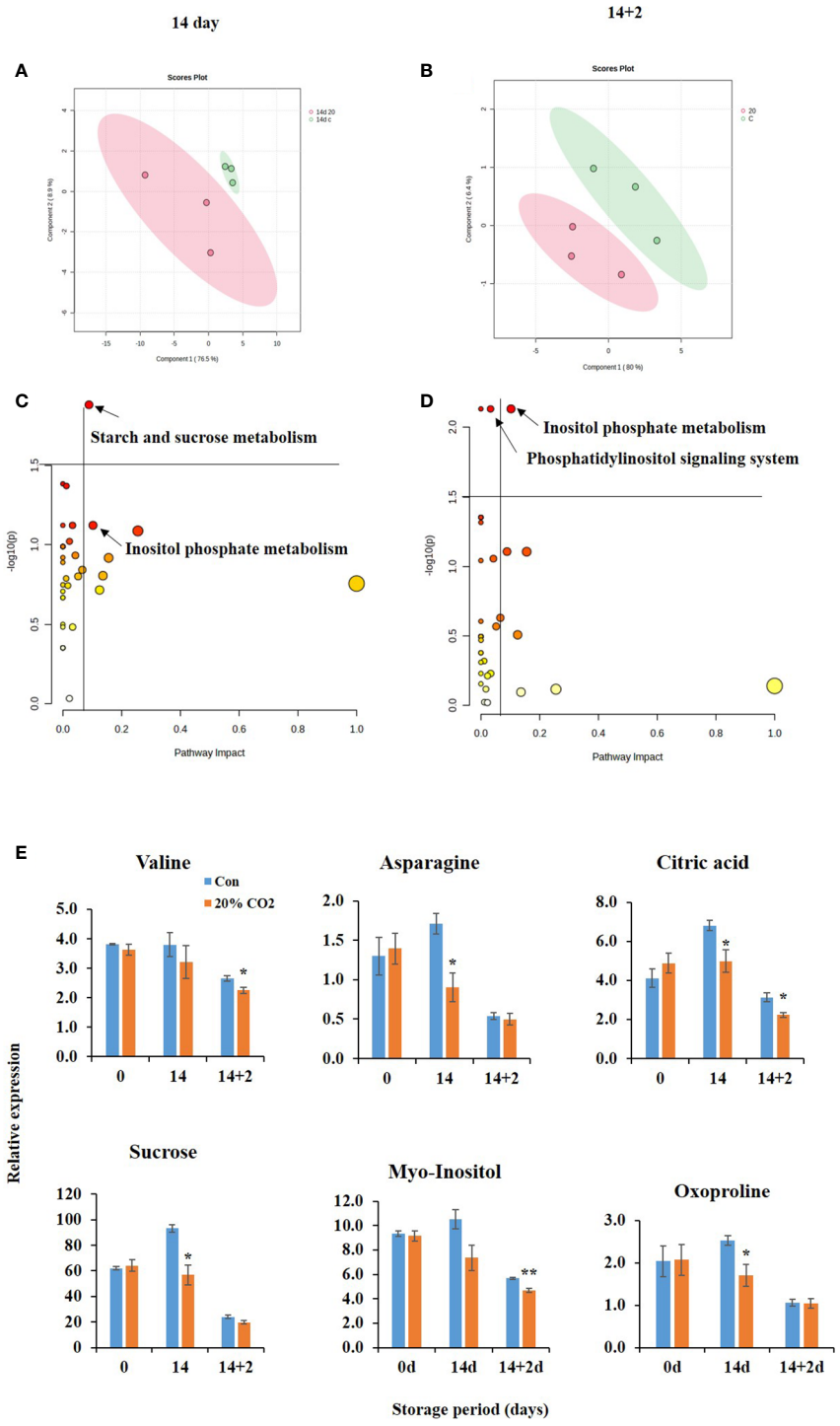

FIGURE 3
Metabolic changes in of CO_2-treated paprika. Scores plot of partial least squares discriminant analysis of water soluble and lipid soluble metabolites at days 14 **(A)** and 14 + 2 **(B)**; Pathway analysis of water soluble and lipid soluble metabolites on days 14 **(C)** and 14 + 2 **(D)**; differential accumulation of metabolites **(E)** in paprika treated with CO_2 and stored at 4°C for 14 days, followed by storage for 2 days at 20°C (14 + 2). *p < 0.1, and **p < 0.01,

overexpression enhances freezing tolerance (Li et al., 2004). Furthermore, DAG can serve as a substrate for the synthesis of various lipids, including membrane phospholipids and TAGs. Diacylglycerol O-acyltransferase 1 (DGAT) transfers a fatty acyl group from a fatty acyl-CoA molecule to a DAG molecule, resulting in the formation of TAG (Wu et al., 2022). In this study, the expression of DEGs encoding DGAT and oleosins, the structural proteins of TAGs, were induced in the CO_2-treated fruits (Table 1; Shimada et al., 2008). The *dgat1* mutant lines exhibited reduced cold tolerance, and DAG and PA levels were significantly increased

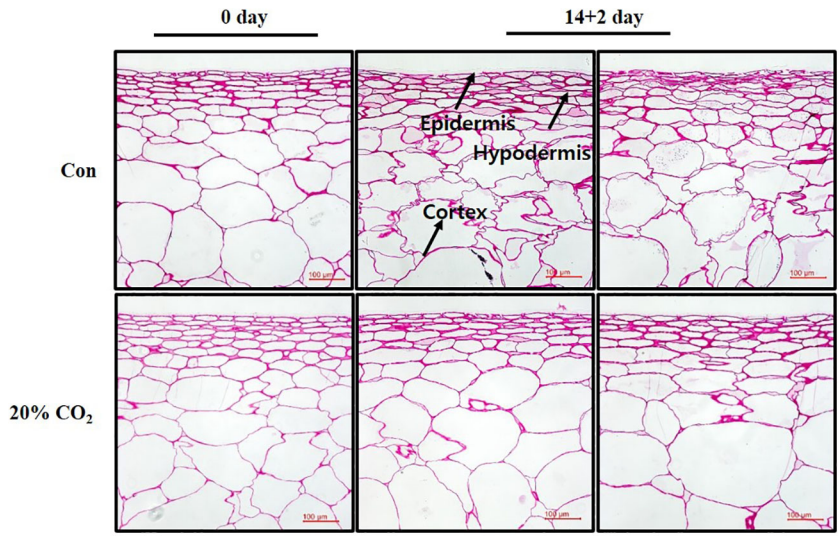

FIGURE 4
Microscopic analysis of pericarp tissues of paprika.

in Arabidopsis (Tan et al., 2018). Moreover, the dynamic balance of PA, DAG, and TAG is an important protective strategy to combat freezing temperatures (Tan et al., 2018).

The ICE–CBF/DREB1 transcriptional cascade has been extensively studied for its role in cold signaling (Chinnusamy et al., 2007). *ICE1* transcription factor directly activates cold-responsive genes by binding to cis-elements in the *CBF3/DREB1a* and *CBF2* (*DREB1C*) promoters (Chinnusamy et al., 2007). In the present study, *DREB1A* and *DREB1C* were expressed at day 0 after CO_2 treatment (Table 2; Figure 2E), indicating the potent impact of CO_2 treatment on the early activation of crucial components of the ICE–CBF/DREB1 pathway. Moreover, PLC and PLD pathways function upstream of the ICE–CBF/DREB1 pathway (Vergnolle et al., 2005). These results indicate that CO_2 treatment may trigger ICE–CBF/DREB1 pathway to regulate chilling stress. Furthermore, the jasmonate signaling pathway acts as a pivotal upstream regulator of the ICE–CBF/DREB1 pathway, and plays a pivotal role in enhancing freezing tolerance in Arabidopsis (Hu et al., 2013). Remarkably, CO_2 treatment induced the expression of jasmonate synthesis-related genes, specifically *alpha-dioxygenase 1*, *9-divinyl ether synthase* (*DES*), *9S-lipoxygenase* (*LOX5*), in the treated fruits (Table 1; Figure 2E). The concurrent induction of *DREBs* and jasmonic acid biosynthesis-related genes strongly suggests the activation of the ICE–CBF pathway following CO_2 treatment. Moreover, CO_2 treatment triggered the expression of known stress-responsive genes, such as *peroxidase 32*, *heatshok protein 70*, *pathogenesis related proteins* (Table 2; Figure 2E), and promoted stress defense mechanisms. The upregulation of stress-related genes may have amplified antioxidant enzyme activity, as confirmed by ABTS and DPPH assays, and enhanced polyphenol content (Supplementary Figure S2). Overall, these results indicate that CO_2 enhances resistance to freezing stress in fruits through a multifaceted approach, thereby improving postharvest quality.

Intricate stress signaling might induce lipid processes, as evidenced by enhanced expression of the membrane integrity associated gene *fatty acid desaturases* (*FADs*) in CO_2-treated fruits (Table 1; Figure 2E), leading to improved membrane stability (Figure 4), which may contribute to extending the shelf life of the fruits. This is of particular significance, considering that the balance of unsaturated fatty acids within the lipid bilayer plays a pivotal role in plant responses to CI (Zhang and Tian, 2010). Moreover, heterologous overexpression of *Eriobotrya japonica's FAD8* in Arabidopsis increased the expression of *ICE-CBF-cold regulated genes* in response to low temperatures (Xu et al., 2023), indicating intricate interaction between lipid process and stress signaling during chilling stress.

4.3 Short-term CO_2 treatment activates metabolites associated with inositol phosphate metabolism and starch and sucrose metabolism

At day 14 of cold storage, starch and sucrose metabolism were remarkably altered, suggesting that high CO_2 exposure may play a role in modulating carbohydrate metabolism in CO_2-treated paprika during cold storage. Starch and sucrose, the principal carbohydrates in plants, play critical roles in energy storage and transfer (Zhu et al., 2023), and alterations in this pathway indicates that short-term CO_2 treatment increases the tricarboxylic acid (TCA) cycle, potentially affecting fruit respiration. Exposing agricultural produce to elevated levels of CO_2, especially for short durations may promote anaerobic metabolism or stress responses. Under these conditions, a reduction in mitochondrial respiration, which in turn limits the availability of ATP for energy-demanding processes. In response to this energy crisis, fruit metabolism adapts by enhancing substrate-level ATP production. This adaptation involves various processes, including the breakdown of soluble sugars and the degradation of starch (Gorin et al., 1978; Planchet et al., 2017; Brizzolara et al., 2020).

Terzoudis et al. (2022) reported that a decrease in oxygen levels was associated with reduced levels of sucrose, citrate, and valine in postharvest peach fruits. Furthermore, under anaerobic conditions, certain amino acids, including valine, can be metabolized via the branched-chain amino acid degradation pathway to produce compounds that feed into the TCA cycle or the electron transport chain (Araújo et al., 2011). This might lead to a decrease in valine levels in CO_2-treated fruits (Figure 3E). Another possible explanation is that a sudden elevation in CO_2 may affect protein synthesis and degradation in cells (Brizzolara et al., 2020). Notably, Tanou et al. (2017) reported differential accumulation of valine was associated with CI tolerance in peach fruits. Similarly, the reduction in citric acid and sucrose levels can be interpreted as continuous metabolism under elevated CO_2 levels. Although it is known that high levels of CO_2 and low O_2 inhibit cell respiration (Kubo et al., 1989), metabolism might increase through the GABA shunt pathway under low O_2 conditions (Li et al., 2021).

IPs and phosphatidylinositol (PI) signaling pathways are involved in several biological processes, including chilling stress. IP3 is generated by PLC-mediated hydrolysis of PtdInsP2, and triggers a set of cellular processes by releasing calcium, which acts as a secondary messenger to transduce cold signals (Sun et al., 2021). In this study, inositol phosphate metabolism was identified at both days 14 and 14 + 2, emphasizing its importance and potential sensitivity to CO_2 exposure. Phosphatidylinositol signaling is pivotal for various cellular processes, including cell growth, differentiation, and motility (Sun et al., 2021). The phosphatidylinositol signaling system and inositol phosphate metabolic pathways are linked to freezing tolerance and CI regulation in plants (Zakharian et al., 2010; Sun et al., 2021). Notably, metabolite changes in CO_2-treated fruits were associated with phosphatidylinositol signaling and inositol phosphate metabolism (Figure 3D), suggesting their potential role in CO_2-induced chilling tolerance in paprika.

Notably, the cellular response to CO_2 in non-climacteric fruits appears to differ from that in climacteric fruits. For instance, treatment with 30% CO_2 for 3 h maintained the quality of tomatoes and protected against CI through associated with transcriptional changes in ethylene-related genes and respiratory-related metabolism (Park et al., 2021), whereas CO_2 treatment maintained the quality of paprika, a non-climacteric fruit, by modulating mainly lipid-related processes, stress responses, and metabolism of starch and inositol phosphates.

5 Conclusion

Short-term CO_2 treatment reduced CI and improved postharvest quality in paprika by activating PA synthesis and its signaling via the PLD and PLC–DK pathways, inducing stress signaling via the ICE–CBF pathway, and enhancing lipid processes and antioxidant defense mechanisms, thereby promoting membrane stability (Figure 5).

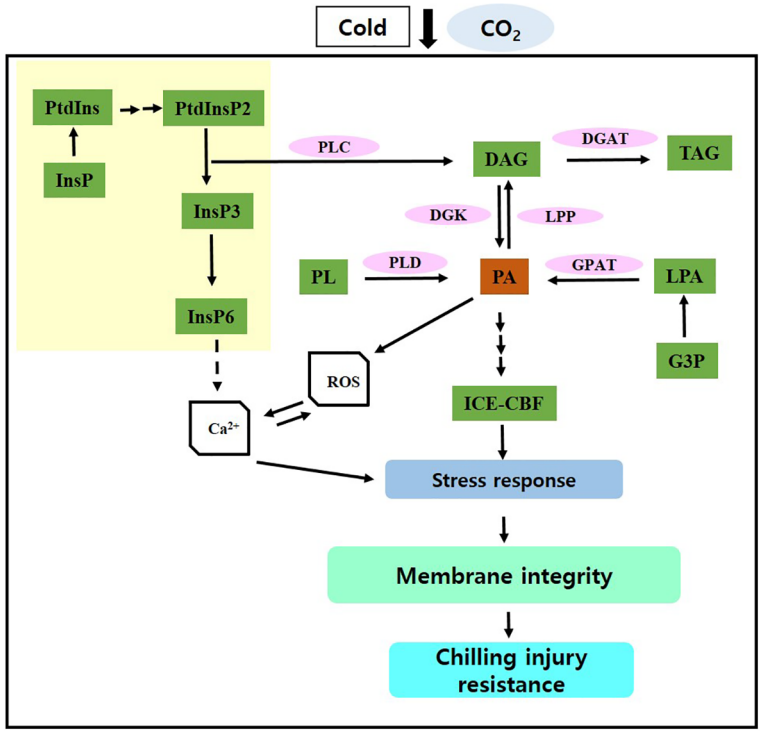

FIGURE 5
Potential molecular mechanism through which CO_2 maintains postharvest quality and protects against chilling injury. InsP, inositol phosphate; PtdIns, phosphatidylinositol; PtdInsP, phosphatidylinositol phosphate; PL, phospholipid; PLD, phospholipase D; PLC, phospholipase C; PA, phosphatidic acid; DAG, diacylglycerol; TAG, triacylglycerol; G3P, glycerol-3-phosphate, LPA, lysophosphatidic acid; DGK, DAG kinase; GPAT, G3P acyltransferase; LPP, LPA phosphatase. Solid arrows represent established pathways; dashed arrows indicate potential pathways; array of arrows indicate multiple steps; yellow region indicate inositol phosphate metabolism.

Overall, these findings contribute to the advancement of innovative strategies for preserving postharvest quality in paprika and minimizing losses. However, further studies are necessary to examine the effects of short-term CO_2 treatment on the postharvest quality of other crop species under cold storage.

Data availability statement

The datasets presented in this study can be found in online repositories. The names of the repository/repositories and accession number(s) can be found here: https://www.ncbi.nlm.nih.gov/bioproject/PRJNA1019830/.

Author contributions

M-HP: Conceptualization, Funding acquisition, Methodology, Project administration, Resources, Supervision, Validation, Visualization, Writing – review & editing. KK: Data curation, Methodology, Supervision, Writing – original draft. K-RD: Data curation, Writing – original draft. HE: Data curation, Software, Writing – original draft. JC: Data curation, Methodology, Writing – original draft. PP: Data curation, Investigation, Resources, Writing – original draft. SM: Conceptualization, Data curation, Formal Analysis, Investigation, Methodology, Software, Supervision, Validation, Visualization, Writing – original draft, Writing – review & editing.

Funding

The author(s) declare financial support was received for the research, authorship, and/or publication of this article. This study was funded by the Cooperative Research Program for Agriculture, Science, and Technology (Project No. PJ01601102) in the Rural Development Administration of the Republic of Korea.

Conflict of interest

The authors declare that the research was conducted in the absence of any commercial or financial relationships that could be construed as a potential conflict of interest.

Publisher's note

Supplementary material

The Supplementary Material for this article can be found online at: https://www.frontiersin.org/articles/10.3389/fpls.2023.1287997/full#supplementary-material

References

Afolabi, A. S., Choi, I.-L., Lee, J. H., Kwon, Y. B., Yoon, H. S., and Kang, H.-M. (2023). Effect of pre-storage CO2 treatment and modified atmosphere packaging on sweet pepper chilling injury. *Plants* 12 (3), 671. doi: 10.3390/plants12030671

Araújo, W. L., Tohge, T., Ishizaki, K., Leaver, C. J., and Fernie, A. R. (2011). Protein degradation–an alternative respiratory substrate for stressed plants. *Trends Plant Sci.* 16 (9), 489–498. doi: 10.1016/j.tplants.2011.05.008

Besada, C., Llorca, E., Novillo, P., Hernando, I., and Salvador, A. (2015). Short-term high CO2 treatment alleviates chilling injury of persimmon cv. Fuyu by preserving the parenchyma structure. *Food Control* 51, 163–170. doi: 10.1016/j.foodcont.2014.11.013

Biswas, P., East, A. R., Hewett, E. W., and Heyes, J. A. (2016). "Chilling injury in tomato fruit," in *Horticultural reviews*, vol. 44, 229–278. doi: 10.1002/9781119281269.ch5

Brizzolara, S., Manganaris, G. A., Fotopoulos, V., Watkins, C. B., and Tonutti, P. (2020). Primary metabolism in fresh fruits during storage [Review]. *Front. Plant Sci.* 11. doi: 10.3389/fpls.2020.00080

Chinnusamy, V., Zhu, J., and Zhu, J.-K. (2007). Cold stress regulation of gene expression in plants. *Trends Plant Sci.* 12 (10), 444–451. doi: 10.1016/j.tplants.2007.07.002

Clément, C., Burrus, M., and Audran, J. C. (1996). Floral organ growth and carbohydrate content during pollen development in Lilium. *Am. J. Bot.* 83 (4), 459–469. doi: 10.1002/j.1537-2197.1996.tb12727.x

Craddock, C. P., Adams, N., Kroon, J. T., Bryant, F. M., Hussey, P. J., Kurup, S., et al. (2017). Cyclin-dependent kinase activity enhances phosphatidylcholine biosynthesis in Arabidopsis by repressing phosphatidic acid phosphohydrolase activity. *Plant J.* 89 (1), 3–14. doi: 10.1111/tpj.13321

del Olmo, I., Romero, I., Alvarez, M. D., Tarradas, R., Sanchez-Ballesta, M. T., Escribano, M. I., et al. (2022). Transcriptomic analysis of CO2-treated strawberries (Fragaria vesca) with enhanced resistance to softening and oxidative stress at consumption [Original Research]. *Front. Plant Sci.* 13. doi: 10.3389/fpls.2022.983976

Dennis, G., Sherman, B. T., Hosack, D. A., Yang, J., Gao, W., Lane, H. C., et al. (2003). DAVID: database for annotation, visualization, and integrated discovery. *Genome Biol.* 4 (9), 1–11. doi: 10.1186/gb-2003-4-9-r60

Eum, H.-L., Han, S.-H., and Lee, E.-J. (2021). High-CO2 treatment prolongs the postharvest shelf life of strawberry fruits by reducing decay and cell wall degradation. *Foods* 10 (7), 1649. doi: 10.3390/foods10071649

Gorin, N., Bonisolli, F., Heidema, F. T., Klop, W., and Williams, A. A. (1978). Changes in starch content and amylase zymograms during storage of Golden Delicious and Cox's Orange Pippin apples. *Z. fur Lebensmittel-untersuchung und-forschung* 166 (3), 157–161. doi: 10.1007/BF01354808

Hong, Y., Zhao, J., Guo, L., Kim, S.-C., Deng, X., Wang, G., et al. (2016). Plant phospholipases D and C and their diverse functions in stress responses. *Prog. Lipid Res.* 62, 55–74. doi: 10.1016/j.plipres.2016.01.002

Hu, Y., Jiang, L., Wang, F., and Yu, D. (2013). Jasmonate regulates the inducer of CBF expression–c-repeat binding factor/DRE binding factor1 cascade and freezing tolerance in Arabidopsis. *Plant Cell* 25 (8), 2907–2924. doi: 10.1105/tpc.113.112631

Kim, D., Langmead, B., and Salzberg, S. L. (2015). HISAT: a fast spliced aligner with low memory requirements. *Nat. Methods* 12 (4), 357–360. doi: 10.1038/nmeth.3317

Kong, X.-m., Zhou, Q., Luo, F., Wei, B.-d., Wang, Y.-j., Sun, H.-j., et al. (2019). Transcriptome analysis of harvested bell peppers (Capsicum annuum L.) in response to cold stress. *Plant Physiol. Biochem.* 139, 314–324. doi: 10.1016/j.plaphy.2019.03.033

Kubo, Y., Inaba, A., and Nakamura, R. (1989). Effects of high CO2 on respiration in various horticultural crops. *J. Japanese Soc. Hortic. Sci.* 58 (3), 731–736. doi: 10.2503/jjshs.58.731

Li, W., Li, M., Zhang, W., Welti, R., and Wang, X. (2004). The plasma membrane–bound phospholipase Dδ enhances freezing tolerance in Arabidopsis thaliana. *Nat. Biotechnol.* 22 (4), 427–433. doi: 10.1038/nbt949

Liao, Y., Smyth, G. K., and Shi, W. (2014). featureCounts: an efficient general purpose program for assigning sequence reads to genomic features. *Bioinformatics* 30 (7), 923–930. doi: 10.1093/bioinformatics/btt656

Lim, C. S., Kang, S. M., Cho, J. L., Gross, K. C., and Woolf, A. B. (2007). Bell Pepper (Capsicum annuum L.) Fruits are Susceptible to Chilling Injury at the Breaker Stage of Ripeness. *HortScience horts* 42 (7), 1659–1664. doi: 10.21273/hortsci.42.7.1659

Lisec, J., Schauer, N., Kopka, J., Willmitzer, L., and Fernie, A. R. (2015). Corrigendum: Gas chromatography mass spectrometry-based metabolite profiling in plants. *Nat. Protoc.* 10 (9), 1457. doi: 10.1038/nprot0915-1457a

Nakamura, Y. (2017). Plant phospholipid diversity: emerging functions in metabolism and protein–lipid interactions. *Trends Plant Sci.* 22 (12), 1027–1040. doi: 10.1016/j.tplants.2017.09.002

Park, M.-H., Kim, S.-J., Lee, J.-S., Hong, Y.-P., Chae, S.-H., and Ku, K.-M. (2021). Carbon dioxide pretreatment and cold storage synergistically delay tomato ripening through transcriptional change in ethylene-related genes and respiration-related metabolism. *Foods* 10 (4), 744. doi: 10.3390/foods10040744

Perlikowski, D., Kierszniowska, S., Sawikowska, A., Krajewski, P., Rapacz, M., Eckhardt, Ä., et al. (2016). Remodeling of leaf cellular glycerolipid composition under drought and re-hydration conditions in grasses from the Lolium-Festuca complex. *Front. Plant Sci.* 7, 1027. doi: 10.3389/fpls.2016.01027

Planchet, E., Lothier, J., and Limami, A. M. (2017). Hypoxic respiratory metabolism in plants: reorchestration of nitrogen and carbon metabolisms. *Plant respiration: Metab. fluxes carbon balance* 43, 209–226. doi: 10.1007/978-3-319-68703-2_10

Rai, A., Kumari, K., and Vashistha, P. (2022). Umbrella review on chilling injuries: Post-harvest issue, cause, and treatment in tomato. *Scientia Hortic.* 293, 110710. doi: 10.1016/j.scienta.2021.110710

Rao, T. V. R., Gol, N. B., and Shah, K. K. (2011). Effect of postharvest treatments and storage temperatures on the quality and shelf life of sweet pepper (Capsicum annum L.). *Scientia Hortic.* 132, 18–26. doi: 10.1016/j.scienta.2011.09.032

Robinson, M. D., McCarthy, D. J., and Smyth, G. K. (2010). edgeR: a Bioconductor package for differential expression analysis of digital gene expression data. *Bioinformatics* 26 (1), 139–140. doi: 10.1093/bioinformatics/btp616

Robinson, M. D., and Oshlack, A. (2010). A scaling normalization method for differential expression analysis of RNA-seq data. *Genome Biol.* 11 (3), 1–9. doi: 10.1186/gb-2010-11-3-r25

Romero, I., Vazquez-Hernandez, M., Escribano, M. I., Merodio, C., and Sanchez-Ballesta, M. T. (2016). Expression profiles and DNA-binding affinity of five ERF genes in bunches of Vitis vinifera cv. Cardinal treated with high levels of CO2 at low temperature. *Front. Plant Sci.* 7, 1748. doi: 10.3389/fpls.2016.01748

Rothan, C., Duret, S., Chevalier, C., and Raymond, P. (1997). Suppression of ripening-associated gene expression in tomato fruits subjected to a high CO2 concentration. *Plant Physiol.* 114 (1), 255–263. doi: 10.1104/pp.114.1.255

Shimada, T. L., Shimada, T., Takahashi, H., Fukao, Y., and Hara-Nishimura, I. (2008). A novel role for oleosins in freezing tolerance of oilseeds in Arabidopsis thaliana. *Plant J.* 55 (5), 798–809. doi: 10.1111/j.1365-313X.2008.03553.x

Song, H.-J., and Ku, K.-M. (2021). Optimization of allyl isothiocyanate sanitizing concentration for inactivation of salmonella typhimurium on lettuce based on its phenotypic and metabolome changes. *Food Chem.* 364, 130438. doi: 10.1016/j.foodchem.2021.130438

Su, W., Raza, A., Zeng, L., Gao, A., Lv, Y., Ding, X., et al. (2021). Genome-wide analysis and expression patterns of lipid phospholipid phospholipase gene family in Brassica napus L. *BMC Genomics* 22 (1), 1–15. doi: 10.1186/s12864-021-07862-1

Sun, S., Lin, M., Qi, X., Chen, J., Gu, H., Zhong, Y., et al. (2021). Full-length transcriptome profiling reveals insight into the cold response of two kiwifruit genotypes (A. arguta) with contrasting freezing tolerances. *BMC Plant Biol.* 21 (1), 1–20. doi: 10.1186/s12870-021-03152-w

Tan, W.-J., Yang, Y.-C., Zhou, Y., Huang, L.-P., Xu, L., Chen, Q.-F., et al. (2018). DIACYLGLYCEROL ACYLTRANSFERASE and DIACYLGLYCEROL KINASE modulate triacylglycerol and phosphatidic acid production in the plant response to freezing stress. *Plant Physiol.* 177 (3), 1303–1318. doi: 10.1104/pp.18.00402

Tanou, G., Minas, I. S., Scossa, F., Belghazi, M., Xanthopoulou, A., Ganopoulos, I., et al. (2017). Exploring priming responses involved in peach fruit acclimation to cold stress. *Sci. Rep.* 7 (1), 11358. doi: 10.1038/s41598-017-11933-3

Taye, A. M., Tilahun, S., Park, D. S., Seo, M. H., and Jeong, C. S. (2017). Effects of continuous application of CO2 on fruit quality attributes and shelf life during cold storage in cherry tomato. *Hortic. Sci. Technol.* 35 (3), 300–313. doi: 10.12972/kjhst.20170033

Terzoudis, K., Hertog, M. L. A. T. M., and Nicolaï, B. M. (2022). Dynamic labelling reveals central carbon metabolism responses to stepwise decreasing hypoxia and reoxygenation during postharvest in pear fruit. *Postharvest Biol. Technol.* 186, 111816. doi: 10.1016/j.postharvbio.2021.111816

Tilahun, S., Jeong, M. J., Choi, H. R., Baek, M. W., Hong, J. S., and Jeong, C. S. (2022). Prestorage high CO2 and 1-MCP treatment reduce chilling injury, prolong storability, and maintain sensory qualities and antioxidant activities of "Madoka" Peach fruit [Original research]. *Front. Nutr.* 9. doi: 10.3389/fnut.2022.903352

Valenzuela, J. L., Manzano, S., Palma, F., Carvajal, F., Garrido, D., and Jamilena, M. (2017). Oxidative stress associated with chilling injury in immature fruit: postharvest technological and biotechnological solutions. *Int. J. Mol. Sci.* 18 (7), 1467. doi: 10.3390/ijms18071467

Vergnolle, C., Vaultier, M.-N., Taconnat, L., Renou, J.-P., Kader, J.-C., Zachowski, A., et al. (2005). The cold-induced early activation of phospholipase C and D pathways determines the response of two distinct clusters of genes in Arabidopsis cell suspensions. *Plant Physiol.* 139 (3), 1217–1233. doi: 10.1104/pp.105.068171

Wu, J., Nadeem, M., Galagedara, L., Thomas, R., and Cheema, M. (2022). Recent insights into cell responses to cold stress in plants: Signaling, defence, and potential functions of phosphatidic acid. *Environ. Exp. Bot.* 203, 105068. doi: 10.1016/j.envexpbot.2022.105068

Xu, X., Yang, H., Suo, X., Liu, M., Jing, D., Zhang, Y., et al. (2023). EjFAD8 enhances the low-temperature tolerance of loquat by desaturation of sulfoquinovosyl diacylglycerol (SQDG). *Int. J. Mol. Sci.* 24 (8), 6946. doi: 10.3390/ijms24086946

Yu, Y., Kou, M., Gao, Z., Liu, Y., Xuan, Y., Liu, Y., et al. (2019). Involvement of phosphatidylserine and triacylglycerol in the response of sweet potato leaves to salt stress. *Front. Plant Sci.* 10, 1086. doi: 10.3389/fpls.2019.01086

Zakharian, E., Cao, C., and Rohacs, T. (2010). Gating of transient receptor potential melastatin 8 (TRPM8) channels activated by cold and chemical agonists in planar lipid bilayers. *J. Neurosci.* 30 (37), 12526–12534. doi: 10.1523/JNEUROSCI.3189-10.2010

Zhang, C., and Tian, S. (2010). Peach fruit acquired tolerance to low temperature stress by accumulation of linolenic acid and N-acylphosphatidylethanolamine in plasma membrane. *Food Chem.* 120 (3), 864–872. doi: 10.1016/j.foodchem.2009.11.029

Zhu, M., Zang, Y., Zhang, X., Shang, S., Xue, S., Chen, J., et al. (2023). Insights into the regulation of energy metabolism during the seed-to-seedling transition in marine angiosperm Zostera marina L.: Integrated metabolomic and transcriptomic analysis. *Front. Plant Sci.* 14, 1130292. doi: 10.3389/fpls.2023.1130292

frontiers | Frontiers in Plant Science

TYPE Original Research
PUBLISHED 16 November 2023
DOI 10.3389/fpls.2023.1233477

OPEN ACCESS

EDITED BY
Shifeng Cao,
Zhejiang Wanli University, China

REVIEWED BY
Yingying Wei,
Ningbo University, China
Haibo Luo,
Nanjing Normal University, China

*CORRESPONDENCE
Ghulam Khaliq
ghulam-khan@live.com

RECEIVED 02 June 2023
ACCEPTED 28 August 2023
PUBLISHED 16 November 2023

CITATION
Khaliq G, Ali S, Ejaz S, Abdi G, Faqir Y, Ma J, Siddiqui MW and Ali A (2023) γ-Aminobutyric acid is involved in overlapping pathways against chilling injury by modulating glutamate decarboxylase and defense responses in papaya fruit. *Front. Plant Sci.* 14:1233477. doi: 10.3389/fpls.2023.1233477

γ-Aminobutyric acid is involved in overlapping pathways against chilling injury by modulating glutamate decarboxylase and defense responses in papaya fruit

Ghulam Khaliq[1]*, Sajid Ali[2], Shaghef Ejaz[2], Gholamreza Abdi[3], Yahya Faqir[4], Jiahua Ma[4], Mohammed Wasim Siddiqui[5] and Asgar Ali[6]

[1]Department of Horticulture, Faculty of Agriculture, Lasbela University of Agriculture, Water and Marine Sciences, Uthal, Pakistan, [2]Department of Horticulture, Faculty of Agricultural Sciences and Technology, Bahauddin Zakariya University, Multan, Pakistan, [3]Department of Biotechnology, Persian Gulf Research Institute, Persian Gulf University, Bushehr, Iran, [4]Engineering Research Center for Biomass Resource Utilization and Modification of Sichuan Province, Southwest University of Science and Technology, Mianyang, China, [5]Department of Food Science and Post-Harvest Technology, Bihar Agricultural University, Sabour, India, [6]Centre of Excellence for Postharvest Biotechnology (CEPB), School of Biosciences, University of Nottingham Malaysia, Semenyih, Malaysia

The effect of γ-aminobutyric acid (GABA) treatment at two concentrations (1 mM or 5 mM) on papaya fruit stored at 4°C and 80%–90% relative humidity for 5 weeks was investigated. The application of GABA at 5 mM apparently inhibited chilling injury, internal browning, electrolyte leakage, malondialdehyde (MDA), hydrogen peroxide (H_2O_2), polyphenol oxidase (PPO), phospholipase D (PLD), and lipoxygenase (LOX) activities of papaya fruit. Fruit treated with 5 mM GABA enhanced the activities of ascorbate peroxidase (APX), catalase (CAT), glutathione reductase (GR), superoxide dismutase (SOD), glutamate decarboxylase (GAD), and phenylalanine ammonia-lyase (PAL). In addition, GABA treatment significantly displayed higher levels of proline, endogenous GABA accumulation, phenolic contents, and total antioxidant activity than the nontreated papaya. The results suggested that GABA treatment may be a useful approach to improving the chilling tolerance of papaya fruit by reducing oxidative stress and enhancing the defense system.

KEYWORDS

papaya, GABA, chilling injury, abiotic stress, proline, GAD

1 Introduction

Papaya (*Carica papaya* L.) fruit is cultivated and consumed worldwide in tropical and subtropical regions. It contains vitamins A and C, thiamine, riboflavin, polyphenolic compounds, and carotenoids (Parven et al., 2020). The main carotenoids in papaya are β-carotene, β-cryptoxanthin, and lycopene. However, papaya is a typical climacteric fruit, and its ripening is accompanied by a high respiration rate and ethylene production that leads to rapid pulp softening and sudden biochemical changes (Gao et al., 2020). All these changes affect the quality and shelf life of papaya fruit during storage and transportation. These postharvest losses adversely affect the grower's income and the papaya fruit industry. Therefore, low-temperature storage is one of the best practices to maintain quality and slow down the biochemical and physiological processes of papaya fruit. Unfortunately, papaya fruit is very vulnerable to chilling temperatures when kept below 10°C (Wu et al., 2019). Papaya fruit shows chilling injury symptoms such as water soaking, surface pitting, shriveling of peel, internal browning, flesh mealiness, and poor aroma and flavor, which leads to a short storage life and lower fruit quality (Pan et al., 2019).

Two main hypotheses were suggested to elucidate the effect of low temperatures on chilling-sensitive plants. The first assumption states that the cell membrane is the main site for chilling injury development (Liang et al., 2020). The biophysical structure of the cell membrane changes under low-temperature stress, which may cause decreased fluidity, loss of membrane function, and deactivation of membrane-bound enzymes, ultimately destroying the membrane (Wolfe, 1978). Lipid peroxidation induces the solidification of saturated fatty acids and increases the ratio of sterol/phospholipid, enhancing membrane fluidity (Marangoni et al., 1996). This reveals that changes in the physical properties of cell membranes are temperature-dependent, and during low-temperature stress, these induced changes can be reversed before irreparable damage to the cell membrane occurs. The second assumption describes that during chilling stress, plants have been shown to produce higher levels of reactive oxygen species (ROS) that comprise hydrogen peroxide, hydroxyl radical, and superoxide anion (Valenzuela et al., 2017). ROS are the main cause of lipid peroxidation, and this leads to cellular disorders and the manifestation of chilling injury symptoms (Liang et al., 2020). Plants have two defense systems to scavenge ROS. The first is antioxidant compounds such as ascorbate, glutathione, vitamin A, phenolics, and anthocyanins. The second system is composed of antioxidant enzymes like APX, CAT, GR, and SOD. In response to oxidative stress, plants raise their enzymatic and nonenzymatic antioxidant defense systems to moderate the severe effects of stress caused by ROS (Li et al., 2019).

A lot of postharvest methods have been developed to maintain the quality and regulate chilling injury of various fruits, including edible coatings (Mendy et al., 2019), low- and high-temperature conditioning (Jin et al., 2014), modified atmosphere (Liang et al., 2020), and elicitors, including exogenous methyl jasmonate (Cao et al., 2010; Chen et al., 2021), melatonin (Mirshekari et al., 2020), nitric oxide (Wang et al., 2016), oxalic acid (Li et al., 2014), and glycine betaine (Luo et al., 2022). All these techniques have played an effective role in reducing chilling injury and maintaining the quality of fruits, but the efficiency of these methods depends on the cultivar, preharvest factors, storage temperature, and duration of storage (Zou et al., 2014). In addition, these methods have limitations due to complicated operations, high energy consumption, chemical residues, and high investment. Modified atmosphere storage is an efficient technique to reduce chilling injury in fruits; however, it changes the gas composition, resulting in undesirable effects like off-flavor and anaerobic respiration. Therefore, it is necessary to discover simple, inexpensive, safe, and efficient approaches to mitigate the chilling injury to papaya fruit. The activation of resistance mechanisms through physical or chemical treatment is attracting great attention for maintaining fruit quality and reducing oxidative damage (Ding et al., 2019).

γ-Aminobutyric acid is a non-protein amino acid and is involved in many physiological processes as a signaling molecule. GABA is a natural compound that regulates oxidative stress responses such as drought, heat, ultraviolet irradiation, and chilling (Ramos-Ruiz et al., 2019). GABA is considered to be involved in the activation of defense mechanisms, induction of nitrate transport, pollen tube growth, cell elongation, anti-chilling protection, and advancement of plant growth and development (Rastegar et al., 2020). GABA is associated with numerous physiological processes like the regulation of cytosolic pH, carbon flux into the tricarboxylic acid cycle, redox status, osmoregulation, and energy production (Ramos-Ruiz et al., 2019). The evidence revealed that GABA treatment inhibited the synthesis of saturated fatty acids and the accumulation of ROS and triggered the antioxidant defense system (Aghdam et al., 2016).

GABA is synthesized through a GABA shunt pathway, which consists of the three enzymes GABA transaminase, glutamate decarboxylase (GAD), and succinic semialdehyde dehydrogenase. GAD activity is primarily responsible for the accumulation of GABA, which contributed to the improvement of chilling tolerance in fruits stored in cold storage (Shang et al., 2011). Through the increase of GAD activity and the regulation of GABA-T activity, exogenous GABA treatment may influence the GABA shunt pathway during cold storage, resulting in GABA accumulation that may help as an adaptive defense mechanism against chilling stress. In addition to participating in the regulation of osmotic balance and enhancing stress tolerance, proline accumulates in plants during chilling stress (Wang et al., 2014). Proline plays a key role in the prevention of chilling injury because higher proline concentrations under chilling stress lead to higher chilling tolerance. Due to increased GAD, pyrroline-5-carboxylate synthetase (P5CS), and ornithine δ-aminotransferase (OAT) activity during storage, proline contents increased in peach fruit during storage. A reduced proline dehydrogenase (PDH) activity is correlated with an increase in proline contents because PDH is the rate-limiting mitochondrial enzyme that catalyzes proline into glutamic acid (Shang et al., 2011). Therefore, treated fruits with higher proline levels and increased GAD activity respond more actively to chilling stress, and their accumulation increases the ability of fruits to improve chilling tolerance during storage.

GABA treatments increased resistance to chilling stress in several fruits, such as peaches (Shang et al., 2011; Yang et al., 2011), bananas (Wang et al., 2014), citrus (Sheng et al., 2017), and pears (Li et al., 2019). It was reported that GABA treatment induced the accumulation of proline contents, activated antioxidant enzymes, and maintained cellular membrane integrity (Malekzadeh et al., 2017). The exogenous application of GABA has similar effects as the endogenous molecule, enabling plants to cope with stress conditions. However, no report is available for the GABA treatment of the chilling injury to papaya fruit. For the first time, the present work provides an innovative insight into the role of exogenous GABA treatment in the regulation of the GABA-shunt pathway by activating proline metabolism and GAD activity in papaya fruit. Therefore, the objectives of this study were to investigate the crucial role of GABA in mediating the resistance mechanism, oxidative stress tolerance, and antioxidant defense system of papaya fruit during low-temperature storage.

2 Materials and methods

2.1 Fruit materials and treatment

Papaya fruit was harvested at the physiologically mature stage from an orchard located in Uthal, Balochistan, Pakistan. After harvest, all fruit were shifted to the laboratory within 1 h. Harvested fruits with uniform size, maturity, color, smooth surface, no disease symptoms or cracks, and free from mechanical damage were selected for the experiment. Based on our preliminary study, GABA was tested at different concentrations; however, 1 mM to 5 mM GABA treatments were found safe and had no adverse effect on papaya. The fruits were divided into three groups of 90 fruits each, and each replicate contained 30 fruits. The first and second groups were immersed in 1 mM and 5 mM GABA solution, respectively, for 5 min. The third group was dipped in distilled water for 5 min and served as a control. Each treatment was replicated three times. All the fruits were then air dried for 1 h and stored at 4°C (80%–90% RH) for 5 weeks. The biochemical observations were measured at 0, 1, 2, 3, 4, and 5 weeks of cold storage. The chilling injury index, internal browning, and electrolyte leakage were determined after 4 h of the sample transferred from cold storage. The flesh tissues of the fruit sample were taken and stored at −80°C (Ultra Low-Temperature Freeze, DW-HL528S, China) for subsequent analysis.

2.2 Measurement of chilling injury and internal brown index

The chilling injury (CI) index was assessed after 4 h of the sample being transferred from cold storage. The chilling injury symptoms were assessed visually on the fruit surface. The chilling injury was measured on each fruit using a five-point scale from 0 to 4: 0 = no symptoms; 1 = trace injury (1%–20%); 2 = slight injury (20%–40%); 3 = moderate injury (40%–60%); and 4 = severe injury (>60%). The chilling injury was estimated using the following formula: CI index = Σ[(CI ranking) × (number of fruit at CI ranking)]/(total number of fruit × highest CI ranking) × 100.

The internal browning (IB) index was measured in the mesocarp area based on the total browning symptoms using the following subjective scale: 0 = no browning; 1 = browning area ranging from 1% to 20%; 2 = browning area ranging from 20% to 40%; 3 = browning area ranging from 40% to 60%; 4 = browning area >60%. The internal browning index was assessed using the following formula: IB index = Σ[(IB ranking) × (number of fruit at IB ranking)]/(total number of fruit × highest IB ranking) × 100.

2.3 Electrolyte leakage

Electrolyte leakage (EL) was determined according to the method of Khaliq et al. (2016) with slight modifications. Using a cork borer with a 10-mm diameter, 15 discs (4 mm thick) of papaya flesh were excised from the middle part of the fruit. The discs were put in 25 mL of deionized water and shaken constantly for 30 min. Electrolyte leakage (L_0) in the solution was assessed using a conductivity meter (BANTE, DDS 12DW, USA). The discs were then placed in a boiling water bath for 15 min. After cooling, the electrolyte leakage (L_1) was remeasured. The results were then estimated using the following formula: EL (%) = (L_0/L_1) × 100.

2.4 Malondialdehyde content

The MDA content was measured according to the method described by Dhindsa et al. (1981). Using a refrigerated centrifuge D3024R, USA, one gram of sample tissue was homogenized with 3 mL of 5% (w/v) trichloroacetic acid before being centrifuged at 12,000×*g* for 20 min at 4°C. Afterwards, 2.5 mL of 0.5% thiobarbituric acid was mixed with the supernatant (1.5 mL). The reaction solution was heated in boiling water for 30 min and then centrifuged at 10,000×*g* for 10 min. The absorbance was measured at 532 nm, 600 nm, and 450 nm using a UV/Vis spectrophotometer (T80, UK). The results were expressed as micromoles per kilogram of fresh weight (FW).

2.5 Determination of hydrogen peroxide

Hydrogen peroxide was determined following the method of Patterson et al. (1984). Two grams of sample tissue was homogenized with 5 mL of ice-cold acetone and centrifuged at 10,000×*g* for 15 min at 4°C. One milliliter of the supernatant was mixed with 0.2 mL of concentrated ammonia and 0.1 mL of 5% titanium sulfate. The peroxide–titanium complex was precipitated. The precipitate was mixed with 4 mL of 2 M sulfuric acid and then centrifuged at 3,000×*g for* 10 *min*. The absorbance was measured at 415 nm. A standard curve was constructed with H_2O_2 at concentrations ranging from 10 µM to 100 µM, and the results were expressed as millimoles per kilogram of FW.

2.6 Endogenous GABA content and GAD activity

The GABA content was measured following the method of Hu et al. (2015). One gram of fruit sample was mixed with 3 mL of 0.05 M lanthanum chloride, and the mixture was centrifuged for 5 min at 12,000×*g* at 4°C. Afterward, the supernatant was added with 200 µL of 2 M potassium hydroxide and again centrifuged for 5 min at 12,000×*g* at 4°C. Consequently, 400 µL of supernatant was mixed with 600 µL of 0.05 M phosphate buffer (pH 10), 5% NaOCl, and 200 µL of 6% concentrated phenol in boiling water for 10 min. Subsequently, 100 µL of 60% alcohol was added to the reaction mixture. The absorbance at 645 nm was monitored using a spectrophotometer. The GABA content was quantified with a standard curve constructed using known amounts of GABA and expressed as milligrams per kilogram of FW.

For GAD enzyme extraction, 2 g of sample tissue was added to 5 mL of extraction Tris-HCl (0.1 M, pH 9.1) buffer containing 10% glycerol, 0.5 mM of pyridoxal phosphate, 1 mM of phenylmethylsulfonyl fluoride, 1 mM of dithiothreitol, and 5 mM of ethylene diamine tetraacetic acid. The mixture was centrifuged at 12,000×*g* for 20 min at 4°C, and the resulting supernatant was used for GAD determination. The activity of the GAD enzyme was assayed according to the method of Deewatthanawong et al. (2010). The enzyme assay contained 0.1 M of potassium phosphate buffer (pH 5.8), 40 µM of pyridoxal phosphate, and 3 mM of L-glutamic acid. The reaction was ended by adding 0.1 mL of 0.5 M hydrochloric acid. GAD activity was expressed as units per gram per hour of fresh weight.

2.7 Proline content

The proline content was determined following the method of Shang et al. (2011). In brief, 1 g of fruit sample was homogenized with 5 mL of 3% (v/v) sulfosalicylic acid and centrifuged at 12,000×*g* for 10 min at 4°C. Two milliliters of the supernatant was added to 3 mL of ninhydrin reagent and 2 mL of glacial acetic acid and boiled at 100° C for 1 h. After cooling, 4 mL of toluene was added to the reaction mixture. The absorbance was recorded at 520 nm. A standard curve was constructed using a known concentration of proline, and the results were expressed as milligrams per kilogram of FW.

2.8 Extraction and assays of antioxidant enzyme

For enzyme extraction, 5 g of flesh samples was homogenized in 10 mL of ice-cold extraction sodium phosphate buffer (100 mM, pH 7.5) containing 2% PVPP and 1 mM ethylene diamine tetraacetic acid. The mixture was centrifuged at 12,000×*g* for 20 min at 4°C, and the resulting supernatant was used for the enzyme assay.

CAT activity was measured according to the method of Zhang et al. (2013). CAT activity was expressed as units per gram per minute. GR activity was analyzed following the method of Ding et al. (2007). GR activity was expressed as units per gram per minute. APX activity was determined following the method of Zhang et al. (2013). APX activity was expressed as units per gram per minute. Superoxide dismutase (SOD) activity was analyzed according to the method of Zhang et al. (2013). SOD activity was expressed as units per gram per hour.

2.9 PAL and PPO activity

PAL activity was assayed following the method of Nguyen et al. (2003). Five grams of sample tissue from the pulp was homogenized in 10 mL of sodium borate buffer (100 mM, pH 8.8) containing 1% PVPP and 5 mM β-mercaptoethanol. The homogenate was centrifuged at 13,000×*g* for 20 min at 4°C, and the resulting supernatants were collected for the enzyme assay. PAL activity was expressed as units per gram per minute. PPO activity was assayed following the protocol of Nguyen et al. (2003). Five-gram sample tissue was mixed with 10 mL of phosphate buffer (100 mM, pH 7.8) and 1% PVPP. The mixture was then centrifuged at 13,000×*g* for 20 min at 4°C. The supernatant was used for the PPO enzyme assay. PPO activity was expressed as units per gram per minute.

2.10 PLD and LOX enzyme activity

The activities of PLD and LOX enzymes were measured in accordance with the procedure outlined by Aghdam et al. (2016). One unit of PLD was defined as the quantity of enzyme required to catalyze the synthesis of 1 nmol D-nitrophenol h^{-1}. One unit of LOX was defined as the amount of enzyme that induced an increase in absorption of 0.01 min^{-1} at 234 nm.

2.11 Measurement of total phenolics and antioxidant activity

Total phenolic contents were estimated following the Folin-Ciocalteu reagent method as described by Farina et al. (2020). The content of total phenols was expressed in terms of grams of gallic acid equivalents per kilogram of sample fresh weight, using gallic acid as a standard. The free radical 2,2-diphenyl-1-picrylhydrazyl (DPPH) scavenging method was assessed to quantify the total antioxidant activity according to Rastegar et al. (2020). DPPH scavenging activity was expressed as a percent.

2.12 Statistical analysis

A two-level factorial completely randomized design (CRD) with three replications was used in this study. Using SAS software, data on the effects of GABA treatment on the biochemical and physiological characteristics of papaya fruit were analyzed. The Fisher's least significant differences (LSD) test was used for *post-hoc* analysis. All model parameters were tested at $p < 0.05$ for significance level.

3 Results

3.1 Chilling injury and internal browning

The chilling injury index of papaya increased after 2 weeks of storage in both GABA-treated and control fruit. However, this increasing trend was postponed when fruit was subjected to GABA treatment. The chilling injury index was significantly reduced in papaya fruit treated with 1 mM or 5 mM GABA compared to the control (Figure 1A). The most effective result was observed in fruit at a concentration of 5 mM GABA treatment. The internal browning appeared after 2 weeks of storage, and afterward, it continuously increased in both control and GABA-treated fruit over the rest of the storage period (Figure 1B). The exogenous application of GABA treatment efficiently inhibited the development of internal browning, which is a typical chilling injury symptom in papaya fruit. GABA treatments not only resulted in a lower chilling injury from 2 to 5 weeks but also inhibited the increase in internal browning during the whole storage period compared to the control fruit (Figure 2).

3.2 Electrolyte leakage

Cell membrane integrity can be measured by electrolyte leakage. Electrolyte leakage increased over the entire storage period, irrespective of the GABA treatments (Figure 1C). After 5 weeks of storage, electrolyte leakage in papaya fruit treated with 1 mM or 5 mM GABA was 29% and 52% lower, respectively, than the control fruit.

3.2 MDA content

The increased production of MDA reflects oxidative deterioration and damage to cell membranes. The amount of MDA increased with increasing the storage period. However, the exogenous application of GABA led to a reduction of lipid peroxidation (Figure 1D). The lowest level of MDA was observed in fruit treated with 5 mM GABA during the entire storage period.

3.4 Hydrogen peroxide

Chilling injury is an oxidative physiological disorder that induces a significant production of ROS, including hydrogen peroxide, and this leads to lipid peroxidation. Excess production of H_2O_2 involves substantial damage to cell membrane stability. Lipid peroxidation caused by ROS generation is revealed by the deterioration of the cell membrane. The control fruit's H_2O_2 level was significantly higher than that of the GABA-treated fruit (Figure 3A). After being stored for 5 weeks, papaya fruit treated

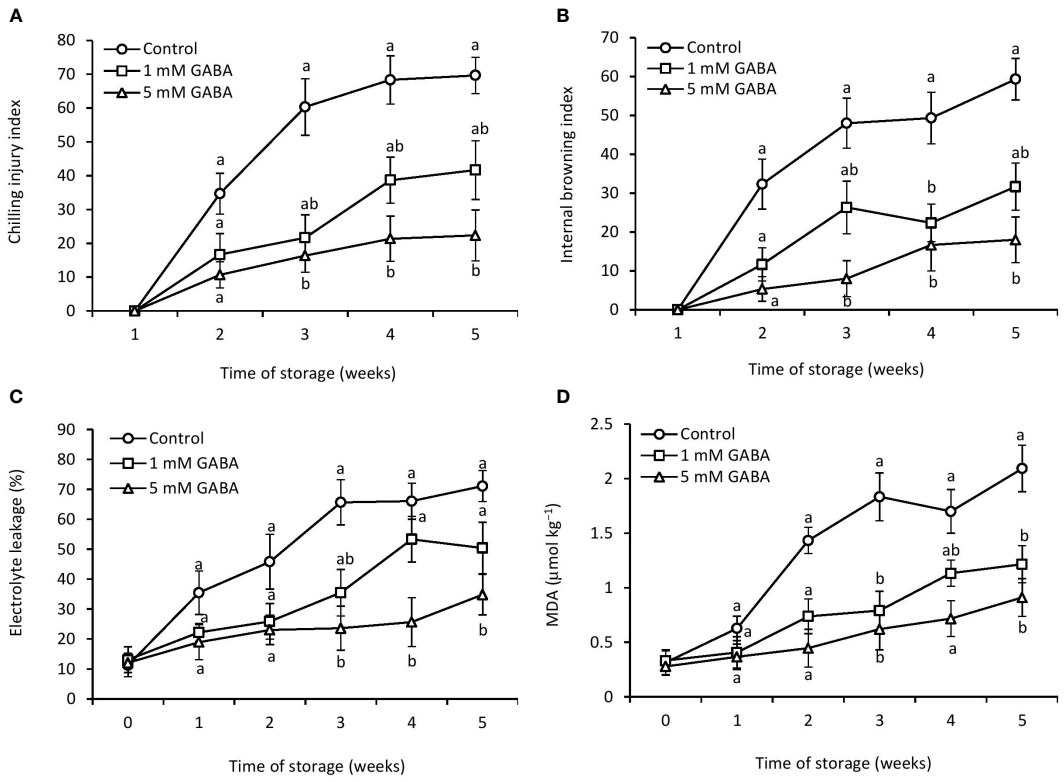

FIGURE 1
Chilling injury **(A)**, internal browning **(B)**, electrolyte leakage **(C)**, and MDA **(D)** of papaya fruit treated with GABA during storage at 4°C for 5 weeks. Vertical bars represent the standard error of the means for three replicates. Means with different letters show significant differences.

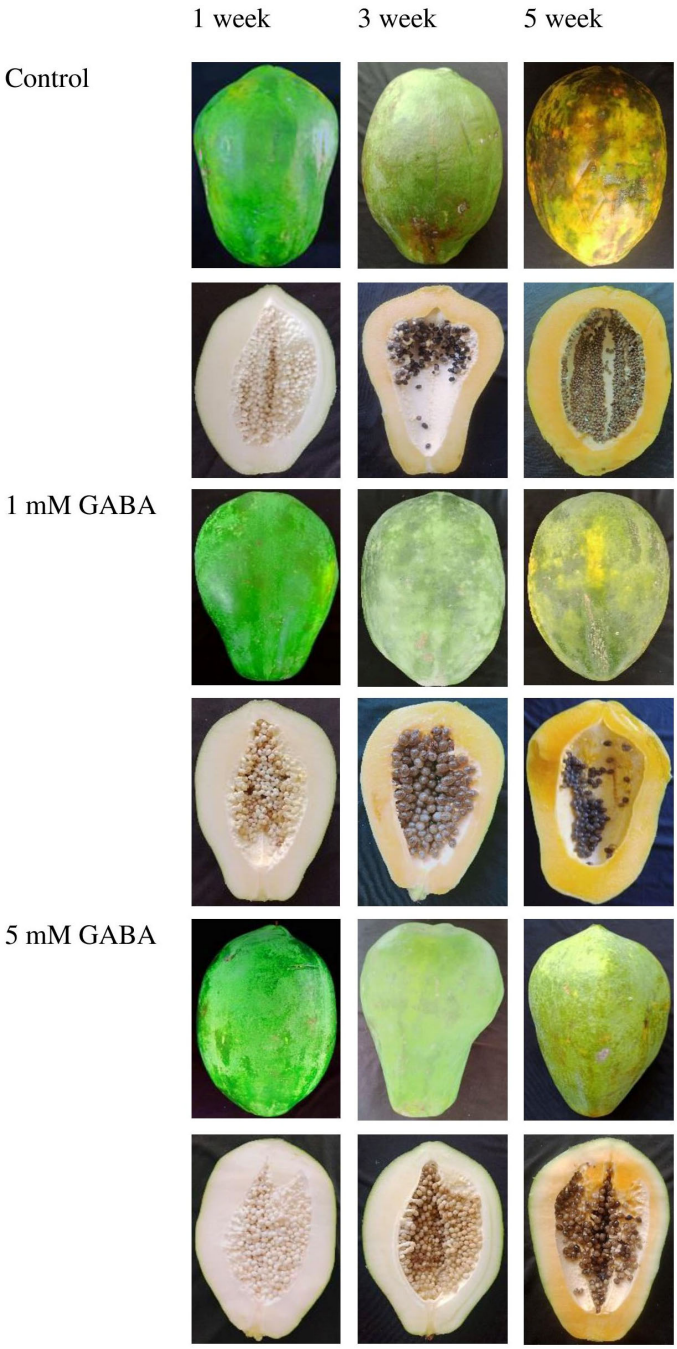

FIGURE 2
Peel and pulp appearance of papaya fruit treated with GABA during storage at 4°C for 1, 3, and 5 weeks.

with 1 mM or 5 mM GABA had H_2O_2 levels that were 46% and 67% lower, respectively, than those in the control fruit.

3.5 GABA content and GAD activity

Throughout the whole storage period, the amount of endogenous GABA in the control and fruit treated with 1 mM or 5 mM GABA gradually increased. After 5 weeks of storage, the GABA-treated fruit had considerably more GABA than the control fruit (Figure 3B). The control fruit showed the lowest endogenous GABA content throughout the storage time. In contrast, the endogenous GABA content of papaya fruit treated with 1 mM or 5 mM GABA was 44% and 48% higher, respectively, than that of the control group after 5 weeks of storage. Exogenous application of GABA treatment potentially affected GAD enzyme activity. Initially, the activity of the GAD enzyme increased from the first week to the third week in both treated and untreated fruit and then declined until the end of cold storage (Figure 3C). However, for the entire storage period, papaya fruit treated with 1 mM or 5 mM

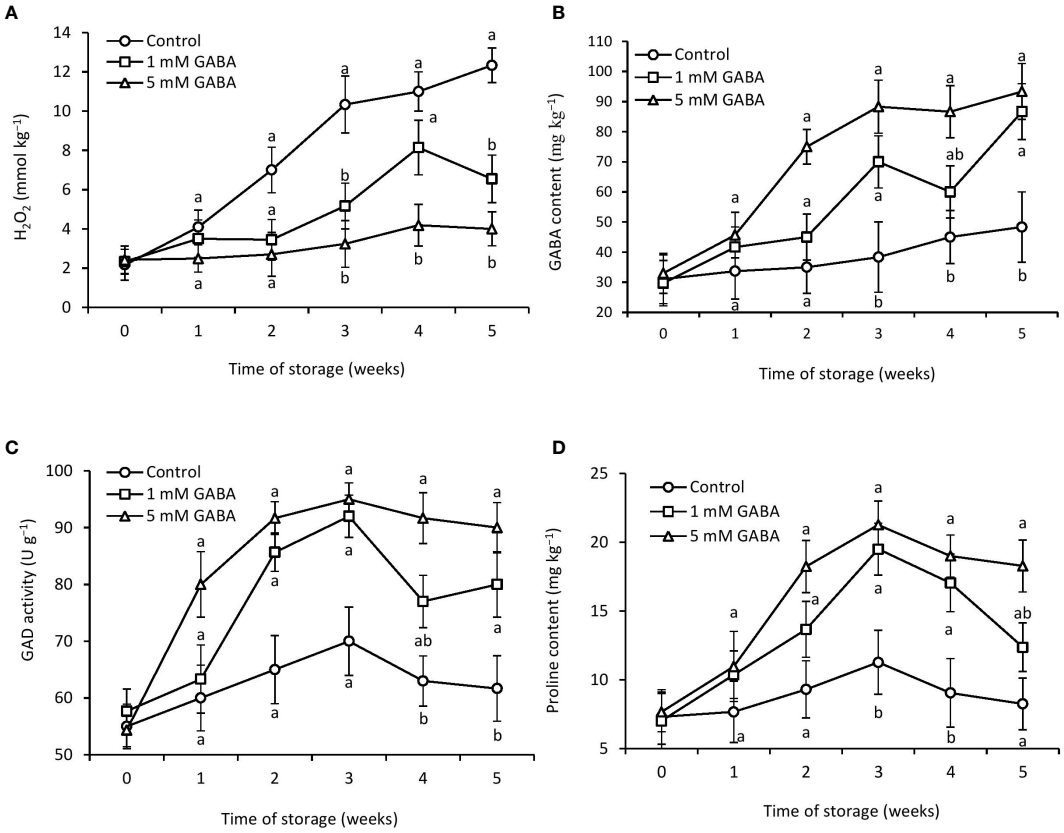

FIGURE 3
H_2O_2 **(A)**, GABA content **(B)**, GAD activity **(D)**, and proline content **(C)** in papaya fruit treated with GABA during storage at 4°C for 5 weeks. Vertical bars represent the standard error of the means for three replicates. Means with different letters show significant differences.

GABA significantly maintained higher GAD activity compared to control fruit.

3.6 Proline content

Proline content of treated and untreated fruit increased until the first 3 weeks of storage and then declined. The proline content was 34% and 54% higher in fruit subjected to 1 mM or 5 mM GABA, respectively, than the control after storage for 5 weeks (Figure 3D).

3.7 Antioxidant enzyme activities

Both treated and untreated papaya fruit initially had higher CAT activity during the first 2 weeks, which then steadily decreased until the end of the storage period (Figure 4A). However, this declining rate was more obvious in the control fruit. Papaya fruit treated with 1 mM or 5 mM GABA substantially maintains a high level of CAT activity. GR plays a key role against ROS in the defense system and actively takes part in the ascorbate-glutathione (ASH-GSH) cycle. The results showed that GR activity was positively affected by GABA treatment (Figure 4B). Firstly, GR activity increased in all papaya fruit, reached its peak after 2 weeks of storage, and then progressively declined during the rest of the storage period. GR activity in papaya fruit treated with 1 mM or 5 mM GABA was 32% and 64% higher, respectively, than the control fruit at 5 weeks of storage period.

In both GABA-treated and control fruit, APX activity increased during the first 2 weeks, then dropped until the end of the storage period (Figure 4C). However, this decreasing rate was more prominent in the control fruit. Papaya fruit treated with 1 mM or 5 mM GABA enhanced APX activity more than that in the control fruit. SOD is considered one of the most important defense-related enzymes and crucial for the detoxification of ROS during stress conditions. Exogenous application of GABA treatment (1 mM or 5 mM) maintained a higher level of SOD activity than that in the control fruit over the entire storage period (Figure 4D).

3.8 PAL and PPO activity

Up to 3 weeks of storage, PAL activity in the GABA-treated and control fruit increased gradually; thereafter, it dropped until the end of the storage period (Figure 5A). Compared with the control fruit, papaya fruit treated with 1 mM or 5 mM GABA triggered PAL activity during the whole storage time. PPO activity gradually increased over the course of 4 weeks in both the GABA-treated and control groups (Figure 5B). After that, it slightly declined in control and fruit treated with 1 mM GABA. The PPO activity of

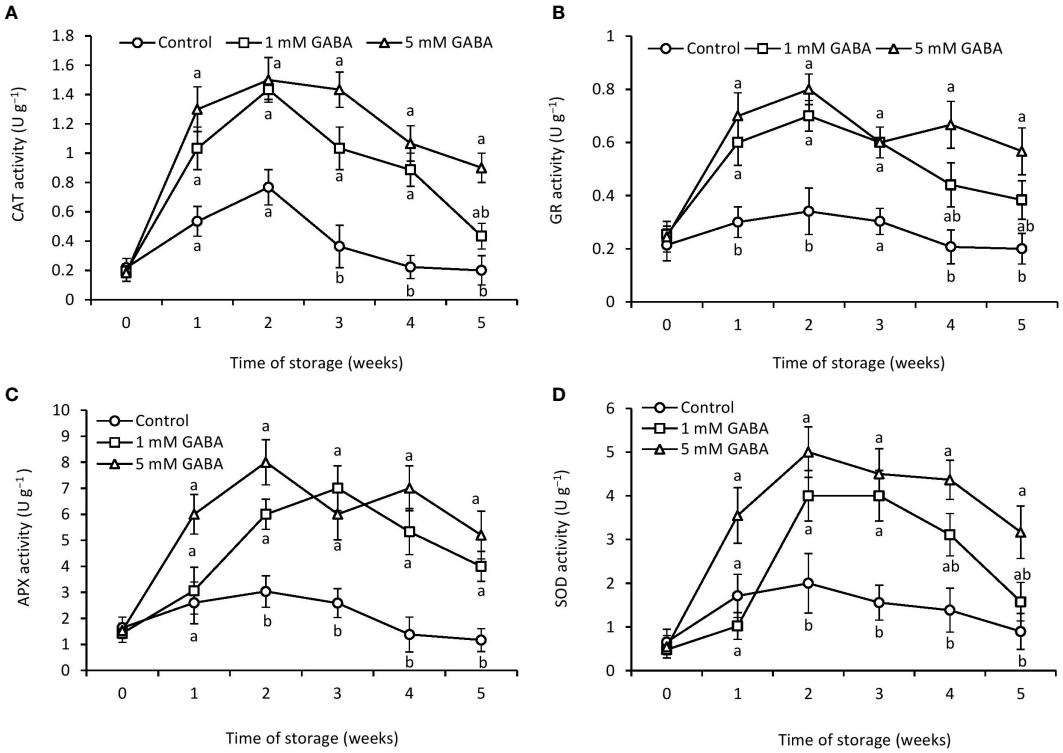

FIGURE 4
Activities of CAT **(A)**, GR **(B)**, APX **(C)**, and SOD **(D)** in papaya fruit treated with GABA during storage at 4°C for 5 weeks. Vertical bars represent the standard error of the means for three replicates. Means with different letters show significant differences.

papaya fruit treated with 1 mM or 5 mM GABA was 21% and 50% lower, respectively, than that of the control group after 5 weeks of storage, which indicated that GABA could limit PPO activity during storage.

3.9 PLD and LOX enzyme activity

PLD activity increased with an increase in the storage period. However, papaya fruit treated with GABA reduced the PLD activity (Figure 5C). For the whole storage period, fruit exposed to 5 mM GABA showed the lowest level of PLD activity. After being stored for 5 weeks, papaya fruit treated with 1 mM or 5 mM GABA may have reduced the LOX activity compared to the control fruit (Figure 5D), which demonstrates that GABA may be able to restrict LOX activity during storage.

3.10 Total phenolics and antioxidant activity

Over the first 3 weeks of storage, phenolic contents steadily increased in all papaya fruit but thereafter decreased (Figure 6A). However, over the entire storage period, the GABA treatment (1 mM or 5 mM) preserved higher levels of total phenolic contents than the control fruit. The DPPH-radical scavenging activity of GABA-treated fruit reached its peak after 3 weeks of storage and then steadily decreased (Figure 6B). However, the highest DPPH activity peak was observed in the control fruit after 2 weeks of storage. The DPPH activity was 26% and 67% higher in fruit exposed to 1 mM or 5 mM GABA, respectively, than the control after storage for 5 weeks.

4 Discussion

The present results indicated that GABA treatments (1 mM or 5 mM) improved the chilling tolerance of papaya fruit during low-temperature storage. The symptoms of chilling injury on the fruit surface and internal browning were clearly inhibited in treated papaya fruit. Similar evidence has been observed in other fruits treated with GABA, such as peach (Shang et al., 2011), banana (Wang et al., 2014), and cucumber (Malekzadeh et al., 2017). The correlation between chilling injury and defense system-related indices of papaya fruit was performed using Pearson correlation analysis. In this study, proline and DPPH were positively correlated with chilling injuries. However, a negative correlation was observed between chilling injury and GABA, GAD, CAT, GR, APX, SOD, and phenolics (Table 1). Exogenous application of GABA enhanced tolerance to chilling stress and improved the GABA shunt pathways in many fruits (Ramos-Ruiz et al., 2019). The cell membrane is the first line of defense to protect the cell during stress. The primary event that happens during chilling stress is the destruction of the plasma membrane (Mditshwa et al., 2023). When chilling-sensitive

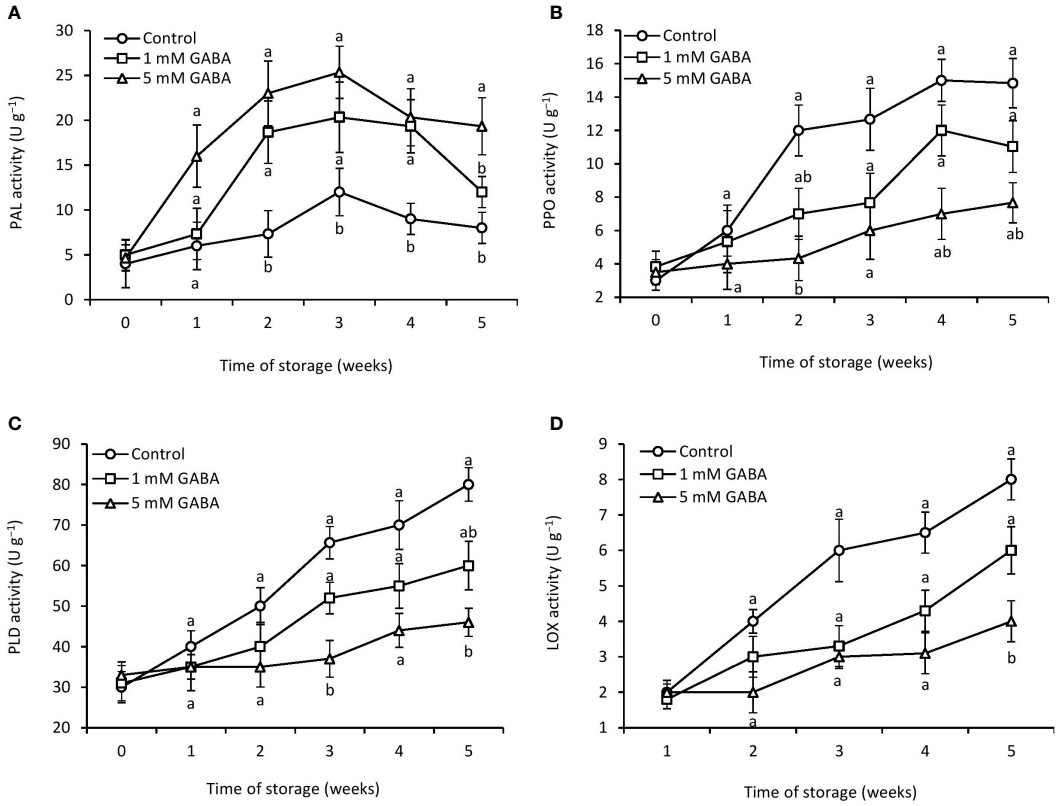

FIGURE 5
Activities of PAL **(A)**, PPO **(B)**, PLD **(C)**, and LOX **(D)** in papaya fruit treated with GABA during storage at 4°C for 5 weeks. Vertical bars represent the standard error of the means for three replicates. Means with different letters show significant differences.

plants are subjected to low-temperature stress, the cell membrane modifies from a flexible structure to a rigid one, and this could cause cracks and leakage of water, ions, and metabolites (Wolfe, 1978). Under cold stress, changes in cell membrane structure have an effect on membrane fluidity and performance (Liang et al., 2020). Electrolyte leakage is used as a parameter for the assessment of cell membrane stability and permeability. Degradation of cell membrane structure occurs by changing the proportion of unsaturated/saturated fatty acids and the increasing level of electrolyte leakage (Marangoni et al., 1996). The involvement of GABA in maintaining cell membrane integrity and fluidity has been widely studied. For example, GABA treatments improved cold tolerance in blood orange and pear fruits by protecting cell membrane structure (Habibi et al., 2019; Li et al., 2019). GABA treatment may inhibit electrolyte leakage and subsequently maintain cell membrane integrity in treated papaya fruit.

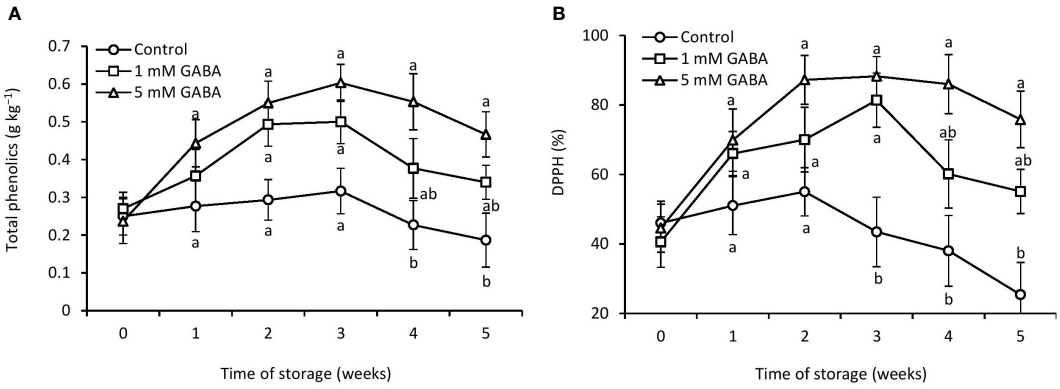

FIGURE 6
Total phenolics **(A)** and DPPH **(B)** in papaya fruit treated with GABA during storage at 4°C for 5 weeks. Vertical bars represent the standard error of the means for three replicates. Means with different letters show significant differences.

TABLE 1 Pearson correlation coefficients between chilling injury and defense system-related indices of papaya fruit during storage.

	GABA	GAD	Proline	CAT	GR	APX	SOD	PAL	Phenolic	DPPH	CI
GABA	–										
GAD	0.48	–									
Proline	0.55	0.68	–								
CAT	0.85	0.54	0.73	–							
GR	0.91	0.61	0.75	0.95	–						
APX	0.92	0.54	0.77	0.73	0.69	–					
SOD	0.39	0.72	0.87	0.89	0.86	0.72	–				
PAL	0.60	0.65	0.89	0.70	0.62	0.69	0.74	–			
Phenolic	0.92	0.82	0.89	0.90	0.91	0.72	0.93	0.67	–		
DPPH	−0.19	−0.08	−0.05	−0.10	−0.09	−0.01	0.06	−0.13	−0.15	–	
CI	−0.41	−0.02	0.01	−0.32	−0.35	−0.08	−0.11	−0.23	−0.28	0.56	–

GABA, γ-aminobutyric acid; GAD, glutamate decarboxylase; CAT, catalase; GR, glutathione reductase; APX, ascorbate peroxidase; SOD, superoxide dismutase; PAL, phenylalanine ammonia lyase; DPPH, 2-diphenyl-1-picrylhydrazyl; CI, chilling injury. $p < 0.01$.

MDA is a byproduct of lipid peroxidation and a stress marker for oxidative cell damage. Peroxidation of cell membrane lipids is one of the primary biochemical signs of chilling injury, and increased MDA generation is a sign that the cell membrane has been damaged (Khaliq, 2015; Ramos-Ruiz et al., 2019). The degradation of lipids and peroxidation of unsaturated fatty acids are the major reasons for membrane breakdown. MDA is the final product of peroxidation that determines membrane deterioration and oxidative damage in response to stress. The main causes of membrane breakdown are lipid degradation and unsaturated fatty acid peroxidation. MDA is responsible for oxidative damage and membrane degradation in response to stress. Evidence has shown that the increased accumulation of MDA and ion leakage is closely associated with chilling stress in plants (Ding et al., 2007). An increase in ion leakage and MDA has been observed in many fruits and vegetables suffering from chilling injury (Valenzuela et al., 2017). Recent studies have revealed that elicitors like nitric oxide, melatonin, and methyl jasmonate inhibited the occurrence of chilling injury and regulated stress responses in various horticultural crops, including banana (Wang et al., 2016), sapota (Mirshekari et al., 2020), and pomegranate (Chen et al., 2021). The same behavior has been found in cornelian cherry fruit, where GABA treatment postponed MDA accumulation and electrolyte leakage (Rabiei et al., 2019). These results indicated that ion leakage and lipid peroxidation intensified the manifestation of chilling injury in control fruit. However, papaya fruit treated with GABA may lessen membrane lipid breakdown and solute leakage, improving the fruit's ability to adapt to low-temperature stress.

Both regular cell metabolism and numerous biotic and abiotic stress conditions result in the production of ROS (Hilal et al., 2023). ROS plays a dual role as both beneficial and harmful, depending on their concentration in plant cells. Low concentrations of ROS function as a secondary messenger in signaling transduction pathways that mediate numerous physiological responses in plants (Apel and Hirt, 2004). However, the disproportionate production of ROS during stress can perturb cell homeostasis and even lead to cell death (Aghdam et al., 2016). Therefore, it is necessary to maintain balanced levels of ROS within a certain range to ensure normal cell metabolism. During chilling stress, overproduction of ROS causes oxidative damage to chloroplasts, mitochondria, and apoplast and decreases the activities of antioxidant enzymes, thus destroying the membrane system, causing metabolic disorders, and ultimately leading to cell lysis (Blokhina et al., 2003). Several evidences have shown that chilling injury in fruits can be partly attributed to the imbalance production of ROS during stress. Chilling stress increases ROS levels that stimulate lipid peroxidation and eventually result in the destruction of cell membranes (Mohammadrezakhani et al., 2019). ROS increases the peroxidation of membrane lipids and oxidative damage by producing hydroxyl radicals (Malekzadeh et al., 2017). GABA treatment decreased the accumulation of H_2O_2 and enhanced the cold adaptation mechanism in blood orange, pear, and anthurium cut flowers (Habibi et al., 2019; Li et al., 2019; Mahjoory et al., 2019). In the present experiment, the trend of H_2O_2 was similar to the results of Rabiei et al. (2019), where cornelian cherry fruit was treated with GABA. These results demonstrated that GABA treatment apparently delayed H_2O_2 in treated fruit. Hence, the results suggest that GABA may scavenge H_2O_2 and other ROS, resulting in less oxidative damage in treated papaya fruit.

In response to biotic and abiotic stresses, plants' endogenous GABA content was found to increase. The biosynthetic pathways of GABA were improved through the exogenous GABA shunt by the provision of carbon skeletons and energy (Ramos-Ruiz et al., 2019). GABA plays a crucial part in several pathways by controlling the generation of ROS, increasing energy status, and enhancing the activities of antioxidant enzymes against stresses (Li et al., 2019). The cytosolic enzyme GAD is mainly responsible for the biosynthesis of endogenous GABA (Sheng et al., 2017). Several studies reported that endogenous GABA accumulation increased in fruits treated with GABA, like cucumber and pear (Malekzadeh et al., 2017; Li et al., 2019). Papaya fruit improves low-temperature

tolerance by enhancing the activities of energy metabolism-related enzymes like GAD (Pan et al., 2019). The GAD enzyme was increased in peach and banana fruits by improving the endogenous GABA content (Shang et al., 2011; Ali et al., 2022). Aghdam et al. (2016) reported that the GABA shunt pathway might be a potent mechanism for enhancing chilling tolerance in fresh produce. In this study, the exogenous GABA treatment could be one of the reasons that induced the GABA-shunt pathway by stimulating GAD enzyme activity in treated papaya fruit.

Proline is the main amino acid that is responsible for membrane stabilization, free-radical scavenging activity, and cellular osmotic regulation in plants. Proline plays an important role during stress and positively contributes to stress responses, such as chilling injuries. Mohammadrezakhani et al. (2019) reported that exogenous proline treatment reduced the deleterious effects of oxidative stress in citrus fruit by activating antioxidant enzyme activities. Proline has a strong role in the mediation of chilling tolerance by regulating defense responses. In plants, pyrroline-5-carboxylate synthetase and ornithine δ-aminotransferase enzymes are responsible for the biosynthesis of proline. Peach fruit treated with GABA enhanced proline content due to increased activity of pyrroline-5-carboxylate synthetase and ornithine δ-aminotransferase enzymes (Shang et al., 2011). Elevated proline content under the regulation of proline metabolism may be linked with chilling stress resistance, as reported in oxalic acid-treated mango fruit (Li et al., 2014) and litchi fruit (Liu et al., 2020). The effect of GABA on regulating the proline content has been observed in several fruits stored under low-temperature stress. Proline content was improved in GABA-treated papaya. Therefore, treated fruit indicated a higher chilling tolerance, which could be partly connected with the induced proline content. These results agree with those of Shang et al. (2011) and Wang et al. (2014), who reported a higher content of proline in peach and banana fruits treated with GABA.

Plant cells contain an enzymatic defense system against the overproduction of ROS during biotic and abiotic stresses (Blokhina et al., 2003). The antioxidant enzymes, e.g. CAT, APX, GR, and SOD are the primary constituents of the defense system that protect fruits against ROS (Apel and Hirt, 2004). Generally, when fruits are exposed to chilling stress, the activities of antioxidant enzymes, including CAT, GR, APX, and SOD, may be induced. Antioxidant enzymes actively participate in the defense mechanism. GR and APX are the key components of the ascorbate-glutathione cycle and play a crucial role in scavenging ROS (Yang et al., 2011). Catalase is an essential antioxidant enzyme for scavenging ROS during stress. CAT is the main part of a defense system that directly dismutases H_2O_2 into water and oxygen (Rabiei et al., 2019). SOD plays a protective role and detoxifies free radicals during stress. SOD catalyzes the superoxide anion to H_2O_2, and that H_2O_2 can be scavenged by APX or CAT. Generally, under low-temperature stress, the increased activities of antioxidant enzymes are correlated with chilling tolerance. The higher activity of antioxidant enzymes in mango, peach, and papaya fruits was positively related to the acquisition of chilling tolerance (Ding et al., 2007; Yang et al., 2011; Shadmani et al., 2015). It was reported that GABA has an essential role in reducing biotic and abiotic stress, regulating metabolic processes, and increasing chilling tolerance (Aghdam et al., 2016). It was known that endogenous GABA concentrations quickly accumulated in response to chilling stress in peach, citrus, and sapota fruits, and the increased level of GABA was involved in cold adaptation mechanisms (Shang et al., 2011; Mohammadrezakhani et al., 2019; Mirshekari et al., 2020). These findings support the idea of Malekzadeh et al. (2017), who found that cucumbers treated with GABA increased resistance to chilling stress by stimulating the activities of antioxidant enzymes. These results can be clarified by the evidence that GABA treatment could enhance the antioxidant enzyme activities, which in turn could scavenge the excess production of ROS and thus protect the papaya fruit from oxidative damage.

PAL is considered a biochemical marker that induces resistance mechanisms in fruits and vegetables during low-temperature stress. PAL activity is increased in response to low-temperature stress in orange fruit (Habibi et al., 2019). PAL is the major enzyme responsible for the biosynthesis of phenols (Nguyen et al., 2003). PAL activity is positively correlated with the phenylpropanoid pathway (Sun et al., 2020). The phenylpropanoid pathway has been involved in the production of phenols such as lignin, hydroxycinnamic acids, flavonoids, isoflavonoids, and coumarins (Anthony et al., 2023). These phenolic metabolites are implicated in the defense system and antioxidant activity. In this study, the stimulation of PAL activity through the application of GABA treatment could be associated with the increased production of metabolites that would help increase chilling tolerance in papaya fruit. PPO is the main enzyme responsible for the flesh and peel browning of fruits and vegetables. Peeling and flesh browning are the prominent symptoms of chilling injury during storage at low temperatures. The major cause of fruit and vegetable browning is the oxidation of phenol by the PPO (Nguyen et al., 2003). Under stress conditions, the PPO enzyme oxidizes monophenol to diphenol and again oxidizes diphenol to quinones, and these react with proteins or amino acids, which results in brown pigmentation (Valenzuela et al., 2017). The increased activity of PPO is closely linked to the advanced chilling injury symptoms in pomegranate stored at low-temperature stress (Chen et al., 2021). It has been reported that exogenous GABA treatments reduced the PPO activity in blood orange (Habibi et al., 2019). The reduced activity of PPO in papaya fruit treated with GABA indicates that it is connected to a low incidence of chilling injury.

During senescence and stress, the activity of PLD increases, which causes membrane breakdown. PLD initiates the hydrolysis of lipids under salt and chilling stresses (Mirshekari et al., 2020). A lipolytic cascade causes membrane damage as PLD and LOX are critical for the breakdown of phospholipids (Bargmann et al., 2009). LOX plays an essential role in the oxidative breakdown of membrane lipids. LOX activity enhances lipid unsaturation and membrane fluidity (Malekzadeh et al., 2017). The stimulation of PLD and LOX results in irreparable membrane destruction and eventually the manifestation of chilling injury (Aghdam et al., 2016). These findings imply that PLD and LOX may contribute to the development of chilling symptoms in papaya fruit. GABA treatments improve chilling tolerance in papaya fruit by reducing

the activity of PLD and LOX enzymes. Thus, it can be inferred that GABA treatment may be an innovative approach to reducing papaya fruit oxidative damage during low-temperature storage due to its reducing effects on PLD and LOX enzyme activity.

Phenolic contents have antioxidant properties and scavenge reactive oxygen species. Phenolic compounds retain the nutritive qualities of fruits and vegetables, for example, flavor, color, bitterness, and astringency (Rastegar et al., 2020). Phenolic compounds present in fruits reveal their physiological role and involvement in antioxidant capacity. The Folin–Ciocalteu method is commonly used for the quantitative investigation of total phenolic content in fruits and vegetables. Phenolic contents in untreated fruit first increased and then decreased with the storage period, although GABA treatments induced the increase in phenolic content. A number of studies showed that postharvest treatments reduced the loss of phenolic content and stimulated antioxidant activity in various fruits during cold storage (Hanif et al., 2020; Khaliq et al., 2021). It was reported that GABA treatment detoxified ROS, triggered DPPH-radical scavenging capacity, and retained the phenolic content of banana fruit (Wang et al., 2014). Similarly, GABA treatment reduced the loss of phenolic content and enhanced DPPH-radical scavenging activity in mango fruit (Rastegar et al., 2020). Phenolic content and DPPH-radical scavenging activity first increased and then declined in papaya fruit during storage (Mendy et al., 2019). There are different kinds of nonenzymatic antioxidant compounds that could contribute to the total antioxidant capacity. However, it is not clear which constituents are mainly responsible for increasing antioxidant activity. In this work, the chilling injury was accompanied by higher flesh browning in the control fruit, which might have happened due to phenol oxidation. GABA treatments can postpone the oxidation of phenolics by preventing the commencement of oxidizing chain reactions. The increased accumulation of phenolics in GABA-treated papaya fruit may enhance antioxidant capacity, consequently inhibiting ROS accumulation and improving chilling tolerance.

5 Conclusions

The present results demonstrated that GABA treatment played a vital role in improving the chilling tolerance of papaya fruit by inducing a defense system and reducing oxidative damage. The exogenous application of GABA treatment reduced lipid peroxidation, ion leakage, H_2O_2, PPO, PLD, and LOX activity. Additionally, the accumulation of proline, endogenous GABA, and total phenolics may be beneficial for maintaining plasma membrane fluidity and integrity. These findings help us better understand the involvement of GABA in the chilling tolerance of papaya stored at low-temperature stress. Therefore, the exogenous GABA treatment is a nontoxic technique to maintain the nutritional value and quality of papaya fruit.

Data availability statement

The raw data supporting the conclusions of this article will be made available by the authors, without undue reservation.

Author contributions

GK and SA: conceptualization and writing—original draft. SE and GA: visualization and writing. YF and JM: formal analysis and data curation. MS and AA: reviewing and editing. All authors contributed to the article and approved the submitted version.

Acknowledgments

The authors would like to thank the Lasbela University of Agriculture, Water and Marine Sciences, Uthal, Pakistan, for providing all the necessary facilities to conduct this research work.

Conflict of interest

The authors declare that the research was conducted in the absence of any commercial or financial relationships that could be construed as a potential conflict of interest.

Publisher's note

References

Aghdam, M. S., Naderi, R., Jannatizadeh, A., Sarcheshmeh, M. A. A., and Babalar, M. (2016). Enhancement of postharvest chilling tolerance of anthurium cut flowers by γ-aminobutyric acid (GABA) treatments. *Scientia Hortic.* 198, 52–60. doi: 10.1016/j.scienta.2015.11.019

Ali, S., Nawaz, A., Naz, S., Ejaz, S., Maqbool, M., Siddiqui, M. H., et al. (2022). Hydrogen sulfide mitigates chilling injury of postharvest banana fruits by regulating γ-aminobutyric acid shunt pathway and ascorbate–glutathione cycle. *Front. Plant Sci.* 13. doi: 10.3389/fpls.2022.941246

Anthony, B. M., Chaparro, J. M., Prenni, J. E., and Minas, I. S. (2023). Carbon sufficiency boosts phenylpropanoid biosynthesis early in peach fruit development priming superior fruit quality. *Plant Physiol. Biochem.* 196, 1019–1031. doi: 10.1016/j.plaphy.2023.02.038

Apel, K., and Hirt, H. (2004). Reactive oxygen species: metabolism, oxidative stress, and signal transduction. *Annu. Rev. Plant Biol.* 55, 373–399. doi: 10.1146/annurev.arplant.55.031903.141701

Bargmann, B. O. R., Laxalt, A. M., Ter Riet, B., Testerink, C., Merquiol, E., Mosblech, A., et al. (2009). Reassessing the role of phospholipase D in the *Arabidopsis* wounding response. *Plant Cell Environ.* 32, 837–850. doi: 10.1111/j.1365-3040.2009.01962

Blokhina, O., Virolainen, E., and Fagerstedt, K. V. (2003). Antioxidants, oxidative damage and oxygen deprivation stress: a review. *Ann. Bot.* 91 (2), 179–194. doi: 10.1093/aob/mcf118

Cao, S., Zheng, Y., Wang, K., Rui, H., and Tang, S. (2010). Effect of methyl jasmonate on cell wall modification of loquat fruit in relation to chilling injury after harvest. *Food Chem.* 118 (3), 641–647. doi: 10.1016/j.foodchem.2009.05.047

Chen, L., Pan, Y., Li, H., Jia, X., Guo, Y., Luo, J., et al. (2021). Methyl jasmonate alleviates chilling injury and keeps intact pericarp structure of pomegranate during low temperature storage. *Food Sci. Technol. Int.* 27 (1), 22–31. doi: 10.1177/1082013220921597

Deewatthanawong, R., Nock, J. F., and Watkins, C. B. (2010). γ-Aminobutyric acid (GABA) accumulation in four strawberry cultivars in response to elevated CO2 storage. *Postharvest Biol. Technol.* 57 (2), 92–96. doi: 10.1016/j.postharvbio.2010.03.003

Dhindsa, R. S., Pulmb-Dhindsa, P., and Thorpe, T. A. (1981). Leaf senescence. Correlated with increased levels of membrane permeability and lipid peroxidation and decreased levels of superoxide dismutase and catalase. *J. Exp. Bot.* 32 (1), 93–101. doi: 10.1093/jxb/32.1.93

Ding, X., Zhu, X., Ye, L., Xiao, S., Wu, Z., Chen, W., et al. (2019). The interaction of CpEBF1 with CpMADSs is involved in cell wall degradation during papaya fruit ripening. *Horticulture Res.* 6 (1), 1–18. doi: 10.1038/s41438-018-0095-1

Ding, Z. S., Tian, S. P., Zheng, X. L., Zhou, Z. W., and Xu, Y. (2007). Responses of reactive oxygen metabolism and quality in mango fruit to exogenous oxalic acid or salicylic acid under chilling temperature stress. *Physiologia Plantarum* 130 (1), 112–121. doi: 10.1111/j.1399-3054.2007.00893

Farina, V., Tinebra, I., Perrone, A., Sortino, G., Palazzolo, E., Mannino, G., et al. (2020). Physicochemical, nutraceutical and sensory traits of six papaya (*Carica papaya* L.) cultivars grown in greenhouse conditions in the Mediterranean climate. *Agronomy* 10 (4), 501. doi: 10.3390/agronomy10040501

Gao, Q., Tan, Q., Song, Z., Chen, W., Li, X., and Zhu, X. (2020). Calcium chloride postharvest treatment delays the ripening and softening of papaya fruit. *J. Food Process. Preserv.* 44 (8), e14604. doi: 10.1111/jfpp.14604

Habibi, F., Ramezanian, A., Rahemi, M., Eshghi, S., Guillén, F., Serrano, M., et al. (2019). Postharvest treatments with γ-aminobutyric acid, methyl jasmonate, or methyl salicylate enhance chilling tolerance of blood orange fruit at prolonged cold storage. *J. Sci. Food Agric.* 99 (14), 6408–6417. doi: 10.1002/jsfa.9920

Hanif, A., Ahmad, S., Shahzad, S., Liaquat, M., and Anwar, R. (2020). Postharvest application of salicylic acid reduced decay and enhanced storage life of papaya fruit during cold storage. *J. Food Measurement Characterization* 14 (6), 3078–3088. doi: 10.1007/s11694-020-00555-5

Hilal, B., Khan, T. A., and Fariduddin, Q. (2023). Recent advances and mechanistic interactions of hydrogen sulfide with plant growth regulators in relation to abiotic stress tolerance in plants. *Plant Physiol. Biochem.* 196, 1065–1083. doi: 10.1016/j.plaphy.2023.03.006

Hu, X., Xu, Z., Xu, W., Li, J., Zhao, N., and Zhou, Y. (2015). Application of γ-aminobutyric acid demonstrates a protective role of polyamine and GABA metabolism in muskmelon seedlings under Ca $(NO_3)_2$ stress. *Plant Physiol. Biochem.* 92, 1–10. doi: 10.1016/j.plaphy.2015.04.006

Jin, P., Duan, Y., Wang, L., Wang, J., and Zheng, Y. (2014). Reducing chilling injury of loquat fruit by combined treatment with hot air and methyl jasmonate. *Food Bioprocess Technol.* 7 (8), 2259–2266. doi: 10.1007/s11947-013-1232-3

Khaliq, G. (2015). *Effects of edible coatings enriched with calcium chloride on physiological, biochemical and quality responses of mango (Mangifera Indica L. cv. Choke Anan) fruit during cold storage* (Serdang, Malaysia: Universiti Putra Malaysia). doi: 10.13140/RG.2.2.33366.60487

Khaliq, G., Mohamed, M. T. M., Ghazali, H. M., Ding, P., and Ali, A. (2016). Influence of gum arabic coating enriched with calcium chloride on physiological, biochemical and quality responses of mango (*Mangifera indica* L.) fruit stored under low temperature stress. *Postharvest Biol. Technol.* 111, 362–369. doi: 10.1016/j.postharvbio.2015.09.029

Khaliq, G., Ullah, M., Memon, S. A., Ali, A., and Rashid, M. (2021). Exogenous nitric oxide reduces postharvest anthracnose disease and maintains quality of custard apple (*Annona squamosa* L.) fruit during ripening. *J. Food Measurement Characterization* 15 (1), 707–716. doi: 10.1007/s11694-020-00658-z

Li, J., Zhou, X., Wei, B., Cheng, S., Zhou, Q., and Ji, S. (2019). GABA application improves the mitochondrial antioxidant system and reduces peel browning in 'Nanguo'pears after removal from cold storage. *Food Chem.* 297, 124903. doi: 10.1016/j.foodchem.2019.05.177

Li, P., Zheng, X., Liu, Y., and Zhu, Y. (2014). Pre-storage application of oxalic acid alleviates chilling injury in mango fruit by modulating proline metabolism and energy status under chilling stress. *Food Chem.* 142, 72–78. doi: 10.1016/j.foodchem.2013.06.132

Liang, S. M., Kuang, J. F., Ji, S. J., Chen, Q. F., Deng, W., Min, T., et al. (2020). The membrane lipid metabolism in horticultural products suffering chilling injury. *Food Qual. Saf.* 4 (1), 9–14. doi: 10.1093/fqsafe/fyaa001

Liu, G., Zhang, Y., Yun, Z., Hu, M., Liu, J., Jiang, Y., et al. (2020). Melatonin enhances cold tolerance by regulating energy and proline metabolism in litchi fruit. *Foods* 9 (4), 454. doi: 10.3390/foods9040454

Luo, M., Sun, H., Ge, W., Sun, Y., Zhou, X., Zhou, Q., et al. (2022). Effect of glycine betaine treatment on aroma production of 'Nanguo'Pears after long-term cold storage–possible involvement of ethylene synthesis and signal transduction pathways. *Food Bioprocess Technol.* 15 (6), 1327–1342. doi: 10.1007/s11947-022-02813-4

Mahjoory, F., Ebrahimzadeh, A., Hassanpouraghdam, M. B., and Aazami Mavaloo, M. A. (2019). Postharvest GABA application effects on some biochemical characteristics of Anthurium cut flowers under cold storage conditions. *J. Ornamental Plants* 9 (2), 115–127.

Malekzadeh, P., Khosravi-Nejad, F., Hatamnia, A. A., and Mehr, R. S. (2017). Impact of postharvest exogenous γ-aminobutyric acid treatment on cucumber fruit in response to chilling tolerance. *Physiol. Mol. Biol. Plants* 23 (4), 827–836. doi: 10.1007/s12298-017-0475-2

Marangoni, A. G., Palma, T., and Stanley, D. W. (1996). Membrane effects in postharvest physiology. *Postharvest Biol. Technol.* 7 (3), 193–217. doi: 10.1016/0925-5214(95)00042-9

Mditshwa, A., Khaliq, G., Hussein, Z., and Ejaz, S. (2023). Sustainable postharvest management practices for fresh produce. *Front. Sustain. Food Syst.* 7, 1143759. doi: 10.3389/fsufs.2023.1143759

Mendy, T. K., Misran, A., Mahmud, T. M. M., and Ismail, S. I. (2019). Application of *Aloe vera* coating delays ripening and extend the shelf life of papaya fruit. *Scientia Hortic.* 246, 769–776. doi: 10.1016/j.scienta.2018.11.054

Mirshekari, A., Madani, B., Yahia, E. M., Golding, J. B., and Vand, S. H. (2020). Postharvest melatonin treatment reduces chilling injury in sapota fruit. *J. Sci. Food Agric.* 100 (5), 1897–1903. doi: 10.1002/jsfa.10198

Mohammadrezakhani, M., Hajilou, J., Rezanejad, F., and Zaare-Nahandi, F. (2019). Assessment of exogenous application of proline on antioxidant compounds in three Citrus species under low temperature stress. *J. Plant Interact.* 14 (1), 347–358. doi: 10.1080/17429145.2019.1629033

Nguyen, T. B. T., Ketsa, S., and Van Doorn, W. G. (2003). Relationship between browning and the activities of polyphenoloxidase and phenylalanine ammonia lyase in banana peel during low temperature storage. *Postharvest Biol. Technol.* 30 (2), 187–193. doi: 10.1016/S0925-5214(03)00103-0

Pan, Y., Zhang, S., Yuan, M., Song, H., Wang, T., Zhang, W., et al. (2019). Effect of glycine betaine on chilling injury in relation to energy metabolism in papaya fruit during cold storage. *Food Sci. Nutr.* 7 (3), 1123–1130. doi: 10.1002/fsn3.957

Parven, A., Sarker, M. R., Megharaj, M., and Meftaul, I. M. (2020). Prolonging the shelf life of papaya (*Carica papaya* L.) using *Aloe vera* gel at ambient temperature. *Scientia Hortic.* 265, 109228. doi: 10.1016/j.scienta.2020.109228

Patterson, B. D., MacRae, E. A., and Ferguson, I. B. (1984). Estimation of hydrogen peroxide in plant extracts using titanium (IV). *Anal. Biochem.* 139 (2), 487–492. doi: 10.1016/0003-2697(84)90039-3

Rabiei, V., Kakavand, F., Zaare-Nahandi, F., Razavi, F., and Aghdam, M. S. (2019). Nitric oxide and γ-aminobutyric acid treatments delay senescence of cornelian cherry fruits during postharvest cold storage by enhancing antioxidant system activity. *Scientia Hortic.* 243, 268–273. doi: 10.1016/j.scienta.2018.08.034

Ramos-Ruiz, R., Martinez, F., and Knauf-Beiter, G. (2019). The effects of GABA in plants. *Cogent Food Agric.* 5 (1), 1670553. doi: 10.1080/23311932.2019.1670553

Rastegar, S., Khankahdani, H. H., and Rahimzadeh, M. (2020). Effect of γ-aminobutyric acid on the antioxidant system and biochemical changes of mango fruit during storage. *J. Food Measurement Characterization* 14 (2), 778–789. doi: 10.1007/s11694-019-00326-x

Shadmani, N., Ahmad, S. H., Saari, N., Ding, P., and Tajidin, N. E. (2015). Chilling injury incidence and antioxidant enzyme activities of *Carica papaya* L.'Frangi'as influenced by postharvest hot water treatment and storage temperature. *Postharvest Biol. Technol.* 99, 114–119. doi: 10.1016/j.postharvbio.2014.08.004

Shang, H., Cao, S., Yang, Z., Cai, Y., and Zheng, Y. (2011). Effect of exogenous γ-aminobutyric acid treatment on proline accumulation and chilling injury in peach fruit after long-term cold storage. *J. Agric. Food Chem.* 59 (4), 1264–1268. doi: 10.1021/jf104424z

Sheng, L., Shen, D., Luo, Y., Sun, X., Wang, J., Luo, T., et al. (2017). Exogenous γ-aminobutyric acid treatment affects citrate and amino acid accumulation to improve fruit quality and storage performance of postharvest citrus fruit. *Food Chemistry 216*, 138–145. doi: 10.1016/j.foodchem.2016.08.024

Sun, Y., Asghari, M., and Zahedipour-Sheshgelani, P. (2020). Foliar spray with 24-epibrassinolide enhanced strawberry fruit quality, phytochemical content, and postharvest life. *J. Plant Growth Regul.* 39 (2), 920–929. doi: 10.1007/s00344-019-10033-y

Valenzuela, J. L., Manzano, S., Palma, F., Carvajal, F., Garrido, D., and Jamilena, M. (2017). Oxidative stress associated with chilling injury in immature fruit: postharvest technological and biotechnological solutions. *Int. J. Mol. Sci.* 18 (7), 1467. doi: 10.3390/ijms18071467

Wang, Y., Luo, Z., Huang, X., Yang, K., Gao, S., and Du, R. (2014). Effect of exogenous γ-aminobutyric acid (GABA) treatment on chilling injury and antioxidant capacity in banana peel. *Scientia Hortic.* 168, 132–137. doi: 10.1016/j.scienta.2014.01.022

Wang, Y., Luo, Z., Mao, L., and Ying, T. (2016). Contribution of polyamines metabolism and GABA shunt to chilling tolerance induced by nitric oxide in cold-stored banana fruit. *Food Chem.* 197, 333–339. doi: 10.1016/j.foodchem.2015.10.118

Wolfe, J. O. E. (1978). Chilling injury in plants—the role of membrane lipid fluidity. *Plant Cell Environ.* 1 (4), 241–247. doi: 10.1111/j.1365-3040.1978.tb02036.x

Wu, Q., Li, Z., Chen, X., Yun, Z., Li, T., and Jiang, Y. (2019). Comparative metabolites profiling of harvested papaya (*Carica papaya* L.) peel in response to chilling stress. *J. Sci. Food Agric.* 99 (15), 6868–6881. doi: 10.1002/jsfa.9972

Yang, A., Cao, S., Yang, Z., Cai, Y., and Zheng, Y. (2011). γ-Aminobutyric acid treatment reduces chilling injury and activates the defence response of peach fruit. *Food Chem.* 129 (4), 1619–1622. doi: 10.1016/j.foodchem.2011.06.018

Zhang, Z., Huber, D. J., and Rao, J. (2013). Antioxidant systems of ripening avocado (*Persea americana* Mill.) fruit following treatment at the preclimacteric stage with aqueous 1-methylcyclopropene. *Postharvest Biol. Technol.* 76, 58–64. doi: 10.1016/j.postharvbio.2012.09.003

Zou, Y., Zhang, L., Rao, S., Zhu, X., Ye, L., Chen, W., et al. (2014). The relationship between the expression of ethylene-related genes and papaya fruit ripening disorder caused by chilling injury. *PLoS One* 9 (12), e116002. doi: 10.1371/journal.pone.0116002

frontiers | Frontiers in Plant Science

TYPE Original Research
PUBLISHED 22 March 2024
DOI 10.3389/fpls.2024.1332583

OPEN ACCESS

EDITED BY
Shifeng Cao,
Zhejiang Wanli University, China

REVIEWED BY
Khalil R. Jahed,
Virginia Tech, United States
Cundong Li,
Hebei Agricultural University, China
Kocsy Gábor,
Hungarian Academy of Sciences (MTA), Hungary
Parviz Heidari,
Shahrood University of Technology, Iran

*CORRESPONDENCE
Yuechen Zhang
zhangyuechen@hebau.edu.cn
Weimin Zhu
yy17@saas.sh.cn

†These authors have contributed equally to this work

RECEIVED 03 November 2023
ACCEPTED 11 March 2024
PUBLISHED 22 March 2024

CITATION
Dai T, Ban S, Han L, Li L, Zhang Y, Zhang Y and Zhu W (2024) Effects of exogenous glycine betaine on growth and development of tomato seedlings under cold stress. *Front. Plant Sci.* 15:1332583. doi: 10.3389/fpls.2024.1332583

Effects of exogenous glycine betaine on growth and development of tomato seedlings under cold stress

Taoyu Dai[1†], Songtao Ban[2†], Liyuan Han[1†], Linyi Li[2], Yingying Zhang[1], Yuechen Zhang[3*] and Weimin Zhu[1,2*]

[1]Shanghai Key Laboratory of Protected Horticulture Technology, The Protected Horticulture Institute, Shanghai Academy of Agricultural Sciences, Shanghai, China, [2]Key Laboratory of Intelligent Agricultural Technology (Yangtze River Delta), Ministry of Agriculture and Rural Affairs, Agricultural Information Institute of Science and Technology, Shanghai Academy of Agricultural Sciences, Shanghai, China, [3]State Key Laboratory of North China Crop Improvement and Regulation/Key Laboratory of Crop Growth Regulation of Hebei Province/College of Agronomy, Hebei Agricultural University, Baoding, Hebei, China

Low temperature is a type of abiotic stress affecting the tomato (*Solanum lycopersicum*) growth. Understanding the mechanisms and utilization of exogenous substances underlying plant tolerance to cold stress would lay the foundation for improving temperature resilience in this important crop. Our study is aiming to investigate the effect of exogenous glycine betaine (GB) on tomato seedlings to increase tolerance to low temperatures. By treating tomato seedlings with exogenous GB under low temperature stress, we found that 30 mmol/L exogenous GB can significantly improve the cold tolerance of tomato seedlings. Exogenous GB can influence the enzyme activity of antioxidant defense system and ROS levels in tomato leaves. The seedlings with GB treatment presented higher Fv/Fm value and photochemical activity under cold stress compared with the control. Moreover, analysis of high-throughput plant phenotyping of tomato seedlings also supported that exogenous GB can protect the photosynthetic system of tomato seedlings under cold stress. In addition, we proved that exogenous GB significantly increased the content of endogenous abscisic acid (ABA) and decreased endogenous gibberellin (GA) levels, which protected tomatoes from low temperatures. Meanwhile, transcriptional analysis showed that GB regulated the expression of genes involved in antioxidant capacity, calcium signaling, photosynthesis activity, energy metabolism-related and low temperature pathway-related genes in tomato plants. In conclusion, our findings indicated that exogenous GB, as a cryoprotectant, can enhance plant tolerance to low temperature by improving the antioxidant system, photosynthetic system, hormone signaling, and cold response pathway and so on.

KEYWORDS

cold stress, tomato seedlings, glycine betaine, hyperspectral phenotyping, cryoprotectant

Introduction

Cold stress is a significant environmental factor that has a detrimental impact on plant growth and productivity (Liu et al., 2012; Ré et al., 2017). When exposed to low temperature, plants undergo physiological and biochemical responses, including the production of reactive oxygen species (ROS), inhibiting photosynthesis and changes in osmotic solutes (Lu et al., 2020; Rahman et al., 2023; Xu et al., 2023). In order to survive under cold stress, plant activates cold response signals and transduction to regulatory networks which initiates multiple responses, including physiological and biochemical responses (Ding et al., 2020). These responses include hormone metabolism and signal transduction, synthesis of various protective compounds (e.g., proline and soluble sugars), enhancement of antioxidant capacity, changes in stabilization of membrane systems, and improvement of cold tolerance (Zhang et al., 2022).

Using multiple exogenous cryoprotectants to enhance plant's tolerance to cold stress is an effective way (Román-Figueroa et al., 2021). The latest research indicates that the regulation mechanisms of cryoprotectants in plants to cold stress are complex processes, including efficiently scavenging ROS, the production of osmotic agents, activation of cold regulating (COR) genes, and so on (Jahed et al., 2023). Exogenous melatonin application improves the cold tolerance of strawberry seedlings by stimulating the expression of downstream genes in the DREB/CBF-COR pathway (Hayat et al., 2022). Moreover, the application of exogenous hormone has a positive effect (Larkindale and Huang, 2005). Abscisic acid (ABA) can increase tolerance to drought and cold stress by decreasing water loss and activating downstream signaling (Heidari et al., 2021a). Brassinosteroids(BRs) can improve the plant heat tolerance in the regulation of ROS metabolism through the expression of many antioxidant genes that enhance the activity of antioxidant enzymes (Ogweno et al., 2008).Additionally, plant secondary metabolites have been found to reduce damage from abiotic stress, such as proline, soluble sugars and so on (Kumar et al., 2011). Therefore, the study of improving plant cold resistance with exogenous substances has important practical production application value.

Glycine betaine (GB) is one of the well-known stress protectants (Park et al., 2006; Yao et al., 2018; Shemi et al., 2021). The accumulation of GB produced by exogenous or transgenic applications can induce the expression of certain stress-responsive genes, including those for enzymes that scavenge reactive oxygen species (Chen and Murata, 2011). *CodA* gene, which encodes a choline oxidase to catalyze the conversion of choline to GB, was transferred into tomato that normally does not accumulate GB. These transgenic plants had accumulated GB and are more tolerant of chilling stress than their wild-type counterparts (Park et al., 2004).Previous studies have revealed that application of exogenous GB enhances the ability to combat abiotic stresses in crops (Khalid et al., 2022). Exogenous-applied GB can improve drought tolerance in wheat during reproductive growth stages (Shemi et al., 2021). Transcriptome analysis showed it improved the plant growth through up-regulating osmoprotection, increasing net photosynthetic rate and the catalase activity, decreasing ion leakage and protecting the antioxidant defense system (Khalid et al., 2022). In tomato, exogenous GB increases the seed germination by reducing ROS formation, altering the contents of metabolites and plant hormones (Zhang et al., 2022).

Tomato is amongst the most widely cultivated vegetables, and it is highly sensitive to chilling stress (Liu et al., 2020a). In this research, we applied exogenous GB to the seedlings to evaluate the impact of GB on the cold stress during the tomato seedling stage. We evaluated the following parameters: high-throughput plant phenotyping, chlorophyll-related parameters and hormone levels, as well as the gene expression related to low temperature response. This study aims to uncover the regulatory mechanism of exogenous GB on the chilling tolerance of tomato seedlings and identified exogenous substances that regulate plant cold tolerance-related genes in order to understand their expression patterns.

Materials and methods

Plants and growth conditions

The material NRP20 used in this experiment is a cold-sensitive species obtained from Shanghai Academy of Agricultural Sciences. Tomato seedlings were grown in greenhouse in controlled conditions (18-h light/6-h dark cycles, 25°Cday/18°C night. And 60% relative humidity) and were treated using exogenous GB (containing 0.01% Tween-20 surfactant) one time at the four-leaf stage in order to do different experiments. Different concentrations of GB, 20 mmol/L, 30 mmol/L, 40 mmol/L, 50 mmol/L were sprayed one time on tomato seedling groups while the control was sprayed with distilled water, each group with 72 seedlings. The plants grew in the normal temperature in the greenhouse for 24 hours after GB treatment and then were subjected to cold stress (4° C) for observing the phenotype and were selected the most suitable concentration of GB. Based on the previous study, the 30 mmol/L GB solution was selected to pretreat tomato seedlings while the control group was pretreated with distilled water. Under the same culturing conditions as the mentioned above, the seedlings grew at room temperature for 24 hours before undergoing low-temperature treatment for the following experiment. They were used for measuring plant hyperspectral phenotyping, enzyme activities, chlorophyll fluorescence, hormone levels, and the gene expression.

Morphological observation and measurement of tomato seedlings

On the 7th day, the growth status of tomato seedlings from different treatments was observed, and the survival rate and embryonic root length were measured using a vernier caliper (72 independent biological replicates were measured).

Determination of antioxidant enzyme activities and DAB chemical staining

Leaves (5th from cotyledon) under GB and water treatment were harvested at different time points according to experimental requirements. The levels of proline content, MDA content,H_2O_2 content,$O_2^{\cdot-}$ content superoxide dismutase (SOD), catalase (CAT), and peroxidase (POD) activities were measured using an enzyme-linked immunosorbent assay (ELISA). Each measurement was performed in triplicate, and the detection methods were performed according to the instructions from Suzhou Kemi Biotechnology Co., Ltd. Tomato seedlings at the same developmental stage were selected for 3-diaminobenzidine (DAB) staining. The 5th leaves were immediately placed in a DAB solution (pH 3.8, 1mg/ml) and subjected to vacuum infiltration until the leaves sank to the bottom. The stained leaves were then incubated at 28°C for 6-10h, during which a dark red precipitate was observed. The stained leaves were subsequently subjected to a series of washes in 95% ethanol, followed by boiling water for 10 minutes, and then subjected to three cycles of washing in 85%, 70%, and 50% ethanol solutions. Finally, the stained leaves were photographed using a camera.

Plant hyperspectral phenotyping

The tomato seedlings was placed on a black light-absorbing background cloth in a darkroom, and a hyperspectral imaging system was used to obtain hyperspectral images of the tomato seedlings. In the environment for visualizing images (ENVI) software, the decision tree classification method was used to separate each tomato seedling area from the background in the hyperspectral image, and the chemical properties of the plant were quantitatively measured at the individual plant level. The average spectral reflectance data of all pixel reflectance in the pure tomato seedling image area were calculated as its spectral reflectance data. The partial least squares discriminant analysis (PLS-DA) was used to analyze the spectral reflectance differences of WR and GR, WL and GL tomato seedlings before and after processing. PLS-DA was used to establish a relationship model between spectral parameters and sample categories to achieve sample category prediction and establish a reliable mathematical model to summarize and generalize the spectral characteristics of the research object. The parameters of the PLS-DA evaluation model are explanatory rate of the model for the X matrices (R^2X), explanatory rate of the model for the Y matrices (R^2Y), and prediction ability of the model (Q^2). The spectral reflectance of each tomato seedling was used to calculate normalized difference vegetation index (NDVI), structure insensitive pigment index (SIPI), carotenoid reflectance index 1 (CRI1), carotenoid reflectance index 2 (CRI2), pigment specific normalized difference a (PSNDa) and pigment specific normalized difference b (PSNDb), which were closely related to the plant physiology (Blackburn, 1998; Gitelson et al., 2002; Vásquez et al., 2018; Rasheed et al., 2020).

Measurement of chlorophyll fluorescence and P700 parameters

The chlorophyll fluorescence imaging system (WALZ, IMAG-MAX/L) was used to observe and analyze the photosynthetic system of tomato leaves at the same location, measure the chlorophyll fluorescence and P700 oxidation-reduction state of the leaves. Before measurement, tomato seedlings were dark-adapted for 15 minutes. The maximum photochemical efficiency of photosystem II (PSII) after dark adaptation (Fv/Fm), the non-photochemical quenching coefficient (NPQ), the apparent photosynthetic electron transport rate (ETR) of PSII, and the photochemical quenching coefficient (qP) were determined by measuring the fluorescence intensity emitted by the PSII antenna during light energy conversion, obtaining information on the operation of PSII. Six leaves at the same location of each treatment were randomly selected, and three points were randomly selected for each leaf, avoiding the veins.

Extraction and determination of plant hormones ABA and GA

The contents of ABA and GA of the samples at different time (0, 24, 48, and 72h) after chilling treatment were determined to use an enzyme-linked immunosorbent assay (ELISA) supplied by China Agricultural University (Zhang et al., 2022). Six independent biological replicates were tested.

RNA extraction and real-time quantitative PCR

Total RNA was extracted from tomato seedling leaves at different time points (0, 1, 2, and 12h) after chilling treatment by the Biospin Plant Total RNA Extraction Kit (Hangzhou Bioer Technology Co., Ltd.). The RNA extraction process followed our laboratory's experimental protocol (Zhang et al., 2022). The extracted RNA was reverse transcribed by the HiScript II One Step RT-PCR Kit (Novogene Corporation) to obtain cDNA. The *EIF* gene was used as an internal reference gene, and qRT-PCR analysis was performed using the Hieff UNICON® Universal Blue qPCR SYBR Green Master Mix (Shanghai Yisheng Biological Technology Co., Ltd.). Each reaction was performed in triplicate, and the relative expression levels were calculated by $2^{-\triangle\triangle CT}$ method. The primer design was conducted using Primer5 software (see ST1).

Statistical analysis

Data were processed with Excel, and statistical analysis was performed with SPSS 22.0 (IBM Corp., Armonk, NY, USA) with a significant level of $P < 0.05$ (Zhang et al., 2022). GraphPad Prism 8

(GraphPad Software, Inc., USA) was used for data visualization. Phenotypic observations were recorded using a Canon camera.

Results

Exogenous application of GB promotes the cold stress tolerance of tomato seedlings

Tomato plants were subjected to water treatment and GB treatment and placed them at 4°C for 7 days. We then performed a phenotypic analysis of the overall growth status and leaf wilting degree of the tomato seedlings. As shown in Figure 1A, after 7 days of cold treatment, the leaves of the tomato plants treated with water had withered, while the plants treated with GB appeared good growth compared to the water-treated plants (Figure 1A). We subsequently measured the root length of the tomato plants with a vernier caliper and calculated their survival rates. The results demonstrated that after cold treatment, the root diameter of the tomato plants treated with water became thinner, and the root length was significantly shorter. In contrast, the survival rates of the tomato plants treated with GB (20mmol/L, 30mmol/L, 40mmol/L, 50mmol/L) were all significantly increased, while the roots of the seedlings were all longer than control ($P < 0.01$) (Figures 1C, D). The treatment effect of the 30mmol/L concentration was superior to that of the other concentration (Figure 1B). This suggested that GB treatment exerted a stimulating influence on the development of tomato seedlings under cold stress. Notably, the seedlings showed the best survival rate under the treatment of GB 30mmol/L. Exogenous GB effectively mitigates the detrimental effects of cold stress on the growth and development of tomato seedlings, fostering the growth of both the aerial and subterranean parts of the seedlings, thereby enhancing their morphological architecture.

GB treatment enhances ROS scavenging capacity of tomato seedlings under cold stress

When plants suffer cold stress, they induce excessive production of ROS. Leaf phenotypes were observed using DAB histochemical staining and the contents of H_2O_2 and O_2^- were measured. The contents of malondialdehyde (MDA) and proline were also measured and compared as indicators of oxidative damage. As shown in Figures 2F–H, there was no obvious difference in the contents of H_2O_2, O_2^-, MDA, and proline in tomato plants at room temperature. Cold stress increased excessive production of ROS. in both treatment groups. However, we found that tomato leaves treated with GB had less accumulation of MDA, H_2O_2, and O_2^-, while a huge increase in proline content with significant differences at the rate of increase ($P < 0.01$). In contrast, the WL treatment reached maximum levels of H_2O_2 and MDA accumulation on the 7th day of cold stress, with a daily decrease in proline content, which reached its lowest value on the 7th day (Figures 2D–H). It indicates that tomato seedlings treated with GB can effectively reduce oxidative stress damage caused by cold stress. Plants initiate protective enzyme systems to scavenge excess ROS and prevent cell damage caused by abiotic stress. At room temperature, no significant differences were discovered among SOD, CAT and POD activities in tomato seedlings. However, the activities of antioxidant enzymes in tomato seedlings were significantly enhanced under cold stress, and the activities of SOD, POD, and CAT were observed to be higher ($P < 0.01$) than in the GB-treated group compared to the WL treatment group (Figures 2A–C). It indicates that under cold stress, the external application of GB externally enhances the ability of tomato seedlings to scavenge excess ROS by strengthening the enzymatic antioxidant defense system to varying degrees, and the effect is the most significant at a concentration of 30mmol/L.

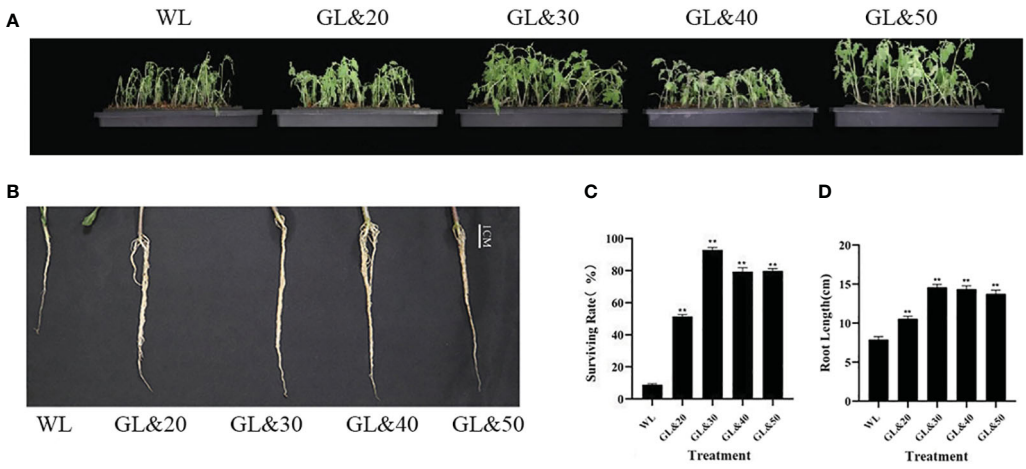

FIGURE 1
Effects of different concentrations of GB on growth of tomato seedlings under cold stress. **(A)** Tomato seedling phenotype. **(B)** Seedling root length and growth at day 7. **(C)** Survival rate of seedlings at day 7. **(D)** Seedling root length at day 7. In all cases, the asterisk indicated a significant difference among the groups according to Tukey's test. (**$P < 0.01$). WL: Tomato seedlings treated with water at low temperature; GL&20: 20mmol/L GB was applied externally at low temperature; GL&30: 30mmol/L GB was applied externally at low temperature. GL&40: 40mmol/L GB was applied externally at low temperature; GL&50: 50mmol/L GB was applied externally at low temperature.

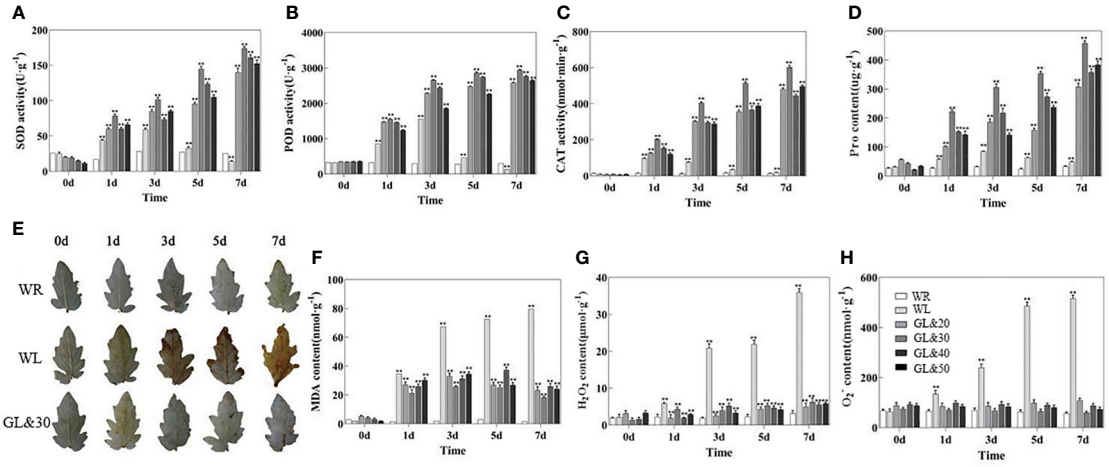

FIGURE 2
Different concentrations of GB on the accumulation of reactive oxygen species (ROS) and the activities of antioxidant enzymes in tomato seedlings at 0, 1, 3, 5 and 7 days of cold treatment **(A)** SOD activity. **(B)** POD activity. **(C)** CAT activity. **(D)** proline (Pro) content. **(E)** DAB staining. **(F)** the accumulation of malondialdehyde (MDA). **(G)** H_2O_2 content. **(H)**O_2^- content. In all cases, the asterisk indicated a significant among the groups according to Tukey's test. (**$P < 0.01$). WR: tomato seedlings treated with water at room temperature; WL: Tomato seedlings treated with water at low temperature; GL&20: 20mmol/L GB was applied externally at low temperature; GL&30: 30mmol/L GB was applied externally at low temperature. GL&40: 40mmol/L GB was applied externally at low temperature; GL&50: 50mmol/L GB was applied externally at low temperature.

Exogenous application of GB enhances the photosynthetic capacity and cold tolerance of tomato seedlings

The photosynthetic system was observed and analyzed by a chlorophyll fluorescence imaging system (WALZ, IMAG-MAX/L) in the same part of tomato leaves. Chlorophyll fluorescence phenotype analysis results showed that the tomato leaves treated with WL were significantly damaged, and the photosystem II (PSII) activity was disrupted. In contrast, tomato plants treated with GB (20mmol/L, 30mmol/L, 40mmol/L, and 50mmol/L) grew well, with no apparent damage (Figure 3A). Subsequently, the data analysis of the fluorescence yield at various points of the OJIP chlorophyll fluorescence kinetics curve of the leaves revealed that the PSII reaction center activity was reduced. Nevertheless, there was almost no difference in the leaves treated with GB at low temperature compared to the control at room temperature, and the leaves appeared a normal physiological phenotype, with the activity of light and PSII significantly improved (Figure 3B). It was found that the application of GB with a concentration of 30mmol/L had the most significant alleviating effect. To further investigate the effects of GB treatment, the chlorophyll fluorescence-related parameters in tomato leaves were measured using the plant efficiency analyzer before and on the sixth day of low-temperature treatment. It shows that the chlorophyll fluorescence-related parameters of the tomato leaves treated with water were all inhibited in photosynthesis. The maximum photochemical efficiency of PSII (Fv/Fm value) decreased significantly ($P < 0.01$), while that of GL treatment increased significantly compared to WL treatment, indicating that GB treatment helps prevent PSII photo-inhibition caused by cold stress (Figure 3C). In addition, NPQ, ETR (II), and qP increased significantly compared to WL treatment ($P < 0.01$) (Figures 3D–F). These results suggest that cold stress reduces the capacity of light energy absorption and the oxygen release of PSII. However, external application GB can maintain the stability of PSII under cold stress by dissipating excess light energy through NPQ, which maintains its structural integrity and reduces light damage caused by cold stress. Furthermore, GB treatment helps in improving the rate of photosynthetic electron transfer, enhancing the photochemical activity under cold stress, which protects PSII from light damage.

Effects of exogenous GB on high-flux plant phenotypes of tomato seedlings under cold stress

A hyperspectral imaging system was used to obtain hyperspectral images of the tomato seedlings (Figure 4A). No significant differences were found in the spectral reflectance in the four treatments before low temperature treatment, as well as between CB treatment and the control for day 6 at normal temperature (Figures 4B, C). Compared with GL treatment, the spectral reflectance of WL treatment was R^2Y=0.899 and R^2Q=0.86, indicating the significant differences of the spectral reflectance of WL treatment and GL treatment under cold stress. The above results showed that tomato leaves were severely damaged under cold stress, and the external application of GB could significantly alleviate the damage. Additionally, the NDVI value of the low temperature treatment group was lower than that of the control group, indicating that the growth was inhibited. However, the NDVI value of GB treatment group was significantly higher ($P < 0.01$) than that of low-temperature water treatment (Figure 4D). Carotenoid content, as measured by SIPI, CRI1 and CRI2, showed a positive correlation with growth accumulation. However, the overall carotenoid content of low-temperature treatment group was lower than that of normal temperature group, while the GB treatment group exhibited higher carotenoid content than the low-temperature water treatment group (Figures 4E–G). Chlorophyll a and b content, as measured by PSNDa and PSNDb, respectively, showed significantly higher levels (*P*

10.3389/fpls.2024.1332583

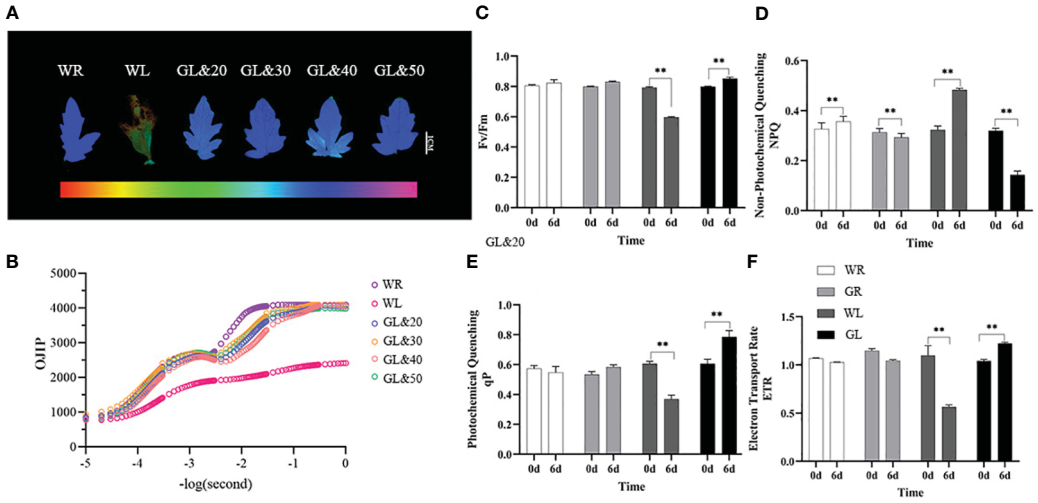

FIGURE 3
Effects of different concentrations of GB on photosynthetic capacity of tomato seedlings under cold stress **(A)** Chlorophyll fluorescence. **(B)** Chlorophyll fluorescence kinetic curve (OJIP) **(C)** Maximum photochemical efficiency of PSII (Fv/Fm). **(D)** Non-photochemical quenching coefficient (NPQ). **(E)** Photochemical quenching coefficient (qP). **(F)** Apparent photosynthetic electron transport rate (ETR). In all cases, the asterisk indicated a significant difference among the groups according to Tukey's test. (**$P < 0.01$). WR: tomato seedlings treated with water alone at room temperature; WL: Tomato seedlings treated with water at low temperature; GL&20: 20mmol/L GB was applied externally at low temperature; GL&30: 30mmol/L GB was applied externally at low temperature. GL&40: 40mmol/L GB was applied externally at low temperature; GL&50: 50mmol/L GBe was applied externally at low temperature; GL: Tomato seedlings treated with 30mmol/L GB at low temperature.

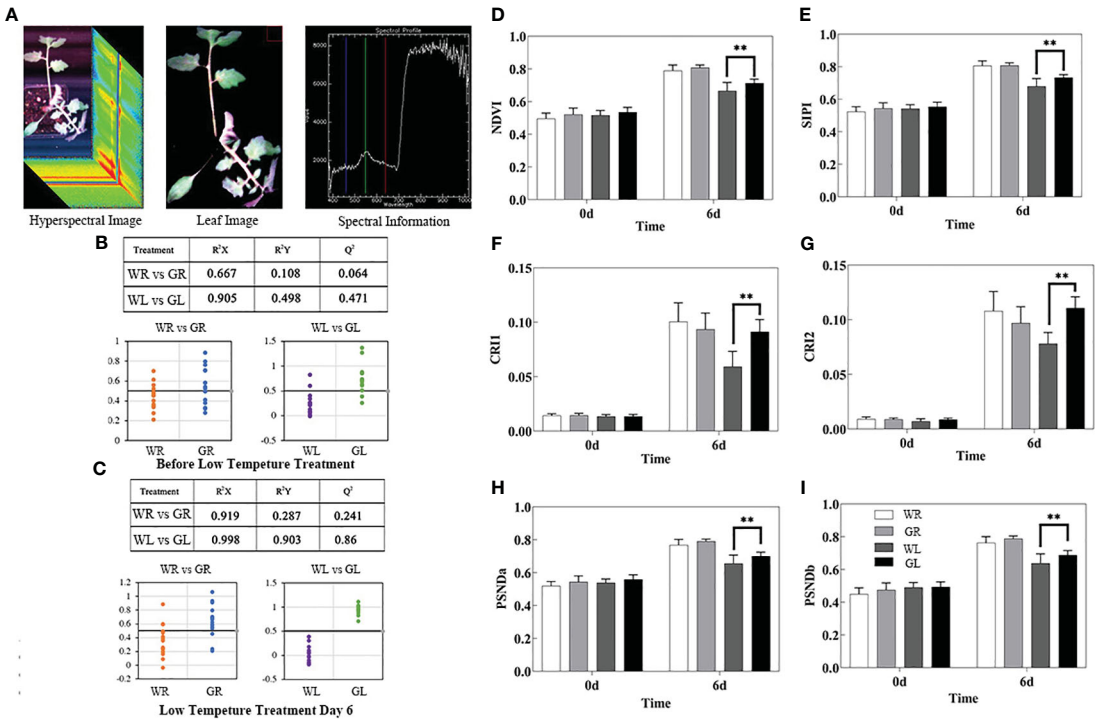

FIGURE 4
Effects of different concentrations of GB applied on high-throughput plant phenotyping of tomato seedlings under cold stress. **(A)** Acquisition and processing of hyperspectral data. **(B)** Classification results of PLS-DA model and PLS-DA model of spectral reflectance before low temperature treatment. **(C)** The spectral reflectance classification results of PLS-DA model and PLS-DA model on the 6th day of low temperature treatment (0.5 was taken as the threshold value, WR and WL categories were set as the value 0, GR and GL categories were set as the value 1, and the y-coordinate was the predicted value of the model for the category values; The closer the predicted value was to the set value, the better classification effect was and the higher distinction between the two categories). **(D)** NDVI biomass growth status. **(E)** SIPI. **(F)** CRI1. **(G)** CRI2. **(H)** PSNDa. **(I)** PSNDb. In all cases, the asterisk indicated a significant difference among the groups according to Tukey's test (**$P < 0.01$). WR: tomato seedlings treated with water at room temperature; GR: tomato seedlings treated with 30mmol/L GB at room temperature; WL: Tomato seedlings treated with water at low temperature; GL: Tomato seedlings treated with 30mmol/L GB at low temperature.

< 0.01) in the GB treatment group compared to low-temperature water treatment group (Figures 4H, I). In conclusion, it highlights the significant damage to tomato seedling leaves under cold stress, and demonstrates that the external application of GB can effectively mitigates the detrimental effects of the cold stress.

The effect of GB on GA and ABA content in tomato seedlings

After cold stress, the GA contents of all plants gradually decreased. As time goes on, the content of GA in the seedlings treated with GB is the lowest ($P < 0.01$) (Figure 5A) ABA content gradually accumulated in tomato seedlings treated with WL and GL, and the ABA content in tomato plants treated with WL began to decrease at 48h of stress, inhibiting ABA compound synthesis. On the contrary, the ABA content in tomato seedlings treated with GL significantly increased compared to WL treatment ($P < 0.01$) (Figure 5B), with an increase of 138.1%, 32.4%, and 97.6% at 24, 48, and 72h of treatment, respectively, and the ABA synthesis pathway was activated, reaching its peak at 72h of cold stress.

Effects of GB on cold-regulated genes expression in tomato seedlings

To further explore the molecular mechanisms of GB on the cold tolerance of tomato seedlings, we analyzed the expression levels of cold-regulated genes under cold stress. Our results showed that the expression levels of *SlGRAS4, ICE1, SlCBF3, Lox2*, and *ZAT12* in tomato plants treated with GB were significantly up-regulated ($P < 0.01$) compared to those treated with water, reaching their maximum levels after 1h, 12h, 2h, 1h, and 12h of cold stress, respectively (Figure 6A). However, the expression of *SlCBF1* and *SlCBF2* genes was not detected due to their low abundance. *SlGRAS4* which plays an important role in tomato cold resistance was also tested and found to be regulated. At the same time, it was also found that the gene expression level in the SlGRAS4 pathway including antioxidant capacity (*SlPOD, GPX/GST, Glut*, and *SlAPX*), calcium signaling pathways (*Cal-ATPase* and *Cam*), photosynthesis (*Rubsico*), and energy metabolism (*PEPCK* and *MDH*), has changed as shown in Figure 6B. Our results demonstrated that during cold stress, the expression levels of genes associated with antioxidant capacity (*SlPOD, GPX/GST, SlAPX*, and *Glut*), photosynthesis (*Rubsico*), and energy metabolism (*PEPCK* and *MDH*) in tomato plants treated with GB were significantly up-regulated compared to those treated with water ($P < 0.01$). The expression of calcium signaling pathways genes (*Cal-ATPase* and *Cam*), was notably significantly up-regulated in GL-treated plants compared to WL-treated plants ($P < 0.01$). Moreover, we measured the expression levels of *Pirin, TBN1*, and *SBT3* which associated with programmed cell death (PCD) and found that the expression levels of three PCD genes were elevated in tomato plants treated with water, reaching their highest levels after 12h of cold stress. Instead, the expression of these three PCD genes was significantly down-regulated ($P < 0.01$) in tomato plants treated with GB, showing significant differences (Figure 6C). Our results indicate that low temperature leads to the expression of genes related to PCD, and GB treatment can mitigate the extent of PCD under cold stress, thereby enhancing the cold tolerance of tomato seedlings.

Discussion

Cold stress is well-known in affecting plant growth and development, resulting in suppressed seed germination, impaired growth, compromised reproductive capacity, reduced crop and yield and quality (Wang et al., 2022). Tomato shows high sensitivity to low temperature at all stages during growth. The use of exogenous agents in agricultural production can enhance cold tolerance, promote growth, and increase crop yield. The application 24-epi-brassinolide (EBR) on tomato seedling induced oxidative stress and changed the content of endogenous phytohormones under low-temperature (Heidari et al., 2021b). In our previous study, exogenous GB was found to successfully enhance the seed germination rate under cold stress (Zhang et al., 2022). Here, the

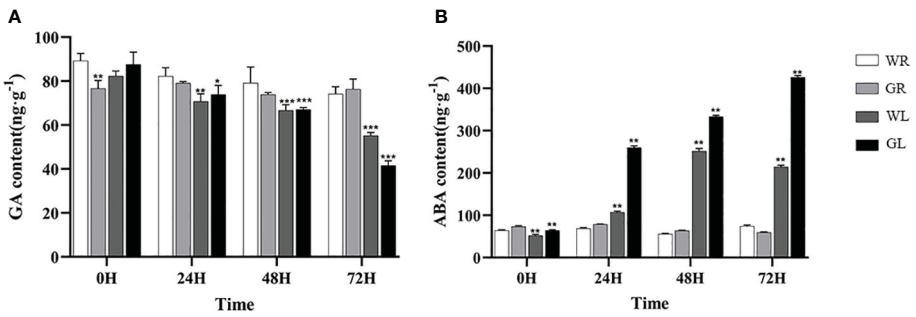

FIGURE 5
Effects of different concentrations of GB on plant hormone levels in tomato seedlings under cold stress **(A)** GA content **(B)** ABA content. In all cases the asterisk indicates a significant difference among the groups according to Tukey's test (*$P < 0.05$, **$P < 0.01$, *** $P < 0.001$). WR: tomato seedlings treated with water alone at room temperature; GR: tomato seedlings treated with 30mmol/L GB at room temperature; WL: Tomato seedlings treated with water at low temperature; GL: Tomato seedlings treated with 30mmol/L GB at low temperature.

appropriate exogenous GB was also found to effectively mitigate the effects of cold stress on tomato seedlings and significantly improve the survival rate.

Cold stress induces physiological and biochemical changes including photosynthesis, respiration, and ROS, including O_2^- and H_2O_2 (Hayat et al., 2022). To counteract the detrimental effects of ROS, plants activate protective enzyme systems, including SOD, POD, and CAT to reduce oxidants and regulate cellular homeostasis (Hasanuzzaman et al., 2020; Kamran et al., 2020). In this study, the accumulation of H_2O_2 in the leaves appeared altered by different treatment under low temperature. The tomato seedling treated with GB had significantly lower levels of H_2O_2, O_2^-, and MDA, as while as higher level of SOD, POD, and CAT than water-treated tomato seedling under cold stress (Figure 2). In addition, we also analyzed the gene expression levels of *SlPOD, GPX/GST, SlAPX*, and *Glut*, which is involved in antioxidant activity regulation. Their expression was significantly up-regulated after treatment of exogenous GB under cold stress compared with the control. The accumulation of proline has also been substantiated to enhance plant resistance (Hayat et al., 2012). We also found the proline content, which was reported to reduce lipid peroxidation and acts as an antioxidant to overcome the oxidative stress created by cold stress (Heidari et al., 2021b), was also significantly increased. Collectively, it can be inferred that exogenous GB can serve as a cryoprotectant to regulate the cold tolerance of plants by activating the enzymatic antioxidant defense system to scavenge excess ROS and alleviate the inhibitory effects of chilling stress.

Plant photosynthesis as a crucial process in plants is highly susceptible to temperature. PSII is recognized as the main component inhibited by temperature stress, while chlorophyll a fluorescence transient has been widely used to study PSII performance in plants under environmental stresses (Devacht et al., 2011; Yan et al., 2013; Kalisz et al., 2016). In our study, the expression of *Rubsico*, the photosystem-related gene, was significantly up-regulated with exogenous GB treatment under cold stress The photoinhibition of PSII in tomato plants treated with exogenous GB was effectively alleviated (Figure 3). Fv/Fm, ETR, and qP in PSII chlorophyll fluorescence were significantly increased, while the value of NPQ was decreased, indicating reduced energy dissipation and enhanced electron transfer activity. Our findings revealed that exogenous cryoprotectants can maintain the stability of PSII under cold stress, maintaining its photochemical activity and enhancing the rate of photosynthetic electron transfer.

In recent years, plant phenomics offers a suite of new technologies to investigate crop breeding and to environmental responses (Pasala and Pandey, 2020; Wang et al., 2023). High-throughput plant phenotyping approaches are developing rapidly and are already helping to bridge the genotype phenotype gap (Hall et al., 2022). Recently, the use of an automated high-throughput phenotyping platform to analyze the dynamics of maize growth provides a valuable tool for molecular design breeding and predicting maize varieties with ideal plant architectures (Wang et al., 2023). Here, we analyzed the effect of GB on tomato seedlings under cold stress using the high-throughput phenotyping tools. Our finding revealed that GB could significantly alleviate the damage caused by low temperature and keep the normal growth and development of seedlings for image analysis. Our high-throughput phenotype data is consistent with other molecular, physiological and metabolic characteristics. Taken together, combining plant phenomics with other methods is a novel approach for dissecting plants characteristics under low temperature stress, which will be useful for studying the mechanisms of abiotic stress in crops.

Phytohormones play central roles in the ability of plants to adapt to changing environments by regulating growth, development, nutrient allocation, and source/sink transitions (Peleg and Blumwald, 2011). The ABA signaling pathway and other hormonal interactions have been identified as crucial roles in enabling plants to respond to various abiotic stresses (Peleg and Blumwald, 2011; Finkelstein, 2013; Rezaul et al., 2019). On the other hand, the balance between GA and ABA mediates plant developmental processes in conferring stress resistance (Vishal and Kumar, 2018). ABA positively regulates transcriptional control and metabolomics alterations enhanced tolerance to cold when maize encountered extreme temperatures (Guo et al., 2021). Under low-temperature conditions, DELLA proteins, as the negative transcription factor in GA pathway, are components of the CBF1-mediated cold stress response and promote plant adaptation to cold stress in rice (Achard et al., 2008). In this study, tomato seedlings treated with GB exhibited higher ABA and less GA levels compared to those in the water treatment group. Consequently, the changing of GA and ABA levels after GB treatment may ultimately enhance the survival and adaptability of tomato plants under cold stress. These results further indicated that the cross-talk between plant hormones plays a crucial role in the response of plants to abiotic stress.

Cold-induced second messengers such as Ca^{2+} signal and ROS activate the expressions of cold-responded genes. OsCNGC9, a cyclic nucleotide-gated channel, positively regulates the cold-induced calcium influx and cytoplasmic calcium elevation to enhance chilling tolerance in rice (Wang et al., 2021). In the current study, the expressions of *Cal-ATPase* and *Cam* involved in calcium signaling pathway were significantly up-regulated under cold stress. Previous studies have revealed that the CBF/DREB1-dependent transcriptional regulatory pathway is essential for plant responses to cold stress (Jaglo-Ottosen et al., 1998; Gilmour et al., 2000; Shi et al., 2018). The expression of *CBFs* rapidly induced by various transcription factors, such as *ICE1* and *GRAS4* under cold stress (Chinnusamy et al., 2003; Kim et al., 2015; Liu et al., 2020b). However, the RNA-seq results of leaf tissues under cold stress showed differences in the gene expression, alternative splicing events, and miRNA between two tomato species with different cold tolerance capacities (Chen et al., 2015). In our study, we have observed significant up-regulation of cold response pathway-related genes, including *SlCBF3*, *SlICE1*, *SlLos2*, *SlGRAS4* and *SlZAT12*, after exposure to cold stress. While, *SlCBF1* and *SlCBF2* genes showed no detectable expression levels. The above results suggested that *CBF* genes were involved in responses to cold stress, but their functions differ little in tomato and GB also probably controls COR

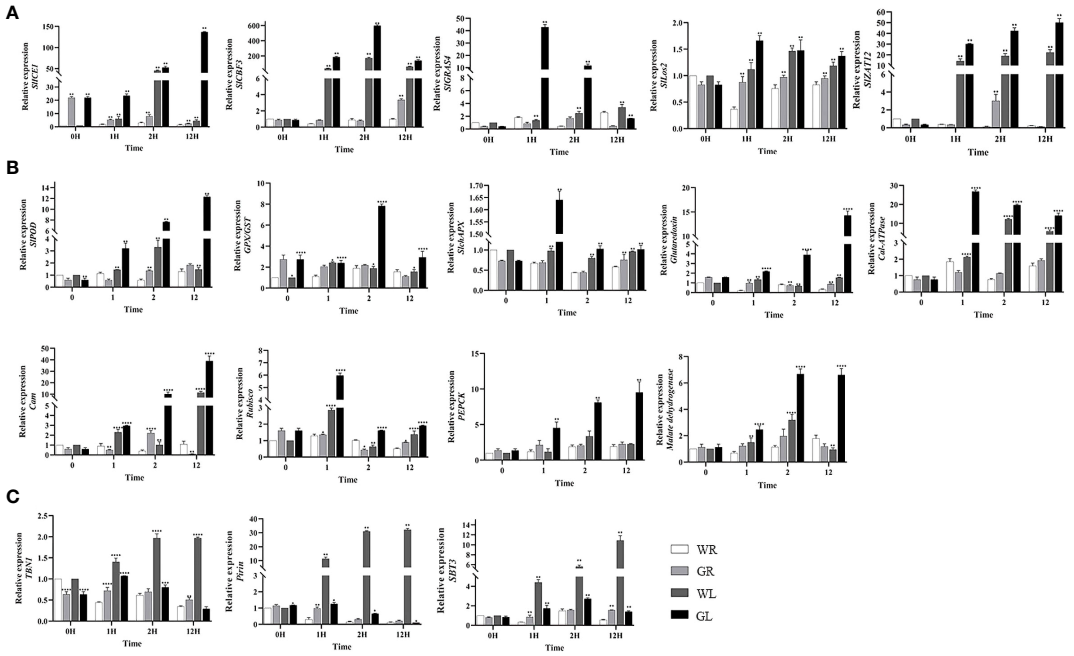

FIGURE 6
Effect of GB treatment on cold regulation genes expression in tomato seedlings under cold stress. **(A)** Cold regulatory genes *SlICE1, SlCBF3, SlGRAS4, Los2, ZAT12*. **(B)** Genes involved in antioxidant capacity (*SlPOD, GPX/GST, SlAPX,Glut*), calcium signaling pathways (*Cal-ATPase*) and calmodulin-binding protein (*Cam*), photosynthesis (*Rubsico*), energy metabolism (*PEPCK*) and *MDH*. **(C)** Genes related to programmed cell death (*Pirin*, *TBN1*, and *SBT3*). The bar is represented as the average of three repeated calculations. In all cases, an asterisk indicated a significant difference among the groups according to Tukey's test (*$P < 0.05$, **$P < 0.01$, *** $P < 0.001$, **** $P < 0.0001$). WR: tomato seedlings treated with water alone at room temperature; GR: tomato seedlings treated with 30mmol/L GB at room temperature; WL: Tomato seedlings treated with water at low temperature; GL: Tomato seedlings treated with 30mmol/L GB at low temperature.

genes through a CBF-dependent pathway in tomato in response to low-temperature stress. Both abiotic and biotic stressors can trigger programmed cell death (PCD) (Lee et al., 2014; Wang et al., 2015). PCD-related genes including *Pirin*, *TBN1*, *SBT3*, play important roles for proper growth, development and biotic/abiotic stress in plants (Orzaez et al., 2001; Koval et al., 2013; Buono et al., 2019). We observed a significant upregulation of the three PCD genes (*Pirin*, *TBN1*, *SBT3*) under WL treatment, while PCD genes were

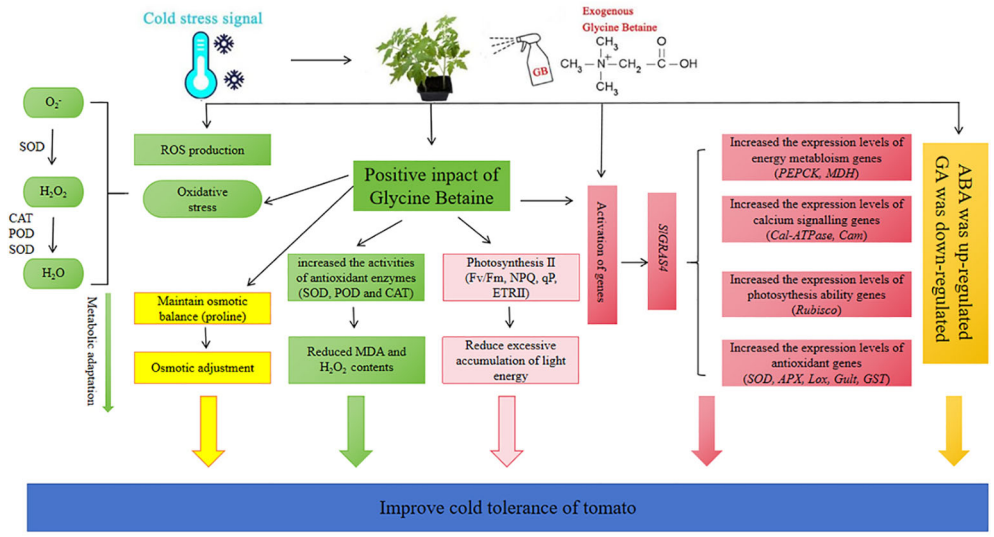

FIGURE 7
A mechanism diagram shows the mechanism of cold stress tolerance in tomato seedlings mediated by GB. Exogenous GB not only regulates antioxidant system, osmotic regulation, hormone levels, light and system II stability; It also enhances cold tolerance in tomato by regulating signal networks to activate stress-responsive genes.

significantly down-regulated after GL treatment. In plants, PCD is a part of the defense responses against environmental stresses (Locato and De Gara, 2018). Overall, changes in the expression patterns of PCD related genes indicate that plant PCD is involved in tomato response to cold stress.

Conclusion

Low temperature is a major limiting factor for the growth and reproduction of crop. Using certain exogenous cryoprotectants to enhance crop tolerance to temperature stress is one of the effective ways to protect plant development and agricultural production. This study investigated the effect of exogenous GB on tomato cold sensitive species under cold stress. A working model illustrated the role and complex mechanism of GB to enhance tomato tolerance under cold stress (Figure 7). Exogenous GB activates the expression of different genes expression. which in turn regulates its target metabolism and signaling pathways, leading to enhanced cold tolerance. The results depicted that GB regulated the expression of antioxidant system, photosynthetic system, calcium signaling, energy metabolism-related and low temperature pathway-related genes and so on in tomato plants. Moreover, GB application increased the content of antioxidant enzymes to reduce ROS and protected the photosynthetic system under cold stress. GB treatment could increase the content of proline, ABA and decrease the content of MDA, GA in response to low-temperature stress. In conclusion, GB, as a cryoprotectant, can improve the growth of tomato seedlings under cold stress through complex biological processes and multifaceted mechanism.

Data availability statement

The original contributions presented in the study are included in the article/Supplementary Material. Further inquiries can be directed to the corresponding authors.

Author contributions

TD: Writing – original draft, Writing – review & editing. SB: Writing – original draft, Writing – review & editing. LH: Writing – original draft, Writing – review & editing. LL: Writing – original draft, Writing – review & editing. YYZ: Writing – original draft, Writing – review & editing. YCZ: Writing – original draft, Writing – review & editing. WZ: Writing – original draft, Writing – review & editing.

Funding

The author(s) declare financial support was received for the research, authorship, and/or publication of this article. This work was funded by grants from National Key Research and Development Program of China (grant no. 2023YFD1201504) and the Natural Science Foundation of Shanghai (22ZR1455100).

Acknowledgments

Due to space limitations, we apologize to our colleagues whose important work are not cited in this review.

Conflict of interest

The authors declare that the research was conducted in the absence of any commercial or financial relationships that could be construed as a potential conflict of interest.

The reviewer CL declared a shared affiliation with the author YCZ to the handling editor at the time of review.

Publisher's note

Supplementary material

The Supplementary Material for this article can be found online at: https://www.frontiersin.org/articles/10.3389/fpls.2024.1332583/full#supplementary-material

References

Achard, P., Gong, F., Cheminant, S., Alioua, M., Hedden, P., and Genschik, P. (2008). The cold-inducible CBF1 factor-dependent signaling pathway modulates the accumulation of the growth-repressing DELLA proteins *via* its effect on gibberellin metabolism. *Plant Cell.* 20, 2117–2129. doi: 10.1105/tpc.108.058941

Blackburn, G. A. (1998). Spectral indices for estimating photosynthetic pigment concentrations: A test using senescent tree leaves. *Int. J. Remote Sensing.* 19, 657–675. doi: 10.1080/014311698215919

Buono, R. A., Hudecek, R., and Nowack, M. K. (2019). Plant proteases during developmental programmed cell death. *J. Exp. Bot.* 70, 2097–2112. doi: 10.1093/jxb/erz072

Chen, H. Y., Chen, X. L., Chen, D., Li, J., Zhang, Y., and Wang, A. (2015). A comparison of the low temperature transcriptomes of two tomato genotypes that differ in freezing tolerance:*Solanum lycopersicum and Solanum habrochaites*. *BMC Plant Biol.* 15, 132. doi: 10.1186/s12870-015-0521-6

Chen, T. H., and Murata, N. (2011). Glycinebetaine protects plants against abiotic stress: mechanisms and biotechnological applications. *Plant Cell Environ.* 34, 1–20. doi: 10.1111/j.1365-3040.2010.02232.x

Chinnusamy, V., Ohta, M., Kanrar, S., Lee, B. H., Hong, X., Agarwal, M., et al. (2003). ICE1: A regulator of cold-induced transcriptome and freezing tolerance in Arabidopsis. *Genes Dev.* 17, 1043–1054. doi: 10.1101/gad.1077503

Devacht, S., Lootens, P., Baert, J., Waes, J. V., Bockstaele, E. V., and Roldán-Ruiz, I. (2011). Evaluation of cold stress of young industrial chicory (Cichorium intybus L.) plants by chlorophyll a fluorescence imaging. I. Light induction curve. *Photosynthetica* 49, 161–171. doi: 10.1007/s11099-011-0015-1

Ding, Y., Shi, Y., and Yang, S. (2020). Molecular regulation of plant responses to environmental temperatures. *Mol. Plant* 13, 544–564. doi: 10.1016/j.molp.2020.02.004

Finkelstein, R. (2013). Abscisic Acid synthesis and response. *Arabidopsis Book.* 11, e166. doi: 10.1199/tab.0166

Gilmour, S. J., Sebolt, A. M., Salazar, M. P., Everard, J. D., and Thomashow, M. F. (2000). Overexpression of the Arabidopsis CBF3 transcriptional activator mimics multiple biochemical changes associated with cold acclimation. *Plant Physiol.* 124, 1854–1865. doi: 10.1104/pp.124.4.1854

Gitelson, A. A., Zur, Y., Chivkunova, O. B., and Merzlyak, M. N. (2002). Assessing carotenoid content in plant leaves with reflectance spectroscopy. *Photochem. Photobiology.* 75, 272–281. doi: 10.1562/0031-8655(2002)0750272ACCIPL2.0.CO2

Guo, Q., Li, X., Niu, L., Jameson, P. E., and Zhou, W. (2021). Transcription-associated metabolomic adjustments in maize occur during combined drought and cold stress. *Plant Physiol.* 186, 677–695. doi: 10.1093/plphys/kiab050

Hall, R. D., D'Auria, J. C., Silva Ferreira, A. C., Gibon, Y., Kruszka, D., and Mishra, P. (2022). High-throughput plant phenotyping: a role for metabolomics? *Trends Plant Sci.* 27, 549–563. doi: 10.1016/j.tplants.2022.02.001

Hasanuzzaman, M., Bhuyan, M. H. M. B., Parvin, K., Bhuiyan, T. F., Anee, T. I., Nahar, K., et al. (2020). Regulation of ROS metabolism in plants under environmental stress: A review of recent experimental evidence. *Int. J. Mol. Sci.* 21, 8695. doi: 10.3390/ijms21228695

Hayat, S., Hayat, Q., AlYemeni, M. N., Wani, A. S., Pichtel, J., and Ahmad, A. (2012). Role of proline under changing environments. *Plant Signaling behavior.* 7, 1456–1466. doi: 10.4161/psb.21949

Hayat, F., Sun, Z., Ni, Z., Iqbal, S., Xu, W., Gao, Z., et al. (2022). Exogenous Melatonin Improves Cold Tolerance of Strawberry (Fragaria × ananassa Duch.) through Modulation of DREB/CBF-COR Pathway and Antioxidant Defense System. *Horticulturae* 8, 194. doi: 10.3390/horticulturae8030194

Heidari, P., Entazari, M., Ebrahimi, A., Ahmadizadeh, M., Vannozzi, A., Palumbo, F., et al. (2021b). Exogenous EBR ameliorates endogenous hormone contents in tomato species under low-temperature stress. *Horticulturae* 7, 84. doi: 10.3390/horticulturae7040084

Heidari, P., Reza Amerian, M., and Barcaccia, G. (2021a). Hormone profiles and antioxidant activity of cultivated and wild tomato seedlings under low-temperature stress. *Agronomy* 11, 1146. doi: 10.3390/agronomy11061146

Jaglo-Ottosen, K. R., Gilmour, S. J., Zarka, D. G., Schabenberger, O., and Thomashow, M. F. (1998). Arabidopsis CBF1 overexpression induces COR genes and enhances freezing tolerance. *Science* 280, 104–106. doi: 10.1126/science.280.5360.104

Jahed, K. R., Saini, A. K., and Sherif, S. M. (2023). Coping with the cold: unveiling cryoprotectants, molecular signaling pathways, and strategies for cold stress resilience. *Front. Plant Sci.* 14. doi: 10.3389/fpls.2023.1246093

Kalisz, A., Jezdinsk, A., Pokluda, R., Skara, A., and Gil, J. (2016). Impacts of chilling on photosynthesis and chlorophyll pigment content in juvenile basil cultivars. *Horticulture Environ. Biotechnol.* 57, 330–339. doi: 10.1007/s13580-016-0095-8

Kamran, M., Parveen, A., Ahmar, S., Malik, Z., Hussain, S., Chattha, M. S., et al. (2020). An overview of hazardous impacts of soil salinity in crops, tolerance mechanisms, and amelioration through selenium supplementation. *Int. J. Mol. Sci.* 21, 148. doi: 10.3390/ijms21010148

Khalid, M., Rehman, H. M., Ahmed, N., Nawaz, S., Saleem, F., Ahmad, S., et al. (2022). Using exogenous melatonin, glutathione, proline, and glycine betaine treatments to combat abiotic stresses in crops. *Int. J. Mol. Sci.* 23, 12913. doi: 10.3390/ijms232112913

Kim, Y. S., Lee, M., Lee, J. H., Lee, H. J., and Park, C. M. (2015). The unified ICE-CBF pathway provides a transcriptional feedback control of freezing tolerance during cold acclimation in Arabidopsis. *Plant Mol. Biol.* 89, 187–201. doi: 10.1007/s11103-015-0365-3

Koval, T., Lipovová, P., Podzimek, T., Matoušek, J., Dušková, J., Skálová, T., et al. (2013). Plant multifunctional nuclease TBN1 with unexpected phospholipase activity: structural study and reaction-mechanism analysis. *Acta Crystallographica: Section D (Wiley-Blackwell).* 69, 213–226. doi: 10.1107/S0907444912043697

Kumar, S., Kaur, R., Kaur, N., Bhandhari, K., Kaushal, N., Gupta, K., et al. (2011). Heat-stress induced inhibition in growth and chlorosis in mungbean (Phaseolus aureus Roxb.) is partly mitigated by ascorbic acid application and is related to reduction in oxidative stress. *Acta Physiologiae Plantarum.* 33, 2091–2101. doi: 10.1007/s11738-011-0748-2

Larkindale, J., and Huang, B. (2005). Effects of abscisic acid, salicylic acid, ethylene and hydrogen peroxide in thermotolerance and recovery for creeping bentgrass. *Plant Growth Regulation.* 47, 17–28. doi: 10.1007/s10725-005-1536-z

Lee, S., Lee, H. J., Huh, S. U., Paek, K. H., Ha, J. H., and Park, C. H. (2014). The Arabidopsis NAC transcription factor NTL4 participates in a positive feedback loop that induces programmed cell death under heat stress conditions. *Plant Science.* 227, 76–83. doi: 10.1016/j.plantsci.2014.07.003

Liu, T., Jiao, X., Yang, S., Zhang, Z., Ye, X., Li, J., et al. (2020a). Crosstalk between GABA and ALA to improve antioxidation and cell expansion of tomato seedling under cold stress. *Environ. Exp. Botany.* 180, 104228. doi: 10.1016/j.envexpbot.2020.104228

Liu, H., Ouyang, B., Zhang, J., Wang, T., Li, H., Zhang, Y., et al. (2012). Differential modulation of photosynthesis, signaling, and transcriptional regulation between tolerant and sensitive tomato genotypes under cold stress. *PloS One* 7, e50785. doi: 10.1371/journal.pone.0050785

Liu, Y., Shi, Y., Zhu, N., Zhong, S., Bouzayen, M., and Li, Z. (2020b). SlGRAS4 mediates a novel regulatory pathway promoting chilling tolerance in tomato. *Plant Biotechnol. J.* 18, 1620–1633. doi: 10.1111/pbi.13328

Locato, V., and De Gara, L. (2018). Programmed cell death in plants: an overview. *Methods Mol. Biol.* 1743, 1–8. doi: 10.1007/978-1-4939-7668-3_1

Lu, J., Wang, Z., Yang, X., Wang, F., Qi, M., Li, T., et al. (2020). Cyclic electron flow protects photosystem I donor side under low night temperature in tomato. *Environ. Exp. Botany.* 177, 104151. doi: 10.1016/j.envexpbot.2020.104151

Ogweno, J. O., Song, X. S., Shi, K., Hu, W. H., Mao, W. H., Zhou, Y. H., et al. (2008). Brassinosteroids alleviate heatinduced inhibition of photosynthesis by increasing carboxylation efficiency and enhancing antioxidant systems in Lycopersicon esculentum. *J. Plant Growth Regul.* 27, 49–57. doi: 10.1007/s00344-007-9030-7

Orzaez, D., de Jong, A. J., and Woltering, E. J. (2001). A tomato homologue of the human protein PIRIN is induced during programmed cell death. *Plant Mol. Biol.* 46, 459–468. doi: 10.1023/a:1010618515051

Park, E. J., Jeknic, Z., and Chen, T. H. (2006). Exogenous application of glycinebetaine increases chilling tolerance in tomato plants. *Plant Cell Physiol.* 47, 706–714. doi: 10.1093/pcp/pcj041

Park, E. J., Jeknić, Z., Sakamoto, A., DeNoma, J., Yuwansiri, R., Murata, N., et al. (2004). Genetic engineering of glycinebetaine synthesis in tomato protects seeds, plants, and flowers from chilling damage. *Plant J.* 40, 474–487. doi: 10.1111/j.1365-313X.2004.02237.x

Pasala, R., and Pandey, B. B. (2020). Plant phenomics: High-throughput technology for accelerating genomics. *J. Biosci.* 45, 111. doi: 10.1007/s12038-020-00083-w

Peleg, Z., and Blumwald, E. (2011). Hormone balance and abiotic stress tolerance in crop plants. *Curr. Opin. Plant Biol.* 14, 290–295. doi: 10.1016/j.pbi.2011.02.001

Rahman, M. A., Song, Y., Hasan, M. M., Jahan, M. S., Siddiqui, M. H., Park, H. S., et al. (2023). Mechanistic basis of silicon mediated cold stress tolerance in alfalfa (Medicago sativa L.). *Silicon* 16, 1057–1069. doi: 10.1007/s12633-023-02697-9

Rasheed, F., Delagrange, S., and Lorenzetti, F. (2020). Detection of plant water stress using leaf spectral responses in three poplar hybrids prior to the onset of physiological effects. *Int. J. Remote Sensing.* 41, 5127–5146. doi: 10.1080/01431161.2020.1727052

Ré, M. D., Gonzalez, C., Escobar, M. R., Sossi, M. L., Valle, E. M., and Boggio, S. B. (2017). Small heat shock proteins and the postharvest chilling tolerance of tomato fruit. *Physiologia Plantarum.* 159, 148–160. doi: 10.1111/ppl.12491159

Rezaul, I. M., Baohua, F., Tingting, C., Weimeng, F., Caixia, Z., Longxing, T., et al. (2019). Abscisic acid prevents pollen abortion under high-temperature stress by mediating sugar metabolism in rice spikelets. *Physiol. Plant* 165, 644–663. doi: 10.1111/ppl.12759

Román-Figueroa, C., Bravo, L., Paneque, M., Navia, R., and Cea, M. (2021). Chemical products for crop protection against freezing stress: A review. *J. Agron. Crop Sci.* 207, 391–403. doi: 10.1111/jac.12489

Shemi, R., Wang, R., Gheith, E. S. M. S., Hussain, H. A., Cholidah, L., Zhang, K., et al. (2021). Role of exogenous-applied salicylic acid, zinc and glycine betaine to improve drought-tolerance in wheat during reproductive growth stages. *BMC Plant Biol.* 21, 574. doi: 10.1186/s12870-021-03367-x

Shi, Y., Ding, ,. Y., and Yang, S. (2018). Molecular regulation of CBF signaling in cold acclimation. *Trends Plant Sci.* 23, 623–637. doi: 10.1016/j.tplants.2018.04.002

Vásquez, C., Inostroza, L., and Acuña, H. (2018). Phenotypic variation of cold stress Resistance-Related traits of white clover populations naturalized in patagonian cold environments. *Crop Science.* 58, 1132–1144. doi: 10.2135/cropsci2017.07.0460

Vishal, B., and Kumar, P. P. (2018). Regulation of seed germination and abiotic stresses by gibberellins and abscisic acid. *Front. Plant Sci.* 9. doi: 10.3389/fpls.2018.00838

Wang, W., Guo, W., Le, L., Yu, J., Wu, Y., Li, D., et al. (2023). Integration of high-throughput phenotyping, GWAS, and predictive models reveals the genetic architecture of plant height in maize. *Mol. Plant* 16, 354–373. doi: 10.1016/j.molp.2022.11.016

Wang, J. C., Ren Y, L., Liu, X., Luo, S., Zhang, X., Liu, X., et al. (2021). Transcriptional activation and phosphorylation of OsCNGC9 confer enhanced chilling tolerance in rice. *Mol. Plant* 14, 315–329. doi: 10.1016/j.molp.2020.11.022

Wang, X., Song, Q., Liu, Y., Brestic, M., and Yang, X. (2022). The network centered on ICEs play roles in plant cold tolerance, growth and development. *Planta* 255, 81. doi: 10.1007/s00425-022-03858-7

Wang, P., Zhao, L., Hou, H., Zhang, H., Huang, Y., and Wang, P. (2015). Epigenetic changes are associated with programmed cell death induced by heat stress in seedling leaves of zea mays. *Plant Cell Physiol.* 56, 965–976. doi: 10.1093/pcp/pcv023

Xu, Z., Zhang, J., Wang, X., Essemine, J., Jin, J., Qu, M., et al. (2023). Cold-induced inhibition of photosynthesis-related genes integrated by a TOP6 complex in rice mesophyll cells. *Nucleic Acids Res.* 51, 1823–1842. doi: 10.1093/nar/gkac1275

Yan, K., Chen, P., Shao, H., Shao, C., Zhao, S., and Brestic, M. (2013). Dissection of photosynthetic electron transport process in sweet sorghum under heat stress. *PloS One* 8, e62100. doi: 10.1371/journal.pone.0062100

Yao, W.-Q., Lei, Y.-K., Yang, P., Li, Q.-S., Wang, L.-L., He, B.-Y., et al. (2018). Exogenous glycinebetaine promotes soil cadmium uptake by edible amaranth grown during subtropical hot season. *Int. J. Environ. Res. Public Health* 15, 1794. doi: 10.3390/ijerph15091794

Zhang, Y., Dai, T., Liu, Y., Wang, J., Wang, J., Wang, Q., et al. (2022). Effect of exogenous glycine betaine on the germination of tomato seeds under cold stress. *Int. J. Mol. Sci.* 23, 10474. doi: 10.3390/ijms231810474

frontiers | Frontiers in Plant Science

TYPE Original Research
PUBLISHED 14 May 2024
DOI 10.3389/fpls.2024.1402521

OPEN ACCESS

EDITED BY
Maria F. Drincovich,
Centro de Estudios Fotosintéticos y Bioquímicos (CEFOBI), Argentina

REVIEWED BY
Yuquan Duan,
Chinese Academy of Agricultural Sciences (CAAS), China
Jianfei Kuang,
South China Agricultural University, China

*CORRESPONDENCE
Lei Wang
freshair928@163.com

RECEIVED 17 March 2024
ACCEPTED 26 April 2024
PUBLISHED 14 May 2024

CITATION
Wang L, Liu L, Huang A, Zhang H and Zheng Y (2024) The metabolism of amino acids, AsA and abscisic acid induced by strigolactone participates in chilling tolerance in postharvest zucchini fruit. *Front. Plant Sci.* 15:1402521. doi: 10.3389/fpls.2024.1402521

The metabolism of amino acids, AsA and abscisic acid induced by strigolactone participates in chilling tolerance in postharvest zucchini fruit

Lei Wang[1]*, Li Liu[1], Anqi Huang[1], Hua Zhang[1] and Yonghua Zheng[2]

[1]College of Agriculture and Agricultural Engineering, Liaocheng University, Liaocheng, China, [2]College of Food Science and Technology, Nanjing Agricultural University, Nanjing, China

Zucchini fruit are notably susceptible to chilling injury when stored at low temperatures. The purpose of this experimental investigation was to assess the influence of strigolactone (ST) (5 μmol L^{-1}) on mitigating chilling injury and the metabolic changes in amino acids, ascorbic acid, and abscisic acid in zucchini fruit stored at 4°C. Research findings demonstrated that ST-treated zucchini fruit displayed a significantly higher tolerance to chilling stress compared to the control group. Postharvest ST treatment led to a decrease in weight loss, accompanied by reduced levels of malondialdehyde and relative ion leakage compared to the untreated group. ST immersion significantly boosted the metabolic pathways associated with proline and arginine, affecting both the enzymatic reactions and gene expressions, thus cumulatively increasing the internal concentrations of these amino acids in zucchini fruit. Zucchini treated with ST exhibited an increased concentration of γ-aminobutyric acid (GABA) as a result of augmented activities and elevated transcriptional levels of glutamate decarboxylase (GAD), GABA transaminase (GAT), and succinate semialdehyde dehydrogenase (SSD). In the ST-treated sample, the elevated enzymatic activities and enhanced gene expressions within the ascorbic acid (AsA) biosynthesis pathway worked together to sustain AsA accumulation. The application of ST resulted in a rise in abscisic acid (ABA) concentration, which correspondingly correlated with the induction of both activities and gene expression levels of crucial enzymes involved in ABA metabolism. Our findings revealed that submerging zucchini fruit in ST could be a highly effective strategy for boosting their chilling tolerance. The alleviation in chilling injury induced by ST may be attributed to the modulation of proline, arginine, GABA, AsA and ABA metabolism.

KEYWORDS

***Cucurbita pepo*, chilling tolerance injury, strigolactone, ABA, physiological metabolism**

1 Introduction

Among the multitude of postharvest preservation techniques for fruit and vegetable, cold storage continues to be recognized as the most efficacious method and is extensively employed for the storage and conservation of horticultural commodities (Valenzuela et al., 2017; Zhang et al., 2019). Cold storage effectively mitigates the metabolic activity in plant cells, postpones senescence, and safeguards the quality of postharvest horticultural goods. Nonetheless, this method poses a challenge for certain fruit and vegetable native to tropical and subtropical regions, as it can induce chilling injury (CI), thereby resulting in a decline in their overall quality (Zhang et al., 2019). Zucchini (*Cucurbita pepo* L.) is a highly nutritious and medicinally valuable vegetable crop that is notably sensitive to chilling temperatures (Palma et al., 2019; Zuo et al., 2021). The manifestations of CI in zucchini fruit are predominantly characterized by the emergence of pits and damaged patches on the outer surface or exocarp tissue (Carvajal et al., 2015). The appearance of these CI symptoms causes zucchini to be very susceptible to disease infection and rot, which directly affects its commercial value. Consequently, exploring methods to prevent or alleviate CI in zucchini fruit has emerged as a pressing research focus within the field of postharvest science. Experimental studies have discovered that specific postharvest treatments are capable of effectively reducing the severity of chilling injury in postharvest fruit and vegetable (Aghdam et al., 2019; Islam et al., 2022). Previous studies have proposed that the potential biochemical mechanism of chilling injury in fruit and vegetable involve several interconnected processes: disruption to cellular membranes, reactive oxygen species (ROS) stress, alterations in unsaturated fatty acid metabolism, perturbations in energy supply, and changes in intracellular sugar metabolism (Wu et al., 2024). Current research also attempts to elucidate the mechanism of CI in terms of the role of internal signaling molecules and functional phytochemicals within fruit and vegetable, such as GABA, proline, and argnine.

Plants inherently hold the potential capacity to cope with adverse environmental situations. Exogenous stimuli can efficaciously activate this complex adaptation process, which unfolds through the meticulous choreography of a wide array of internal signaling molecules. Strigolactone (ST), a category of phytohormones derived from carotenoids, serve as vital small signaling molecules governing various developmental stages and responding to a multitude of environmental cues (Soliman et al., 2022). Beyond their established functions in modulating plant growth and nutrient distribution within plants, ST' positive influence on the postharvest physiological processes of fruits has garnered escalating interest in their scientific investigation (Wu et al., 2022; Liu et al., 2024a). During refrigerated storage at 0°C, ST enhanced fruit quality in strawberries by bolstering the antioxidant defense system and regulating the metabolic pathways involving phenylpropanoids, nitric oxide, and hydrogen sulfide (Huang et al., 2021a). Physiological evaluations demonstrated that the use of ST significantly alleviated the progression of CI in postharvest litchi fruit (Liu et al., 2024a). Ferrero et al. (2018) highlighted the involvement of ST in enhancing the accumulation of anthocyanins within grapevine berries through synergistic interactions with other phytohormones. It is becoming increasingly clear that ST is finding broader applications in agriculture contexts (Li et al., 2023; Kapoor et al., 2024). Considering the extensive applications of ST in agricultural practices, obtaining a thorough comprehension of its multifaceted roles across a broad range of plant species is essential. Up until now, no scientific research has been published detailing the effects of ST immersion treatments in reducing chilling damage during the postharvest period for zucchini fruit. This study aimed to explore the efficacy of ST in diminishing chilling injury in zucchini fruit during cold storage. Concurrently, we scrutinized the metabolic changes in amino acids, ascorbic acid and abscisic acid to shed light on the potential biochemical mechanisms responsible for the improved chilling tolerance in postharvest zucchini fruit during cold storage treated with ST.

2 Materials and methods

2.1 *ST treatment and* sample collection

Fruit (*Cucurbita pepo* L. cv. Zaoqing) were meticulously handpicked from a farm situated in the outskirts of Liaocheng at their commercial maturity stage. Any fruit found to have defects were carefully discarded to ensure only top-quality produce was used. Subsequently, we selected fruit that displayed consistent size and uniform coloration. All zucchini fruit were divided randomly into two sets of 150 pieces each. Based on a preliminary screening test conducted over a range of concentrations (0, 1, 5, 10, 20 μM), one set was treated by immersing them in a solution consisting of 5 μM ST (Solarbio Science and Technology Co., Ltd., Beijing, China) for a period of ten minutes. This experimental process validated that the chosen concentration of 5 μM ST exerted the most efficacious results. Another batch was treated with sterile water instead, functioning as the control group. Thereafter, all the fruit were left to dry out gently at the ambient temperature of 20°C for around an hour. The fruit were then stored at 4°C for a span of sixteen days, under conditions where the relative humidity was consistently held at 90%. A total of 30 fruit from each batch were shifted to 20°C for a 2-day shelf life simulation before undergoing physio-biochemical index assessments and chilling injury measurements every four days. For each replicate, the sample tissue of ten fruit without chilling injury symptom was mixed together and stored in liquid nitrogen for subsequent physio-biochemical parameter analysis. Each treatment had three biological replicates at every assessment point, and the entire experiment was repeated twice.

2.2 Assessment of chilling injury in cold-stored zucchini

The severity of chilling injury was determined by evaluating the external surface pitting areas in zucchini fruit. The classification system for assessing the severity of chilling injury was structured as follows: At Grade 0, there were no discernible symptoms of pitting. Grade 1 denoted that the affected area covered less than 10% of the

fruit's total surface. In Grade 2, the pitting extended across 11% to 25% of the fruit's skin. Grade 3 represented a pitting area ranging from 26% to 50% of the fruit's surface. Lastly, Grade 4 signified that the pitting had spread over more than 50% of the fruit's exterior. The Chilling Injury Index was calculated using the following formula: ∑(chilling injury level × quantity of fruit at corresponding level)/(4 × total fruit number).

2.3 Quantifications of malondialdehyde (MDA) and relative and ion leakage

To assess the MDA content and ion leakage in the experimental fruit, we adhered to the detailed protocol outlined by Wang et al. (2023). A sample of fruit pulp was ground in a 15 mL of TCA solution. The resultant mixture was then centrifuged at 10,000 g for a duration of 15 minutes. Following this, the absorbance of the extracted supernatant was measured spectrophotometrically at three distinct wavelengths, namely 450, 532, and 600 nm. The MDA concentration was computed using the following formula: $6.45\times(Ab_{532}-Ab_{600})-0.56\times Ab_{450}$. To determine ion leakage, four grams of uniformly sliced zucchini cylinders (with a thickness of 2 mm) taken from the cuticular layer of ten fruits were soaked in 30 mL of deionized water for a period of ten minutes. The initial electrical conductivity (D_i) was then recorded. Next, the samples were boiled for another ten minutes before cooling down to 20°C. Upon reaching this temperature, the final electroconductivity (D_f) was measured in another 30 mL of deionized water. The ion leakage percentage was derived from the ratio of initial to final conductivity values, expressed as: $(D_i/D_f)\times 100\%$.

2.4 Measurement of proline content and the activities of enzymes involved in proline metabolism

The determination of proline content was carried out according to the previous research of Wang et al. (2023). Tissue sample was homogenized in 20 mL of sulphosalicylic acid and then subjected to water bath incubation at 100°C for tenminutes. Following a 10-minute centrifugation at 15,000 g, the supernatant was retrieved and mixed with methylbenzene (5 mM), ninhydrin (2%, v/v), and acetic acid (5%, v/v). The absorbance of the reaction mixture was measured at 520 nm by spectrophotometry, with results presented in terms of mg/kg of tissue sample.

Ornithine-δ-aminotransferase (OAT) activity was measured following the procedure outlined in the research of Wang et al. (2023). Tissue sample was homogenized in tripotassium phosphate buffer containing dithiothreitol, and the mixture was subsequently centrifuged at 15,000 g for 12 minutes at 4°C. The assay mixture was composed of crude enzyme (0.8 mL), 1.3 mL of Orn (35 mM), 0.2 mL of ninhydrin (2%, w/v), and 1.7 mL of phosphopyridoxal (0.15 mM). One unit of enzyme activity is defined as an increment of 0.01 absorbance units at 510 nm per minute, which is recorded in U/kg tissue sample.

Tissue sample was crushed in Tris-HCl buffer solution including PVP, EDTA, and dithiothreitol, which was then centrifuged at 15,000 g for 15 minutes at 4°C. Reaction mixture for measuring PCS (pyrroline-5-carboxylate synthase) consisted of enzyme supernatant, $MgCl_2$, Tris-HCl buffer, and ATP. Reaction mixture for measuring PDH (proline dehydrogenase) consisted of enzyme supernatant, proline, Na_2CO_3-$NaHCO_3$ buffer, and NAD^+ (Wang et al., 2023). One unit of activity of the above two enzymes is defined as the change in absorbance by 0.001 per minute at a wavelength of 340 nm.

2.5 Measurements of GABA content and the activities of enzymes involved in GABA metabolism

GABA concentration was determined following the analytical methods outlined by Madebo et al. (2021). Zucchini tissue was homogenized in a 50 mM lanthanum chloride solution, and the mixture was subsequently centrifuged at 15,000 g for 12 minutes at 4°C. The assay blend included 0.6 mL boracic acid buffer (pH 9.0), 0.8 mL phenyl hydroxide, 0.6 mL $NaClO_4$, 0.4 mL potassium hydroxide, and 2.6 mL obtained supernatant. The absorbance of the assay blend was measured spectrophotometrically at a wavelength of 645 nm, with results presented in terms of milligrams per kilogram of tissue sample.

Glutamate decarboxylase (GAD) activity was measured following the procedure outlined in the research of Madebo et al. (2021). Zucchini tissue was crushed in Tris-HCl buffer solution, which was then centrifuged at 15,000 g for 15 minutes at 4°C. The assay mixture consisted of tripotassium phosphate buffer (0.25 M), glycerol (0.1 mM), phosphopyridoxal (0.07 mM), dithiothreitol (0.1 mM). One unit of enzyme activity is defined as the production of one microgram of GABA within one minute. GABA transaminase (GAT) activity was measured following the procedure outlined in the research of Madebo et al. (2021). Zucchini tissue was crushed in PBS buffer, which was then centrifuged at 15,000 g for 15 minutes at 4°C. The assay mixture consisted of GABA (0.1 mM), DTT (0.2 mM), ethylene diamine tetraacetic acid (0.03 M), acetonate (0.05 mM), phosphopyridoxal (0.05 mM), Tris-HCI buffer (0.2 M), obtained supernatant (0.6 mL). The reaction was terminated by adding sulfosalicylic acid, and the absorbance of the solution was subsequently determined spectrophotometrically at a wavelength of 450 nm. The determination of succinate semialdehyde dehydrogenase (SSD) activity was conducted in adherence to the guidelines provided in the Plant SSD ELISA Kit from Jiangsu Boshen Biotechnology Co., LTD. Tissue sample was crushed in PBS buffer (pH 7.3), which was then centrifuged at 15,000 g for 15 minutes at 4°C. The assay mixture consisted of POD, DTT, tetramethylbenzidine, and obtained supernatant. The absorbance of the mixture was measured spectrophotometrically at a wavelength of 450 nm, with results presented in terms of units per gram of tissue sample.

2.6 Measurements of AsA content and the activities of enzymes involved in AsA metabolism

The determination of AsA concentration in zucchini fruit was guided by the methods outlined in the work of Wang et al. (2016).

To measure the AsA concentration, four grams of fruit tissues were finely ground in 15 milliliters of prechilled oxalic acid. Subsequently, the AsA content was determined through a titration process using 2,6-dichlorophenol indophenol as the titrating agent. The result was reported in units of grams per kilogram of tissue. The measurement of ascorbate peroxidase (APX) activity was conducted according to the protocol laid out by Li et al. (2019). The composition of the reaction blend included enzyme suspension, sodium phosphate buffer (1.5 mL, 50 mM, pH 7.0), AsA (50 μL, 9 mM), and H_2O_2 (15 μL, 30%). The unit defining enzyme activity was considered as the amount of enzyme that caused a decrement in absorbance at a wavelength of 290 nm min^{-1}. The quantification of monodehydroascorbate reductase (MDR) activity was performed according to the methodologies prescribed by Liu et al. (2024b). Zucchini tissue was homogenized in prechilled Tris-HCl buffer that included polyvinylpyrrolidone (5%, w/v), ethylenediaminetetraacetic acid, Triton X-100, and dithiothreitol. Following this, the mixture was subjected to centrifugation at 11,000 g (4°C). The composition of the reaction mixture included HEPES-KOH buffered solution, NADH, ascorbate, ascorbate oxidase enzyme, and 0.8 milliliters of the supernatant derived from the enzyme preparation. The result was determined by measuring absorbance at a wavelength of 340 nm using a spectrophotometer. The assessment of ascorbate oxidase (ACO) activity in the fruit tissue was conducted in accordance with the methodology prescribed by Yun et al. (2020). Fruit pulp were finely ground in a pre-cooled sodium phosphate buffer solution (pH 6.5). The reaction blend primarily comprised ascorbic acid, glutathione, and the supernatant fraction. The composition of the reaction mixture included glutathione, AsA, and supernatant derived from the enzyme preparation. One unit of ACO activity was established as the measure of the oxidative transformation of ascorbic acid occurring per second, and the results were expressed in terms of μmol s^{-1} kg^{-1} protein.

2.7 Measurements of arginine content and the activities of enzymes involved in arginine metabolism

The determination of arginine content within zucchini tissue was estimated following the method of Jin et al. (2019). Tissue sample was pulverized with hydrochloric acid solution (0.2 M), and the mixture was subsequently centrifuged at 8,000 g for 12 minutes at 4°C to collect the supernate. The residue was extensively rinsed with hydrochloric acid solution (0.2 M) and subsequently subjected to centrifugation at 8,000 g. The resulting supernatant was combined and mixed with 5-sulfosalicylic acid. After undergoing ultrasonic treatment and subsequent centrifugation at 8,000 g, the reaction system was meticulously filtered using a 0.22 μM aqueous phase filter. The filter liquor was detected with a Hitachi L-8800 amino acid analyzer and the concentration of arginine was quantified following the manufacturer's standard procedures. Arginase (ARG) activity was measured following the procedure outlined in the research of Zhang et al. (2013). Tissue sample was crushed in Tris-HCl buffer solution including ME (2-mercaptoethanol), PMSF, and PVP, which was then centrifuged at 15,000 g for 15 min at 4°C. Reaction solution included crude enzyme, arginine, Gly-NaOH, and manganese chloride. The reaction was ceased by the addition of $HClO_4$. The resulting solution was combined with another liquid containing both sulfuric and phosphoric acids, and then the mixture was incubated in boiling water bath for 60 minutes. The absorbance of reaction mixture was recorded at 520 nm. One unit of ARG activity was defined as the production of one milligram of urea per minute per gram of tissue sample. The activities of arginine decarboxylase (ADC) and ornithine decarboxylase (ODC) were performed following the protocol provided by Zhang et al. (2013). Tissue sample was crushed in sodium phosphate buffer solution including DTT, PMSF, EDTA, and AsA, which was then centrifuged at 15,000 g for 15 min at 4°C. Reaction solution included crude enzyme, PLP, EDTA, and DTT. The assay reactions were commenced by introducing 100 μL of arginine for ADC activity measurement or L-ornithine for ODC activity assessment, and the resulting mixtures were then maintained at 37°C for 30 minutes. Termination of the reaction was achieved by adding perchloric acid, following which the mixture was centrifuged at 10,000 g to collect the supernate. The absorbance of assay blend was recorded at 254 nm. Enzyme activities were represented by the variation of 0.01 units in absorbance per minute for every gram of tissue sample.

2.8 Measurements of ABA content and the activities of enzymes involved in ABA metabolism

The evaluation of ABA content in the frozen zucchini tissues was conducted in accordance with the standards delineated by Siebeneichler et al. (2022). To do this, 2.0 grams of zucchini tissues were thoroughly pulverized in a pre-chilled 80% methanol solution. The resulting mixtures were centrifugated at 13,000 g for 30 minutes (4°C). The resulting supernatant was passed through a 0.22-micron syringe filter for purification. After eliminating polar constituents using a Sep-Pak C18 cartridge, ABA content was measured using the enzyme-linked immunosorbent assay (ELISA) kits provided by Adanti Biotechnology Co., Ltd., Hubei, China, and expressed as μg kg^{-1} sample. Abscisic acid aldehyde oxidase (AAO) activity was determined as directed by Zuo et al. (2021). In this process, 2.5 grams of fruit specimen were ground in 10 mL prechilled phosphoric acid buffer. The resulting mixtures were subjected to centrifugation at 12,000 g for a duration of fifteen minutes at 4°C. The AAO activity was assayed spectrophotometrically at 450 nm following the producer's instructions for AAO ELISA technique; with one unit of AAO activity defined as the generation of one nmol of ABA under the given assay conditions. The 9-cis-epoxycarotenoid dioxygenase (ECD) activity was assessed following the direction of Huang et al. (2021c). A 2.5 gram portion of fruit tissue was crushed in 15 mL prechilled PBS buffer solution and centrifuged at 12,000 g at 4°C. ECD activity was subsequently quantified spectrophotometrically at

450 nm, adhering to the instructions provided by the ELISA kit from Mlbio, Shanghai, China.

2.9 RNA extraction and quantitative analysis of genes expressions

RNA extraction from zucchini tissues was conducted following the methodology described by Liu et al. (2024b). First, 5.0 grams of fruit sample were ground into powder in liquid nitrogen. Total RNA was retrieved by employing a CTAB-based extraction solution containing 2% (v/v) β-mercaptoethanol. The quantity and quality of the isolated RNA were assessed utilizing a Thermo NanoDrop 2000 spectrophotometer. Subsequently, cDNA synthesis was performed through reverse transcription in adherence to the protocol recommended by Yeasen Biotechnology Co., Ltd., Shanghai. Real-time quantitative PCR (qPCR) was carried out following the instructions accompanying the GoTaq® qPCR Master Mix kit from Promega. Each reaction solution consisted of the cDNA template, 2.5 microliters specific primers for each target gene, 5 microliters of double-distilled water, and 15 microliters of the qPCR Master Mix. Based on the NCBI database, the primer sequences employed in this study were carefully selected and are exhaustively detailed in Table 1. Relative transcript abundance of the target genes and the housekeeping gene were calculated according to 2−ΔΔCT formula.

2.10 Statistical analysis

The present investigation was designed and performed following a thorough randomization method. Statistical analysis of the collected data was carried out using ANOVA model. Statistical comparisons among the treatments were conducted utilizing Duncan's Multiple Range Test, with a significance threshold set at p-value less than 0.05.

TABLE 1 Primer sequences for gene expression in qRT-PCR analysis.

Genes	Gene ID	Primer sequence (5′→3′)	Length (bp)
CpPCS	111805552	ACTTCATCAGAAGCGGCCAA CCAAGCATAATGCACCACATCT	162
CpPDH	111809051	AATCTTGCTGTCTCTCCGGC ACGAGCCAACTCAACATCCA	186
CpOAT	111783359	TTCCTCCCCAAGTGATCCCA ATCCCACAGTGTGAGTCTACG	178
CpARG	111807154	TTCAACCCTCAGCGAGACAC ACCTTGGCTCATCACTCTCAC	187
CpADC	111794938	GGATAGCTCTCTTCCGTCGC CGAACGGTCATGTTCCCAGA	192
CpODC	111798957	CCAACATGGCCTCCTCCATT GGGTTGGGGTTGCATTTGAC	168
CpGAD	111808603	CCGTCGAAGGCCGATATCAA GCTCATCCGCTCTCACTTCA	176
CpGAT	111809776	CGTGGACTAAGGGTTGGAGTT ATGTGCGACAGACTGAGACC	200
CpSSD	111796065	CTTGGTCGGGAAGGATCCAA GGCCTCTGCCTATCTGGTTT	175
CpAPX	111782837	GCTAGTGGCATGGGGAGATG TCCAAAGAGACAGGGAGACCA	171
CpMDR	111809047	CGTTTGAGCAAGTGGGGTTG TGACACAATGCTGAGCCGAT	183
CpACO	111793728	AGGGAGCCTAACTTCCTCGT GCTCGAATCGTAGGTCCAGG	182
CpAAO	111789967	TGACGGCCTCAGAAAGTTCC CCGCCGACGATTATGACAGA	150
CpECD	111809781	ATGGATTCCGGCAGGAACAG CCCGCTGCAAGAAATTCCAC	169
CpACTIN	111787537	TCGGTGCCGAACGTTTTAGA AACCACCGGAGAGGACGATA	159

3 Results

3.1 Chilling injury index, weight loss, MDA content and relative electrolyte leakage in zucchini fruit subjected to cold storage

Throughout a 16-day period of cold storage at 4°C, a steady escalation in the chilling injury index was noticed in zucchini fruit. Zucchini fruit subjected to ST treatment exhibited a notably slower increase in the chilling injury index relative to untreated controls. After the 4th day of storage, the chilling injury index in ST-treated zucchinis was significantly less than in untreated ones (Figure 1A). The application of ST proved effective in curbing the surge of the chilling injury index. As the storage duration extended, there were gradual upsurges in weight loss rate, MDA content, and relative electrolyte leakage levels within zucchini fruit (Figures 1B–D). The findings from our experiments indicated that ST intervention significantly deterred the escalation of above three physiological parameters over time.

3.2 Proline content, metabolic enzymatic activities related to proline, and associated gene expression in zucchini fruit subjected to cold storage

Throughout the entire storage period, proline content in zucchini fruit consistently rose (Figure 2A). Notably, this ascending trend was augmented in fruit that subjected to ST treatment. PCS activity in treated fruit initially displayed a pattern of rising before declining, reaching its peak at the eighth day of observation. Throughout the entire storage period, the control group consistently exhibited lower PCS activity levels compared to those in the ST-treated group (Figure 2B). Comparable patterns were also observed in the

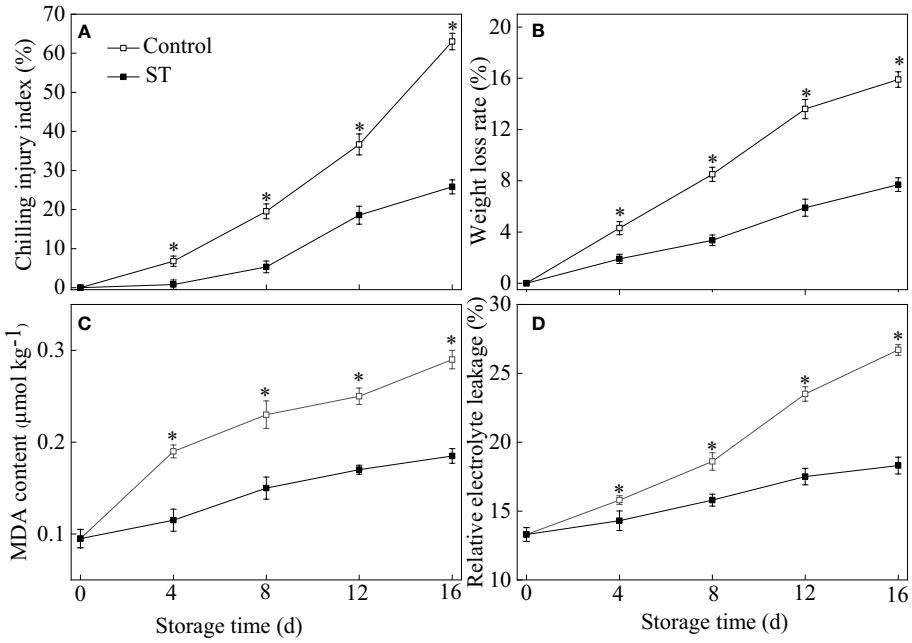

FIGURE 1
Variations of chilling injury index **(A)**, weight loss **(B)**, MDA content **(C)** and relative electrolyte leakage **(D)** in control and 5 μM ST treated zucchini fruit during cold storage. Vertical bars indicate the standard error of the mean values. Asterisks imply statistically significant differences ($p < 0.05$) between the control and ST treated group in the same day.

transcription abundance of *CpPCS* across both control and treated group (Figure 2C). PDH activity showcased a downward trend in zucchini fruit throughout the storage duration (Figure 2D). The expression of the *CpPDH* gene in zucchini fruit initially ascended before subsequently declining (Figure 2E). Remarkably, both the activity and transcription abundance of PDH were lower in the treated fruit compared to their counterparts in the control group. OAT activity in the ST-treated fruit registered a sharp rise during the initial four days of storage, followed by a gradual decrease over the rest of the storage timeframe (Figure 2F). Throughout the storage period, the expression of the *CpOAT* gene was consistently higher in the treated zucchini fruit compared to the control group (Figure 2G).

3.3 Arginine content, metabolic enzymatic activities related to arginine, and associated gene expression in zucchini fruit subjected to cold storage

As can be observed in Figure 3A, a general decrease trend in arginine content is recorded during the course of storage duration (Figure 3A). Activities of ARG and ADC in treated fruit exhibited similar trajectories of ascent before descending, peaking at day 12. Over the entire storage period, the untreated fruit consistently presented with lower activities of ARG and ADC when compared to the treated counterparts (Figures 3B, D). ST treatment significantly increased the relative expression of *CpARG* and *CpADC* in zucchini fruit during cold storage (Figures 3C, E). Compared with the control group, ST treatment significantly promoted the increase of ODC activity and the relative expression of *CpODC* in zucchini fruit during cold storage (Figures 3F, G).

3.4 GABA content, metabolic enzymatic activities related to GABA, and associated gene expression in zucchini fruit subjected to cold storage

The content of GABA in control zucchini fruit consistently reduced over the course of their storage period. Conversely, in the ST-treated group, GABA levels peaked at day 4 and thereafter began to diminish (Figure 4A). GABA content in treated zucchini fruit was notably higher in comparison to the control fruit. The activity of GAD and expression of the *CpGAD* gene in zucchini fruit initially rose before declining later on. From the fourth day of storage onwards, both GAD activity and gene expression levels were significantly elevated in the treated fruit relative to the control fruit (Figures 4B, C). ST treatment resulted in a considerable enhancement of GAT activity and the expression of the *CpGAT* gene throughout the entire storage period (Figures 4D, E). The activity of SSD initially showed a significant increase followed by a slight diminution in both the control and treated group as storage duration extended (Figure 4F). In treated fruit, the relative expression of *CpSSD* consistently increased with prolonged storage, whereas in the control group, it initially decreased and then slightly rose as storage time lengthened (Figure 4G).

10.3389/fpls.2024.1402521

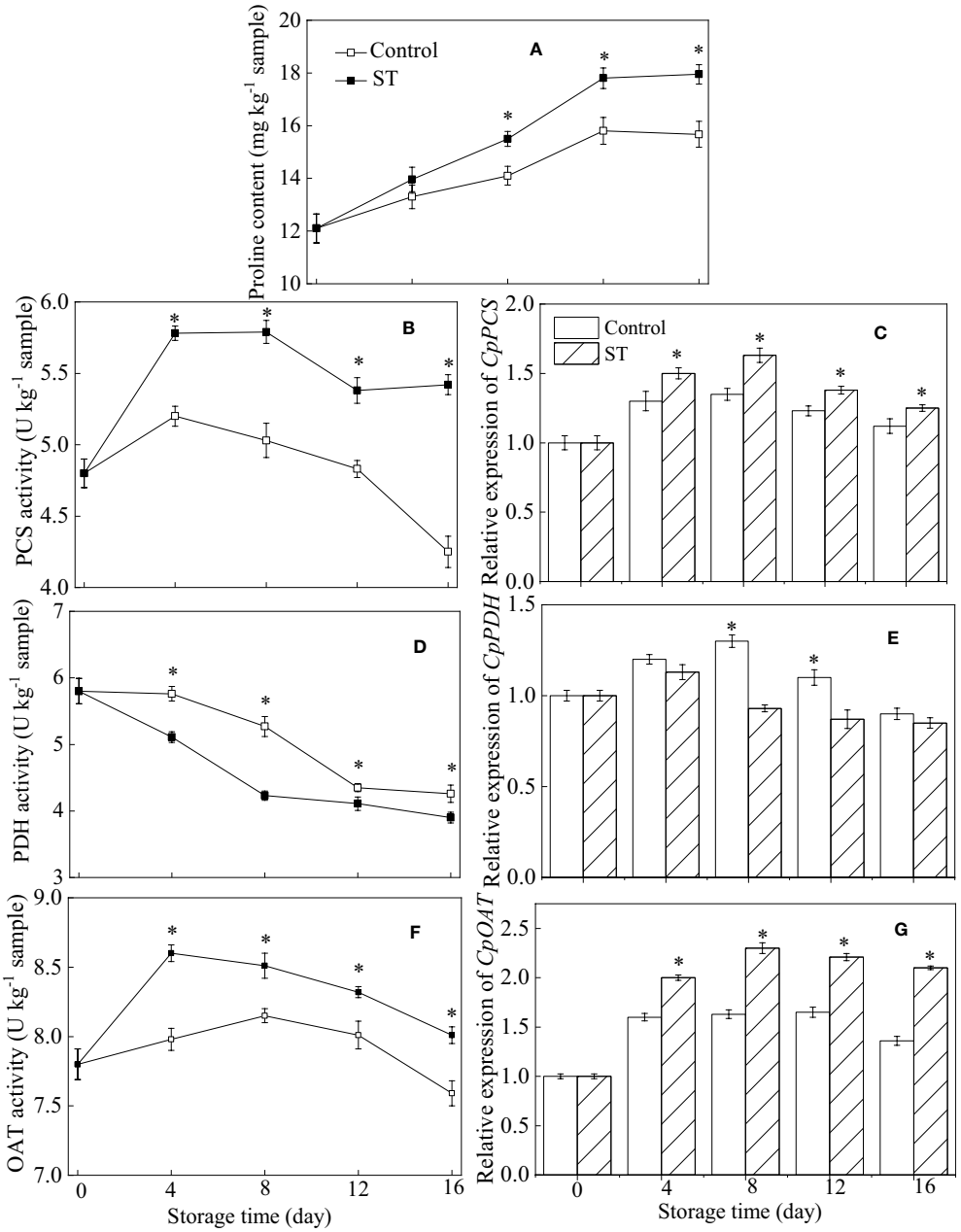

FIGURE 2
Variations of proline content **(A)**, metabolic enzymatic activities related to proline **(B, D, F)** and associated gene expression in control **(C, E, G)** and 5 mM ST treated zucchini fruit during cold storage. Vertical bars indicate the standard error of the mean values. Asterisks imply statistically significant differences ($p < 0.05$) between the control and ST treated group in the same day.

3.5 AsA content, metabolic enzymatic activities related to AsA, and associated gene expression in zucchini fruit subjected to cold storage

Over the course of storage, AsA content in zucchini fruit continuously diminished (Figure 5A). Nevertheless, the application of ST prior to storage served to alleviate this decline in AsA levels. In the ST-treated zucchini fruit, the activities of APX and MDR initially surged significantly before experiencing a modest decline as storage time progressed, consistently maintaining levels that were notably higher than those found in the control group (Figures 5B, D). Comparable trends in expression were also observed for the genes *CpAPX* and *CpMDR* in both control and treated zucchini fruit (Figures 5C, E). ACO activity in zucchini fruit exhibited a progressive decline throughout the entire storage period. Starting from the eighth day of storage, control samples displayed a notably higher ACO activity level compared to the ST-treated group (Figure 5F). The expression of *CpACO* gene in zucchini samples decreased over time (Figure 5G). However, after eight days of storage, the transcription level of *CpACO* was significantly downregulated in the ST-treated samples as opposed to the control fruit.

10.3389/fpls.2024.1402521

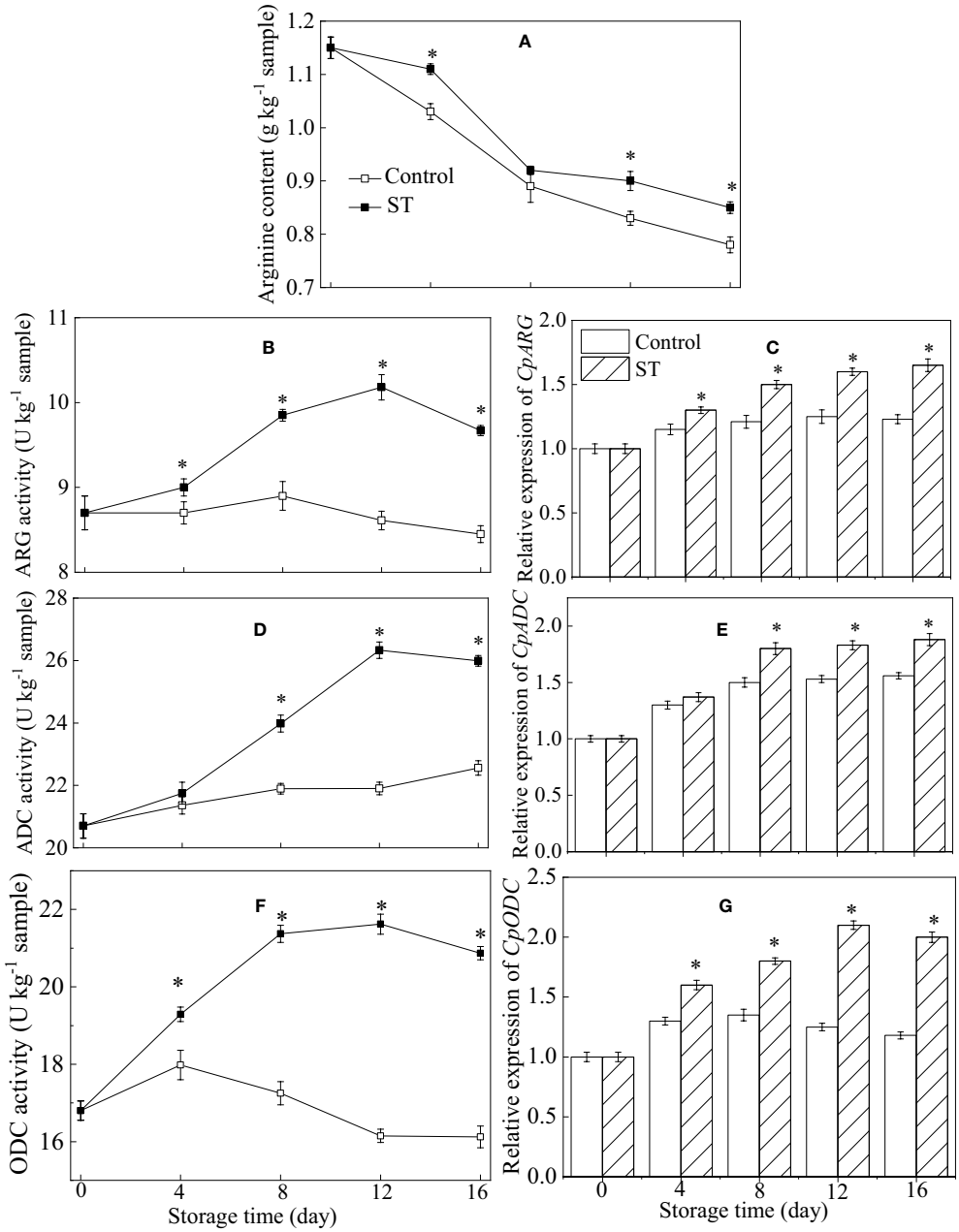

FIGURE 3
Variations of arginine content **(A)**, metabolic enzymatic activities related to arginine **(B, D, F)** and associated gene expression in control **(C, E, G)** and 5 mM ST treated zucchini fruit during cold storage. Vertical bars indicate the standard error of the mean values. Asterisks imply statistically significant differences ($p < 0.05$) between the control and ST treated group in the same day.

3.6 ABA content, metabolic enzymatic activities related to ABA, and associated gene expression in zucchini fruit subjected to cold storage

The results showed that ABA content rose continuously in both the ST-treated and control group, yet it was significantly higher in the ST-treated group specifically between the 12th and 16th days of the trial (Figure 6A). The activity of AAO in treated zucchini fruit initially rose before declining later on (Figure 6B). The expression of *Cp*AAO gene in zucchini samples increased gradually over time (Figure 6C). Starting from the eighth day of storage, ST treatment significantly heightened AAO activity and corresponding gene expression levels compared to the control fruit. During the complete storage span, activity of ECD and expression of *CpECD* gene in zucchini fruit consistently decreased over time. ST treatment induced a marked enhancement in ECD activity between the fourth and eighth days of the experiment (Figure 6D). In comparison to the control, the ST treatment notably augmented the increase in *CpECD* expression starting from the eighth day of storage (Figure 6E).

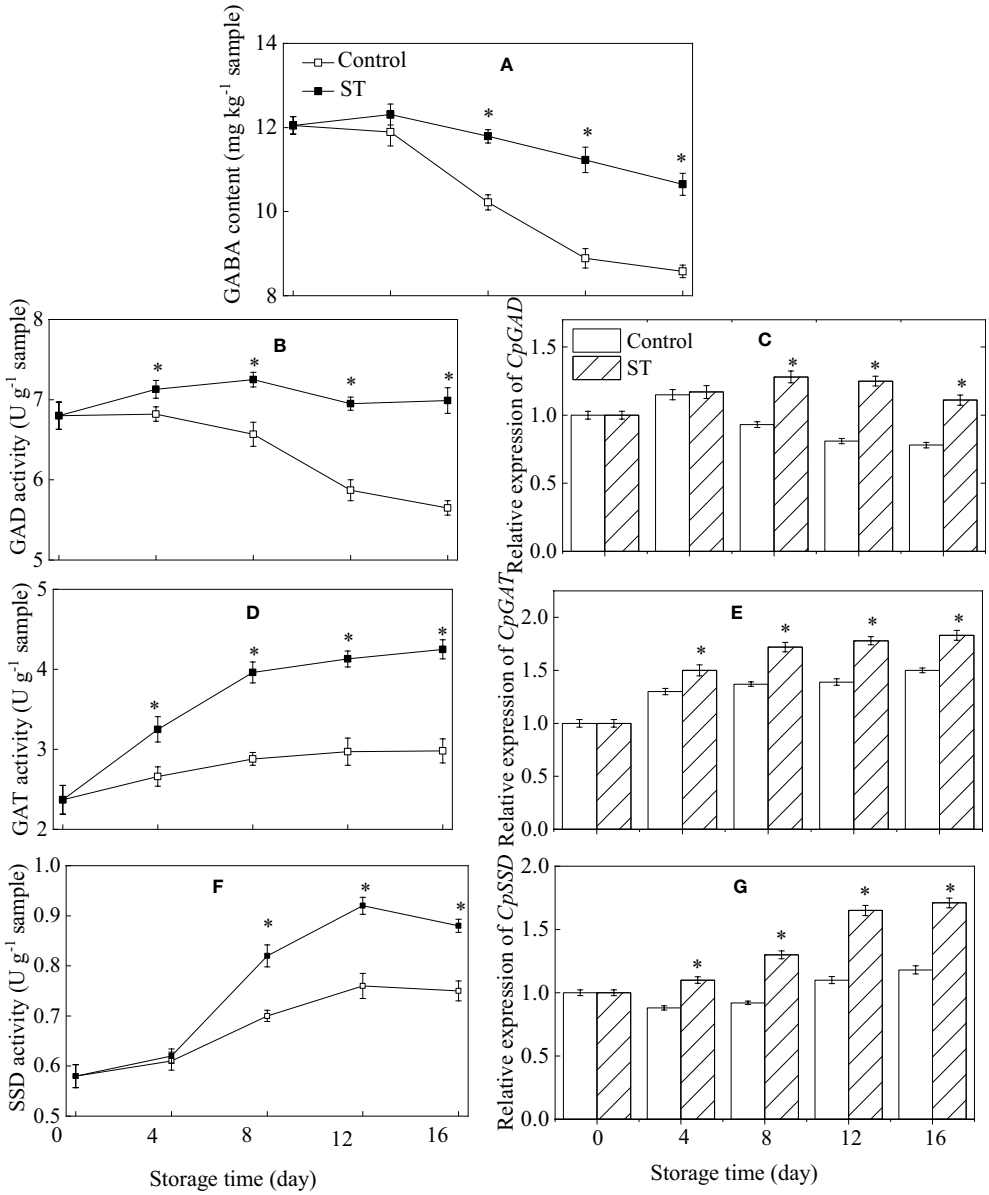

FIGURE 4
Variations of GABA content **(A)**, metabolic enzymatic activities related to GABA **(B, D, F)** and associated gene expression in control **(C, E, G)** and 5 mM ST treated zucchini fruit during cold storage. Vertical bars indicate the standard error of the mean values. Asterisks imply statistically significant differences ($p < 0.05$) between the control and ST treated group in the same day.

4 Discussion

Zucchini is a highly favored fruit enjoyed worldwide with perennial high consumer demand. Unfortunately, zucchini fruit displays an exceptional sensitivity to chilling injury when subjected to conventional cold storage methods. Chilling injury experienced by zucchini fruit during refrigeration is an irreversible physiological issue that significantly impacts its market worth and ability to resist diseases (Palma et al., 2019). Implementing effective postharvest strategies to prevent the progression of chilling injury is critically important for safeguarding the interests of the fruit sector. Growing body of robust evidence suggests that applying ST positively influences the activation of defense mechanisms and aids in mitigating various stress conditions (Marzec, 2016; Soliman et al., 2022). There is a rising interest in the metabolic pathways of internal signaling molecules and functional metabolites in relation to cold storage of horticultural commodities, given their integral participation in diverse physiological functions (Zhang et al., 2021). Earlier research has documented the favorable effects of ST treatment in diminishing chilling injury in several types of fruits, including litchi and pea (Cooper et al., 2018; Liu et al., 2024a). In our current investigation, we observed that immersing zucchini fruit in a solution containing 5 μM ST effectively reduced the occurrence of chilling injury during refrigeration.

It is widely accepted that the development of chilling injury in fruit and vegetable largely stems from cellular membrane damage occurring during the postharvest storage phase (Zhang et al., 2021). The cell membrane constitutes the principal location where chilling

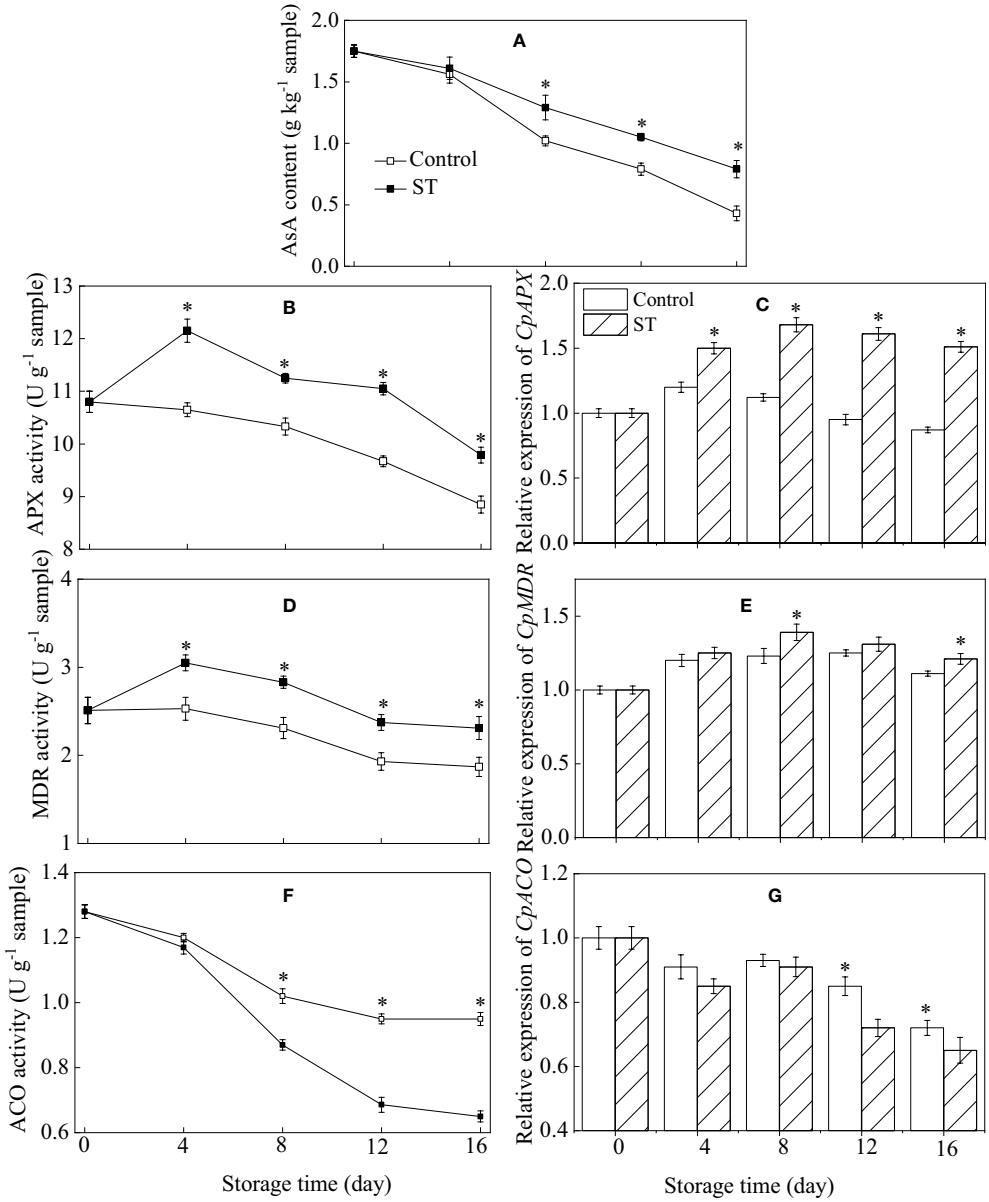

FIGURE 5
Variations of AsA content **(A)**, metabolic enzymatic activities related to AsA **(B, D, F)** and associated gene expression in control **(C, E, G)** and 5 mM ST treated zucchini fruit during cold storage. Vertical bars indicate the standard error of the mean values. Asterisks imply statistically significant differences ($p < 0.05$) between the control and ST treated group in the same day.

injury takes root. When cell membranes undergo a transition from their fluid, liquid-crystalline state to a rigid, solid-gel structure under chilling temperatures, it significantly raises the likelihood of compromised regulated semi-permeability, leading to potential cell membrane dysfunction (Liu et al., 2016). The incidence of chilling injury is frequently linked with oxidative damage, which can be biochemically evidenced by the presence of MDA—a key marker representing the endpoint of lipid peroxidation processes. Both electrolyte leakage and MDA accumulation are well-regarded proxies for assessing the extent of damage to semipermeable membranes, typically caused by oxidative degradation of membrane lipids. These parameters are frequently utilized in determining the functional integrity of the cell membrane (Wang et al., 2023). Increased relative electrolyte leakage in plants promotes more efficient interactions between enzymes and substrates, thereby accelerating intracellular oxidation reactions. Malondialdehyde content serves as an indicator of the severity of oxidative stress endured by the plant (Mohammadi et al., 2023). A wealth of research literature decisively suggested that a reduction in relative electrolyte leakage and MDA accumulation could significantly bolster the chilling tolerance of a variety of horticultural commodities. Zhang et al. (2023) substantiated that a decrease in relative electrolyte leakage and MDA levels jointly contributed to alleviating chilling injury in cucumber fruit when exposed to fucoidan. Our findings showed a consistent rise in electrolyte leakage and MDA levels across both control and treated zucchini fruit. Nonetheless, the application of ST significantly postponed this escalation, consequently attenuating

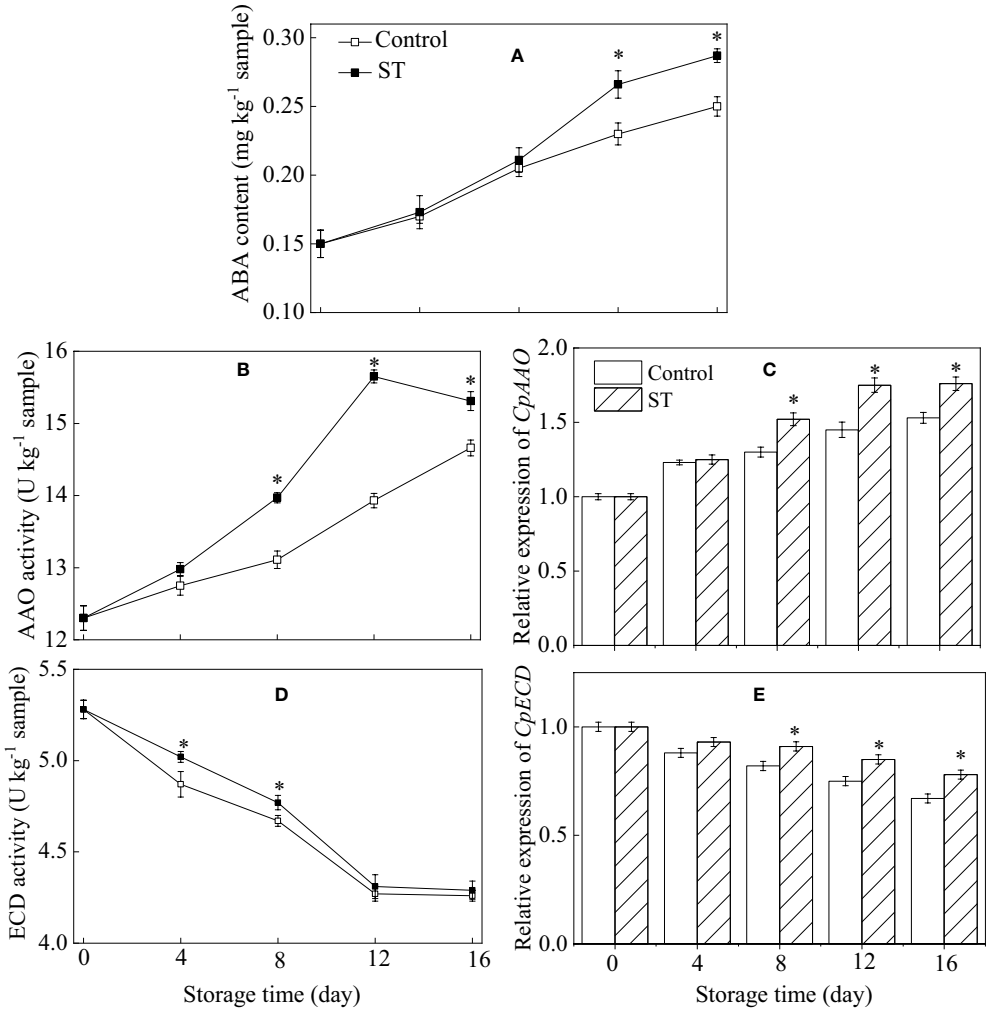

FIGURE 6
Variations of ABA content **(A)**, metabolic enzymatic activities related to ABA **(B, D)** and associated gene expression in control **(C, E)** and 5 mM ST treated zucchini fruit during cold storage. Vertical bars indicate the standard error of the mean values. Asterisks imply statistically significant differences ($p < 0.05$) between the control and ST treated group in the same day.

the progression of chilling injury in the treated zucchini fruit. It can be deduced that the application of ST likely contributes to enhancing chilling resistance in zucchini fruits by virtue of its ability to reduce electrolyte leakage and MDA levels.

Within plant organisms, proline operates as a signaling agent that engages in numerous biochemical reactions, particularly during adverse environmental stress scenarios. Not only does proline serve as an effective osmoprotectant through its compatibility as a solute, but there is compelling evidence suggesting that it also plays crucial roles in neutralizing free radicals, regulating cellular redox status, sequestering metal ions, and instigating protective responses within plants (Raza et al., 2023). Proline is widely recognized for its capacity to augment plant resilience against chilling stress. Ample research supports the involvement of multiple enzymes in proline metabolism, which is crucial for sustaining a fundamental equilibrium in plants. The formation of proline from either glutamate or ornithine is catalyzed by different enzymes; PCS operates in the cytosol while OAT functions in plastids. In parallel, proline breakdown takes place within mitochondria, involving several interconnected metabolic steps driven by a series of enzymes, such as PDH among others (Mattioli et al., 2009). A pronounced accumulation of proline represents a significant adaptive physiological trait contributing to plant resilience against various stress conditions. Notably, in plants susceptible to cold stress, a heightened proline buildup can alleviate the detrimental effects of chilling injury (Wang et al., 2023). There is a mounting body of evidence indicating that the modulation of enzyme activities and gene expression, which in turn affects proline levels, can help mitigate CI in harvested horticultural products during postharvest storage. Aghdam et al. (2019) discovered that melatonin treatment conferred chilling resistance to tomato fruit through the regulation of enzymes associated with proline metabolism, ultimately impacting proline levels. Islam et al. (2022) also reached comparable conclusions, suggesting that the augmented proline levels resulting from heightened PCS and OAT activities and suppressed PDH activity were instrumental in boosting chilling tolerance in pomegranate subjected to 24-epibrassinolide treatment. Significantly, the upregulated expression of genes related to proline metabolism has been shown to confer greater resilience to

environmental stressors. This correlation extends to the response of pear fruit to chilling injury. Sun et al. (2020) discovered that glycine betaine induced chilling tolerance in pear fruit was linked with heightened transcriptional levels of *PuPCS* and *PuOAT*, alongside reduced expression of *PuPDH*, all of which are genes connected to proline metabolism. Increasing proline level during cold storage within plants is a common phenomenon and arises as a net result of augmented biosynthesis and altered degradation processes. The elevated proline levels observed in zucchini fruit during cold storage can be attributed to its innate defense mechanism against cold stress, which stimulates the metabolic pathway of proline synthesis. The observed enhancement seems to stem from the zucchini fruit's reaction to cold stress, compounded by the influence of ST treatment, which further induces proline metabolism. Thus, it is reasonable to infer that ST treatment's positive impact on elevating enzyme activities and gene expressions leads to increased proline accumulation, which in turn aids in reducing the severity of chilling injury.

Arginine, a fundamental building block of proteins and a source for generating certain bioactive substances in higher plants, is a pivotal amino acid deeply integrated into various metabolic processes and actively engaged in the stress response mechanisms of these plants (Nasr et al., 2022). As arginine possesses a high carbon-to-nitrogen ratio, it not only supplies plants with essential nitrogen but also sustains cellular functions and boosts tolerance to diverse abiotic stresses. Its metabolism provides a platform for several ornithine-dependent pathways, such as the production of polyamines and proline, which contribute to stress adaptation (Alcázar et al., 2010). Arginine has drawn widespread interest in research due to its proven effectiveness in improving cold tolerance in harvested crops during postharvest storage. A variety of enzymes participate in the breakdown of arginine, such as arginase and arginine decarboxylase (ADC). ADC enzymatically converts arginine into polyamines; meanwhile, arginase breaks down arginine into urea and ornithine. Ornithine serves as a precursor for both polyamines and proline production through two separate pathways—ornithine decarboxylase (ODC) generates polyamines, while ornithine aminotransferase contributes to proline biosynthesis (Zhang et al., 2013). Additionally, an elevation in arginine content and augmented arginase activity could play a part in ensuring regular cell operations and preserving structural stability (Bokhary et al., 2020). Enhancing chilling tolerance in zucchinis upon application of hot water treatment may be attributed to the increased accumulation of endogenous arginine, facilitated by heightened expression of ADC and ODC genes and corresponding enzyme activities (Bokhary et al., 2020). Similar findings were also seen in papaya fruit treated with arginine, indicating that the acquired chilling tolerance was a result of the synergistic regulation of ARG, ODC, and ADC enzyme activities (Huang et al., 2021b). In our research, we found that the application of ST treatment to zucchini fruit under cold storage conditions led to augmented activities of ARG, ODC, and ADC enzymes, accompanied by a corresponding increase in the expression of their respective genes. Moreover, the elevated enzyme activities and corresponding gene expressions in ST-treated zucchini fruit resulted in higher arginine content, ultimately contributing to enhanced chilling tolerance during refrigerated storage. Based on the aforementioned findings, we could deduce that compared to control fruit, the augmented activities and gene expressions of ARG, ADC, and ODC enzymes in ST-treated zucchini lead to a higher arginine content, which may significantly contribute to the improved chilling tolerance regulated by ST in harvested zucchini fruit.

Several research studies have convincingly demonstrated the complex and diverse roles that endocellular GABA plays in plant growth and development, acting as a signaling agent that influences a wide array of physiological processes. These functions encompass stress responses to growth control, extending to challenges posed by both living organisms and environmental factors (Kinnersley and Turano, 2010; Bown and Shelp, 2016). GABA is also recognized as a stress-responsive metabolite and maintains a strong connection with other intrinsic phytohormones (Palma et al., 2019). In the context of plants, GABA is produced through a specialized metabolic route known as the GABA shunt pathway, a process meticulously managed by a sequence of enzymes—chief among them being SSD, GAT, and GAD (Tarkowski et al., 2020). The enzyme GAD plays a core role in GABA metabolism by facilitating the enzymatic reaction that converts glutamate into GABA. Subsequently, GABA experiences breakdown via the process of transamination. On the other hand, GAT enzyme plays a crucial role in reversibly transforming GABA into succinic semialdehyde via deamination. The ensuing succinic semialdehyde is then converted into succinic acid by SSD. Finally, succinic acid gets processed within the TCA cycle (Tarkowski et al., 2020). The fluctuations in GABA concentration are intricately linked with adverse conditions, such as chilling injury, in a wide array of horticultural species. An increase in GABA levels during cold storage represents a natural physiological adaptation, emerging from the delicate equilibrium between its production and breakdown processes. Multiple researches have convincingly revealed that augmenting chilling tolerance in harvested produce involves stimulation of enzyme activities and the activation of genes encoding for elements of the GABA shunt pathway. In the case of Pyrus ussuriensis, treating the fruit postharvest with $CaCl_2$ has been proven to enhance its resistance to chilling stress by influencing the enzymes and genes tied to GABA metabolic processes (Li et al., 2020). Analogously, it was discovered that loquats treated with phytosulfokine α (PSKα) showed augmented activities of GAD and GAT, which were instrumental in combating postharvest chilling stress (Liu et al., 2024c). In present investigation, we observed that ST treatment in zucchini fruit undergoing cold storage significantly boosted the activity levels of the enzymes of SSD, GAT, and GAD, concurrent with an increase in the expression of the corresponding genes. This upregulation corresponded to a heightened GABA content in the ST-treated zucchini fruit, which was pivotal in fostering enhanced chilling tolerance during storage under low temperature. The findings indicated that ST treatment led to an increased accumulation of GABA in zucchinis potentially by stimulating the activities and gene expressions of GAD, GAT, and SSD, effectively mitigating chilling stress impacts.

Ascorbic acid, commonly referred to as vitamin C, is an essential antioxidant abundantly present in plant life. It significantly influences fruit ripening processes and stress resilience, and exerts a crucial regulatory function in fruit maturation and preservation during

postharvest storage (Smirnoff, 2018). Increasing levels of AsA within fruit not only enrich the trophic profile of the fruit but also bolster its resistance against a broad spectrum of environmental stress factors. The AsA content in fruit tissues is influenced not just by its synthesis but also by its degradation and regeneration, where the ascorbate–glutathione cycle can potentially stimulate AsA accumulation (Liu et al., 2024b). An accumulating body of evidence indicates that a suite of recycling enzymes play a significant role in the AsA metabolic pathway. Utilizing ascorbate as a reactant, the enzyme APX effectively neutralizes excessive hydrogen peroxide, thus guarding cells against oxidative stress damage. Additionally, APX orchestrates the chemical transition of AsA into monodehydroascorbic acid. Simultaneously, monodehydroascorbic acid can revert back to AsA through the enzymatic action of MDR. Ascorbate oxidase, an enzyme of the ascorbate oxidase family, also contributes to the conversion of a portion of AsA into monodehydroascorbic acid through its catalytic action (Luo et al., 2022). Experimental data has convincingly shown a profound interconnection between the incidence of chilling injury and the metabolic processes involving AsA in postharvest horticultural products. According to our previous investigation, the application of melatonin on harvested *Pyrus bretschneideri* fruit led to an improvement in their cold resistance. This enhancement was linked to the increased enzyme activities and gene expression of APX and MDR, which in turn resulted in a rise in ascorbic acid (AsA) content (Liu et al., 2024b). There is evidence suggesting that, in comparison with the biosynthesis of AsA, the cyclic degradation pathways play a potentially more significant role in sustaining the AsA levels within postharvest fruit (Luo et al., 2022; Zheng et al., 2022). For example, Luo et al. (2022) disclosed that subjecting kiwifruit to melatonin treatment led to a decrease in the expression of *AcACO* and increase in the transcriptional level of *AcAPX* and *AcMDR* related to AsA metabolism during cold storage, consequently postponing the onset of chilling injury. In this study, ST treatment was found to enhance the chilling tolerance of zucchini fruit, a process that coincided with heightened activities and gene expressions of APX and MDR enzymes, reduced ACO activity and gene expression, and elevated AsA concentration. Based on these findings, it is hypothesized that the AsA metabolism triggered by ST treatment plays a critical role in inducing improved chilling tolerance in zucchini fruit stored under cold conditions.

Abscisic acid (ABA), a key plant hormone, exerts a vital influence over multiple stages of plant growth and development. Serving as a central regulatory element, ABA orchestrates plants' resistance and adaptive responses to a variety of environmental stressors, particularly those that lead to dehydration, including drought, high salinity, and low temperatures (Chen et al., 2020). The synthesis of ABA progresses through a chain of precisely orchestrated enzymatic steps. The enzyme ECD facilitates the oxidative breakage of 9'-cis-neoxanthin and 9'-cis-violaxanthin, giving rise to xanthoxin. Next, this precursor molecule is converted into abscisic aldehyde via the catalytic action of a short-chain alcohol dehydrogenase. Ultimately, AAO enzyme performs the oxidative reaction that transforms abscisic aldehyde into the final product, ABA (Wu et al., 2023). ECD stands out among these enzymes as a pivotal regulatory component that significantly influences the pace of ABA biosynthesis, acting as a pivotal rate-controlling enzyme in the process. Research indicates that there is a positive correlation between an increase in the internal production of ABA and a decrease in the severity of chilling damage experienced by litchis and zucchinis (Zuo et al., 2021; Liu et al., 2024a). Carvajal et al. (2017) highlighted that during cold storage, zucchini fruit exhibited an upsurge in the inherent abscisic acid levels as well as an enhancement in the activity of AAO, an enzyme integral to ABA biosynthesis. The experimental observations strongly suggest that ABA serves as the key phytohormone contributing to the enhancement of cold tolerance in harvested zucchini fruit during postharvest storage (Carvajal et al., 2017; Zuo et al., 2021). On the contrary, the results presented by Xu et al. (2019) have established that UV-C treatment efficiently postpones the senescence of strawberry fruit by downregulating the expression of genes related to ABA biosynthesis, thereby reducing ABA levels. This variation can be explained by considering the distinct attributes of individual fruit cultivars along with the inherent peculiarities of the diverse fruit tissues. Our research revealed that soaking zucchini fruit in ST solution led to an elevation in ABA concentration, concurrent with increases in both the activities and transcriptional abundance of AAO and ECD enzymes. On this basis, we conjecture that the abscisic acid metabolic alterations induced by ST application contribute to alleviating chilling injury in zucchini fruit during refrigerated storage.

5 Conclusions

In summary, our experimental findings validated that applying ST after harvest proved to be effective in diminishing the effects of chilling injury in zucchini fruit during storage at the low temperature of 4°C. ST treatment led to a decline in the rate of weight loss and a reduction in both relative electrolyte leakage and MDA content in zucchini fruit stored under cold condition for a duration of 16 days. ST treatment triggered an elevation in the levels of proline, arginine, AsA, GABA, and ABA, which was accomplished by means of modulating the enzymatic activities and transcriptional levels of corresponding genes within the zucchini fruit. The foregoing findings suggest that the postharvest application of ST presents a viable strategy to alleviate CI in zucchini fruit when stored under low temperature condition.

Data availability statement

The original contributions presented in the study are included in the article/Supplementary Material. Further inquiries can be directed to the corresponding author.

Author contributions

LW: Data curation, Formal analysis, Investigation, Validation, Writing – original draft. LL: Data curation, Formal analysis, Methodology, Writing – original draft. AH: Formal analysis, Investigation, Methodology, Writing – review & editing. HZ: Formal analysis, Methodology, Project administration, Writing – review & editing. YZ: Conceptualization, Supervision, Writing – review & editing.

Funding

The author(s) declare financial support was received for the research, authorship, and/or publication of this article. Funding support for this research was provided by National Natural Science Foundation of China (No. 31601521) and Shandong Provincial Natural Science Foundation (Project No. ZR2021MC185).

Conflict of interest

The authors declare that the research was conducted in the absence of any commercial or financial relationships that could be construed as a potential conflict of interest.

Publisher's note

Supplementary material

The Supplementary Material for this article can be found online at: https://www.frontiersin.org/articles/10.3389/fpls.2024.1402521/full#supplementary-material

References

Aghdam, M. S., Luo, Z., Jannatizadeh, A., Sheikh-Assadi, M., Sharafi, Y., Farmani, B., et al. (2019). Employing exogenous melatonin applying confers chilling tolerance in tomato fruits by upregulating ZAT2/6/12 giving rise to promoting endogenous polyamines, proline, and nitric oxide accumulation by triggering arginine pathway activity. *Food Chem.* 275, 549–556. doi: 10.1016/j.foodchem.2018.09.157

Alcázar, R., Altabella, T., Marco, F., Bortolotti, C., Reymond, M., Koncz, C., et al. (2010). Polyamines: Molecules with regulatory functions in plant abiotic stress tolerance. *Planta* 231, 1237–1249. doi: 10.1007/s00425-010-1130-0

Bokhary, S. U. F., Wang, L., Zheng, Y., and Jin, P. (2020). Pre-storage hot water treatment enhances chilling tolerance of zucchini (*Cucurbita pepo* L.) squash by regulating arginine metabolism. *Postharvest Biol. Technol.* 166, 111229. doi: 10.1016/j.postharvbio.2020.111229

Bown, A. W., and Shelp, B. J. (2016). Plant GABA: not just a metabolite. *Trends Plant Sci.* 21, 811–813. doi: 10.1016/j.tplants.2016.08.001

Carvajal, F., Palma, F., Jamilena, M., and Garrido, D. (2015). Preconditioning treatment induces chilling tolerance in zucchini fruit improving different physiological mechanisms against cold injury. *Ann. Appl. Biol.* 166, 340–354. doi: 10.1111/aab.2015.166.issue-2

Carvajal, F., Palma, F., Jiménez-Muñoz, R., Jamilena, M., Pulido, A., and Garrido, D. (2017). Unravelling the role of abscisic acid in chilling tolerance of zucchini during postharvest cold storage. *Postharvest Biol. Technol.* 133, 26–35. doi: 10.1016/j.postharvbio.2017.07.004

Chen, K., Li, G. J., Bressan, R. A., Song, C. P., Zhu, J. K., and Zhao, Y. (2020). Abscisic acid dynamics, signaling, and functions in plants. *J. Integr. Plant Biol.* 62, 25–54. doi: 10.1111/jipb.12899

Cooper, J. W., Hu, Y., Beyyoudh, L., Dasgan, H. Y., Kunert, K., Beveridge, C. A., et al. (2018). Strigolactones positively regulate chilling tolerance in pea and in Arabidopsis. *Plant Cell Environ.* 41, 1298–1310. doi: 10.1111/pce.13147

Ferrero, M., Pagliarani, C., Novák, O., Ferrandino, A., Cardinale, F., Visentin, I., et al. (2018). Exogenous strigolactone interacts with abscisic acid-mediated accumulation of anthocyanins in grapevine berries. *J. Exp. Bot.* 69, 2391–2401. doi: 10.1093/jxb/ery033

Huang, Y., Cai, S., Ruan, X., Xu, J., and Cao, D. (2021c). CSN improves seed vigor of aged sunflower seeds by regulating the fatty acid, glycometabolism, and abscisic acid metabolism. *J. Adv. Res.* 33, 1–13. doi: 10.1016/j.jare.2021.01.019

Huang, Q., Song, H., Pan, Y., and Zhang, Z. (2021b). Exogenous arginine enhances the chilling tolerance in postharvest papaya fruit by regulating arginine and proline metabolism. *J. Food Process. Pres.* 45, e15821. doi: 10.1111/jfpp.15821

Huang, D., Wang, Y., Zhang, D., Dong, Y., Meng, Q., Zhu, S., et al. (2021a). Strigolactone maintains strawberry quality by regulating phenylpropanoid, NO, and H2S metabolism during storage. *Postharvest Biol. Technol.* 178, 111546. doi: 10.1016/j.postharvbio.2021.111546

Islam, M., Ali, S., Nawaz, A., Naz, S., Ejaz, S., Shah, A. A., et al. (2022). Postharvest 24-epibrassinolide treatment alleviates pomegranate fruit chilling injury by regulating proline metabolism and antioxidant activities. *Postharvest Biol. Technol.* 188, 111906. doi: 10.1016/j.postharvbio.2022.111906

Jin, L., Cai, Y., Sun, C., Huang, Y., and Yu, T. (2019). Exogenous L-glutamate treatment could induce resistance against *Penicillium expansum* in pear fruit by activating defense-related proteins and amino acids metabolism. *Postharvest Biol. Technol.* 150, 148–157. doi: 10.1016/j.postharvbio.2018.11.009

Kapoor, R. T., Alam, P., Chen, Y., and Ahmad, P. (2024). Strigolactones in plants: from development to abiotic stress management. *J. Plant Growth Regul.* 43, 903–919. doi: 10.1007/s00344-023-11148-z

Kinnersley, A. M., and Turano, F. J. (2010). Gamma aminobutyric acid (GABA) and plant responses to stress. *Crit. Rev. Plant Sci.* 19, 479–509. doi: 10.1080/07352680091139277

Li, M., Li, X., Han, C., Ji, N., Jin, P., and Zheng, Y. (2019). Physiological and metabolomic analysis of cold plasma treated fresh-cut strawberries. *J. Agric. Food Chem.* 67, 4043–4053. doi: 10.1021/acs.jafc.9b00656

Li, M., Yang, M., Liu, X., Hou, G., Jiang, Y., She, M., et al. (2023). Pre-harvest application of strigolactone (GR24) accelerates strawberry ripening and improves fruit quality. *Agronomy* 13, 2699. doi: 10.3390/agronomy13112699

Li, J., Zhou, Q., Zhou, X., Wei, B., Zhao, Y., and Ji, S. (2020). Calcium treatment alleviates pericarp browning of 'Nanguo' pears by regulating the GABA shunt after cold storage. *Front. Plant Sci.* 11. doi: 10.3389/fpls.2020.580986

Liu, J., Bao, Y., Liu, S., Zhu, L., Xu, X., Jiang, G., et al. (2024a). Physiological and transcriptomic analyses reveal mechanisms of exogenous strigolactones to regulate cold tolerance in litchi fruit. *Postharvest Biol. Technol.* 210, 112764. doi: 10.1016/j.postharvbio.2024.112764

Liu, Y., Hou, Y., Yi, B., Zhao, Y., Bao, Y., Wu, Z., et al. (2024c). Exogenous phytosulfokine α alleviates chilling injury of loquat fruit via regulating sugar, proline, polyamine and γ-aminobutyric acid metabolisms. *Food Chem.* 436, 137729. doi: 10.1016/j.foodchem.2023.137729

Liu, L., Huang, A., Wang, B., Zhang, H., Zheng, Y., and Wang, L. (2024b). Melatonin mobilizes the metabolism of sugars, ascorbic acid and amino acids to cope with chilling injury in postharvest pear fruit. *Sci. Hortic.* 323, 112548. doi: 10.1016/j.scienta.2023.112548

Liu, Z., Li, L., Luo, Z., Zeng, F., Jiang, L., and Tang, K. (2016). Effect of brassinolide on energy status and proline metabolism in postharvest bamboo shoot during chilling stress. *Postharvest Biol. Technol.* 111, 240–246. doi: 10.1016/j.postharvbio.2015.09.016

Luo, Z., Zhang, J., Xiang, M., Zeng, J., Chen, J., and Chen, M. (2022). Exogenous melatonin treatment affects ascorbic acid metabolism in postharvest 'Jinyan' kiwifruit. *Front. Nutr.* 9. doi: 10.3389/fnut.2022.1081476

Madebo, M. P., Luo, S., Wang, L., Zheng, Y., and Jin, P. (2021). Melatonin treatment induces chilling tolerance by regulating the contents of polyamine, γ-aminobutyric acid, and proline in cucumber fruit. *J. Integr. Agr.* 20, 3060–3074. doi: 10.1016/S2095-3119(20)63485-2

Marzec, M. (2016). Strigolactones as part of the plant defence system. *Trends Plant Sci.* 21, 900–903. doi: 10.1016/j.tplants.2016.08.010

Mattioli, R., Costantino, P., and Trovato, M. (2009). Proline accumulation in plants. *Plant Signal. Behav.* 4, 1016–1018. doi: 10.4161/psb.4.11.9797

Mohammadi, M., Eghlima, G., and Ranjbar, M. E. (2023). Ascorbic acid reduces chilling injury in anthurium cut flowers during cold storage by increasing salicylic acid biosynthesis. *Postharvest Biol. Technol.* 201, 112359. doi: 10.1016/j.postharvbio.2023.112359

Nasr, F., Razavi, F., Rabiei, V., Gohari, G., Ali, S., and Hano, C. (2022). Attenuation of chilling injury and improving antioxidant capacity of persimmon fruit by arginine application. *Foods* 11, 2419. doi: 10.3390/foods11162419

Palma, F., Carvajal, F., Jimenez-Munoz, R., Pulido, A., Jamilena, M., and Garrido, D. (2019). Exogenous gamma-aminobutyric acid treatment improves the cold tolerance of zucchini fruit during postharvest storage. *Plant Physiol. Bioch.* 136, 188–195. doi: 10.1016/j.plaphy.2019.01.023

Raza, A., Charagh, S., Abbas, S., Hassan, M. U., Saeed, F., Haider, S., et al. (2023). Assessment of proline function in higher plants under extreme temperatures. *Plant Biol.* 25, 379–395. doi: 10.1111/plb.13510

Siebeneichler, T. J., Crizel, R. L., Reisser, P. L., Perin, E. C., Messias, R. S., Rombaldi, C. V., et al. (2022). Changes in the abscisic acid, phenylpropanoids and ascorbic acid metabolism during strawberry fruit growth and ripening. *J. Food Compos. Anal.* 108, 104398. doi: 10.1016/j.jfca.2022.104398

Smirnoff, N. (2018). Ascorbic acid metabolism and functions: a comparison of plants and mammals. *Free Radical Bio. Med.* 122, 116–129. doi: 10.1016/j.freeradbiomed.2018.03.033

Soliman, S., Wang, Y., Han, Z., Pervaiz, T., and El-kereamy, A. (2022). Strigolactones in plants and their interaction with the ecological microbiome in response to abiotic stress. *Plants* 11, 3499. doi: 10.3390/plants11243499

Sun, H., Luo, M. L., Zhou, X., Zhou, Q., Sun, Y., Ge, W. Y., et al. (2020). Exogenous glycine betaine treatment alleviates low temperature-induced pericarp browning of 'Nanguo' pears by regulating antioxidant enzymes and proline metabolism. *Food Chem.* 306, 125626. doi: 10.1016/j.foodchem.2019.125626

Tarkowski, Ł.P., Signorelli, S., and Höfte, M. (2020). γ-Aminobutyric acid and related amino acids in plant immune responses: emerging mechanisms of action. *Plant Cell Environ.* 43, 1103–1116. doi: 10.1111/pce.13734

Valenzuela, J. L., Manzano, S., Palma, F., Carvajal, F., Garrido, D., and Jamilena, M. (2017). Oxidative stress associated with chilling injury in immature fruit: postharvest technological and biotechnological solutions. *Int. J. Mol. Sci.* 18, 1467. doi: 10.3390/ijms18071467

Wang, L., Zhang, H., Jin, P., Guo, X., Li, Y., Fan, C., et al. (2016). Enhancement of storage quality and antioxidant capacity of harvested sweet cherry fruit by immersion with β-aminobutyric acid. *Postharvest Biol. Technol.* 118, 71–78. doi: 10.1016/j.postharvbio.2016.03.023

Wang, B., Zhang, H., Li, Y., Zheng, Y., and Wang, L. (2023). Elevated level of chilling tolerance in cucumber fruit was obtained by β-aminobutyric acid via the regulation of antioxidative response and metabolism of energy, proline and unsaturated fatty acid. *Sci. Hortic.* 307, 111521. doi: 10.1016/j.scienta.2022.111521

Wu, W., Cao, S., Shi, L., Chen, W., Yin, X., and Yang, Z. (2023). Abscisic acid biosynthesis, metabolism and signaling in ripening fruit. *Front. Plant Sci.* 14. doi: 10.3389/fpls.2023.1279031

Wu, F., Gao, Y., Yang, W., Sui, N., and Zhu, J. (2022). Biological functions of strigolactones and their crosstalk with other phytohormones. *Front. Plant Sci.* 13. doi: 10.3389/fpls.2022.821563

Wu, J., Tang, R., and Fan, K. (2024). Recent advances in postharvest technologies for reducing chilling injury symptoms of fruits and vegetables: A review. *Food Chem. X.* 21, 101080. doi: 10.1016/j.fochx.2023.101080

Xu, Y., Charles, M. T., Luo, Z., Mimee, B., Tong, Z., Roussel, D., et al. (2019). Preharvest UV-C treatment affected postharvest senescence and phytochemicals alternation of strawberry fruit with the possible involvement of abscisic acid regulation. *Food Chem.* 299, 125138. doi: 10.1016/j.foodchem.2019.125138

Yun, Z., Gao, H., Chen, X., Chen, Z., Zhang, Z., Li, T., et al. (2020). Effects of hydrogen water treatment on antioxidant system of litchi fruit during the pericarp browning. *Food Chem.* 336, 127618. doi: 10.1016/j.foodchem.2020.127618

Zhang, W., Jiang, H., Cao, J., and Jiang, W. (2021). Advances in biochemical mechanisms and control technologies to treat chilling injury in postharvest fruits and vegetables. *Trends Food Sci. Technol.* 113, 355–365. doi: 10.1016/j.tifs.2021.05.009

Zhang, Y., Lin, D., Yan, R., Xu, Y., Xing, M., Liao, S., et al. (2023). Amelioration of chilling injury by fucoidan in cold-stored cucumber via membrane lipid metabolism regulation. *Foods* 12, 301. doi: 10.3390/foods12020301

Zhang, M., Liu, W., Li, C., Shao, T., Jiang, X., Zhao, H., et al. (2019). Postharvest hot water dipping and hot water forced convection treatments alleviate chilling injury for zucchini fruit during cold storage. *Sci. Hortic.* 249, 219–227. doi: 10.1016/j.scienta.2019.01.058

Zhang, X., Shen, L., Li, F., Meng, D., and Sheng, J. (2013). Amelioration of chilling stress by arginine in tomato fruit: Changes in endogenous arginine catabolism. *Postharvest Biol. Technol.* 76, 106–111. doi: 10.1016/j.postharvbio.2012.09.012

Zheng, X., Gong, M., Zhang, Q., Tan, H., Li, L., Tang, Y., et al. (2022). Metabolism and regulation of ascorbic acid in fruits. *Plants* 11, 1602. doi: 10.3390/plants11121602

Zuo, X., Cao, S., Zhang, M., Cheng, Z., Cao, T., Jin, P., et al. (2021). High relative humidity (HRH) storage alleviates chilling injury of zucchini fruit by promoting the accumulation of proline and ABA. *Postharvest Biol. Technol.* 171, 111344. doi: 10.1016/j.postharvbio.2020.111344

frontiers | Frontiers in Plant Science

TYPE Original Research
PUBLISHED 15 August 2024
DOI 10.3389/fpls.2024.1435066

OPEN ACCESS

EDITED BY
Isabel Lara,
Universitat de Lleida, Spain

REVIEWED BY
Xiaoxu Li,
Chinese Academy of Agricultural Sciences (CAAS), China
Ke Wang,
Anhui Agricultural University, China

*CORRESPONDENCE
Ting Min
minting1323@163.com

†These authors have contributed equally to this work and share first authorship

RECEIVED 19 May 2024
ACCEPTED 30 July 2024
PUBLISHED 15 August 2024

CITATION
Lu K, Wu X, Yuan R, Yi Y, Wang L, Ai Y, Wang H and Min T (2024) Mechanism of exogenous methyl jasmonate in regulating the quality of fresh-cut Chinese water chestnuts.
Front. Plant Sci. 15:1435066.
doi: 10.3389/fpls.2024.1435066

Mechanism of exogenous methyl jasmonate in regulating the quality of fresh-cut Chinese water chestnuts

Keyan Lu[1†], Xinping Wu[1†], Ruimin Yuan[1], Yang Yi[1,2], Limei Wang[3], Youwei Ai[1], Hongxun Wang[2,3] and Ting Min[1,2*]

[1]College of Food Science and Engineering, Wuhan Polytechnic University, Wuhan, China, [2]Hubei Key Laboratory for Processing and Transformation of Agricultural Products (Wuhan Polytechnic University), Wuhan, China, [3]School Biology and Pharmaceutical Engineering, Wuhan Polytechnic University, Wuhan, China

Fresh-cut Chinese water chestnuts (CWCs) are susceptible to yellowing and browning during storage due to mechanical damage and the loss of protective outer skin, adversely affecting their marketability and shelf life. Methyl jasmonate (MeJA) is currently extensively used for food preservation, but it has not been used in Chinese water chestnuts. This study investigated the effect of MeJA treatment on the quality of fresh-cut CWCs. Fresh-cut CWCs immersed in 20 μM MeJA solution for 10 min and stored at 10°C for 5 d effectively delayed the yellowing process, reduced the respiration rate, and minimized the weight and soluble solids loss during storage. In addition, MeJA treatment induced the activities of superoxide dismutase (SOD) and catalase (CAT), which improved the antioxidant capacity of fresh-cut CWCs and inhibited the generation of reactive oxygen species (ROS). Meanwhile, MeJA treatment inhibited the activities of phenylalanine aminotransferase (PAL), polyphenol oxidase (PPO) and peroxidase (POD). The results of quantitative real-time PCR (qRT-PCR) showed that MeJA down-regulated the expression of *CwCHS1*, *CwCHS2*, *CwCHS3* and *CwCHI2* in freshly cut CWCs and inhibited the accumulation of flavonoids, thus delaying the surface discoloration of freshly cut CWCs.

KEYWORDS

fresh-cut, Chinese water chestnut, methyl jasmonate, yellowing, quality

1 Introduction

Chinese water chestnut (CWC, Eleocharis Tuberosa) is a commonly found aquatic plant known for its edible bulb with a sweet, juicy, and crisp texture, which is highly popular in China (Song et al., 2019). However, CWC bulbs tend to be covered in muddy outer purplish-brown skin, necessitating cleaning and peeling before consumption. Manual cleaning and peeling processes are time-consuming and escalate labor costs. To address

these challenges and provide convenience to consumers, the industry has introduced sorting machines, cleaning machines, and peelers (Zhou et al., 2022) to achieve standardized processing of fresh-cut CWCs and enhance production efficiency. Despite these advancements, removing the outer skin during processing exposes the meat of fresh-cut CWCs to mechanical damage, rendering its cells vulnerable. Consequently, fresh-cut CWCs are highly susceptible to yellowing during storage, leading to a rapid decline in organoleptic quality and a loss of commercial value (Li et al., 2022).

The phenomenon of browning, which occurs in many freshly cut fruits and vegetables, primarily results from enzymatic activity (Hasan et al., 2020). In the presence of oxygen, phenolic compounds in these produce items are transformed into quinones through the action of PPO and POD. These quinones polymerize into brown pigments (Teng et al., 2020). Additionally, the presence of excessive ROS, such as superoxide anion ($O_2\cdot^-$) and hydrogen peroxide (H_2O_2), accelerates browning and can lead to membrane lipid peroxidation, causing increased permeability (Zhu et al., 2022a). The disruption of cell membrane integrity accelerates the reaction of phenolics and other substances with oxygen and enzymes, resulting in the rapid deterioration of the appearance of fruits and vegetables (Zha et al., 2022).

As described by previous authors, discoloration of fresh-cut CWCs is primarily due to specific metabolites on the surface, with yellowing substances mainly identified as flavonoids, such as eriodictyol and naringenin (Pan et al., 2015). The synthesis of flavonoids involves key enzymes in the phenylpropanoid pathway, such as PAL, chalcone isomerase (CHI), and chalcone synthase (CHS) (Li et al., 2022). It is now understood that PAL serves as a bridge between primary and phenylpropanoid metabolism, initiating the catalysis of phenylpropanoid metabolism. This metabolic pathway generates secondary compounds like phenols, lignin, and flavonoids, which are susceptible to enzymatic browning and can transform into brown substances under the influence of PPO and POD (Teng et al., 2020).

Much research has been conducted to retard the quality deterioration of fresh-cut CWCs. Early approaches involved chitosan coating (Pen and Jiang, 2003), citric acid (Jiang et al., 2004), and hydrogen peroxide (Peng et al., 2008) to inhibit yellowing. In consideration of environmental friendliness and food safety, more recent studies have explored soaking treatments with ascorbic acid and ferulic acid (Song et al., 2019), hydrogen sulfide (Dou et al., 2021), melatonin (Xu et al., 2022), and hydrogen-rich water (Li et al., 2022). We are also investigating convenient postharvest techniques to inhibit the yellowing of fresh-cut CWCs. A literature review revealed that methyl jasmonate, a naturally occurring plant compound, is currently under investigation for food preservation (Wang et al., 2021).

Methyl jasmonate (MeJA) is a volatile phytohormone with robust biological activity (Cheong and Do Choi, 2003). As a signaling molecule, MeJA plays a pivotal role in various physiological and biochemical processes in plants and regulates the synthesis of other hormones (Per et al., 2018). While storing numerous postharvest fruits and vegetables, MeJA has been shown to maintain quality and enhance systemic acquired resistance (Wang et al., 2021). Studies have demonstrated that exogenous MeJA increases the production of volatiles, phenolics, and unsaturated fatty acids in postharvest fruits and vegetables. MeJA promotes the release of aroma-related lactones in peaches (Cai et al., 2020), significantly elevates carotenoid content in cherry tomatoes after harvest (Liu et al., 2018b), induces the synthesis of ripening aromatic volatiles (Qin et al., 2017), enhances ester synthesis capacity in Nanguo pears (Luo et al., 2021), and improves the flavor quality of postharvest fruits. MeJA also contributes to color and firmness improvement, delays aging, and reduces or prevents cold damage symptoms by boosting antioxidant enzyme activity and promoting antioxidant production in postharvest fruits and vegetables (Dong et al., 2016; Wang et al., 2019b; Zhu et al., 2022b). Concha et al. (2013) found that MeJA promotes fragaria chiloensis fruit ripening and defense-related processes through up-regulation of anthocyanin-related genes (*CHS*, *CHI*, *F3H*). In addition, ethephon and 1-methylcyclopropene were found to inhibit flavonoid accumulation in fresh-cut CWCs by down-regulating *CwCHS1* and *CwCHI1* expression in fruit (Xu et al., 2023b). However, MeJA has hitherto not been applied to fresh-cut CWCs preservation.

Given the various factors contributing to the yellowing of fresh-cut CWCs, including enzymatic browning, active oxygen metabolism, membrane lipid metabolism, and flavonoid accumulation (Pan et al., 2015; Zhu et al., 2022a), we hypothesized that MeJA may delay changes in the appearance of fresh-cut CWCs through these pathways. Consequently, the aim of our study was to assess the effect of MeJA on fresh-cut CWCs and its mechanisms by measuring basic quality indicators, relevant indicators of antioxidant system and reactive oxygen species metabolism, and expression of genes related to the phenylpropane metabolic pathway. We also provided insights that may prove valuable for the application of MeJA in preserving the quality of other food products.

2 Materials and methods

2.1 Materials and treatment

CWCs were procured from a local market and pre-cooled at 4°C for 24 h. The laboratory was sterilized with ozone under completely closed conditions for two hours before commencing the experiment. Following washing and peeling, fresh CWCs with intact, thick, hard, and dark brown peels, measuring 35–45 cm in diameter and devoid of external damage, internal diseases, or pests, were selected for subsequent experiments. Based on prior experiments, we established an immersion duration of 10 minutes (Xu et al., 2020; Duan et al., 2022). We subsequently conducted experiments to determine the optimal MeJA concentration. Fresh-cut CWCs were immersed in MeJA solutions at 10, 20, 50, and 100 μM for 10 min, with 20 μM MeJA yielding superior inhibition of yellowing compared to other groups. Subsequent experiments were conducted in accordance with this result.

The selected CWCs were randomly divided into treatment and control groups after immersing them in a 0.1% NaClO solution for

5 minutes. The treatment group was immersed in a 20 μM MeJA solution (containing 1% anhydrous ethanol for dissolution), while the control group was immersed in distilled water containing 1% anhydrous ethanol. After 10 min of immersion, all CWCs were removed to allow drying. Each group of two CWCs was sealed in a polyethylene bag (200 × 280 mm) containing a polyethylene tray (180 × 120 × 25 mm) (Xu et al., 2023a). Subsequently, all samples were stored at 10°C and analyzed daily. The sample tissues were frozen in liquid nitrogen and stored in -80°C for backup.

2.2 Appearance and degree of browning

Camera photography was employed to assess the appearance of fresh-cut CWCs using images (Canon, EOS550D). The L^*, a^*, and b^* values were determined using a JZ-300 colorimeter (Shenzhen Jinzhun Instrument Equipment Co., Ltd., China). The color difference (,E) was calculated using the following equation:

$$\Delta E = \sqrt{(L^* - L_0^*)^2 + (a^* - a_0^*)^2 + (b^* - b_0^*)^2}$$

While L_0, a_0, and b_0 were all values on the 0th day, L*, a*, and b* were readings at each sampling point during the storage period. Measurement of the degree of browning was in accordance with the method of Min et al. (2017) and was expressed as $A_{410\ nm} \times 10$.

2.3 Weight loss rate, total soluble solids content, O_2 and CO_2 content in bags

Weight loss rates of fresh-cut CWCs were evaluated using the weighing method as described by Wu et al. (2024). The measurement of total soluble solid content was referenced from a study by Xu et al. (2022). Tissues weighing 10 g were manually ground and filtered through a fine cotton gauze. Subsequently, total soluble solids were assessed using a portable refractometer (Wu et al., 2024).

According to Wu et al. (2024), O_2 and CO_2 contents in bags of fresh-cut CWCs were determined using a portable headspace analyzer (Checkpoint 3, Mocon, Denmark).

2.4 Total phenolics, total flavonoid, and soluble quinone content

The total phenolics content (TPC) was determined using the method of Min et al. (2017), and the results were quantified with standard gallic acid samples, presented in $mg \cdot kg^{-1}$. The determination of soluble quinone and total flavonoid content (TFC) followed the procedure outlined by Xu et al. (2022). Their absorbance was measured at 437 nm and 510 nm, and the results were presented as $A_{437\ nm} \cdot g^{-1}$ and $mg \cdot kg^{-1}$, respectively.

2.5 PAL, PPO, and POD activities

PAL, PPO and POD activities were assessed according to previous descriptions (Min et al., 2019). The variation of PAL, PPO and POD activities were measured at 290, 420 and 470 nm per minute. Defined as the amount of enzyme required per gram of fresh weight for a change in absorbance value (0.1, 0.001 and 0.01), respectively, the results were expressed as $U \bullet g^{-1}$.

2.6 $O_2\bullet^-$ and $OH\bullet^-$ generation rate, H_2O_2 and malondialdehyde (MDA) content

$O_2 \cdot^-$ generation rate was performed as described by Chen et al. (2022), and the results are rendered in $nmol \cdot g^{-1} \cdot min^{-1}$. $OH \cdot^-$ generation rate and H_2O_2 content were evaluated using $OH \cdot^-$ and H_2O_2 kits (Nanjing Jianjian Bioengineering Research Institute Co., Ltd., Nanjing, China), and the results are presented in $mmol \cdot g^{-1} \cdot min^{-1}$ and $mmol \cdot g^{-1}$, respectively. MDA content was measured in accordance with Xu et al. (2022) and expressed in $\mu mol \cdot g^{-1}$.

2.7 SOD and CAT activities

Based on the description of Chen et al. (2022), changes in activity were evaluated using SOD and CAT kits (Nanjing Jianjian Bioengineering Research Institute Co., Ltd., Nanjing, China), and the results are rendered in $U \bullet g^{-1}$.

2.8 Expression of genes related to phenylpropane metabolic pathway

According to our previous study, the sequences of genes encoding key enzymes of the phenylpropanoid pathway were obtained based on the NCBI database (*CwCHS1*、*CwCHS2*、*CwCHS3*、*CwCHI2*) (Xu et al., 2023b). Extraction of RNA from CWCs and cDNA synthesis and qRT-PCR reactions were performed as described by Xu et al. (2023b). Three biological replicates were performed for each sampling site. The internal reference gene in this study was *CwActin* (MG742687.1). Primer sequences were designed using Primer 5.0 software (Supplementary Table 1).

2.9 Statistical analysis

The experiment was repeated three times and the results were expressed as mean ± standard error. Comparisons of means between groups were analyzed by one way analysis of variance (ANOVA) using SPSS 19 followed by Duncan's test. $p < 0.05$ indicates statistical significance.

3 Results

3.1 The effect of MeJA on appearance, color change, and browning degree

Appearance quality and color of fruits are critical factors in assessing its quality (Zhu et al., 2022b) and significantly influence consumer purchasing decisions. As shown in Figure 1A, fresh-cut CWCs exhibited significant yellowing during storage. The CWCs in the control group displayed pronounced yellowing on the third day, while CWCs soaked in MeJA exhibited less discoloration. Severe yellowing appeared on the surface of the control group in the last two days, whereas discoloration in the MeJA-treated group was significantly inhibited. As shown in Figure 1B, the browning degree of fresh-cut CWCs gradually increased with time. On day 5, the browning degree increased 2.26-fold in the MeJA group and 3.24-fold in the CK group compared to day 0. The MeJA group consistently exhibited significantly less browning than the control group.

The color difference values reflect the color change of fresh-cut CWCs in numerical form (Wu et al., 2024). The L^* value of fresh-cut CWCs decreased continuously during storage, but the MeJA-treated group remained consistently higher than the control group ($p < 0.05$) (Figure 1C). As shown in Figures 1D, E, the a^* and b^* values of CWCs increased continuously, and those of the MeJA group were significantly lower than the control group in the last three days. Compared to the control, MeJA significantly suppressed the decrease in L^* values as well as the increase in a^* and b^* values of fresh-cut CWCs. During storage, the ,E value of the MeJA treatment group was always lower than that of the CK group, with an overall increasing trend, which was consistent with the appearance and browning results (Figure 1F). The results indicated that MeJA treatment could effectively delay the browning of fresh-cut CWCs.

3.2 The effect of MeJA on soluble solids content, weight loss rate, and headspace gas composition in bags

The transition from fruit ripening to aging is often accompanied by decreased soluble solids content (Wu et al., 2024). As shown in Figure 2A, the soluble solid content initially increased and then decreased. The CK group reached its peak on day 2 and then experienced a sharp decline, while fresh-cut water chestnuts treated with MeJA soaking peaked on the third day. On day 5, the soluble solid content of the MeJA group decreased by 5.20% compared to the initial value, while that of the CK group decreased by 20.55%. MeJA resulted in a smoother and delayed decrease in the soluble solid content of CWCs compared to the control. The weight loss rate continuously increased, as depicted in Figure 2B, but MeJA suppressed this trend compared to the CK group. In summary, MeJA could effectively inhibit the reduction of weight and soluble solids in fresh-cut CWCs.

The headspace gas in the bags can indirectly reflect the respiration intensity of fresh-cut CWCs (Chen et al., 2022). Fresh-cut CWCs showed a gradual decrease in O_2 content and a gradual increase in CO_2 content (Figures 2C, D). Starting from day 3, MeJA effectively suppressed this change compared to the control, indicating that MeJA could effectively inhibit the respiration of fresh-cut CWCs.

3.3 The effect of MeJA on TPC, soluble quinone content, and TFC

Phenolic compounds can be converted to quinones through reactions catalyzed by PPO and POD in the presence of oxygen, forming brown pigments (Teng et al., 2020). Both TPC and soluble quinone contents of freshly cut CWCs exhibited an increasing trend, but those of the MeJA group increased to a lesser extent than the control (Figures 3A, B).

Pan et al. (2015) proposed that the yellowing of fresh-cut CWCs was due to the accumulation of flavonoids. In Figure 3C, the TFC of freshly cut CWCs increased rapidly with time. On day 5, TFC in the CK group increased by 69.44% compared to day 0, while the MeJA-treated group had only increased by 50.71%. MeJA significantly inhibited the increase in TFC compared to the control ($p < 0.05$). In conclusion, MeJA could delay the surface yellowing of fresh-cut CWCs by reducing the accumulation of soluble quinone and TFC.

3.4 The effect of MeJA on PAL, PPO, and POD activities

When plants experience mechanical damage, the activity of PAL in their tissues increases, enabling plants to produce more phenolics (Min et al., 2017). These phenolics react with O_2 to produce quinones, catalyzed by PPO and POD, leading to the browning of fruits and vegetables (Liu et al., 2018a). According to Figures 4A–C, PAL and POD activities showed an increasing trend, while PPO activities continued to decrease. On day 5, PAL and POD activity in the control group increased by 4.75-fold and 2.35-fold compared to the initial values, while in the MeJA group, they increased by only 3.39-fold and 1.48-fold. Except for day 0, MeJA consistently and significantly maintained PAL, PPO, and POD activities at lower levels than the control throughout this period.

3.5 The effect of MeJA on $O_2^{\bullet-}$ and $OH^{\bullet-}$ generation rate, H_2O_2 and malondialdehyde (MDA) content

An increasing body of evidence suggests that abiotic stress, such as mechanical injury or cold, induces the production of ROS in plants, including $O_2\cdot^-$, $OH\cdot^-$, H_2O_2, and lipid peroxides, disrupting metabolic homeostasis and potentially causing oxidative stress an·d cell damage (Xu et al., 2023a). Excess ROS can increase cell membrane permeability, lipid peroxidation, and DNA mutation, resulting in oxidative stress and cell damage (Apel and Hirt, 2004). Oxidative stress can stimulate the biosynthesis of flavonoids (Li et al., 2022), further promoting the yellowing of fresh-cut CWCs.

As shown in Figure 5A, the $OH\cdot^-$ production rate reached its peak or sub-peak on the first day due to mechanical damage. The

production rate of both groups decreased substantially on the first day and reached essentially the same level. From the first day, the $OH^{\cdot}$ production rate increased sharply in both treatment groups, although it consistently remained significantly lower in the MeJA group than the CK group. Both groups exhibited a fluctuating decrease in the $O_2^{\cdot-}$ generation rate (Figure 5B). From day 0 to day 2, the $O_2^{\cdot-}$ generation rate decreased continuously and then increased. The MeJA group began to decline on the third day, while the CK group began to decline after peaking on the fourth day. MeJA significantly inhibited the $O_2^{\cdot-}$ generation rate compared to the control.

The H_2O_2 content increased with time (Figure 5C). Ultimately, the H_2O_2 content in the MeJA group was 2.20-fold higher than on day 0, whereas that in the control group was 3.18-fold higher. MeJA significantly inhibited the accumulation of H_2O_2 from the first day. MDA is used to characterize the extent of oxidative damage to cell membranes (Wu et al., 2024). The MDA content of fresh-cut CWCs increased during storage (Figure 5D). MeJA significantly inhibited the accumulation of MDA in fresh-cut CWCs during storage, except on the first day. At the end of storage (5d), the MDA content of the CK group was 1.50 times higher as compared to the MeJA-treated group.

3.6 The effect of MeJA on SOD and CAT activities

Excessive ROS can lead to cellular damage and even apoptosis, while highly active antioxidant enzymes can mitigate the damage caused by ROS and maintain the relative balance of ROS metabolism. SOD catalyzes the conversion of $O_2^{\cdot-}$ to H_2O_2, and CAT can convert H_2O_2 to O_2 and H_2O, helping maintain the cellular environment's relative stability and protect cells from ROS (Kong et al., 2020). Both SOD and CAT activities exhibited a wave-like decreasing trend (Figure 6). SOD activity decreased sharply during the early storage stages, then increased and decreased slightly from day 3 to 5 (Figure 6A). Overall, MeJA enhanced the SOD activity of fresh-cut CWCs.

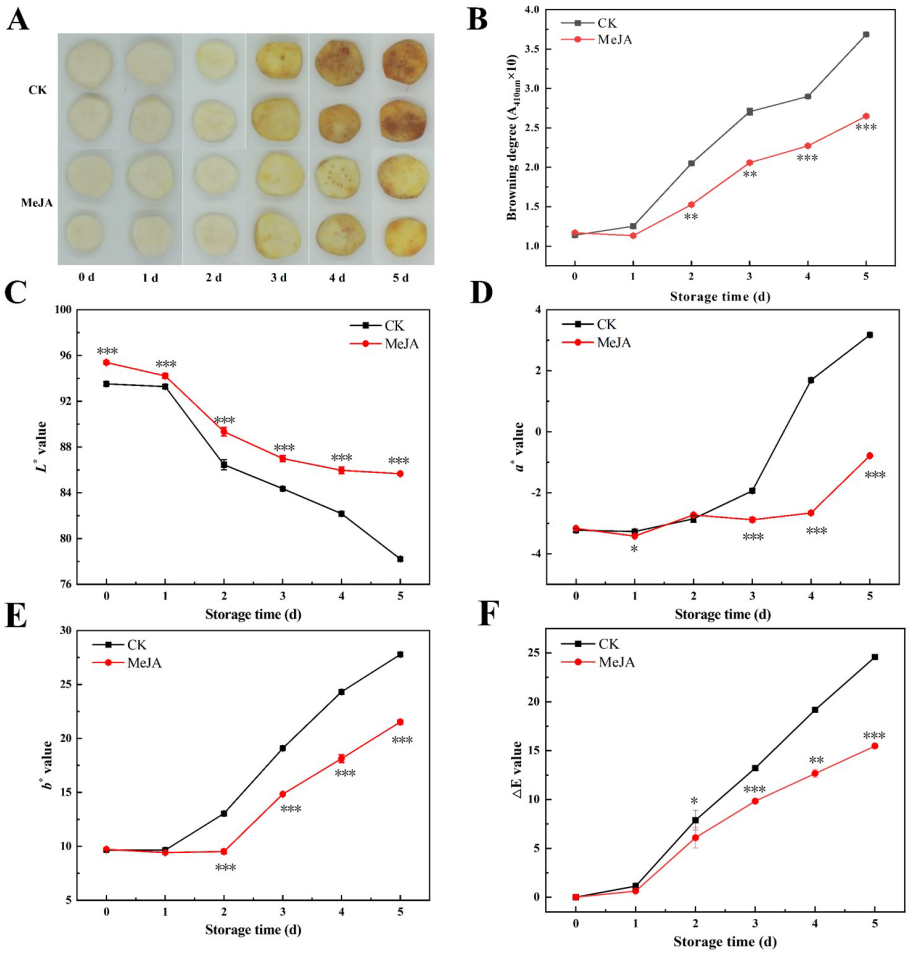

FIGURE 1
The effect of MeJA treatment on the appearance **(A)**, browning degree **(B)**, color change **(C-E)**, and ΔE value **(F)** of fresh-cut CWCs. Error bars represent the standard error of three biological replicates. *、 **、 ***: represent the level of difference between MeJA group and CK group is $p < 0.05$、$p < 0.01$、$p < 0.001$, respectively.

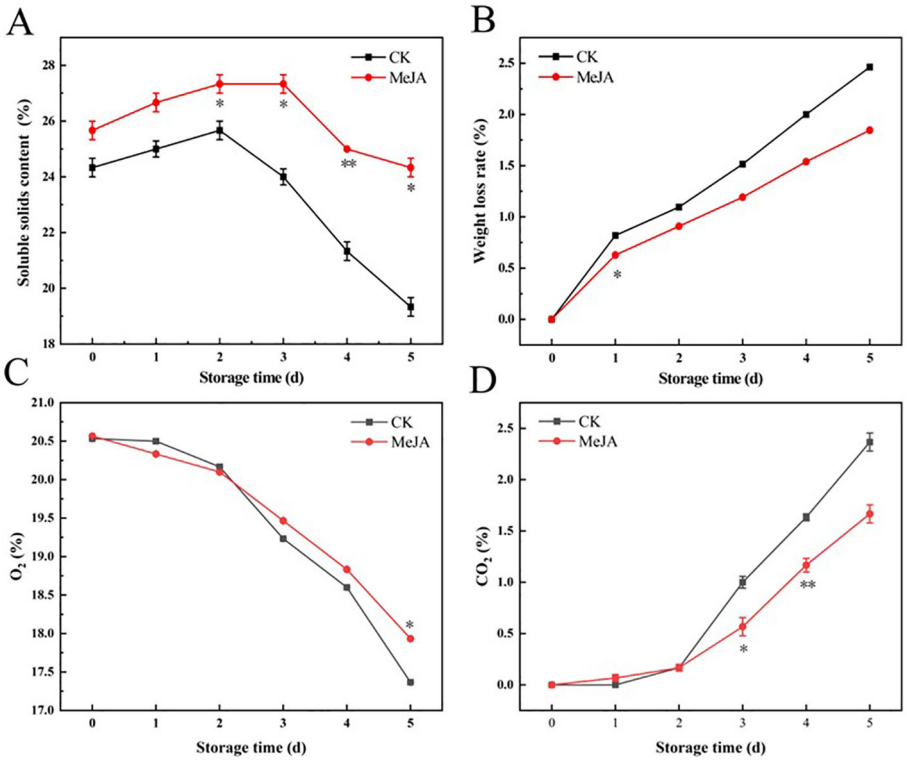

FIGURE 2
The effect of MeJA treatment on the soluble solids content **(A)**, weight loss rate **(B)**, O_2 content **(C)** and CO_2 content **(D)** of fresh-cut CWCs. Error bars represent the standard error of three biological replicates. *、 **、 ***: represent the level of difference between MeJA group and CK group is $p < 0.05$、$p < 0.01$、$p < 0.001$, respectively.

As shown in Figure 6B, CAT activity in the MeJA group was significantly higher than that in the CK group as a whole and peaked at day 4.In short, MeJA also improved the CAT activity of fresh-cut CWCs.

3.7 Gene expression levels

In this experiment, in order to investigate the mechanism by which MeJA can delay surface discoloration and quality deterioration of fresh-cut CWCs during storage, *CwCHS* and *CwCHI2* genes were obtained for qPCR analysis using the materials of this experiment (fresh-cut CWCs). In the phenylpropane pathway, *CHS* and *CHI* are important precursors and key enzymes for flavonoid synthesis (Song et al., 2019). During the storage period, the expression levels of *CwCHS1* and *CwCHI2* genes showed an overall increasing trend, but were significantly lower in the MeJA-treated group compared with the CK group (Figure 7). As can be seen from Figures 7A, C, the MeJA group significantly down-regulated the expression of *CwCHS1* and *CwCHS3* genes in fresh-cut CWCs compared to the CK group (2–5 d). However, the expression level of *CwCHS2* gene was significantly higher in the CK group than in the MeJA group except for day 2, and the MeJA group significantly down-regulated the expression of *CwCHI2* gene in the later stages of storage (3–5 d). The *CwCHS2* and *CwCHI2* gene expression levels in the CK group were 5.02 and 2.97 times higher than those in the MeJA group (5 d), respectively (Figures 7B, D). The results indicated that MeJA inhibited the accumulation of flavonoids in fresh-cut CWCs probably by down-regulating the expression of *CwCHS1*, *CwCHS2*, *CwCHS3* and *CwCHI2*, which delayed the surface discoloration of fresh-cut CWCs.

4 Discussion

People generally assess the freshness of fruits and vegetables based on sensory qualities such as appearance, smell, texture, and taste (Xu et al., 2023a), a principle that especially applies to fresh-cut products. Due to mechanical damage and the loss of their protective outer layer after peeling, water chestnuts are prone to browning when exposed to air, significantly shortening their shelf life (Xu et al., 2022). Among our findings, the immersion of fresh-cut CWCs in 20 μM MeJA for 10 min notably suppressed yellowing, supported by the L^*, a^*, b^* values and the degree of browning. MeJA treatment has also been observed to effectively inhibit browning in other produce, such as litchi fruit (Deshi et al., 2021), thereby corroborating our findings.

The enhanced respiration and transpiration in fresh-cut CWCs, resulting from loss of their outer skin protection, make them more vulnerable to water loss during storage. Mechanical damage compromises cellular integrity, accelerating the loss of internal

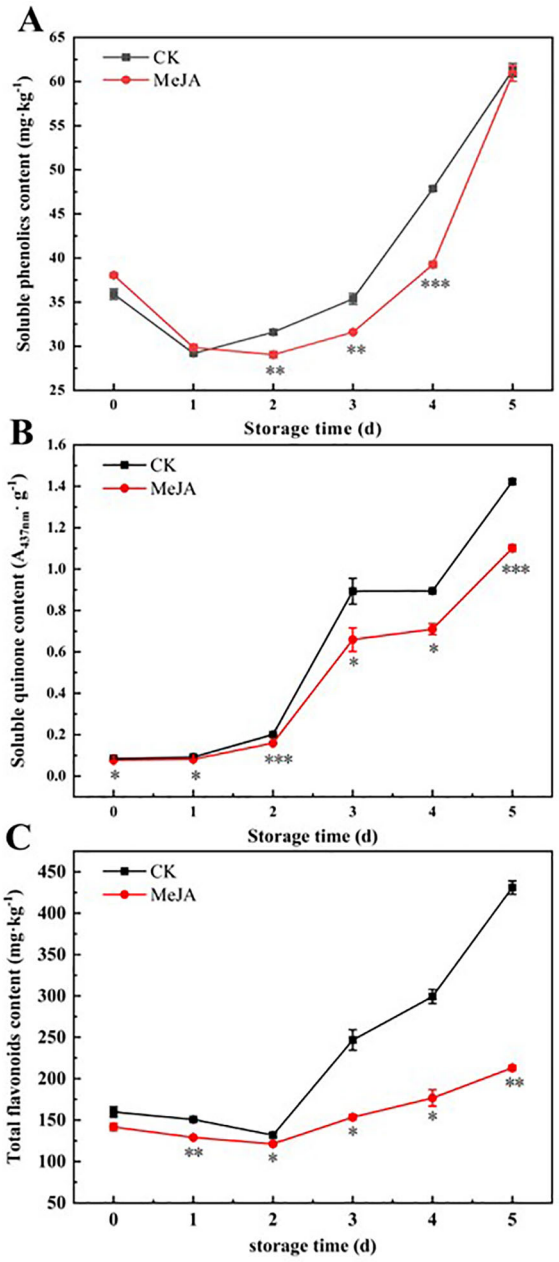

FIGURE 3
The effect of MeJA treatment on the soluble phenolics content **(A)**, soluble quinone content **(B)**, and total flavonoid content **(C)** of fresh-cut CWCs. Error bars represent the standard error of three biological replicates. *、**、***: represent the level of difference between MeJA group and CK group is $p < 0.05$、$p < 0.01$、$p < 0.001$, respectively.

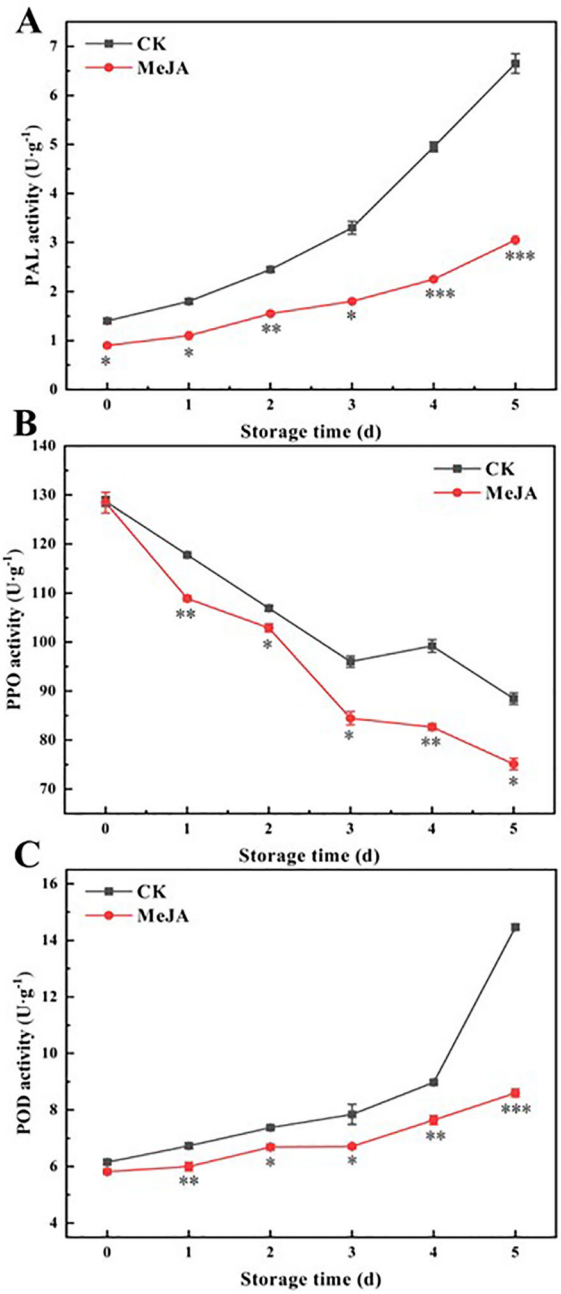

FIGURE 4
The effect of MeJA treatment on the activities of PAL **(A)**, PPO **(B)**, and POD **(C)** of fresh-cut CWCs. Error bars represent the standard error of three biological replicates. *、**、***: represent the level of difference between MeJA group and CK group is $p < 0.05$、$p < 0.01$、$p < 0.001$, respectively.

nutrients and exacerbating weight loss. Soluble solids content has been acknowledged to be a vital quality indicator (Liu et al., 2023). O_2 and CO_2 content can reflect respiratory intensity to a certain extent (Chen et al., 2022). MeJA has previously been shown to attenuate respiration and delay the weight loss of pomegranates (Garcia-Pastor et al., 2020). Our study also found that MeJA inhibited the respiration of fresh-cut CWCs, reducing weight loss and suppressing changes in soluble solid content, consistent with findings from studies on MeJA-treated 'Kinnow' mandarins (Baswal et al., 2020), and jujubes (Dong et al., 2016).

The increase in PAL activity promotes the formation and accumulation of phenolic compounds (Pen and Jiang, 2004; Kong et al., 2021). Our study observed a concurrent rise in PAL activity and TPC in fresh-cut CWCs, consistent with existing literature (Xu et al., 2022). Enzymatic browning results in the increased soluble quinone

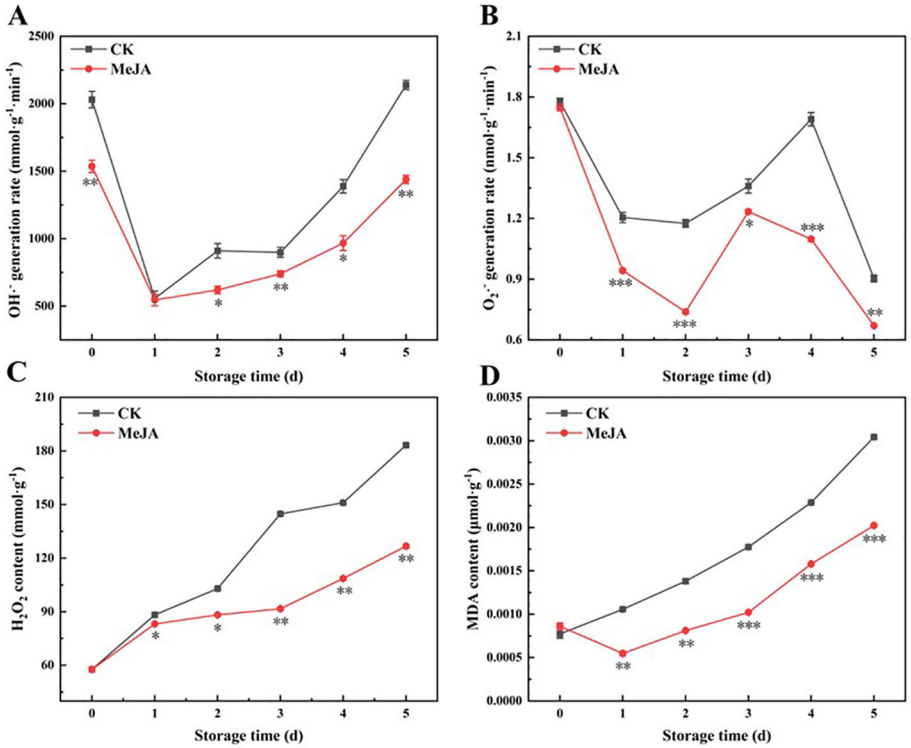

FIGURE 5
The effect of MeJA treatment on the $OH^{\cdot -}$ generation rate **(A)**, $O_2^{\cdot -}$ generation rate **(B)**, H_2O_2 content **(C)** and MDA content **(D)** of fresh-cut CWCs. Error bars represent the standard error of three biological replicates. *、 **、 ***: represent the level of difference between MeJA group and CK group is $p < 0.05$、$p < 0.01$、$p < 0.001$, respectively.

content in plant tissues (Teng et al., 2020). Numerous studies have shown that the total flavonoid content of fresh-cut CWCs increases with progressing yellowing (Li et al., 2016). In our study, the soluble quinone content, TPC, and TFC of fresh-cut CWCs gradually increased, yet MeJA suppressed this trend, maintaining a significantly lower degree of yellowing in appearance compared to the control. Several studies have suggested that the reduction of relevant pigment substances in plants, including flavonoids, carotenoids, total phenolics, chlorophylls, and anthocyanins, is the primary cause of postharvest discoloration in certain fresh produce (Zhang et al., 2023b). Huang et al. (2022) indicated that combining malic acid and lycopene could effectively alleviate the reduction of anthocyanins, flavonoids, and phenols, resulting in a more vibrant litchi peel. Similarly, Zhang et al. (2023a) concluded that salicylic acid inhibits the degradation of pigments, resulting in Longan peel containing more flavonoids, total phenols, carotenoids, and other

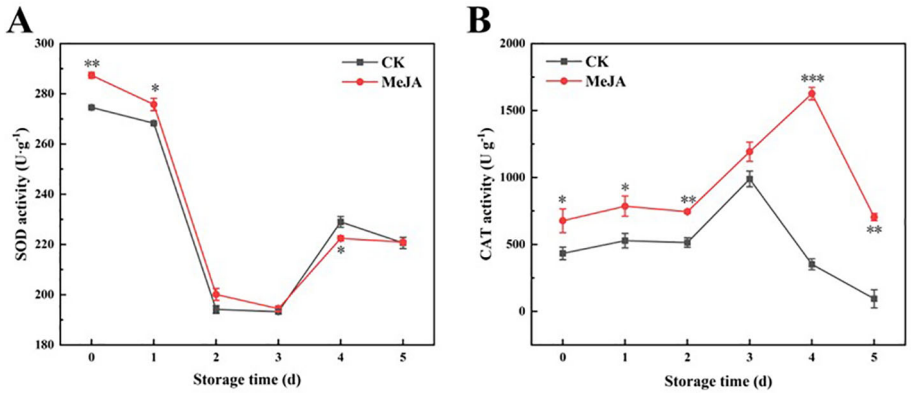

FIGURE 6
The effect of MeJA treatment on the activities of SOD **(A)** and CAT **(B)** of fresh-cut CWCs. Error bars represent the standard error of three biological replicates. *、 **、 ***: represent the level of difference between MeJA group and CK group is $p < 0.05$、$p < 0.01$、$p < 0.001$, respectively.

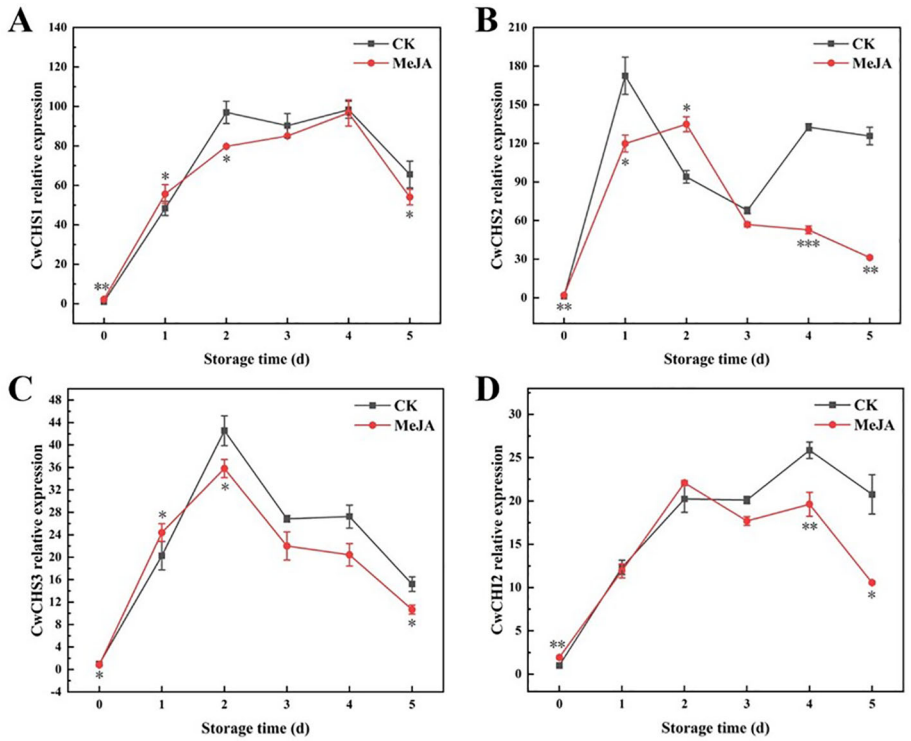

FIGURE 7
Gene expression of *CwCHS1* **(A)**, *CwCHS2* **(B)**, *CwCHS3* **(C)**, and *CwCHI2* **(D)** in MeJA-treated fresh-cut CWCs. *、**、***: represent the level of difference between MeJA group and CK group is $p < 0.05$、$p < 0.01$、$p < 0.001$, respectively.

pigment substances, thereby maintaining stable peel color. To some extent, these studies support our findings, suggesting that the reduction of TPC and TFC can delay the yellowing of fresh-cut CWCs, and MeJA seems effective in this regard.

Song et al. (2019)showed that PPO and POD, as key enzymes in the oxidation of phenolics, are one of the main causes of browning degree in fresh-cut fruits and vegetables. Meanwhile, SOD as an antioxidant enzyme played a key role in delaying the quality decline of fresh-cut fruits and vegetables. PPO exhibits high activity in damaged fruits and vegetables, promoting the conversion of polyphenols to quinones. On the other hand, POD catalyzes the oxidative polymerization of phenolics and flavonoids in fruits and vegetables in the presence of H_2O_2, leading to browning (Liu et al., 2018a). Studies on eugenol emulsion inhibiting the yellowing of fresh-cut CWCs by reducing enzyme activities (PPO, POD, especially PAL) and decreasing phenolic and quinone formation have been documented (Teng et al., 2020). Cai et al. (2024) showed that MeJA-loaded biofilm treatment inhibited POD activity and MDA content in loquat fruits, thereby slowing down their quality deterioration, which is similar to the results of the present study. Chitosan coating has been reported to effectively inhibit the discoloration of fresh CWCs, mainly by reducing the oxygen supply to freshwater chestnuts and inhibiting PAL, PPO, and POD activities (Pen and Jiang, 2003). Zhang et al. (2022) found that Aurone inhibited the yellowing of CWCs by reducing POD activity. Our research observed that MeJA inhibited PAL, PPO, and POD activities, accompanied by a decrease in TPC, TFC, and soluble quinones. Song et al. (2019) showed that ferulic acid treatment of fresh-cut CWCs significantly down-regulated the expression levels of *CwCHI1*, *CwCHS1*, and *CwCHS2*, which delayed the cut surface yellowing of fresh-cut CWCs. In this study, we found that the expression of *CwCHS1*, *CwCHS2*, *CwCHS3* and *CwCHI2* was significantly down-regulated in MeJA-treated freshly cut CWCs (Figure 7). This is consistent with the results of Xu et al. (2023b). We hypothesized that *CwCHS1*, *CwCHS2* and *CwCHS3* might be the key genes involved in the regulation of flavonoid accumulation by MeJA treatment. And *CwCHI2* may play a role in the late storage stage, thus inhibiting flavonoid accumulation in fresh-cut CWCs and achieving the purpose of delaying the surface discoloration of fresh-cut CWCs.

Plants naturally produce some reactive oxygen species during normal physiological metabolism (You et al., 2012). For example, as oxygen enters plant cells through respiration, it receives electrons to produce $O_2\cdot^-$, which then transforms into H_2O_2 and $OH\cdot^-$. The content of ROS is usually balanced by the antioxidant system (Kong et al., 2020). However, certain stresses lead to a significant generation of ROS, disrupting the ROS balance and resulting in cell membrane damage, accelerating fruit oxidation and quality deterioration (Wang et al., 2023). SOD can catalyze the transformation of $O_2\cdot^-$ into H_2O_2, while CAT can convert H_2O_2 into O_2 and H_2O, reducing cell membrane damage (Liu et al., 2023). During storage, the production rate of $OH\cdot^-$and the content of H_2O_2 and MDA in fresh-cut CWCs increased continuously, but those in the MeJA group were consistently lower than in the control. The $O_2\cdot^-$ generation rate trend differed from other substances, showing an increase followed by a decrease. When analyzed in conjunction with the results, it could be explained by the initial decrease and subsequent increase in SOD activity. MeJA increased SOD activity, facilitating the conversion of $O_2\cdot^-$, resulting in a slower $O_2\cdot^-$

generation rate in the MeJA group. The increase in CAT activity in the MeJA group promoted the decrease in H_2O_2 content. In summary, the reduction of ROS and the enhancement of antioxidant capacity mitigated the oxidative damage to cell membranes, consequently reducing the production of MDA in the MeJA group. MeJA has been reported to activate SOD and CAT activities to maintain the quality of produce, such as blueberries (Wang et al., 2019a), which aligns with our results.

5 Conclusions

In conclusion, immersing freshly cut CWCs in 20 μM MeJA for 10 minutes effectively delays surface yellowing, inhibits respiration, reduces weight loss, and maintains soluble solid content during storage. MeJA also reduces the accumulation of TPC, soluble quinones by suppressing PAL, PPO, and POD activities, and significantly slows down the generation rates of $O_2\cdot^-$ and $OH\cdot^-$, reduces H_2O_2 and MDA content by increasing SOD and CAT activities. Also, MeJA inhibited the synthesis of flavonoids in fresh-cut CWCs by down-regulating the expression of genes related to the phenylpropane metabolic pathway (*CwCHS1*, *CwCHS2*, *CwCHS3* and *CwCHI2*). Ultimately, MeJA effectively retards surface yellowing and maintains the quality of fresh-cut CWCs by reducing flavonoid production and enhancing antioxidant capacity.

Data availability statement

The datasets presented in this study can be found in online repositories. The names of the repository/repositories and accession number(s) can be found in the article/Supplementary Material.

Author contributions

KL: Data curation, Methodology, Software, Validation, Visualization, Writing – original draft. XW: Data curation, Methodology, Software, Validation, Visualization, Writing – original draft. RY: Methodology, Writing – review & editing. YY: Validation, Writing – review & editing. LW: Validation, Writing – review & editing. YA: Writing – review & editing. HW: Writing – review & editing. TM: Funding acquisition, Methodology, Resources, Supervision, Writing – original draft, Writing – review & editing.

Funding

The author(s) declare financial support was received for the research, authorship, and/or publication of this article. This research was financially supported by the National Natural Science Foundation of China (32001764).

Conflict of interest

The authors declare that the research was conducted in the absence of any commercial or financial relationships that could be construed as a potential conflict of interest.

Publisher's note

Supplementary material

The Supplementary Material for this article can be found online at: https://www.frontiersin.org/articles/10.3389/fpls.2024.1435066/full#supplementary-material

References

Apel, K., and Hirt, H. (2004). Reactive oxygen species: metabolism, oxidative stress, and signal transduction. *Annu. Rev. Plant Biol.* 55, 373–399. doi: 10.1146/annurev.arplant.55.031903.141701

Baswal, A. K., Dhaliwal, H. S., Singh, Z., Mahajan, B. V. C., and Gill, K. S. (2020). Postharvest application of methyl jasmonate, 1-methylcyclopropene and salicylic acid extends the cold storage life and maintain the quality of 'Kinnow' mandarin (Citrus nobilis L. X C. deliciosa L.) fruit. *Postharvest Biol. Technol.* 161, 111064. doi: 10.1016/j.postharvbio.2019.111064

Cai, H., Han, S., Yu, M., Ma, R., and Yu, Z. (2020). The alleviation of methyl jasmonate on loss of aroma lactones correlated with ethylene biosynthesis in peaches. *J. Food Sci.* 85, 2389–2397. doi: 10.1111/1750-3841.15339

Cai, Z., Huang, W., Zhong, J., Jin, J., Wu, D., and Chen, K. (2024). Methyl jasmonate-loaded composite biofilm sustainably alleviates chilling lignification of loquat fruit during postharvest storage. *Food Chem.* 444, 138602. doi: 10.1016/j.foodchem.2024.138602

Chen, J., Xu, Y., Yi, Y., Hou, W., Wang, L., Ai, Y., et al. (2022). Regulations and mechanisms of 1-methylcyclopropene treatment on browning and quality of fresh-cut lotus (Nelumbo nucifera Gaertn.) root slices. *Postharvest Biol. Technol.* 185, 111782. doi: 10.1016/j.postharvbio.2021.111782

Cheong, J. J., and Do Choi, Y. (2003). Methyl jasmonate as a vital substance in plants. *Trends Genet.* 19, 409–413. doi: 10.1016/S0168-9525(03)00138-0

Concha, C. M., Figueroa, N. E., Poblete, L. A., Oñate, F. A., Schwab, W., and Figueroa, C. R. (2013). Methyl jasmonate treatment induces changes in fruit ripening by modifying the expression of several ripening genes in Fragaria chiloensis fruit. *Plant Physiol. Biochem.* 70, 433–444. doi: 10.1016/j.plaphy.2013.06.008

Deshi, V., Homa, F., Tokala, V. Y., Mir, H., Aftab, M. A., and Siddiqui, M. W. (2021). Regulation of pericarp browning in cold-stored litchi fruit using methyl jasmonate. *J. King Saud University-Science* 33, 101445. doi: 10.1016/j.jksus.2021.101445

Dong, Y., Zhi, H. H., Xu, J., Zhang, L. H., Liu, M. P., and Zong, W. (2016). Effect of methyl jasmonate on reactive oxygen species, antioxidant systems, and microstructure

of Chinese winter jujube at two major ripening stages during shelf life. *J. Hortic. Sci. Biotechnol.* 91, 316–323. doi: 10.1080/14620316.2016.1159924

Dou, Y., Chang, C., Wang, J., Cai, Z., Zhang, W., Du, H., et al. (2021). Hydrogen sulfide inhibits enzymatic browning of fresh-cut Chinese water chestnuts. *Front. Nutr.* 8. doi: 10.3389/fnut.2021.652984

Duan, W., Yang, C., Cao, X., Zhang, C., Liu, H., Chen, K., et al. (2022). Transcriptome and DNA methylome analysis reveal new insights into methyl jasmonate-alleviated chilling injury of peach fruit after cold storage. *Postharvest Biol. Technol.* 189, 111915. doi: 10.1016/j.postharvbio.2022.111915

Garcia-Pastor, M. E., Serrano, M., Guillén, F., Giménez, M. J., Martínez-Romero, D., Valero, D., et al. (2020). Preharvest application of methyl jasmonate increases crop yield, fruit quality and bioactive compounds in pomegranate 'Mollar de Elche' at harvest and during postharvest storage. *J. Sci. Food Agric.* 100, 145–153. doi: 10.1002/jsfa.10007

Hasan, S. K., Ferrentino, G., and Scampicchio, M. (2020). Nanoemulsion as advanced edible coatings to preserve the quality of fresh-cut fruits and vegetables: a review. *Int. J. Food Sci. Technol.* 55, 1–10. doi: 10.1111/ijfs.14273

Huang, H., Wang, L., Bi, F., and Xiang, X. (2022). Combined application of Malic acid and lycopene maintains content of phenols, antioxidant activity, and membrane integrity to delay the pericarp browning of litchi fruit during storage. *Front. Nutr.* 9. doi: 10.3389/fnut.2022.849385

Jiang, Y., Pen, L., and Li, J. (2004). Use of citric acid for shelf life and quality maintenance of fresh-cut Chinese water chestnut. *J. Food Eng.* 63, 325–328. doi: 10.1016/j.jfoodeng.2003.08.004

Kong, M., Murtaza, A., Hu, X., Iqbal, A., Zhu, L., Ali, S. W., et al. (2021). Effect of high-pressure carbon dioxide treatment on browning inhibition of fresh-cut Chinese water chestnut (Eleocharis tuberosa): Based on the comparison of damaged tissue and non-damaged tissue. *Postharvest Biol. Technol.* 179, 111557. doi: 10.1016/j.postharvbio.2021.111557

Kong, X. M., Ge, W. Y., Wei, B. D., Zhou, Q., Zhou, X., Zhao, Y. B., et al. (2020). Melatonin ameliorates chilling injury in green bell peppers during storage by regulating membrane lipid metabolism and antioxidant capacity. *Postharvest Biol. Technol.* 170, 111315. doi: 10.1016/j.postharvbio.2020.111315

Li, F., Hu, Y., Shan, Y., Liu, J., Ding, X., Duan, X., et al. (2022). Hydrogen-rich water maintains the color quality of fresh-cut Chinese water chestnut. *Postharvest Biol. Technol.* 183, 111743. doi: 10.1016/j.postharvbio.2021.111743

Li, Y. X., Pan, Y. G., He, F. P., Yuan, M. Q., and Li, S. B. (2016). Pathway analysis and metabolites identification by metabolomics of etiolation substrate from fresh-cut Chinese water chestnut (Eleocharis tuberosa). *Molecules* 21, 1648. doi: 10.3390/molecules21121648

Liu, Y., Liu, Y., Chen, Q., Yin, F., Song, M., Cai, W., et al. (2023). Methyl jasmonate treatment alleviates chilling injury and improves antioxidant system of okra pod during cold storage. *Food Sci. Nutr.* 11, 2049–2060. doi: 10.1002/fsn3.3241

Liu, H., Meng, F., Miao, H., Chen, S., Yin, T., Hu, S., et al. (2018b). Effects of postharvest methyl jasmonate treatment on main health-promoting components and volatile organic compounds in cherry tomato fruits. *Food Chem.* 263, 194–200. doi: 10.1016/j.foodchem.2018.04.124

Liu, C., Zheng, H., Sheng, K., Liu, W., and Zheng, L. (2018a). Effects of melatonin treatment on the postharvest quality of strawberry fruit. *Postharvest Biol. Technol.* 139, 47–55. doi: 10.1016/j.postharvbio.2018.01.016

Luo, M., Zhou, X., Hao, Y., Sun, H., Zhou, Q., Sun, Y., et al. (2021). Methyl jasmonate pretreatment improves aroma quality of cold-stored 'Nanguo' pears by promoting ester biosynthesis. *Food Chem.* 338, 127846. doi: 10.1016/j.foodchem.2020.127846

Min, T., Bao, Y., Zhou, B., Yi, Y., Wang, L., Hou, W., et al. (2019). Transcription profiles reveal the regulatory synthesis of phenols during the development of lotus rhizome (Nelumbo nucifera Gaertn). *Int. J. Mol. Sci.* 20, 2735. doi: 10.3390/ijms20112735

Min, T., Xie, J., Zheng, M., Yi, Y., Hou, W., Wang, L., et al. (2017). The effect of different temperatures on browning incidence and phenol compound metabolism in fresh-cut lotus (Nelumbo nucifera G.) root. *Postharvest Biol. Technol.* 123, 69–76. doi: 10.1016/j.postharvbio.2016.08.011

Pan, Y. G., Li, Y. X., and Yuan, M. Q. (2015). Isolation, purification and identification of etiolation substrate from fresh-cut Chinese water-chestnut (Eleocharis tuberosa). *Food Chem.* 186, 119–122. doi: 10.1016/j.foodchem.2015.03.070

Pen, L. T., and Jiang, Y. M. (2003). Effects of chitosan coating on shelf life and quality of fresh-cut Chinese water chestnut. *LWT-Food Sci. Technol.* 36, 359–364. doi: 10.1016/S0023-6438(03)00024-0

Peng, L., and Jiang, Y. (2004). Effects of heat treatment on the quality of fresh-cut Chinese water chestnut. *Int. J. Food Sci. Technol.* 39, 143–148. doi: 10.1046/j.0950-5423.2003.00767.x

Peng, L., Yang, S., Li, Q., Jiang, Y., and Joyce, D. C. (2008). Hydrogen peroxide treatments inhibit the browning of fresh-cut Chinese water chestnut. *Postharvest Biol. Technol.* 47, 260–266. doi: 10.1016/j.postharvbio.2007.07.002

Per, T. S., Khan, M. I. R., Anjum, N. A., Masood, A., Hussain, S. J., and Khan, N. A. (2018). Jasmonates in plants under abiotic stresses: Crosstalk with other phytohormones matters. *Environ. Exp. Bot.* 145, 104–120. doi: 10.1016/j.envexpbot.2017.11.004

Qin, G. H., Wei, S. W., Tao, S. T., Zhang, H. P., Huang, W. J., Yao, G. F., et al. (2017). Effects of postharvest methyl jasmonate treatment on aromatic volatile biosynthesis by 'Nanguoli' fruit at different harvest maturity stages. *New Z. J. Crop Hortic. Sci.* 45, 191–201. doi: 10.1080/01140671.2016.1272470

Song, M., Wu, S., Shuai, L., Duan, Z., Chen, Z., Shang, F., et al. (2019). Effects of exogenous ascorbic acid and ferulic acid on the yellowing of fresh-cut Chinese water chestnut. *Postharvest Biol. Technol.* 148, 15–21. doi: 10.1016/j.postharvbio.2018.10.005

Teng, Y., Murtaza, A., Iqbal, A., Fu, J., Ali, S. W., Iqbal, M. A., et al. (2020). Eugenol emulsions affect the browning processes, and microbial and chemical qualities of fresh-cut Chinese water chestnut. *Food Bioscience* 38, 100716. doi: 10.1016/j.fbio.2020.100716

Wang, Y., Gao, L., Wang, Q., and Zuo, J. (2019b). Low temperature conditioning combined with methyl jasmonate can reduce chilling injury in bell pepper. *Scientia Hortic.* 243, 434–439. doi: 10.1016/j.scienta.2018.08.031

Wang, S. Y., Shi, X. C., Liu, F. Q., and Laborda, P. (2021). Effects of exogenous methyl jasmonate on quality and preservation of postharvest fruits: A review. *Food Chem.* 353, 129482. doi: 10.1016/j.foodchem.2021.129482

Wang, H., Wu, Y., Yu, R., Wu, C., Fan, G., and Li, T. (2019a). Effects of postharvest application of methyl jasmonate on physicochemical characteristics and antioxidant system of the blueberry fruit. *Scientia Hortic.* 258, 108785. doi: 10.1016/j.scienta.2019.108785

Wang, H., Zhang, Y., Pu, Y., Chen, L., He, X., Cao, J., et al. (2023). Composite coating of guar gum with salicylic acid alleviates the quality deterioration of vibration damage in 'Huangguan' pear fruit through the regulation of antioxidant metabolism. *Postharvest Biol. Technol.* 205, 112476. doi: 10.1016/j.postharvbio.2023.112476

Wu, X., Li, Q., Yi, Y., Wang, L., Hou, W., Ai, Y., et al. (2024). Cinnamaldehyde affects the storage quality of freshly cut water chestnuts through the regulation of reactive oxygen species and the AsA-GSH cycle. *Scientia Hortic.* 332, 113199. doi: 10.1016/j.scienta.2024.113199

Xu, Y., Bao, Y., Chen, J., Yi, Y., Ai, Y., Hou, W., et al. (2023a). Mechanisms of ethanol treatment on controlling browning in fresh-cut lotus roots. *Sci. Hortic.* 310, 111708. doi: 10.1016/j.scienta.2022.111708

Xu, Y., Yi, Y., Ai, Y., Hou, W., Wang, L., Wang, H., et al. (2023b). Ethephon and 1-methylcyclopropene regulate storage quality and browning of fresh-cut Chinese water chestnuts. *Postharvest Biol. Technol.* 200, 112331. doi: 10.1016/j.postharvbio.2023.112331

Xu, Y., Yu, J., Chen, J., Gong, J., Peng, L., Yi, Y., et al. (2022). Melatonin maintains the storage quality of fresh-cut Chinese water chestnuts by regulating phenolic and reactive oxygen species metabolism. *Food Qual. Saf-Oxford.* 6, fyac002. doi: 10.1093/fqsafe/fyac002

Xu, D., Zuo, J., Li, P., Yan, Z., Gao, L., Wang, Q., et al. (2020). Effect of methyl jasmonate on the quality of harvested broccoli after simulated transport. *Food Chem.* 319, 126561. doi: 10.1016/j.foodchem.2020.126561

You, Y., Jiang, Y., Sun, J., Liu, H., Song, L., and Duan, X. (2012). Effects of short-term anoxia treatment on browning of fresh-cut Chinese water chestnut in relation to antioxidant activity. *Food Chem.* 132, 1191–1196. doi: 10.1016/j.foodchem.2011.11.073

Zha, Z., Tang, R., Wang, C., Li, Y. L., Liu, S., Wang, L., et al. (2022). Riboflavin inhibits browning of fresh-cut apples by repressing phenolic metabolism and enhancing antioxidant system. *Postharvest Biol. Technol.* 187, 111867. doi: 10.1016/j.postharvbio.2022.111867

Zhang, A., Mu, L., Shi, Y., Liu, Y., Deng, Y., Lao, Y., et al. (2022). The effects of aurone on the yellowing of fresh-cut water chestnuts. *Food Chemistry: X* 15, 100411. doi: 10.1016/j.fochx.2022.100411

Zhang, H., Shan, T., Chen, Y., Lin, M., Chen, Y., Lin, L., et al. (2023a). Salicylic acid treatment delayed the browning development in the pericarp of fresh longan by regulating the metabolisms of ROS and membrane lipid. *Scientia Hortic.* 318, 112073. doi: 10.1016/j.scienta.2023.112073

Zhang, Y., Tang, H., Lei, D., Zhao, B., Zhou, X., Yao, W., et al. (2023b). Exogenous melatonin maintains postharvest quality in kiwiberry fruit by regulating sugar metabolism during cold storage. *LWT* 174, 114385. doi: 10.1016/j.lwt.2022.114385

Zhou, X., Hu, W., Li, J., Iqbal, A., Murtaza, A., Xu, X., et al. (2022). High-pressure carbon dioxide treatment and vacuum packaging alleviate the yellowing of peeled Chinese water chestnut (Eleocharis tuberosa). *Food Packaging Shelf Life* 34, 100927. doi: 10.1016/j.fpsl.2022.100927

Zhu, L., Hu, W., Murtaza, A., Iqbal, A., Li, J., Zhang, J., et al. (2022a). Eugenol treatment delays the flesh browning of fresh-cut water chestnut (Eleocharis tuberosa) through regulating the metabolisms of phenolics and reactive oxygen species. Food Chemistry. *X* 14, 100307. doi: 10.1016/j.fochx.2022.100307

Zhu, L., u, H., Dai, X., Yu, M., and Yu, Z. (2022b). Effect of methyl jasmonate on the quality and antioxidant m ncapacity by modulating ascorbate-glutathione cycle in peach fruit. *Scientia Hortic.* 303, 111216. doi: 10.1016/j.scienta.2022.111216

frontiers | Frontiers in Plant Science

TYPE Original Research
PUBLISHED 22 August 2024
DOI 10.3389/fpls.2024.1419719

OPEN ACCESS

EDITED BY
Shifeng Cao,
Zhejiang Wanli University, China

REVIEWED BY
Yun Xiang,
Lanzhou University, China
Jiejie Li,
Beijing Normal University, China

*CORRESPONDENCE
Che Wang
wangwangche@163.com
Shaobin Zhang
zsb@syau.edu.cn
Ming He
lnyhming@163.com
Yue Gao
gyue1217@syau.edu.cn

†These authors have contributed equally to this work

RECEIVED 18 April 2024
ACCEPTED 02 August 2024
PUBLISHED 22 August 2024

CITATION
Lv Y, Liu S, Zhang J, Cheng J, Wang J, Wang L, Li M, Wang L, Bi S, Liu W, Zhang L, Liu S, Yan D, Diao C, Zhang S, He M, Gao Y and Wang C (2024) Genome-wide identification of actin-depolymerizing factor family genes in melon (*Cucumis melo* L.) and CmADF1 plays an important role in low temperature tolerance.
Front. Plant Sci. 15:1419719.
doi: 10.3389/fpls.2024.1419719

Genome-wide identification of actin-depolymerizing factor family genes in melon (*Cucumis melo* L.) and CmADF1 plays an important role in low temperature tolerance

Yanling Lv[1,2,3†], Shihang Liu[1†], Jiawang Zhang[3], Jianing Cheng[1], Jinshu Wang[1], Lina Wang[1], Mingyang Li[1], Lu Wang[1], Shuangtian Bi[1], Wei Liu[3], Lili Zhang[3], Shilei Liu[3], Dabo Yan[1], Chengxuan Diao[1], Shaobin Zhang[1*], Ming He[3*], Yue Gao[1*] and Che Wang[1*]

[1]College of Bioscience and Biotechnology, Shenyang Agricultural University, Shenyang, China, [2]College of Horticulture, Shenyang Agricultural University, Shenyang, China, [3]Institute of Vegetable, Liaoning Academy of Agricultural Sciences, Shenyang, China

Actin depolymerizing factors (ADFs), as the important actin-binding proteins (ABPs) with depolymerizing/severing actin filaments, play a critical role in plant growth and development, and in response to biotic and abiotic stresses. However, the information and function of the ADF family in melon remains unclear. In this study, 9 melon ADF genes (CmADFs) were identified, distributed in 4 subfamilies, and located on 6 chromosomes respectively. Promoter analysis revealed that the CmADFs contained a large number of cis-acting elements related to hormones and stresses. The similarity of CmADFs with their Arabidopsis homologue AtADFs in sequence, structure, important sites and tissue expression confirmed that ADFs were conserved. Gene expression analysis showed that CmADFs responded to low and high temperature stresses, as well as ABA and SA signals. In particular, CmADF1 was significantly up-regulated under above all stress and hormone treatments, indicating that CmADF1 plays a key role in stress and hormone signaling responses, so CmADF1 was selected to further study the mechanism in plant tolerance low temperature. Under low temperature, virus-induced gene silencing (VIGS) of CmADF1 in oriental melon plants showed increased sensitivity to low temperature stress. Consistently, the stable genetic overexpression of CmADF1 in Arabidopsis improved their low temperature tolerance, possibly due to the role of CmADF1 in the depolymerization of actin filaments. Overall, our findings indicated that CmADF genes, especially CmADF1, function in response to abiotic stresses in melon.

KEYWORDS

genome-wide identification, CmADF1, low temperature, oriental melon, Arabidopsis

Introduction

Melon (*Cucumis melo* L.), originated from tropical zone, is a worldwide fruit with high edible value and economic value, and is sensitive to low temperature. Under the influence of the environment and climate in the northern region, the oriental melon cultivated in facilities in winter and spring is often affected by low temperature, which seriously deteriorates their edible quality and commercial value, and even no harvest (Zhang Y. P., et al., 2017). Low temperature has become an important limiting factor for facility cultivation of oriental melon in winter and spring.

In the process of resisting unfavorable conditions, plants have evolved strategies to protect themselves (Ding et al., 2019). The cytoskeleton is closely related to various environmental stimuli (Wang et al., 2011; Sengupta et al., 2019; Byun et al., 2021). Actin filaments are a major member of cytoskeleton and play an important role in stress responses (Zhang et al., 2010; Wang et al., 2011; Ye et al., 2013; Fan et al., 2016). Depolymerization of actin filaments in *Arabidopsis* plants under salt and osmotic stress can improve plant tolerance (Zhang et al., 2010; Wang et al., 2011; Ye et al., 2013). Pokorná et al. (2004) found that in 3-day-old BY-2 cells exposed at 0°C for 12 hours, actin filaments disintegrated completely, or turned into few in number, short, and sometimes branched filaments, actin bars or dots. The findings of Fan et al. (2015; 2016) suggest that actin cytoskeleton plays a key role in the tolerance of *Arabidopsis* seedlings to low temperature and heat stress, and specific members of actin depolymerizing factors (ADFs) may be involved in regulating plant response to low temperature and heat stress. Destabilizers of actin filaments and microtubules cause the activation of cold-inducible *Brassica napus BN115* (Sangwan et al., 2001). However, the molecular mechanism of the dynamic change of actin filaments under low temperature is poorly understood.

The dynamic reorganization of intracellular actin filaments is regulated by a large number of ABPs with different functions (Hussey et al., 2006; Huang et al., 2011; Roland et al., 2008), in which ADFs are considered to be an important regulator of actin filaments changes (Maciver and Hussey, 2002; Bamburg and Bernstein, 2008). ADF is abundant and highly conserved in all eukaryotes, and plays an important role in plant growth and development as well as in response to multiple biotic and abiotic stresses (Andrianantoandro and Pollard 2006; Dong et al., 2001, 2013). The functions of ADFs in Arabidopsis have been studied *in vivo* extensively. For example, AtADF1 can affect plants growth, development and morphogenesis (Dong et al., 2001), and participate in high temperature and salt stress processes (Wang et al., 2021, 2023). AtADF2 is required for normal cell growth and plant development, and its mediated actin dynamic is essential for root-knot nematode infection of Arabidopsis (Clément et al., 2009). AtADF4 relates to plants growth and development (Peng and Huang, 2006), plays a role in regulating hypocotyl growth, response to osmotic (Yao et al., 2022) and drought stresses (Zhao et al., 2016), and improves disease resistance of *Arabidopsis* to bacterium DC3000AvrPphB (Tian et al., 2009). AtADF5 is important for pollen germination and pollen tube growth (Zhu et al., 2017), promotes stomatal closure by regulating actin cytoskeleton remodeling under ABA and drought stresses (Qian et al., 2019), and improves the basal and acquired freezing resistance of *Arabidopsis* (Zhang et al., 2021). AtADF7 and AtADF10 are involved in pollen development and pollen tube growth (Daher and Geitmann, 2012; Zheng et al., 2013). Under osmotic stress, AtADF7 inhibited actin bundling protein VILLIN1 regulation of root hair formation (Bi et al., 2022). In addition, ADFs from barley and wheat have been shown to be related to plant resistance to various pathogens (Miklis et al., 2007; Fu et al., 2014; Inada et al., 2016). TaADF4 and TaADF7 from wheat play a stimulative role in resistance to the stripe rust infection (Zhang B. et al., 2017; Fu et al., 2014). TaADF3 negatively regulates wheat resistance against Puccinia striiformis (Tang et al., 2016). Increasing evidence has shown that ADFs play an important role in response and tolerance to various stresses (Huang et al., 2012; Xu et al., 2021). Drought resistance of *OsADF3* in rice transgenic *Arabidopsis* is enhanced (Huang et al., 2012). AtADF5 improves the basal and acquired freezing resistance of *Arabidopsis* (Zhang et al., 2021). Overexpression of *TaADF16* significantly improved the tolerance of transgenic plants to freezing stress (Xu et al., 2021). DaADF3 in *Deschampsia antarctica* enhanced the cold tolerance of transgenic rice plants (Byun et al., 2021). In the process of wheat cold acclimation, an *ADF* gene is induced, and the increased resistance to freezing shows that the ADF protein may be required in reorganization of the cytoskeleton under low temperatures (Ouellet et al., 2001). In short, more and more plant ADFs have been functionally characterized, while ADFs in oriental melon have not been reported.

In this study, we identified 9 *CmADF* genes in oriental melon and found that they were similar to homologue *AtADF* genes in sequence, structure, important site and tissue expression through analysis of their biological information and tissue expression. Further stress expression patterns showed that CmADFs responded to low temperature, high temperature, ABA and SA signals, especially under SA treatment, all CmADFs were dramatically up-regulated by approximately ten to hundreds of times. *CmADF1* was significantly upregulated under all the above treatments, especially during 24 h of low temperature treatment, and maintained high expression, which provides the functional implication of CmADF1 in low temperature response. Further studies on the phenotype and actin filaments organization of *Arabidopsis* seedlings overexpressing *CmADF1* under low temperature, as well as phenotype analysis and physiological identification of *CmADF1* gene silenced oriental melon seedlings, indicated that CmADF1 affected the process of actin filaments depolymerization and played an important role in plant adaptation to low temperature stress.

Materials and methods

Plant materials, growth conditions, and stress treatments

The low temperature tolerant genotype Oriental melon ' LT-6 ' was provided by the Vegetable Research Institute of Liaoning Academy of Agricultural Sciences, and the *CmADF1* silent plant

was obtained by VIGS technology. The Oriental melon grew at 25/20°C (light 16 h/darkness 8 h) to two-leaf stage and was subjected to low temperature (4°C), high temperature (40°C), ABA (100 μM) and SA (100 μM) treatment for stress expression analysis. The second true leaves were sampled at 0, 3, 6, 12 and 24 h after treatment. Tissues of two-month-old plants, including roots, stems, young leaves, pistillate and staminate flowers, were collected for tissue expression analysis. The silenced plants of *CmADF1* (TRV-A) were treated at 4°C at the two-leaf stage to observe the phenotype and analyze the physiological indexes.

The *Arabidopsis thaliana* plants used in this study have a Columbia background. *Atadf1* (The T-DNA insertion mutant) (SALK_144459) was obtained from ABRC, and the *fABD2-GFP* material was donated by China Agricultural University (Wang et al., 2021). The *Arabidopsis* overexpression materials (*CmADF1*-OE and *pCmADF1*::GUS) were constructed by our laboratory. The seeds of WT and *CmADF1*-OE with 4°C vernalization for 3 days were seeded on 1/2 MS medium (Wang et al., 2023), and cultured in a 22°C incubator with a light/dark cycle of 16 h/8 h. After 14 days, the seedlings were placed in incubators at 22°C and 4°C for 0, 24 and 48h respectively, and the leaf area was counted by Image J software. WT and *CmADF1*-OE plants grown under normal conditions for 9 days were treated at 4°C for 12 h, and the morphology of actin filaments in leaves was observed.

Identification of the *ADF* gene family in oriental melon

To identify the *ADF* gene family members in oriental melon, amino acid sequences of 11 *ADFs* in *Arabidopsis* with ADF-H (Actin-Depolymerizing Factor Homology) domain were used as query sequences to search against the entire melon genome database (http://melonomics.net/) with the threshold $E \leq e^{-20}$ and default parameters by performing a BLASTP analysis. Then, the candidate sequences of ADF proteins in the melon genome were used repeatedly to search new ADFs. The longest protein sequence were selected when there were more than one predicted ADF proteins resulting from the alternative splicing by one gene. All identified ADF proteins were checked if they contained ADF-H domain by SMART (http://smart.embl-heidelberg.de/) analysis and hidden Markoy model analysis with PF00241 (http://pfam.xfam.org/family/PF00241). The protein sequences and genome sequences of CmADFs are downloaded from the Melon Genome database. CmADF paralogous genes to AtADF were named for the corresponding AtADFs. Molecular weight (kDa) and isoelectric points (pI) were calculated by the pI/Mw tool at online ProtParam (http://web.expasy.org/protparam/). Subcellular localization was predicted by WoLF PSORT (https://www.genscript.com/tools/psort). We predicted the tertiary structure of the CmADF protein using SWISS-MODEI (http://swissmodel.expasy.org/) and displayed the images using PyMOL V2.3.2 software. The genomic DNA sequence of 2000 bp upstream of gene initiation codon (ATG) was used as the promoter sequence and submitted to the promoter analysis system PlantCARE (http://bioinformatics.psb.ugent.Be/webtools/plantcare/html/) to find all potential cis-acting elements.

Sequence alignment and phylogenetic analysis

The ADF amino acid sequences of melon, *Arabidopsis*, cucumber, watermelon, *Cucurbita maxima* and *Cucurbita pepo* were aligned using ClustalX 2.1 (Larkin et al., 2007). ESpript3.0 (http://espript.ibcp.fr/ESPript/cgi-bin/ESPript.cgi) was used for image display. The unrooted phylogenetic tree was generated in MEGA6.0 using the neighbor-joining (NJ) method with 1000 bootstrap replicates (Tamura et al., 2013).

Chromosome localization and gene duplication

The chromosomal locations for each *CmADF* were determined according to melon genome information. Tandem and segmental duplications were determined using CoGe (https://genomevolution.org/CoGe/) online tool. Duplicated genes were linked using Circos software (http://circos.ca/). The non-synonymous substitution rate (Ka) and synonymous substitution rate (Ks) were calculated by DnaSp V5.0 (Librado and Rozas, 2009) software. The approximate time of each duplication event ($T=Ks/2\lambda$, $\lambda=6.1\times10^{-9}$) (Lynch and Conery, 2000) was estimated by Ks value.

Gene structure and conserved motif analysis of ADF in melon and *Arabidopsis*

According to structural information of *ADF* genes obtained from the gff3 files of melon and *Arabidopsis* genome databases, the intron-exon structures of each gene were drawn using GSDS (http://gsds.cbi.pku.edu.cn) online tool. MEME4.10.2 software (http://meme-suite.Org/tools/meme) was used to analyze the conserved motifs of *ADF* genes in melon and *Arabidopsis*. The maximum value of searched motif was set to 10, the length of motif was between 6 and 50, and other parameters were default values.

Total RNA extraction and real-time fluorescence quantitative PCR analysis

All total RNA was extracted by EasyPure Plant RNA Kit (Beijing Quanshi Jin Biotechnology Co., LTD.). 18S was selected as the internal control for RT-qPCR analysis. The primer sequences are shown in Supplementary Table 3. Roche Light Cycler 480 was used to detect the relative expression level of *ADFs*.

Overexpression and subcellular localization of CmADF1

The full-length CDS of *CmADF1* was respectively cloned into the pSuper1300-GFP and pCAMBIA 1300 vectors to generate *35S::CmADF1*-GFP and *35S::CmADF1*, which were then introduced into the Agrobacterium tumefaciens strain GV3101. The primer sequences are listed in Supplementary Table 3. T3 transgenic homozygous lines were screened for confocal microscope observation and low temperature study. *35S::CmADF1*-GFP was used to observe subcellular localization. *35S::CmADF1*was used in subsequent low temperature stress studies.

Promoter activity analysis

CmADF1 promoter fragment containing the first intron of *CmADF1* was cloned in pCAMBIA1300-221 vector to generate *pADF1*::GUS. Homozygous lines were used for promoter activity analysis. The positive seedlings growing for 9 days were treated at 4 °C for 0, 6, and 12 h, and GUS staining was performed. The primer sequences are listed in Supplementary Table 3.

Visualization and quantitative analysis of actin filaments

As previously reported, *CmADF1*-OE#8 plants were hybridized with *fABD2-GFP* plants, and homozygous plants were selected for subsequent experiments. Confocal microscopy (Nikon A1) with a 40×objective was used to observe actin filaments in pavement cells of cotyledons with a 488-nm laser. Image J was used to measure skewness, density, length and actin cables applied to quantify actin filaments in previous reports. All experiments were repeated 3 times. 30 individual seedlings from different genotypes and treatments were screened to collect more than 200 cells from 60 images.

Western blot assays

10-day-old *CmADF1-GFP* overexpressing Arabidopsis seedlings were used for Western Blot. As previously reported (Liu et al., 2013; Wang et al., 2020), GFP (a labeled protein) was analyzed by SDS-PAGE. Rubisco bands were used as loading controls.

Vector construction and infection of virus-induced gene silencing

The CmADF1 gene in oriental melon were silenced by VIGS. The specific primers containing EcoRI/KpnI cleavage sites were designed to generate *pTRV2-CmADF1* (Supplementary Table 3 for the sequence of primers). The method of cotyledon infection was used. The cotyledons of the germinated oriental melon seeds were fully expanded about 5 days after sowing, and they could be infected. The detailed infection process was carried out according to the method of Liao et al. (2019). About 60 infected plants were randomly divided into 3 groups, and each plant was sampled separately after treatment at 4°C for 0, 6 and 12 h. The expression of *CmADF1* in the leaves of VIGS plants was detected by agarose gel electrophoresis and RT-qPCR, and the plants with transcription level lower than 50% of that of the control plants were selected for subsequent experiments.

Determination of physiological and biochemical indexes and water loss rate

Relative electrolyte leakage (REL) and water loss was measured as described previously (Xing et al., 2020). The contents of soluble protein, proline, malondiald ehyde (MDA) and the activities of SOD, CAT and POD were determined with the relevant kit of Suzhou Mengxi Biomedical Technology Co., LTD. All experiments were repeated three times.

Results

Genome-wide identification and bioinformatics analysis of ADF gene family members in oriental melon

The ADF family member from *Arabidopsis* with the ADF-H domain (PF00241) was used for Blast search in the entire melon genome. 11 non-redundant putative ADF proteins were found, 3 of them were produced by one gene, which was subject to differential splicing, so we selected the longest protein sequence. Finally, 9 *CmADF* genes were identified by SMART and Pfam analysis, and they were named with the same names as their homologue *AtADF* genes. CmADF proteins contain 132 (CmADF8) to 146 (CmADF6) amino acids, and their physicochemical properties are shown in Supplementary Table 1.

To clarify the phylogenetic relationships and functional divergence of *CmADF* gene family members, amino acid sequences of ADF from *Arabidopsis*, melon and other Cucurbitaceae species (cucumber, watermelon, *Cucurbita maxima* and *Cucurbita pepo*) were used to construct the phylogenetic tree (Figure 1A). Accession numbers of the *ADF* genes in each species were shown in Supplementary Table 1. The results showed that 9 CmADFs were distributed in 4 subfamilies and located on six of the 12 melon chromosomes (Figure 1B). Two pairs of segmentally duplicated genes *ADF7/10* and *ADF1/4* were detected (Figure 1B).

As previously reported (Bowman et al., 2000), there are 5 β-strands and 3 central α-helices in the predicted tertiary structures of CmADFs (Supplementary Figure 1). A comparative analysis of the protein sequence and gene structure of the ADFs from melon and *Arabidopsis* showed that they contain the conserved serine-6 residue at the N-terminus (except *CmADF5* and *AtADF5* of which were replaced by threonine, and *CmADF8* of which was deleted), conserved actin binding sites (R98/135/137 and K82/100 in AtADF1) (Dong et al., 2013) (Figure 1C), as well as conserved

10.3389/fpls.2024.1419719

motifs (Supplementary Figure 2) and gene structure (Figure 1D). Exon-intron structures of *ADFs* in melon and *Arabidopsis* is very conservative (Figure 1D). The homologous *ADFs* of the two species were comprised three exons and two introns (except CmADF8) and same number of amino acids in the exons (except CmADF8 and AtADF1). The first exons of CmADFs and AtADFs in Subclass I and II (except CmADF8 and AtADF1) contained only 3 amino acids (start codon ATG), followed by a longer first intron

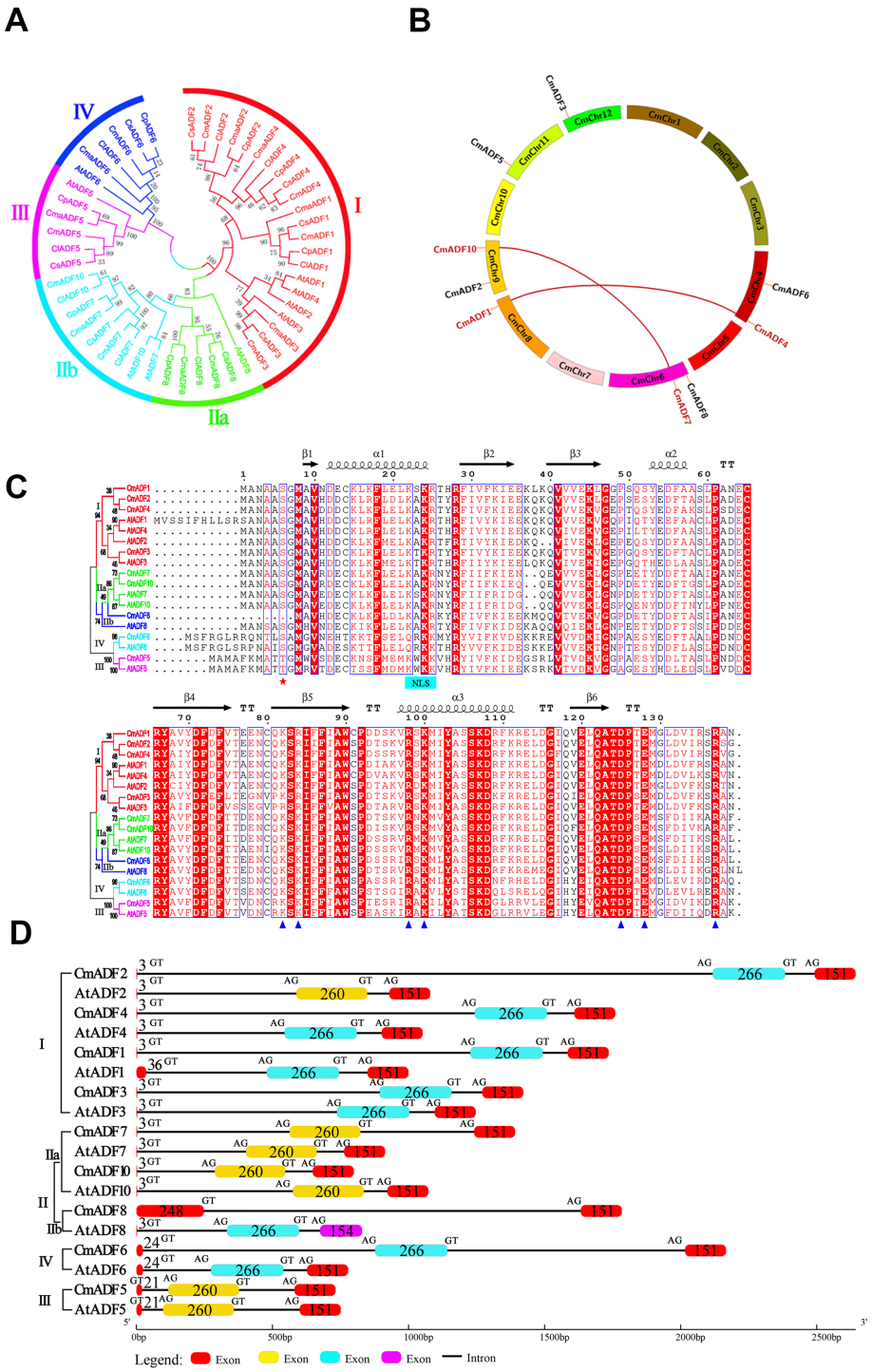

FIGURE 1
Phylogenetic relationship, Chromosomal location and duplication events, Sequence alignment, exon-intron structures of *CmADFs*. **(A)** Phylogenetic tree of ADF proteins from melon and other plants. Cucumis melon, *Arabidopsis thaliana*, *Cucumis sativus*, *Citrullus lanatus subsp*, *Cucurbita maxima var*, *Cucurbita pepo subsp* were represented by Cm, At, Cs, Cla, Cma and Cp, respectively. **(B)** Location and duplication events of 9 *CmADF* genes onto six melon chromosomes. The segmentally duplicated genes are linked by red lines. **(C)** Sequence alignment of CmADF and AtADF proteins. Pentagons indicate conserved sites that may bind to G-actin and F-actin, blue pentagons indicate the 6th serine site, and blue bar indicates the nuclear localization signal. **(D)** Exon-intron structures of *ADFs* in melon and *Arabidopsis*. The numbers indicates the length of exon. GT and AG indicate splicing sites.

(Figure 1D), while the ones of *CmADFs* and *AtADFs* in Subclass III and IV increased to 21 and 24 amino acids due to the alteration of the intron conserved clipping site (GT) after ATG (Figure 1D) and intron sliding (Nan et al., 2017).

Analysis of promoter sequences showed that in addition to many light response elements in all members, *CmADF* promoters contained several key defense and stress responsiveness, low-temperature responsiveness, and heat stress cis-acting elements and elements involved in the response to various hormones, such as abscisic acid (ABA), salicylic acid (SA), gibberellins (GA), auxin (IAA), ethylene, and methyl jasmonate (MeJA) (Supplementary Figure 3). It also contained DRE and MYB binding sites.

Expression pattern analysis of *CmADFs* in different oriental melon tissues

RT-qPCR was performed for analyzing the expression of *CmADFs* in different oriental melon tissues. The expression of *CmADFs* was clearly divided into two categories: *CmADFs* from subclass I, III and IV were expressed in all tissues, while *CmADFs* from subclass II were specifically expressed in flowers (Figure 2). Only *CmADF1* was highly expressed in leaves, the other *ADFs* showed higher expression levels in male flowers and female flowers than that in roots, stems, and leaves. Compared with other *CmADFs*, *CmADF2*, *CmADF3* and *CmADF6* had extremely higher expression levels in all tissues.

Expression pattern analysis of *CmADFs* under low and high temperature stress

Temperature change is one of the main environmental stressors affecting the growth and yield of melon (Korkmaz and Dufault, 2004). In order to gain an insight into the potential function of CmADFs in unfavorable temperature conditions, we analyzed the expression of *CmADFs* in leaves of oriental melon seedlings at two-leaf stage under low and high temperature stress. The results showed that except for CmADF3/7/8, the expression of other CmADFs was induced by low temperature stress (Figure 3A). Among them, *CmADF6* expression was the highest, and *CmADF1* expression was high and stable. Under high temperature stress, the expression of *CmADF1/3/4/7/8/10* was significantly induced, and the expression of *CmADF10* increased the highest, while the expression of *CmADF2/5/6* decreased, and *CmADF2* continued to be significantly down-regulated, indicating that the expression of *CmADFs* was complex under high temperature stress (Figure 3B). Under low and high temperature, the expression of *CmADF1/4/10* was all induced, but only *CmADF1* was significantly up-regulated.

Expression pattern analysis of *CmADFs* in ABA and SA stress

Considering that ABA and SA are the main hormones in plant adaptation to stresses, we analyzed the expression of *CmADFs* in leaves under ABA and SA stress. The results showed that after ABA treatment, only *CmADF2* expression was down-regulated, and all the other *CmADFs* were up-regulated. Other genes reached the highest expression level at 6 h after treatments, except for *CmADF8*, which reached the peak value at 24 h (Figure 4A). Under SA stress, all *CmADFs* responded sharply at the beginning, increasing their expression with approximately 13-770 folds, and continued to be highly expressed until 24 h (Figure 4B). These results reveal that *CmADFs* respond to SA and ABA induction. Overall, CmADF1 was significantly upregulated in response to temperature and hormonal signals. At the same time, *CmADF1* expression levels was high and stable under low temperature stress, indicating that CmADF1 plays an important role in environmental and hormonal signals. Therefore, CmADF1 was selected for the study of low temperature tolerance in plants.

Subcellular localization of *CmADF1*

Transgenic *Arabidopsis* plants in T3 were observed by laser scanning confocal microscope for the localization and actin filaments binding of *CmADF1*. As shown in Figure 5, a large number of actin filaments bundle structures formed by *CmADF1*-

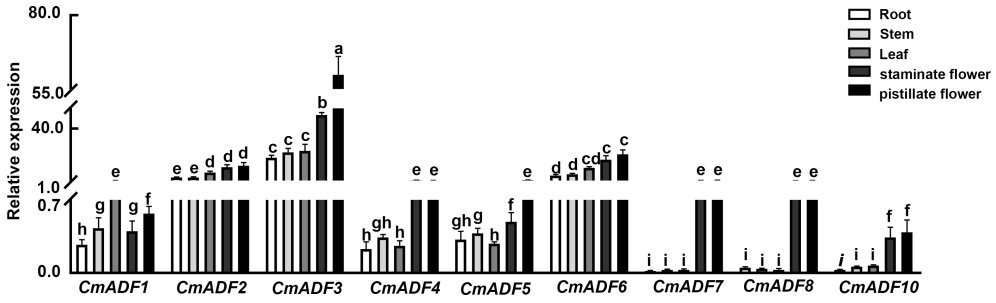

FIGURE 2
The expression of *CmADFs* in different Oriental melon tissues. The relative expression of *CmADFs* were determined by RT-qPCR, and *18S* was used as an internal control. All values used for statistical analysis were the mean ± SD of three independently replicated experiments, and then a Tukey's *post-hoc* test was performed using one-way ANOVA. Different lowercase letters indicate a significant difference.

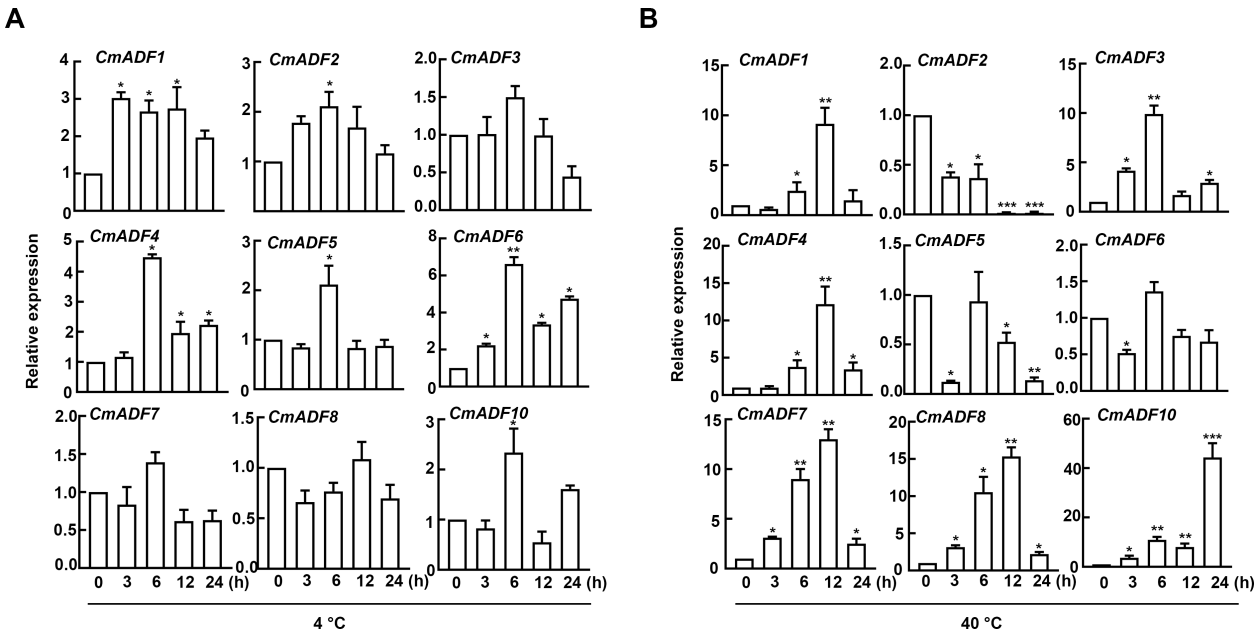

FIGURE 3
The expression of *CmADFs* under low (4°C) **(A)** and high (40°C) **(B)** temperature treatments according to RT-qPCR. *18S* was used as an internal control. The values are means ± SD from three independent replicate experiments (Student's t-test, *P < 0.05,** p < 0.01,***P < 0.001). The significant difference is represented by asterisks.

GFP green fluorescent protein in the paver cells in the control group (Figures 5A, B). These actin filaments in the paver cells were shortened or disappeared after 50 nM LatB (microfilament depolymerization drug) treatment (Figure 5A). Moreover, the filamentous structure did not change after 50 nM Oryzalin (a microtubule depolymerization drug) treatment (Figure 5B), further indicating that CmADF1 specifically binds to actin filaments rather than microtubules in *Arabidopsis*.

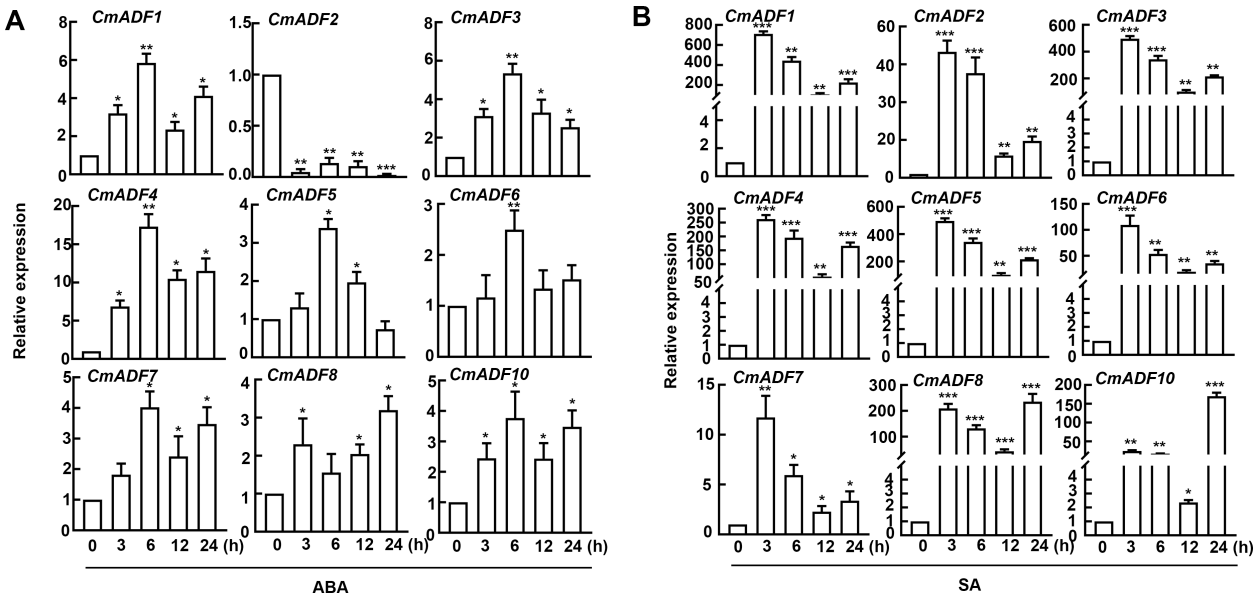

FIGURE 4
The expression of *CmADFs* under ABA (0.1 mM) **(A)** and SA (0.1 mM) **(B)** treatments according to RT-qPCR. *18S* was used as an internal control. The values are means ± SD from three independent replicate experiments (Student's t-test, *P < 0.05,** p < 0.01,***P < 0.001). The significant difference is represented by asterisks.

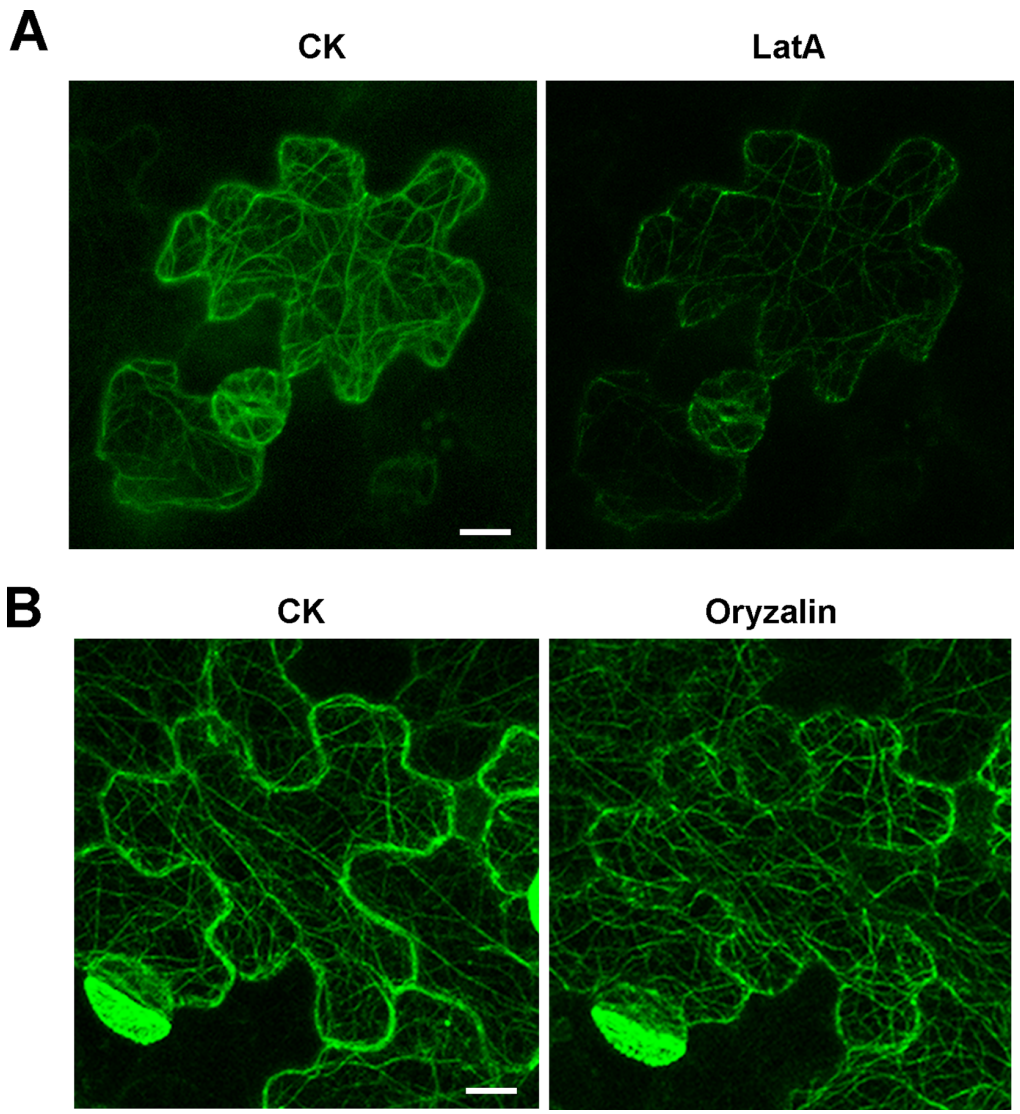

FIGURE 5
CmADF1 localization on actin filaments in melon. The leaves of 5-day transgenic *Arabidopsis* homozygous T3 plants were used for observation. **(A)** The actin filaments skeleton formed by *CmADF1*-GFP before (CK) and after Lat B treatment (50 nM). **(B)** The actin filaments skeleton formed by *CmADF1*-GFP before (CK) and after oryzalin treatment (50 nM). Scale bar = 25 μm.

Promoter activity analysis of *CmADF1*

It has been reported that *AtADF1* plays an important role in stresses such as salt and high temperature stress (Wang et al., 2021, 2023). Our results showed that *CmADF1* maintained a high expression in melon under low temperature conditions. Therefore, we investigated the mechanism of CmADF1 in melon adaptation to low temperature stress. Firstly, GUS staining was used to detect the effect of low temperature on the activity of CmADF1 promoter, and to further verify the expression pattern of *CmADF1* gene under low temperature stress. After 4°C treatment, the color of p*CmADF1*::GUS plants deepened with the prolongation of treatment time, and the expression of *CmADF1* was significantly up-regulated (Figure 6), demonstrating that low temperature promoted the activity of CmADF1 promoter.

CmADF1 overexpression affects actin filaments stability under low temperature stress

ADF1 is an actin filament depolymerizing protein. To explore whether *CmADF1* can regulate actin filaments under low temperatures, we constructed transgenic *Arabidopsis* overexpressed T3 homozygous lines (*CmADF1*-OE#6 and *CmADF1*-OE#8) (Supplementary Figure 4). The homozygous offsprings (*CmADF1*-OE#8) of *CmADF1*-OE#8 × *fABD2-GFP* were selected to observe actin filaments. Compared with WT, *CmADF1*-OE#8 seedlings had fewer actin filaments bundles, and more short filaments under both normal and low temperatures (Figures 7A, B). Consistent with the morphology of actin filaments, quantitative analysis of actin filament organization showed that the skewness value, bunting rate,

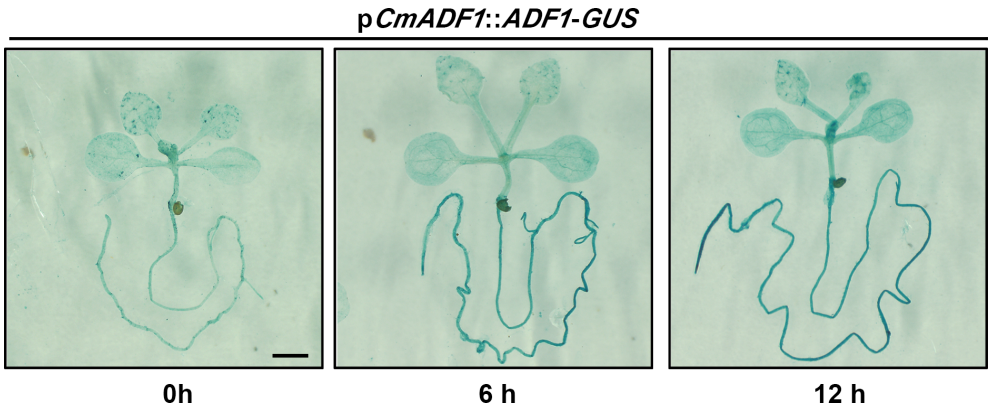

FIGURE 6
CmADF1 promoter activity analysis under low temperature treatment. Staining of *pCmADF1*::GUS transgenic *Arabidopsis* plants under low temperature for 0 h, 6 h and 12 h. Scale bar = 1 mm.

fluorescence density and length of actin filaments in *CmADF1*-OE#8 were significantly lower than those in WT (Figure 7B), indicating that overexpression of *CmADF1* caused the instability of actin filaments. Compared with normal conditions, the actin filaments in WT were shorter and finer under low temperature, indicating that low temperature induced the instability of intracellular actin filaments.

CmADF1 overexpression enhance the low temperature tolerance in Arabidopsis

T3 *CmADF1*-OE#6 and T3 *CmADF1*-OE#8 seedlings were used to analyze the function of CmADF1 under low temperature (Figure 8). The phenotypes of 14-day-old WT, *CmADF1*-OE#6 and *CmADF1*-OE#8 seedlings were observed under normal (22°C) and low temperature (4°C) stress for 0, 24 and 48 h. There was no significant difference between WT and overexpressed plants before low temperature treatment. After treatment for 24 and 48 h, the leaves of WT plants shrunk significantly in size (Figures 8A–C) and lost more water (Figure 8D), compared with those of overexpressed plants. WT plants were more severely damaged than overexpressed plants after 48 h of treatment, with water-soaked spots on the leaves (Figure 8C).

CmADF1-OE seedlings showed superior resistance by less damage to low temperature stress with more fine actin bundles

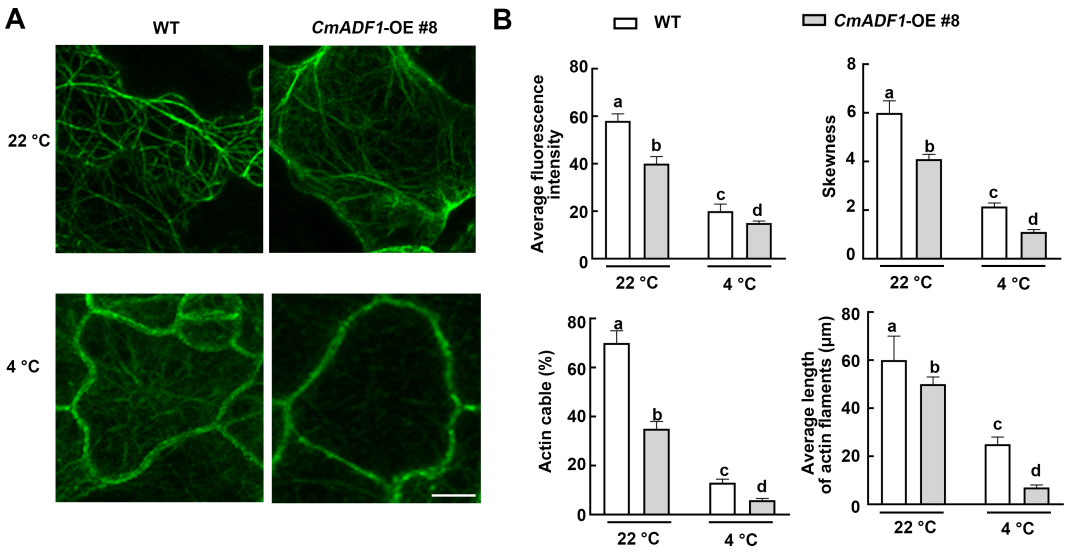

FIGURE 7
CmADF1 increases the instability of actin filaments under low temperatures. The organization **(A)**, Average fluorescence density, actin cable and average length **(B)** of actin filaments in WT and *CmADF1*-OE#8 plants under low temperature treatment. Indicators in **(B)** are measured based on images in **(A)**. Values are means ± SD (At least 30 individual seedlings from different genotypes and treatments were used to collect more than 300 images). One-way ANOVA followed by a Tukey's *post-hoc* test is used for statistical analysis. Different lowercase letters denoted significant differences. Scale bar= 25 μm.

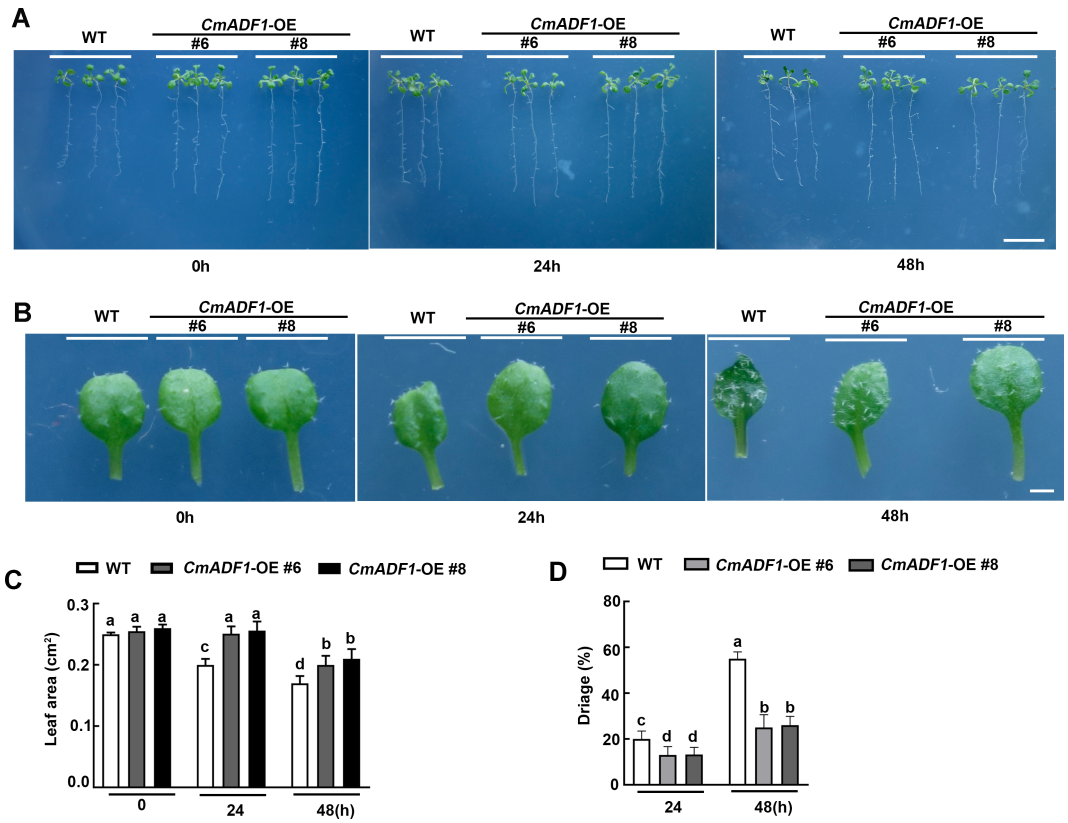

FIGURE 8
CmADF1-OE positively regulates low temperature tolerance of *Arabidopsis*. Plant Phenotype **(A)**, Leaves Phenotype **(B)**, Leaves Area **(C)**, Water loss rate of plants **(D)** of *CmADF1* transgenic seedlings under low temperature treatment. 14-day-old seedlings of WT, *CmADF1*-OE#6 and *CmADF1*-OE#8 were placed in normal temperature (22°C) and low temperature (4°C) chamber for 0, 24 and 48 h. At least 60 leaves from 30 seedlings were measured in **(C)** and at least 400 seedlings were measured in **(D)**. One-way ANOVA followed by a Tukey's *post-hoc* test is used for statistical analysis. Different lowercase letters denoted significant differences. Scale bar=1cm in **(A)**, Scale bar=1mm in **(B)**.

and short filaments than WT seedlings (Figures 7A, B), which implicated that *CmADF1* enhanced plant tolerance to low temperature by regulating actin filaments organization.

CmADF1-Silenced Plants are Sensitive in response to Low Temperature

The expression level of *CmADF1* was detected by RT-qPCR when the *CmADF1* gene silencing (TRV-A) plants obtained by VIGS technology had two leaves, and TRV-A plants with high silencing efficiency were selected for subsequent research (Figure 9A). Under optimal temperature control conditions, no significant difference in growth between TRV-A and control plants was observed (TRV-0) (Figure 9B). After treatment at 4° C for 6 and 12 h, TRV-A plants suffered more serious damage than TRV-0 plants, and their leaves shrunk more seriously and lost more water (Figures 9B–D). Compared with TRV-0 plants, the relative electrolyte leakage (REL) and malondialdehyde content of TRV-A plants were higher, while the contents of soluble protein and proline and the activities of SOD, POD and CAT were lower, reaching a significant level at 12 h (except for REL) (Figure 9E), illustrating that silencing *CmADF1* reduced the low temperature tolerance of oriental melon.

Discussion

Highly conservative *CmADF* genes in oriental melon

Since the *ADF* gene was discovered in the early 1980s, more and more ADFs had been found gradually in different species. In eukaryotic cells, ADFs were encoded by polygene families, which were abundant in plants (Maciver and Hussey, 2002). The reported plant ADF families includes 11 *ADFs* in *Arabidopsis* (Ruzicka et al., 2007), rice (Feng et al., 2006) and tobacco (Khatun et al., 2016), 13 *ADFs* in maize (Huang et al., 2020), 25 *ADFs* in wheat (Xu et al., 2021) and 18 *ADFs* in soybean (Sun et al., 2023). The ADF gene family is considered to be structurally and functionally conserved in plants (McCurdy et al., 2001). In our study, 9 *ADF* genes were

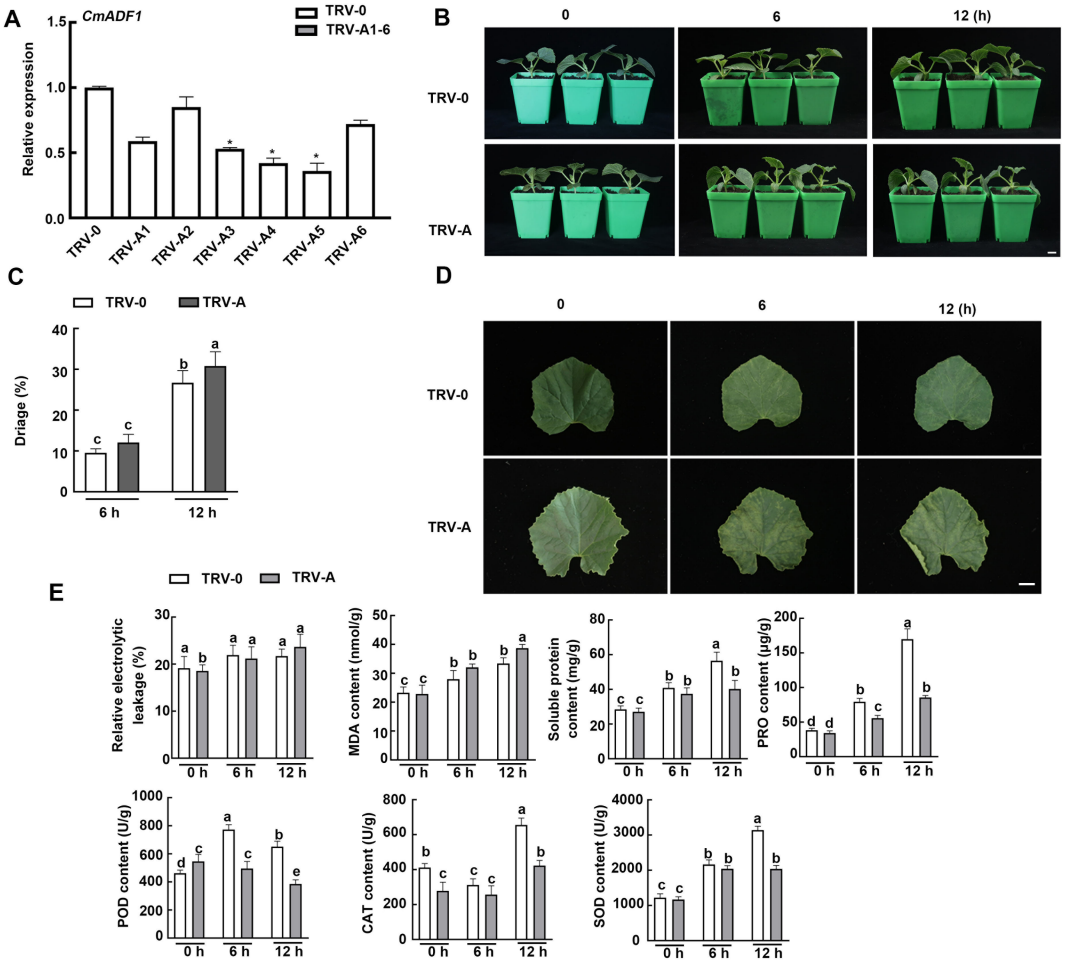

FIGURE 9
The silencing of *CmADF1* in oriental melon seedlings by virus-induced gene silencing (VIGS) increased its sensitivity to low temperature. *CmADF1* expression **(A)**, Plant phenotype **(B)**, Water loss rate of leaves **(C)**, Leaves **(D)**, the relative electrolyte leakage (REL), malondialdehyde (MDA), Soluble protein and proline content (PRO), SOD, POD and CAT activity **(E)** of TRV-0 (control) plants and TRV-A (*CmADF1*-silenced) plants under low temperature treatment. Scale bar=1 cm.

identified in oriental melon for the first time, and they were distributed to four subclasses as in *Arabidopsis*. Moreover, they were almost the same as their homologue AtADFs in intron-exon structure, number of amino acids contained in exons, as well as type and number of motifs. There were also some important conserved sites in CmADFs, such as the serine at position 6 of N-terminal (S6), actin binding sites (Figure 1C). The activity of ADF protein was regulated by phosphorylation of N-terminal conserved serine or threonine. The S6 mutant of ZmADF3 lost its ability to bind to G-actin and F-actin (Smertenko et al., 1998). The S6 activity of LlADF1 decreased after phosphorylation, and the binding and disassembly F-actin activities were lost (Allwood et al., 2002). The base residues (K82, R135, R137) on β-chain and α-helix form actin binding sites, which is important for G-and F-actin binding (Dong et al., 2013). These results indicate that *ADF* family genes are structurally conserved.

The ADFs in flowering plants probably evolved from a common ancestor (Nan et al., 2017). Fragments and tandem gene duplication are considered to be the major driving forces in the evolution of large gene families (Cannon et al., 2004). Duplicate gene pairs in *Arabidopsis* and wheat are likely caused by tandem duplication, while two pairs of segmentally duplicated genes *ADF7/10* and *ADF1/4* were observed (Figure 1B; Supplementary Table 4) in melon as in tomato (Khatun et al., 2016), maize (Huang et al., 2020), and soybean (Xu et al., 2021). The ADF gene family has been differentiated in expression pattern and function during a long evolutionary process (Kijima et al., 2016). The angiosperm *ADF* gene family consists of four very conserved subfamilies, which are divided into two classes: reproductive or constitutive/vegetative (Ruzicka et al., 2007). In our study, tissue expression patterns of *ADFs* in melon were similar to those in *Arabidopsis*. *CmADFs* in Subclass I, III, and IV are expressed in all tissues examined and may

play a critical role in growth and development (Figure 2). *CmADFs* in Subclass II specifically expressed in flowers may contribute to reproductive development (Figure 2). Unlike *AtADF8*, which is mainly expressed in roots and root hairs, *CmADF8* is specifically expressed in flowers, indicating that different species are relatively independent in the subsequent evolutionary process. In general, ADF family genes were quite conserved in the long-term evolution of plants.

A large number of CmADFs respond to temperature stress and hormone signals

Expression analysis of *ADF* gene families in tomato, maize, wheat and soybean revealed that the expression of *ADFs* would change significantly under abiotic stresses such as heat, cold, drought, high salt, abscisic acid (ABA), jasmonic acid (JA) and injury (Khatun et al., 2016; Huang et al., 2020; Xu et al., 2021; Sun et al., 2023). Many ADFs in tomatoes were induced by cold, heat, drought, NaCl, ABA, JA, and injury treatment (Khatun et al., 2016). In maize, ZmADF1 was significantly up-regulated under all abiotic stresses, and ZmADF2 and ZmADF3 were significantly induced under high temperature, drought and ABA treatment (Huang et al., 2020). The expression of *GmADFs* in soybean changed under high temperature, low temperature, drought and salt stresses, and *GmADF2/5/9/12/13/16/18* were significantly induced by heat stress (Sun et al., 2023). *TaADF16/17/18* in wheat promoted the freezing resistance of wheat plants acclimated to the cold (Xu et al., 2021). ADF1 in Arabidopsis has been shown to participate in high temperature and salt stresses, and is also the most important member of *Arabidopsis* ADF family involved in stress.

In present study, *CmADF1* was significantly induced in all treatments (Figures 3, 4), suggesting that, similar to *Arabidopsis*, ADF1 in melon may have an important effect on stress tolerance. Under low temperature, *CmADF1* was stably and highly expressed (Figure 3), while *AtADF1* was not induced, but *AtADF5* and *AtADF9* in Subclass III were significantly up-regulated (Fan et al., 2016). This indicates that *ADF* genes in different plants are functionally differentiated. Members of a gene family from the same group may have similar functions (Huang et al., 2020). *CmADF1/3/4* from Subclass I and *CmADF7/8/10* from Subclass II were both significantly induced under high temperature, ABA, and SA treatments (Figures 3, 4), suggesting that they may confer plants tolerance to these stresses. Studies have shown that actin depolymerization can increase plant resistance to pathogens, and that SA is crucial to this process (Leontovyčová et al., 2019). The expression of *CmADFs* was increased several hundred-fold under SA treatments, which may enhance resistance to biotic stress by depolymerizing actin filaments dependent on SA signaling pathway. *CmADF2* was sensitive to high temperature and ABA treatments, indicating the diversity and complexity of functions among family members in resistance to stress. A large number of *ADFs* respond to different abiotic stresses, and the function of some of them in stresses has been proven, so it is necessary for us to further study ADFs.

CmADF1 plays an important role in plant low temperature tolerance

Low temperature is an important factor affecting the yield of Oriental melon. The detail molecular mechanism of dynamic changes of actin filaments under low temperature is still uncovered, the only thing we know is that low temperature treatment leads to the depolymerization of actin filaments like the other abiotic stresses do, such as salt, high temperature, and osmotic stress (Pokorná et al., 2004; Wang et al., 2011; Fan et al., 2015). Byun et al. (2021) found that DaADF3 functions to depolymerize F-actin into G-actin in transgenic rice plants overexpressing *DaADF3*, and observed cytoskeleton structural changes in *D. antarctica* seedlings in response to cold stress treatment, which imply that DaADF3 regulates the cytoskeleton structure to adapt to changing environmental conditions, especially cold stress in *D. antarctica*. ADF members in Subclass I have functions in resisting biotic/abiotic stresses (Huang et al., 2020). *ADF1* in Subclass I is highly expressed in all tissues and is most closely related to salt stress and high temperature stress (Wang et al., 2021, 2023).

Our study found that *CmADF1* is the only gene in the melon ADF family with highly stable up-regulated under low temperatures (Figure 3A), and GUS staining (Figure 6) confirmed this result. Therefore, CmADF1 may be a primary protein responding to low temperature stress in the CmADF family. Previous studies have found that some ADFs are involved in responding to low temperature, however there is still a lack of in-depth study on actin filament dynamics. Our studies revealed that low temperature stress induced actin filaments instability (Figure 8), which is consistent with the ADF family that is functionally characterized by depolymerization and cutting actin filaments. Our results further indicated that *CmADF1*-OE transgenic seedlings with low temperature-promoted the depolymerization of actin filaments showed more resistant to low temperature (Figure 7A). These suggests that the actin filaments morphology of *CmADF1*-OE under low temperature is directly caused by the function of CmADF1 to depolymerize and cut single actin filament, and CmADF1 regulates remodeling of the actin cytoskeleton to adapt to low temperature stress in melon.

Actin filaments depolymerization have been proved to play a positive regulatory role in salt, osmotic, high temperature and drought stress (Wang et al., 2011; Fan et al., 2015). Xu et al. (2021) found that *TaADF16*-OE transgenic *Arabidopsis* plants suffered less freezing damage in comparison with WT, and had higher POD and SOD activities and more soluble sugar accumulation after a 24h incubation at 4°C. They believed that overexpression of *TaADF16* may contributes to the positive effects on ROS scavenging and osmotic regulation, and enhances the freezing resistance of *Arabidopsis* plants. In our experiment, *CmADF1*-OE conferred *Arabidopsis* better growth status under low temperature compared with WT and *Atadf1*, demonstrating that *CmADF1* enhanced the low temperature tolerance of seedlings and promoted seedlings growth. Meanwhile, *CmADF1*-silenced oriental melon seedlings showed that the contents of soluble protein and proline, and the activities of superoxide dismutase (SOD), peroxidase (POD) and Catalase (CAT) were

significantly lower than those in the control. Thus, CmADF1 is a key protein that triggers low-temperature induced actin filament depolymerization in melon, which improves the plant's low-temperature tolerance. Zhang et al. (2021) found that *AtADF5*, as a downstream target gene of C-repeat binding factor (CBF) signaling pathway, is involved in plant response and resistance to low temperature stress by regulating the dynamics of actin filaments. Overexpression of *TaADF16* induces the expression of cold-responsive genes, which may regulate cold tolerance through interaction with ICE (inducer of *CBF* expression)-CBF-related genes (Xu et al., 2021). Synthetic nucleotides designed based on the DRE element contained in the DaADF3 promoter have a high binding affinity with DaCBF7 (Byun et al., 2015, 2021). We also found the DRE binding site in the *CmADF1* promoter (Supplementary Figure 3). Whether the CBF protein is an important factor affecting the transcription level of CmADF1 in oriental melon with low temperature tolerance will be our next work. Together, our results demonstrate that CmADF1 plays an important role in plant adaptation to low temperature by leading to depolymerization of actin filaments, providing breakthrough insights into the molecular basis for melon adaptation to low temperature stress.

Conclusion

In this study, 9 *ADF* genes were identified in Oriental melon, which were clustered into four subfamilies and their proteins contain one conserved ADF-H domain specific to ADF family genes by phylogenetic tree and conserved domain analysis (Figures 1A, C). The comparative analysis of *ADFs* in *Arabidopsis* and melon showed that *ADFs* of these two species were highly similar in phylogenetic evolution, tertiary structure, conserved motifs and key conserved sites binding to actin, indicating that plant ADF genes are very conserved in the long-term evolution process (Figures 1A, C, D; Supplementary Figures 1, 2). Various *CmADFs* displayed specific tissue expression patterns (Figure 2), some were induced by temperature and hormone signals (Figures 3, 4). *CmADF1/2/4/5/6/10 and CmADF1/3/4/7/8/10* were induced under low/high temperature stress, respectively (Figure 3). All *CmADFs* responded to SA and ABA signals (Figure 4). These results suggested that *CmADFs* may be involved in melon response to stress. *CmADF1* had high and stable expression levels under low temperature stress (Figure 3A). *CmADF1* overexpressing plants promoted the instability of actin filaments and enhanced the resistance growth to low temperature treatments (Figures 7, 8), suggesting that CmADF1 plays an important role in low temperature stress in melon. Because the expression of *CmADF1* gene was significant induced by low temperature, and the *CmADF1* gene promoter contained the binding sites of MYB and CBF (Supplementary Figure 3), the key transcription factors in plants tolerance low temperature stress, we speculate the role of CmADF1 in low temperature may be regulated by MYB and/or CBF class transcription factors. We will look for upstream transcription factors of the *CmADF1* gene to explore the molecular mechanisms of CmADF1 in low temperature in future research.

Data availability statement

The original contributions presented in the study are included in the article/Supplementary Material. Further inquiries can be directed to the corresponding authors.

Author contributions

YL: Data curation, Formal analysis, Investigation, Writing – original draft, Writing – review & editing, Conceptualization, Methodology, Project administration, Validation. SHL: Conceptualization, Investigation, Data curation, Formal analysis, Writing – review & editing. JZ: Resources, Supervision, Validation, Formal analysis, Writing – review & editing. JC: Data curation, Formal analysis, Validation, Writing – review & editing. JW: Formal analysis, Validation, Visualization, Writing – review & editing. LiW: Data curation, Validation, Visualization, Writing – review & editing. ML: Formal analysis, Validation, Writing – review & editing. LuW: Formal analysis, Visualization, Writing – review & editing. SB: Validation, Visualization, Writing – review & editing. WL: Formal analysis, Writing – review & editing. LZ: Validation, Writing – review & editing. SLL: Investigation, Writing – review & editing. DY: Formal analysis, Writing – review & editing. CD: Writing – review & editing, Investigation. SZ: Conceptualization, Project administration, Supervision, Writing – review & editing. MH: Conceptualization, Funding acquisition, Project administration, Supervision, Writing – review & editing. YG: Funding acquisition, Project administration, Supervision, Writing – review & editing. CW: Conceptualization, Funding acquisition, Project administration, Supervision, Writing – review & editing.

Funding

The author(s) declare financial support was received for the research, authorship, and/or publication of this article. This research was supported by the National Key Research and Development Program of China (2022YFE0108200), Liaoning Provincial Natural Science Foundation of China (Grant No. 2022-BS-165), the National Natural Science Foundation of China (31970183), Comprehensive Experimental Station Project of National Watermelon and Melon Industry Technology System (CARS-25), Seed Industry Innovation Project of Shenyang (22-318-2-14), Liaoning Revitalization Talents Program (XLYC2002065), and Graduate Innovation Cultivation Fund of Shenyang Agricultural University (Nos. 2021YCXB09 and 2022YCXS19). Partly supported by the open funds of the State Key Laboratory of Plant Physiology and Biochemistry (SKLPPBKF1905), the PhD Start-up Fund of Liaoning Province (2022-BS-045), and President's Fund of Liaoning Academy of Agricultural Sciences (2022BS0702).

Acknowledgments

The authors thank Researcher Wen Changlong and his team from Beijing Academy of Agriculture and Forestry Sciences for their guidance and opinions on the experiment.

Conflict of interest

The authors declare that the research was conducted in the absence of any commercial or financial relationships that could be construed as a potential conflict of interest.

Publisher's note

All claims expressed in this article are solely those of the authors and do not necessarily represent those of their affiliated organizations, or those of the publisher, the editors and the reviewers. Any product that may be evaluated in this article, or claim that may be made by its manufacturer, is not guaranteed or endorsed by the publisher.

Supplementary material

The Supplementary Material for this article can be found online at: https://www.frontiersin.org/articles/10.3389/fpls.2024.1419719/full#supplementary-material

References

Allwood, E. G., Anthony, R. G., Smertenko, A. P., Reichelt, S., Drobak, B. K., Doonan, J. H., et al. (2002). Regulation of the pollen-specific actin depolymerizing factor LlADF1. *Plant Cell* 14, 2915–2927. doi: 10.1105/tpc.005363

Andrianantoandro, E., and Pollard, T. D. (2006). Mechanism of actin filament turnover by severing and nucleation at different concentrations of ADF/cofilin. *Molecular cell* 24 (1), 13–23. doi: 10.1016/j.molcel.2006.08.006

Bamburg, J. R., and Bernstein, B. W. (2008). ADF/cofilin. *Curr. Biol. CB* 18, R273–R275. doi: 10.1016/j.cub.2008.02.002

Bi, S., Li, M., Liu, C., Liu, X., Cheng, J., Wang, L., et al. (2022). Actin depolymerizing factor ADF7 inhibits actin bundling protein VILLIN1 to regulate root hair formation in response to osmotic stress in Arabidopsis. *PloS Genet.* 18, e1010338. doi: 10.1371/journal.pgen.1010338

Bowman, G. D., Nodelman, I. M., Hong, Y., Chua, N. H., Lindberg, U., Schutt, C. E., et al. (2000). A comparative structural analysis of the ADF/cofilin family. *Proteins.* 41, 374-384. doi: 10.1002/1097-0134(20001115)41:3<374::aid-prot90>3.0.co;2-f

Byun, M. Y., Cui, L. H., Lee, A., Oh, H. G., Yoo, Y. H., Lee, J., et al. (2021). Abiotic stress-induced *actin-depolymerizing factor 3* from *deschampsia Antarctica* enhanced cold tolerance when constitutively expressed in rice. *Front. Plant Sci.* 12. doi: 10.3389/fpls.2021.734500

Byun, M. Y., Lee, J., Cui, L. H., Kang, Y., Oh, T. K., Park, H., et al. (2015). Constitutive expression of DaCBF7, an Antarctic vascular plant Deschampsia Antarctica CBF homolog, resulted in improved cold tolerance in transgenic rice plants. *Plant Sci.* 236, 61–74. doi: 10.1016/j.plantsci.2015.03.020

Cannon, S. B., Mitra, A., Baumgarten, A., Young, N. D., and May, G. (2004). The roles of segmental and tandem gene duplication in the evolution of large gene families in Arabidopsis thaliana. *BMC Plant Biol.* 4, 10. doi: 10.1186/1471-2229-4-10

Clément, M., Ketelaar, T., Rodiuc, N., Banora, M. Y., Smertenko, A., Engler, G., et al. (2009). Actin-depolymerizing factor2-mediated actin dynamics are essential for root-knot nematode infection of Arabidopsis. *Plant Cell* 21, 2963–2979. doi: 10.1105/tpc.109.069104

Daher, F. B., and Geitmann, A. (2012). Actin depolymerizing factors ADF7 and ADF10 play distinct roles during pollen development and pollen tube growth. *Plant Signal. Behav.* 7, 879–881. doi: 10.4161/psb.20436

Ding, Y., Shi, Y., and Yang, S. (2019). Advances and challenges in uncovering cold tolerance regulatory mechanisms in plants. *New Phytol.* 222, 1690–1704. doi: 10.1111/nph.15696

Dong, C. H., Tang, W. P., and Liu, J. Y. (2013). Arabidopsis AtADF1 is functionally affected by mutations on actin binding sites. *J. Integr. Plant Biol.* 55, 250–261. doi: 10.1111/jipb.12015

Dong, C. H., Xia, G. X., Hong, Y., Ramachandran, S., Kost, B., and Chua, N. H. (2001). ADF proteins are involved in the control of flowering and regulate F-actin organization, cell expansion, and organ growth in Arabidopsis. *Plant Cell* 13, 1333–1346. doi: 10.1105/tpc.13.6.1333

Fan, T. T., Ni, J. J., Dong, W. C., An, L. Z., Xiang, Y., and Cao, S. Q. (2015). Effect of low temperature on profilins and ADFs transcription and actin cytoskeleton reorganization in Arabidopsis. *Biol. Plant* 59, 793–796. doi: 10.1007/s10535-015-0546-6

Fan, T., Wang, R., Xiang, Y., An, L., and Cao, S. (2016). Heat stress induces actin cytoskeletal reorganization and transcript profiles of vegetative profilins and actin depolymerizing factors (ADFs) in *Arabidopsis*. *Acta Physiol. Plant* 38, 37. doi: 10.1007/s11738-016-2061-6

Feng, Y., Liu, Q., and Xue, Q. (2006). Comparative study of rice and Arabidopsis actin-depolymerizing factors gene families. *J. Plant Physiol.* 163, 69–79. doi: 10.1016/j.jplph.2005.01.015

Fu, Y., Duan, X., Tang, C., Li, X., Voegele, R. T., Wang, X., et al. (2014). TaADF7, an actin-depolymerizing factor, contributes to wheat resistance against Puccinia striiformis f. sp. tritici. *Plant Journal: Cell Molecu Lar Biol.* 78, 16–30. doi: 10.1111/tpj.12457

Huang, Y. C., Huang, W. L., Hong, C. Y., Lur, H. S., and Chang, M. C. (2012). Comprehensive analysis of differentially expressed rice actin depolymerizing factor gene family and heterologous overexpression of OsADF3 confers Arabido psis Thaliana drought tolerance. *Rice (New York N.Y.)* 5, 33. doi: 10.1186/1939-8433-5-33

Huang, J., Sun, W., Ren, J., Yang, R., Fan, J., Li, Y., et al. (2020). Genome-wide identification and characterization of actin-depolymerizing factor (ADF) family genes and expression analysis of responses to various stresses in zea mays L. *Int. J. Mol. Sci.* 21, 1751. doi: 10.3390/ijms21051751

Huang, S., Xiang, Y., and Ren, H. (2011). "Actin-binding proteins and actin dynamics in plant cells," in *The Plant Cytoskeleton*, vol. 2 . Ed. B. Liu (Springer-Verlag New York Inc: Springer, New York, NY), 57–80. doi: 10.1007/978-1-4419-0987-9_3

Hussey, P. J., Ketelaar, T., and Deeks, M. J. (2006). Control of the actin cytoskeleton in plant cell growth. *Annu. Rev. Plant Biol.* 57, 109–125. doi: 10.1146/annurev.arplant.57.032905.105206

Inada, N., Higaki, T., and Hasezawa, S. (2016). Nuclear function of subclass I actin-depolymerizing factor contributes to susceptibility in arabidopsis to an adapted powdery mildew fungus. *Plant Physiol.* 170, 1420–1434. doi: 10.1104/pp.15.01265

Khatun, K., Robin, A. H., Park, J. I., Kim, C. K., Lim, K. B., Kim, M. B., et al. (2016). Genome-Wide Identification, Characteriz- ation and Expression Profiling of ADF Family Genes in Solanum lycopersicum L. *Genes* 7, 79. doi: 10.3390/genes7100079

Kijima, S. T., Hirose, K., Kong, S. G., Wada, M., and Uyeda, T.Q. (2016). Distinct biochemical properties of arabidopsis thaliana actin isoforms. *Plant & cell physiology* 57 (1), 47-56. doi: 10.1093/pcp/pcv176

Korkmaz, A., and Dufault, R. (2004). Differential cold stress duration and frequency treatment effects on muskmelon seedling and field growth and yield. *Eur. J. Hortic. Sci.* 69, 12–20.

Larkin, M. A., Blackshields, G., Brown, N. P., Chenna, R., McGettigan, P. A., McWilliam, H., et al. (2007). Clustal W and clustal X version 2.0. *Bioinf. (Oxford England)* 23, 2947–2948. doi: 10.1093/bioinformatics/btm404

Leontovyčová, H., Kalachova, T., Trdá, L., Pospíchalová, R., Lamparová, L., Dobrev, P. I., et al. (2019). Actin depolymerization is able to increase plant resistance against pathogens via activation of salicylic acid signalling pathway. *Sci. Rep.* 9, 10397. doi: 10.1038/s41598-019-46465-5

Liao, J. J., Wang, C. H., Xing, Q. J., Li., Y. P., Liu, X. F., and Qi, H. Y. (2019). Overexpression and VIGS system for functional gene validation in oriental melon (Cucumis melo var. makuwa Makino). *Plant Cell Tissue Organ Culture (PCTOC)* 137, 275–284. doi: 10.1007/s11240-019-01568-9

Liu, X., Qin, T., Ma, Q., Sun, J., Liu, Z., Yuan, M., et al. (2013). Light-regulated hypocotyl elongation involves proteasome-dependent degradation of the microtubule regulatory protein WDL3 in Arabidopsis. *Plant Cell* 25, 1740–1755. doi: 10.1105/tpc.113.112789

Lynch, M., and Conery, J. S. (2000). The evolutionary fate and consequences of duplicate genes. *Sci. (New York N.Y.)* 290, 1151–1155. doi: 10.1126/science.290.5494.1151

Maciver, S. K., and Hussey, P. J. (2002). The ADF/cofilin family: actin-remodel ing proteins. *Genome Biol.* 3, 1-12. doi: 10.1186/gb-2002-3-5-reviews3007

McCurdy, D. W., Kovar, D. R., and Staiger, C. J. (2001). Actin and actin-binding proteins in higher plants. *Protoplasma* 215, 89–104. doi: 10.1007/BF01280306

Miklis, M., Consonni, C., Bhat, R. A., Lipka, V., Schulze-Lefert, P., and Panstruga, R. (2007). Barley MLO modulates actin-dependent and actin-independent antifungal defense pathways at the cell periphery. *Plant Physiol.* 144, 1132–1143. doi: 10.1104/pp.107.098897

Nan, Q., Qian, D., Niu, Y., He, Y., Tong, S., Niu, Z., et al. (2017). Plant actin-depolymerizing factors possess opposing biochemical properties arising from key amino acid changes throughout evolution. *Plant Cell* 29, 395–408. doi: 10.1105/tpc.16.00690

Ouellet, F., Carpentier, E., Cope, M. J., Monroy, A. F., and Sarhan, F. (2001). Regulation of a wheat actin- depolymerizing factor during cold acclimation. *Plant Physiol.* 125, 360–368. doi: 10.1104/pp.125.1.360

Peng, S. Q., and Huang, D. F. (2006). Expression of an Arabidopsis actin-depolymerizing factor 4 gene (AtADF4) in tobacco causes morphological change of plants. *J. Plant Physiol. Mol. Biol.* 32, 52–56.

Pokorná, J., Schwarzerová, K., Zelenková, S., Petrášek, J., Janotová, I., Čapková, V., et al. (2004). Sites of actin filament initiation and reorganization in cold-treated tobacco cells. *Plant Cell Environ.* 27, 641–653. doi: 10.1111/j.1365-3040.2004.01186.x

Qian, D., Zhang, Z., He, J., Zhang, P., Ou, X., Li, T., et al. (2019). Arabidopsis ADF5 promotes stomatal closure by regulating actin cytoskeleton remodeling in response to ABA and drought stress. *J. Exp. Bot.* 70, 435–446. doi: 10.1093/jxb/ery385

Roland, J., Berro, J., Michelot, A., Blanchoin, L., and Martiel, J. L. (2008). Stochastic severing of actin filaments by actin depolymerizing factor/cofilin controls the emergence of a steady dynamical regime. *Biophys. J.* 94, 2082–2094. doi: 10.1529/biophysj.107.121988

Ruzicka, D. R., Kandasamy, M. K., McKinney, E. C., Burgos-Rivera, B., and Meagher, R. B. (2007). The ancient subclasses of Arabidopsis Actin Depolymerizing Factor genes exhibit novel and differential expression. *Plant Journal: Cell Mol. Biol.* 52, 460–472. doi: 10.1111/j.1365-313X.2007.03257.x

Sangwan, V., Foulds, I., Singh, J., and Dhindsa, R. S. (2001). Cold-activation of Brassica napus BN115 promoter is mediated by structural changes in membranes and cytoskeleton, and requires Ca^{2+} influx. *Plant Journal: Cell Mole- Cular Biol.* 27, 1–12. doi: 10.1046/j.1365-313x.2001.01052.x

Sengupta, S., Mangu, V., Sanchez, L., Bedre, R., Joshi, R., Rajasekaran, K., et al. (2019). An actin-depolymerizing factor from the halophyte smooth cordgrass, Spartina alterniflora (SaADF2), is superior to its rice homolog (OsADF2) in conferring drought and salt tolerance when constitutively overexpressed in rice. *Plant Biotechnol. J.* 17, 188–205. doi: 10.1111/pbi.12957

Smertenko, A. P., Jiang, C. J., Simmons, N. J., Weeds, A. G., Davies, D. R., and Hussey, P. J. (1998). Ser6 in the maize actin-depolymerizing factor, ZmADF3, is phosphorylated by a calcium-stimulated protein kinase and is essential for the control of functional activity. *Plant Journal: Cell Mol. Biol.* 14, 187–193. doi: 10.1046/j.1365-313x.1998.00107.x

Sun, Y., Wang, D., Shi, M., Gong, Y., Yin, S., Jiao, Y., et al. (2023). Genome-wide identification of actin-depolymerizing factor gene family and their expression patterns under various abiotic stresses in soybean (*Glycine max*). *Front. Plant Sci.* 14. doi: 10.3389/fpls.2023.1236175

Tamura, K., Stecher, G., Peterson, D., Filipski, A., and Kumar, S. (2013). MEGA6: molecular evolutionary genetics analysis version 6.0. *Mol. Biol. Evol.* 30, 2725–2729. doi: 10.1093/molbev/mst197

Tang, C., Deng, L., Chang, D., Chen, S., Wang, X., and Kang, Z. (2016). TaADF3, an actin-depolymerizing factor, negatively modulates wheat resistance against puccinia striiformis. *Front. Plant Sci.* 6. doi: 10.3389/fpls.2015.01214

Tian, M., Chaudhry, F., Ruzicka, D. R., Meagher, R. B., Staiger, C. J., and Day, B. (2009). Arabidopsis actin-depolymerizing factor AtADF4 mediates defense signal transduction triggered by the Pseudomonas syringae effector AvrPphB. *Plant Physiol.* 150, 815–824. doi: 10.1104/pp.109.137604

Wang, X., Bi, S., Wang, L., Li, H., Gao, B. A., Huang, S., et al. (2020). GLABRA2 regulates actin bundling protein VILLIN1 in root hair growth in response to osmotic stress. *Plant Physiol.* 184, 176–193. doi: 10.1104/pp.20.00480

Wang, L., Cheng, J., Bi, S., Wang, J., Cheng, X., Liu, S., et al. (2023). Actin depolymerization factor ADF1 regulated by MYB30 plays an important role in plant thermal adaptation. *Int. J. Mol. Sci.* 24, 5675. doi: 10.3390/ijms24065675

Wang, L., Qiu, T., Yue, J., Guo, N., He, Y., Han, X., et al. (2021). Arabidopsis ADF1 is regulated by MYB73 and is involved in response to salt stress affecting actin filament organization. *Plant Cell Physiol.* 62, 1387–1395. doi: 10.1093/pcp/pcab081

Wang, C., Zhang, L. J., and Huang, R. D. (2011). Cytoskeleton and plant salt stress tolerance. *Plant Signaling Behav.* 6, 29–31. doi: 10.4161/psb.6.1.14202

Xing, Q., Liao, J., Cao, S., Li, M., Lv, T., and Qi, H. (2020). CmLOX10 positively regulates drought tolerance through jasmonic acid-mediated stomatal closure in oriental melon (*Cucumis melo* var. *makuwa Makino*). *Sci. Rep.* 10, 17452. doi: 10.1038/s41598-020-74550-7

Xu, K., Zhao, Y., Zhao, S., Liu, H., Wang, W., Zhang, S., et al. (2021). Genome-wide identification and low temperature responsive pattern of actin depolymerizing factor (ADF) gene family in wheat (*Triticum aestivum* L.). *Front. Plant Sci.* 12. doi: 10.3389/fpls.2021.618984

Yao, H., Li, X., Peng, L., Hua, X., Zhang, Q., Li, K., et al. (2022). Binding of 14-3-3κ to ADF4 is involved in the regulation of hypocotyl growth and response to osmotic stress in Arabidopsis. *Plant science: an Int. J. Exp. Plant Biol.* 320, 111261. doi: 10.1016/j.plantsci.2022.111261

Ye, J., Zhang, W., and Guo, Y. (2013). Arabidopsis SOS3 plays an important role in salt tolerance by mediating calcium-dependent microfilament reorganization. *Plant Cell Rep.* 32, 139–148. doi: 10.1007/s00299-012-1348-3

Zhang, B., Hua, Y., Wang, J., Huo, Y., Shimono, M., Day, B., et al. (2017). TaADF4, an actin- depolymerizing factor from wheat, is required for resistance to the stripe rust pathogen Puccinia striiformis f. sp. tritici. *Plant Journal: Cell Mol. Biol.* 89, 1210–1224. doi: 10.1111/tpj.13459

Zhang, P., Qian, D., Luo, C., Niu, Y., Li, T., Li, C., et al. (2021). Arabidopsis ADF5 acts as a downstream target gene of CBFs in response to low-temperature stress. *Front. Cell Dev. Biol.* 9. doi: 10.3389/fcell.2021.635533

Zhang, Y. P., Yao, X. Q., Yang, S. J., Xv, S., and Chen, Y. Y. (2017). Effects of low temperature treatment and recovery on the photosynthesis and antioxidantcharacteristics in melon seedlings. *Acta Agriculturae Shanghai* 33, 41–49.

Zhang, L., Yuan, M., Ge, Y., Liu, Y., Fan, J., Ruan, Y., et al. (2010). The microfilament cytoskeleton plays a vital role in salt and osmotic stress tolerance in Arabidopsis. *Plant Biol. (Stuttgart Germany)* 12, 70–78. doi: 10.1111/j.1438-8677.2009.00201.x

Zhao, S., Jiang, Y., Zhao, Y., Huang, S., Yuan, M., Zhao, Y., et al. (2016). CASEIN KINASE1-LIKE PROTEIN2 regulates actin filament stability and stomatal closure via phosphorylation of actin depolymerizing factor. *Plant Cell* 28, 1422–1439. doi: 10.1105/tpc.16.00078

Zheng, Y., Xie, Y., Jiang, Y., Qu, X., and Huang, S. (2013). Arabidopsis actindepolymerizing factor7 severs actin filaments and regulates actin cable turnover to promote normal pollen tube growth. *Plant Cell* 25, 3405–3423. doi: 10.1105/tpc.113.117820

Zhu, J., Nan, Q., Qin, T., Qian, D., Mao, T., Yuan, S., et al. (2017). Higher-ordered actin structures remodeled by arabidopsis ACTIN-DEPOLYMERIZING FACTOR5 are important for pollen germination and pollen tube growth. *Mol. Plant* 10, 1065–1081. doi: 10.1016/j.molp.2017.06.001

frontiers | Frontiers in Plant Science

TYPE Original Research
PUBLISHED 09 September 2024
DOI 10.3389/fpls.2024.1413716

OPEN ACCESS

EDITED BY
Shifeng Cao,
Zhejiang Wanli University, China

REVIEWED BY
Lijun Sun,
Nantong University, China
Hongyan Qi,
Shenyang Agricultural University, China

*CORRESPONDENCE
Yusong Luo
523622643@qq.com

RECEIVED 07 April 2024
ACCEPTED 10 June 2024
PUBLISHED 09 September 2024

CITATION
Sun S, Yang Y, Hao S, Liu Y, Zhang X, Yang P, Zhang X and Luo Y (2024) Comparison of transcriptome and metabolome analysis revealed cold-resistant metabolic pathways in cucumber roots under low-temperature stress in root zone.
Front. Plant Sci. 15:1413716.
doi: 10.3389/fpls.2024.1413716

Comparison of transcriptome and metabolome analysis revealed cold-resistant metabolic pathways in cucumber roots under low-temperature stress in root zone

Shijun Sun[1,2,3], Yan Yang[4], Shuiyuan Hao[1,3], Ye Liu[1,3], Xin Zhang[1,3], Pudi Yang[1,3], Xudong Zhang[1,3] and Yusong Luo[5]*

[1]Hetao College, Department of Agronomy, Bayannur, China, [2]Key Laboratory of Urban Agriculture, Ministry of Agriculture and Rural Affairs, Shanghai, China, [3]Hetao Green Agricultural Product Safety Production and Warning Control Laboratory, Hetao College, Bayannur, China, [4]Urat Middle Banner Green Industry Development Center, Bayannur, China, [5]Department of Horticulture, Hunan Agricultural University, Changsha, Hunan, China

Introduction: Low ground temperature is a major factor limiting overwintering in cucumber cultivation facilities in northern alpine regions. Lower temperatures in the root zone directly affect the physiological function of the root system, which in turn affects the normal physiological activity of plants. However, the importance of the ground temperature in facilities has not attracted sufficient attention.

Methods: Therefore, this study tested the cucumber variety Jinyou 35 under three root zone temperatures (room temperature, 20–22°C; suboptimal temperature, 13– 15°C; and low temperature, 8–10°C) to investigated possible cold resistance mechanisms in the root of cucumber seedlings through hormone, metabolomics, and transcriptomics analyses.

Results and discussion: The results showed that cucumber roots were subjected to chilling stress at different temperatures. Hormone analysis indicated that auxin content was highest in the roots. Jasmonic acid and strigolactone participated in the low-temperature stress response. Auxin and jasmonate are key hormones that regulate the response of cucumber roots to low temperatures. Phenolic acid was the most abundant metabolite in cucumber roots under chilling stress. Additionally, triterpenes may play an important role in chilling resistance. Differentially expressed genes and metabolites were significantly enriched in benzoxazinoid biosynthesis in the room temperature vs. suboptimal temperature groups and the room temperature vs. low temperature groups. Most differentially expressed transcription factor genes in AP2/ERF were strongly induced in cucumber roots by both suboptimal and low-temperature stress conditions. These results provide guidance for the cultivation of cucumber in facilities.

KEYWORDS

cucumber, root, cold-resistant, transcriptome, metabolome

1 Introduction

Cucumbers originated in the tropical rainforests of the southern foothills of the Himalayas and now exhibit a wide distribution, large cultivation area, high yield, and high economic value. According to FAO data (https://www.fao.org/zh), the area harvested in 2020 of cucumber reached 1,311,461 ha, and the yield reached 58,947.4 $kg{\cdot}ha^{-1}$ in China. Cucumber is a typical thermophilic plant with high-temperature requirements throughout its entire life cycle, especially for seedlings, which are more sensitive to low temperatures (Walters, 1989). In addition, different varieties of cucumber have different resistance to low temperature stress (Li et al., 2022). In northern China, cucumbers are often used for early spring and overwinter cultivation. The seedling stage or early planting date is often affected by low temperatures (such as the late spring coldness in March and April in Northern China), which affect plant growth and development, delay the fruit listing period, and may cause economic losses (Li et al., 2022).

At present, most horticultural facilities in northern China are relatively simple, and modern technology applications are limited. Therefore, crops grown in facilities are always grown under adverse environmental conditions, resulting in low yields, poor quality, and limited economic benefits (Sun et al., 2010). Environmental factors such as temperature, light, moisture, and CO_2 concentration are of great significance for plant growth. Among these factors, root zone temperature plays a crucial role in plant growth (Sun et al., 2016). The adaptation range of cucumber root to temperature was narrow. Damage to root cells will affect the function of root and growth of aerial portion. Low-temperature root stresses can be categorized as chilling injury (cold injury above 0°C) and freezing injury (freezing injury below 0°C) (Jan et al., 2009; Chen et al., 2020). Previous studies have indicated that chilling injury affects the structure and function of cell membranes, enhancing membrane permeability and solute ion exudation, thereby changing the balance of ion concentrations inside and outside the cells (Bai et al., 2021). It also affects enzyme activity, leading to metabolic disorders (Zhao et al., 2021). While freezing injury can cause freezing inside and outside plant cells, salt toxicity, membrane protein degradation, and biofifilm system damage (Xu et al., 2023). In severe cases freezing injury may lead to the death of the whole plant (Saadati et al., 2021). Chilling and freezing injuries differ in their mechanisms and outcomes (Lijing Chen et al., 2014; Gong et al., 2020). In addition, chilling injuries account for the main issues occurring under low temperatures that must be solved in cucumber production facilities.

To develop a method for protecting cucumber crops from low-temperature stress and support future cultivation, we must first understand the mechanisms of low-temperature stress responses at the molecular level. In order to survive in low temperatures, plants transduce the cold signals into downstream components, thereby inducing appropriate defense mechanisms. Low temperature stress lead to the change of the lipids conformation and proteins in membrane, increases membrane permeability, inhibits ion transport and energy conversion pathways and cause damage to the ultrastructure of cells. Then the Ca^{2+} and other second messenger would be activates and amplified the signal in a cascade. These will eventually affecting the genes expression and biosynthesis of secondary metabolite involve in defense mechanisms modules (Zhu, 2016). The endogenous hormones plays an important role in response to low temperature stress in plant though participate in signal transduction and leads to expression of downstream genes (Xiang et al., 2017). Plant hormones, such as abscisic acid (ABA), brassinosteroid (BR), gibberellin (GA), and jasmonic acid (JA), have been reported to mediate plant adaptations to cold stress (Hu et al., 2013; Ding et al., 2015; Eremina et al., 2016; Li et al., 2017; Lantzouni et al., 2019).

With the rapid development of sequencing technology, transcriptomic and metabolomic analyses have been widely used to explore the molecular mechanisms by which plants cope with low-temperature stress (Bahrman et al., 2019; Xu et al., 2023). Transcriptomics and metabolomics analyses on 1-year-old branches of the cold-resistant cultivar Hanfu and the cold-sensitive apple cultivar Changfuji No. 2 revealed that Hanfu accumulated 4-aminobutyric acid, spermidine, and ascorbic acid to scavenge reactive oxygen species. The transcription factors apetala 2/ethylene responsive factor (AP2/ERF) and WRKY were strongly induced under freezing stress (Xu et al., 2023). Besides, the NAC family transcription factor were also involve in cold resistance. The CsNAC1 was induced by cold and ABA in both leaves and roots of citrus (*Citrus reshni*) (Mauch-Mani and Flors, 2009). A combination analysis on peach cultivars Donghe No.1 and 21st Century subjected to different temperatures (-5 to -30°C) for 12 h revealed that that soluble sugar, flavone, lignin biosynthesis-associated genes, and several key genes (e.g., COMT, CCR, CAD, PER, and F3'H) may play key roles in cold tolerance in peach (Li et al., 2023). Under low-temperature stress, the expression levels of some genes associated with plant hormones and MAPK pathways were significantly upregulated, and flavonoid metabolites were significantly enriched in waxy corn inbred lines N28 compared to those in N67. These genes and metabolites may help N28 improve cold resistance (Jiang et al., 2023). The During the cold treatment phase, the biological process changes mainly focus on antioxidant, and during the recovery period, a wide range of cold resistance reactions can be found, such as the accumulation of large amounts of amino acids. The combination analysis on 2 cold-resistant rice varieties (Nipponbare and 93–11) in different cold treatment stage reveled that during the metaphase of cold treatment, antioxidation-related compounds appeared earlier in Nipponbare, while ROS levels were higher in 93–11. Compared with CBF/DREB, ROS regulated genes were more active in Nipponbare stress response. Therefore, during the recovery period, metabolites related to cold resistance were more easily expressed in the cold-tolerant Nipponbare variety, while compounds related to aging were more easily accumulated in 93–11 (Zhang et al., 2016).

According to previous study, the best root zoom temperature for cucumber is 20–25°C. When the root zone temperature is lower than 15°C, the development and growth of cucumber root will be affected by low temperature (Xue et al., 2015). The aim of the present study was to evaluate the hormone change in the root of cucumber cultivar Jinyou 35 under three root zone temperatures

(room temperature, 20–22°C; suboptimal temperature, 13–15°C; and low temperature, 8–10°C). The main metabolic pathways activated in response to chilling stress in cucumber roots were investigated using a combination of transcriptomics and metabolomics. Differentially expressed genes (DEGs) and their metabolites (DEMs) were identified. Identifying cold tolerance–related genes and analyzing the regulatory mechanisms of cold response in cucumbers using modern biological methods can provide theoretical support for the cultivation of cold-tolerant varieties.

2 Materials and methods

2.1 Plant materials

The 'Jinyou 35' cucumber cultivar was selected for analysis. 'Jinyou 35' is widely used in early spring cultivation for its good quality and cold resistance and it used to occupied more than 70% of the early spring cucumber cultivation area in China (around year 2010), and it is still widely used in Inner Mongolia province until now (https://www.taas.ac.cn) (Sun et al., 2016; Sun et al., 2018). The experiment was carried out in the Crop Cultivation Laboratory of Hetao College, Bayannaoer, Inner Mongolia Province (40°34′-41°17′N, 107°6′-107°44′E). Three root zone temperatures were set: room temperature, 20–22°C; suboptimal temperature, 13–15°C; and low temperature, 8–10°C. A peat, vermiculite, and perlite mix with a volume ratio of 6:3:1 was used as the substrate for plant culture. Seedlings were planted in soil containing temperature controllers in mid-July 2022. The planting density was set at a line interval of 12 cm and a row interval of 18 cm.

To control the soil temperature, a temperature control line was laid at 15–18 cm depth below the soil, and the temperature-sensing probe was buried approximately 8 cm deep in the soil layer. Root zone temperatures were regulated from 22:00 to 6:00 the following day. After transplantation, cucumber seedlings were placed under low-temperature conditions. The room temperature setting (20–22°C) was used as the control (CK). The suboptimal (13–15°C) and low temperatures (8–10°C) were used as the treatment conditions. Each treatment group comprised 60 seedlings. Random sampling was used. Twenty days after transplantation, the root samples were immediately frozen in liquid nitrogen. The samples were sent to Wuhan Mai Tver Biotechnology Co., Ltd. to detect endogenous hormone content and conduct transcriptomic and metabolomic analysis. The root samples were named RR (root samples under room temperature conditions), SR (root samples under suboptimal temperature conditions), and LR (root samples under low-temperature conditions). Each test was performed in triplicate.

According to our previous studies, the root length, surf area, volume, tips and forks of cucumber under low temperature stress in the root zone is shown in Table 1 (Sun et al., 2017).

2.2 Determination of endogenous hormones

High performance liquid chromatography–grade acetonitrile and methanol were purchased from Merck (Darmstadt, Germany). Milli-Q water (Millipore, Bradford, USA) was used for all experiments. All standards were purchased from Olchemim Ltd. (Olomouc, Czech Republic) and IsoReag (Shanghai, China). Acetic and formic acids were purchased from Sigma-Aldrich (St. Louis, MO, USA). Standard stock solutions (1 mg/mL) were prepared in methanol. All stock solutions were stored at -20°C. The stock solutions were diluted with methanol to obtain working solutions prior to analysis.

After freezing in liquid nitrogen, root samples were ground into powder (30 Hz, 1 min) and stored at -80°C until needed. Root samples (50 mg) were weighed into a 2 mL plastic microtubes, frozen in liquid nitrogen, and dissolved in 1 mL methanol/water/formic acid (15:4:1, V/V/V). As internal standards for quantification, 10 µL of the internal standard mixed solution (100 ng/mL) was added to the extract. The mixture was vortexed for 10 min and centrifuged for 5 min (12000 r/min, and 4°C). Then, the supernatant was transferred to clean plastic microtubes, evaporated to dryness, dissolved in 100 µL 80% methanol (V/V), and filtered through a 0.22 µm membrane filter for further LC-MS/MS analysis (Cai et al., 2014; Floková et al., 2014; Niu et al., 2014; Li et al., 2016).

The root sample extracts were analyzed using an UPLC-ESI-MS/MS system (UPLC, ExionLC™ AD https://sciex.com.cn/; MS, Applied Biosystems 6500 Triple Quadrupole, https://sciex.com.cn/). The analytical conditions were as lay out in Supplementary Table 1.

Linear ion trap and triple quadrupole (QQQ) scans were acquired on a triple quadrupole–linear ion trap mass spectrometer (QTRAP), QTRAP® 6500+ LC-MS/MS System equipped with an ESI Turbo Ion Spray interface, operating in both positive and negative ion modes and controlled by Analyst 1.6.3 software (Sciex). The ESI source operation parameters were as follows: ion source, ESI +/-; source temperature, 550°C; ion spray voltage, 5500 V (positive) and -4500 V (negative); curtain gas (CUR), 35 psi. Phytohormones were analyzed using scheduled multiple reaction monitoring (MRM). Data acquisition was performed using Analyst 1.6.3 software (Sciex). Multiquant 3.0.3

TABLE 1 Effects of low root zone temperature on root morphology of cucumber (Sun et al., 2017).

Sample	Length	Surf Area	Root Volume	Tips	Forks
RR	315.71 ± 66.37aA	39.91 ± 4.38aA	0.59 ± 0.029aA	652 ± 97aA	3827 ± 593aA
SR	170.47 ± 67.71bB	25.86 ± 5.45bB	0.54 ± 0.032bB	305 ± 102bB	2150 ± 498bB
LR	82.34 ± 27.56cC	15.28 ± 4.69cC	0.27 ± 0.023cC	112 ± 38cC	836 ± 139cC

Lowercase letters indicates significant difference (0.05>P≥0.01) and uppercase letters represents extremely significant difference (P<0.01).

software (Sciex) was used to quantify all metabolites. Mass spectrometry parameters, including the declustering potentials (DPs) and collision energies (CEs) for individual MRM transitions, were performed with further DP and CE optimization. A specific set of MRM transitions were monitored for each period according to the metabolites eluted within this period (Pan et al., 2010; Cui et al., 2015; Šimura et al., 2018).

2.3 Metabolite profiling and data analyses

Root samples were freeze-dried using a vacuum freeze-dryer (Scientz-100F). The freeze-dried samples were crushed using a mixer mill (MM 400, Retsch) with zirconia bead for 1.5 min at 30 Hz. The lyophilized powder (50 mg) was powder in 1.2 mL of 70% methanol solution and vortexed for 30 s every 30 min for six rounds total. Following centrifugation at 12000 rpm for 3 min, the extracts were filtrated (SCAA-104, 0.22 μm pore size; ANPEL, Shanghai, China, http://www.anpel.com.cn/) before UPLC-MS/MS analysis.

The sample extracts were analyzed using an UPLC-ESI-MS/MS system (UPLC, ExionLC™ AD, https://sciex.com.cn/; MS, Applied Biosystems 4500 Q TRAP, https://sciex.com.cn/). The analytical conditions were as follows, UPLC: column, Agilent SB-C18 (1.8 μm, 2.1 mm * 100 mm); The mobile phase was consisted of solvent A (pure water with 0.1% formic acid) and solvent B (acetonitrile with 0.1% formic acid). Sample measurements were performed using a gradient program that employed starting conditions of 95% A and 5% B. Within 9 min, a linear gradient of 5% A and 95% B was programmed, and a composition of 5% A and 95% B was maintained for 1 min. Subsequently, the composition was adjusted to 95% A and 5.0% B within 1.1 min and kept for 2.9 min. The flow velocity was set as 0.35 mL per min; The column oven was set to 40°C; The injection volume was 4 μL. The effluent was alternately connected to an ESI-triple quadrupole–linear ion trap-MS (QTRAP)-MS.

The ESI source operation parameters were as follows: source temperature, 550°C; ion spray voltage, 5500 V (positive) and -4500 V (negative); ion source gas I (GSI), gas II (GSII), and CUR at 50, 60, and 25 psi, respectively; and high collision-activated dissociation. QQQ scans were acquired in the MRM experiments with a collision gas (nitrogen) in the medium. The DP and CE for individual MRM transitions were determined with further DP and CE optimization. A specific set of MRM transitions was monitored for each period according to the metabolites eluted within this period.

Unsupervised principal component analysis (PCA) was performed using the prcomp statistical function in R (www.R-project.Org/). The data were unit variance scaled before unsupervised PCA.

Hierarchical cluster analysis (HCA) results of samples and metabolites were presented as heatmaps with dendrograms, whereas Pearson correlation coefficients (PCC) between samples were calculated using the cor function in R and presented only as heatmaps. Both HCA and PCC were performed using the R package, Complex Heatmap. For the HCA, the normalized signal intensities of the metabolites (unit variance scaling) were visualized as a color spectrum.

For two-group analysis, differential metabolites were determined by VIP (VIP ≥ 1) and absolute Log2FC (|Log2FC|≥ 1.0). VIP values were extracted from the OPLS-DA results, which also contained score plots and permutation plots, and were generated using the R package MetaboAnalystR. The data were log-transformed (log2) and mean-centered before OPLS-DA. A permutation test (200 permutations) was performed to avoid overfitting.

Identified metabolites were annotated using the KEGG Compound Database (http://www.kegg.jp/XXXeg/compound/), and annotated metabolites were mapped to the KEGG Pathway Database (http://www.kegg.jp/XXXeg/pathway.html). Pathways with mapped significantly regulated metabolites were then fed into metabolite set enrichment analysis, and their significance was determined using hypergeometric test p-values.

2.4 RNA-seq and data analysis

Root samples were immediately frozen in liquid nitrogen and stored at −80°C. Total RNA was extracted from roots using the RNAprep Pure Polyphenol Plant Total RNA Extraction Kit (TIANGEN, China). A cDNA library was constructed and sequenced on an Illumina HiSeq4000 system supplied by Mateware. The adapters and low-quality sequences were removed using Fastp with default parameters, and clean reads were mapped to the reference genome of the ChineseLonggenomev3.fa.gz using HISAT2. The number of mapped reads and transcript lengths were normalized. The fragments per kilobase million (FPKM) were used as indicators of transcript or gene expression. The Pearson correlation coefficient and PCA were used to evaluate the correlation and repetitiveness among samples. Differential expression analysis was performed using DESeq2 (|log2- old change| ≥1, and FDR < 0.05) to obtain differentially expressed genes between two samples. Heat maps and Venn diagrams were drawn using the Tbtools software. Three biological replicates were used for each root sample.

Nonredundant transcript sequences identified as genes were further analyzed by Gene Ontology (GO) annotation (http://www.ge-neontology.org/) to identify GO terms among DEGs with significant differences, and the Kyoto Encyclopedia of Genes and Genomes (KEGG) database (http://www.genome.jp/XXXeg/) was used to identify significantly enriched pathways.

To verify the accuracy of RNA-seq data, q-RT-PCR validation was performed using frozen root samples. First, strand c DNA was synthesized using TAKARA PrimeScript™ RTMaster Mix (Perfect Real Time). Real-time quantitative PCR was performed using a QTOWER Real-time fluorescence quantitative PCR instrument (ANALYTIKJENA, Germany) using Talent qPCR PreMix (SYBR Green). The cucumber actin gene was used as an internal control. Each reaction was performed in triplicate with are action volume of 20 μL. Cycling parameters were 96°C for 10 min, 40 cycles of 95°C for 15 s, 58°C for 20 s and 72°C for 30 s, final extension at 72°C for 10 min. Quantitative data were calculated as $2^{-\triangle\triangle}$CT.

Primer sequences are listed in Supplementary Table 2. Each test was performed in triplicate.

2.5 Statistical analyses

Each treatment was performed in triplicate, and the data are presented as the mean ± standard deviation. Significant differences ($P < 0.05$) were evaluated using SPSS Statistics (version 26.0; SPSS Inc., Chicago, IL, USA) and one-way analysis of variance with Duncan's test. The comparison groups of endogenous hormones, metabolites, and RNA-seq data were divided into RR vs. SR, RR vs. LR, and SR vs. LR groups.

3 Results

3.1 Endogenous hormone responses of cucumber roots to chilling stress

In this study, roots of the cucumber cultivar Jinyou 35 were subjected to different degrees of low temperature stress. We identified 17 differentially accumulated endogenous hormones among RR vs. SR, RR vs. LR, and SR vs. LR (Figure 1). Detailed information on differentially accumulated endogenous hormones is listed in Supplementary Table 3. Differentially accumulated endogenous hormones can be classified into six categories. As the temperature decreased, ABA and cytokinin (CK) content decreased, while auxin, GA, and JA content increased. Strigolactone (SL) content increased in SR and decreased in LR compared with RR. The hormone with the highest accumulation in cucumber roots was auxin. The proportions of SR (74%) and LR (74%) were higher than that of RR (50%), indicating that auxin is important not only in root development, but also in response to chilling injury. The accumulation trend of CK was opposite to that of auxin, indicating that the relationship between auxin and CK is stress resistant under low-temperature stress. Auxins can increase the GA levels in plants. The accumulation trend of GA was similar to that of auxin but was much lower in content. The ABA content decreased as temperature decreased, and the ratio decreased from 18% in RR to 2% in LR. There was a stress-resistance relationship between GA and ABA in cucumber roots under low-temperature stress. The JA content increased sharply in LR and was hardly detected in RR and SR, indicating that JA might play an important role in low-temperature stress. The SL content in LR was significantly higher than in RR and SR; however, the ratio in LR (22%) was lower than that in RR.

Venn diagrams show that 9, 12, and 11 differentially accumulated endogenous hormones were obtained for RR vs. SR, RR vs. LR, and SR vs. LR, respectively. These hormones may play key roles in chilling stress response. One hormone (2MeSiP) was accumulated in all groups (Figure 1B). These hormones may be associated with low root zone temperature responses in cucumber roots.

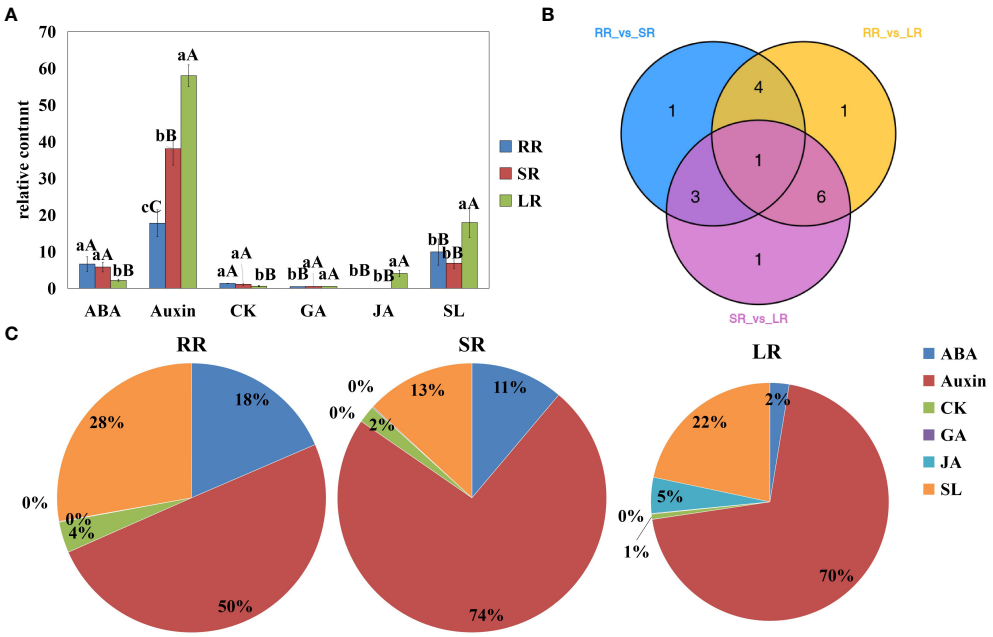

FIGURE 1
Content of differentially accumulated endogenous hormones **(A)**, Venn diagram **(B)**, and pie chart **(C)** RR, SR and LR. Values are average on three replicates. Significant differences are indicated by letters, lowercase letter indicates significant difference (0.05>P≥0.01), uppercase letter represents extremely significant difference (0.01>P≥0.001). RR: The cucumber root samples under room temperature condition; SR: The cucumber root samples under suboptimal temperature condition LR: The cucumber leaf samples under low temperature condition. The same below.

3.2 Metabolite identification in cucumber root

To further study the difference in the response of cucumber to suboptimal and low temperatures compared to that under room temperature, metabolomic analyses were performed. LC-MS/MS was used for targeted metabolomic analysis. MRM detection, PCA, and correlation analyses showed that the data quality met the requirements for subsequent analyses (Supplementary Figures S1A-D). Of the 995 metabolites screened for each comparison group under the VIP, FC, and P-value triple screening conditions, 119 were DEMs in RR vs. SR (75 upregulated and 44 downregulated), 152 were DEMs in RR vs. LR (96 upregulated and 56 downregulated), and 120 were DEMs in SR vs. LR (60 upregulated and 60 downregulated) (Supplementary Figures S1F-H). To better understand the metabolic response mechanisms of cucumber roots under low-temperature stress, we analyzed the DEMs identified in each comparison group. The Venn diagram analysis further showed there were 55 DEMs common to RR vs. SR and RR vs. LR. Most DEMs are flavonoids and phenolic acids that improve the suboptimal and low-temperature tolerance of plants by increasing the activity of antioxidant enzymes. Five DEMs were common to all three groups. All five DEMs were flavonoids, with two isoflavones and three flavones identified.

As shown in Figure 2, the contents of phenolic acids, plumerane, alkaloids, and organic acids were significantly higher than those of the other metabolites. The detail information of metabolites in phenolic acids, plumerane, alkaloids, organic acids and triterpene class was shown in Supplementary Table 4. Phenolic acid was the most abundant compound. The percentages of SR (36%) and LR (37%) were almost the same and higher than that of RR (30%). The main phenolic acids that accumulated in the cucumber roots were p-Coumaryl alcohol, benzaldehyde, and isoferulic acid* (Figure 2C), the relative contents of which are listed in Supplementary Table 4. The downward trends of plumerane (21% in RR, 14% in SR, and 10% in LR) and alkaloids (21% in RR, 13% in SR, and 11% in LR) with temperature were almost the same. The main components of plumerane were 3-Indoleacrylic acid, indole-3-carboxaldehyde, and methoxyindoleacetic acid. The alkaloids used were 3-amino-2-naphthoic acid and cyclohexylamine. Organic acids (15% in RR, 20% in SR, and 31% in LR) increased sharply with decreasing temperature, especially in SR and LR. 2-Isopropylmalic acid, iminodiacetic acid, and JAs are the main organic acids accumulated in cucumber roots. Additionally, the triterpene (isomangiferolic acid and ursolic acid) content in SR was significantly higher than in RR (269 times) and LR (195102 times), which may play an important role in the chilling resistance process.

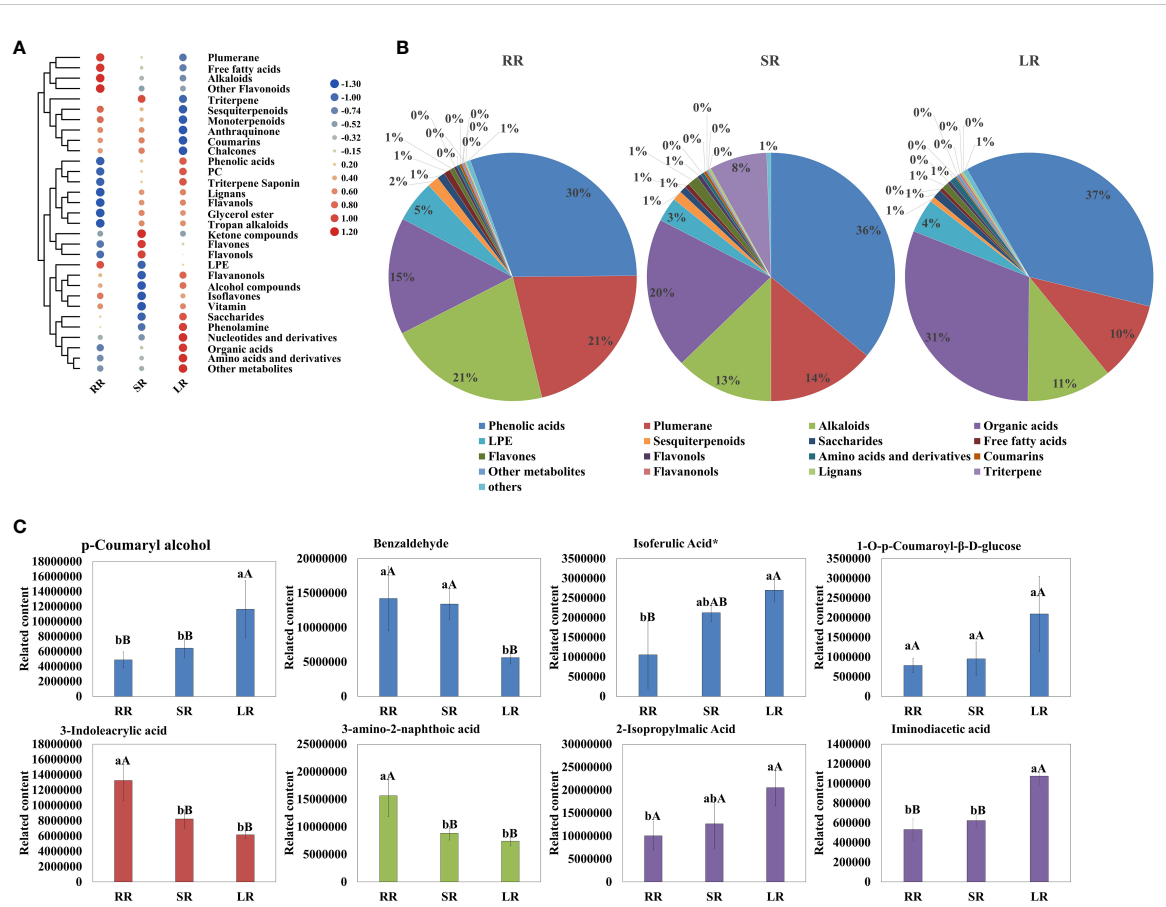

FIGURE 2
Cluster heatmap **(A)** and pie chart **(B)** of metabolites classified by Class II. Main content of phenolic acids, plumerane, alkaloids, and organic acids **(C)**.

3.3 Transcriptomic analysis in cucumber root

To further study the difference in response to suboptimal and low temperatures compared to that under room temperature in cucumber, transcriptomic analyses were performed. We prepared nine cDNA libraries. The Q20 and Q30 values of each cDNA library were greater than 97% and 92%, respectively; the base error rate was 0.03%, the average G/C content was 42.61%, and the average base number was 6.56 Gb (Supplementary Table 5). The proportion of clean reads that mapped to the reference genome was > 95%. In addition, the correlation coefficients between the samples were calculated based on the FPKM values of all genes in each sample, and PCA was performed. The results showed that the square of the correlation coefficient (R2) was greater than 0.92 and that the samples were scattered between groups and gathered within them (Supplementary Figures S2A, C). Cluster analysis revealed a clear separation between the samples, whereas replicate samples from each treatment clustered together (Supplementary Figure S2B). Three biological replicates were analyzed for each cucumber root sample group. Most DEGs were found in the RR vs. LR comparison (1136; 761 upregulated and 375 downregulated genes), followed by those in SR vs. LR (366; 287 upregulated and 79 downregulated genes); RR vs. SR had the lowest number of DEGs (189; 150 upregulated and 39 downregulated genes). Interestingly, the number of upregulated DEGs in each comparison group was higher than that of the downregulated DEGs (Supplementary Figure S2D). In addition, Venn diagram analysis revealed 141 common DEGs between the RR vs. SR and RR vs. LR groups (Supplementary Figure S2E). In total, 256 common DEGs were identified between RR vs. SR and SR vs. LR. Only six DEGs were common between the RR vs. SR and SR vs. LR groups. Ten common DEGs were expressed in all three groups.

3.4 Comparative analysis of DEGs and DEMs in cucumber root under low-temperature stress

To compare the low-temperature response differences under different temperature conditions, the enrichment of DEGs and DEMs was analyzed in the three comparison groups. The GO enrichment results showed that the DEGs in RR vs. SR were significantly enriched in plant organ morphogenesis (GO:1905392), cell development (GO:0048468), and plant epidermis development (GO:0090558) (Figure 3A). The DEGs in RR vs. LR were significantly enriched in tetrapyrrole binding (GO:0046906), polysaccharide metabolic processes (GO:0005976), and enzyme regulator activity (GO:0030234) (Figure 3B). The DEGs in SR vs. LR were significantly enriched in tetrapyrrole binding (GO:0046906), thylakoids (GO:0009579), and apoplasts (GO:0048046) (Figure 3C).

KEGG enrichment analysis of the DEGs showed that 118 DEGs were enriched in 47 pathways in RR vs. SR, while 1 043 DEGs were enriched in 111 pathways in RR vs. LR (Figures 3D, E). Plant hormone signal transduction (ko04075) and benzoxazinoid biosynthesis (ko00402) were significantly enriched in the two comparison groups, indicating that cucumber roots responded to suboptimal and low-temperature stress through these two basic metabolic pathways. In total, 392 DEGs were enriched in 82 pathways in SR vs. LR (Figure 3F). Photosynthesis-antenna proteins (ko00196), isoquinoline alkaloid biosynthesis (ko00950), the MAPK signaling pathway (ko04016), phenylpropanoid biosynthesis (ko00940), pentose and glucuronate interconversions (ko00040), and cyanoamino acid metabolism (ko00460) were significantly enriched in the RR vs. LR and SR vs. LR comparison groups. The results showed that cucumber roots might respond exclusively to low-temperature stress through these metabolic pathways.

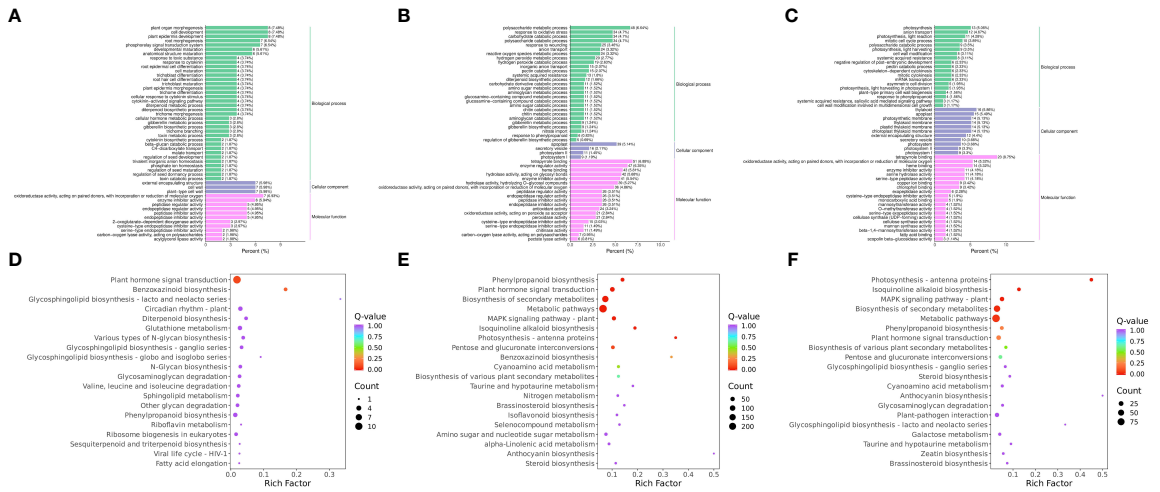

FIGURE 3
GO enrichment of DEGs in RR vs. SR **(A)**, RR vs. LR **(B)** and SR vs. LR **(C)**. KEGG enrichment of DEGs in RR vs. SR **(D)**, RR vs. LR **(E)** and SR vs. LR **(F)**.

In RR vs. SR, 52 DEMs were enriched in 27 pathways, while 75 DEMs were enriched in 33 pathways in RR vs. LR (Figures 4A, B). Benzoxazinoid biosynthesis (ko00402); stilbenoid, diarylheptanoid, and gingerol biosynthesis (ko00945); flavone and flavonol biosynthesis (ko00944); flavonoid biosynthesis (ko00941); and isoflavonoid biosynthesis (ko00943) were significantly enriched in the two comparison groups, indicating that these DAMs may be key metabolites that respond to suboptimal and low-temperature stress in cucumber roots. For RR vs. SR, the DEGs and DEMs were significantly enriched in the benzoxazinoid biosynthesis pathway. In SR vs. LR, 80 DEMs were enriched in 33 pathways (Figure 4C). Stilbenoid, diarylheptanoid, gingerol, and flavonoid biosynthesis were the main pathways enriched in this group.

Association analysis of transcriptomics and metabolomics allows the prediction of changes in metabolites at the transcriptional level and verifies the results of gene transcription at the metabolic level. Also it further analyzing the relationship between metabolic and transcriptional spectra and the metabolic mechanisms of various biological systems of plant (Cavill et al., 2016). The DEGs and DEMs mapped to the KEGG pathway database were compared to obtain information on common pathways. In the RR vs. SR, RR vs. LR, and SR vs. LR comparison groups, 8, 28, and 21 pathways were co-enriched by DEGs and DEMs, respectively. For RR vs. SR, DEGs and DEMs were significantly enriched in the benzoxazinoid biosynthesis pathway (Figure 4D). In RR vs. LR, DEGs and DEMs were significantly enriched in benzoxazinoid biosynthesis, phenylpropanoid biosynthesis, plant hormone signal transduction, and other pathways (Figure 4E). In SR vs. LR, DEGs and DEMs were significantly enriched in some biosynthesis pathways such as stilbenoid, diarylheptanoid, gingerol, flavonoid, and phenylpropanoid biosynthesis (Figure 4F). In summary, these common enrichment pathways may be the transcriptomic and metabolic bases for low-temperature resistance in cucumber roots.

3.5 DEGs and DAMs involved in phenylpropanoid biosynthesis

The phenylpropanoid biosynthesis pathway exists widely in higher plants and leads to the production of many secondary metabolites related to low-temperature stress, such as flavonoids, terpenoids, and phenolic acids. Most DEGs in the phenylpropanoid biosynthesis pathway increased with decreasing temperature (Figure 5). The other ten genes showed the opposite trend. The cytochrome P450 gene, CsaF5H, showed the highest expression in the SR. Two phenolic acids, DAMs, p-Coumaryl alcohol and coniferyl alcohol, are involved in phenylpropanoid biosynthesis. CsaPER52 (CsaV36G002170), which regulates the conversion of p-Coumaryl alcohol to p-Hydroxyphenyl lignin, is highly related to the content of p-Coumaryl. While CsaPER5, which participates in the conversion of coniferyl alcohol to guaiacyl lignin, is highly related to coniferyl alcohol content. The increasing trend of these DAMs and DEGs may promote cucumber root response to low-temperature stress.

3.6 Key transcription factors associated with low-temperature stress

Weighted gene co-expression network analysis (WGCNA) was used to identify the characteristic genes of a module, key genes in the module, association between modules, and sample phenotypes (Langfelder and Horvath, 2008). Using WGCNA, all genes in the nine cucumber root samples (RR, SR, and LR with three biological replicates) were divided into 52 coexpression modules (Figure 6A, Supplementary Table S6). We identified 1052 coexpressed genes in the green module, which had a significantly positive correlation with IPA (r = 0.92, P = 0.00044), while 798 coexpressed genes were identified in the pink module and had a positive correlation with IA

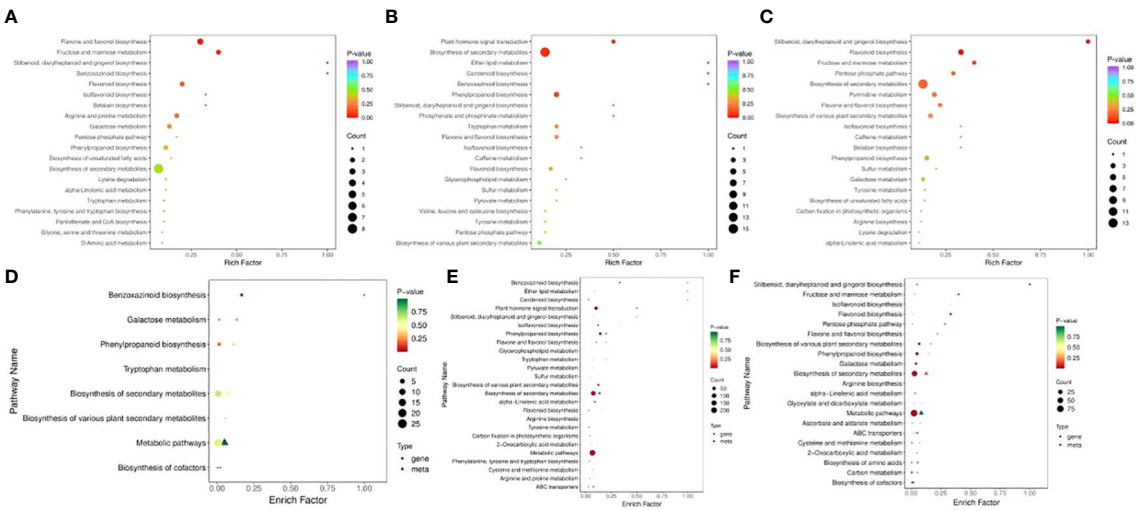

FIGURE 4
KEGG enrichment of DAMs in RR vs. SR **(A)**, RR vs. LR **(B)**, and SR vs. LR **(C)**. The KEGG enrichment of DEGs and DAMs in RR vs. SR **(D)**, RR vs. LR **(E)**, and SR vs. LR **(F)**.

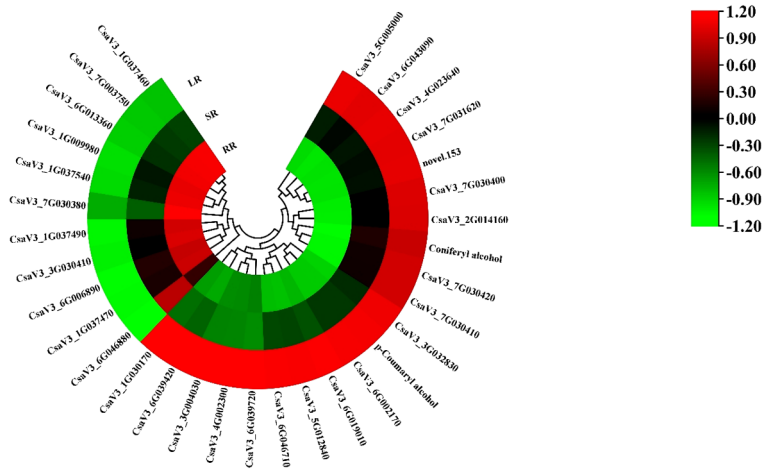

FIGURE 5
The heatmap of DEGs and DAMs involved in phenylpropanoid biosynthesis.

(r = 0.99, P = 3.3e-07), TRA (r = 0.99, P = 3.3e-07), and OPC-6 (r = 0.99, P = 3.3e-07) (Figure 6B). The gene expression patterns of the green module were significantly correlated with the hormone with the highest content in the SR group, which might relate to suboptimal temperature stress. The gene expression patterns of the pink module were significantly correlated with hormone with the highest content in the LR group, which might be related to low-temperature stress.

When PCC was set as ≥0.90 or ≤−0.90, 1052 and 798 DEGs were used to construct a coexpression network of green and pink modules, respectively (Supplementary Table S7). The expression levels of 37 genes from the green and pink modules that were highly correlated with hormone content in cucumber roots may be regarded as highly connected genes (hub genes) and were involved in two categories: plant hormone signal transduction (16) and transcription factors (TFs) (21) (Figures 6C, D; Supplementary Table S8).

According to the expression patterns of DEGs in the plant hormone signal transduction pathway, some TFs may be involved in the regulation of hormone content in cucumber roots, resulting in responses to low-temperature stress. Previous studies have demonstrated that AP2/ERF, bHLH, WRKY, and other genes play important roles in the response of plants to low-temperature stress (Yonghong Li et al., 2023; Xu et al., 2023). In green and pink modules, 21 differentially expressed TF genes (DETFs) were identified in the gene coexpression network.

The DETF in the green module were involved in three categories, the AP2/ERF (CsaV32G035630, CsaV33G003840, CsaV36G028510, CsaV36G032480, CsaV36G042200, CsaV37G003470), bHLH (CsaV31G039160, CsaV32G005070, CsaV32G007370, CsaV33G000850, CsaV33G042970, CsaV37G003870) and WRKY family (CsaV32G002020, CsaV33G012180, CsaV36G050320, CsaV37G026330, CsaV37G031980, CsaV37G033570, and CsaV36G044340). The DETF in the pink module belong to the AP2/ERF family (CsaV33G002570 and CsaV36G012590). These results indicated that the WRKY family and CBF1 genes mainly responded to suboptimal temperature stress. Different DETFs in the AP2/ERF family may regulate the response to suboptimal and low-temperature stress in cucumber roots.

In addition, in the plant hormone signal transduction pathway, 18 DEGs (one AUX1, four AUX/IAA, three ARF, 3 GH3 and seven SAUR) participated in auxin signal transduction (Figure 6D). Seven DEGs (2 B-ARRs and 5 A-ARRs) affected CK signal transduction. Seven DEGs (two GID1, three DELLA, and two PIF3) regulated the GA signal transduction. Eight DEGs (four BRI1, one BKI1, one BSK, one TCH4, and one CYCD3) were associated with BR signal transduction. One and two DEGs (TGA and two JAZ) were associated with salicylic acid and jasmonic acid (JA) signal transduction, respectively. Interestingly, no DEGs were detected during ABA or ethylene signal transduction. This indicates that these two hormones may have little effect on the response to chilling stress in cucumber roots.

To further analyze the TFs related to the response to low-temperature stress in cucumber roots, we created a heat map of DETFs in the AP2, bHLH, MYB, NAC, and WRKY families (Figure 7A). Most DETFs were upregulated with a decrease temperature in AP2 family. Additionally, DREB/CBF (C-repeat binding/dehydration-responsive element-binding protein, *CsaV33G016760*) in the AP2/ERF-ERF Subfamily was downregulated in SR and LR compared to RR. The other DREB (dehydration-responsive element-binding protein, CsaV32G002020) gene was upregulated in SR and downregulated in LR, whereas in the bHLH and WRKY families, most DETFs were downregulated in LR compared with RR. The upregulated DETF in WRKY family is WRKY75 (*CsaV34G003030*). Half of the DEGs were downregulated in the MYB and NAC families. The qRT-PCR results for the key genes are presented in Figure 7B. The results of q-RT-PCR were basically consistent with those of transcriptome sequencing, which proved that the sequencing was reliable.

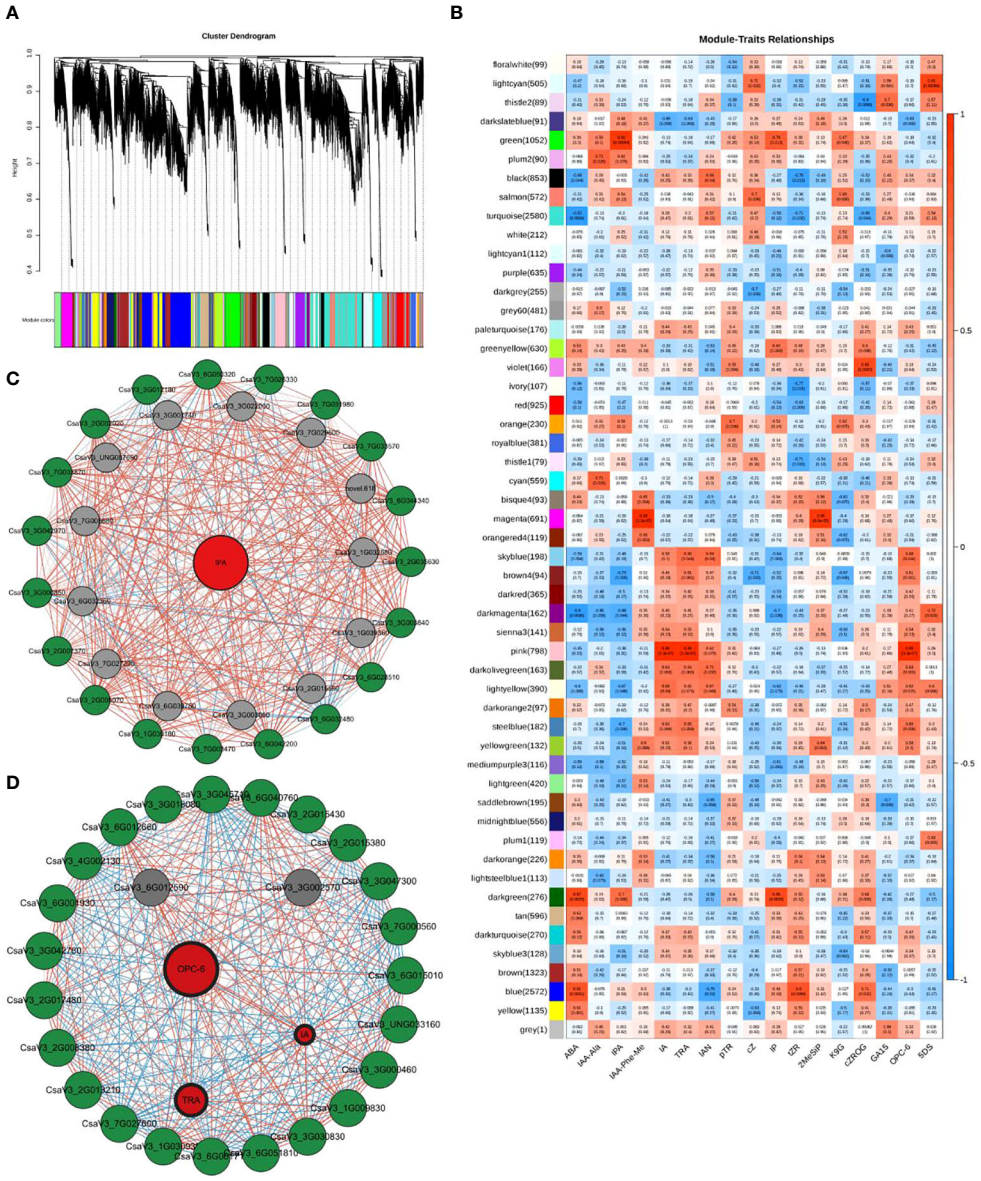

FIGURE 6
WGCNA results. **(A)** Tree maps of 22,551 genes were constructed by hierarchical clusters with topological overlap dissimilarity. Each gene was represented by leaves in the tree branch. The coexpression distance between two genes represents the height on the y-axis. The first and second lines below the tree indicate the module members identified by the dynamic tree using the cutting method and the combined dynamic tree identity with a 0.85 merge threshold, respectively. The main branches comprise 52 coexpression modules. **(B)** Relationships between differentially accumulated endogenous hormones in cucumber roots (column) and module characteristic genes (MEs, row). The color indicates intensity and direction. The numbers in parentheses are partial Pearson correlations and corresponding P-values. **(C)** Subnetwork of IPA and putative transcription factors (TFs) and structural genes related to Plant hormone signal transduction from the green module. **(D)**: Subnetwork of three plant hormones and structural genes related to Plant hormone signal transduction and putative TFs and from the pink module. Red circles denote metabolite, green circles denote pathway genes, and gray circles denote TFs. The lines between the two dots indicate their interactions. The colors of lines represent the positive or negative relationship between two genes or metabolite and gene. The width of lines represents the strength of correlations between the two genes; the wider the stronger and the thinner the weaker the interactions. The width of label lines represents the FC between two inbred lines; the wider the larger stronger and the thinner the smaller the multipliers.

4 Discussion

Under suboptimal low temperature stress, the biomass of cucumber root decreased significantly compared with room temperature. Increasing evidence suggests that specific hormones play an important role in plant responses to low-temperature stress, including ABA, JA, salicylic acid (SA), GA, brassinolactone (Br), CK, ethylene and so on (D. Chen, Wang, Yue, & Zhao, 2016). Auxin is a common factor in most hormone regulatory networks (Chen et al., 2016; Xiao, et al., 2018). It is not only involved in the whole process of plant development but also participates in regulating plant adaptability to environmental change (Chen et al., 2016; Zhang et al., 2020). In cucumber root, auxin plays a key role in maintaining the root growth (Su and Masson, 2019). In our study, auxin

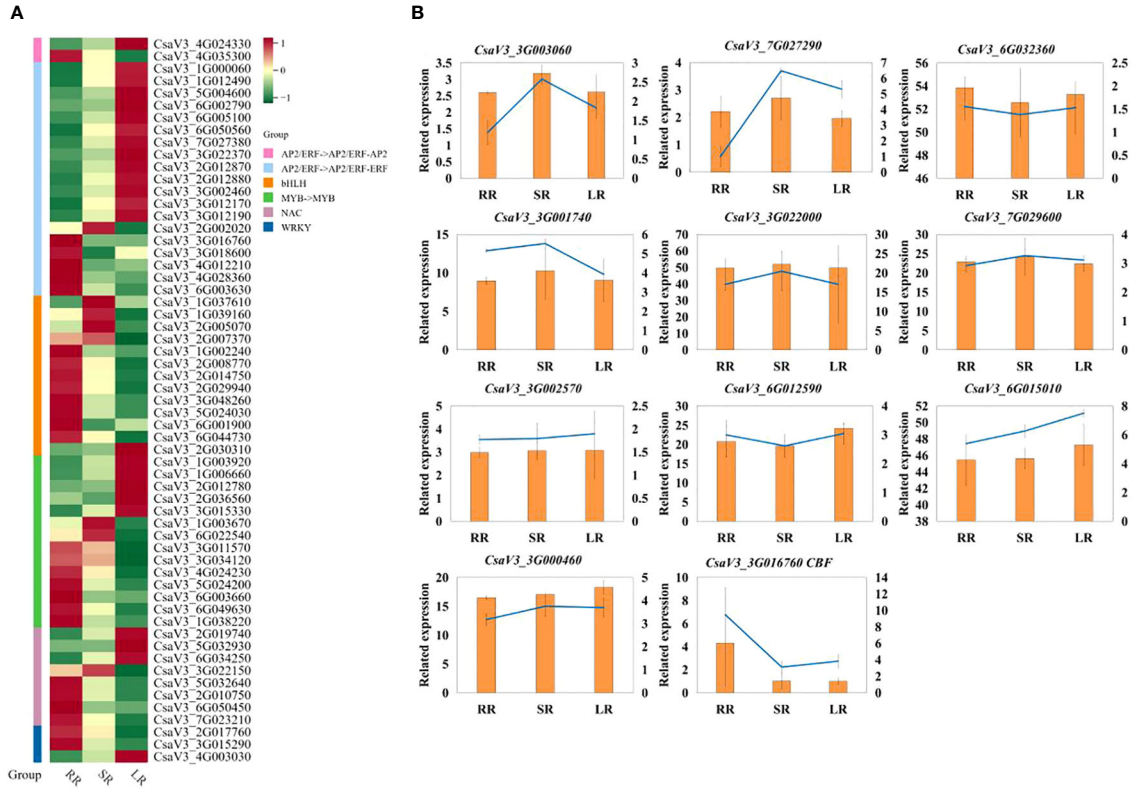

FIGURE 7
(A) Heat map of DETFs in AP2, bHLH, MYB, NAC and WRKY family. **(B)** q-RT-PCR result.

accumulated abundantly under low-temperature conditions, and its content was higher than that of all other hormones. Studies on ABA have demonstrated that it is an important regulator of the whole plant life cycle and is involved in regulating many abiotic stress responses (Li et al., 2022). However, in our study, ABA was not the main hormone that determined the response to chilling stress in cucumber roots. JA also regulates the response of cucumber roots to low-temperature stress. These two hormones are key regulators of root development. Studies on the relationship between JA and low-temperature stress have mainly focused on fruits. The mechanism by which JA signal transduction responds to chilling stress in cucumber roots requires further investigation. Studies on cucumber cold-resistant cultivars Zhongnong37 and cold-sensitive cultivars Shuyanbailv under low-temperature condition reveal that the IAA, ABA, and JA content in cold-resistant cultivars was higher than cold-sensitive cultivars under three low-temperature treatment conditions (15–10, 12–8, and 9–5°C) (Amin et al., 2022). After H2S treatment, a sharp increase in endogenous IAA content was observed in cucumbers, which enhanced tolerance to cold stress. Conversely, NPA application significantly compromised cucumber defense against cold by decreasing endogenous IAA and H2S contents (2020). These studies indicate that auxin plays a key role in cold stress and enhances the resistance to cold injury in cucumbers.

The contents of phenolic acids, plumerane, alkaloids, and organic acids were significantly higher than those of other metabolites accumulated in the cucumber roots. Phenolic acid was the most abundant compound. The accumulation of soluble phenolic acids is also involved in cold stress responses in plants. In rice, the phenolic constituents of phenols, polyphenols, flavonoids, and phenolic acids have different bound forms in Japonica and Indica subtypes, and these may have a positive role under chilling stress (Rayee et al., 2020). Plumerane and alkaloids were positively correlated with temperature, whereas organic acids were negatively correlated with temperature. Alkaloids are secondary metabolites produced by the interaction between plants and the external ecological environment. As chemical defense substances, alkaloids play an important role in resisting the influence of adverse environment such as high-temperature and drought (Li et al., 2012). But there are few study on function of alkaloids in low temperature resistance in cucumber root. Organic acids affect plant resistance during exposure to low temperature. The accumulation of fumaric acid and azelaic acid were crucial for response to cold stress in *Arabidopsis* (Xu et al., 2011; Dyson et al., 2016). In our study, 2-Isopropylmalic acid, iminodiacetic acid, and JA were the main organic acids accumulated in cucumber roots, indicating that they were important for the response of cucumber roots to cold stress. Additionally, triterpenes may play an important role in cold resistance. Benzoxazinoid and phenylpropanoid biosyntheses were the main differential pathways in response to chilling injury in cucumber roots and are both involved in plant abiotic stress responses. The final product of phenylpropanoid biosynthesis is coumaric acid, which is the precursor of downstream pathways, such as flavonoid-related pathways and lignin synthesis. This has also been introduced by temperature (Dong and Lin, 2020). Benzoxazinoid

biosynthesis has garnered significant research attention for its role in defensive process (disease resistance, insect resistance,etc) and allelopathy (Gao et al., 2017). However, its relationship with the low-temperature stress requires further investigation.

TFs play crucial roles in plant growth, development, and adaptation to stress. AP2/ERF and WRKY play important roles in plant responses to low-temperature stress (Xu et al., 2023). Therefore, this study mainly analyzed the expression patterns of AP2/ERF and WRKY and found that, WRKY (contain WRKY15, WRKY2, WRKY57, WRKY13, WRKY6, and PER40) were strongly induced by suboptimal temperature stress. AP2/ERF was strongly induced by both suboptimal and low-temperature stresses in cucumber roots. Furthermore, we found that CBF1 responded mainly to suboptimal temperature stress. WRKY6 is induced by freezing stress in apple branches (Xu et al., 2023). In cucumbers, CsWRKY21 and CsWRKY46 positively regulate the response to cold stress in different ways. CsWRKY21 is involved in the CBF-mediated cold response signaling pathway. CsWRKY46 enhances the expression of ABI5, a key transcription factor in the ABA signaling pathway. This activates the expression of RD29A and COR47 and participates in the ABA-dependent cold response regulation pathway (Ying et al., 2016). Therefore, it is important to analyze the expression patterns of AP2/ERF and WRKY in cucumber roots under low-temperature stress as well as the molecular expression networks of key genes regulated by these TFs.

Cold response signaling pathways in plants are distinguished by whether the regulation of signal transduction relies on CBF. Numerous studies have demonstrated that CBFs proteins play a central role in cold acclimation. Cold-responsive signals in plants are mainly regulated by the ICE-CBF-COR (ICE, CBF expression protein inducer; COR, cold-responsive gene) mode (Ramezani et al., 2017; Tang et al., 2022). The transcription level was significantly upregulated by ICE. It also activates the expression of downstream cold-responsive genes (CORs) by binding to the cis-elements in their promoters (Liu et al., 2018). However, current studies show that some TFs in the AP2/ERF and WRKY families are involved in the regulation of plant hypothermia responses through a pathway that is independent of CBF. In this study, the CBF transcription factor (*CsaV33G016760*), which had been identified in cucumber, was downregulated in cucumber roots in response to low-temperature stress. However, most DETFs were upregulated in the AP2 family and were strongly induced by both suboptimal and low-temperature stresses. This suggests that the regulatory pathway of the response to low-temperature stress in cucumber roots mainly depends on the AP2/ERF family, without dependence on CBF. However, this conclusion requires further investigation.

5 Conclusion

In the present study, cucumber cultivars were subjected to cold stress at different temperatures. By combining transcriptomics and metabolomics data, DEGs and DEMs responding to chilling stress were identified in the cucumber root samples RR, SR, and LR. Hormone detection indicated that auxin had the highest content in the roots. Thus, JA may play an important role in low-temperature stress. Furthermore, under chilling stress, the highest phenolic acid content was observed in the cucumber roots. The main phenolic acids accumulated in cucumber roots are p-coumaryl alcohol, benzaldehyde, and isoferulic acid. The downward trends of plumerane and alkaloids with temperature were similar. The organic acid content increased sharply with decreasing temperature. 2-Isopropylmalic acid, iminodiacetic acid, and JAs are the main organic acids accumulated in cucumber roots. Additionally, triterpenes may play an important role in chilling resistance. DEGs and DEMs were significantly enriched in benzoxazinoid biosynthesis in the RR vs. SR and RR vs. LR groups. DEGs and DEMs were significantly enriched in phenylpropanoid biosynthesis in the RR vs. LR and SR vs. LR groups. Most DETFs in the AP2/ERF family were strongly induced by both suboptimal and low-temperature stresses in cucumber roots. In conclusion, these results explain the response to chilling stress in cucumber roots, but further studies on the differential expression patterns of the components of these pathways are needed to reveal the mechanisms of low temperatures in cucumbers.

Data availability statement

Original datasets are available in a publicly accessible repository: The original contributions presented in the study are publicly available. This data can be found at the NCBI with accession number: PRJNA1135659.

Author contributions

SJS: Data curation, Formal analysis, Funding acquisition, Project administration, Writing – original draft, Writing – review & editing. YY: Resources, Writing – review & editing. SYH: Formal analysis, Investigation, Writing – review & editing. YL: Formal analysis, Investigation, Writing – review & editing. XZ: Formal analysis, Investigation, Writing – review & editing. PY: Data curation, Formal analysis, Writing – review & editing. XDZ: Data curation, Investigation, Writing – review & editing. YSL: Data curation, Formal analysis, Writing – original draft, Writing – review & editing.

Funding

The author(s) declare financial support was received for the research, authorship, and/or publication of this article. This work was supported by Open Foundation of Key Laboratory of Urban Agriculture, Ministry of Agriculture and Rural Areas (NO.008), National Natural Science Foundation of Inner Mongolia (2021BS03009) and Scientific research program of HETAO College (HYHB202301).

Conflict of interest

The authors declare that the research was conducted in the absence of any commercial or financial relationships that could be construed as a potential conflict of interest.

Publisher's note

All claims expressed in this article are solely those of the authors and do not necessarily represent those of their affiliated organizations, or those of the publisher, the editors and the reviewers. Any product that may be evaluated in this article, or claim that may be made by its manufacturer, is not guaranteed or endorsed by the publisher.

Supplementary material

The Supplementary Material for this article can be found online at: https://www.frontiersin.org/articles/10.3389/fpls.2024.1413716/full#supplementary-material

References

Amin, B., Atif, M. J., Meng, H., Ghani, M. I., Ali, M., Wang, X., et al. (2022). Biochemical and physiological responses of cucumis sativus cultivars to different combinations of low–Temperature and high humidity. *J. Plant Growth Regul.* 42, 390–406. doi: 10.1007/s00344-021-10556-3

Bahrman, N., Hascoët, E., Jaminon, O., Dépta, F., Hû, J.-F., Bouchez, O., et al. (2019). Identification of genes differentially expressed in response to cold in Pisum sativum using RNA sequencing analyses. *Plants (Basel)* 8, 288. doi: 10.3390/plants8080288

Bai, C., Fang, M., Zhai, B., Ma, L., Fu, A., Gao, L., et al. (2021). Regulations of m6A methylation on tomato fruit chilling injury. *Hortic. Plant J.* 7, 434–442. doi: 10.1016/j.hpj.2021.05.005

Cai, B.-D., Zhu, J.-X., Gao, Q., Luo, D., Yuan, B.-F., and Feng, Y.-Q. (2014). Rapid and high-throughput determination of endogenous cytokinins in Oryza sativa by bare Fe_3O_4 nanoparticles-based magnetic solid-phase extraction. *J. Chromatogr. A* 1340, 146–150. doi: 10.1016/j.chroma.2014.03.030

Cavill, R., Jennen, D., Kleinjans, J., and Briede´, J. J. (2016). Transcriptomic and metabolomic data integration. *Briefings Bioinf.* 17, 891–901. doi: 10.1093/bib/bbv090

Chen, D., Wang, W., Yue, Q., and Zhao, Q. (2016). Research progress of plant auxin as a regulator of cold stress response. *Plant Physiol. J.* 52, 989–997. doi: 10.13592/j.cnki.ppj.2016.0042

Chen, L., Hu, W., Mishra, N., Wei, J., Lu, H., Hou, Y., et al. (2020). AKR2A interacts with *KCS1* to improve VLCFAs contents and chilling tolerance of *Arabidopsis thaliana*. *Plant J.* 103, 1575–1589. doi: 10.1111/tpj.14848

Chen, L., Xiang, H., Miao, Y., Zhang, L., Guo, Z. F., Zhao, X. H., et al. (2014). An overview of cold resistance in plants. *J. Agron. Crop Sci.* 200, 237–245. doi: 10.1111/jac.12082

Cui, K., Lin, Y., Zhou, X., Li, S., Liu, H., Zeng, F., et al. (2015). Comparison of sample pretreatment methods for the determination of multiple phytohormones in plant samples by liquid chromatography–electrospray ionization-tandem mass spectrometry. *Microchemical J.* 121, 25–31. doi: 10.1016/j.microc.2015.02.004

Ding, Y., Li, H., Zhang, X., Xie, Q., Gong, Z., and Yang, S. (2015). *OST1* kinase modulates freezing tolerance by enhancing ICE1 stability in *arabidopsis*. *Dev. Cell* 32, 278–289. doi: 10.1016/j.devcel.2014.12.023

Dong, N., and Lin, H. (2020). Contribution of phenylpropanoid metabolism to plant development and plant–environment interactionsFA. *J. Integr. Plant Biol.* 63, 180–209. doi: 10.1111/jipb.13054

Dyson, B. C., Miller, M. A. E., Feil, R., Rattray, N., Bowsher, C. G., Goodacre, R., et al. (2016). FUM2, a cytosolic fumarase, is essential for acclimation to low temperature in *Arabidopsis thaliana*. *Plant Physiol.* 2016, 172, 118–127. doi: 10.1104/pp.16.00852

Eremina, M., Unterholzner, S. J., Rathnayake, A. I., Castellanos, M., Khan, M., Kugler, K. G., et al. (2016). Brassinosteroids participate in the control of basal and acquired freezing tolerance of plants. *Proc. Natl. Acad. Sci.* 11477, 113. doi: 10.1073/pnas.1611477113

Floková, K., Tarkowská, D., Miersch, O., Strnad, M., Wasternack, C., and Novák, O. (2014). UHPLC-MS/MS based target profiling of stress-induced phytohormones. *Phytochemistry* 105, 147–157. doi: 10.1016/j.phytochem.2014.05.015

Gao, H., Li, S., Wang, H., Lin, F., zhang, C., and Lang, Z. (2017). Progress on function and biosynthesis of benzoxazinoids. *China Biotechnol.* 37, 104–109. doi: 10.13523/j.cb.20170815

Gong, Z., Xiong, L., Shi, H., Yang, S., Herrera-Estrella, L. R., Xu, G., et al. (2020). Plant abiotic stress response and nutrient use efficiency. *Sci. China Life Sci.* 63, 635–674. doi: 10.1007/s11427-020-1683-x

Hu, Y., Jiang, L., Wang, F., and Yua, D. (2013). Jasmonate regulates the INDUCER OF CBF Expression–C-REPEAT BINDING FACTOR/DRE BINDING FACTOR1 cascade and freezing tolerance in *Arabidopsis*. *Plant Cell* 25, 2907–2924. doi: 10.1105/tpc.113.112631

Jan, N., Mahboob-ul-Hussain,, and Andrabi, K. I. (2009). Cold resistance in plants: A mystery unresolved. *Electronic J. Biotechnol.* 12, 1–15. doi: 10.2225/vol12-issue3-fulltext-3

Jiang, F., Lv, S., Zhang, Z., Chen, Q., Mai, J., Wan, X., et al. (2023). Integrated metabolomics and transcriptomics analysis during seed germination of waxy corn under low temperature stress. *BMC Plant Biol.* 23, 190. doi: 10.1186/s12870-023-04195-x

Langfelder, P., and Horvath, S. (2008). WGCNA: an R package for weighted correlation network analysis. *BMC Bioinf.* 9, 559. doi: 10.1186/1471-2105-9-559

Lantzouni, O., Alkofer, A., Falter-Braun, P., and Schwechheimer, C. (2019). Growth-regulating factors interact with DELLAs and regulate growth in cold stress. *Plant Cell* 32, 1018–1034. doi: 10.1105/tpc.19.00784

Li, Q., Li, L., Hou, J., Luo, R., Wang, R., Hu, J., et al. (2022). Advances on mechanism of cucurbit crops in response to low temperature stress (in Chinese). *Acta Hortic. Sin.* 49, 1382–1394. doi: 10.16420/j.issn.0513-353x.2021-0575

Li, Y., Tian, Q., Wang, Z., Li, J., Liu, S., Chang, R., et al. (2023). Integrated analysis of transcriptomics and metabolomics of peach under cold stress. *Front. Plant Sci.* 14. doi: 10.3389/fpls.2023.1153902

Li, H., Ye, K., Shi, Y., Cheng, J., Zhang, X., and Yang, S. (2017). BZR1 positively regulates freezing tolerance *via* CBF-dependent and CBF-independent pathways in *Arabidopsis*. *Mol. Plant* 10, 545–559. doi: 10.1016/j.molp.2017.01.004

Li, Y., Zhou, X., Lou, Z., and Xiao, X. (2012). Review of plant secondary metabolites and the factors that influence its accumulation (in Chinese). *Jiangxi Forestry Sci. Technol.* 3, 54–60. doi: 10.3969/j.issn.1006-2505.2012.03.018

Li, Y., Zhou, C., Yan, X., Zhang, J., and Xu, J. (2016). Simultaneous analysis of ten phytohormones in *Sargassum horneri* by high-performance liquid chromatography with electrospray ionization tandem mass spectrometry. *J. Separation Sci.* 39, 1804–1813. doi: 10.1002/jssc.201501239

Liu, J., Shi, Y., and Yang, S. (2018). Insights into the regulation of CBF cold signaling in plants: Regulation of CBF cold signaling. *J. Integr. Plant Biol.* 60(9), 1–39. doi: 10.1111/jipb.12657

Mauch-Mani, B., and Flors, V. (2009). The ATAF1 transcription factor: at the convergence point of ABA-dependent plant defense against biotic and abiotic stresses. *Cell Res.* 19, 1322~1323. doi: 10.1038/cr.2009.135

Niu, Q., Zong, Y., Qian, M., Yang, F., and Teng, Y. (2014). Simultaneous quantitative determination of major plant hormones in pear flowers and fruit by UPLC/ESI-MS/MS. *Analytical Methods* 6, 1766. doi: 10.1039/C3AY41885E

Pan, X., Welti, R., and Wang, X. (2010). Quantitative analysis of major plant hormones in crude plant extracts by high-performance liquid chromatography–mass spectrometry. *Nat. Protoc.* 5, 986–992. doi: 10.1038/nprot.2010.37

Ramezani, M., Rahmani, F., and Dehestani, A. (2017). Comparison between the effects of potassium phosphite and chitosan on changes in the concentration of Cucurbitacin E and on antibacterial property of *Cucumis sativus*. *BMC Complementary Altern. Med.* 17, 295. doi: 10.1186/s12906-017-1808-y

Rayee, R., Xuan, T. D., Tran, H. D., Fakoori, N. A., Khanh, T. D., and Dat, T. D. (2020). Responses of flavonoids, phenolics, and antioxidant activity in rice seedlings between Japonica and Indica subtypes to chilling stress. *Int. Lett. Natural Sci.* 77, 41–50. doi: 10.56431/v-1ns7w4

Saadati, S., Baninasab, B., Mobli, M., and Gholami, M. (2021). Foliar application of potassium to improve the freezing tolerance of olive leaves by increasing some osmolite compounds and antioxidant activity. *Scientia Hortic.* 276, 109765. doi: 10.1016/j.scienta.2020.109765

Šimura, J., Antoniadi, I., Široká, J., Tarkowská, D., Strnad, M., Ljung, K., et al. (2018). Plant hormonomics: multiple phytohormone profiling by targeted metabolomics. *Plant Physiol.* 177, 476–489. doi: 10.1104/pp.18.00293

Su, S.-H., and Masson, P. H. (2019). A new wrinkle in our understanding of the role played by auxin in root gravitropism. *New Phytol.* 224, 761–774. doi: 10.1111/nph.16140

Sun, S., Cui, S., Song, Y., Fu, C., Pan, L., and Sun, Q. (2016). Effect of different root zone temperature on growth and photosynthetic parameters of grafting cucumber (in Chinese). *Northern Horticulture* 22), 1–5. doi: 10.11937/bfyy.201622001

Sun, S., Fu, C., Cui, S., Song, Y., Gao, Y., and Liu, Q. (2018). Effects of root zone temperature on Carbon and Nitrogen metabolism and activities of related enzymes of cucumber seedlings. *J. Northwest A&F Univ.* 46, 71–80. doi: 10.13207/j.cnki.jnwafu.2018.08.010

Sun, S., Fu, C., Song, Y., Wu, R., Xue, Y., and Cui, S. (2017). Effect of low root-zone temperature on growth and ^{15}N uptake and distribution characteristics in grafted cucumber seedling root (in Chinese). *Plant Physiol. J.* 53, 1545–1552. doi: 10.13592/j.cnki.ppj.2017.0150

Sun, J., Liu, J., and Li, Y. (2010). Analysis and research of monitoring and control on greenhouse environment in installation agriculture(in Chinese). *Hunan Agric. Machinery: Acad. Edition* 37, 41–46. doi: CNKI:SUN:HNNJ.0.2010-05-024

Tang, B., Xie, L., Yang, H., Li, X., Chen, Y., Zou, X., et al. (2022). Analysis of the expression and function of key genes in pepper under low-temperature stress. *Front. Plant Sci.* 13. doi: 10.3389/fpls.2022.852511

Walters, T. W. (1989). Historical overview on domesticated plants in China with special emphasis on the. *Cucurbitaceae Economic Bot.* 43, 297–313. doi: 10.1007/BF02858729

Xiang, H. T., Wang, T. T., Zheng, D. F., Wang, L. Z., Feng, Y. J., Luo, Y., et al. (2017). ABA pretreatment enhances the chilling tolerance of a chilling-sensitive rice cultivar. *Braz. J. Bot.* 40, 853–860. doi: 10.1007/s40415-017-0409-9

Xiao, H.-M., Cai, W.-J., Ye, T.-T., Ding, J., and Feng, Y.-Q. (2018). Spatio-temporal profiling of abscisic acid, indoleacetic acid and jasmonic acid in single rice seed during seed germination. *Analytica Chimica Acta* 1031, 119–127. doi: 10.1016/j.aca.2018.05.055

Xu, G., Li, L., Zhou, J., Lyu, D., Zhao, D., and Qin, S. (2023). Comparison of transcriptome and metabolome analysis revealed differences in cold resistant metabolic pathways in different apple cultivars under low temperature stress. *Hortic. Plant J.* 9, 183–198. doi: 10.1016/j.hpj.2022.09.002

Xu, Z. Y., Zhang, X., Schlappi, M., and Xu, Z. Q. (2011). Cold-inducible expression of *AZI1* and its function in improvement of freezing tolerance of *Arabidopsis thaliana* and *Saccharomyces cerevisiae*. *J. Plant Physiol.* 168, 1576–1587. doi: 10.1016/j.jplph.2011.01.023

Xue, H., Duan, Z., Dong, J., Wang, A., Li, X., and Xing, P. (2015). Effects of root zone temperature on cucumber growth, yield and nitrogen use efficiency. *Soils* 47, 842–846. doi: 10.13758/j.cnki.tr.2015.05.004

Ying, Z., Hongjun, Y., Xueyong, Y., Qiang, L., Jian, L., Hong, W., et al. (2016). CsWRKY46, a WRKY transcription factor from cucumber, confers cold resistance in transgenic-plant by regulating a set of cold-stress responsive genes in an ABA-dependent manner. *Plant Physiol. Biochem.* 108, 478–487. doi: 10.1016/j.plaphy.2016.08.013

Zhang, X., Liu, F., Zhai, J., Li, F., Bi, H., and Ai, X. (2020). Auxin acts as a downstream signaling molecule involved in hydrogen sulfideinduced chilling tolerance in cucumber. *Planta* 251, 69. doi: 10.1007/s00425-020-03362-w

Zhang, J., Luo, W., Zhao, Y., Xu, Y., Song, S., and Chong, K. (2016). Comparative metabolomic analysis reveals a reactive oxygen species-dominated dynamic model underlying chilling environment adaptation and tolerance in rice. *New Phytol.* 211, 1295–1310. doi: 10.1111/nph.14011

Zhao, Y., Song, C., Brummell, D. A., Qi, S., Lin, Q., Bi, J., et al. (2021). Salicylic acid treatment mitigates chilling injury in peach fruit by regulation of sucrose metabolism and soluble sugar content. *Food Chem.* 358, 129867. doi: 10.1016/j.foodchem.2021.129867

Zhu, J. K. (2016). Abiotic stress signaling and responses in plants. *Cell* 167, 313–324. doi: 10.1016/j.cell.2016.08.029

frontiers | Frontiers in Plant Science

TYPE Original Research
PUBLISHED 28 November 2024
DOI 10.3389/fpls.2024.1420431

OPEN ACCESS

EDITED BY
Maria F. Drincovich,
Centro de Estudios Fotosintéticos y Bioquímicos (CEFOBI), Argentina

REVIEWED BY
Rudo Ngara,
University of the Free State, South Africa
Bin Wang,
Shaoguan University, China
Weirong Xu,
Ningxia University, China

*CORRESPONDENCE
Enhua Xia
xiaenhua@gmail.com
Wenjie Wang
wwj00@126.com

†These authors have contributed equally to this work

RECEIVED 20 April 2024
ACCEPTED 31 October 2024
PUBLISHED 28 November 2024

CITATION
Wu Q, Jiao X, Liu D, Sun M, Tong W, Ruan X, Wang L, Ding Y, Zhang Z, Wang W and Xia E (2024) *CsWAK12*, a novel cell wall-associated receptor kinase gene from *Camellia sinensis*, promotes growth but reduces cold tolerance in *Arabidopsis*.
Front. Plant Sci. 15:1420431.
doi: 10.3389/fpls.2024.1420431

CsWAK12, a novel cell wall-associated receptor kinase gene from *Camellia sinensis*, promotes growth but reduces cold tolerance in *Arabidopsis*

Qiong Wu[1†], Xiaoyu Jiao[1†], Dandan Liu[1], Minghui Sun[1], Wei Tong[2], Xu Ruan[1], Leigang Wang[1], Yong Ding[1], Zhengzhu Zhang[1], Wenjie Wang[1*] and Enhua Xia[2*]

[1]Tea Research Institute, Anhui Academy of Agricultural Sciences, Hefei, Anhui, China, [2]State Key Laboratory of Tea Plant Biology and Utilization, Anhui Agricultural University, Hefei, China

Cold significantly impacts the growth and development of tea plants, thereby affecting their economic value. Receptor-like kinases (RLKs) are thought to play a pivotal role in signaling the plant's response to cold and regulating cold tolerance. Among the RLK subfamilies, wall-associated receptor-like kinases (WAKs) have been investigated across various plant species and have been shown to regulate cell growth and stress responses. However, the function of WAK genes in response to cold stress in tea has yet to be studied. In a previous investigation, we identified the *WAK* gene family from Camellia sinensis and isolated a specific *WAK* gene, *CsWAK12*, which is induced by abiotic stresses. Here, we demonstrate that CsWAK12 is involved in the regulation of cold tolerance in tea plants. CsWAK12 was rapidly induced by cold, peaking at 3 hours after treatment at 4°C (10-fold increase). Heterologous overexpression of *CsWAK12* (35S:*CsWAK12*) in *Arabidopsis* promoted plant growth by enhancing root length and seed size under normal conditions, although it reduced cold resistance compared to the wild type. Under cold stress, the transgenic plants exhibited a lower survival rate and significantly altered levels of superoxide dismutase (SOD) activity and malondialdehyde (MDA) content compared to the wild type (WT). Furthermore, the expression of C-repeat/dehydration-responsive element binding factor (CBF) genes was diminished in CsWAK12-overexpressing transgenic Arabidopsis plants following cold treatment. Transcriptome analysis revealed that genes associated with the CBF pathway, such as transcription factor genes (ERF53, ERF54, and DREB2A) were markedly reduced in the overexpression line. These data suggest that CsWAK12 acts as a negative regulator, reducing the cold tolerance of transgenic Arabidopsis by mediating the CBF pathway. Therefore, CsWAK12 may serve as a candidate gene for the molecular breeding of cold resistance in tea plants.

KEYWORDS

***Camellia sinensis*, wall-associated kinases (WAKs), plant growth, CBF, cold stress**

1 Introduction

Wall-associated kinases (WAKs) constitute a distinct subfamily of receptor-like kinases (RLKs). Their extracellular domains are tightly bound to the pectin of the cell wall and play a crucial role in the plant's response to stress (He et al., 1996; Anderson et al., 2001). In recent years, the *WAK* gene family has been identified in various plants, including *Arabidopsis*, tobacco, cotton, tomato, rice, and barley, and has been confirmed to be involved in plant growth and development, pathogen response, abiotic stress response, and other physiological processes (Dou et al., 2021; Zhang et al., 2005; Tripathi et al., 2020; He et al., 1999; Kurt et al., 2020; Yu et al., 2022). Antisense *WAK2* or *WAK4* in *Arabidopsis*, which resulted in a 50% decrease in WAK protein levels, led to reduced cell elongation, blocked lateral root development, and dwarfed plants (Lally et al., 2001; He et al., 1999). *OsWAK10* in temperate *Oryza japonica* accessions regulates cellulose synthesis in the secondary cell wall by sensing pectic cell wall components, thereby controlling plant height and stem strength in rice (Cai et al., 2023). The cotton gene *GhWAK7A* mediates chitin-induced signaling pathways, activating downstream gene expression by phosphorylating lysin-motif-containing receptor-like kinases (LYKs/CERK1), specifically GhLYK5 and modulating the chitin-induced association between GhLYK5-GhCERK1 to enhance resistance against the infections of *Verticillium dahliae* and *Fusarium oxysporum f.* sp. *vasinfectum* (Lin et al., 2020). The overexpression of *OsWAK112* in rice and *Arabidopsis* significantly decreased plant survival under salt stress, while the knockdown of *OsWAK112* in rice enhanced plant survival under the same condition. This indicates that *OsWAK112* negatively regulates plant salt responses by inhibiting ethylene production, possibly through direct binding with OsSAMS1/2/3 (Lin et al., 2021). Additionally, silencing *CaWAKL20* improved the heat tolerance of pepper; however, *Arabidopsis CaWAKL20*-OE lines exhibited decreased sensitivity to abscisic acid (ABA), resulting in increased heat sensitivity. This suggests that *CaWAKL20* negatively modulates plant thermotolerance by reducing the expression of ABA-responsive genes (Wang et al., 2019).

Tea [*Camellia sinensis* (L.) O. Ktze] is a traditional plant renowned for producing a popular beverage in China, celebrated for its refreshing qualities, pleasant aroma, and lively palate. With the rise of new-style tea consumption, the value of tea plantations in China has increased significantly. However, temperature variations associated with warm and cold climates pose limitations on the cultivation and growth of the tea plant, which is typically classified as a tropical and subtropical crop. Low temperatures can cause the freezing of cell membranes, leading to cell death, leaf damage, and restricted growth. In recent years, significant advancements have been made in identifying cold stress-responsive RLKs and their associated signaling networks. For instance, *Arabidopsis* PHLOEM INTER-CALATED WITH XYLEM-LIKE 1 (AtPXL1) is induced by cold and heat stress, but not by drought (Jung et al., 2015). The overexpression of the brassinosteroid receptor (BRI1) gene *AtBRI1* resulted in a higher germination frequency of *Arabidopsis* seeds under cold stratification, while the mutant exhibited reduced sensitivity to cold stratification (Kim et al., 2019). However, the roles of WAKs in response of tea plant to cold stress have not yet been reported.

In our previous research, we identified the tea *WAK* gene family through *in silico* analysis and examined its expression patterns using a microarray dataset (Jiao et al., 2023). In this study, we isolated a previously identified *WAK* gene, designated *CsWAK12* (CSS0006198), which exhibited significant cold sensitivity in tea plants. We further characterized the *CsWAK12* gene to assess its expression at a chilling temperature of 4°C and investigated plants that heterogeneously overexpressed this gene when subjected to sub-zero temperatures of −8°C. The CsWAK12 protein was localized to the membrane. Additionally, the ectopic expression of *CsWAK12* in *Arabidopsis* resulted in a notable decrease in cold tolerance in the transgenic plants. Specifically, superoxide dismutase (SOD) activity was reduced, and malondialdehyde (MDA) content was inhibited in the *CsWAK12* transgenic lines in *Arabidopsis*. Furthermore, quantitative real-time PCR and transcriptome analysis revealed that *AtCBFs* were significantly influenced by *CsWAK12*.

2 Materials and methods

2.1 Plant materials and stress treatment

The tea cultivar "Shu Cha Zao" (SCZ) was cultivated in the Experimental Tea Garden of the Tea Research Institute at the Anhui Academy of Agricultural Sciences, located in Huangshan, Anhui (118.26E, 29.69N). To analyze the tissue expression pattern, apical buds, young leaves, stems, roots, and flowers were collected from the same SCZ plant in the garden in its natural state. Tender branches, approximately 15–20 cm in length, were collected from SCZ and inserted into water-saturated flower mud for cold treatment in a 4°C culture chamber. Conditions in the chamber were maintained at 60% relative humidity, with a 12-h photoperiod and a light intensity of 2,000 lux. Control samples were placed in a tissue culture room at 28°C, also under 60% relative humidity and a 12-h photoperiod with the same light intensity. Young leaves were collected after 0, 3, 6, 12, 24, and 48 h of each treatment. All samples were processed in the morning at 10:00 a.m., wrapped in foil, immediately frozen in liquid nitrogen, and stored at −80°C.

2.2 RNA isolation, cDNA synthesis, and quantitative real-time PCR analysis

Total RNA was extracted from plant materials using the RNAprep Pure Plant Plus Kit (Tiangen, Beijing, China) and subsequently subjected to reverse transcription using PrimeScript™ RT Master Mix (TAKARA, Tokyo, Japan), following the manufacturer's instructions. Quantitative reverse transcription polymerase chain reaction (qRT-PCR) was conducted on a LightCycler® 96 Instrument (Roche, California, USA) utilizing SYBR® Green Pro Taq HS Premix (AGBIO, Hunan, China) by a three-step PCR reaction procedure. The reaction

volume was set to 20 µL, and the thermal cycling program consisted of an initial denaturation step at 95°C for 30 s, followed by 40 cycles of denaturation at 95°C for 5 s and annealing/extension at 60°C for 30 s. Each sample was technically replicated three times and the relative expression levels were normalized to the *CsACTIN* gene (Shen et al., 2019). The primers used for qRT-PCR are detailed in Supplementary Table S1A.

2.3 Plant transformation and generation of overexpressing *Arabidopsis* plants

The complete coding sequence of *CsWAK12* was ligated into the binary vector pCAMBIA3301 (Pyeast, Shaanxi, China), which contains EcoRI and BamHI restriction sites and is regulated by the CaMV35S promoter, utilizing specific primers (Supplementary Table S3B). The relative expression levels were normalized to those of the *AtUBQ10* gene. The recombinant plasmid was introduced into the *Agrobacterium tumefaciens* strain GV3101 (Tsingke, Beijing, China) using the freeze–thaw method. A transgenic *Arabidopsis* strain was generated by transforming wild-type (WT) *Arabidopsis* (Columbia-0) through the floral dip method. T1 plants were screened on 1/2 Murashige-Skoog (MS) Modified Plant Media containing 0.05% glufosinate after sterilization with 20% NaClO and 75% alcohol and were confirmed via PCR. T3 transgenic progeny were selfed from T1 for at least two generations and verified by sequencing (Tsingke, Beijing, China).

In brief, plants were grown in a controlled growth chamber under a 16-h light and 8-h dark cycle, maintained at temperatures of 23/22°C and 60% relative humidity for optimal growth. T3 transgenic and WT Arabidopsis seeds were sown on the surface of the aforementioned 1/2 MS Media. The total root growth of 10-day-old seedlings was measured using vernier calipers. Ten seedlings were taken from each strain, with three replicates for each. To compare the seed length of various Arabidopsis types, seeds harvested at the same time were measured and recorded using ImageJ (Schneider et al., 2012). A minimum of 30 seeds from each line were measured.

2.4 Evaluation of cold tolerance in transgenic *Arabidopsis* seedlings

Following the previously reported protocol, the freezing assay was conducted with minor modifications (Xie et al., 2018; Yang et al., 2023). To evaluate the survival rates of different types of *Arabidopsis* types under cold stress and tolerance, seedlings were cultivated on medium under normal conditions for 2 weeks before exposure to −8°C for 2 h. Subsequently, all seedlings were kept in the dark at 4°C for at least 12 h post-chilling and then returned to normal conditions for 6 days. After the recovery period, the presence of new young leaves was considered indicators of viable seedlings.

To assess the phenotypic changes in different *Arabidopsis* types under cold stress, 10-day-old seedlings were transferred to nutrient soil composed of vermiculite and perlite in a 2:1:1 ratio. These 3-week-old seedlings were then subjected to 4°C for 1 week for cold acclimation, followed by exposure to −15°C for 1.5 h, hereinafter referred to as CA. The 4-week-old seedlings in soil were divided into three groups: one group was treated at the low temperature of −8°C for 2 h (NA1), another group was treated at −15°C for 1 h (NA2), and the remaining group was maintained under normal conditions as a control.

To investigate the physiological changes in different *Arabidopsis* types, 4-week-old seedlings under normal conditions were transferred to −6°C for 0, 1.5, 3, and 6 h to measure SOD activity and MDA content. SOD activity was measured using the SOD Activity Assay Kit (WST-1 Method), while MDA content was assessed using the MDA Content Assay Kit (Solarbio, Beijing, China) to evaluate the cold tolerance of transgenic *Arabidopsis* seedlings over various durations.

2.5 RNA-seq analyses of cold–related genes in transgenic *Arabidopsis* seedlings

To investigate the mechanistic network of *CsWAK12* in response to cold, comparative transcriptomic analyses were conducted using 4-week-old seedlings from transgenic *Arabidopsis* lines and WT plants. These seedlings were subjected to −6°C for 3 h, with normal conditions serving as the control. Total RNA was extracted from both overexpressing *Arabidopsis* and WT plants using the Total RNA Extractor (Trizol) and quantified with the Qubit® 2.0 Fluorometer (Invitrogen, CA, USA) employing Qubit™ RNA High Sensitivity Kits (Invitrogen, CA, USA) for transcriptome analyses. Sequencing was performed on the Illumina Hiseq X Ten platform, and the resulting reads were mapped to the reference genome of *A. thaliana* (TAIR10) using HISAT2 (Kim et al., 2015). Transcript expression was assessed using RSeQC, and transcript abundance was estimated in transcripts per million (TPM) (Wang et al., 2012). Differentially expressed genes (DEGs) were analyzed with DESeq2 and selected based on Student's *t*-test, applying a significance threshold of $p < 0.05$ and a fold change (FC) greater than 2. A Gene Ontology (GO) enrichment analysis was performed using topGO (Alexa et al., 2006). Kyoto Encyclopedia of Genes and Genomes (KEGG) pathway enrichment analysis of DEGs was conducted using the R package clusterProfiler (Yu et al., 2012).

C-repeat/dehydration-responsive element binding factor (CBF) genes, including *AtCBF1* (*AT4G25490*), *AtCBF2* (*AT4G25470*), and *AtCBF3* (*AT4G25480*), were quantified by qRT-PCR. Additionally, the expression level of *CsWAK12* in transgenic lines was measured. *Arabidopsis AtUBQ10* (*AT4G05320*) served as the reference gene in qRT-PCR (Liu et al., 2022). The primer sequences for the genes utilized are listed in Supplementary Table S3E. Relative gene expression values were calculated using the $2^{-\Delta\Delta Ct}$ method.

2.6 Statistical analysis

All experiments were conducted with a minimum of three biological replicates. Statistical analyses were performed using

Microsoft Excel (Microsoft, Washington, USA) and IBM SPSS Statistics 20 (IBM, New York, USA). The data are presented as mean ± standard deviation (SD). Different letters indicate significant differences at $p < 0.05$, while the symbol ** denotes significant differences at $p < 0.01$, as determined by one-way ANOVA.

3 Results

3.1 Molecular characteristics of *CsWAK12* and homoeologous genes

The *CsWAK12* open reading frame (ORF) was isolated from the tea variety SCZ based on the available putative sequence information in the TPIA database (Gao et al., 2023). Our previous study indicated that *CsWAK12* is located on chromosome 4 of the tea plant (Xiao-Yu et al., 2023). The isolated full-length mRNA of *CsWAK12* (accession no. PP739783) consists of 2,265 nucleotides (nt) that encode a protein of 754 amino acids with an estimated molecular mass of 83.39 kDa and an isoelectric point of 5.70.

The protein BLAST analysis of the complete amino acid sequences revealed the presence of at least three domains in the CsWAK12 protein, including the wall-associated receptor kinase galacturonan-binding domain, the epidermal growth factor-like domain, and the catalytic domain (Figure 1A). This finding is consistent with homologous genes from *Arabidopsis thaliana* (NP173549.1), *Actinidia chinensis* (PSS00108.1), *Camellia lanceoleosa* (KAI8015626.1), *Hibiscus trionum* (GMI82953.1), *Melia azedarach* (KAJ4700806.1), *Nicotiana tabacum* (XP016513667.1), *Oryza sativa* (XP015635765.1), and *Vitis vinifera* (RVW51064.1). These results suggest that the structure of *CsWAK12* and homologous genes is relatively conserved, implying that they may perform similar functions. Furthermore, the phylogenetic analysis indicated that the CsWAK12 protein shares greater similarities with CsWAK2 from *Camellia lanceoleosa* (Figure 1B).

3.2 Expression patterns of *CsWAK12* in tea plant

To investigate the potential functions of *CsWAK12*, we examined its relative expression across various tissues of naturally growing tea plants. We performed qRT-PCR to analyze the expression patterns of *CsWAK12* in different tissues of SCZ, including bud, leaf, stem, root, and flower. The results indicated that the *CsWAK12* gene exhibited the highest expression in young leaves and the lowest expression in apical buds. Notably, *CsWAK12* was expressed in all examined organs, with the highest levels found in leaves, and the lowest in flowers, suggesting that *CsWAK12* plays significant roles in leaf development (Figure 1C).

To further explore the potential function of *CsWAK12* in the cold response of tea, we subjected long fresh shoots of SCZ to low-temperature conditions (4°C) for indoor simulated cold stress. qRT-PCR analysis revealed that *CsWAK12* was upregulated under cold stress, exhibiting more than a twofold increase in relative expression values. Notably, *CsWAK12* transcripts peaked at 3 h at 4°C, reaching approximately a 10-fold increase compared to the control treatment (Figure 1D). This increased expression was also significantly greater at 6, 24, and 36 h post-treatment (Figure 1E–I), while a significant decrease at 48 hours (Figure 1J).

3.3 Overexpression of *CsWAK12* improves the growth of *Arabidopsis*

The *CsWAK12* gene, driven by the CaMV35S promoter, was successfully transformed into *Arabidopsis*. Eleven overexpression lines of *CsWAK12* were obtained from which three lines exhibiting notably high expression levels were selected: OE-*CsWAK12*#9, OE-*CsWAK12*#13, and OE-*CsWAK12*#14, referred to as OE9, OE13, and OE14, respectively (Figure 2A). These lines were chosen from T3 homozygous lines for further characterization. Phenotypic analysis of the transgenic lines indicated that *CsWAK12* promotes growth in *Arabidopsis*, as evidenced by increased root length and seed size (Figure 2B). Notably, the average root length of OE14 was 7.34 mm longer than that of the WT. The average seed lengths measured 460.51 μm for OE14, 442.98 μm for OE9, and 428.06 μm for OE13, while the WT measured 395.65 μm (Figures 2C, D).

3.4 Overexpression of *CsWAK12* reduces the cold tolerance of *Arabidopsis*

To assess the cold tolerance of *CsWAK12* transgenic lines, 2-week-old WT and transgenic seedlings grown on 1/2 MS plates were transferred to −15°C for 1 h (Figure 3A). Additionally, 4-week-old WT and transgenic seedlings grown in nutrient soil were subjected to −8°C for 2 h and −15°C for 1 h. We observed that the overexpression of *CsWAK12* resulted in an altered cold tolerance phenotype (Figure 3B). All three transgenic lines exhibited reduced cold tolerance, as evidenced by lower survival rates. While the survival rates of WT and transgenic lines were compared under normal growth conditions, they differed significantly following cold treatment. Specifically, 59% of WT *Arabidopsis* survived exposure to −8°C for 2 h, whereas only 27% of transgenic *Arabidopsis* survived (Figure 3C). In summary, the survival rate of transgenic plants without cold acclimation was significantly lower than that of WT plants. These transgenic plants exhibited stunted growth, shorter root lengths, reduced plant height, and wilted, yellowing rosette leaves after exposure to freezing conditions. Although cold-acclimated transgenic plants demonstrated some degree of cold resistance, their growth rate remained slower, and their survival rate was still diminished. Furthermore, transgenic *Arabidopsis* demonstrated significantly altered levels of SOD activity and MDA (Figures 3D, E). The activity of SOD in WT plants gradually decreased with prolonged cold treatment while the transgenic lines exhibited an overall increase in activity. In contrast, the MDA content in WT plants increased steadily with extended cold exposure. In the transgenic

10.3389/fpls.2024.1420431

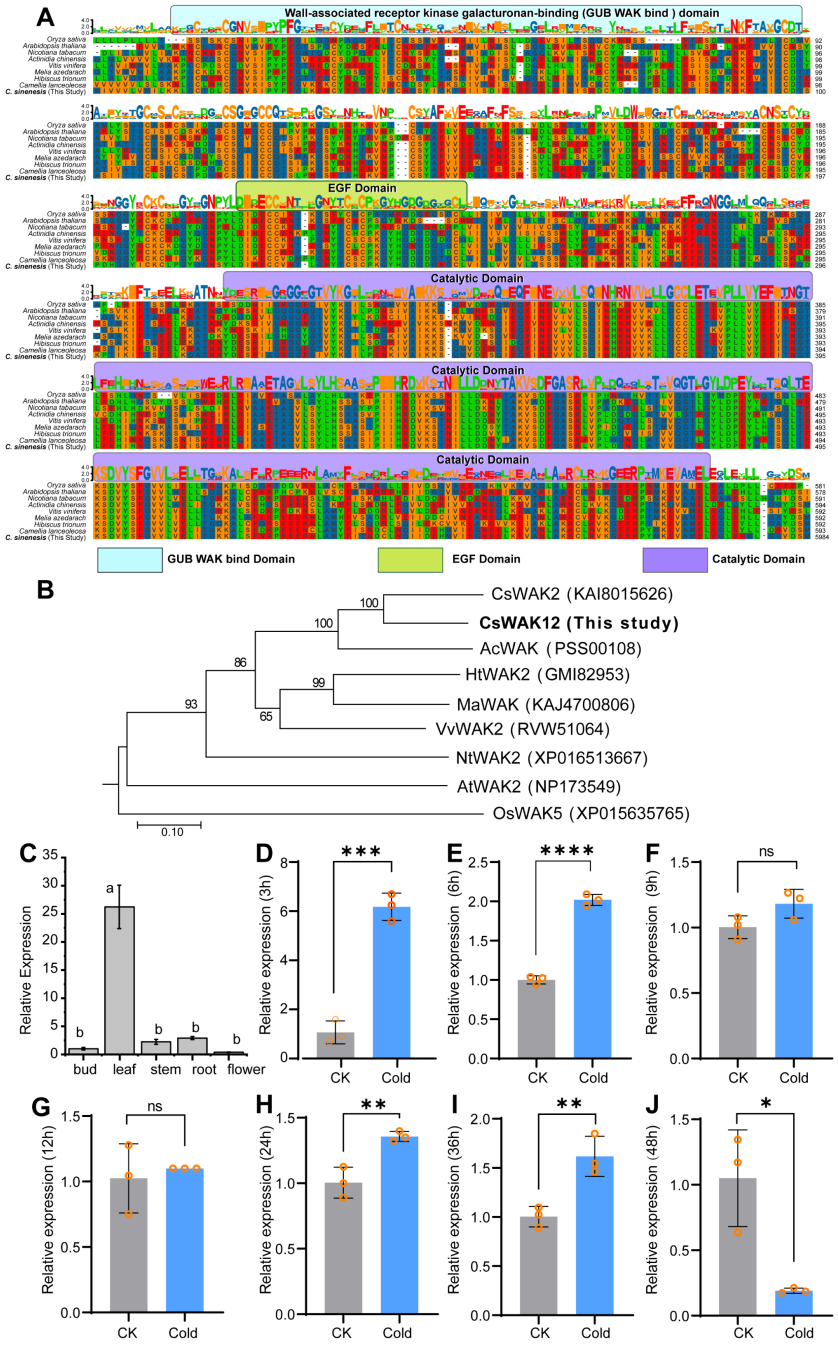

FIGURE 1
Sequence alignment, phylogenetic analysis, and expression pattern of *CsWAK12*. **(A)** Multiple sequence alignment of homologous genes of *CsWAK12*. Different domains are represented by different colors, where the GUB WAK bind domain is light blue, the EGF domain is green, and the catalytic domain is purple. **(B)** The phylogenic tree of *CsWAK12* in different plant species was plotted by the MegAlign software. **(C)** qRT-PCR analysis of the *CsWAK12* transcript in different tissues of SCZ. The total RNA was isolated from the samples of bud, leaf, stem, roots, and flowers. **(D–J)** The expression levels of *CsWAK12* in tea leaves under low-temperature treatment. Error bars represent ± SD (n = 3). Different letters indicate significant differences at $p < 0.05$ according to two-way ANOVA (Duncan's multiple range test). Statistically significant differences were indicated by $*p < 0.05$; $**p < 0.01$; $***p < 0.001$;$****p < 0.0001$ according to unpaired t-test.

line OE9, MDA levels rose rapidly within the first 3 h but subsequently decreased. The transgenic line OE13 exhibited a similar trend to the WT, albeit with a higher growth rate. Additionally, MDA levels in line OE14 displayed an inhibition pattern after exposure to cold (Supplementary Table S4A).

3.5 *CsWAK12* affects the expression of cold-responsive genes in *Arabidopsis*

The signal transmission of cold stress is closely correlated to the core CBF (C-REPEAT BINDING FACTOR) regulatory pathway,

10.3389/fpls.2024.1420431

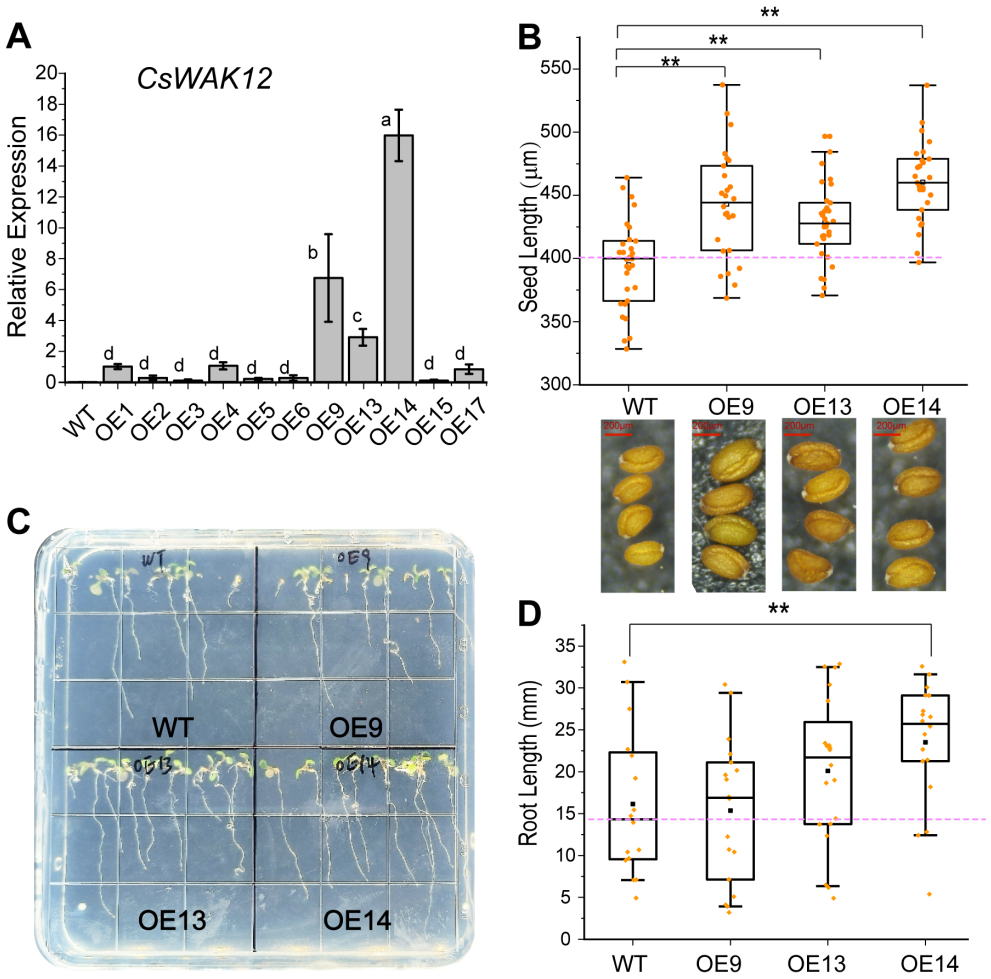

FIGURE 2
Overexpression of *CsWAK12* promotes the growth in transgenic *Arabidopsis*. **(A)** The transcription level of the *CsWAK12* gene in different lines. **(B)** The boxplot showed the seed size of transgenic lines. The lower graph showed the seed of transgenic lines. **(C)** The phenotypes of *CsWAK12* transgenic lines grown on medium. **(D)**The boxplot showed the root length of transgenic lines. The error bars indicate the SDs from three biological replicates. ** indicates a significant difference at the 0.01 level. Different lowercase letters indicate significant difference (P−0.05).

which plays an important role in the plant cold stress response (Liu et al., 2018). To understand the potential mechanisms of altered cold tolerance in *CsWAK12* transgenic plants, we examined the relative expression of *CsWAK12* and *AtCBFs* (*AtCBF1*, *AtCBF2*, and *AtCBF3*) genes in WT and transgenic *Arabidopsis* under −6°C treatment with different duration by qRT-PCR and the normal condition as control. In general, *AtCBFs* in transgenic lines were suppressed before the cold treatment and rapidly induced by cold at 1.5 h. It was noteworthy that *AtCBF2* was significantly inhibited in transgenic lines at 3 h, while the differences in performance of *AtCBF1* and *AtCBF3* were insignificant between transgenic lines and WT. After 6 h, the expression of *AtCBFs* tended to be consistent eventually (Supplementary Table S4B). Owing to the expression changes of *AtCBFs*, we detected the relative expression of *AtICE1*, which was considered as the core transcriptional regulatory element of *AtCBFs*. It was not surprising that the expression level of *AtICE1* was stable and the differences between transgenic lines and WT were relatively subtle (Figure 4). Additionally, we examined several key cold response genes associated with *AtCBFs*, including *AtKIN1*, *AtCOR15A*, *AtCOR15B*, *AtCOR47*, and *AtRD29A*, using qRT-PCR (Supplementary Figure 1). These genes displayed distinct expression patterns, indicating that CsWAK12 may be involved in complex cold response mechanisms. For instance, the fluctuations in *AtCOR15A* expression were minimal in the WT, whereas they were significantly elevated in the transgenic lines. Furthermore, the expression of *AtCOR15B* in the transgenic line OE14 was higher than that of the WT under normal conditions, but decreased to levels comparable to the WT under cold treatment.

3.6 Transcriptome analysis of *CsWAK12* transgenic *Arabidopsis*

To investigate the potential molecular roles of *CsWAK12* in cold stress responses, we conducted a comparative transcriptome analysis of both WT and OE14 under normal growth conditions (N) and cold stress (C) using the Illumina Hiseq X Ten sequencing platform. A total of 99.33 GB raw reads were obtained from all tested samples.

10.3389/fpls.2024.1420431

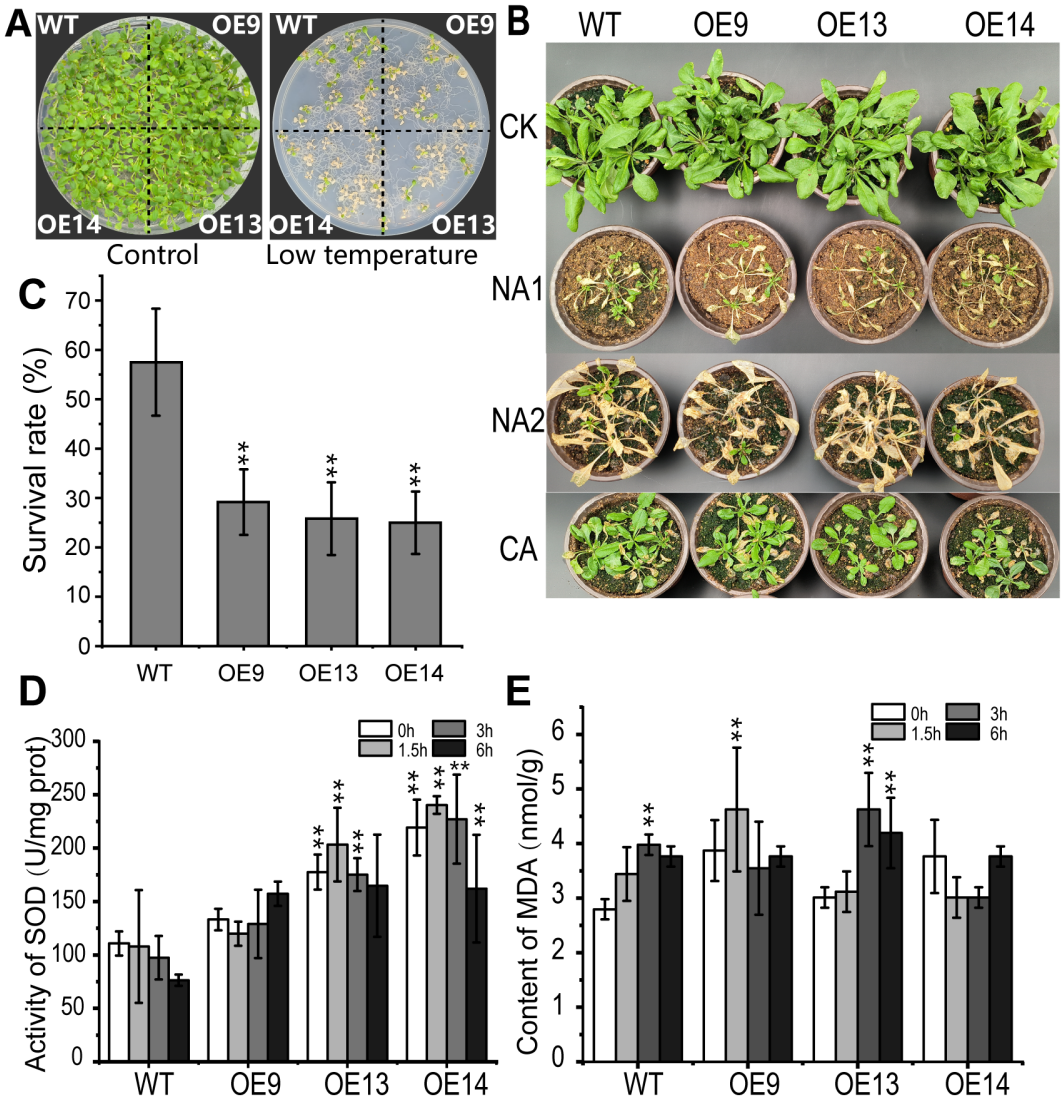

FIGURE 3
Overexpression of *CsWAK12* in *Arabidopsis* reduced cold tolerance. **(A)** The left panel shows the phenotypes of wild-type and transgenic plants growing normally for 2 weeks, while the right panel illustrates the phenotypes of wild-type and transgenic plants after cold treatments at −8°C for 2 (h) **(B)** Phenotypes of the transgenic lines and WT plants after freezing. Four-week-old pot-grown *Arabidopsis* plants were treated with −8°C for 2 h (NA1) and −15°C for 1 h (NA2), after which they were recovered for 7 days. **(C)** Survival rate of WT and transgenic Arabidopsis lines under cold stress. **(D)** Activity of SOD and **(E)** content of MDA of the transgenic lines and WT plants after −6°C. The error bars indicate the SDs from three biological replicates. ** indicates a significant difference at the 0.01 level.

More than 87.86 GB average clean data ratio was above 95% (Q20 > 97.64% and Q30 > 93.73%) (Supplementary Table S5).

DEGs were analyzed between each sequential stage (WT N/C and OE14 N/C) based on fragments per kilobase of transcript per million mapped reads (FPKM), applying thresholds of false discovery rate (FDR) < 0.01 and FC > 2. In WT, we identified 1,221 upregulated and 897 downregulated genes, while in OE14, there were 1,905 upregulated and 685 downregulated genes (Figure 5A). Overall, a total of 3,349 DEGs were identified between the two comparison groups, with 759 DEGs specific to WT and 1,231 DEGs specific to OE14 (Figure 5B). To further clarify the function categories of the DEGs induced by cold stress, we conducted a GO and Kyoto Encyclopedia of Genes and Genomes (KEGG) enrichment analysis. Generally, a corrected *p*-value (*Q*-value) of less than 0.05 indicates significant enrichment of functions. As presented in Supplementary Table S6, the GO terms associated with DEGs in OE14 N/C significantly differ from those in WT N/C. Notably, the biological regulation of biological processes (GO:0065007, *Q*-value = 1.89E-14), the extracellular region of cellular components (GO:0005576, *Q*-value = 5.13E-12), and the catalytic activity of molecular functions (GO:0003824, *Q*-value = 7.54E-05) were particularly prominent. Furthermore, KEGG enrichment analysis of DEGs in OE14 N/C indicated that CsWAK12 may be involved in secondary metabolic pathways such as phenylpropanoid biosynthesis (ko00940, *Q*-value = 1.42E-05), alpha-linolenic acid metabolism (ko00592, *Q*-value = 5.40E-05), and glucosinolate biosynthesis (ko00966, *Q*-value = 6.63E-03) (Supplementary Table S7). These results suggest that the cold

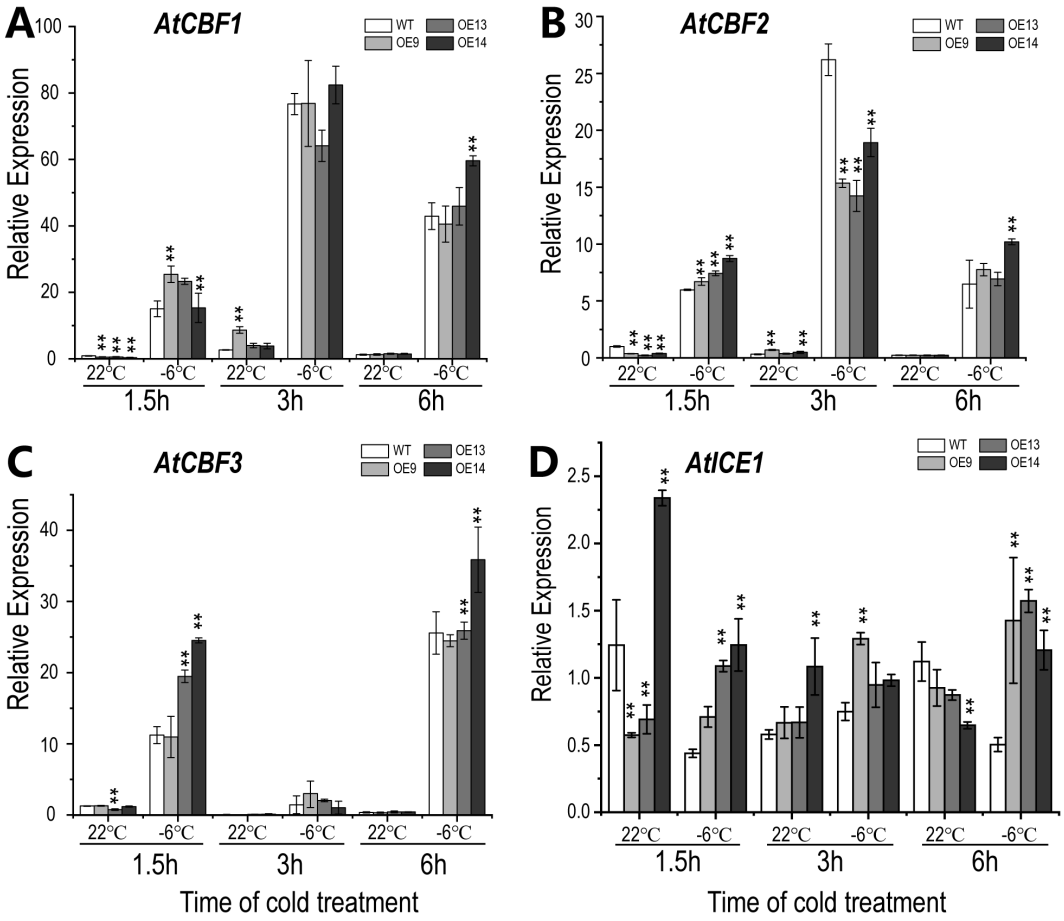

FIGURE 4
Expression pattern of *CsWAK12* and cold-related genes in *Arabidopsis* plants. The expression of *AtCBF1* **(A)**, *AtCBF2* **(B)**, *AtCBF3* **(C)**, and *AtICE1* **(D)** in transgenic lines and WT. The error bars indicate the SDs from three biological replicates. ** indicates a significant difference compared with WT under each treatment at the 0.01 level.

response mechanisms regulated by CsWAK12 in plants are complex.

The specific DEGs in OE14 N/C were predicted using iTAK, revealing 17 transcription factors (TFs) and 17 protein kinases (PKs) that exhibited significant expression changes under cold stress (Figures 5C, D). The expression of TFs such as MAF5 (AT5G65080) and FLC (AT5G10140) was significantly inhibited under cold stress, whereas MYB34 (AT2G31010), WRKY28 (AT4G18170), and JAZ10 (AT5G13220) were significantly activated (Supplementary Table S8A). Notably, ERF (AT4G28140) expression was reduced in WT under cold stress but was highly induced in the overexpressing (OE) line. Regarding PKs, genes such as MAPK3 (AT2G31010) were significantly inhibited under cold stress, while FRK1 (AT2G19190) and WAK1 (AT1G21250) were significantly activated (Supplementary Table S8B).

The genes involved in the CBF pathway contribute to the formation of cold resistance in plants (Supplementary Table S10) (Kidokoro et al., 2021, 2023). To investigate the underlying mechanisms of cold sensitivity in transgenic plants, we analyzed the expression patterns of 40 genes associated with the CBF pathway using transcriptome data (Supplementary Table S11). The result showed that the expression of circadian clock-related genes, such as *REVEILLE 4* (*RVE4*), *Central Circadian Oscillator 1* (*CCA1*), *Late Elongate Hypocotyl* (*LHY*), and *Night Light-inducible and Clock-Regulated* (*LNKs*), was significantly induced in the OE line. In contrast, several TF genes, including *ERF53/54*, *CBFs*, and *DREB2A*, were markedly reduced in the OE line (Supplementary Figure 3). These findings suggest that CsWAK12 may play a role in the biological processes related to plant biorhythms, thereby influencing plant cold tolerance by inhibiting the expression of positive regulatory TFs.

4 Discussion

Multiple RLKs have been confirmed to play a role in the response to cold stress. CRPK1 (Cold-responsive protein kinase 1) negatively regulates cold tolerance by phosphorylating 14-3-3λ, which has been shown to promote the destabilization of CBF proteins via the 26S proteasome pathway in *Arabidopsis* (Liu et al., 2017). Overexpression of *MRLK2* (FERONIA gene) in apple enhances the expression of the cold-responsive genes and anthocyanin biosynthesis-related genes, resulting in increased cold tolerance in the OE lines (Jing et al., 2023). Moreover, overexpressing *BRI1* in *Arabidopsis* facilitates seed

10.3389/fpls.2024.1420431

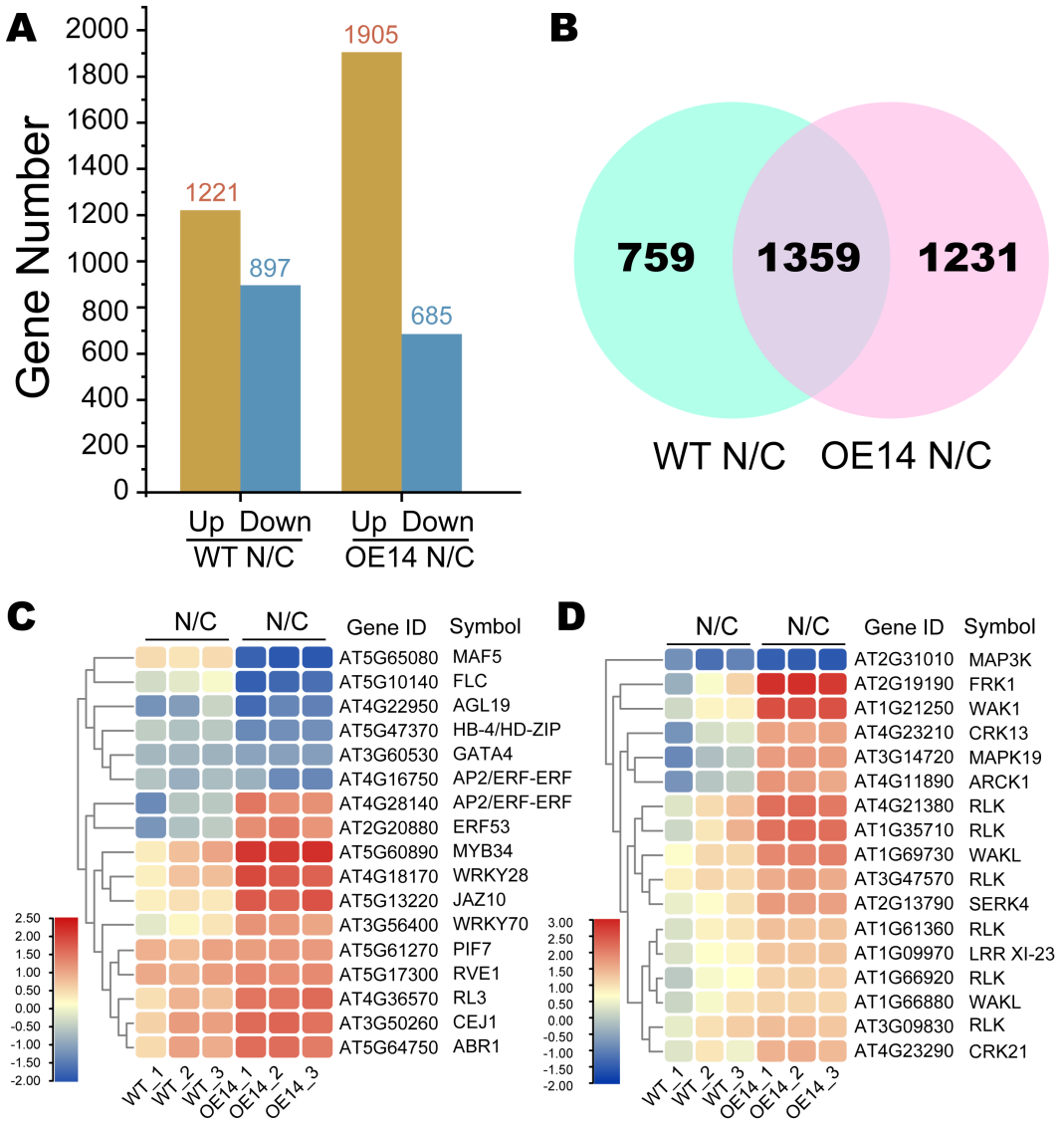

FIGURE 5
Classification of the assembled transcripts and the differentially expressed genes (DEGs). **(A)** Histogram of DEGs in two comparison groups between WT and OE14. **(B)** Venn diagram of OE14-specific DEGs in two comparison groups between WT and OE14. **(C)** Heatmaps of OE14-specific DEGs classified as TF. **(D)** Heatmaps of DEGs classified as PK. Log_2(TPM Fold Change) ≥ 1 or ≤−1 and $p < 0.05$ were used as the standard for screening DEGs. The symbol "N/C" refers to a comparative transcriptome analysis of *Arabidopsis* plants under normal growth conditions (N) and cold stress **(C)**.

germination under cold stratification, whereas the *bri1-5* mutant exhibits significantly reduced sensitivity to cold stratification and inhibits the expression of CBF1/2 genes (Kim et al., 2019). It is intriguing to consider whether the WAK gene is also involved in cold response functionality. In this study, we report that a cell wall-associated RLK from tea plant, *CsWAK12*, serves as a potential negative regulator of the cold stress response. *CsWAK12* is induced by cold in the tea plant and reduces cold tolerance in *Arabidopsis* lines overexpressing *CsWAK12*, as evidenced by decreased seedling survival rates, SOD activity, and MDA content.

WAKs are considered as physical connections between the cell walls and the plasma membrane in higher plant. Gold conjugated secondary antibodies targeting the WAK1 antiserum localize to the surfaces of *Arabidopsis* leaf cells, particularly in the cell wall region, which can be visualized using both light and electron microscopy (He et al., 1996). Green fluorescence was observed along the edge of the cells after the transformation of the GFP-tagged CaWAKL20 coding sequence from pepper into onion epidermal cells (Wang et al., 2019). Similarly, in the case of the tea plant, the fusion protein CsWAK12-GFP was localized to the cell membrane after being introduced into tobacco leaves in this study (Supplementary Figure 2).

WAK proteins have been shown to play a significant role in plant growth and development. Antisense expression of *WAK* in *Arabidopsis* leaves, which resulted in a 50% reduction in total WAK protein levels, led to smaller leaf cells and consequently to dwarf plants (Lally et al., 2001; Kohorn et al., 2006). In rice, various WAK genes regulate growth through distinct mechanisms. *OsWAK10* and its variants modulate cell wall signals to control the amplitude of

secondary wall cellulose synthesis by amplifying pectin-derived signals, which, in turn, influences the height of rice stems (Cai et al., 2023). Conversely, OsWAK11 negatively regulates the stature, leaf angle, and seed length of rice plants by phosphorylating and repressing OsBRI1 activity, a crucial regulatory site for rice architecture (Yue et al., 2022). Therefore, WAKs may exhibit differential roles in plant growth and development. In our study, *CsWAK12* was found to promote growth in *Arabidopsis* OE lines, enhancing root length, seed size, and overall growth potential (Figure 3). It is acknowledged that plants may suppress growth to redirect energy toward defense against environmental stress. Regarding the specific function of the *CsWAK12* gene, it appears to inhibit the cold stress response while simultaneously promoting growth, indicating heightened sensitivity to cold. The intriguing functional model of *CsWAK12* in relation to cold stress and physiological growth warrants further elucidation.

To investigate the functional model in depth, we analyzed the relationship between *CsWAK12* and the classical cold response CBF pathway. CBFs play crucial roles in plant response to cold stress, as their expression is rapidly induced by cold conditions. This induction enables CBFs to bind to the promoter regions of Cold-Regulated (COR) genes, activating their expression and thereby positively regulating cold resistance in plants. In our research, we observed the expression of CBF genes in WT and OE lines during cold treatment. Notably, the expression of *CBFs* in OE lines was suppressed at 1.5 h but induced at 3 h under normal conditions. Although cold stress induced *CBF* expression, we noted considerable variation in the magnitude of these changes between WT and OE lines. These results suggest that CsWAK12 may be involved in the CBF pathway, potentially reducing cold resistance by interfering with the transcriptional activity of *CBFs*. Inducer of CBF expression 1 (ICE1) is a master regulator of CBFs, encoding an MYC-like bHLH TF, that binds to canonical MYC cis-elements in *CBF* promoters, thereby positively regulating *CBF* gene expression (Miura et al., 2007). As a core component of the CBF signaling pathway, the transcriptional level of *ICE1* is not induced by low temperature; however, its protein level is regulated by various modifications, including ubiquitination and phosphorylation (Ye et al., 2019). In our study, the relative expression of *ICE1* was only slightly affected by low temperature in both WT and transgenic lines, consistent with previous findings. We speculate that *CsWAK12* may play a role in the post-translational modification of ICE1, which subsequently influences the expression of *CBFs*.

Numerous reliable studies have confirmed that TFs such as MYB, WRKY, ERF, and JAZ are involved in the cold stress response in plant (Xu et al., 2018; Li et al., 2023; An et al., 2022). MdMYB308L interacts with MdbHLH33, enhancing its binding to the promoters of *MdCBF2* and *MdDFR* in apple (Xie et al., 2018). *Arabidopsis* plants overexpressing PbMYB1L from pear exhibited significant anthocyanin accumulation in leaves following cold treatment, which significantly induced the expression of *AtCBF* genes, resulting in enhanced cold tolerance (Zhou et al., 2024). WRKY33 in both wild and cultivated tomatoes positively regulates cold tolerance (Guo et al., 2022). In rice, WRKY53 mediates the crosstalk between brassinosteroid (BR) signaling and the MAPK pathway to regulate plant architecture and seed size, while negatively regulating rice cold tolerance at the booting stage by fine-tuning anther gibberellin levels (Tang et al., 2022; Tian et al., 2021). Our previous research found that transgenic *Arabidopsis* lines overexpressing CsWRKY29 and CsWRKY37 genes exhibited higher survival rates and lower MDA levels under freezing treatment compared to WT plants (Zhao et al., 2022). In this study, we also observed that *CsWAK12* altered the expression of several TF genes. MYB34, WRKY28, and WRKY70 were inhibited in transgenic lines under normal conditions but were more strongly induced by low temperatures (Supplementary Table S5A). These results suggest that CsWAK12 plays a negative role in activating cold response TF genes. Therefore, it would be interesting to investigate the downstream cooperators of CsWAK12 to elucidate the cold response pathway.

Mitogen-activated protein kinases (MAPKs) represent a crucial signaling link between cell surface receptors and both transcriptional and enzymatic regulation in eukaryotes. Evidence suggests a role for MAPKs in WAK signaling. Protoplasts from plants homozygous for the null allele wak2-1 exhibited a reduction in the activation of MPK3 (Kohorn et al., 2009). MPK6 is likely a target of WAK2cTAP, a dominant allele of WAK2, which serves a distinct function compared to MPK3 (Kohorn et al., 2012). Our research demonstrated that MAP3K was highly induced in the OE line, while MAPK19 was inhibited under normal growth conditions. However, MAPK19 was induced by cold in the OE line. These results indicate a role for MAPKs in CsWAK12 signaling during cold stress. Furthermore, the expression of *WAK1* in the OE line was initially inhibited but was subsequently strongly induced by cold, whereas *CsWAK12* exhibited the opposite pattern. This suggests that CsWAK12 has an antagonistic relationship with WAK1 in response to cold. Future studies will be intriguing to explore the potential complementary functions of the *CsWAK12* and *WAK1* genes.

5 Conclusion

In this study, we report that tea CsWAK12 possesses conserved domains characteristic of the WAK family and is localized to the plasma membrane. The expression of CsWAK12 is upregulated in response to cold stress. Overexpression of CsWAK12 promotes plant growth but decreases *Arabidopsis* tolerance to cold stress. Additionally, overexpressing CsWAK12 reduces the cold-induced expression of CBF genes under normal conditions, although their expression is more strongly induced by cold stress. Therefore, we suggest that CsWAK12 negatively modulates plant cold tolerance by interfering with the transcriptional activity of *CBFs*. Our results lay a foundation for further understanding the functional mechanisms of WAKs in plant adaptation to environmental stress.

Data availability statement

The RNA-seq raw data for all samples are accessible at NCBI BioProject PRJNA1102880, which includes an accession number for SRX24324921~SRX24324932. The isolated full-length mRNA of

CsWAK12 is available at NCBI Nucleotide Datasets under the accession number PP739783. The original contributions presented in the study are included in the article/Supplementary Material, further inquiries can be directed to the corresponding author/s.

Author contributions

QW: Conceptualization, Investigation, Writing – original draft, Data curation, Formal analysis, Funding acquisition, Methodology, Project administration. XJ: Methodology, Validation, Writing – review & editing, Data curation. DL: Methodology, Visualization, Writing – review & editing. MS: Writing – review & editing. WT: Writing – review & editing. XR: Writing – review & editing. LW: Writing – review & editing. YD: Funding acquisition, Writing – review & editing. ZZ: Writing – review & editing. WW: Funding acquisition, Writing – review & editing. EX: Funding acquisition, Writing – review & editing.

Funding

The author(s) declare financial support was received for the research, authorship, and/or publication of this article. This work was supported by the Open Fund of State Key Laboratory of Tea Plant Biology and Utilization (SKLTOF20220120), the National Natural Science Foundation of China (32261133519), the Achievements Transformation Project of Anhui Academy of Agricultural Sciences (2024YL041), and the China Agricultural Research System (CARS-19).

Conflict of interest

The authors declare that the research was conducted in the absence of any commercial or financial relationships that could be construed as a potential conflict of interest.

Publisher's note

Supplementary material

The Supplementary Material for this article can be found online at: https://www.frontiersin.org/articles/10.3389/fpls.2024.1420431/full#supplementary-material

References

Alexa, A., Rahnenführer, J., and Lengauer, T. (2006). Improved scoring of functional groups from gene expression data by decorrelating GO graph structure. *Bioinformatics* 22, 1600–1607. doi: 10.1093/bioinformatics/btl140

An, J.-P., Xu, R.-R., Liu, X., Su, L., Yang, K., Wang, X.-F., et al. (2022). Abscisic acid insensitive 4 interacts with ICE1 and JAZ proteins to regulate ABA signaling-mediated cold tolerance in apple. *J. Exp. Bot.* 73, 980–997. doi: 10.1093/jxb/erab433

Anderson, C. M., Wagner, T. A., Perret, M., He, Z.-H., He, D., and Kohorn, B. D. (2001). WAKs: cell wall-associated kinases linking the cytoplasm to the extracellular matrix. *Plant Mol. Biol.* 47, 197–206. doi: 10.1023/A:1010691701578

Cai, W., Hong, J., Liu, Z., Wang, W., Zhang, J., An, G., et al. (2023). A receptor-like kinase controls the amplitude of secondary cell wall synthesis in rice. *Curr. Biol.* 33, 498–506. doi: 10.1016/j.cub.2022.12.035

Dou, L., Li, Z., Shen, Q., Shi, H., Li, H., Wang, W., et al. (2021). Genome-wide characterization of the WAK gene family and expression analysis under plant hormone treatment in cotton. *BMC Genomics* 22, 85. doi: 10.1186/s12864-021-07378-8

Gao, Q., Wei, T., Li, F., Wang, Y., Wu, Q., Wan, X., et al. (2023). TPIA2: an updated tea plant information archive for *camellia* genomics. *Nucleic Acids Res.* 52, D1661–D1667. doi: 10.1093/nar/gkad701

Guo, M., Yang, F., Chenxu, L., Zou, J., Qi, Z., Fotopoulos, V., et al. (2022). A single nucleotide polymorphism in WRKY33 promoter is associated with the cold sensitivity in cultivated tomato. *New Phytol.* 236, 989–1005. doi: 10.1111/nph.v236.3

He, Z.-H., Cheeseman, I., He, D., and Kohorn, B. D. (1999). A cluster of five cell wall-associated receptor kinase genes, WAK1-5, are expressed in specific organs of *Arabidopsis*. *Plant Mol. Biol.* 39, 1189–1196. doi: 10.1023/A:1006197318246

He, Z.-H., Fujiki, M., and Kohorn, B. D. (1996). A cell wall-associated, receptor-like protein kinase. *J. Biol. Chem.* 271, 19789–19793. doi: 10.1074/jbc.271.33.19789

Jiao, X.-Y., Wu, Q., Liu, D.-D., Sun, M.-H., and Wang, W.-J. (2023). Identification and expression analysis of the wall-associated kinase gene family in *Camellia sinensis*. *J. Agric. Biotechnol.* 31, 1816–1831. 10.3969/j.issn.1674-7968.2023.09.004

Jing, Y., Pei, T., Chunrong, L., Wang, D., Wang, Q., Chen, Y., et al. (2023). Overexpression of the feronia receptor kinase mdMRLK2 enhances apple cold tolerance. *Plant J.* 115, 236–252. doi: 10.1111/tpj.16226

Jung, C. G., Hwang, S.-G., Park, Y. C., Park, H. M., Kim, D. S., Park, D. H., et al. (2015). Molecular characterization of the cold- and heat-induced *arabidopsis* PXL1 gene and its potential role in transduction pathways under temperature fluctuations. *J. Plant Physiol.* 176, 138–146. doi: 10.1016/j.jplph.2015.01.001

Kidokoro, S., Hayashi, K., Haraguchi, H., Ishikawa, T., Soma, F., Konoura, I., et al. (2021). Posttranslational regulation of multiple clock-related transcription factors triggers cold-inducible gene expression in *Arabidopsis*. *Proc. Natl. Acad. Sci.* 118, e2021048118. doi: 10.1073/pnas.2021048118

Kidokoro, S., Konoura, I., Soma, F., Suzuki, T., Miyakawa, T., Tanokura, M., et al. (2023). Clock-regulated coactivators selectively control gene expression in response to different temperature stress conditions in *Arabidopsis*. *Proc. Natl. Acad. Sci.* 120, e2216183120. doi: 10.1073/pnas.2216183120

Kim, D., Langmead, B., and Salzberg, S. L. (2015). HISAT: a fast spliced aligner with low memory requirements. *Nat. Methods* 12, 357–360. doi: 10.1038/nmeth.3317

Kim, S. Y., Warpeha, K. M., and Huber, S. C. (2019). The brassinosteroid receptor kinase, BRI1, plays a role in seed germination and the release of dormancy by cold stratification. *J. Plant Physiol.* 241, 153031. doi: 10.1016/j.jplph.2019.153031

Kohorn, B. D., Johansen, S., Shishido, A., Todorova, T., Martinez, R., Defeo, E., et al. (2009). Pectin activation of MAP kinase and gene expression is WAK2 dependent. *Plant J.* 60, 974–982. doi: 10.1111/j.1365-313X.2009.04016.x

Kohorn, B. D., Kobayashi, M., Johansen, S., Riese, J., Huang, L. F., Koch, K., et al. (2006). An *Arabidopsis* cell wall-associated kinase required for invertase activity and cell growth. *Plant J.* 46, 307–316. doi: 10.1111/j.1365-313X.2006.02695.x

Kohorn, B. D., Kohorn, S. L., Tanya, T., Baptiste, G., Stansky, K., and McCullough, M. (2012). A dominant allele of *arabidopsis* pectin-binding wall-associated kinase induces a stress response suppressed by MPK6 but not MPK3 mutations. *Mol. Plant* 5, 841–851. doi: 10.1093/mp/ssr096

Kurt, F., Kurt, B., and Filiz, E. (2020). Wall Associated Kinases (WAK) Gene Family in Tomato (*Solanum lycopersicum*): Insights into Plant Immunity. *Gene Rep.* 21, 100828. doi: 10.1016/j.genrep.2020.100828

Lally, D., Ingmire, P., Tong, H.-Y., and He, Z.-H. (2001). Antisense expression of a cell wall-associated protein kinase, WAK4, inhibits cell elongation and alters morphology. *Plant Cell* 13, 1317–1332. doi: 10.1105/tpc.13.6.1317

Li, B., Wang, X., Wang, X., and Xi, Z. (2023). An AP2/ERF transcription factor VvERF63 positively regulates cold tolerance in Arabidopsis and grape leaves. *Environ. Exp. Bot.* 205, 105124. doi: 10.1016/j.envexpbot.2022.105124

Lin, Z., Jamieson, P., Zhang, L., Zhao, Z., Babilonia, K., et al. (2020). The cotton wall-associated kinase ghWAK7A mediates responses to fungal wilt pathogens by complexing with the chitin sensory receptors. *Plant Cell* 32, 3978–4001. doi: 10.1105/tpc.19.00950

Lin, W., Yuehua, W., Liu, X., Shang, J.-X., and Zhao, L. (2021). OsWAK112, a wall-associated kinase, negatively regulates salt stress responses by inhibiting ethylene production. *Front. Plant Sci.* 12, 751965. doi: 10.3389/fpls.2021.751965

Liu, Z., Hou, S., Rodrigues, O., Wang, P., Luo, D., Munemasa, S., et al. (2022). Phytocytokine signaling reopens stomata in plant immunity and water loss. *Nature* 605, 332–339. doi: 10.1038/s41586-022-04684-3

Liu, Z., Jia, Y., Ding, Y., Shi, Y., Li, Z., Guo, Y., et al. (2017). Plasma membrane CRPK1-mediatedPhosphorylation of 14-3-3 proteins induces their nuclear import to fine-tune CBF signaling during cold response. *Mol. Cell* 66, 117–128. doi: 10.1016/j.molcel.2017.02.016

Liu, J., Yiting, S., and Yang, S. (2018). Insights into the regulation of CBF cold signaling in plants. *J. Integr. Plant Biol.* 60, 780–795. doi: 10.1111/jipb.12657

Miura, K., Jin, J. B., Lee, J., Yoo, C. Y., Stirm, V., Miura, T., et al. (2007). SIZ1-mediated sumoylation of ICE1 controls CBF3/DREB1A expression and freezing tolerance in *Arabidopsis*. *Plant Cell* 19, 1403–1414. doi: 10.1105/tpc.106.048397

Schneider, C. A., Rasband, W. S., and Eliceiri, K. W. (2012). NIH Image to ImageJ: 25 years of image analysis. *Nat. Methods* 9, 671–675. doi: 10.1038/nmeth.2089

Shen, J., Zhang, D., Zhou, L., Zhang, X., Liao, J., Duan, Y., et al. (2019). Transcriptomic and metabolomic profiling of camellia sinensis L. cv. 'Suchazao' Exposed to temperature stresses reveals modification in protein synthesis and photosynthetic and anthocyanin biosynthetic pathways. *Tree Physiol.* 39, 1583–1599. doi: 10.1093/treephys/tpz059

Tang, J., Tian, X., Mei, E., He, M., Gao, J., Yu, J., et al. (2022). WRKY53 negatively regulates rice cold tolerance at the booting stage by fine-tuning anther gibberellin levels. *Plant Cell* 34, 4495–4515. doi: 10.1093/plcell/koac253

Tian, X., He, M., Mei, E., Zhang, B., Tang, J., Xu, M., et al. (2021). WRKY53 integrates classic brassinosteroid signaling and the mitogen-activated protein kinase pathway to regulate rice architecture and seed size. *Plant Cell* 33, 2753–2775. doi: 10.1093/plcell/koab137

Tripathi, R. K., Aguirre, J. A., and Singh, J. (2020). Genome-wide analysis of wall associated kinase (WAK) gene family in barley. *Genomics* 113, 523–530. doi: 10.1016/j.ygeno.2020.09.045

Wang, H., Niu, H., Liang, M., Zhai, Y., Huang, W., Ding, Q., et al. (2019). A wall-associated kinase gene caWAKL20 from pepper negatively modulates plant thermotolerance by reducing the expression of ABA-responsive genes. *Front. Plant Sci.* 10, 591. doi: 10.3389/fpls.2019.00591

Wang, L., Wang, S., and Li, W. (2012). RseQC: quality control of RNA-seq experiments. *Bioinformatics* 28, 2184–2185. doi: 10.1093/bioinformatics/bts356

Xie, Y., Chen, P., Yan, Y., Bao, C., Li, X., Wang, L., et al. (2018). An atypical R2R3 MYB transcription factor increases cold hardiness by CBF- dependent and CBF-independent pathways in apple. *New Phytol.* 218, 201–218. doi: 10.1111/nph.14952

Xu, H., Yang, G., Zhang, J., Wang, Y., Zhang, T., Wang, N., et al. (2018). Overexpression of a repressor mdMYB15L negatively regulates anthocyanin and cold tolerance in red-fleshed callus. *Biochem. Biophys. Res. Commun.* 500, 405–410. doi: 10.1016/j.bbrc.2018.04.088

Yang, J., Guo, X., Mei, Q., Qiu, L., Chen, P., Li, W., et al. (2023). MdbHLH4 negatively regulates apple cold tolerance by inhibiting MdCBF1/3 expression and promoting MdCAX3L-2 expression. *Plant physiology* 191, 789–806. doi: 10.1093/plphys/kiac512

Ye, K., Li, H., Ding, Y., Shi, Y., Song, C., Gong, Z., et al. (2019). BRASSINOSTEROID-INSENSITIVE2 negatively regulates the stability of transcription factor ICE1 in response to cold stress in *arabidopsis*. *Plant Cell* 31, 2682–2696. doi: 10.1105/tpc.19.00058

Yu, G., Wang, L.-G., Han, Y., and He, Q.-Y. (2012). clusterProfiler: an R package for comparing biological themes among gene clusters. *OMICS: A J. Integr. Biol.* 16, 284–287. doi: 10.1089/omi.2011.0118

Yu, H., Zhang, W., Kang, Y., Fan, Y., Yang, X., Shi, M., et al. (2022). Genome-wide identification and expression analysis of wall-associated kinase (WAK) gene family in potato (*Solanum tuberosum* L.). *Plant Biotechnol. Rep.* 16, 317–331. doi: 10.1007/s11816-021-00739-5

Yue, Z.-L., Liu, N., Deng, Z.-P., Zhang, Y., Wu, Z.-M., Zhao, J.-L., et al. (2022). The receptor kinase osWAK11 monitors cell wall pectin changes to fine-tune brassinosteroid signaling and regulate cell elongation in rice. *Curr. Biol.* 32, 2454–2466. doi: 10.1016/j.cub.2022.04.028

Zhang, S., Chen, C., Li, L., Meng, L., Singh, J., Jiang, N., et al. (2005). Evolutionary expansion, gene structure, and expression of the rice wall-associated kinase gene family. *Plant Physiol.* 139, 1107–1124. doi: 10.1104/pp.105.069005

Zhao, H., Mallano, A. I., Li, F., Li, P., Wu, Q., Wang, Y., et al. (2022). Characterization of csWRKY29 and csWRKY37 transcription factors and their functional roles in cold tolerance of tea plant. *Beverage Plant Res.* 2, 15. doi: 10.48130/BPR-2022-0015

Zhou, X., Lei, D., Yao, W., Li, S., Wang, H., Lu, J., et al. (2024). A novel R2R3-myb transcription factor pbMYB1l of *pyrus bretschneideri* regulates cold tolerance and anthocyanin accumulation. *Plant Cell Rep.* 43, 34. doi: 10.1007/s00299-023-03117-3

Frontiers in
Plant Science

Cultivates the science of plant biology and its applications

The most cited plant science journal, which advances our understanding of plant biology for sustainable food security, functional ecosystems and human health.

Discover the latest Research Topics

See more →

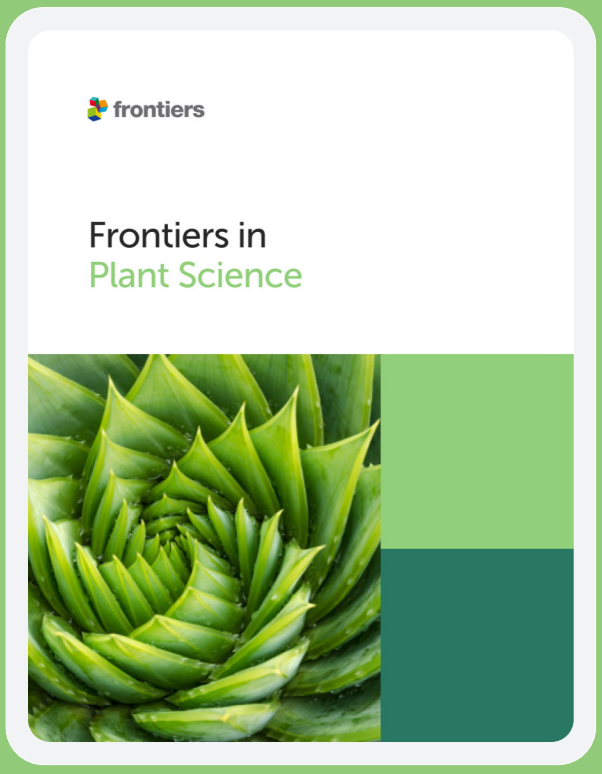

Frontiers

Avenue du Tribunal-Fédéral 34
1005 Lausanne, Switzerland
frontiersin.org

Contact us

+41 (0)21 510 17 00
frontiersin.org/about/contact